

VOL. 707 NO. 2 21 JULY 1995

THIS ISSUE COMPLETES VOL. 707

including

**11th International Symposium on  
Preparative and Industrial Chromatography,  
Baden-Baden, October 3-6, 1994**

JOURNAL OF

# CHROMATOGRAPHY A

INCLUDING ELECTROPHORESIS AND OTHER SEPARATION METHODS

## EDITORS

U.A.Th. Brinkman (Amsterdam)  
R.W. Giese (Boston, MA)  
J.K. Haken (Kensington, N.S.W.)  
C.F. Poole (London)  
L.R. Snyder (Orinda, CA)  
S. Terabe (Hyogo)

EDITORS, SYMPOSIUM VOLUMES,  
E. Heftmann (Orinda, CA), Z. Deyl (Prague)

## EDITORIAL BOARD

D.W. Armstrong (Rolla, MO)  
W.A. Aue (Halifax)  
P. Boček (Brno)  
P.W. Carr (Minneapolis, MN)  
J. Crommen (Liège)  
V.A. Davankov (Moscow)  
G.J. de Jong (Weesp)  
Z. Deyl (Prague)  
S. Dilli (Kensington, N.S.W.)  
Z. El Rassi (Stillwater, OK)  
H. Engelhardt (Saarbrücken)  
M.B. Evans (Hatfield)  
S. Fanali (Rome)  
G.A. Guiochon (Knoxville, TN)  
P.R. Haddad (Hobart, Tasmania)  
I.M. Hais (Hradec Králové)  
W.S. Hancock (Palo Alto, CA)  
S. Hjertén (Uppsala)  
S. Honda (Higashi-Osaka)  
Cs. Horváth (New Haven, CT)  
J.F.K. Huber (Vienna)  
J. Janák (Brno)  
P. Jandera (Pardubice)  
B.L. Karger (Boston, MA)  
J.J. Kirkland (Newport, DE)  
E. sz. Kováts (Lausanne)  
C.S. Lee (Ames, IA)  
K. Macek (Prague)  
A.J.P. Martin (Cambridge)  
E.D. Morgan (Keele)  
H. Poppe (Amsterdam)  
P.G. Righetti (Milan)  
P. Schoenmakers (Amsterdam)  
R. Schwarzenbach (Dübendorf)  
R.E. Shoup (West Lafayette, IN)  
R.P. Singhal (Wichita, KS)  
A.M. Siouffi (Marseille)  
D.J. Strydom (Boston, MA)  
T. Takagi (Osaka)  
N. Tanaka (Kyoto)  
K.K. Unger (Mainz)  
P. van Zoonen (Bilthoven)  
R. Verpoorte (Leiden)  
Gy. Vigh (College Station, TX)  
J.T. Watson (East Lansing, MI)  
B.D. Westerlund (Uppsala)

## EDITORS, BIBLIOGRAPHY SECTION

Z. Deyl (Prague), J. Janák (Brno), V. Schwarz (Prague)

ELSEVIER

# JOURNAL OF CHROMATOGRAPHY A

INCLUDING ELECTROPHORESIS AND OTHER SEPARATION METHODS

**Scope.** The *Journal of Chromatography A* publishes papers on all aspects of **chromatography, electrophoresis** and related methods. Contributions consist mainly of research papers dealing with chromatographic theory, instrumental developments and their applications. In the *Symposium volumes*, which are under separate editorship, proceedings of symposia on chromatography, electrophoresis and related methods are published. *Journal of Chromatography B: Biomedical Applications*—This journal, which is under separate editorship, deals with the following aspects: developments in and applications of chromatographic and electrophoretic techniques related to clinical diagnosis or alterations during medical treatment; screening and profiling of body fluids or tissues related to the analysis of active substances and to metabolic disorders; drug level monitoring and pharmacokinetic studies; clinical toxicology; forensic medicine; veterinary medicine; occupational medicine; results from basic medical research with direct consequences in clinical practice.

**Submission of Papers.** The preferred medium of submission is on disk with accompanying manuscript (see *Electronic manuscripts* in the Instructions to Authors, which can be obtained from the publisher, Elsevier Science B.V., P.O. Box 330, 1000 AH Amsterdam, Netherlands). Manuscripts (in English; four copies are required) should be submitted to: Editorial Office of *Journal of Chromatography A*, P.O. Box 681, 1000 AR Amsterdam, Netherlands, Telefax (+31-20) 485 2304, or to: The Editor of *Journal of Chromatography B: Biomedical Applications*, P.O. Box 681, 1000 AR Amsterdam, Netherlands. Review articles are invited or proposed in writing to the Editors who welcome suggestions for subjects. An outline of the proposed review should first be forwarded to the Editors for preliminary discussion prior to preparation. Submission of an article is understood to imply that the article is original and unpublished and is not being considered for publication elsewhere. For copyright regulations, see below.

**Publication information.** *Journal of Chromatography A* (ISSN 0021-9673): for 1995 Vols. 683–714 are scheduled for publication. *Journal of Chromatography B: Biomedical Applications* (ISSN 0378-4347): for 1995 Vols. 663–674 are scheduled for publication. Subscription prices for *Journal of Chromatography A*, *Journal of Chromatography B: Biomedical Applications* or a combined subscription are available upon request from the publisher. Subscriptions are accepted on a prepaid basis only and are entered on a calendar year basis. Issues are sent by surface mail except to the following countries where air delivery via SAL is ensured: Argentina, Australia, Brazil, Canada, China, Hong Kong, India, Israel, Japan, Malaysia, Mexico, New Zealand, Pakistan, Singapore, South Africa, South Korea, Taiwan, Thailand, USA. For all other countries airmail rates are available upon request. Claims for missing issues must be made within six months of our publication (mailing) date. Please address all your requests regarding orders and subscription queries to: Elsevier Science B.V., Journal Department, P.O. Box 211, 1000 AE Amsterdam, Netherlands. Tel.: (+31-20) 485 3642; Fax: (+31-20) 485 3598. Customers in the USA and Canada wishing information on this and other Elsevier journals, please contact Journal Information Center, Elsevier Science Inc., 655 Avenue of the Americas, New York, NY 10010, USA, Tel. (+1-212) 633 3750, Telefax (+1-212) 633 3764.

**Abstracts/Contents Lists** published in Analytical Abstracts, Biochemical Abstracts, Biological Abstracts, Chemical Abstracts, Chemical Titles, Chromatography Abstracts, Current Awareness in Biological Sciences (CABS), Current Contents/Life Sciences, Current Contents/Physical, Chemical & Earth Sciences, Deep-Sea Research/Part B: Oceanographic Literature Review, Excerpta Medica, Index Medicus, Mass Spectrometry Bulletin, PASCAL-CNRS, Referativnyi Zhurnal, Research Alert and Science Citation Index.

**US Mailing Notice.** *Journal of Chromatography A* (ISSN 0021-9673) is published weekly (total 52 issues) by Elsevier Science B.V., (Sara Burgerhartstraat 25, P.O. Box 211, 1000 AE Amsterdam, Netherlands). Annual subscription price in the USA US\$ 5389.00 (US\$ price valid in North, Central and South America only) including air speed delivery. Second class postage paid at Jamaica, NY 11431. **USA POSTMASTERS:** Send address changes to *Journal of Chromatography A*, Publications Expediting, Inc., 200 Meacham Avenue, Elmont, NY 11003. Airfreight and mailing in the USA by Publications Expediting.

**See inside back cover** for Publication Schedule, Information for Authors and information on Advertisements.

© 1995 ELSEVIER SCIENCE B.V. All rights reserved.

0021-9673/95/\$09.50

No part of this publication may be reproduced, stored in a retrieval system or transmitted in any form or by any means, electronic, mechanical, photocopying, recording or otherwise, without the prior written permission of the publisher, Elsevier Science B.V., Copyright and Permissions Department, P.O. Box 521, 1000 AM Amsterdam, Netherlands.

Upon acceptance of an article by the journal, the author(s) will be asked to transfer copyright of the article to the publisher. The transfer will ensure the widest possible dissemination of information.

**Special regulations for readers in the USA**—This journal has been registered with the Copyright Clearance Center, Inc. Consent is given for copying of articles for personal or internal use, or for the personal use of specific clients. This consent is given on the condition that the copier pays through the Center the per-copy fee stated in the code on the first page of each article for copying beyond that permitted by Sections 107 or 108 of the US Copyright Law. The appropriate fee should be forwarded with a copy of the first page of the article to the Copyright Clearance Center, Inc., 222 Rosewood Drive, Danvers, MA 01923, USA. If no code appears in an article, the author has not given broad consent to copy and permission to copy must be obtained directly from the author. The fee indicated on the first page of an article in this issue will apply retroactively to all articles published in the journal, regardless of the year of publication. This consent does not extend to other kinds of copying, such as for general distribution, resale, advertising and promotion purposes, or for creating new collective works. Special written permission must be obtained from the publisher for such copying.

No responsibility is assumed by the Publisher for any injury and/or damage to persons or property as a matter of products liability, negligence or otherwise, or from any use or operation of any methods, products, instructions or ideas contained in the materials herein. Because of rapid advances in the medical sciences, the Publisher recommends that independent verification of diagnoses and drug dosages should be made.

Although all advertising material is expected to conform to ethical (medical) standards, inclusion in this publication does not constitute a guarantee or endorsement of the quality or value of such product or of the claims made of it by its manufacturer.

Ⓢ The paper used in this publication meets the requirements of ANSI/NISO Z39.48-1992 (Permanence of Paper).

Printed in the Netherlands

## CONTENTS

(Abstracts/Contents Lists published in Analytical Abstracts, Biochemical Abstracts, Biological Abstracts, Chemical Abstracts, Chemical Titles, Chromatography Abstracts, Current Awareness in Biological Sciences (CABS), Current Contents/Life Sciences, Current Contents/Physical, Chemical & Earth Sciences, Deep-Sea Research/Part B: Oceanographic Literature Review, Excerpta Medica, Index Medicus, Mass Spectrometry Bulletin, PASCAL-CNRS, Referativnyi Zhurnal, Research Alert and Science Citation Index)

11TH INTERNATIONAL SYMPOSIUM ON PREPARATIVE AND INDUSTRIAL CHROMATOGRAPHY  
BADEN-BADEN, OCTOBER 3-6, 1994

Combined continuous and preparative chromatographic separation by K.H. Row (Inchon, South Korea) . . . . .	105
Scale-up of liquid chromatography for industrial production of parenteral antibiotic E1077 by M. Kodama, S. Ishizawa, A. Koiwa and T. Kanaki (Ibaraki, Japan) and K. Shibata and H. Motomura (Kanagawa, Japan) . . . . .	117
Production of rare-earth oxides of high purity by Z. Zheng, D. Ling and Y. Sun (Changzhou, China) . . . . .	131
Hydrophobic interaction chromatography of <i>Chromobacterium viscosum</i> lipase (Short communication) by J.A. Queiroz (Covilhã, Portugal), F.A.P. Garcia (Coimbra, Portugal) and J.M.S. Cabral (Lisboa, Portugal) . . . . .	137
(end of symposium papers)	

## REVIEW

Carbon sorbents and their utilization for the preconcentration of organic pollutants in environmental samples by E. Matisová and S. Škrabáková (Bratislava, Slovak Republic) (Received 9 March 1995) . . . . .	145
---	-----

## REGULAR PAPERS

*Column Liquid Chromatography*

Study of aroma compound-natural polymer interactions by dynamic coupled column liquid chromatography by S. Langourieux and J. Crouzet (Montpellier, France) (Received 18 January 1995) . . . . .	181
Analysis of colloids. VIII. Concentration- and memory effects in size exclusion chromatography of colloidal inorganic nanometer-particles by C.-H. Fischer and T. Siebrands (Berlin, Germany) (Received 31 December 1994) . . . . .	189
Molecular imprinting of acetylated carbohydrate derivatives into methacrylic polymers by K.G.I. Nilsson (Lund, Sweden), K. Sakaguchi (Tokyo, Japan), P. Gemeiner (Bratislava, Slovak Republic) and K. Mosbach (Lund, Sweden) (Received 20 February 1995) . . . . .	199
Capability of a polymeric C <sub>30</sub> stationary phase to resolve <i>cis-trans</i> carotenoid isomers in reversed-phase liquid chromatog- raphy by C. Emenhiser (Raleigh, NC, USA), L.C. Sander (Gaithersburg, MD, USA) and S.J. Schwartz (Raleigh, NC, USA) (Received 6 March 1995) . . . . .	205
Normal-phase high-performance liquid chromatography using enhanced-fluidity liquid mobile phases by S.T. Lee and S.V. Olesik (Columbus, OH, USA) (Received 8 February 1995) . . . . .	217
Purification of antibody Fab fragments by cation-exchange chromatography and pH gradient elution by R. Mhatre, W. Nashabeh, D. Schmalzing, X. Yao, M. Fuchs, D. Whitney and F. Regnier (Framingham, MA, USA) (Received 27 February 1995) . . . . .	225
Peptide chiral purity determination: hydrolysis in deuterated acid, derivatization with Marfey's reagent and analysis using high-performance liquid chromatography-electrospray ionization-mass spectrometry by D.R. Goodlett, P.A. Abuaf, P.A. Savage, K.A. Kowalski, T.K. Mukherjee, J.W. Tolan, N. Corkum, G. Goldstein and J.B. Crowther (Annandale, NJ, USA) (Received 28 February 1995) . . . . .	233

Contents (continued)

- Simultaneous determination of enalapril, felodipine and their degradation products in the dosage formulation by reversed-phase high-performance liquid chromatography using a Spherisorb C<sub>8</sub> column  
by X.-Z. Qin, J. DeMarco and D.P. Ip (West Point, PA, USA) (Received 10 March 1995) . . . . . 245

*Gas Chromatography*

- Investigation of the use of oxygen doping of the electron-capture detection for determination of atmospheric halocarbons  
by G.A. Sturrock, P.G. Simmonds and G. Nickless (Bristol, UK) (Received 9 January 1995) . . . . . 255
- Endogenous alkaloids in man. XXI. Analysis of glyoxylate-derived 1,3-thiazolidines and their precursors after trimethylsilylation by gas chromatography-mass spectrometry  
by G. Bringmann, C. Hesselmann and D. Feineis (Würzburg, Germany) (Received 3 March 1995) . . . . . 267
- Multi-residue pesticide analysis in environmental water samples using solid-phase extraction discs and gas chromatography with flame thermionic and mass-selective detection  
by T.A. Albanis and D.G. Hela (Ioannina, Greece) (Received 6 March 1995) . . . . . 283
- Determination of permethrin and cyfluthrin in water and sediment by gas chromatography-mass spectrometry operated in the negative chemical ionization mode  
by G.A. Bonwick, C. Sun, P. Abdul-Latif and P.J. Baugh (Salford, UK), C.J. Smith (Deeside, UK), R. Armitage (Leeds, UK) and D.H. Davies (Salford, UK) (Received 13 March 1995) . . . . . 293

*Supercritical Fluid Chromatography*

- Packed capillary column supercritical fluid chromatography using SE-54 polymer encapsulated silica  
by Y. Shen, A. Malik, W. Li and M.L. Lee (Provo, UT, USA) (Received 7 March 1995) . . . . . 303

*Electrophoresis*

- Determination of  $\beta$ -cyclodextrin inclusion complex constants for 3,4-dihydro-2-*H*-1-benzopyran enantiomers by capillary electrophoresis  
by Ph. Baume, Ph. Morin, M. Dreux, M.C. Viaud, S. Boye and G. Guillaumet (Orléans, France) (Received 6 March 1995) . . . . . 311
- Determination of isoflavones using capillary electrophoresis in combination with electrospray mass spectrometry  
by M.A. Aramendia, I. García, F. Lafont and J.M. Marinas (Córdoba, Spain) (Received 7 March 1995) . . . . . 327
- Determination of sugars by capillary electrophoresis with electrochemical detection using cuprous oxide modified electrodes  
by X. Huang and W.Th. Kok (Amsterdam, Netherlands) (Received 2 March 1995) . . . . . 335
- Migration behaviour of alkali and alkaline-earth metal ion-EDTA complexes and quantitative analysis of magnesium in real samples by capillary electrophoresis with indirect ultraviolet detection  
by T. Wang and S.F.Y. Li (Singapore, Singapore) (Received 28 February 1995) . . . . . 343
- Free-solution capillary electrophoretic resolution of chiral amino acids via derivatization with homochiral isothiocyanates.  
Part I  
by R. Bonfichi, C. Dallanoce, S. Lociuoro and A. Spada (Gerenzano (VA), Italy) (Received 7 February 1995) . . . . . 355

SHORT COMMUNICATIONS

*Column Liquid Chromatography*

- Quantitative structure-retention relationships of acyclovir esters using immobilised albumin high-performance liquid chromatography and reversed-phase high-performance liquid chromatography  
by D.S. Ashton, C. Beddell, A.D. Ray and K. Valkó (Kent, UK) (Received 7 March 1995) . . . . . 367
- Determination of biogenic amines and their precursor amino acids in wines of the Vallée du Rhône by high-performance liquid chromatography with precolumn derivatization and fluorimetric detection  
by T. Bauza (Montpellier and Avignon, France), A. Blaise (Montpellier, France), F. Daumas (Avignon, France) and J.C. Cabanis (Montpellier, France) (Received 2 March 1995) . . . . . 373
- Direct separation of carboxylic acid and amine enantiomers by high-performance liquid chromatography on reversed-phase silica gels coated with chiral copper(II) complexes  
by N. Ôi, H. Kitahara and F. Aoki (Osaka, Japan) (Received 21 February 1995) . . . . . 380

Use of $\beta$ -diketonate anions as eluent in non-suppressed ion chromatography: 1,3-cyclohexanedionate as acidic eluent by N. Hirayama, M. Maruo, A. Shiota and T. Kuwamoto (Kyoto, Japan) (Received 7 March 1995) . . . . .	384
<i>Gas Chromatography</i>	
Use of a trio of modified cyclodextrin gas chromatographic phases to provide structural information on some constituents of volatile oils by T.J. Betts (Perth, Australia) (Received 1 March 1995) . . . . .	390
<i>Electrophoresis</i>	
Analysis of recombinant human growth hormone and its related impurities by capillary electrophoresis by P. Dupin, F. Galinou and A. Bayol (Labège, France) (Received 24 February 1995) . . . . .	396
AUTHOR INDEX . . . . .	401



**11TH INTERNATIONAL SYMPOSIUM ON  
PREPARATIVE AND INDUSTRIAL CHROMATOGRAPHY**

*Baden-Baden, October 3-6, 1994*

*Guest Editor*

**K.K. UNGER**

(Mainz, Germany)







ELSEVIER

Journal of Chromatography A, 707 (1995) 105–116

JOURNAL OF  
CHROMATOGRAPHY A

# Combined continuous and preparative chromatographic separation

Kyung Ho Row

*Department of Chemical Engineering, INHA University, 253 Yonghyun-Dong, Nam-Ku, Incheon, South Korea*

## Abstract

A combined continuous and preparative gas–liquid chromatographic system was considered for the separation of the close-boiling components diethyl ether and dichloromethane. The characteristics of the combined continuous and preparative gas–liquid chromatographic system were investigated in terms of the experimental operating conditions. It was experimentally confirmed that the additional column length and the desorbent velocity were the most important factors to ensure the continuous separation of the feed mixture. The theoretical concentration profiles were calculated by a mathematical model with the assumptions of uniform film thickness and linear partition equilibrium. Although small deviations between the calculated profiles and the experimental data were observed, the model might be used as a predictive tool for determining the optimum operating conditions for the combined continuous and preparative chromatographic system.

## 1. Introduction

Gas chromatography is a separation method based on differences in the partition coefficients of substances distributed between a stationary liquid phase (SLP) and a mobile phase. Since the introduction of gas chromatography [1], over the past 30 years much efforts have been made to increase the throughput capabilities. Until now, attempts have been made to scale up lab-sized chromatographic units to treat larger quantities of substances and to bring these systems to preparative or process-scale operation [2,3].

Generally the chromatographic processes fall into two main categories, i.e. batch and continuous. Batch-type processes were first developed in 1953 and commercial units are now available [4]. Continuous systems were introduced soon after 1955 and in recent years work on this type of system has mainly concentrated on increasing

their throughputs [1,2,5]. Among the systems to meet the conditions of high throughput, the UOP (Universal Oil Products) process is widely acknowledged as a useful system [6]. As an improved preparative chromatography, Wankat [7] and Ha et al. [8,9] developed moving feed point chromatography. This was later combined with moving product withdrawal chromatography, and moving port chromatography was suggested [10]. Wankat properly used a local equilibrium model to analyze the characteristics of the system. Two mathematical models of the moving bed adsorber, an intermittent moving bed and a continuous moving bed type, were presented by Hashimoto et al. for calculating the concentration profiles of glucose and fructose [11,12].

Such mixtures as various hydrocarbons, dextran, and saccharoids were separated using series of semicontinuous counter-current refiners (SCCR) [13–15] and a mathematical model

based on the theoretical plate concept was used to simulate the performance of the unit [16]. For the SCCR unit and the UOP process, Ching and Ruthven have proposed a theoretical model for simulated counter-current operation as an equivalent counter-current cascade of theoretical equilibrium stages under steady-state condition and obtained the analytical concentration profile [17,18].

In this paper, a continuous separation method is utilized in which binary feed mixtures are separated by the combined continuous and preparative chromatographic system in two steps (partition and desorption). Although the system is equipped with segmented columns and the less-absorbed or less-adsorbed component can be obtained in pure form in the partition or adsorption section as in other continuous systems, the remaining components in the columns can also be separated in the desorption section by changing the operating conditions such as column length and desorbent velocity. Mathematical models for this combined continuous and preparative chromatography have been developed and used to investigate the usefulness of the system and the effects of operating conditions on the resolution of the two close-boiling components by prediction of their concentration profiles. We also compared the experimental data with the calculated values to confirm the mathematical models.

## 2. Operational principles of the system [19]

In the present system, binary feed mixtures of diethyl ether (DEE) and dichloromethane (DCM), are separated continuously with the combined continuous and preparative chromatography taking place in two sections, i.e. the partition and desorption sections.

When a feed mixture is injected into a single column, the less-absorbed component (DEE) is eluted initially by the solubility difference between the feed mixture and the SLP. After a while, as the more-absorbed component (DCM) also begins to be eluted, the components are eluted from the column in a composition which is

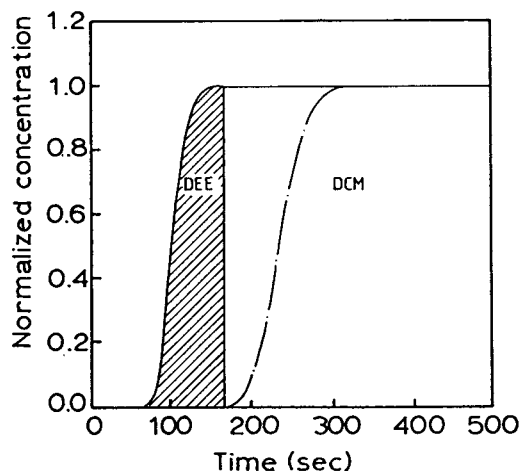


Fig. 1. Theoretical concentration profile in case of step input.

the same as that of the feed mixture. As shown in Fig. 1, the less-absorbed component is eluted as a pure product (the shaded portion in the figure) until the second component starts to elute, so during that time pure DEE can be collected. Here, we define the normalized concentration used in the system as the ratio of the concentration of a component in the mobile phase to the concentration of that component at the inlet of the column,  $c/c_0$ .

Fig. 2 shows the arrangement of the columns and solenoid valves. During operation of this system, two streams, i.e. the carrier gas with feed and the desorbent, enter the system, and two product streams leave the system through the partition section and the desorption section.

The principles of the combined continuous and preparative chromatographic system are based on switching the configuration of the columns. The less-absorbed component can be obtained in pure form before the elution of the more-absorbed component in the partition section starts. During that time, in the desorption section, the less-absorbed component remains in the column while the more-absorbed component can be separated by adjusting the additional column length and the desorbent velocity. If the above two steps can be simultaneously completed within a certain time (switching time), the binary feed

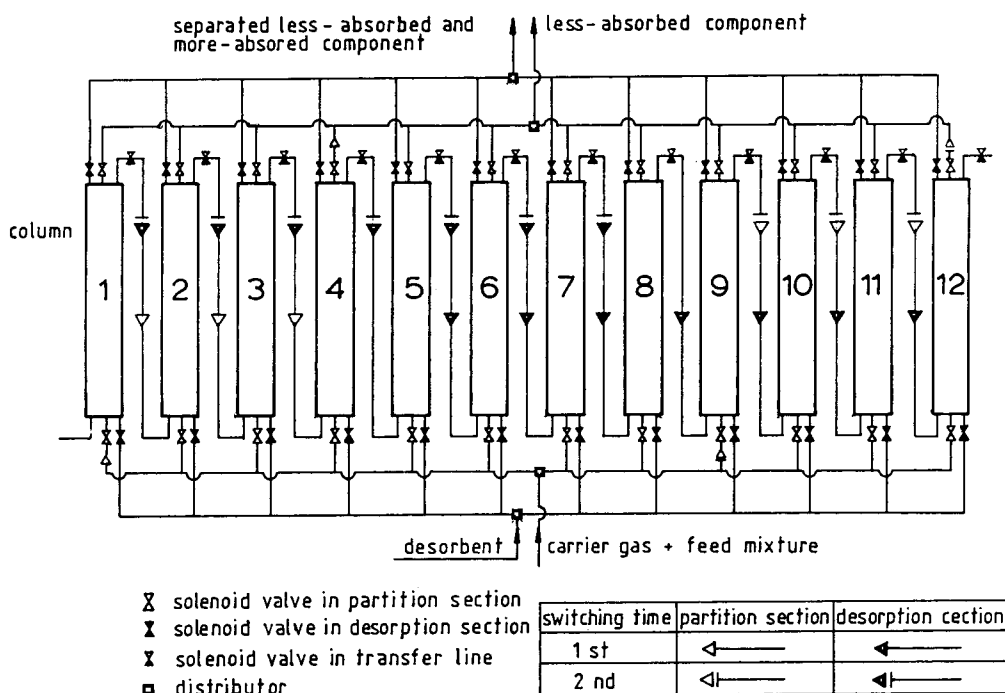


Fig. 2. Configuration of columns and solenoid valves.

mixture can be separated continuously. The switching time depends on the characteristic combination of the stationary liquid and the feed mixture. In the desorption section, the remaining components should be separated within the switching time by changing the operating conditions.

For example, the partition section consists of four columns (e.g. columns 1–4) and the desorption section of eight columns (columns 5–12). During the first switching time, the feed mixture is continuously injected into the inlet of column 1, and the less-absorbed component is obtained in pure form at the outlet of column 4. Just before the elution of the more-absorbed component, within the second switching time, the feed mixture is injected into the inlet of column 9, which is the starting column of a new partition section (columns 9–12). At the same time, in the desorption section (columns 1–8), the desorbent is injected into the inlet of column 1, and at the outlet of column 8, the remaining less-absorbed

component and the more-absorbed components are obtained separately within the switching time.

The segmented columns can be configured and switched by a microprocessor according to the characteristics of feed mixture. The system is a binary separation process, but by the careful selection of the SLP and the operating conditions it can be extended to various feed mixtures.

### 3. Mathematical models

The distribution of the stationary liquid phase on the solid support appears to be very complex because of irregularities in pore size and shape. The assumptions for establishing the governing equations of the processes are a uniformly distributed stationary liquid phase on the surface of the inert solid particles, a linear partition isotherm, negligible sorption and pressure drop effects, and a spherical shape of the solid par-

ticles [20,21]. As the concept of the uniform film thickness simplifies the phenomena of porous particles coated with the stationary liquid phase, transient material balances for a component are

$$\frac{\partial c}{\partial t} + u \frac{\partial c}{\partial z} = \frac{E \partial^2 c}{\epsilon \partial z^2} - \frac{3}{r_p} \frac{1-\epsilon}{\epsilon} D_e \frac{\partial q}{\partial r} \Big|_{r=r_p} \quad (1)$$

for the mobile phase,

$$\epsilon_p \frac{\partial q}{\partial t} = D_e \frac{1}{r^2} \frac{\partial}{\partial r} \left( r^2 \frac{\partial q}{\partial r} \right) - A_p k_g \left( q - \frac{n|_{x=\delta}}{K} \right) \quad (2)$$

for the intraparticle phase, and

$$\frac{\partial n}{\partial t} = D_1 \frac{\partial^2 n}{\partial x^2} \quad (3)$$

for the SLP

The initial and boundary conditions are:

$$c = q = n = 0 \quad (\text{for } t = 0, z > 0) \quad (4)$$

$$c = c_0(t) \quad (\text{for } t > 0, z = 0) \quad (5)$$

$$c = \text{finite} \quad (\text{for } t > 0, z \rightarrow \infty) \quad (6)$$

$$\frac{\partial q}{\partial r} = 0 \quad (\text{for } t > 0, r = 0) \quad (7)$$

$$\frac{\partial n}{\partial x} = 0 \quad (\text{for } t > 0, x = 0) \quad (8)$$

$$D_e \frac{\partial q}{\partial r} = k_f(c - q) \quad (\text{for } t > 0, r = r_p) \quad (9)$$

$$D_1 \frac{\partial n}{\partial x} = k_g \left( q - \frac{n}{K} \right) \quad (\text{for } t > 0, x = \delta) \quad (10)$$

It is assumed that the partition effect is dominant to the adsorption effect with a linear equilibrium isotherm. In terms of a given axial distance,  $z$ , the solution of Eqs. 1–10 in the Laplace domain is

$$C(s) = C_0(s) \exp \left( \frac{z}{2} \left[ \frac{u_0}{E} - \left\{ \left( \frac{u_0}{E} \right)^2 + 4\lambda \right\}^{1/2} \right] \right) \quad (11)$$

where

$$\lambda = \frac{\epsilon}{E} \left( s + \frac{3(1-\epsilon)}{r_p \epsilon} k_f \left\{ 1 - \frac{\sinh(\lambda_2 r_p)}{r_p} \lambda_1 \right\} \right) \quad (12)$$

$$\lambda_1 = \frac{r_p k_f}{D_e \lambda_2 \cosh(\lambda_2 r_p) + \left( k_f - \frac{D_e}{r_p} \right) \sinh(\lambda_2 r_p)} \quad (13)$$

$$\lambda_2 = \left( \frac{1}{D_e} \left[ \{ \epsilon_p s + A_p k_g \} - \frac{A_p k_g^2 \cosh \lambda_3}{D_e K \sqrt{\frac{s}{D_1} \lambda_3 + D_e k_g \cosh \lambda_3}} \right] \right)^{1/2} \quad (14)$$

$$\lambda_3 = \delta \sqrt{\frac{s}{D_1}} \quad (15)$$

The usual method of operating fixed beds for preparative scale is to use a large input pulse of feed onto the column followed by a longer period of flow of carrier gas. In case of pulse input,  $C_0(s)$  has the following form:

$$C_0(s) = \frac{1 - e^{-st_0}}{s} \quad (16)$$

where  $t_0$  is the time of feed injection. Then Eq. 11 becomes at the bed exit,  $z = L$ ,

$$C(s) = \frac{1 - e^{-st_0}}{s} \times \exp \left( \frac{L}{2} \left\{ \frac{u_0}{E} - \left[ \left( \frac{u_0}{E} \right)^2 + 4\lambda \right]^{1/2} \right\} \right) \quad (17)$$

Eq. 17 can be used to predict the concentration profile of a feed component in the partition section. It is assumed that in the desorption section the components are partitioned initially with the inlet concentration of the feed,  $c_0$ . The governing equations are the same as in the partition section. However, some of the initial and boundary conditions are different from those of the partition section. The initial condition and the boundary condition in the desorption section are changed as follows:

$$c = q = c_0 \quad (\text{for } t = 0, z > 0) \quad (18)$$

$$n = Kc_0 \quad (\text{for } t = 0, z > 0) \quad (19)$$

$$c = 0 \quad (\text{for } t > 0, z = 0) \quad (20)$$

Under these conditions, the solution in the

Laplace domain is at a given length  $z$  in the desorption section,

$$C(s) = \gamma \left( \exp \left\{ \frac{z}{2} \left( \frac{u_0}{E} - \left[ \left( \frac{u_0}{E} \right)^2 + 4\gamma_1 \right]^{1/2} \right) \right\} - 1 \right) \quad (21)$$

where

$$\gamma = \left( -\frac{\epsilon_p c_0}{E} + \frac{3(1-\epsilon_p)}{r_p E} k_f \left\{ \frac{\gamma_2 \sinh(\sqrt{\gamma_4} r_p)}{r_p} + \frac{\gamma_5}{\gamma_4} \right\} \right) / \gamma_1 \quad (22)$$

$$\gamma_1 = -\frac{\epsilon s}{E} + \frac{3(1-\epsilon)}{r_p E} k_f \left\{ 1 - \frac{\gamma_3 \sinh(\sqrt{\gamma_4} r_p)}{r_p} \right\} \quad (23)$$

$$\gamma_2 = -\gamma_5 k_f / \gamma_4 (D_e \{ \sqrt{\gamma_4} r_p \cosh(\sqrt{\gamma_4} r_p) - \sinh(\sqrt{\gamma_4} r_p) \} / r_p^2 + k_f \sinh(\sqrt{\gamma_4} r_p) / r_p) \quad (24)$$

$$\gamma_3 = \frac{-\gamma_4}{\gamma_5 \gamma_2} \quad (25)$$

$$\gamma_4 = \frac{1}{D_e} (\epsilon_p s + A_p k_g) \frac{A_p k_g^2 \cosh \left( \sqrt{\frac{s}{D_1}} \delta \right)}{D_e K \{ \sqrt{D_1} s \sinh \left( \sqrt{\frac{s}{D_1}} \delta \right) + k_g \cosh \left( \sqrt{\frac{s}{D_1}} \delta \right) / K \}} \quad (26)$$

$$\gamma_5 = \frac{A_p k_g}{D_e K} \left\{ \frac{K c_0}{s} - \frac{\frac{k_g c_0}{s} \cosh \left( \sqrt{\frac{s}{D_1}} \delta \right)}{\sqrt{D_1} s \sinh \left( \sqrt{\frac{s}{D_1}} \delta \right) + k_g \cosh \left( \sqrt{\frac{s}{D_1}} \delta \right) / K} \right\} + \frac{c_0}{D_e} \quad (27)$$

Eq. 21 is used for predicting the concentration profiles in the desorption section, and it is also used as an input function for the inlet of additional columns of the desorption section. That is,

$$C_0(s) = \gamma \left( \exp \left\{ \frac{L}{2} \left( \frac{u_0}{E} - \left[ \left( \frac{u_0}{E} \right)^2 + 4\gamma_1 \right]^{1/2} \right) \right\} - 1 \right) \quad (28)$$

The governing equations, initial conditions and other boundary conditions are the same as

those in the partition section. Therefore, the solution of the desorption section of the column length,  $L$ , with the additional column length ( $L'$ ) in the  $s$ -domain is

$$C(s) = \gamma \left( \exp \left\{ \frac{L}{2} \left( \frac{u_0}{E} - \left[ \left( \frac{u_0}{E} \right)^2 + 4\gamma_1 \right]^{1/2} \right) \right\} - 1 \right) \times \exp \left( \frac{L'}{2} \left\{ \frac{u_0}{E} \left[ \left( \frac{u_0}{E} \right)^2 + 4\lambda \right]^{1/2} \right\} \right) \quad (29)$$

The resulting Laplace transformed equations (Eqs. 17, 21, and 29) should be converted into the real time domain. For an approximation technique, the equations are inverted numerically with the curve fitting procedure suggested by Dang and Gibilaro [22]. In the numerical inversion, the infinite upper integration limit is taken as the corresponding value of the frequency to the amplitude ratio of the Laplace transformed equations of 0.001, and it takes just about 15 s using HP Vectra (Model 486/66VL) to transform the equations into the real time domain. The kinetic constants and other parameters in the mathematical models are listed in Table 1 [20]. The % liquid loading in the table is defined by the percentage ratio of the weight of stationary liquid phase to that of uncoated solid packings.

#### 4. Experimental

Diethyl ether and dichloromethane were used as feed mixture, and their boiling points are 34.5°C and 40.0°C, respectively. The partition coefficients of DEE and DCM were evaluated on an analytical chromatographic column over wider temperature ranges [23]. Nitrogen was used as carrier gas and desorbent.

Twelve columns were arranged in a circular form. The columns were made of stainless steel, 1 cm I.D., 30 cm height, with a packed height of 25 cm. At both ends of the columns, glass wool was used to keep the solid particles in place. The columns were packed with Chromosorb A (Alltech Associates) which has a sufficient capacity to load the stationary phase and the surface of which is not highly adsorptive, so it is mainly used for preparative-scale separation [24]. Chromosorb A of three different particle sizes (60/80,

Table 1  
The kinetic constants and other parameters used in the simulations

$$k_f = (D_M)/(2r_p)(2 + 1.45Re^{0.50}Sc^{0.33})$$

$$k_g = 12.5(D_M(1 - \epsilon_p))/(r_p \epsilon_p)$$

Mesh size	60/80			45/60			20/30			
$r_p$ (cm)	0.00996			0.01360			0.03140			
% Liquid loading	25	20	15	25	20	15	25	20	15	
$\epsilon_p$	0.62	0.66	0.69	0.62	0.66	0.69	0.50	0.54	0.57	
% Liquid loading	25			20			15			
$\delta$ ( $\mu\text{m}$ )	0.1270			0.0955			0.0650			
Temperature	DEE			DCM						
$^{\circ}\text{C}$	$D_1$ $10^{-6} \text{ cm}^2/\text{s}$			$K$			$D_1$ $10^{-6} \text{ cm}^2/\text{s}$			$K$
25	0.471			184.2			0.595			437.1
35	0.650			126.3			0.901			297.1
45	1.090			88.7			1.275			206.8
$D_c$ ( $\times 10^{-3} \text{ cm}^2/\text{s}$ )	1.00			2.00						
$\epsilon$	0.41									
$A_p$ ( $\text{cm}^2/\text{cm}^3$ )	1300000.0									

45/60, and 20/30 mesh) was commercially available. A rotavapor (Brinkmann Co.) was used to coat dinonylphthalate on the particles, and the percentage liquid loading was set at 20% in the experiments with all particle sizes. Each column has four openings, two for entering streams and two for withdrawing streams, and it was covered with ceramic insulation to keep the column temperature constant.

A schematic diagram of the main chromatographic system is shown in Fig. 3 [19,25]. Five solenoid valves (CKD, AB 31-01-4) were arranged around a column. The twelve columns, sixty solenoid valves, and four distributors were fixed to a support and the complete set-up was enclosed in a steel cover to maintain a desired temperature in the system. The four distributors, two for entering streams and two for withdrawing streams, were installed. Each distributor was

of a cylindrical type whose upper side had one central bore, and the side of the distributor had twelve screwed openings. The entering stream passed through the central bore and went into one of the openings in the distributor, and then it entered the inlet of the column through the solenoid valve connected with the opening. Conversely, the withdrawing stream through the solenoid valve from the outlet of the column went through one of the openings and the central bore in the distributor, and was finally sent to the analyzer.

The inlet feed mixtures and the two outlet streams from the main system were analyzed by a conventional gas chromatograph (Gow Mac 550P thermal conductivity detector) with a syringe (Hamilton Co.) and a ten-port multi-functional sampling valve (Valco Instruments Co.), respectively. Pressure gauges were set at the















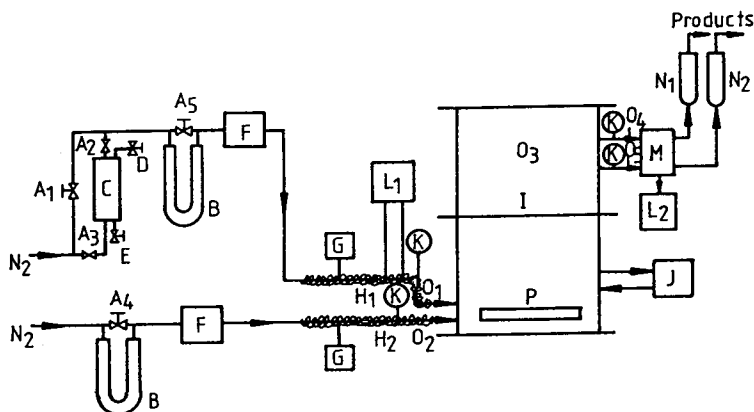


Fig. 3. Schematic diagram of the main chromatographic unit. (A<sub>1</sub>, A<sub>4</sub>, A<sub>3</sub>) Microneedle valves, (A<sub>2</sub>, A<sub>3</sub>) solenoid valves, (B) manometers for adjustment of flow-rates, (C) feed reservoir, (D) inlet of feed, (E) outlet of feed, (F) preheaters for carrier gas and desorbent, (G) temperature controller, (H<sub>1</sub>, H<sub>2</sub>) heating wires, (I) main chromatographic system, (J) programmable controller, (K) pressure gauges, (L<sub>1</sub>, L<sub>2</sub>) gas chromatographs, (M) multifunctional sampling valves, (N<sub>1</sub>, N<sub>2</sub>) bubble flow meters for carrier gas and desorbent, (O<sub>1</sub>–O<sub>5</sub>) thermocouples, (P) electric heater.

inlet and outlet of the main system, so the pressure drops of the two sections were recorded. The dead volume of the system was determined from the measurement of the retention time of a helium sample.

The sixty solenoid valves in the main chromatographic system were controlled by a programmable controller. Flow paths of the partition and desorption sections were initially set by the controller, and then they were automatically and consecutively turned to the next step after a switching time.

## 5. Results and discussion

In a gas chromatographic column, the gas flows through the narrow interstices between the solid support particles packed in the column. The local changes in the viscosity and flow velocity of the gaseous mixture result in the pressure gradient along the column [26]. The smaller the particles the higher the pressure drop (Fig. 4). The velocity gradient will be changed by pressure changes in the column. The average velocity, i.e. the abscissa in Fig. 4,  $u_{ave}$ , is the velocity corrected by the compressibility factor

as suggested by James and Martin [1]. A pressure drop of 30–90 cmHg was observed in the present experimental set-up. The gas velocity will be more uniform at a low inlet-to-outlet pressure ratio. Therefore, it is desirable to use a rather larger particle size and low flow-rates of the carrier gas or the desorbent in order to separate the feed efficiently.

The total elution volumes of the DEE and DCM mixture are plotted versus the feed concentration and the column temperature in Fig. 5.

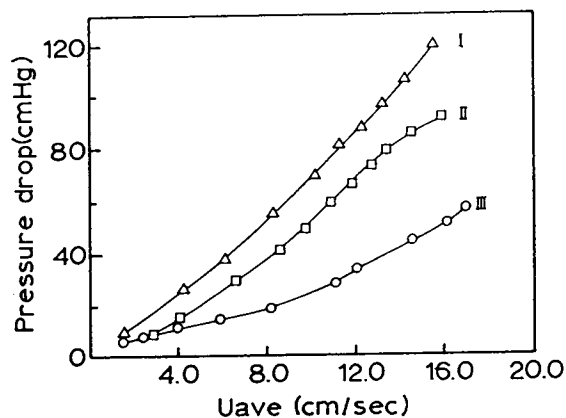


Fig. 4. Effect of particle size on pressure drop; (I) 60/80 mesh,  $L = 100$  cm, (II) 20/30 mesh,  $L = 200$  cm, (III) 20/30 mesh,  $L = 100$  cm.

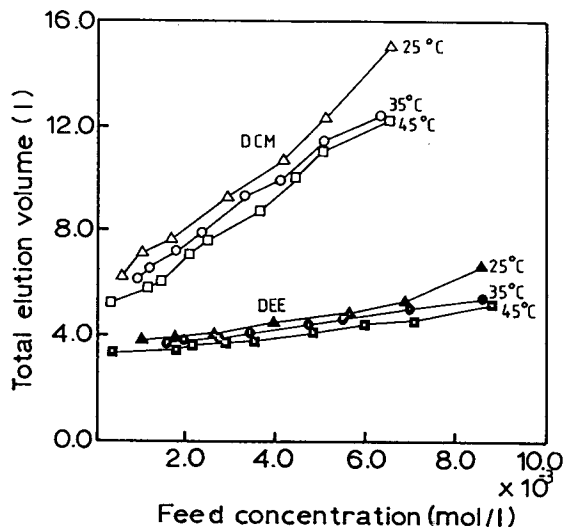


Fig. 5. Effect of feed concentration on total elution volume with column temperatures. (20/30 mesh,  $u_{ave} = 9.53$  cm/s,  $L = 100$  cm, switching time, 300 s).

The total elution volume is the quantity of gas that can elute the components completely from the length of the column. The slope of each component can also be seen in this figure. Although the slope of the elution profile for DEE is low and that for DCM is high, the bandwidth of both components was observed to be wider with increasing feed concentration and decreasing column temperature which resulted from the limited vaporization capacity when feed mixtures with a higher concentration were injected (see Fig. 6). Here,  $c_0$  indicates the inlet concentration of the feed.

The calculated curves in the following figures are the numerical inversion of Eqs. 17, 21, and 29, for the partition section, the desorption section, and the desorption section with additional column length, respectively. The experimental concentration profile for DEE is compared to the calculated values in the partition section (Fig. 7). DCM was not eluted in the partition section, and the agreement between the two profiles was good. The performance of the system in the partition section did not vary greatly with respect to particle size, because the

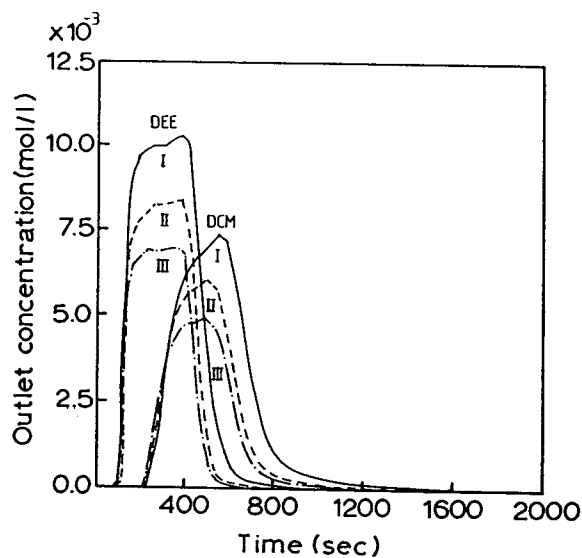


Fig. 6. Effect of feed concentration on elution profile. (I)  $c_{0,DEE} = 10.0 \cdot 10^{-3}$  mol/l, (II)  $8.3 \cdot 10^{-3}$  mol/l, (III)  $6.8 \cdot 10^{-3}$  mol/l; (I)  $c_{0,DCM} = 7.3 \cdot 10^{-3}$  mol/l, (II)  $6.3 \cdot 10^{-3}$  mol/l, (III)  $4.9 \cdot 10^{-3}$  mol/l; 20/30 mesh, 25°C,  $u_{ave} = 9.53$  cm/s,  $L = 100$  cm, switching time, 300 s.

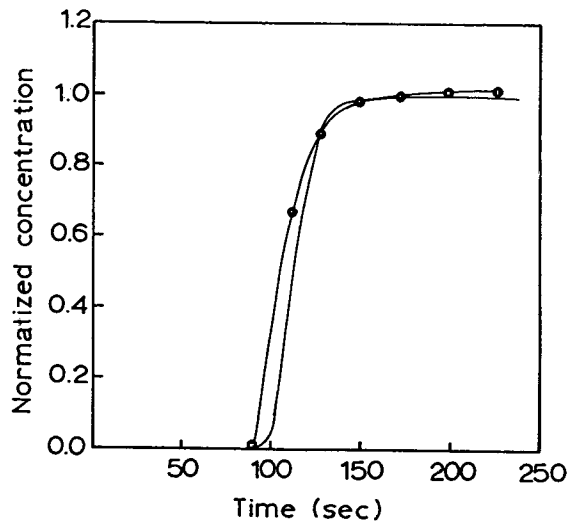


Fig. 7. Comparison of experimental data (●) with calculated values (solid line) for DEE. ( $c_{0,DEE} = 0.98 \cdot 10^{-3}$  mol/l,  $c_{0,DCM} = 0.91 \cdot 10^{-3}$  mol/l, 45/60 mesh, 35°C,  $u_{ave} = 8.80$  cm/s,  $L = 100$  cm, switching time, 240 s).

Table 2  
Switching times (s) with operating conditions

Temp. (°C)	20/30 mesh		45/60 mesh		60/80 mesh		
	L(cm)	100	150	100	150	100	150
25		270	480	300	480	300	480
35		240	360	240	360	240	360
45		180	270	180	300	180	300

switching time was almost constant for the particle sizes used (see Table 2).

Fig. 8 shows the concentration profiles of DEE and DCM in the desorption section. In the model equations (Eqs. 18–20), the initial concentrations were assumed to be proportional to the inlet concentrations of the feed,  $c_0$ . This assumption seems to be valid for the less-absorbed component (DEE), but does not seem to hold exactly for the more-absorbed component (DCM). This means that in the partition section, which is to become the desorption section after a switching time, DCM is not uniformly distributed and more likely maldistributed around the

inlet of the column, because its partition coefficient is large.

The two components were not fully resolved in the desorption section as shown in Fig. 8. If the desorption section is used exclusively without an additional column, the more-absorbed component can be obtained in pure form after the unseparated mixture is recycled in a batch-type process. Continuous operation, however, can be achieved by connecting the additional columns to the end of the desorption section. As shown in Fig. 9, the resolution between the two components was improved by an additional column

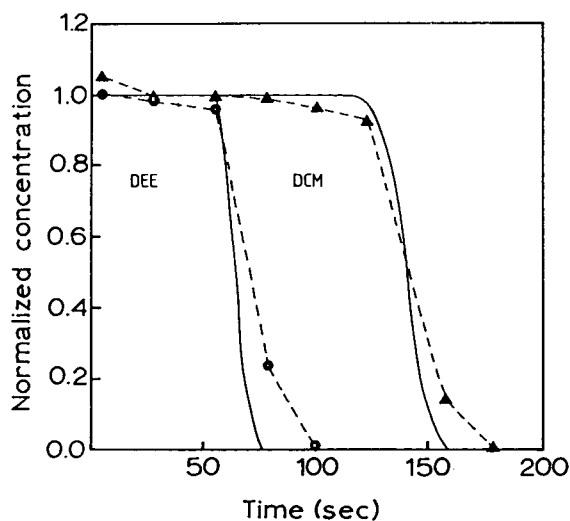


Fig. 8. Comparison of experimental data of DEE (●) and DCM (▲) with calculated values (solid line). ( $c_{0,DEE} = 0.94 \cdot 10^{-3}$  mol/l,  $c_{0,DCM} = 0.78 \cdot 10^{-3}$  mol/l, 45/60 mesh, 45°C,  $u_{ave} = 11.30$  cm/s,  $L = 100$  cm, switching time 180 s).

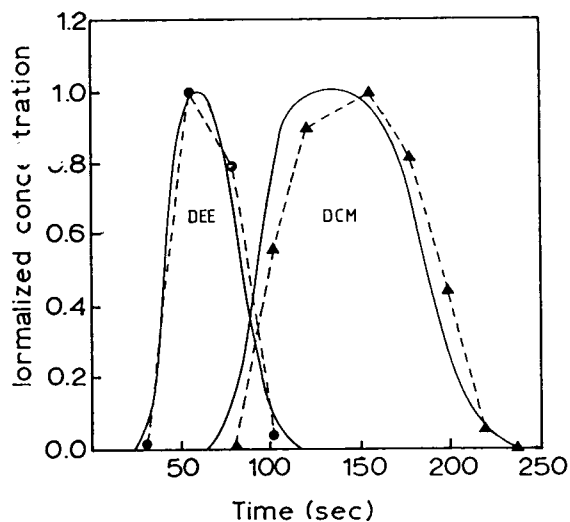


Fig. 9. Comparison of experimental data of DEE (●) and DCM (▲) with calculated values (solid line). ( $c_{0,DEE} = 0.61 \cdot 10^{-3}$  mol/l,  $c_{0,DCM} = 0.57 \cdot 10^{-3}$  mol/l, 20/30 mesh, 35°C,  $u_{ave} = 19.90$  cm/s,  $L = 100$  cm,  $L' = 100$  cm, switching time 240 s).

length of 100 cm. The small differences in the trailing edge of the concentration profile of DEE and in the leading edge of the DCM profile may be partly caused by the assumption of a linear partition equilibrium. With adjustment of only the desorbent velocity, the components remaining in the desorption section with the additional column length can be controlled within the switching time of 240 s.

Flow-rates between 5 and 10 cm<sup>3</sup>/h yielded pure DEE and almost completely separated DEE and DCM with column lengths of 100 cm for the partition and the desorption section, 20/30 mesh particle size, 35°C column temperature, and an additional column length of 100 cm [19].

The pressure drop by the smaller particle size and the longer column length caused variation in the gas velocity, and the higher feed concentrations along the length of the column were necessarily accompanied by changes in the velocities. In the present system, the assumption that the velocity of the carrier or the desorbent remained constant throughout the column was compensated by the average gas velocity. Although small differences between the calculated concentration profiles and the experimental data were observed, the uniform thickness model may be used as a suitable estimation of the optimum operating conditions for the combined continuous and preparative chromatographic system.

To investigate the optimum operating conditions by the operating principle of the system, impurity is defined as the ratio of the overlapped to unoverlapped areas of the two peaks in the desorption section. An increase in the percentage liquid loading decreases the impurity, but it increases the total elution time (Fig. 10). Because higher temperature decreases the total elution time, the impurity increases due to the fast elution of the components. It can also be seen that with higher loading of the SLP, the intersections of the two lines for one loading percentage (the solid line and the interrupted line in the figure) are shifted to higher temperature. In determining the operating conditions in the desorption section with an additional column, another significant factor is the desorbent velocity. Based on the previous results for col-

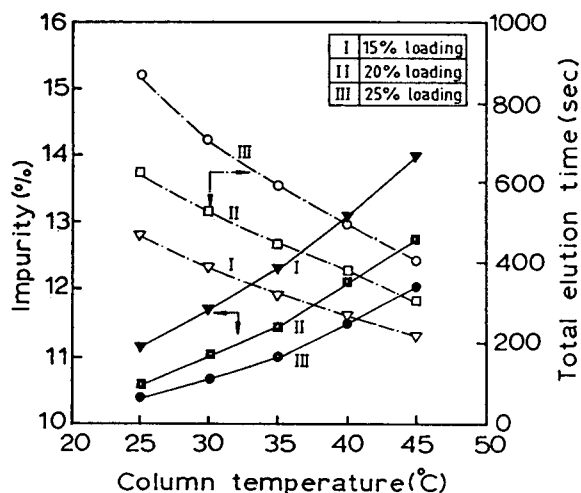


Fig. 10. Effect of column temperature on impurity and total elution time with liquid loading in desorption section. (20/30 mesh,  $u_0 = 10$  cm/s,  $L = 100$  cm,  $L' = 50$  cm).

umn temperature and percentage liquid loading in Fig. 10, the effects of desorbent velocity on impurity and total elution time with the additional column lengths are shown in Fig. 11 at 35°C, 20% liquid loading, and a switching time of 240 s. In terms of additional column length ( $L'$ ), the

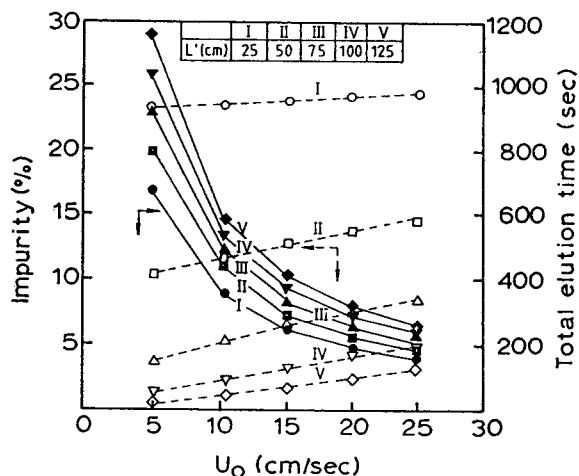


Fig. 11. Effect of desorbent velocity on impurity with additional column length in desorption section. (20/30 mesh, 35°C,  $L = 100$  cm, 20% liquid loading).



solid lines show the relation between the desorbent velocity,  $u_0$ , and the total elution time, while the interrupted lines show the relation between the desorbent velocity,  $u_0$ , and the impurity. When the desorbent velocity is increased, the total elution time is increased, but the impurity is improved. When the allowable impurity is assumed to be 10%, optimum operating conditions exist for a the total elution time of less than 400 s. The optimum total elution time will be set as the switching time.

## 6. Conclusions

Based on the operational principle of the combined continuous and preparative chromatographic system, the experimental conditions were mainly affected by the additional column length and the desorbent velocity. The increased pressure drop caused by the longer column length and higher gas velocity could be minimized by using larger particles, and the variation of the velocity along the column was simply corrected by the average gas velocity. Because the differences between the elution profiles of the pure materials and mixtures were relatively small in this gas chromatographic system, the assumption of a linear partition relation was reasonable.

The switching time for good separation was experimentally determined, and it was mainly affected by the column temperature and column length. In spite of the small deviations caused by the assumptions of constant gas velocity and linear partition isotherm, the theoretical concentration profiles were in relatively good agreement with the experimental data. For the combined continuous and preparative chromatographic system, therefore, the uniform film thickness model can be used for the proper estimation of the optimum operating conditions.

When the feed concentration is increased, the separation mechanism in the column becomes more complex, and generally information on the nonlinear isotherms is necessary to develop the mathematical models.

## Acknowledgement

The author gratefully acknowledges the financial support of INHA university in preparing this manuscript.

## List of symbols

$A_p$	Surface area of porous particle per unit volume, $\text{cm}^2/\text{cm}^3$
$c$	Concentration of solute in mobile phase, mol/l
$c_0$	Inlet concentration of solute, mol/l
$C(s)$	Laplace transform of $c(t)$
$D_e$	Effective intraparticle diffusion coefficient, $\text{cm}^2/\text{s}$
$D_l$	Diffusion coefficient in stationary liquid phase, $\text{cm}^2/\text{s}$
$D_M$	Molecular diffusivity, $\text{cm}^2/\text{s}$
$E$	Effective axial dispersion coefficient, $\text{cm}^2/\text{s}$
$k_f$	Interparticle mass transfer coefficient, cm/s
$k_g$	Intraparticle mass transfer coefficient with respect to stationary liquid phase-film, cm/s
$K$	Partition coefficient
$L$	Column length in partition section and desorption section, cm
$L'$	Additional column length in desorption section, cm
$n$	Concentration of solute in stationary liquid phase, mol/l
$q$	Concentration of solute in the pore space, mol/l
$r$	Radial distance measured from the center of particle, cm
$r_p$	Radius of spherical porous particle, cm
$Re$	Particle Reynolds number
$s$	Variable of Laplace transform with respect to time
$Sc$	Schmidt number
SLP	Stationary liquid phase
$t$	Time, s
$t_0$	Time of feed-injection, s
$T$	Column temperature, K

$u$	Interstitial mean linear velocity of carrier gas or desorbent, cm/s
$u_0$	Superficial velocity of carrier gas or desorbent, cm/s
$u_{ave}$	Average velocity of carrier gas or desorbent, cm/s
$x$	Distance perpendicular to surface of porous particle, cm
$z$	Axial distance, cm

### Greek letters

$\gamma, \gamma_1, \gamma_2,$ $\gamma_3, \gamma_4, \gamma_5$	Values defined by Eqs. 22–27
$\delta$	Film thickness of stationary liquid phase, $\mu\text{m}$
$\epsilon$	Interparticle void fraction of chromatographic column
$\epsilon_p$	Intraparticle void fraction with presence of stationary liquid phase
$\lambda, \lambda_1, \lambda_2, \lambda_3$	Values defined by Eq. 12–15

### References

- [1] A.T. James and A.J.P. Martin, *Analyst*, 77 (1952) 915.
- [2] Eli Grushka (Editor), *Preparative-Scale Chromatography*, Marcel Dekker, New York and Basel, 1989.
- [3] G. Subramanian, *Preparative and Process-Scale Liquid Chromatography*, Ellis Horwood, New York, 1991.
- [4] R.G. Bonmati, G. Chapelet-Letourneux and J.R. Margulis, *Chem. Eng.*, 87 (1989) 70.
- [5] P.E. Barker, in C.H. Knapman (Editor), *Developments in Chromatography*, Applied Science Publisher, London, 1978.
- [6] D.B. Broughton, *Chem. Eng. Pro.*, 64 (1969) 60.
- [7] P.C. Wankat, *Ind. Eng. Chem. Fundam.*, 16 (1977) 468.
- [8] H.Y. Ha, K.H. Row and W.K. Lee, *Sep. Sci. Technol.*, 22 (1987) 141.
- [9] H.Y. Ha, K.H. Row and W.K. Lee, *Sep. Sci. Technol.*, 22 (1987) 1281.
- [10] P.C. Wankat, *Ind. Eng. Chem. Fundam.*, 23 (1984) 256.
- [11] K. Hashimoto, S. Adachi, H. Noujima and A. Maruyama, *J. Chem. Eng. Jpn.*, 16 (1983) 400.
- [12] K. Hashimoto, S. Adachi, H. Noujima and Y. Udea, *Biotechnol. Bioeng.*, 25 (1983) 2371.
- [13] P.E. Barker and R.E. Deeble, *Anal. Chem.*, 45 (1973) 1121.
- [14] P.E. Barker, F.J. Ellison and B.W. Hatt, *Ind. Eng. Chem. Process Des. Dev.*, 17 (1978) 302.
- [15] P.E. Barker and C.H. Chuah, *Chemical Engineer*, Aug./Sept. (1981) 389.
- [16] P.E. Barker, K. England and G. Vlachogiannis, *Chem. Eng. Res. Des.*, 61 (1983) 241.
- [17] C.B. Ching and D.M. Ruthven, *Chem. Eng. Sci.*, 40 (1985) 877.
- [18] C.B. Ching and D.M. Ruthven, *Chem. Eng. Sci.*, 40 (1985) 1411.
- [19] K.H. Row and W.K. Lee, *Sep. Sci. Technol.*, 22 (1987) 1761.
- [20] K.H. Row and W.K. Lee, *J. Chem. Eng. Jpn.*, 19 (1986) 173.
- [21] M.A. Alkarasani and B.J. McCoy, *Chem. Eng. J.*, 23 (1982) 81.
- [22] N.D.P. Dang and L.G. Gibilaro, *Chem. Eng. J.*, 8 (1974) 157.
- [23] I. Moon, K.H. Row and W.K. Lee, *Korean J. Chem. Eng.*, 2 (1985) 155.
- [24] H.M. McNair and A.J.P. Bonelli, *Basic Gas Chromatography*, Varian Aerograph, Berkeley, CA, 1969.
- [25] K.H. Row and W.K. Lee, in N.P. Cheremisinoff (Editor), *Separation by Gas-Liquid Chromatography, Handbook of Heat and Mass Transfer, Vol. 3: Catalysis, Kinetics, and Reactor Engineering*, Ch. 22, Gulf Publishing Company, Houston, TX, 1989.
- [26] A. Littlewood, *Gas Chromatography*, Academic Press, New York, 1970.



ELSEVIER

Journal of Chromatography A, 707 (1995) 117-129

JOURNAL OF  
CHROMATOGRAPHY A

# Scale-up of liquid chromatography for industrial production of parenteral antibiotic E1077

Masato Kodama<sup>a</sup>, Shouzou Ishizawa<sup>a</sup>, Atsushi Koiwa<sup>a</sup>, Takeo Kanaki<sup>a</sup>,  
Ken Shibata<sup>b</sup>, Hirotohi Motomura<sup>b,\*</sup>

<sup>a</sup>Eisai Chemical Co., Ltd., 22 Sunayama Hasaki-machi, Kashima-gun, Ibaraki 314-02, Japan

<sup>b</sup>Kurita Water Industries, Ltd., 7-1 Morinosato-Wakamiya, Atsugi-shi, Kanagawa 243-01, Japan

## Abstract

Purification is a key process for the commercialization of new chemical compounds. This is especially the case of pharmaceutical compounds, which require high quality. Optimization of the purification process is a primary concern. An industrial-scale process was developed for synthesizing a new cephalosporin, 3-aminopropenyl-7-fluoromethoxyiminothiadiazolylcephem (E-1077). Column chromatography was applied to purify this product. Optimum conditions for production were determined on the basis of analytical-scale studies. The process was then scaled up to the pilot production of samples. In order to achieve successful scale-up of industrial chromatography, it is necessary to consider the chemical nature of the crude compound and optimization of each step in the total production process.

## 1. Introduction

Many recently developed pharmaceutical compounds have a complex structure and are chemically unstable. At the same time, the quality requirements for pharmaceutical compounds continue to become even more stringent. As a result, the choice of purification processes and the optimization of purification conditions have become increasingly important. A new cephalosporin antibiotic, E1077 [1-5], currently under development by Eisai, was purified by small-scale octadecylsilica gel (ODS) column chromatography in the early development and synthesis stages. ODS was selected because it is effective with regard to high-purity refinement of com-

pounds that are highly soluble in water, such as E1077. However, the amounts of purified E1077 required, which increased with each stage of development, were difficult to obtain using small-scale chromatography. The quality requirements also become more severe, so the purification conditions had to be improved.

The major problems encountered in improving the purification conditions were as follows:

(1) Minute amounts of coloured components contaminated the purified compound. Coloured components with various properties are included in crude E1077, and although low- and high-polarity coloured components are removed by ODS, some coloured components cannot be removed.

(2) Ignition residues which were mainly silica derived from ODS contaminated the purified compound.

\* Corresponding author.

(3) The HPLC purity of the purified material was low.

(4) A large pressure difference between column inlet and outlet caused low productivity. It took nearly 1 day to carry out the step of chromatographic purification.

(5) Multiple batches were required owing to the small lot size.

Development was undertaken to solve these problems and construct a pilot-scale preparative chromatographic system. High quality, high yield and an easy purification procedure were the goals of development. In addition, recycling of the solvent was taken into consideration, and a pilot system was designed based on the targeted full-scale production system. The system combined different separation media for each function rather than a single separation medium for all functions, because numerous impurities such as by-products and starting materials of chemical synthesis with various properties are contained in crude E1077. Use of a column was considered to improve the concentration of the purified solution. The evaluation of each purification process is relatively simple in a system made up of single functions, so the effectiveness of the purification parameters was easy to examine. As each function was investigated, the causes of problems that arose in actual operation could be easily identified and dealt with quickly.

The parameters of the purification process, including solvent, temperature linear velocity and loading capacity, were investigated using the procedure described below. First, owing to the instability of E1077, the ranges of purification parameters necessary to maintain high quality, such as temperature and solvent, were confirmed. Next, in order to attain high HPLC purity, various separation media were tested in the main purification column, resulting in the selection of ODS. Following the selection of the main column, a colour-removal column for removing minute amounts of coloured components contained in the ODS purified solution and a concentration column for producing the target material in high concentration were investigated. As a result, a purification system consisting of

three columns was developed. This paper describes the investigations and procedures used in this development.

## 2. Experimental

### 2.1. Equipment

An LC-6A pump, SPD-6A ultraviolet detector, C-R4A integrator (all from Shimadzu, Kyoto, Japan) and a UA-100 isothermal water-bath (Tokyo Rika, Tokyo, Japan) were used to determine the parameters for the small-scale column purification and HPLC analysis. An SIL-6B autosampler (Shimadzu, Kyoto, Japan) was used to inject sample amounts of 100  $\mu\text{l}$  or less, and a 5-ml sample loop (constructed in the authors' laboratory) was connected to a Model 7125 sample injector (Rheodyne Cotati, CA, USA) for injecting sample amounts greater than 100  $\mu\text{l}$ .

The confirmation experiment for the system design used an LC-8A pump (Shimadzu), an SPD-6A ultraviolet detector (Shimadzu) and a U-228 recorder (Nihon Denshi Kagaku, Tokyo, Japan). The LC-8A pump was used for sample injection. A UV-2200 recording spectrophotometer (Shimadzu) was used when absorbance was measured to determine the colour of the E1077 solution.

### 2.2. Crude materials and reagents

Crude and purified E1077 were prepared by Eisai Chemical. The structure of E1077 is shown in Fig. 1. The organic solvents used in the experiment with small-volume columns were all of special reagent grade (Kishida Kagaku, Osaka, Japan). Ultra-pure water with a total organic carbon (TOC) level of 2–3 ppb was used. In the confirmation experiment for the column system, special-reagent grade organic solvents (Wako, Osaka, Japan) and "purified"-grade water were used.

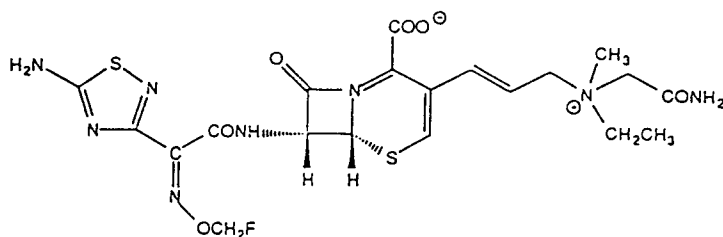


Fig. 1. Structure of E-1077: (-)-(6*R*,7*R*)-7-{2-(5-amino-1,2,4-thiazol-3-yl)-2-[(*Z*)-fluoromethoxyimino]acetamido}-3-[(*E*)-3-[(*RS*)-(carbamoylmethyl)ethylmethylammonio]-1-propenyl]-8-oxo-5,5-thia-1-azabicyclo[4.2.0]oct-2-ene-2-carboxylate ( $C_{20}H_{25}N_8O_6S_2F$ ,  $M_r = 556.6$ ).

### 2.3. Packing

In the small-scale experiment, YMC GEL ODS-A120-S10 (YMC, Kyoto, Japan) was used. In the confirmation experiment of the system design, YMC GEL ODS-AQ-S50 (YMC) was used. MP950A Type I strongly basic anion-exchange resin (Bayer Japan, Tokyo, Japan), Diaion A50 Type II strongly basic anion-exchange resin (Mitsubishi Kasei, Tokyo, Japan), Diaion SK1B strongly acidic cation-exchange resin (Mitsubishi Kasei) and Diaion FP-HG-13 methacrylate resin (Mitsubishi Kasei) were investigated as colour-removal media. In addition, Diaion SP207 and HP20 (Mitsubishi Kasei) were investigated as concentration resins. Both SP207 and HP 20 are styrene-divinylbenzene copolymers having macropores. SP207 has 100-Å pores and HP20 has 200–300-Å pores [6]. These two resins have no functional groups, such as ion-exchange groups, and adsorb various organic materials using Van der Waals forces. SP207 includes a substituted Br group in order to enhance the hydrophobicity over that of HP20.

### 2.4. Column

Stainless-steel columns of 150 mm L × 6 mm I.D. were used in the small-scale experiment. The column used for ODS was an AQ-312-10 packed column (YMC) packed with YMC GEL ODS-A120-S10. The colour-removal column was packed in the laboratory with a packing selected in the adsorption equilibrium experiment de-

scribed later. The concentration column was packed in the laboratory with either SP207 or HP20. For packing in the laboratory, resin soaked in water was poured into the top of the column, then water was pumped through the column and the packing was supplemented to fill any voids that remained. This process was repeated until all voids were eliminated.

For the system confirmation experiment, the selected packings were packed into 20 mm I.D. columns. The column used for ODS was an SH-345-50 packed column (YMC) packed with YMC GEL ODS-AQ-S50. The colour-removal and concentration columns were each packed in the laboratory with the selected packing materials. The relationship between linear velocity (*LV*) and the operating pressure of the ODS column was confirmed using an LC-110 axial compression column (Kurita Water Industries, Tokyo, Japan).

### 2.5. Determination of purity, concentration and colour

The purity and concentration of the target material, E1077, were confirmed by HPLC analysis. Using an Inertsil-ODS-2 (GL Science, Tokyo, Japan) column (150 mm × 4.6 mm I.D.), a mobile phase consisting of acetonitrile, 1 mM sodium dodecyl sulfate (SDS) and phosphoric acid (330:670:5) was eluted at a rate of 1 ml/min, and detection was carried out at 254 nm. The colour of E1077 was defined as the absorption at 450 nm with a concentration of 10% in

aqueous solution, and was calculated from the E1077 concentration found by HPLC analysis and the absorbance measured at 450 nm.

### 2.6. Evaluation of properties of E1077

The influence of temperature on the colour and purity of the E1077 solution was evaluated together with the influence of the type of organic solvent on purity. The influence of temperature was confirmed by changes in solution colour and purity with time when a 15% aqueous solution of purified E1077 was allowed to stand at 5, 10 and 20°C. The influence of the type of organic solvent was confirmed by observing changes in HPLC purity with time at 20°C after preparing various aqueous and organic solvent solutions containing 10% E1077 of 98.4% purity.

### 2.7. Investigation of ODS column

The investigations with the small ODS column were carried out at flow-rates of 2 ml/min and theoretical plate numbers of 4000. The relationship between the mobile phase concentration and the capacity factor was confirmed using a mobile phase with acetonitrile concentrations of 2.5–10% and by loading 10  $\mu$ l of 1% aqueous purified E1077 solution on to the column. The maximum loading capacity that realizes the target purity and yield was estimated at each mobile phase concentration based on the relationship between load and the purity–yield curve. The relationship was found based on preparative experiments at load levels of 2–3 steps. Crude aqueous E1077 solution with an E1077 concentration of 5% was applied for the preparative experiments.

### 2.8. Confirmation of relationship between LV and operating pressure of ODS column

The maximum flow-rate was compared at the theoretical plate number of 4000 when ODS packings of 10 and 50  $\mu$ m were applied. The theoretical plate number and operating pressure of a 1 m length column were confirmed at each LV.

### 2.9. Investigation of colour-removal column

The resin for colour removal was evaluated for E1077 yield and colour-removal rate by an adsorption equilibrium experiment. A 0.5-g amount of each resin was added to 5 ml of ODS-purified solution, the solution was allowed to soak for 1 h with occasional stirring at 0°C, the supernatant was filtered through a GL Chromatodisc 25N 0.45- $\mu$ m filter, (GL Science) and then the amount of target material and the colour of the filtrate solution were determined. The colour adsorption capacity and E1077 yield were evaluated using a 150 mm  $\times$  6 mm I.D. column with continuous loading of ODS-purified E1077 at LV between 0.25 and 4.0 m/h.

### 2.10. Investigation of concentration column

The capacity of the concentration column was calculated from the breakthrough curve obtained when a 7% acetonitrile solution of purified E1077 was loaded at various concentrations on to a 150 mm  $\times$  6 mm I.D. column at a rate of 0.1 ml/min. The concentration of the eluate from the concentration column was evaluated by examining the elution peak width when E1077 was eluted at each concentration after a fixed amount of purified E1077 was already adsorbed in the column.

## 3. Results and discussion

### 3.1. Properties of E1077

The increase in the colour of the solution is shown in Fig. 2 as a function of temperature. The decrease in HPLC purity at each temperature is shown in Fig. 3. It is clear that this compound is unstable at higher temperatures. Although the product quality deteriorates considerably at 20°C, the compound is relatively stable at 5 and 10°C. From the viewpoint of stability, a lower temperature is preferable, but taking into account the issues related to cooling control during actual manufacture in the plant, purification at 10°C was selected.

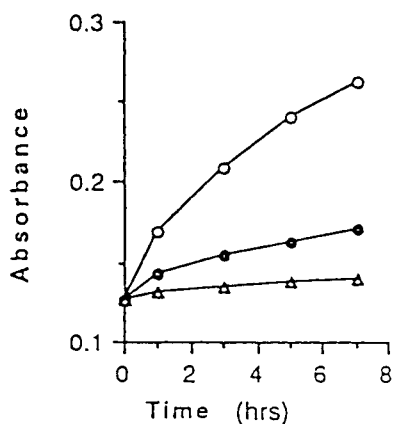


Fig. 2. Influence of temperature on colour of E1077 solution. Increase in absorbance at 450 nm with time of 10% conversion of E1077 concentration using 150 mg/ml of purified E1077 in aqueous solution. O = 20°C; ● = 10°C; Δ = 5°C.

Regarding organic solvents, the compound is unstable in the presence of lower alcohols, and the HPLC purity deteriorates as shown in Fig. 4. On the other hand, the compound was stable in acetone and acetonitrile. However, acetone is not suitable for UV monitoring in preparative chromatography because the UV absorption of acetone at lower wavelengths is greater than that of acetonitrile. Acetone also presents problems when attempting to analyse the purified solution, so acetonitrile was selected as the mobile phase.

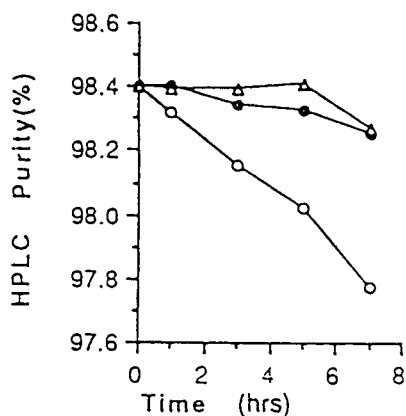


Fig. 3. Influence of temperature on HPLC purity of E1077 solution. Decrease in HPLC purity with time of 150 mg/ml of purified E1077 in aqueous solution. O = 20°C; ● = 10°C; Δ = 5°C.

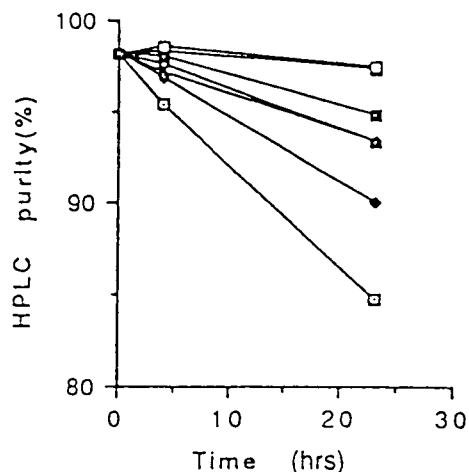


Fig. 4. HPLC purity in aqueous solution. Decrease in HPLC purity with time in different aqueous-organic solvent mixtures (1:1) of 150 mg/ml of purified E1077 in aqueous solution. 1 = Acetonitrile; 2 = acetone; 3 = 2-propanol; 4 = 1-propanol; 5 = THF; 6 = EtOH; 7 = MeOH.

### 3.2. Purification column

E1077 is an antibiotic requiring high purity and high yield, so the purification column is very important. With this in mind, ODS was selected as the packing because of its high resolution and performance, both confirmed in our previous work with a small-scale column. An axial compression column was used because an industrial scale was assumed and this column has been shown to maintain consistent performance over long periods [7,8].

ODS S-50  $\mu\text{m}$  was chosen as the packing because it demonstrates high productivity on the industrial scale and is relatively inexpensive. As shown in Fig. 5, when a comparison is made at the same theoretical plate number, ODS S-50  $\mu\text{m}$  provides a higher flow-rate than ODS S-10  $\mu\text{m}$ . In other words, high productivity can be achieved. The theoretical plate number was set at 4000 after considering the difficulty of purification and the actual capabilities of the device for industrial-scale separation. Taking the column length as 1.2 m, the maximum flow rate was  $LV = 3.0$  m/h owing to the pressure resistance of the column (pressure difference 30  $\text{kgf/cm}^2$ ) [9,10].

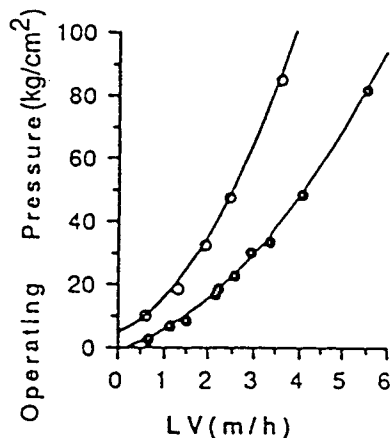


Fig. 5. Relationship between  $LV$  and operating pressure at a theoretical plate number of 4000 for ODS columns of (○) 10 and (●) 50  $\mu\text{m}$ . The column length resulting in a theoretical plate number of 4000 was calculated for each  $LV$ ; the operating pressure was also calculated. Although the operating pressure was found for 10% acetonitrile at 10°C, the above plate number was valid because the pressure difference was very small (10% or less) within the range of acetonitrile concentration 0–20%.

The relationship between the mobile phase concentration and the capacity factor of the target material for a small-scale column is shown in Fig. 6. The column temperature was 10°C as determined earlier. Based on previous experience, the maximum productivity was often

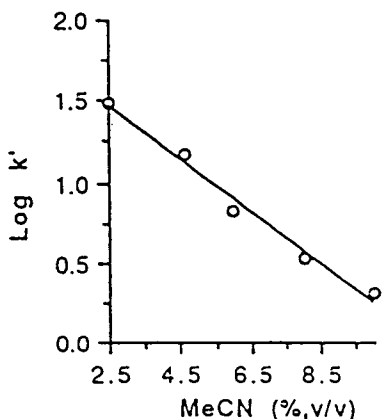


Fig. 6. Relationship between acetonitrile concentration in mobile phase and  $\log k'$  of E1077 in ODS column. YMC AQ-312-10 column (150 mm  $\times$  6 mm I.D.); 10°C; 2 ml/min; injection of 10  $\mu\text{l}$  of 10 mg/ml purified E1077 in aqueous solution.

obtained with a capacity factor of 20 or less. Therefore, the maximum loading capacity was investigated in the capacity factor range 0.2–15 and an acetonitrile concentration range of 4–20%. As shown in Fig. 7, the highest loading capacity was obtained at an acetonitrile concentration of 7%. In determining the parameters for column purification, solvent consumption, production efficiency and number of batches were used as indices.

Fig. 8 shows the relationship between the mobile phase concentration and productivity. Productivity is defined as the loading capacity divided by the solvent consumption. In calculating the solvent consumption, the 50% acetonitrile used for column flushing after purification was taken to be three bed volumes of column. Productivity was maximized and solvent consumption was minimized when the acetonitrile concentration was 13%. On the other hand, an acetonitrile concentration of 7% provided the greatest loading capacity, and therefore the lowest number of batches. The difference in solvent consumption between acetonitrile concentrations of 7 and 13% is less than 25%, so

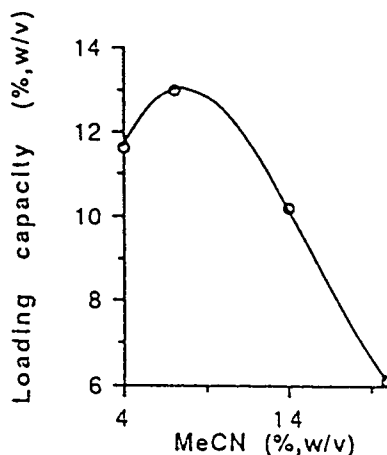


Fig. 7. Relationship between mobile phase concentration and loading capacity in ODS column. The ordinate shows the maximum value of the loading capacity that will achieve the target purity and yield. The loading capacity is shown as mass of E1077 in loaded crude material relative to volume of ODS (% w/v). YMC AQ-312-10 column (150 mm  $\times$  6 mm I.D.); 10°C; 2 ml/min; aqueous solution of crude E1077 material loaded.



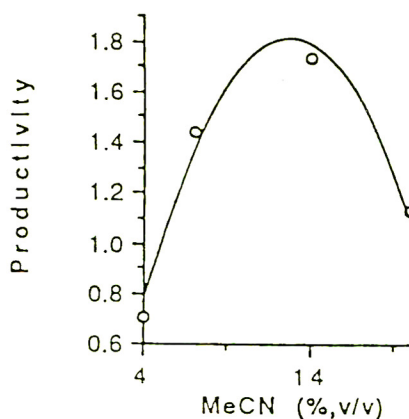


Fig. 8. Relationship between mobile phase concentration and productivity required for E1077 purification on ODS column. Productivity is defined as loading capacity divided by solvent consumption. The amount of solvent consumed combines both mobile phase for purification and three column bed volumes of 50% acetonitrile for flushing after purification.

emphasizing the minimum number of batches, an acetonitrile concentration of 7% was selected.

### 3.3. Colour-removal column

In order to remove minute coloured components that contaminate the purified solution and to attain a target absorbance, the purification conditions of the colour-removal column were investigated. First, the resin was selected and the location of the colour-removal column was investigated to determine whether to place this column before or after the ODS column. The column was tentatively placed after the ODS column and the ODS-purified solution was used to evaluate the decolorizing effects and E1077 yield for each type of resin in an adsorption equilibrium experiment. The results, shown in Fig. 9, indicate that anion ion-exchange resin (Type I) is the most effective.

The column was next placed before the ODS column, and the same experiment was carried out using a crude aqueous solution. When the total decolorization rate combining the ODS and colour-removal columns is considered, the results are about the same. However, placing the colour-removal column before the ODS column

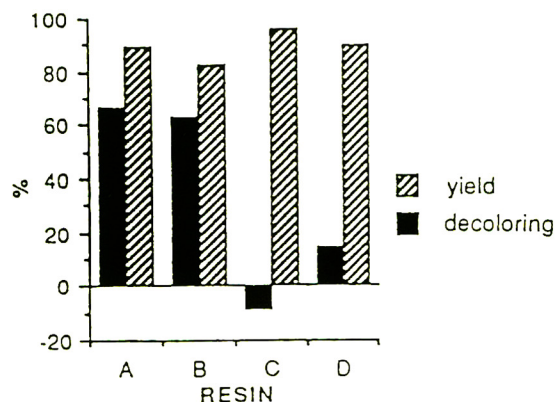


Fig. 9. Adsorption equilibrium for ODS-purified solution to select decolorizing resin. A 0.5-g amount of each resin was added to 5 ml of ODS solution purified from crude E1077 material, the solution was shaken at a temperature lower than the freezing point and the E1077 yield and decolorization rate were confirmed. (A) Strongly basic anion-exchange resin I; (B) strongly basic anion-exchange resin II; (C) strongly acidic anion-exchange resin; (D) methacrylate resin.

is thought to exert a negative influence on the purification of impurities owing to diffusion of the loaded solution. Therefore, it was decided to place the colour-removal column after the ODS column. Next, to determine the column dimensions, the capacity for adsorbing coloured components was confirmed by investigation of the breakthrough capacity using ODS-purified solution. The minute amounts of coloured components did not break through even when a solution with a load factor of 2000% (w-E1077/v-column) was passed through the column. As shown in Fig. 10, even when the flow-rate for the column was varied within an *LV* range of 0.25–4.0 m/h, no influence on the yield of E1077 and the rate of decolorization was observed. Therefore, the column diameter was designed to accommodate the flow-rate within this range.

### 3.4. Concentration column

The concentration of E1077 in the ODS-purified solution is dilute and the volume of the solution is large. Therefore, parameters for concentrating the solution in a column system were investigated. Initially, the packing of the small-

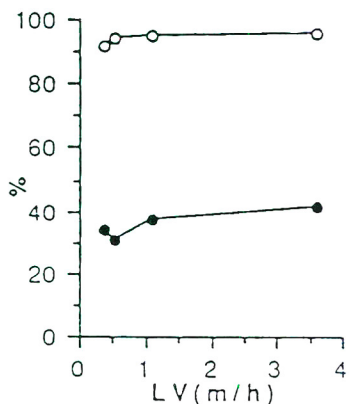


Fig. 10. Relationship between E1077 yield and decolorization to LV in colour removal column. Decolorizing resin packed in a 150 mm  $\times$  6 mm I.D. column; 10°C; ODS-purified crude E1077 material loaded.  $\circ$  = Yield;  $\bullet$  = decolorization.

scale concentration column was the same ODS as used in the purification column. However, the elution of ignition residues from the ODS was a problem. This occurred when a high water content in the mobile phase caused silica gel to dissolve at about 10 ppm. This gel could not be eliminated in the post-processes and contaminated the final product as an ignition residue. As a result, the packing material of the concentration column was changed to a synthetic adsorption resin that did not cause elution of ignition residues. Finally, use of hydrophobic adsorption resin SP207 or HP20 was considered because these resins exhibit high adsorption capacities and are widely used in large-scale applications.

As shown in Fig. 11, the adsorption capacity relative to E1077 was found to be much larger for SP207 than for HP20. Therefore, SP207 was selected. The column dimensions were also set according to the adsorption capacity corresponding to the E1077 concentration of the ODS-purified solution. Next, the acetonitrile concentration used to elute the adsorbed E1077 from the resin was determined after considering the solubility of E1077 and the elution peak width or, in other words, the amount of eluent. As shown in Fig. 12, the elution peak widths broaden when the acetonitrile concentration is

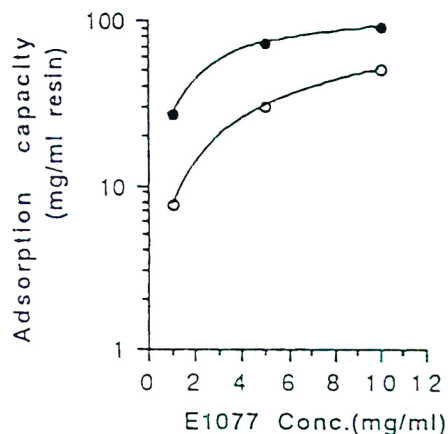


Fig. 11. Adsorption capacity of ( $\bullet$ ) SP207 and ( $\circ$ ) HP20. The resins were packed into individual 150 mm  $\times$  6 mm I.D. columns at 10°C and an aqueous solution of purified E1077 was loaded. The adsorption capacity was determined from the breakthrough curve.

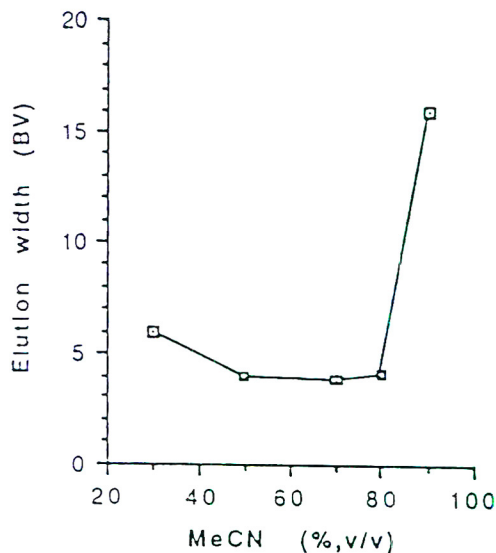


Fig. 12. Relationship between acetonitrile concentration in eluent and peak width of SP207 concentration column. SP207 packed into a 150 mm  $\times$  6 mm I.D. column; 10°C; a fixed amount of purified E1077 in aqueous solution was loaded, elution was carried out at each concentration of acetonitrile and peak widths were confirmed by UV monitoring of the solution from the column outlet.

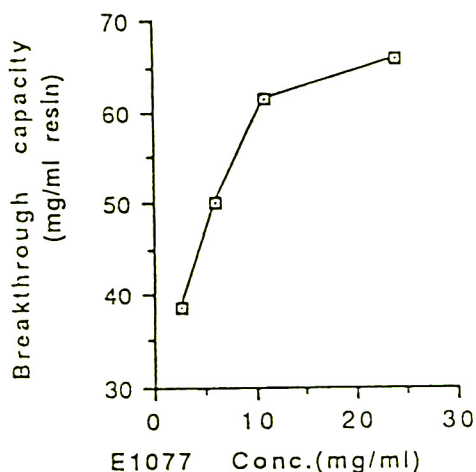


Fig. 13. Relationship between E1077 concentration and breakthrough capacity of SP207 concentration column. SP207 packed into a 150 mm × 6 mm I.D. column; 10°C; each concentration of purified E1077 in aqueous solution was sequentially loaded and the breakthrough capacity was found from the breakthrough curve obtained by UV monitoring of the solution from the column outlet.

either less than 50% or greater than 80%. In particular, when the concentration is 80% or more, the broadening is abrupt. The reason for this is the deposition of E1077 due to low solubility at higher concentrations of acetonitrile. As a result of this investigation, a concentration range of 50–80% was determined to be suitable. Considering the operations after column purification, E1077 deposition and ease of concentration after chromatographic purification, a higher acetonitrile concentration was thought to be desirable. Therefore, an acetonitrile concentration of 70% was selected.

### 3.5. New problems with concentration column

After the adsorption and elution parameters of the concentration column had been set according to the results of the experiments described above, the quality of the concentrated solution and the yield were investigated. In this experiment, aqueous E1077 solution was loaded on to the concentration column, E1077 was eluted and the concentrated solution was analysed. As a result, although the HPLC purity and yield satisfied the target values, the colour of the solution, as shown in Table 1, clearly deteriorated after concentration in the concentration column. Although a recheck was made using the cephalosporin compound E1040 which has the same betaine structure [11,12], the results were the same.

These results indicate that some component in the SP207 used in the concentration column caused the solution colour to deteriorate. As the SP207 was sufficiently batch-flushed with acetone before use, it was assumed that the unknown component could not be eliminated by acetone flushing. Finally, iron ions present during resin synthesis were proposed as the cause, and an experiment was carried out for confirmation.

As the stability of E1077 is very poor and evaluation of experimental results using E1077 is difficult, a preparatory experiment was performed using E1040, which is relatively stable and has a similar structure. The relationship between the amount of iron eluting from the SP207, as measured before the experiment, and the colour of the concentrated E1040 solution is shown in Table 2. The colour of the solution is

Table 1  
Colour of E1077 and E1040 solutions after SP207 concentration

Cephalosporin	Colour (AU <sup>a</sup> )		Colour increase (AU <sup>a</sup> )
	Before concentration	After concentration	
E-1077	0.092	0.357	0.265
E-1040	0.130	0.204	0.074

SP207 was flushed with acetone and packed in a 500 mm × 10 mm I.D. column. Aqueous solutions of purified E1077 and E1040 were loaded and the colour of the eluate with 70% acetonitrile was measured.

<sup>a</sup> AU = absorbance unit.

Table 2

Colour and iron content of E1040 concentrated from the SP207 column

No.	Eluted Fe (mg/l resin)	Colour of E1040 (AU)
1	<0.28	0.071
2	1.15	0.217

SP207 was packed in a 500 nm × 10 mm I.D. column, aqueous solutions of purified E1077 were loaded and the colour and iron content of the eluate with 70% acetonitrile were measured. Iron was measured by atomic absorption spectrometry.

stronger with higher levels of iron. Next, the solution colour change with time when iron ions were mixed with various types of cephalosporin compounds was observed. Although iron(III) chloride is used as a catalyst when synthesizing SP207, iron(II) chloride was used for this experiment because iron(III) chloride solution interferes with the observation of colour change.

Fig. 14 shows the results of the investigation into the influence of iron(II) chloride on the colour of various types of cephalosporin compound solutions. The structures of the compounds are shown in Fig. 15 [13]. For each cephalosporin compound, although there were differences in degree, higher iron ion concen-

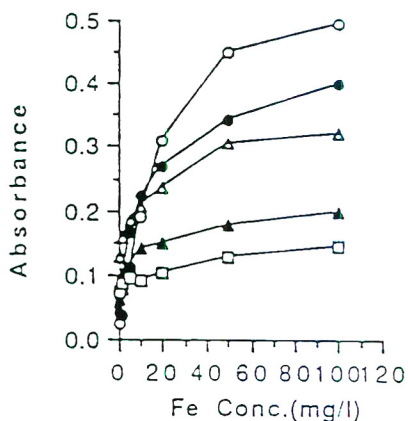


Fig. 14. Influence of iron(II) ion on colour of cephalosporin solution. Each aqueous iron(II) chloride solution was mixed 1:1 (v/v) with 2 mg/ml of aqueous cephalosporin solution to obtain each concentration. ○ = E-1040; ● = E-1077; △ = CTX; ▲ = CER; ◻ = CET.

trations resulted in poor solution colour. These results confirm the negative influence of the iron ions on solution colour. With these results in mind, development of a resin washing method was initiated. This development resulted in washing with added solvents such as (triethylamine) (TEA) and (ethylenediamine) (EDA), as shown in Fig. 16. The colour deterioration of the concentrated solution was shown to be greatly reduced by these methods, and an appropriate method for washing resins before use in purification was developed [14].

### 3.6. System design

A confirmation experiment was carried out using a laboratory-scale system of 20 mm I.D. columns with the purification parameters determined in previous investigations. An outline of the system is shown in Fig. 17. The dimensions of the colour-removal column in this system were balanced with the other columns and set to withstand the continuous use of multiple runs because the dimensions corresponding to one run were very small. An outline of the purification process is given below.

(1) Crude E1077 solution is highly purified by the ODS separation column.

(2) The ODS-purified solution is routed directly to the connected colour-removal column, and minute amounts of coloured components are adsorbed and removed. E1077, not adsorbed in the colour-removal column, is routed to the concentration column and adsorbed there. Ignition residues (silica) are not adsorbed by the concentration column, so they pass through and are eliminated.

(3) The E1077 adsorbed in the concentration column is eluted and a concentrated, purified E1077 solution is obtained. To improve the concentration effect when eluting, the concentration column is isolated from the system when elution is carried out. In the confirmation experiment with the laboratory-scale system, the estimates for both quality and yield were attained. Therefore, a pilot plant was designed and constructed, and the capabilities were realized as expected.

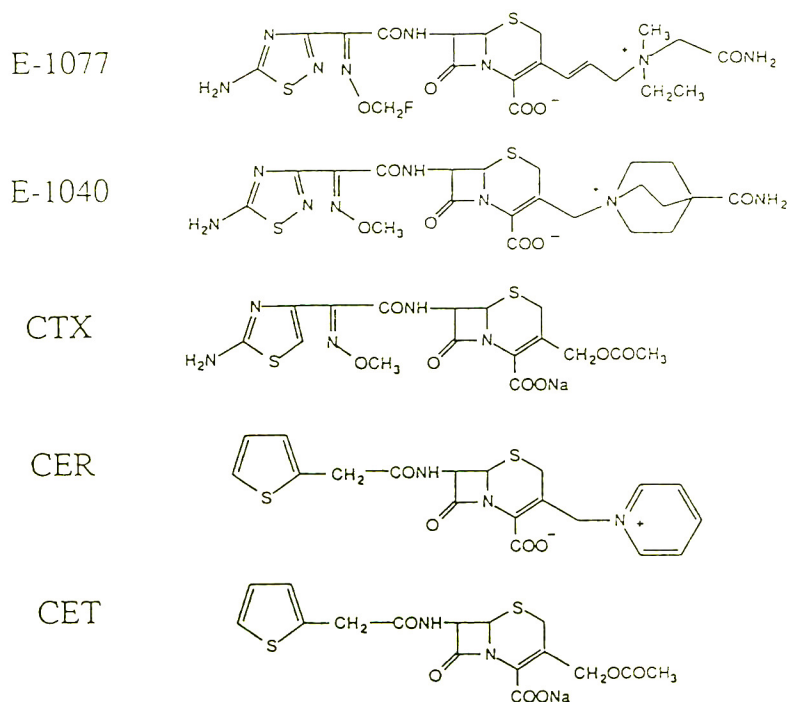


Fig. 15. Structural formulae of cephalosporin compounds. CTX = cefotaxime; CER = cephaloridine; CET = cephalothin.

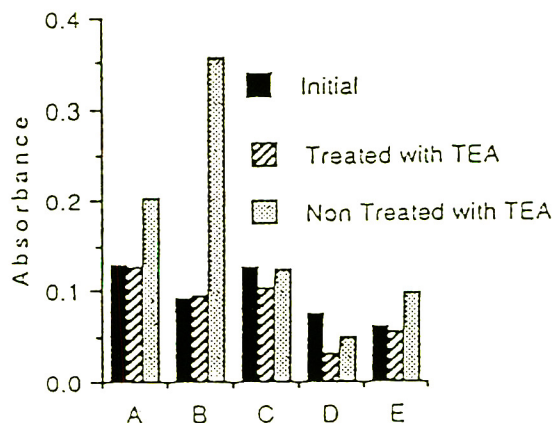


Fig. 16. Colour of SP207 concentrated cephalosporin solution before and after treatment of SP207 with TEA. TEA-treated SP207 and untreated SP207 were packed into individual 500 mm  $\times$  10 mm I.D. columns; aqueous solutions of each purified cephalosporin were loaded, elution was performed using 70% aqueous acetonitrile and the eluate colour was measured. (A) E1077; (B) E1040; (C) CTX; (D) CER; (E) CET.

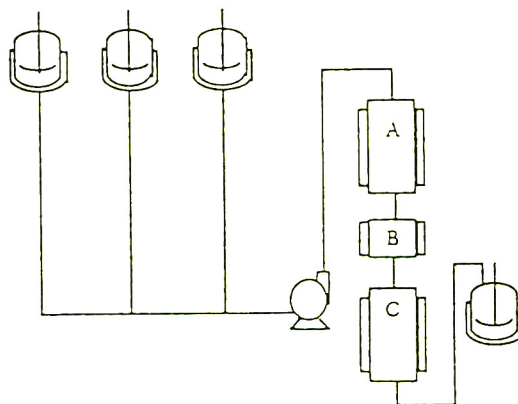


Fig. 17. Outline of pilot-plant design based on experimental results. The system consists of three columns including a purification column for achieving target high purity, a colour-removal column for achieving target solution colour and a concentration column. (A) ODS column; (B) MP-500A column; (C) SP-207 column.

The most important of the many advantages that have been realized by using this system are listed below:

(1) Unstable E1077 was highly purified. In particular, minute amounts of coloured components, which were difficult to remove by ODS purification alone, were eliminated. Also, the problem of ignition residue contamination was resolved.

(2) The yield was increased and cost was greatly reduced.

(3) The number of working steps was reduced because most of the purification operations are performed by a column system which is sequential and closed. System control was also simplified.

(4) All of the fluids passing through the system are either aqueous or single organic solvent solutions, and most of the organic solvent is reusable by distillation during production.

#### 4. Conclusion

Bulk pharmaceuticals require extremely high quality, and as these compounds have continued to become complex, so purification has become more difficult. The applicability of crystallization for purification is a key for developing organic synthetic pharmaceuticals of simple molecules. Crystallization is beneficial because large amounts of high-quality material can be processed in a short time, facilities are simple, special equipment is not required and the target material can be obtained at low cost because, generally, large amounts of various solvents are not necessary.

Purification methods using liquid chromatography are generally used for initial research and organic synthesis on a small scale. However, because disadvantages are thought to attend complex operations that use large amounts of solvents and large-scale facilities, the method is generally thought to be inapplicable to production. As a result, much of the investment in many pharmaceuticals has been in research with the goal of converting to purification by crystallization.

E1077 used in this experiment has a complex

structure and is unstable. Purification by crystallization was unsuccessful in our previous work and, as high quality must be maintained for its intended use as a pharmaceutical, there was no effective procedure other than chromatography. Without column chromatography, development of this compound would not have been possible. The chromatographic purification system was constructed in response to the challenge presented by this problem, and the possibility of production with column purification was demonstrated.

In the future, new active materials that are even more complex and unstable will be developed and the quality required can be expected to increase even further. Therefore, the column purification method, which can extract target compounds with high purity and in high yield, will continue to satisfy expectations in the future. The demand for chromatographic purification in pharmaceutical synthesis will probably increase in the future in accordance with improvements in column technology and the development of column-related facilities and separating materials.

#### References

- [1] T. Kamiya, T. Naito, Y. Kai, Y. Komatsu, M. Sasho, N. Sato, T. Nakamura and S. Negi, in Abstracts of Interscience Conference on Antimicrobial Agents and Chemotherapy, Atlanta, GA, October 1990, American Society for Microbiology, Washington, DC, 1990, p. 160.
- [2] S. Kamiya, T. Naito, S. Negi, Y. Komatsu, T. Kai, T. Nakamura, I. Sugiyama and Y. Machida, Jpn. Kokai Tokkyo Koho, JP1 156984.
- [3] K. Hata, M. Otsuki and T. Nishino, *Antimicrob. Agents Chemother.*, 36 (1992) 1894.
- [4] N. Watanabe, R. Hiruma and K. Katsu, *Antimicrob. Agents Chemother.*, 36 (1992) 589.
- [5] T. Toyosawa, S. Miyazaki, A. Tsuji and K. Yamaguchi, *Antimicrob. Agents Chemother.*, 37 (1993) 60.
- [6] *The Basic Manual for Ion-Exchange and Synthetic Adsorption Resins of Diaion*, Mitsubishi-Kasei, Tokyo, 1990, p. 123.
- [7] Y. Kinoshita and H. Motomura, *Chem. Eng.*, 33 (1988) 56.
- [8] H. Motomura and S. Sakuma, in K. Suda (Editor), *Ekitai Chromatography Kougyouka Gijyutstu Sougousiryoku Syuusei*, NTS, Tokyo, 1987, Ch. 7, p. 521.

- [9] Y. Kinoshita, 1992 Report of the Working Group 2 of Bio-separation Engineering, Society of Chemical Engineers, Tokyo, 1992, Ch. 5, p. 36.
- [10] Y. Kinoshita and H. Motomura, in Abstracts of the 7th International Symposium on Preparative Chromatography, Gent, April 1990, p. 151.
- [11] Y. Yamauchi, I. Sugiyama, I. Saitoh, S. Nomoto, T. Kamiya and S. Negi, Jpn. Koukoku Tokkyo Koho, JP6 33286.
- [12] N. Watanabe, K. Katsu, M. Moriyama and K. Kitoh, *Antimicrob. Agents Chemother.*, 32 (1988) 693.
- [13] K. Sakai, Saisin Kouseizai Youran, Yakugyou-Jihousiya, Tokyo, 1988, p. 51 and 64.
- [14] S. Ishizawa, M. Kodama, A. Koiwa, T. Kanai, K. Shibata and H. Motomura, in Proceedings of the 67th Spring Meeting of Chemical Society of Japan, Tokyo, March 1994, p. 663.







ELSEVIER

Journal of Chromatography A, 707 (1995) 131–135

JOURNAL OF  
CHROMATOGRAPHY A

# Production of rare-earth oxides of high purity

Zuying Zheng, Daren Ling\*, Ying Sun

*Department of Applied Chemistry, Jiangsu Institute of Petrochemical Technology, Changzhou, 213016, China*

## Abstract

A novel industrial technology for producing rare earth oxides of high purity (>99.99%) by temperature pressurized ion-exchange displacement chromatography is reported. It was concluded from the technological parameters that the concentration of complex agent in the eluent can be several times higher than that used in the classical ion-exchange method if a certain amount of buffer is present; the height equivalent to a theoretical plate (HETP) decreases linearly with increase in the operating temperature, increases slightly with increase in the flow-rate of the eluent and depends on the particle size of the ion exchanger. Rare earth oxides of high purity were manufactured on an industrial scale using a solution of special composition as eluent, and enriched rare earth mixtures or single rare earth oxides with low grade as raw and processed material on a temperature pressurized ion-exchange multi-column operating system containing polytetrafluoroethylene as the inner liner.

## 1. Introduction

Ion-exchange displacement chromatography with an amino-carboxylic complex agent as the eluent has been an important and effective method for industrially separating rare earth mixtures. However, because of its intrinsic shortcomings, such as long run period, low eluate concentration of rare earths and high production costs, its application in industry is limited. Recently, the temperature pressurized ion-exchange technique has been improved [1–3]. Owing to the patenting of the key techniques for processing, the separation of rare earths on an industrial scale has rarely been reported [4–6]. This paper briefly reports a novel industrial technology for producing rare earth oxides of high purity (>99.99%) by temperature pressurized ion-exchange displacement chromatography.

## 2. Experimental

The experiments were carried out using a temperature pressurized stainless-steel multi-column system [7], which consisted of five pressurized columns with jackets, three tanks for storing feed, eluent and ion exchanger sludge, three types of pumps (reciprocating pump, pressure air pump and vacuum pump), two types of valves (needle cut-off valve and safety valve) and five pipelines for vacuum, exhaust, feed, eluent and ion-exchanger sludge. In addition, another simple temperature pressurized glass multi-column system was built for parts of the experiments [8].

In the separation of rare earths by the temperature pressurized ion-exchange method, the factors that affect the efficiency of the separation are mainly the composition of eluent, the volume ratio of adsorption column and displacement column, the type of ion exchanger and its par-

\* Corresponding author.

Table 1  
Calculation of acidity of eluent with simulated titration curve

Resin	Composition of eluent			pH of eluate	
	$C_c^0$ (M) <sup>a</sup>	$C_b^0$ (M) <sup>a</sup>	pH	Calculated	Measured
D01 × 8	0.015	0	8.8	3.0	3.0
D01 × 8	0.015	0.114	6.5	5.4	5.4
D01 × 8	0.015	0.022	6.2	3.9	4.0
D01 × 12	0.015	0.114	6.5	5.4	5.4
D001 × 8	0.015	0.114	6.5	5.4	5.4
D001 × 8	0.015	0.022	6.2	3.9	4.0

<sup>a</sup>  $C_c^0$  = concentration of complexing agent in the eluent;  $C_b^0$  = concentration of buffer agent in the eluent.

ticle size, the flow-rate of the eluent, the operating temperature and the carrier ions. In this work, a strongly acidic cation exchanger with a cross-linked polystyrene structure (degree of crosslinking is 8%, crosslinking with divinylbenzene) was used. The particle diameter of the ion exchanger was between 30 and 90  $\mu\text{m}$ . Copper ion and hydrogen ion were the carrier ions.

### 2.1. Eluent

When the light rare earths were separated with an eluent of 0.015 M complexing agent (pH 8.8) at 60°C, precipitation occurred in the lanthanum region [9]. The pH in this region was 3.0. If the pH of the eluent was not suitably controlled, failure of the separation occurred owing to blocking of the columns. However, the precipitation disappeared if a buffer salt formed by a weak acid and a weak base was added to the eluent. The amount added and its corresponding buffering capacity can be determined from simu-

lated titration curves. From this, the pH of the eluate can be controlled [9]. A comparison is shown in Table 1.

When the buffer agent was added, it changed the composition of the eluent and the concentration of rare earths, the complex formability and the pH of the eluate. Table 2 gives the results of the separation of Eu(II) using eluents with the different composition.

As shown in Table 2, because of the added buffer agent, it is possible to use a solution with a high concentration of a complexing agent as the eluent. Under these conditions, the concentration of the driving ion increases considerably, which makes the migration rate of the band and the rare earth concentration in the eluate increase proportionally, although the complex formability ( $C_f$ ) decreases slightly [3]. Observing the values of the slopes ( $s$ ) of the displacement curves at the rear boundaries, the boundaries did not collapse; to the contrary, they became sharp. This conclusion has been tested and verified in many experiments.

Table 2  
Effect of composition of eluent on complex formability of Eu(II)

$C_c^0$ (M)	$C_b^0$ (%)	pH	$k$	$C_f$ (%)	$v$	$s$
0.015	Moderate	8.0	30	86	970	3
0.050	Moderate	8.0	11	74	400	4
0.075	Moderate	8.0	6.2	73	230	7

pH = pH of the eluent;  $k$  = column distribution ratio;  $C_f$  = complex formability;  $v$  = volume of eluent consumed;  $s$  = slope of displacement curve at rear boundary.

## 2.2. Temperature

In order to study the effect of temperature on the separation, Sm–Nd and Gd–Tb were separated at flow-rates of 13 and 3.6 cm/min, respectively, on a Cu–H resin bed. The eluent was a solution of pH 7.5 containing 0.050 M complexing agent and a moderate amount of buffer agent (Table 3). HETP was used to express the separation efficiency, which was calculated according to the boundary equation based on the distillation equilibrium plate model [2].

As shown in Table 3, the calculated values of HETP are lower at an operating temperature of 75°C than at lower temperatures according to the boundaries of the displacement curves of the Nd–Sm pair. When the temperature was decreased to 25°C, the HETP increased, the boundary of the curve collapsed and the separation efficiency became worse. The effect of temperature on the separation of Gd–Tb exhibited the same tendency.

In the process of ion exchange without chemical reaction at a low reaction rate, the diffusion rate of ions depends on the liquid film diffusion and interparticle diffusion. When an ion exchanger of micrometre particle diameter is used as the packing of column, the controlling step of the ion-exchange rate is the rate of liquid film diffusion [2]. Therefore, an increase in the operating temperature undoubtedly increases the diffusion of ions, decreases HETP and gives a good separation efficiency. However, in practice, it would not be convenient to operate at high temperatures. The column temperature is suitably controlled below 80°C when Cu–H columns are used as the carrier ion beds.

Table 3  
Effect of temperature on separation efficiency

Parameter	Nd–Sm				Gd–Tb		
Carrier ion	Cu–H				Cu–H		
Eluent	$C_c^0 = 0.050 M$ , pH = 7.5, buffer = moderate						
Flow-rate (cm/min)	13				3.6		
Temperature (°C)	75	70	50	25	75	50	25
HETP (cm)	1.6	1.6	2.2	2.8	0.7	3.3	6

## 2.3. Flow-rate and particle size

The results of the experiments at different linear flow-rates of the eluent and particle sizes of the ion exchanger are given in Tables 4 and 5, respectively. As shown, HETP increases only slightly with the increase in flow-rate from 16 to 25 cm/min. Comparing the efficiency of separation of Sm–Y on columns filled with ion exchangers of particle diameter 30–40  $\mu\text{m}$  and 40–60  $\mu\text{m}$ , the former is better.

It has been reported that the relationship between HETP and the flow-rate ( $V$ ) and the particle size of ion exchanger ( $r$ ) follows the expression  $\text{HETP} = CV^a r^b$ , where  $C$  is a constant,  $0.3 < a < 0.6$  and  $1.4 < b < 1.8$  [10]. In this work, the calculated values of  $a$  and  $b$  were about 0.5 and 1.7, respectively, in good agreement with the above values.

In addition, an increase in the flow-rate in-

Table 4  
Relationship between HETP and linear flow-rate of eluent ( $V$ )

$V$ (cm/min)	HETP (Eu–Sm) (cm)	HETP (Sm–Y) (cm)
16	0.53	0.17
20	0.80	0.19
25	0.84	0.20

Table 5  
Relationship between HETP and particle size of ion exchanger ( $r$ )

$r$ ( $\mu\text{m}$ )	$V$ (cm/min)	HETP (Sm–Y) (cm)
30–40	20	0.18
40–60	20	0.43

creases the HETP slightly and leads to a decrease in column efficiency to a certain extent; however, the production time is considerably shortened. A decrease in particle size can obviously enhance the efficiency of the column, but it will greatly increase the resistance of the column, which is not advantageous for practical operation if an ion exchanger with too small a particle size is used as the column packing.

### 3. Industrial production of rare earth oxides of high purity

A flow diagram of the scheme for the industrial production of rare earth oxides of high purity by temperature pressurized ion-exchange chromatography is shown in Fig. 1.

Fig. 2 shows the scheme of the temperature pressurized multi-column system. It consists of columns with different diameters ( $600 \times 3000$  mm,  $300 \times 1500$  mm), pressurized reciprocating pumps, valves and pipelines with different functions. The columns, the pipelines and the parts of valves were lined with PTFE. The packing in the columns was an ion exchanger with micrometre particle diameter which was hydrodynamically sieved. Ion exchangers of different particle sizes were filled into the different columns according to the functions of the columns.

The enriched rare earth mixture or a single rare earth of low grade was dissolved in the acidic solution. The feed solution was pumped

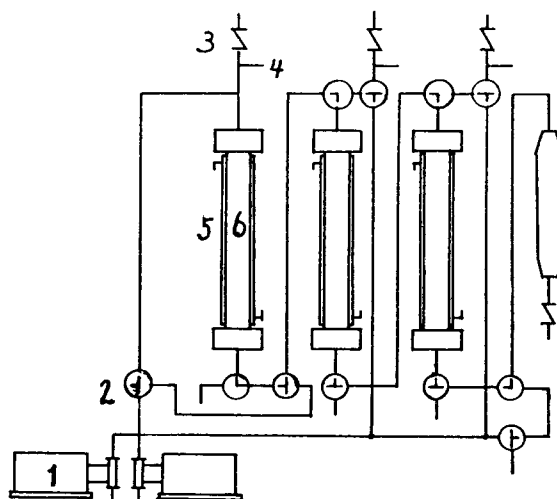


Fig. 2. Temperature pressurized ion-exchange multi-column system. 1 = Reciprocating pump; 2 and 3 = valves; 4 = pressure indicator; 5 = water jacket; 6 = column.

into the adsorption column after the acidity of the feed solution had been adjusted. After washing the column with deionized water, the rare earth adsorption band was eluted to the Cu-H carrier columns with an eluent of the special composition. According to the separation factor of the rare earths, the different displacement distances (the column ratio) were chosen.

The solution of the carrier agent from the columns was treated to recover the carrier agent and the complexing agent by electrolysis and precipitation, respectively. The solutions collected at the overlap areas were returned to the column system in the next run. The solutions of the rare earths were acidified in order to recover the complexing agent, then the rare earths were precipitated and scorified to the oxides as the products. Some measurement results for Er and Y products are given in Table 6. The measurements were made using a JY-38-Plus inductively coupled plasma instrument.

The production capacity for a run (2–3 days) was over 100 kg of rare earth oxides in an industrial plant (Wuxi TIO Ultrapure Materials Company, Wuxi, Jiangsu, China).

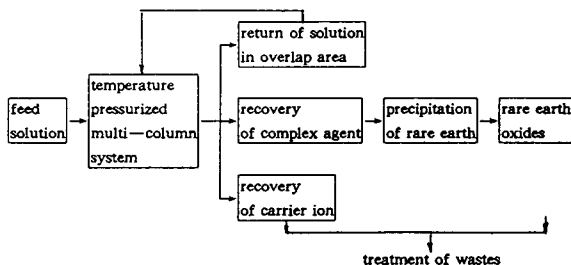


Fig. 1. Flow diagram of scheme for products of rare earth oxides.

Table 6  
Some measurement results for rare earth products

Element	Impurity (ppm) <sup>a</sup>							
	Gd	Tb	Dy	Ho	Er	Tm	Yb	Y
Er	–	–	0	0	–	0	0	0
	–	–	0	0	–	0	0	0
	–	–	0	0	–	13	0	0
Y	0	0.4	0.07	–	0	0.05	0	–
	0	0.4	1.1	–	0	0.03	0	–
	0	0.5	0	–	0	0.03	0	–

<sup>a</sup> Value 0 indicates an amount lower than the detection limit of the instrument.

#### 4. Conclusion

The technology reported here overcomes the intrinsic shortcomings of the classical ion-exchange method (CIEM). The concentration of rare earths in the eluate is several times higher than that obtained with CIEM. The production time per run is much shorter than that using CIEM. In comparison with CIEM, the characteristics for the present process are a shorter production period, much less reagent consumption and waste, higher concentration of rare earths in the eluate and higher column efficiency.

#### References

- [1] D.O. Campbell, *Sep. Purif. Methods*, 1 (1976) 97.
- [2] D. Ling, L. Qiu, et al., *Chem. J. Chin. Univ.*, 1 (1981) 1.
- [3] L. Qiu, D. Ling, et al., in: R.M. Lambrecht and N. Morcos, (Editors), *Applications of Nuclear Radiochemistry*, Pergamon Press, Oxford, 1984, pp. 397–423.
- [4] S. Vijavan, et al., *Min. Eng.*, 41 (1989) 1.
- [5] *Jpn. Pat.* 90111822.
- [6] *Jpn. Pat.* 88215512 and 88270312.
- [7] L.-Q. Cheng, D. Ling and L. Qiu, *Sci. Technol. At. Energ.*, 3 (1980) 366.
- [8] Z.-Y. Zheng, Y.-C. Jiang and D. Ling, *Rare Earths*, 3 (1990) 1.
- [9] D. Ling, A.-M. Zhao and L. Qiu, *J. Lanzhou Univ.*, 2 (1981) 39.
- [10] A. Jardy, et al., *J. Chromatogr.*, 83 (1973) 195.





ELSEVIER

Journal of Chromatography A, 707 (1995) 137–142

JOURNAL OF  
CHROMATOGRAPHY A

Short communication

## Hydrophobic interaction chromatography of *Chromobacterium viscosum* lipase

J.A. Queiroz<sup>a</sup>, F.A.P. Garcia<sup>b</sup>, J.M.S. Cabral<sup>c,\*</sup>

<sup>a</sup>Departamento de Química, Universidade da Beira Interior, 6200 Covilhã, Portugal

<sup>b</sup>Departamento de Eng<sup>a</sup> Química, Universidade de Coimbra, 3000 Coimbra, Portugal

<sup>c</sup>Laboratório de Eng<sup>a</sup> Bioquímica, Instituto Superior Técnico, 1000 Lisboa, Portugal

### Abstract

The influence of mobile phase composition on the chromatographic behaviour of *Chromobacterium viscosum* lipase was studied by using an epoxy-activated spacer arm as a ligand in hydrophobic interaction chromatography. The retention of lipase depends on the salt used and increased with ionic strength, indicating that the interaction of lipase with the stationary phase is of a hydrophobic nature. Using 20% (w/v) ammonium sulphate in the eluent a total retention of lipase on the column was obtained and by washing with 10 mM phosphate buffer a recovery of 79% protein and 89% lipolytic activity were achieved.

### 1. Introduction

Hydrophobic interaction chromatography (HIC) is a very powerful separation technique that is widely used in protein purification. In HIC, the addition of salting-out salts to the equilibration buffer (and sample solution) decreases the availability of water molecules in solution, increases the surface tension and enhances the ligand–protein interactions [1]. Elution and separation, according to differences in the surface hydrophobicity of proteins [2], are in general brought about by decreasing the salt concentration of the eluent.

The main parameters to consider for separation processes using HIC are: the type of

ligand and matrix, the type and concentration of salt, pH, temperature, and additives [3].

Strong hydrophobic interactions sometimes result in almost irreversible adsorption or denaturation during elution with harsh conditions (organic solvents, detergents, chaotropic agents, etc.). An example is the hydrophobic interaction between the lipase of *Chromobacterium viscosum* and a phenyl-Superose column, where elution is only obtained with a gradient of 0–65% (v/v) ethyleneglycol [4]. Therefore, ligands with intermediate hydrophobic character are of great interest, as they provide an adequate binding strength without the drawbacks mentioned above. This can be achieved by the use of bisoxiranes. Bisoxiranes have also been used for the introduction of reactive oxirane groups into agarose and for simultaneous stabilization of the gel by simultaneous cross-linking [5].

\* Corresponding author.

This work aims to study the influence of mobile phase composition on the chromatographic behaviour of *C. viscosum* lipase using bisoxirane (1,4-butanediol diglycidyl ether) with intermediate hydrophobicity as a ligand in HIC. The effectiveness of some salting-out salts (in different concentrations) at various pH values to increase lipase–adsorbent interaction is described.

## 2. Experimental

### 2.1. Materials

Sepharose CL-6B was obtained from Pharmacia (Uppsala, Sweden) and 1,4-butanediol diglycidyl ether from Sigma (St. Louis, MO, USA). All other reagents were of analytical grade.

### 2.2. Lipolytic preparation

A commercial lipolytic preparation of *Chromobacterium viscosum* lipases (3880 U/mg) from Toyo Jozo was used.

### 2.3. Protein determination

The concentration of protein in the samples was determined by the method of Bradford [6].

### 2.4. Activity measurement

Lipase activity was measured in an oil–water emulsion medium [7]. Amounts of 20 g of olive oil, 20 g of Triton X-100 and 60 ml of distilled water were mixed and magnetically stirred for 30 min. A volume of 5 ml of the resulting emulsion and 2 ml of water were preincubated at 37°C for temperature stabilization. The reaction was started by adding 0.5 ml of lipase solution, allowed to progress for 20 min, and stopped by adding 16 ml of an acetone–ethanol (1:1) mixture. The free fatty acids were then assayed by titration with 50 mM NaOH.

### 2.5. Preparation of gel

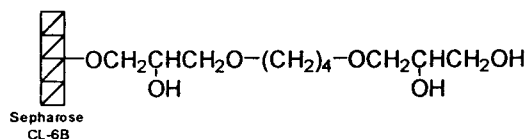
The gel was prepared by coupling 1,4-butanediol diglycidyl ether to Sepharose CL-6B according to Sundberg and Porath [5]. The amount of epoxy groups bound was around 500  $\mu\text{mol/g}$  dry gel. The gel thus obtained was subsequently treated with 1 M sodium hydroxide overnight at room temperature to inactivate the free epoxy groups.

### 2.6. Chromatographic method

The gel (about 5 ml) was packed in a column (10  $\times$  1 cm I.D.) and equilibrated with the desired mobile phase at a flow-rate of 4.5 ml/h. After the lipolytic extract (300  $\mu\text{l}$ , 3 mg) was applied, the elution profile was obtained by continuous measurement of the absorbance at 254 nm. Fractions of 1 ml were collected and the lipolytic activity and protein concentration were determined.

## 3. Results and discussion

In this work the HIC of *C. viscosum* lipase using an epoxy-activated spacer arm with intermediate hydrophobicity as a ligand is studied. The stationary phase was prepared by covalent immobilization of 1,4-butanediol diglycidyl ether on Sepharose CL-6B. This carbohydrate gel was selected because of its chemical stability and its large pore size (to rule out as far as possible the interference of gel-permeation phenomena). The schematic structure of the gel obtained is



The effect of some salts, their concentrations, and the influence of pH on lipase–adsorbent interaction was analysed.

Experiments carried out with different salting-



out salts (Fig. 1) indicate that the nature of the ions can play a significant role in the fractionation process. For sodium chloride, e.g., a small percentage of lipase was retained on the column, using a high concentration of the salt in the buffer. According to Melander et al. [8] an increase in salt molality or change of salt in the mobile phase to one of greater molal surface tension increment (in the absence of special binding effects) will result in increased retention of proteins in HIC. Sodium chloride is the salt used with the smallest molal surface tension increment [2].

The hydrophobic interactions are known to increase with the ionic strength of the medium [8,9]. In this way, as shown in Fig. 2, the progressive increase in ammonium sulphate concentration leads to a parallel increase in the amount of bound lipase. By this procedure, the

total retention of lipase on the column was obtained with 20% (w/v) ammonium sulphate.

The effect of pH on protein retention in HIC is not well defined. For the analysis of pH effect in our system, the buffer concentration was 10 mM for all pH values and 20% (w/v) ammonium sulphate was used to induce hydrophobic interactions. As can be seen in Fig. 3, no significant influence of pH was observed on the adsorption of lipase to the matrix. The retention of *C. viscosum* lipase was not strongly affected in the pH 4–9 range, whether the net charge of the lipase is negative or positive ( $pI$  6.9 [10]). This suggests that the hydrophobic interactions play a major role in the retention of the lipase rather than ionic interactions. However, Hjertén et al. [11] have found that the retention of proteins change more drastically at pH values above 8.5 and/or below 5 than in the pH 5–8.5 range.

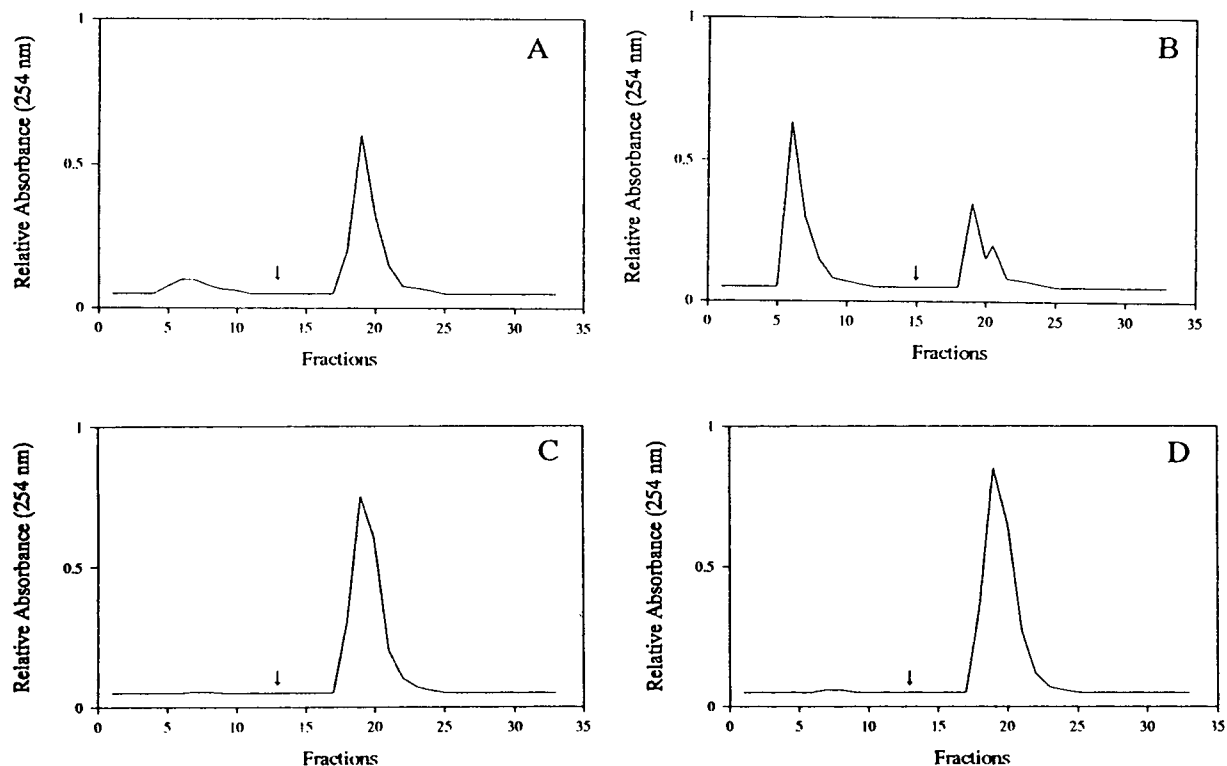


Fig. 1. Hydrophobic interaction chromatography on Sepharose CL-6B column modified with 1,4-butanediol diglycidyl ether (see text). Buffer: (A) 15% (w/w) potassium phosphate, pH 8; (B) 4 M NaCl; (C) 15% (w/v)  $\text{Na}_2\text{SO}_4$ ; and (D) 20% (w/v)  $(\text{NH}_4)_2\text{SO}_4$  in 10 mM phosphate, pH 7. Desorption ( $\downarrow$ ) is obtained with 10 mM phosphate buffer, pH 7.

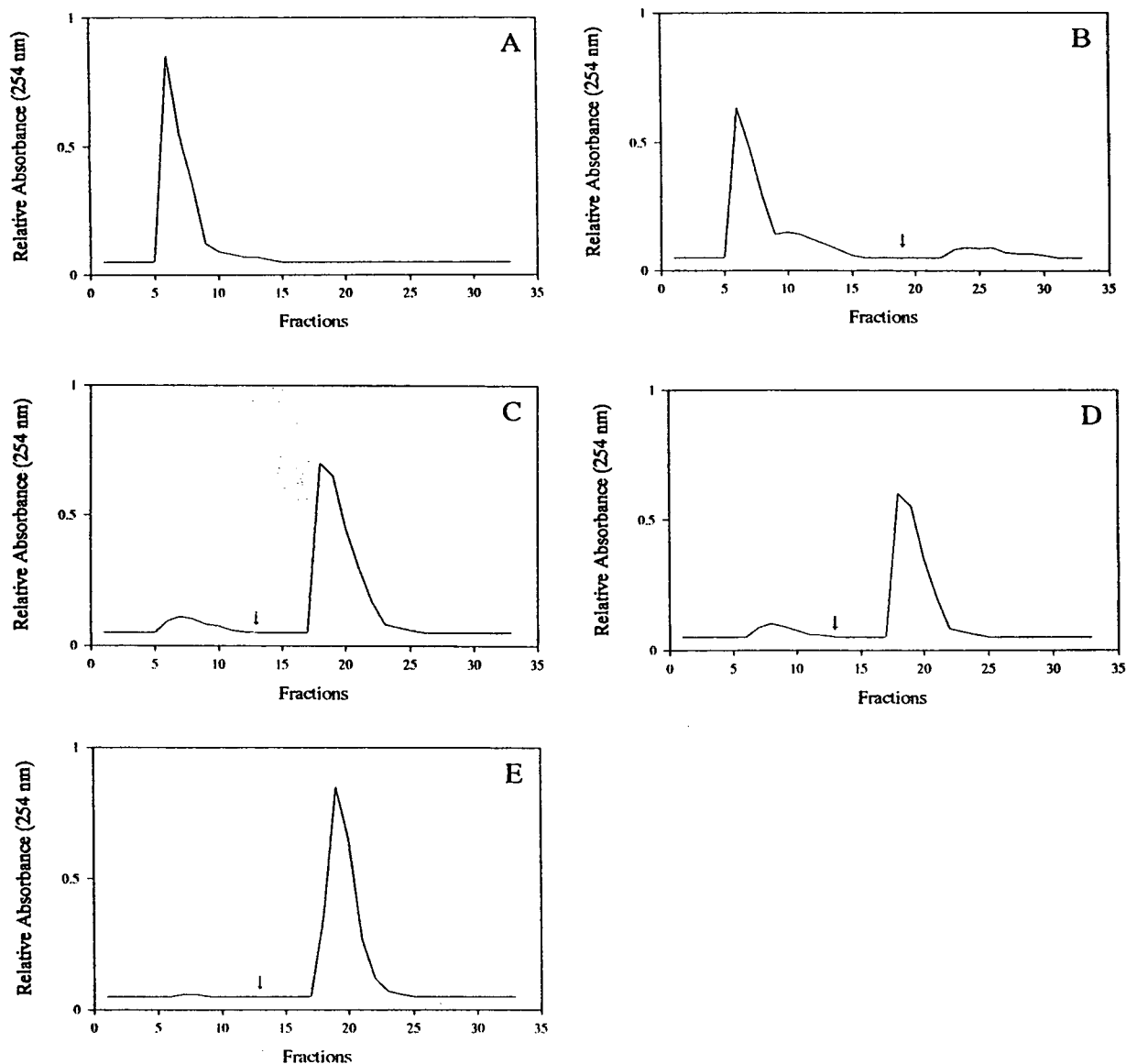


Fig. 2. Hydrophobic interaction chromatography on Sepharose CL-6B column modified with 1,4-butanediol diglycidyl ether (see text). Buffers: 10 mM phosphate, pH 7 (A), containing 10% (B), 15% (C), 17.5% (D) and 20% (E) (w/v)  $(\text{NH}_4)_2\text{SO}_4$ . Desorption ( $\downarrow$ ) is obtained with 10 mM phosphate buffer, pH 7.

However, the magnitude of these alterations in the retention is different for different proteins.

In ideal HIC a decrease in the ionic strength of the buffer might therefore increase desorption. By washing the adsorbent with phosphate buffer (10 mM), after total retention of lipase in the gel, a good recovery yield was obtained: about

79% for protein and 89% for the lipolytic activity. The opposite, as mentioned earlier, occurs when the hydrophobic interaction of *C. viscosum* lipase takes place with a phenyl-Superose column, where the elution is only obtained with a gradient of 0–65% (v/v) ethyleneglycol [4]. An 1.3-fold increase of specific activity was obtained

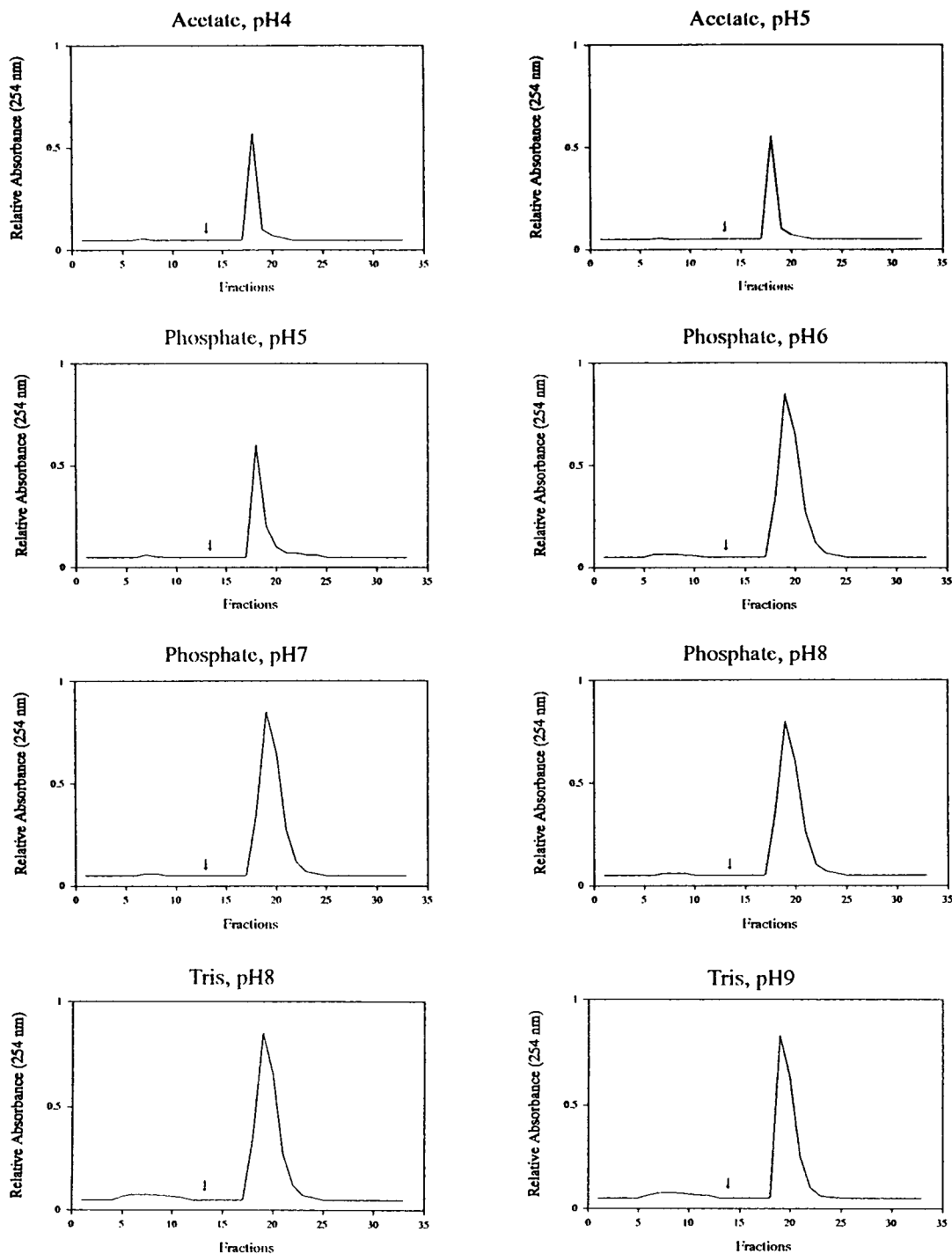


Fig. 3. Hydrophobic interaction chromatography on Sepharose CL-6B column modified with 1,4-butanediol diglycidyl ether (see text). Buffer: 20% (w/v)  $(\text{NH}_4)_2\text{SO}_4$  in 10 mM acetate, phosphate or Tris. Desorption ( $\downarrow$ ) is obtained with the respective buffer (10 mM).

and no further purification could be achieved probably due to the high purity of the initial lipolytic mixture used.

Control experiments carried out using undervivatized Sepharose CL-6B, or modified by covalent immobilization of 1,3-butadiene diepoxide [without  $(\text{CH}_2)_4$ ], did not result in any retention of lipase in the column. This shows that the fractionation of lipase in the gel is not due to the properties of the Sepharose or to the epoxy groups of the ligand. On the other hand, some precipitation of lipase on the top of column (about 10%) may occur, but if a centrifugation step is included before injection of the sample, no change in the chromatographic behaviour of lipase is obtained.

In conclusion, all the experimental results obtained support the hypothesis that the lipase–matrix interaction consisted of hydrophobic binding. In fact, Mathis et al. [12] have assumed that the hydrophobic interaction takes place with the  $-(\text{CH}_2)_4$ -units of the immobilized epoxy-activated spacer arm. The interaction of lipase with the stationary phase is apparently selective and the extent of retention of lipase is significantly affected by the salt used and by the ionic strength. HIC with the gel used seems to provide an interesting approach for lipase fractionation.

## References

- [1] S. Ree, in E.L.V. Harris and S. Angal (Editors), *Protein Purification Methods: a practical approach*, IRL Press, Oxford, 1989, p. 175.
- [2] W. Melander and Cs. Horváth, *Arch. Biochem. Biophys.*, 183 (1977) 200.
- [3] *Hydrophobic Interaction Chromatography — Principles and Methods*, Pharmacia BioProcess Technology, Uppsala, 1993.
- [4] M.A. Taipa, P. Moura-Pinto and J.M.S. Cabral, *Biotechnol. Tech.*, 8 (1994) 27.
- [5] L. Sundberg and J. Porath, *J. Chromatogr.*, 90 (1974) 87.
- [6] M.M. Bradford, *Anal. Biochem.*, 72 (1976) 248.
- [7] Y. Horiuti, H. Koga and S. Gocho, *J. Biochem.*, 80 (1976) 367.
- [8] W. Melander, D. Corradini and Cs. Horváth, *J. Chromatogr.*, 317 (1984) 67.
- [9] S. Hjertén, *J. Chromatogr.*, 87 (1973) 325.
- [10] M. Sugiura and M. Isobe, *Biochim. Biophys. Acta*, 341 (1974) 195.
- [11] S. Hjertén, K. Yao, K.-O. Eriksson and B. Johansson, *J. Chromatogr.*, 359 (1986) 99.
- [12] R. Mathis, P. Hubert and E. Dellacherie, *J. Chromatogr.*, 347 (1985) 291.

**END OF SYMPOSIUM PAPERS**





ELSEVIER

Journal of Chromatography A, 707 (1995) 145–179

JOURNAL OF  
CHROMATOGRAPHY A

## Review

# Carbon sorbents and their utilization for the preconcentration of organic pollutants in environmental samples

Eva Matisová\*, Svetlana Škrabáková

*Department of Analytical Chemistry, Faculty of Chemical Technology, Slovak Technical University, Radlinského 9, 812 37 Bratislava, Slovak Republic*

First received 16 September 1994; revised manuscript received 9 March 1995; accepted 9 March 1995

### Abstract

This review deals with carbon sorbents and their utilisation to trace analysis of organic pollutants in environmental samples. The first sections are devoted to the general characteristics of various kinds of carbon sorbents, carbon formation, the structure of carbon, their classification and characterisation (activated charcoal, graphitized carbon black, carbon molecular sieves and porous carbon). Information is given on the development of carbonaceous adsorbents, their characteristics and properties, development of various preconcentration techniques, off-line or on-line combination with the analytical measuring system (GC and HPLC), and the application of carbon sorbents to the enrichment of analytes is evaluated. The main use of carbon materials as a preconcentration/preseparation step has been in the sampling and trapping of volatile organic compounds (VOCs) from air and water matrices. An other field of application is the trapping of semi-volatile and non-volatile compounds and/or their separation into subclasses. According to the characteristics of the sampled components, carbon sorbents have been utilised in single-bed or multi-bed arrangement (combination of various carbon sorbents or combinations of carbon sorbents with other non-carbonaceous materials) to achieve quantitative trapping of trace components from environmental samples, followed by their desorption for subsequent identification and quantitation. Various achievements and problems, particularly in multicomponent-mixture analysis, are discussed. The physico-chemical properties of recently developed carbon adsorbents are superior compared to those of the “traditional” sorbent materials. Over the recent years much attention has been paid to the application of carbon sorbents for the on-site automated analysis and monitoring of trace pollutants.

### Contents

1. Introduction	146
2. Carbon formation	146
3. Structure of carbon	147
4. Types of carbon sorbents	148
4.1. Activated carbon	149

\* Corresponding author.

4.2. Molecular sieves .....	149
4.3. Graphitized carbon black .....	149
4.4. Porous carbon .....	150
5. Classification and characterization of sorbents .....	151
6. Application of carbon sorbents .....	152
6.1. Choice of the proper sorbent .....	152
6.2. Preconcentration of air contaminants .....	154
6.2.1. Sampling .....	155
6.2.2. Sorption from the gaseous phase–desorption into liquid phase .....	155
6.2.2.1. Activated charcoal–“classical” sampling bed .....	155
6.2.2.2. Activated charcoal–miniaturised sampling bed .....	157
6.2.2.3. Porous carbon .....	158
6.2.3. Sorption from the gaseous phase–desorption into supercritical fluid .....	158
6.2.4. Sorption from the gaseous phase–desorption into gaseous phase .....	159
6.2.4.1. Single-bed sorbents .....	159
6.2.4.1.1. Comparison of graphitized carbons with porous polymers .....	160
6.2.4.2. Multi-bed sorbents .....	162
6.2.4.3. Miniaturized sorbent(s) bed .....	167
6.3. Preconcentration of water contaminants .....	168
6.3.1. Sorption from the liquid phase–desorption into liquid phase .....	169
6.3.2. Sorption from the gaseous phase–desorption into liquid phase .....	173
6.3.3. Sorption from the gaseous phase–desorption into gaseous phase .....	173
7. Conclusions .....	176
References .....	176

## 1. Introduction

Most of the analyses that have to be performed with respect to the control of organic pollutants in the environment, can not be done without the application of preconcentration and sample pretreatment techniques. Samples are very often not compatible with direct injection onto the chromatographic system, analysed components are usually present in matrices incompatible with the gas and/or liquid chromatographic system (soil, sediments), or the concentration of the analytes is lower than the detection limit. Thus, it is necessary to perform sample preparation steps prior to analysis. This mainly consists of preconcentration of the analytes, isolation of the analytes from the matrix and removal of interfering compounds. Nowadays also materials with selective sorption properties are being utilized to a large extent for this purpose. Besides to broad spectrum sorbents, much attention is given to tailored sorbents, which allow the optimal solution of a particular separation problem. Carbonaceous sorbents, the matrix of which mainly consists of carbon,

belong to the group of materials of interest. The main advantage of the carbon sorbents is their high chemical inertness and thermal stability. In contrast to sorbents with a SiO<sub>2</sub> matrix (silica gel, porous glass) their use is not limited by pH and compared with organic polymer sorbents they withstand much higher temperatures. Sorbents with a carbon matrix may also serve as carriers for various functional groups.

In the following sections we present an overview on carbon sorbents and their application to the preconcentration of organic pollutants from environmental samples and their subsequent analysis, particularly of volatile organic compounds by gas chromatography. Preconcentration with carbon sorbents is applicable also to other separation techniques, mainly in the analysis of semivolatiles and non-volatile compounds by HPLC.

## 2. Carbon formation

In principle four consecutive stages may be distinguished in the formation of carbons from



naturally occurring or synthetic precursors: homogenization, carbonization, volatilization of inorganic impurities, and graphitization [1,2].

The term “homogenization” covers all operations which lead to an improved ordering of the structure of any solid or liquid carbonaceous starting material. It usually consists of a thermal treatment of the starting material at 450–700°C in an inert atmosphere. It is well known that the degree of structural order of the carbon precursor essentially determines the extent to which the penultimate material is converted into a graphitic or an amorphous carbon, which represent the two limiting cases.

Carbonization covers a number of processes including coking, charring and reaction with oxidising gases such as oxygen, carbon dioxide and water vapour. It is carried out between 700 and 1200°C. Carbonization increases the percentage of carbon content and introduces pores. The products so formed are termed active carbons and possess a high adsorptive capacity. Carbonization also covers processes whereby a gaseous hydrocarbon is pyrolysed between 1000 and 1700°C to yield dense non-porous layers of pyrolytic carbon [3].

Active carbons may still contain inorganic impurities such as sulphur and silica depending upon their origin. These can be removed by volatilization at 1200–1700°C. This process leaves a large number of defect sites in the structure and causes a disordering of the mutual arrangement of layers. Microscopic holes may even be formed within the particles.

Graphitization covers the subsequent heat-treatment in an inert atmosphere at 1700–3000°C. Such heat treatment brings about densification with concurrent removal of structural defects, and forms a three-dimensionally ordered graphitic structure. The degree of graphitization of any carbon brought about by high temperature treatment depends strongly on its initial structure. Thus treatment of some active carbons at a temperature as low as 1200°C can greatly reduce or even completely eliminate the porosity of the material, whereas some glassy carbons may not convert to graphite even on heating to 3000°C.

### 3. Structure of carbon

Many varieties of carbon are produced industrially on a large scale [4]. The most important of these are: electrographite (for industrial electrodes), nuclear graphite (as a moderator in nuclear reactors), active carbons or charcoals (for adsorption of vapours, extraction of organics from water, decolourising), carbon blacks (fillers in rubber), graphitized carbons, and carbon fibres.

The term “graphitized carbon” generally means that a particular carbon has been heated to a temperature in the region of 3000°C in a graphitizing furnace. In crystallographic terms, the degree of graphitization of such a carbon may fall within wide limits, supposedly “graphitized” carbons ranging from almost amorphous materials to perfect three-dimensional crystalline graphites. There are, in fact, three distinct forms of carbon to which the term “graphitized” can reasonably be applied and which have well-defined crystal structures. The Bernal structure of perfect three-dimensional graphite [5] (Fig. 1) consists of layers of carbon atoms, organized in a hexagonal array and ordered ABABAB... This form of graphite is termed hexagonal graphite. A rarer form of three-dimensional graphite, the Lipson–Stokes form, also exists, but here the layers are ordered ABCABC... This is termed rhombohedral graphite [6]. In both crystalline forms the layer spacing is 3.35 Å and the atomic spacing within the layers is 1.42 Å. Perfect graphite is rarely formed synthetically from amorphous solid carbon, since the bonding between the carbon atoms within the graphitic planes is extremely strong, while the interlayer bonding is weak. Thus graphitization tends to develop by the formation of graphitic sheets which are initially randomly oriented. The reorganization of these sheets into ordered three-dimensional graphite requires such a high activation energy that formation of three-dimensional crystalline graphite is generally impossible below 3000°C. Thus, most synthetic carbons, when heated to about 3000°C, assume the two-dimensional graphite (Warren structure, Fig. 1) in which graphitic sheets are randomly oriented

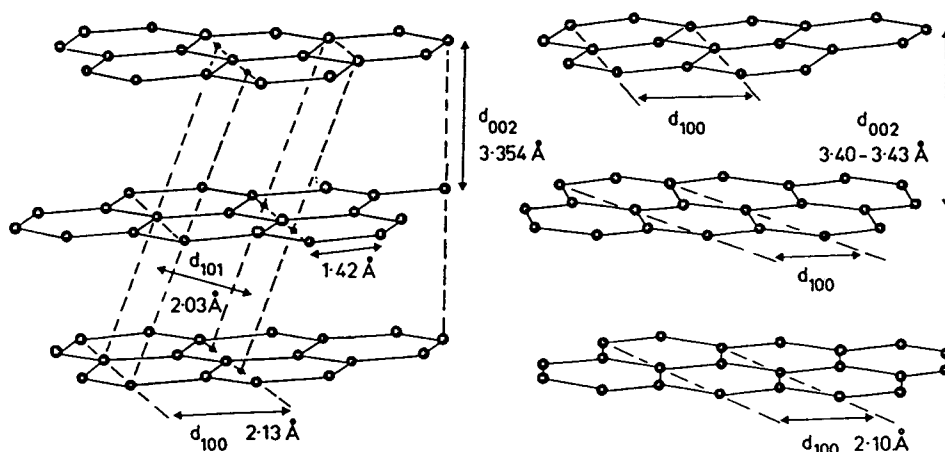


Fig. 1. Atomic structures of graphites. Left: Bernal structure of perfect 3-dimensional graphite with ABAB layer registration. Right: Warren structure of two-dimensional turbostratic graphite with no layer registration. (Reproduced from Ref. [4]).

relative to one another. In two-dimensional graphites the layer spacing is slightly greater than in three-dimensional graphites at 3.40–3.43 Å, and the atomic spacing within the layers is slightly less. Two-dimensional graphites are often said to have a turbostratic structure [7].

While three-dimensional graphites rarely arise from heating of amorphous solid carbons, they can nevertheless arise by high temperature pyrolytic deposition from organic vapours in the gas phase [8]. Presumably, properly oriented layers are laid down in the first place, and no reorganization is required.

#### 4. Types of carbon sorbents

Various kinds of carbon sorbent are available that may be utilized for the enrichment of analytes:

- activated carbon
- molecular sieves
- graphitized carbon black
- porous carbon.

They differ in their physico-chemical characteristics, such as pore size and shape, surface area, size, volume of pores, functionality of surface, and chemical inertness. Kinetic and thermodynamic properties of carbon sorbents (breakthrough volumes, adsorption isotherms,

equation of state, intermolecular interaction mechanisms occurring at the adsorbate/carbon sorbent interface) strongly influence the preconcentration and/or preseparation step. The extent to which these often conflicting characteristics can be achieved will be dependent upon:

- type of starting material
- procedure chosen for preparation of the product
- conditions under which it is used.

The development of carbon sorbents suitable for the enrichment of analytes has generally paralleled the development of chromatographic sorbents. Active carbon adsorbents have long been an obvious choice for the studies in classical liquid chromatography [9]. With the advent of gas chromatography attention turned to graphitized thermal carbon blacks (GTCB) [10], which were found to be suitable nonpolar adsorbents either for gas–solid chromatography [11] or, when coated with a small percentage of liquid phase as a “tailing reducer”, for gas–liquid/solid chromatography [12–14], and to novel active carbons, prepared e.g. by the reduction of polytetrafluoroethylene by lithium amalgam [15,16].

Interest in preparation of the novel carbonaceous adsorbents has recently increased because of the theoretical non-polar character of these materials for HPLC, their applicability over a wide pH range, and the better defined surface prop-

erties in comparison to activated carbon. This is connected with the development of porous carbon packings [1,17] and porous glassy carbon [4,18].

#### 4.1. Activated carbon

Activated carbons have been used since the time of the ancient Egyptians, when charcoals were employed for medicinal purposes. Industrial applications originated in the late 18th century, when it was discovered that activated carbons could adsorb gases and remove colour bodies from solution. A stimulus to industrial production was the development of protective gas masks after the introduction of chemical weapons. Activated carbons are now used extensively in diverse applications [19]: potable and waste water treatment; respirators; solvent recovery from process streams; air and gas purification; prevention of gasoline vapour emissions from automobiles. More specialized applications, sometimes involving the addition of impregnants, can be found in catalysis, medicine, military gas masks and gold recovery.

Commercial sources for activated carbons include biomass materials: wood, coconut shell and fruit pits; and fossilized plant matter: peats, lignites and all ranks of coal; or synthetic polymers [20]. Adsorbent carbons are usually produced by a two-step process of carbonization and then activation by partial gasification. The highly porous structure produced during activation provides the extensive surface area of an activated carbon on which its usefulness as an adsorbent depends.

Problems in using carbon for analytical work are related to the large variations in the physical and chemical properties of the different sources of carbon, the greater difficulty in obtaining low background contamination levels compared to other sorbents, and the fact that many organic compounds are adsorbed so strongly that desorption is only accomplished in very low yields. Activated carbon has a very complex surface structure containing a wide range of functional groups including phenolic, carboxylic, carbonylic, aldehydic, etheric, peroxidic, quinone

and lactone groups [21]. The principal binding mechanisms include hydrophobic interactions, charge-transfer complexation, hydrogen bonding, cation exchange and another specific interactions. The surface of such carbons possesses a high sorption capacity, but it is very heterogeneous. Low recovery of many organic solutes is often associated with the strength of multiple binding interactions, which provide an efficient adsorption mechanism accompanied by inefficient solvent elution, leading to a low overall recovery. Irreversible adsorption can occur in some cases as well as catalytic transformations to different products.

#### 4.2. Molecular sieves

Carbon molecular sieves are formed by the controlled pyrolysis of suitable polymeric materials (e.g. polyvinylchloride) or petroleum pitch materials at temperatures usually above 400°C. They have a highly porous structure with almost uniform micropores [22,23]. They are comprised of very small crystallites crosslinked to yield a disordered cavity–aperture structure.

Carbon molecular sieves are microporous and have a high surface area, with a very pronounced retention of organic compounds, but they can be very easily contaminated by impurities from air. The structure, the purity of the starting polymer material and the technology used for carbonization dictate the particle size and the distribution and size of the pores of the final product. The presence of polymer impurities substantially decreases the homogeneity of the porous structure.

#### 4.3. Graphitized carbon black (GCB)

GCBs as adsorbent for GC were studied in the sixties by Kiselev and his coworkers [10], as well as Horvath [24] and Guichon and coworkers [25].

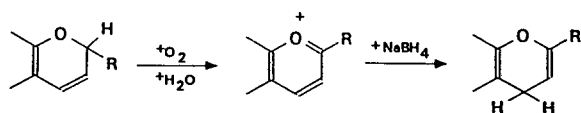
Graphitized carbons are materials with a homogeneous surface and without micropores, they adsorb compounds on their external surfaces based on the molecular size and shape of the adsorbed molecule. GCBs are prepared by

heating ordinary carbon blacks to about 3000°C in an inert gas atmosphere [26–29]. This eliminates volatile, tarry residues and induces the growth of graphite crystallites, particles in which graphite crystals are arranged in the form of polyhedrons. At the same time various functional groups originally present on the carbon black surface are destroyed. The surface of the graphitized carbon blacks is almost completely free of unsaturated bonds, lone electron pairs, free radicals and ions.

The trapping of compounds on GCBs can be explained on the basis of the availability of two types of adsorption sites [27,30]. The vast majority of the surface sites are nonpolar and correspond to a graphite-like array of carbon atoms. These sites show no tendency to interact preferentially with molecules carrying functional groups and dispersive interactions dominate the retention behaviour. Polar adsorption sites are few in number but they can establish specific, strong interactions with polar compounds. Preliminary treatment of the adsorbent may be used to reduce their number. For example, heating to 1000°C in a stream of hydrogen has been used to minimize those active sites associated with the presence of surface oxygen complexes [30–32] while washing with perchloric or phosphoric acid eliminates basic carbonium–oxygen complexes and sulfur present as sulfide [33].

Oxygen complexes with a chromene-like structure may be present as burnt-off residues [34] originating from the heating of carbon blacks. In the presence of water these surface groups are rearranged to form benzopyrylium salts, which are promptly reduced to benzopyrans under mild conditions (see Scheme 1).

Benzopyrylium salts are responsible for binding anions via electrostatic forces [34]. The presence of these positively charged chemical impurities on their surface enables the GCBs to act as both an anion exchanger and a non-specific sorbent. The ion-exchange capacity of non-graphitized carbon black was found to be about twice that of the GCB surface. It seems that carbon blacks are graphitized at very high temperatures at which any surface organic chemical groups should be



Scheme 1.

decomposed. Probably chemical heterogeneities are partially reformed during cooling of the carbonaceous material after the graphitization process [35].

GCBs are composed of loosely aggregated particles of colloidal dimensions. They are hydrophobic. The affinity for water vapour is dependent on the chemical structure of the surface and can be enhanced as a result of oxidation or hydration [36].

#### 4.4. Porous carbon

Porous carbon adsorbents [1,4,17,18,37–39] are materials with a homogeneous hydrophobic surface. They attracted attention because of their stability over a wide pH range and their mechanical stability. They are produced by impregnating a suitable silica gel or another porous template with a phenol–formaldehyde resin mixture, phenol–hexamine mixture, saccharose or another material [18,40,41]. After polymerization within the pores of the template material the polymer is converted to glassy carbon by heating in an inert atmosphere to about 1000°C. The silica template is then removed by alkali to give porous graphitic carbon (PGC). Finally, the material is fired in an inert atmosphere at a high temperature in the range 2000–2800°C to anneal the surface, remove micropores and, depending upon the temperature, produce some degree of graphitization. The particle size, shape, porosity and pore size are determined by the choice of the template material; the surface chemistry is determined by the final heat treatment and any subsequent chemical treatment. It is thus possible in principle to produce PGCs with a range of pore and surface properties tailored to specific requirements [42].

Table 1  
Classification of adsorbents

Class	Adsorbent	Surface
Class I	Graphitized carbon black	Graphitic carbon
Class II	Activated silica gel	Oxides of silica gel
Class III	Activated charcoal Carbon molecular sieves  Porous polymers	–Oxides of amorphous carbon –Amorphous carbon (weak Class III, can approach Class I) –Organic “plastics” (weak-strong Class III)

### 5. Classification and characterisation of sorbents

According to the classification scheme of Kiselev [10,43], there are three classes of sorbents (Table 1). Class I adsorbent is an adsorbent which interacts non-specifically with the four groups of adsorbates (groups A, B, C, D), whereas class II and III adsorbents interact both non-specifically (i.e. London forces, van der Waals forces) and specifically (i.e. strong dipole–dipole interactions). Only class I interacts non-specifically with all groups of adsorbates (Table 2).

Examples of the four groups of adsorbates are: group A molecules—*n*-alkanes; group B molecules—aromatic hydrocarbons, chlorinated hydrocarbons; group C molecules—organo-metallic compounds; and group D molecules—primary alcohols, organic acids, organic bases. The classification of some typical adsorbents assists in determining the adsorbate/adsorbent interactions occurring between the two surfaces.

Kinetic and thermodynamic properties of the solid surface could be characterized by the dynamic gas–solid chromatographic (GSC) technique [43–45]. The physico-chemical measure-

Table 2  
Classification of adsorbates

Group	Molecules	Adsorbents	
		Class I	Class II and III
A	–Spherically symmetrical shells – $\sigma$ -bonds	Nonspecific interaction Dispersion forces	
B	–Electron density concentrated on bonds/links – $\pi$ -bonds	Nonspecific interaction	Nonspecific
C	–( + )-Charge on peripheral links	interaction	+
D	–Concentrated electron densities –( + )-Charge on peripheral links		specific interaction

ments by GSC could be used to obtain the breakthrough volumes, the adsorption isotherms, equation of state, to interpret the mechanism of intermolecular interactions [28,46,47], to study the heterogeneity of the surface [48]. Another physico-chemical characterization of carbons can be performed through particle size analysis, shape determination via electron microscopy, diffuse reflectance FT-IR spectroscopy and IR-PBDS (photothermal beam deflection spectroscopy) [40,49–53], optical microscopy, X-ray microscopy for resolving inorganic impurities in carbon black, transmission electron microscopy for particle/aggregate size and shape distributional information [54], scanning tunnelling microscopy [55], surface area measurements, high-resolution thermogravimetry to obtain information on total porosity, adsorption capacity of porous solids and detection of the active sites present on the carbon surface [56].

Evaluation of the sorbent characteristics and the suitability of a sorbent to trap organic compounds is usually focused on calculation of the specific retention volumes, adsorption coefficients, and equilibrium sorption capacities [43].

The specific retention volume, or breakthrough volume, is the calculated volume of a mobile phase passing through an adsorbent bed that causes a “challenge slug” of adsorbate molecules to migrate from the front of the adsorbent bed to the back of the bed. The challenge slug is introduced via a typical gas and/or liquid chromatographic technique and is detected after it migrates through the adsorbent bed, via a suitable detector. The elution volume is divided by the weight of the adsorbent bed to obtain the specific retention volume, expressed in  $\text{cm}^3/\text{g}$ . This specific retention volume value can be used in constructing an adsorbent tube that possesses known breakthrough characteristics for known adsorbent bed weights.

## 6. Application of carbon sorbents

For the solution of analytical problems in trace analysis, particularly in the analysis of multi-component mixtures, various preconcentration

and/or pre-separation steps have been utilised dependent on the sample matrix. The application of carbon materials for these purposes is related with the development of sorbents with (a) physicochemical properties, and (b) adsorption-desorption properties which provide effective sample enrichment. Carbon sorbents have been applied in various enrichment techniques, particularly in solid-phase extraction (SPE), the purge-and-trap technique and head-space analysis.

In environmental samples the target of the qualitative and quantitative analysis may be the complete multicomponent trace analysis in various matrices, or only the analysis of individual trace component(s). The whole preconcentration/pre-separation procedure differs accordingly. The need for enrichment of trace analytes generally depends on a combination of:

- the volume injected for the analysis,
- the nature and concentration of the compounds analysed,
- the nature of the sample matrix,
- the minimum detectable amount characteristic for the selected sample introduction, separation and detection system.

### 6.1. Choice of the proper sorbent

The use of different carbons (single bed) depends strongly on the applications, but also on the techniques used. Depending on gases, volatile, semi-volatile or non-volatile compounds, both the sorbents and the techniques differ. Different techniques do not require the same characteristics of the carbons.

At present commercially available types of carbon sorbents are active charcoal, graphitized carbon black, molecular sieves and porous carbon. Their specific surface areas range from 5 to  $1200 \text{ m}^2/\text{g}$ . The main types of carbon sorbents used for preconcentration of organic compounds and their further determination predominantly by GC and/or HPLC are listed in Table 3.

The general physico-chemical characteristics which are taken into account for the choice of an adsorbent are functionality, particle size and

Table 3  
Carbon sorbents for preconcentration of organic compounds

Type	Name	Particle size (mesh)	Porosity (nm)	Surface area (m <sup>2</sup> /g)	Producer	
Activated charcoal			1.8–2.2	500–1200		
Molecular sieve	Carbosieve B		1–1.2	1174	King's Lynn, Norfolk	
	Carbosieve S-III	60/80	1.3	1000	Supelco, Inc.	
	Carbosieve S-II	60/80	3.9	1000	Supelco, Inc.	
	Carboxen 1000	60/80	7	1200	Supelco, Inc.	
	Carboxen 1001	60/80		500	Supelco, Inc.	
	Carboxen 1002	60/80		1100	Supelco, Inc.	
	Carboxen 563	20/45		510	Supelco, Inc.	
	Carboxen 564	20/45		400	Supelco, Inc.	
	Carboxen 569	20/45		485	Supelco, Inc.	
	Purasieve	20/40		1070	Union Carbide,	
	Spherocarb	60/80	1.5	1200	Analabs, Inc. (Norwalk, CT, USA)	
	Sortophase					
		Carbosphere	80/100			Alltech, Assoc.
		Saran Carbon				
	Ambersorb					
Porous carbon	Carb I			1200	Polymers	
	Carb II			400	Institute SAS	
	Hypercarb			150–200	Shandon, Runcorn,	
	TSK–Gel Carbon 500			150–200		
Graphitized carbon black	Carbopack F	60/80		5	Supelco, Inc.	
	Carbotrap F	20/40		5	Supelco, Inc.	
	Carbograph 3			6–7	Alltech, Assoc.	
	Carbopack C	60/80		12	Supelco, Inc.	
	Carbotrap C	20/40		12	Supelco, Inc.	
	Carbograph 2			10–12	Alltech, Assoc.	
	Carbopack B	60/80		100	Supelco, Inc.	
	Carbotrap B	20/40		100	Supelco, Inc.	
	Carbograph 1			80–100	Alltech, Assoc.	
	Graphtrap			80–100	Alltech, Assoc.	
	Graphtrap 5			80–100	Alltech, Assoc.	
	Graphon, Spheron			80–100		

shape, surface area, pore size, and chemical inertness.

Functionality plays the main role in the choice of a sorbent for various organic compounds. It is an expression of the affinity of the sorbent for various organic compounds. The classification of some typical adsorbents (section 5) assists in determining the adsorbate/adsorbent interactions occurring between the two surfaces, the

graphitized carbon blacks, or graphitized carbons, behaving as class I adsorbents. The carbon molecular sieves, or amorphous carbons, behave as weak class III adsorbents and may approach a class I classification. Activated charcoal, due to the carbon oxides present on the adsorbent (amorphous carbon) surface, is classified as a class III adsorbent. Chemical inertness is a very important parameter, as the quality of the sor-

bent surface influences the recovery and the reproducibility of the accumulation procedure.

Particle size and shape influence the hydrodynamic conditions in the bed of a sorbent, and are related to the value of the surface area. Smaller particles have a larger surface area, and columns packed with these particles yield a higher performance.

Sorbents having a higher surface area per mass unit have a higher number of active accumulation sites. The surface area can be increased by a porous structure of the sorbent. The factor of pore size is inversely proportional to the surface area. The pores should be as small as possible for effective accumulation, but the size of the analyte molecules should not hinder the penetration of the molecules into the pores.

## 6.2. Preconcentration of air contaminants

The use of gas–solid chromatographic techniques for the characterisation of the kinetic and thermodynamic properties of carbon sorbents provides insight into the adsorbent characteristics [26,57]. A small gas chromatographic column is an effective tool for determining the interactions occurring between contaminants and adsorbent (adsorbate/adsorbent interactions). Using such a column to evaluate adsorbent/adsorbate interactions allows for quick and effective extraction of data that can be applied to the reconstruction of a sampling tube with known sampling parameters. These interactions in the low coverage (Henry's law) region, provide information such as adsorbent surface homogeneity, adsorbate specific retention volume (i.e. analyte breakthrough), and adsorbent capacity for the chosen adsorbate. The choice of water as adsorbate also provides valuable information about the hydrophobic surface properties of the adsorbent, since high humidity sampling conditions can affect the validity of air sampling data.

Specific retention volumes and/or breakthrough volumes (BTVs) which relate to the adsorbent capacity have been studied by several authors [26,43,45,57,58] for a number of carbon sorbents. This specific retention volume value

can be used in constructing an adsorbent tube that possesses known breakthrough characteristics for known adsorbent bed weights. Specific retention volume data can be utilised to obtain the adsorption coefficient, which is a measure of the equilibrium distribution of the introduced adsorbate between the gas and solid phases. Similarly, the equilibrium sorption capacity can be extracted from the specific retention volume data. Equilibrium sorption capacity data are a measure of the adsorbent's capacity for the adsorbate.

The specific retention volume data obtained for the non-specific graphitized carbon black adsorbents (Carbotrap B, Carbotrap C, Carbopack F) [43] and the group A (*n*-alkanes), group B (aromatic and chlorinated hydrocarbons), and group D (oxygenated compounds) adsorbates illustrate the typical interactions occurring between an adsorbate molecule and the surface of a graphitic carbon. The higher surface area of graphitic carbon and the increase in the molecular length results in an increase in the surface-to-surface interactions. This increase is noted as a progressive increase in the specific retention volumes (tested with C<sub>4</sub>–C<sub>14</sub> alkanes). A similar trends is found for group B and D molecules; the molecular size and shape of the adsorbate molecules lend themselves to predictable retention data.

Experts monitoring volatiles and airborne contaminants in various sampling modes must decide which adsorbent will provide the best adsorption/desorption efficiencies for the adsorbates of interest. Carbon molecular sieves are used to trap the more volatile C<sub>5</sub> and smaller compounds. With carbon molecular sieves the diameter of the micropores and the percentage of micropores present are directly responsible for variations in specific retention volume, adsorption coefficient, and equilibrium sorption capacity data. In a systematic study by Betz et al. [57] nine molecular sieves and activated charcoal were evaluated to determine their interactions with four adsorbates—water, ethane, vinylchloride, and dichloromethane. The data obtained from this evaluation reveal trends in both the adsorbent working range and the adsorbents



hydrophobic properties. First the breakthrough volumes for the adsorbate dichloromethane (the adsorbate with the largest molecular size) provide the order of the adsorption strength of the molecular sieves and charcoal tested. The ordering shows that Carbosieve S-III and Carboxen-569 (commercially available Carbosieve and Carboxen types of sieves, Supelco, Bellefonte, PA, USA) followed by activated charcoal, possess the highest affinity for dichloromethane.

Water adsorption is important during sampling under high humidity conditions in the workplace, when competition for the adsorbent surface is occurring between the chosen adsorbate and water. Carboxen-569 and Carboxen-564 possess the smallest breakthrough volumes for water. The hydrophobic properties are a function of the pyrolysis temperature used to prepare these sieves and of the subsequent non-specific surface interactions. The hydrophobic properties of these sieves are, therefore, a function of the tailorability of the carbon molecular sieves. In comparison, the largest water breakthrough volume value is noted for activated charcoal. This greater water/adsorbent interaction for charcoal is a function of the polar functional groups such as carbonyl and carboxyl groups present on the adsorbent surface and the presence of metallic and ionic salt impurities in the adsorbent. This provides insight into the differences between a weak class III adsorbent such as Carboxen-569 and a strong class III adsorbent such as activated charcoal [43].

It was also found that microporous carbon molecular sieves (a polymer-based Carbosieve B and others tested) are potential adsorbents for diffusive sampling of hydrocarbons with more than four carbon atoms [59]. Hydrocarbons with more than seven carbon atoms have extremely high specific retention volumes (20°C) which show that diffusive sampling may not be suitable for these sorbents.

### 6.2.1. Sampling

Sorbents with a large specific surface area have been utilised for the sampling of very volatile organic compounds, such as dichloromethane and vinylchloride; sorbents with a small surface

area are convenient for semi-volatile compounds. Adsorptive sampling of organic pollutants in industrialised and remote areas (emission and immission measurements) on non-polar polymers and carbon adsorption traps has been widely used in single-bed and multi-bed cartridge arrangements. This largely solves the problem of moisture affecting the chromatography compared to canister sampling [60].

Preconcentration tubes containing sorbent, which are the most efficient and cheapest samplers, are widely used in the sampling of industrial atmospheres and ambient air. These are most frequently glass tubes (cartridges) containing about 100–300 mg of solid sorbent in the primary section and 50 mg in the rear (control) section, separated by an inert plug (e.g. silanized glass wool, carbon wool, etc.). Trapped components are desorbed from individual sections separately with a convenient solvent, in the case of activated charcoal most frequently with CS<sub>2</sub> [61,62]. The sorbent in the rear section is often placed in a separate tube when recovery is effected through thermal desorption or in order to detect the migration of the concentrated analyte during storage [63]. Besides the utilisation of “the standard robust” adsorption traps, there is a tendency in recent years to develop miniaturised sorbent traps, particularly for in situ monitoring and on-line automated systems.

### 6.2.2. Sorption from the gaseous phase—desorption into liquid phase

There are general requirements with regard to the solvents used for liquid desorption, to obtain high desorption yields, high purity and with respect to the injector used with capillary GC (splitless, on-column) giving good peaks shapes.

#### 6.2.2.1. Activated charcoal—“classical” sampling bed

Adsorption by means of activated charcoal is the most widely employed sampling method for volatile airborne pollutants in the field of industrial hygiene, both by active and passive sampling devices. Carbon disulphide is recommended for solvent desorption because of its good properties, low gas chromatographic re-

tention time and very low response on a flame ionization detector (FID). Working with CS<sub>2</sub>, however, poses some health problems because of its high toxicity.

Standard Practice for Sampling Atmospheres to Collect Organic Vapours (Activated Charcoal Tube Adsorption method) [62] covers a method for determining the presence of up to 100 certain organic vapours, particularly hydrocarbons, halogenated hydrocarbons and oxygenated compounds (alcohols, ethers, esters). The range of boiling points of compounds commonly collected from air on activated charcoal is from –28°C (dichlorodifluoromethane) to 259°C (naphthalene). A relative humidity higher than 60% can reduce the adsorptive capacity of activated charcoal for some chemicals to 50%. The presence of condensed water droplets in the sample tube indicates a suspect sample. The desorption efficiency, dependent on the nature of the analyte, is in most cases over 90% for non-polar and slightly polar compounds. However, the recovery is known to be influenced also by several other thermodynamic and kinetic factors: the amount of analyte, the presence of other adsorbed substances, the humidity of the sampled air, the ratio between the amount of charcoal and the desorbing liquid, the time and the temperature of contact, the particular batch of charcoal, etc. The recovery of polar compounds from activated charcoal may be incomplete, therefore in some cases binary solvent mixtures were recommended, such as CS<sub>2</sub>–water, or with polar organic solvents, e.g. 2-propanol, methanol, 2-butanol, dimethylformamid [62,63].

Precision and bias in this type of analytical procedure are dependent upon the precision and bias of the analytical procedure for each solvent analyte of concern and the precision and bias of the sampling process [64]. When the errors involving determination of desorption efficiency, sampling, analysis (GC), and pump calibration are combined, the state-of-the-art indicated a relative precision of ±15% at the 95% confidence level for most solvent vapours.

Charcoal is a sorbent adsorbing most organic and inorganic pollutants. Permanent gases (O<sub>2</sub>, N<sub>2</sub>, H<sub>2</sub>, CO) and CH<sub>4</sub>, however, are not ad-

sorbed on charcoal. Ethylene, formaldehyde, and other gases with a boiling point between –100 and 0°C, are only partially adsorbed, whereas gases with boiling points above 0°C are readily adsorbed [63]. Mercury vapour is effectively adsorbed by charcoal, but water vapour only slightly, although moisture reduces the sorption of other substances by charcoal. The physical properties of this popular adsorbent depend to the great extent on its source and subsequent treatment. Charcoal is an excellent sorbent for numerous compounds, but their desorption is often difficult.

With the application of activated charcoal series of problems are encountered, as it is not possible to prepare absolutely identical batches of active charcoal, adsorption is dependent on the size of the carbon particles, micropores, the time of contact with analyte, carbon does not adsorb all organic components and recovery in some cases is small. Activated charcoal obtained from coconut shells is considered to be an almost all-purpose sorbent. The adsorption capacity is an exclusive function of the micropore structure. The best grades of charcoal used for adsorption of air contaminants have a specific surface of ca. 1000 m<sup>2</sup>/g with 70–75% of the surface area containing pores smaller than 2 nm in diameter [63]. On the surface of activated charcoal reactions may occur (isomerisation, hydrolysis—the large carbon surface functions as catalysator), and therefore the desorbed compounds are not always identical with the original analyte.

The on-column injection of charcoal extracts has some advantages for this type of analysis [65]. One is that discrimination effects can be reduced if the technique is handled correctly, particularly with multi-component mixtures. Another advantage is, of course, the increased sensitivity over that of the split technique and/or combination of larger injection volumes. However, also with the split injection regime for emission measurements sufficiently low determination limits could be obtained (e.g. 30-l sample volume and split ratio 1:50, benzene 6.7 μg/m<sup>3</sup> [66]; acrylonitrile 15 μg/m<sup>3</sup> [67]). An example of a chromatogram of the analysis of benzene emission measurement is given in Fig. 2.

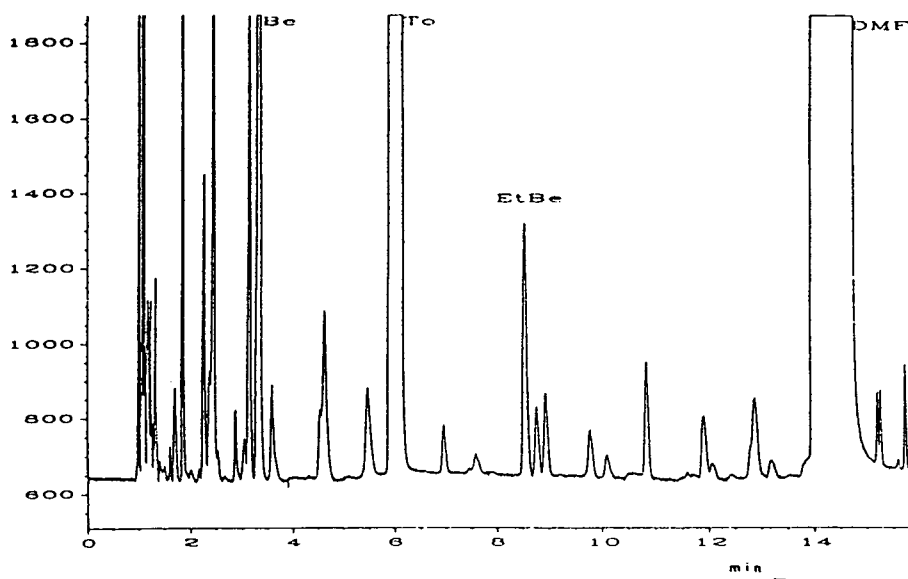


Fig. 2. Chromatogram of analysis of benzene emission measurement; (fused-silica capillary column SP-Nuocol, Supelco); sampling on activated charcoal; DMF desorption; split injection (1:50), FID; Peaks: Be = benzene, To = toluene, EtBe = ethylbenzene, DMF = dimethylformamid. (Reproduced from Ref. [66]).

Sampling on pre-treated charcoal tubes allows control of some airborne contaminants, e.g. methylbromide in concentrations ranging from a few  $\text{mg}/\text{m}^3$  (about 1 ppm) to  $1 \text{ g}/\text{m}^3$  (250 ppm) after liquid desorption and FID–GC analysis [68]. The use of electron-capture detection (ECD) slightly reduces the detection limit. Charcoal must be pre-treated in order to reduce the chemical reaction of  $\text{CH}_3\text{Br}$  with the support and improve the recovery. For high hygrometer levels or low concentrations, the trapping capacity of treated charcoal is reduced. However by using 900-mg charcoal tubes, a minimum sampling of about 10 l is possible without breakthrough. Samples must be kept refrigerated and analysed within 14 days. Sampling with eight different porous polymers (including Tenax GC and TA, Chromosorbs) and three mineral molecular sieves showed that the trapping capacity of those sorbents was poor. The unsatisfactory results of thermal desorption from pre-treated charcoal were found to be due to reactions between the pollutants, the support and the atmospheric water.

#### 6.2.2.2. Activated charcoal–miniaturised sampling bed

An other approach in the development of methods for the preconcentration of analytes is the use of a miniaturised bed of adsorbent combined with off-line liquid desorption, where the high sorption capacity of charcoal has been utilised; the main advantage of this technique is the increased sensitivity of the method and vice versa the decreased limit of quantitation—via the decreased overall volume of solvent used for the extraction. An other advantage is the lower material consumption which leads to less expensive analysis. A disadvantage is the handling of small volumes and the possible introduction of significant errors in quantitation, which however may be reduced by application of internal standards.

A charcoal preconcentration technique was developed for the enrichment of volatile organic compounds from multiliter volumes of air (1–100 l) [69,70]. The method preconcentrates analytes on a 5-mg charcoal trap in a glass tube ( $65 \times 6 \text{ mm O.D.} \times 2 \text{ mm I.D.}$ ); the charcoal bed is

typically 2–3 mm long (Paxton Scientific Glass, Lowland, OH, USA). Analytes are desorbed from the charcoal with a small volume of solvent (several tens of  $\mu\text{l}$ ) and analysed by HRCGC. Laboratory and field tests have been performed to evaluate method precision, analyte breakthrough, and compound recovery from the charcoal. Tests verified that the sampling/analytical system is free from artefact formation under clean to moderately polluted conditions, but further tests are required for areas with a high concentration of hydrocarbons,  $\text{NO}_x$ , and oxidants. The method was developed for alkylnitrates and halocarbons and allows measurement of  $\geq \text{C}_3$  alkylnitrates and  $\text{C}_1$ – $\text{C}_2$  halocarbons at concentrations in the pptv range. Most halocarbons and alkylnitrates showed good recoveries of analytes spiked into the gas stream ranging from 200–1000 pg per compound (a 600-pg spike corresponds to atmospheric concentrations of about 3–6 pptv depending on the compound in 20-l sample). Experiments indicate loss of 30–40% of most analytes over a 48-h period storage at room temperature. Freezing the sample tube improved recovery of the analytes. The samples stored frozen remained reasonably intact for at least 1 month. Despite of the small quantity of charcoal used in the trap, the retention of halocarbons and alkylnitrates from multiliter volumes of air was generally excellent (high relative humidity, air temperature  $\sim 28$ – $30^\circ\text{C}$ ). As traps are repeatedly used and reused, collection efficiency may be lost. Prior to sampling traps are precleaned with solvents. No heat treatment of the charcoal is necessary. Over a concentration range from  $\sim 0.05$  to 10 pptv, the average error of alkylnitrate measurement was estimated at  $\pm (0.1 \pm 8\%)$  pptv; for halocarbons  $\pm (0.1 \pm 5\%)$  pptv.

The extremely high capacity of charcoal was also utilized for retaining VOCs in air or head-space gas (e.g. food) in miniaturised charcoal coated open tubular traps (COT)—glass capillary pieces some 5 cm in length and with an internal diameter approximately corresponding to the capillary separation column coated with a layer of fine charcoal particles [71–73]. Due to their small size, these traps are well suited to capillary GC; such traps placed in the GC injector can be

extracted with ca. 2  $\mu\text{l}$  of solvent [74,75]. Alternatively thermal desorption is possible at capillary GC gas flow-rates, and minimised dilution of the traps with carrier gas results in sharp peaks, even for volatile components; no cold-trapping or refocusing is necessary (e.g. 20 ml of gas can be sucked through this trap in 20 s). Detection limits in 20 ml of air or head-space gas sucked through the trap by a syringe were found to be for benzene 1–3  $\mu\text{g}/\text{m}^3$  and 0.05  $\mu\text{g}/\text{m}^3$  for chlorinated compounds. The total weight of activated charcoal particles (10–18  $\mu\text{m}$ ) was 0.05–0.1 mg. This technique was shown to be convenient for the analysis of compounds with boiling points in the range 90– $235^\circ\text{C}$  [76]. The capacity of COT for highly volatile compounds can be improved by increasing the length of the trap up to 1 m [77–79] or utilising traps with a thick film of crosslinked methylsilicones [80], where highly volatiles are, however, not effectively retained. Decomposition of thermally labile compounds during the desorption from a COT presents a problem.

#### 6.2.2.3. Porous carbon

With the advanced technology of carbon adsorption traps, specially tailored porous carbon materials suitable for the preconcentration of various organic groups have been tested. The preparation of porous carbon is based on the pyrolysis of organic precursors (saccharose) in the matrix of silica gel. This and a similar kind of sorbent were found to be convenient materials for the enrichment of VOCs (hydrocarbons, halocarbons) [81–84] in simulated and real air samples at various concentration levels. By studying recovery data with liquid (and thermal) desorption also of polar compounds—alcohols, aldehydes, ketones [84]—significantly lower recovery data than 100% indicate the presence of residual polar groups on the sorbent, which is in agreement with an FT-IR spectroscopy study of this type of sorbents [40].

#### 6.2.3. Sorption from the gaseous phase—desorption into supercritical fluid

Supercritical fluid extraction (SFE) of organic adsorbents represents a powerful alternative to traditional methods of sample preparation. SFE

exhibits densities similar to those of a liquid, yet with solvent diffusivities and viscosities closer to those of a gas; these properties facilitate mass transfer of solutes resulting in rapid and efficient extractions at relatively mild conditions, thus minimising chemical changes. Determination of volatile and semi-volatile mutagenes in air using solid adsorbents and SFE ( $\text{CO}_2$ ) has been described [85]. Solid adsorbents, activated charcoal, Carbosieve S-III and XAD-4 (styrene-divinylbenzene copolymer) were compared in their trapping efficiencies for dichloromethane (DCH), ethylene dibromide (EDB), 4-nitro-biphenyl, 2-nitrofluorene, fluoranthene. Extraction of different spikes of compounds from adsorbents resulted in >90% recovery of EDB and 60–92% recovery of the aromatics. For more volatile compounds (such as DCH) alternative techniques are necessary to quantitatively recover extracted analytes using SFE due to their volatilisation in the expanding  $\text{CO}_2$  stream.

#### 6.2.4. Sorption from the gaseous phase—desorption into gaseous phase

An interesting alternative to the use of a solvent is desorption with a carrier gas at elevated temperature, followed by on-line introduction of the desorbed analytes onto the gas chromatographic column. This technique requires a compromise between the demands of desorption and those of injection of the sample. In fact, while complete desorption would be favoured by the use of a large amount of carrier gas, for a good chromatographic separation it is mandatory to introduce the analytes onto the column in the form of a narrow band. One can overcome this difficulty by a large amount of carrier gas for the desorption and by concentrating the analytes either on the top of the GC column held at sub-ambient temperature or in an intermediate device, which in turn can be a cold trap or a smaller desorption tube. In the last years ballistic heating of the trap has been applied with cryogenic refocusing of the volatile analytes on the top of the capillary GC column and/or in combination with a thick film of stationary phase in a capillary column. Thermal desorption has the advantage over solvent desorption of greater sensitivity and the absence of

a solvent peak which could potentially mask analyte peaks.

An inherent limitation of the thermal desorption methods is that they do not allow a repetition of the analysis. They are, therefore, not very suitable if complete qualitative information on the pollutants present in the sampled air is not available beforehand and if the order of magnitude of their concentration is not known at least approximately. For these reasons, the thermal desorption methods have been primarily employed for the determination of pollutants, the presence of which could be anticipated.

With thermodesorption reasonably low blanks are required. The problem of low blanks is particularly important for sampling very low ppt–ppb concentrations of organic compounds in ambient air from remote areas. Tenax TA or GC, which has been the most frequently used adsorbent for  $\text{C}_5$ – $\text{C}_{15}$  substances in air, is difficult to clean. Blanks of a few ppt which are stable for weeks, are essential for sampling in remote areas since transport of the non-exposed and exposed solid adsorbent tubes to the laboratory can be very time-consuming. It has been shown that sufficiently low blanks of carbon materials (Carbotrap) could be maintained for a storage period of at least one week [86]. However, this required a careful selection of suitable sealing and tube material. Sampled VOCs (on GCBs in multi-bed arrangement and/or in combination with carbon molecular sieves) stored in a sealed glass container were found to be stable for more than two months [87–91].

##### 6.2.4.1. Single-bed sorbents

Thermal desorption of analytes from activated charcoal is problematic, particularly due to the slow desorption of analytes and the high catalytic activity in comparison with polymeric sorbents. The necessary desorption temperature is so high that many compounds decompose. In spite of that several methods have been published of thermal desorption of pollutants from activated charcoal, e.g. microwave heating of the sorbent up to 700°C, which is convenient for stable analytes [92], heating the adsorbent and sucking the released pollutants into an evacuated gas sampling bulb [93,94], and others. It was found

that the gram size of a given charcoal does not influence the desorption properties, that the maximum temperature needed for complete desorption is independent of the loading and that the members of a homologous series (*n*-alkanes) obey some regularities [95]. Accumulation of thermally desorbed analytes in a reservoir allows repeated GC analysis of sample aliquots [96]. The desorption yields and especially their reproducibility compare favourably with literature data for the standard solvent technique. Even strongly polar analytes can be desorbed satisfactorily, although the yields and their reproducibility are not as good, probably because of decomposition processes. For more polar compounds, the variation of recovery with concentration is significant and should be taken into account if accurate results are required. Application of graphitized sorbents reduces many problems of thermal desorption.

6.2.4.1.1. *Comparison of graphitized carbons with porous polymers* Porous polymers, introduced into analytical practice more than 20 years ago are used no less extensively than activated charcoal. They are relatively inert, hydrophobic and normally have large surface areas. Most porous polymers poorly retain volatile compounds, water and solvent vapour, but this is turned into an advantage if a sample is collected in an atmosphere with a high content of water and solvent vapour [63]. Porous polymers such as Tenax GC, Porapak, Chromosorbs, XAD resins and polyurethane foam are most successfully used to trap toxic agents of high molecular mass and non-volatile substances such as pesticides. Many of the limitations associated with the application of porous polymers are the result of their batch-to-batch variations. Various applications of polymer sorbents, in particular those used for the concentration of toxic substances from air, have been considered in reviews [63]. Certain disadvantages of these sorbents create a number of problems: (1) displacement of the more volatile compounds especially by CO<sub>2</sub>; (2) irreversible adsorption of some compounds, e.g., amines and glycols; (3) oxidation, hydrolysis and polymerization of the sample; (4) contamination of the sorbent due to chemical reactions in the

presence of reactive gases and vapour, e.g., oxides of nitrogen and sulphur, inorganic acids; (5) formation of new compounds arising from reactions and thermal desorption; (6) limited retention capacity; (7) thermal instability; and (8) limitations of sampling volume, rate and time.

Tenax GC, a polymer based on 2,6-diphenyl-*p*-phenylene oxide commercially available with a specific surface area of 19–30 m<sup>2</sup>/g, is preferred in the last years by many analytical chemists for the preconcentration of volatile and non-volatile organic pollutants from atmospheric and water samples because of its high thermal limit (350–400°C), which facilitates thermal desorption.

Owing to its high thermal stability and its ability to trap compounds of various molecular masses and polarity, Tenax is used more often than other sorbents for the recovery of pollutants from environmental samples, particularly air and water. However, it should be born in mind that Tenax, while efficiently trapping non-polar high-molecular-mass compounds, is less efficient with respect to volatile polar compounds, such as alcohols, ketones, ethers and chloro-hydrocarbons [63]. The convenience of enriching atmospheric samples on Tenax GC has been questioned and it was found that this material may be a serious source of interferences, when strong oxidants and inorganic pollutants commonly found in the atmosphere and in industrial emissions come into contact with the polymer. In the presence of ozone, water, SO<sub>2</sub>, and NO<sub>2</sub> Tenax GC undergoes chemical decomposition, giving rise to substantial amounts of organic compounds that can simulate the presence of pollutants in the sample [87,97–99].

Because of the problems encountered with the use of Tenax, particularly in ultra-trace analysis, one started to look for the application of very inert sorbents. A comparison between the collection efficiency of Carbpac B (graphitized carbon black material, which is a relatively pure form of carbon [100]) and Tenax GC in the sampling of C<sub>6</sub>–C<sub>10</sub> hydrocarbons from both simulated and real atmospheres [87], indicates that Carbpac B is the more efficient sorbent (Fig. 3); it does not give rise to sampling ar-

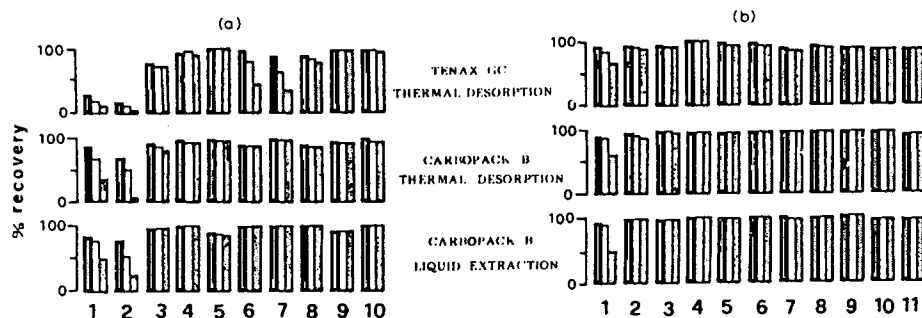


Fig. 3. Percentage of test compounds recovered from Carbopack B and Tenax GC when 2 (closed bars), 5 (open bars) and 10 l (shaded bars) of air were passed through the adsorption traps. (a) Olefins and monoterpenes: 1 = 1-hexene; 2 = bicycloheptadiene; 3 = 1-heptene; 4 = vinylcyclohexene; 5 = 1-octene; 6 = *cis,cis*-octadiene; 7 =  $\alpha$ -pinene; 8 = carene; 9 =  $\alpha$ -terpinene; 10 = limonene. (b) Benzene and alkylbenzenes: 1 = benzene; 2 = toluene; 3 = ethylbenzene; 4 = *o*-xylene; 5 = *m*-xylene; 6 = *p*-xylene; 7 = 1,3,5-trimethylbenzene; 8 = *n*-butylbenzene; 9 = 1,3-diethylbenzene; 10 = 1,3,4,5-tetramethylbenzene; 11 = 1,2,3,4-tetramethylbenzene. (Reproduced from Ref. [87]).

tefacts in the presence of oxidants and acidic pollutants, which are shown to cause decomposition of the Tenax GC polymeric matrix. Enrichment on Carbopack B adsorbent traps was proposed as a suitable method for the evaluation of organic compounds present at ppm–ppt levels in atmospheric samples. The technique has been applied to the determination of organics dispersed in a suburban atmosphere, dissolved in rain water or volatilized from particulate matter emitted from an industrial emission and diesel engine exhaust. With regard to the adsorption efficiencies of Tenax GC and Carbopack B, it was clearly shown, that the latter is a material better suited for the enrichment of low-boiling compounds and particularly of natural hydrocarbons (e.g.  $\alpha$ -pinene, carene). In the presence of 500 ppb of ozone in simulated air samples serious decomposition of the polymeric matrix of Tenax GC was observed and a substantial amount of interfering compounds was detected by GC–MS analysis. The major decomposition products arising from the oxidation of the polymeric matrix were found to be acetophenone and benzaldehyde (Fig. 4). The presence of these compounds is in complete agreement with the results presented by other authors [101], but there is some contradiction with regard to the presence of water, which is according to Krost et al. [101] equally important in producing de-

composition of the polymer. According to Ciccioli et al. [87] water was always present during sample collection at 50% relative humidity, but the production of benzaldehyde, phenol, and benzophenone was observed when ozone was added to the mixture. It is likely that water becomes effective when other pollutants (such as  $\text{NO}_2$  and  $\text{SO}_2$ ) are added to the air stream. The study on Tenax decomposition was also performed in a real atmosphere (ozone conc. < 100–200 ppb) and the formation of artefacts was confirmed. From experiments it follows that ozone is likely to be the main cause of decomposition of the Tenax GC adsorbent and traps packed with Tenax GC can lead to erroneous results in the evaluation of organics in air. The possibility of sampling artefacts is also increased by the fact that in the atmosphere free acids (e.g.  $\text{HNO}_2$ ,  $\text{HNO}_3$ ,  $\text{H}_2\text{SO}_4$ ) can be observed concurrently with high levels of ozone. It must be also recollected that benzaldehyde is an extremely important compound in the photochemical pollution cycle, as it is one of the main products of the reaction of alkylbenzene hydrocarbons with OH radicals.

According to a study by Ciccioli et al. [87] the chemical inertness of Carbopack B permits the determination of organic compounds in anthropogenic emissions, where large amounts of  $\text{NO}_2$ , water, ozone and strong acids are present.

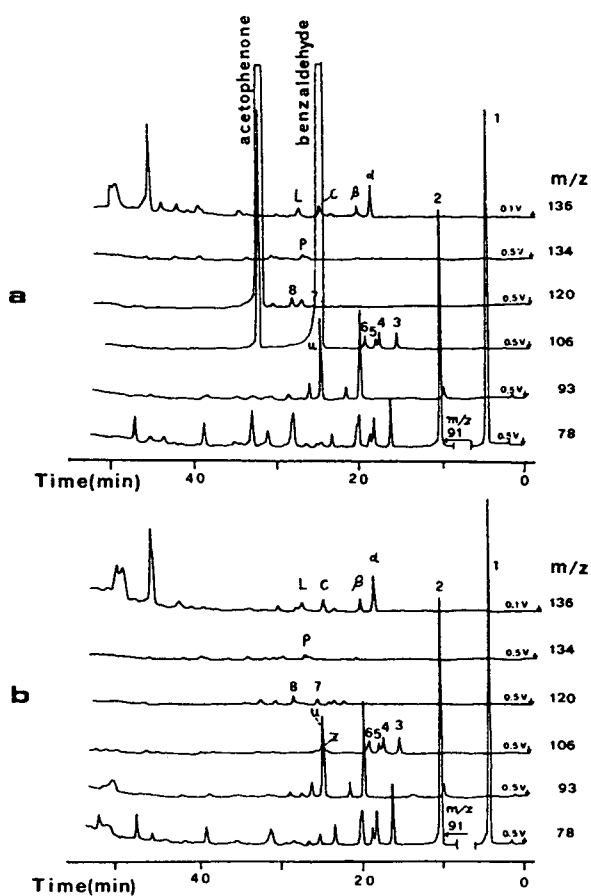


Fig. 4. Selected-ion chromatographic profiles obtained by analysing 10 l of an air sample collected at noon in a pine forest. (a) Tenax GC; (b) Carbotrap B. Peaks: 1 = Benzene; 2 = toluene; 3 = ethylbenzene; 4 = *m*-xylene; 5 = *p*-xylene; 6 = *o*-xylene; 7 = 2-ethyltoluene; 8 = 1,2,4-trimethylbenzene;  $\alpha$  =  $\alpha$ -pinene;  $\beta$  =  $\beta$ -pinene; c = carene; L = limonene; p = *p*-cymene; u = unknown; z = benzaldehyde. The individual concentrations of compounds ranged between 0.09 and 0.004 ppb. (Reproduced from Ref. [87]).

Comparison of Tenax TA (a further development of Tenax GC, which is stable up to 280°C and produces less artefacts than Tenax GC) and Carbotrap B [102] for sampling and analysis of volatile organic compounds in air on the bases of recovery data shows (desorption temperature of Tenax 260°C, Carbotrap 320°C), that many VOCs (toluene, *n*-alkanes C<sub>7</sub>–C<sub>13</sub>, styrene, aniline, dimethylformamide, phenol, butylacetate) with boiling points up to 270°C and occur-

ring in trace amounts could be desorbed quantitatively from Tenax TA, but not from Carbotrap;  $\alpha$ -pinenes and aldehydes (acrolein, hexanal) show some reactivity on Carbotrap. For very volatile compounds and various polar VOCs, substantial losses, most probably due to breakthrough, were observed. With aldehydes similar results were obtained by other authors [103], who found a stronger decomposition of the aldehydes at a desorption temperature of 300°C. When desorbing  $\alpha$ -pinene from Carbotrap, additional peaks were found [102]; GC-MS investigation suggests that rearrangement to other terpenes had taken place; the recoveries of polar compounds, such as acetic acids, isopropanol and 1,2-ethanediol, were unsatisfactory on both sorbents. With Tenax TA a decrease in capacity for volatile compounds was observed when using the same Tenax tubes more than five times; the adsorptive properties of Carbotrap do not change even after being used 30 times. On Tenax TA benzaldehyde and acetophenone were found in small quantities—due to sorbent decomposition. According to results presented by Supelco [104] for Carbotrap, recovery of 1-butanol and 2-ethoxyethylacetate and other compounds is virtually complete both by liquid desorption (CS<sub>2</sub>) and thermodesorption.

The applicability of stainless steel canister and solid adsorbent sampling (Tenax TA and Carbotrap) was studied for very low concentration (>15 ppt) of compounds  $\geq$ C<sub>6</sub> in ambient air samples from remote areas (Arctic) [86]. Different cleaning methods were tested to get sufficiently low blank values for the solid adsorbent Tenax TA and Carbotrap. It was shown that sufficiently low blanks could be obtained for a storage period of at least 1 week. Both sampling techniques were suitable for very low ppt concentrations of benzene and toluene, but their application is complementary. The maximal sampling volume for Tenax tube was 10 l, for Carbotrap 60 l.

#### 6.2.4.2. Multi-bed sorbents

A number of adsorbent materials have shown utility for trapping organics and for desorption particularly by thermal techniques [105]. How-



ever, none of these materials can individually fully accommodate a complete range of organic volatilities or polarities, and thus they must be used in combination with each other. It is apparent from published results, that no single sorbent material is practical for collecting all solutes. In some instances this is because the sorbents do not retain low-molecular-mass materials (Carbotrap C); in other cases it is because the analytes are too strongly retained to be easily desorbed of the heavier solvents (activated charcoal).

Given the lack of a universal sorbent, the best approach to the problem was to construct tubes containing several different materials to attain the desired collection and desorption characteristics, the so-called multi-bed sorbents, where the principle of sequential trapping is taking place [57,106–109]. The scheme of a multi-bed adsorbent tube is given in Fig. 5. The materials would ideally have the ability to stand up to repeated use and heating without changing their characteristics and should additionally give a low background on a chromatogram. It is also desirable that they would have a low affinity for water. The adsorption layers are arranged in such a way that compounds with the lowest molecular mass go through the initial layer(s) and are trapped on the last layer. The initial layer(s) protect the next layer(s) from compounds which could be adsorbed irreversibly. It is important that the flow during sample collection enters the sorbent tube at the least active layer and leaves through the most tenacious layer. Each layer of adsorbent material protects the succeeding more active layer. The direction of the flow during desorption is the reverse of that during sample collection. Consequently,

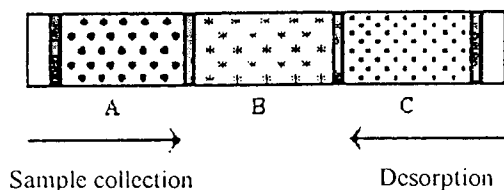


Fig. 5. Multi-bed adsorption tube scheme; A,B,C = different adsorbents with various specific surface area (A = small; B = middle; C = large).

when the tube is heated to desorb the sample, the heat energy required for volatilisation is kept to a minimum, since each molecular mass range is trapped on an appropriate sorbent material from which it is easily released.

Trapping material selections are based on the collection efficiency, the ability to retain a particular class of analytes, and on the desorption efficiency, i.e. the ability to quickly release the trapped compounds. In recent years various combinations of carbonaceous and non-carbonaceous sorbents for trapping organic pollutants from air and other environmental samples (water and soil) were tested.

Supelco produces several combinations of carbon sorbents in multi-bed adsorbent tubes (Table 4), which should be effective for trapping volatile and semi-volatile organic compounds with a broad range in boiling points. Thus one tube would be sufficient instead of several traps for special or multitask applications. Adsorbents of the Carbotrap type comprise various arrangements of several layers of graphitized carbon black with a specific surface area in the range of 5–100 m<sup>2</sup>/g, carbon molecular sieves with a specific surface area of 400–1200 m<sup>2</sup>/g and glass beads. In many applications these traps are used to refocus the analytes after thermal desorption without the need of cryofocusing. The sample is transferred from a sampling 4-mm I.D. tube into a tube with a narrower diameter before desorption onto the GC column. Using a low flow-rate during the transfer step provides for less deeply adsorbed components. Also, the narrower inside diameter provides for a greater linear velocity across the tube when desorbing at the same flow-rate. This technique is certainly effective and less costly than the cryogenic technique. Using a 2-mm I.D. tube to desorb the sample onto the GC column, as opposed to a 4-mm I.D. tube, quadruples the linear velocity with which the desorption flow passes through the tube. Direct sampling with the narrower I.D. tube would lead to a decrease of the sampling tube volume by a factor of 4, giving only 1/4 of the amount of adsorbent in the tube. Challenging that smaller amount of adsorbent with four times the linear velocity, at identical sampling flow-

Table 4  
Multi-bed sorbents commercially available from Supelco

Name	Adsorbents	Use
Carbotrap 150	70/80 glass beads (200 mg)/ 20/40 Carbotrap C (425mg)	Large molecules (PCBs, alkylbenzenes) in air, aqueous samples, suspensions of solid materials
Carbotrap 200	70/80 glass beads (80 mg)/ 20/40 Carbotrap B (200 mg)/ 60/80 Carbosieve S-III (350 mg)	C <sub>2</sub> –C <sub>14</sub> compounds in air
Carbotrap 201	60/80 Carbotrap B (11.5 mg)/ 60/80 Carboxen 1000 (12.5 mg)	Focus very volatile, semi-volatile compounds
Carbotrap 300	20/40 Carbotrap C (300 mg)/ 20/40 Carbotrap B (200 mg)/ 60/80 Carbosieve S-III (125 mg)	C <sub>2</sub> and heavier compounds in air
Carbotrap 301	60/80 Carbopack C (12 mg)/ 60/80 Carbopack B (7 mg)/ 60/80 Carboxen 1000 (8 mg)	Focus volatile, semi-volatile compounds
Carbotrap 302	60/80 Carbopack C (125 mg)/ 60/80 Carbopack B (150 mg)/ 60/80 Carboxen 1001 (200 mg)	Volatile compounds in aqueous samples
Carbotrap 370	60/80 Carbopack F (40 mg)/ 60/80 Carbopack C (50 mg)/ 60/80 Carbopack B (20 mg)	C <sub>5</sub> –C <sub>30</sub> compounds thermally extracted from solid samples; focus semi-volatile compounds
Carbotrap 400	20/40 Carbotrap F (150 mg)/ 20/40 Carbotrap C (150 mg)/ 20/40 Carbotrap B (125 mg)/ 20/40 Carboxen 569 (125mg)	C <sub>2</sub> and heavier compounds in aqueous samples, soils
VOCARB 3000	Carbopack B/Carboxen 1000/ Carboxen 1001/	VOCs from water
VOCARB 4000	Carbopack C/Carbopack B/ Carboxen 1000/Carboxen 1001	Alcohols, ketones, polar oxygenated compounds, VOCs from water
CONCAWE	Chromosorb 106 (200 mg)/ activated charcoal (300 mg)	C <sub>1</sub> –C <sub>4</sub> from air
BTEXTRAP	Carbopack C/Carbopack B	Benzene, toluene, xylenes from water, soil

rate, would increase sample breakthrough by at least 8-fold.

Various applications of multi-bed sorbents (combinations of carbonaceous and non-carbonaceous sorbents) for sampling of organic compounds in air are summarised in Table 5. It was shown in scientific and commercial literature that combination of carbon sorbents allows the sampling of a large variety of compounds differ-

ing in polarity (non-polar/polar compounds) and volatility (C<sub>2</sub>–C<sub>15</sub>) at various concentration levels (ng–mg/m<sup>3</sup>). From the listed papers in Table 5 the most important are considered to be the papers of Bishop and Valis [105] and Ciccioi et al. [88,90].

In their study Bishop and Valis [105] evaluated a number of sorbents (Tenax TA, Carbotrap, Amborsorb XE-340, activated charcoal, Car-

Table 5  
Application of multi-bed sorbents for sampling organic compounds in air samples with subsequent GC determination

Multi-bed sorbent	Analysed compounds	Volatility range b.p. (°C)	Sample volume (l)	Detector	Concentration level MLD <sup>c</sup>	Reference
Tenax GC/molecular sieve SA/Carbosieve S-II	C <sub>2</sub> -C <sub>10</sub> hydrocarbons	-88-220	1-2	FID	0.7-95.5 ppbC <sup>c</sup> 0.1-0.2 ppbC	110
Carbopack/Carbosieve S-III	Halocarbons	-24.2-174	0.35	ECD	2; 200 ppbv	111
	Aromatic hydrocarbons	80-168		FID		
Tenax TA/Carbotrap/Carbosieve S-III	C <sub>2</sub> -C <sub>6</sub> alkenes	-104-69	0.1-2	FID/PID	4-3700 µg/m <sup>3</sup>	112
Tenax TA/Carbotrap/Carbosieve S-III <sup>a</sup>	C <sub>2</sub> -C <sub>8</sub> hydrocarbons	-104-142	0.5	FID/MS	9-630 µg/m <sup>3</sup>	113
Tenax TA/Ambersorb XE-340/activated charcoal	Non-polar and polar compounds	78-174	1-2	MSD	10-200 µg/m <sup>3</sup> <sup>c</sup> 5 ng	105
Carbotrap C/Carbotrap/Carbosieve S-II	C <sub>4</sub> -C <sub>14</sub> compounds	-0.5-254	1-2	FID/MSD	0.02-107 µg/m <sup>3</sup> <sup>c</sup> 0.01 µg/m <sup>3</sup>	88
Chromosorb 106/Carbotrap/Carbosieve S-III	Hydrocarbons					
Carbotrap C/Carbotrap	Halocarbons					
Carbotrap C/Carbotrap/Carbosieve S-III	Oxygenated compounds					
Carbotrap 200	C <sub>2</sub> -C <sub>4</sub> hydrocarbons	-104	0.5-1.2	FID	0.1-1 mg/m <sup>3</sup> <sup>c</sup> 1 µg/m <sup>3</sup>	114
Carbotrap 300	C <sub>2</sub> -C <sub>12</sub> hydrocarbons	-104-216.2	3-30		1-4330 µg/m <sup>3</sup> <sup>c</sup> 0.5 ng/m <sup>3</sup>	115
	Hydrocarbons					
	Halocarbons					
	Oxygenated compounds					
	Sulfides					
Carbotrap 400 <sup>b</sup>	Non-polar and polar compounds	-0.5-448	6	FID/NPD/ MSD		116
	C <sub>3</sub> -C <sub>15</sub>					
	Aliphatic and branched hydrocarbons					
	Alkylbenzenes					
	PAH					
	Heterocompounds (O, N, S)					

<sup>a</sup> Vehicle emissions, tobacco smoke.

<sup>b</sup> Chimney emissions.

<sup>c</sup> MLD = method detection limit.

bosieve S-III) in single-bed and particularly various multi-bed layer arrangements for their ability to retain and thermally desorb an assortment of solvent vapours. The amounts of analyte vapour recovered from the tubes were quantitated using a GC-MS detection. The method is seen to be precise in its reproducibility of the results and it is sensitive (5 ng of a compound in air sample). Of the tubes tested, the design based on Tenax/Amborsorb/charcoal clearly has the broadest potential for successful sampling of a wide range of solvents at various concentrations and under conditions of high humidity. The tubes based on Carbotrap/Carbosieve may also be used but are limited in their ability to retain low-molecular-mass polar compounds (ethanol having the lowest overall recovery), especially under humid conditions. With regard to storage stability, severe losses of the more volatile polar compounds occur with the studied multi-bed tubes. Whether the losses arise from migration, moisture, long-term effects from coadsorption of multiple compounds, oxidation, or other factors is not certain [117]. Water could cause breakthrough of some of the analytes during transfer and also creates problems with MSD operation [105]. The authors tested two approaches to accomplish water removal; the application of drying tubes such as calcium chloride, anhydrous sodium sulfate, and calcium sulfate placed in front of the sampling tubes and the use of tube conditioning. The drying tubes helped to reduce the level of moisture, but trapped some of the analytes. Application of tube conditioning in conjunction with the use of low sample volumes (1–2 l) should minimize the problem of moisture interferences for both types of traps. The sampling tubes were designed to monitor low levels of atmospheric contaminants, often of an unknown identity.

Ciccioli and co-workers contributed to a large extent to the identification and determination of biogenic and anthropogenic volatile organic compounds in urban, forest areas and remote sites [87–91]. They developed a method for the analysis of multicomponent mixtures of polar and non-polar  $C_4$ – $C_{14}$  hydrocarbons belonging to different classes (over 140 components) involved in photochemical smog formation [88]. The num-

ber and amount of oxygenated compounds in investigated environments highlight the importance of these components to the investigation of the mechanism leading to the formation of photochemical smog. They used multi-bed carbon adsorption traps combined with HRCGC-MS. Two different combinations of carbon adsorbent were tested and used for enrichment of hydrocarbons, halocarbons, aldehydes, alcohols, ketones and aliphatic acids: Carbotrap C/Carbotrap and Carbotrap C/Carbotrap/Carbosieve III. Experiments performed in real atmospheres (air samples with a relative humidity ranging from 40 to 90%) showed that the presence of Carbosieve S-III led to enrichment of water to such an extent that plugging of the fused-silica liner of the commercially available desorption unit was observed when the relative humidity was higher than 50%. Insertion of Nafion dryer, desiccants (sodium carbonate and sodium sulfate), and cryogenic traps at  $-10^\circ\text{C}$  resulted in severe losses ( $>50\%$ ) of the high boiling alcohols and aldehydes, especially nonanal and decanal and some terpenes. Quantitation was restricted to components with a carbon atom number greater than 4, as a drastic reduction of the adsorption properties of the carbon material was observed when 2-l samples were collected on the trap when the relative humidity was high. Restriction of sampling volume to 500 ml worked well with FID, but the amount of water and carbon dioxide collected by Carbosieve S-III was still large enough to hinder the collection of mass spectra of a large portion of the chromatogram. Identification of the components by GC-MS was possible only when sample enrichment was performed on the traps filled with two types of graphitized carbon black, as these showed little affinity for either water or carbon dioxide. The minimum amounts detectable in 2-l samples are in the order of 0.01 ng/l, which enables the determination of components present at the tenths of pptv level. The difference between the performance of ten traps used for sampling in parallel was small ( $<10\%$ ). The analysis of samples characterized by substantial amounts of polar components was stated to be extremely useful from the methodological point of view, as it showed the capability of carbon traps to retain

and release in a quantitative way very polar organic compounds with a wide range of carbon numbers (Fig. 6) [90]. Sufficiently low blanks were obtained after cleaning and sealing the traps and storing under a prescribed conditions. Sampled VOCs stored in the sealed traps closed in the glass container were found to be stable for more than 2 months.

Analysing air samples with standard robust adsorption traps and evaluating published results, some general problems become apparent, the main problem being humidity affecting the adsorption phenomena and/or the chromatography (GC-MS). Various approaches of selective removal of water [88,105,110,111] from sampled air have been connected with the losses of some components [88,105]. Supelco proposed a combination of GCBs with molecular sieves for monitoring volatile and semi-volatile compounds as they enable sampling in highly humid conditions, e.g. Carbotrap and Carbosieve S-III [115,118]. There is, however, contradictory information in

the literature in this regard, that Carbosieve S-III would lead to enrichment of water [88,105].

The other problem is related to the trapping capabilities of carbons sorbents for the low-molecular-mass compounds. Sampling  $C_2$  saturated and unsaturated hydrocarbons exhibited some limitations [114]. Collection of  $C_2$  hydrocarbons occurred mainly on Carbosieve S-III in the multi-bed adsorbent tube Carbotrap 200 [118]. Compared to the Supelco data significantly lower breakthrough volumes were found for  $C_2$  hydrocarbons on the Carbosieve S-III [114]. For  $C_1$  and  $C_2$  hydrocarbons, canister sampling is still the method of choice unless direct-sampling GCs are available on site.

#### 6.2.4.3. Miniaturized sorbent(s) bed

An other approach in the development of methods for the preconcentration of analytes in air samples is the utilization of miniaturized beds of adsorbents combined on-line with thermodesorption giving the possibility of automated

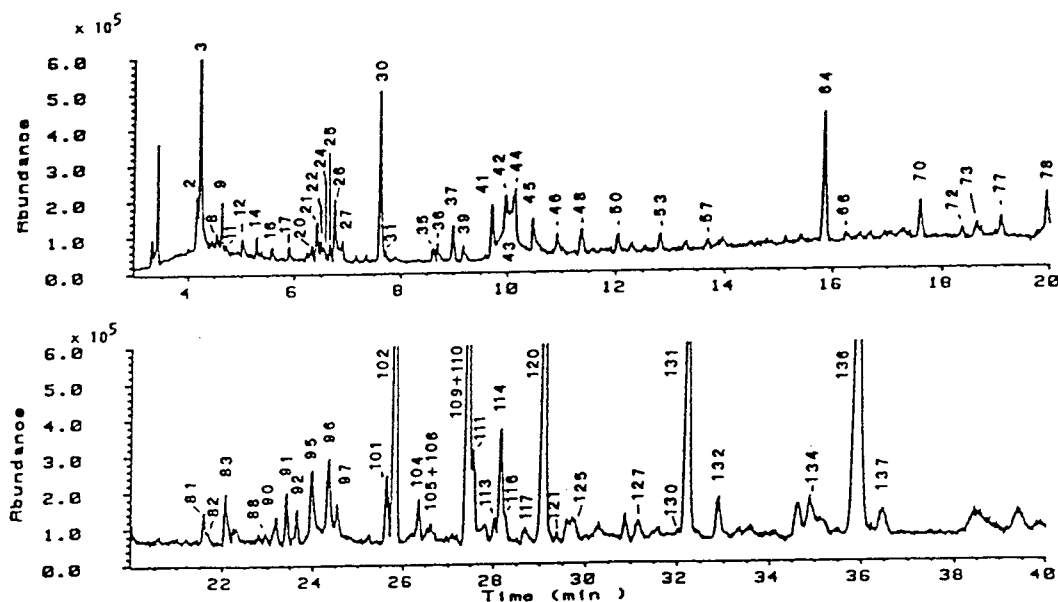


Fig. 6. GC-MS profile of a sample collected in a Northern European pine forest. The trace is the reconstructed chromatogram obtained by using a mass window ranging from  $m/z$  34 to 200. Peaks: 9,21,27,30,46,50,53,97,132,137, alkanes; 8,11,72, alkenes; 41,64,81,83,88,90,105,106,113,121, arenes; 102,104,111,116,120,125,130, monoterpenes; 14,37,42,73, alkyl halides and CFCs; 12,31,36,45,95,96,134, alcohols; 2,16,17,24,39,48,70,91,101,114,131,136, aldehydes; 3,22,26,66,78,92,109,117, ketones; 20, propane, 2-methoxy-2-methyl-; 82, butanoic acid, 3-methyl-; 77, acetic acid, butyl ester; 35,44,57,127, cycloalkanes; 110, phenol. (Reproduced from Ref. [90]).

and continuous monitoring of low-concentration sample streams.

Air samples can be collected at ambient temperature on on-line microtraps [75,119,120], which are made of a few cm long small diameter tubing with a carbon adsorbent (e.g. 0.53-mm I.D. fused-silica capillaries with sorbent held in place with plugs of silanized quartz wool [119]). The sample containing the analyte is introduced onto the analytical column (coated with a thick film of a suitable stationary phase) through the microtrap. The analytes are trapped in the microtrap and can be thermally desorbed by electrical heating. When the heating is rapid enough, the “desorption pulse” serves as an injection for the GC column. Due to the small size and thermal mass of the microtrap, it heats and cools rapidly, and frequent injections can be made as long the GC separation is completed [120]. Automated on-line analysis may be performed even for very volatile compounds (e.g. chlorofluoromethanes) when traps are adopted to have a flow optimum similar to that of the separation capillary without cryogenic peak focusing [119,121,122] (Figs. 7, 8). The precision is comparable to that of other injection devices [120]. The minimum required air sample volume depends upon the noise voltage of the detector, the peak width, the required signal-to-noise ratio, and is inversely proportional to the concentration of the respective analyte and the detector sensitivity [121]; e.g. trichlorofluoromethane has the lowest ambient air concentration of 1.3 pg/ml (1.3  $\mu\text{g}/\text{m}^3$ ). As the ECD response is high, about 60  $\mu\text{l}$  of air is sufficient for analysis; in contrast about 100 ml of air sample is required for trichloroethene (ambient level at 0.1  $\mu\text{g}/\text{m}^3$ ).

Complete trapping and efficient band-focusing may be achieved at ambient temperature with microtraps packed with suitable sorbents. Two approaches have been evaluated by Frank and Frank [119]: if the boiling points of the analytes are within a range of about 100°C, a single-sorbent trap and direct coupling to the GC column are recommended; for samples containing components with widely different volatilities, a trap composed of two or more segments with complementary affinities and coupling to the

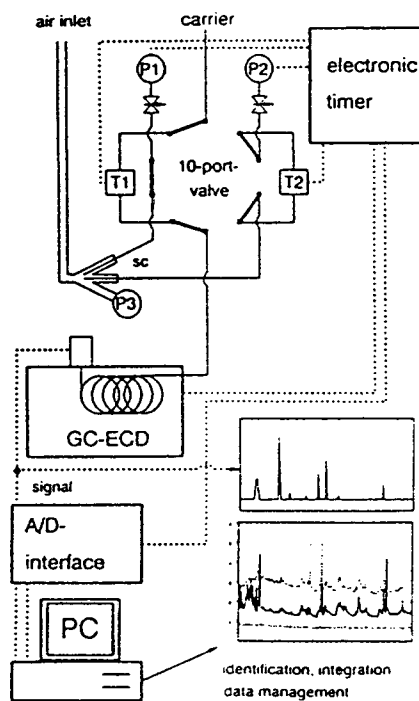


Fig. 7. Schematic presentation of instrumentation for automated sampling and gas chromatographic analysis of volatile trace pollutants in ambient air. Valve position: thermodesorption from trap 1- T1, sample collection on trap 2- T2; P1,P2,P3-membrane pumps. (Reproduced from Ref. [121]).

chromatographic column under carrier gas flow reversion is preferable. Examples of application of carbon sorbents in microtraps are presented in Table 6.

### 6.3. Preconcentration of water contaminants

The above sections summarise the development and application of single-bed and multi-bed carbon sorbents for the preconcentration of volatile and semi-volatile compounds, particularly in air matrices, and the achievements and problems of enrichment of analytes present in air samples, mainly in mixtures, are discussed. From the point of view of environmental analysis water is one of the other very important matrices. Therefore, the following deals with the problem of organic pollutant enrichment from aqueous solutions.

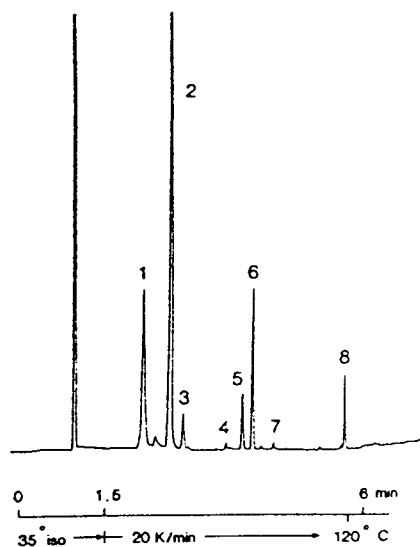


Fig. 8. Gas chromatographic separation of the major  $C_1$ - and  $C_2$ -halocarbons in 40 ml of ambient air on a thick-film (2  $\mu\text{m}$ ) capillary coated with crosslinked SE-54 after automated sampling and thermodesorption. Peaks: 1 =  $\text{CCl}_2\text{F}_2$ ; 2 =  $\text{CCl}_3\text{F}$ ; 3 =  $\text{C}_2\text{Cl}_3\text{F}_3$ ; 4 =  $\text{CHCl}_3$ ; 5 =  $\text{CH}_3\text{CCl}_3$ ; 6 =  $\text{CCl}_4$ ; 7 =  $\text{C}_2\text{HCl}_3$ ; 8 =  $\text{C}_2\text{Cl}_4$ . The retention time of the peak following  $\text{CCl}_2\text{F}_2$  corresponds to  $\text{COCl}_2$ . (Reproduced from Ref. [121]).

The investigation of the contamination of water with low concentrations of compounds is a complex problem that can only be solved using

isolation and preconcentration procedures prior to the determination. There are many techniques that can be used for the isolation and preconcentration of the considered pollutants from environmental samples (for reviews see Refs. [125–130]). Over the past twenty years carbon materials have been utilised for the analysis of aqueous samples, of volatiles (stripping techniques, purge-and-trap techniques, head-space analysis), but also for semi-volatiles and non-volatiles (dynamic stripping, steam distillation, SPE with liquid desorption).

### 6.3.1. Sorption from the liquid phase—desorption into liquid phase

In many environmental procedures trace enrichment is still often carried out by means of liquid–liquid extractions; nevertheless, recoveries are low for polar analytes and this technique cannot be applied to hydrophilic compounds, which are more soluble in water than in the usual organic solvents. The solid-phase extraction technique has gained interest as an alternative to the laborious and time-consuming liquid–liquid extraction.

Until recently, various types of activated carbon were the most commonly used sorption media for the preconcentration of pollutants from aqueous phases [126]. Most pollutants

Table 6  
Miniaturised bed of sorbents for automated and continuous monitoring of low concentration of volatile trace components in air sample stream; sampling at ambient temperature

Microtrap	Trap dimensions I.D. $\times$ length (mm)	Analysed compounds	Volatility range b.p. ( $^{\circ}\text{C}$ )	Sample amount (ml)	Detector	Concentration level MLD	Reference
Haysed D/Carbosphere	1.2 $\times$ 100	$C_1$ – $C_2$ halocarbons	–30–147	0.06–100	ECD	0.03–1.3 [ $\mu\text{g}/\text{m}^3$ ]	121
Haysed D/Carbosphere Charcoal/Graphtrap	0.53 $\times$ 47	$C_1$ – $C_2$ halocarbons	–28–121	60	ECD	0.8–100 [ $\mu\text{g}/\text{m}^3$ ]	122
Carboxen materials <sup>a</sup> 569; 1000	0.5 $\times$ 270 (300)	Chlorofluorocarbons	–48.4––9.8	2000	MS	1.5 ppm	124
Carboxen 1000/1003 <sup>b</sup>		Halocarbons	–48.4–28	2000–3000	MS	1 pttv	123
Carbotrap C	0.33 $\times$ 65	BTX, hexane	80–135	0.04–40	FID	ppbv–ppmv	120

<sup>a</sup> Trapping temperature  $-40^{\circ}\text{C}$ .

<sup>b</sup> Trapping temperature  $-50^{\circ}\text{C}$ .

adsorbed from water on activated carbon are recoverable by liquid extraction.  $\text{CS}_2$  is the most frequently used extractant. Some compounds are resistant, particularly at low loading. The adsorption isotherms of organic pollutants are strongly concave with respect to the concentration axis, i.e. extraction efficiency decreases sharply with decreasing loading. The apparent irreversibility of the adsorption of some substances on activated carbon has been a hindrance to its use for the determination of trace pollutants.

The development of new types of sorbents for SPE is growing rapidly [126,128]. Among the sorbents that have been investigated in recent years are the tailored sorbents. They have attracted attention because of their potential for the optimum solution of separation problems. Sorbents with a predominantly carbonaceous matrix should be mentioned in this context. The advantage of these materials are their thermal stability, chemical resistance and stability over a wide pH range. Non-volatile organics require the use of a homogeneous surface, because only these types of surfaces can provide a linear isotherm, and more or less symmetrical adsorption and desorption. If a large volume is required for the analysis, the robustness or the resistance to the pressure of the carbons has to be taken into account. All these requirements are met by GBCs and/or PGCBs, that are non-polar, inert adsorbents with prevailing hydrophobic properties.

Graphitized carbon black cartridges have successfully been applied for SPE of various pollutants such as polynuclear aromatic hydrocarbons (PAHs), chlorinated pesticides, phthalates and herbicides from water [26]. Carbo-pack B, having a nonporous, substantially nonpolar, and homogeneous surface with an area of about  $100 \text{ m}^2/\text{g}$ , has proved to be a valuable adsorbent for SPE. Cartridges can be easily cleaned and reused without any limitation. The compounds of interest trapped from water are eluted from the cartridge by using the right volume of a suitable solvent (or solvent mixture). Recoveries obtained by spiking Carbo-pack B (at ng level) and the water (at ppt level) with the components of

interest, in general, are very good except for the heavier PAHs. This problem may be solved by using GCBs with a lower surface area. Also Carbo-pack B was successfully utilised by several authors for the preconcentration of non-volatile pesticides [26,131], organochlorine insecticides, triazine, phenoxyacids herbicides and various base-neutral and acidic pesticides [132,133]. For the extraction of phenols [134], chloroanilines [135] and pesticides [133] Carbo-pack B cartridges proved to be more efficient than  $\text{C}_{18}$  silica [134,135] with higher accuracy [133]. A comparison of pesticides recovery data on both sorbents [133] is presented in Table 7. Di Corcia and Marchetti [133,136] elaborated a multiresidue method for a wide range of pesticides in drinking water using GCB cartridge extraction and liquid chromatographic analysis (Fig. 9). The simple and rapid procedure involves passing up to a 2-l sample through a 250-mg Carbo-pack B cartridge. With respect to chemically bonded silica, an apparent weakness of GCB is that its surface framework is contaminated by few oxygen complexes, having a structure similar to benzpyrylium salts [34]. This apparent weakness is, in fact, an advantage in that acidic analytes can be completely isolated from base-neutral ones by first passing through the sorbent bed a solvent system for elution of the nonacidic compounds and then a suitable basified solvent mixture for desorption of the acidic analytes, which are collected separately. In this way, not only extraction and concentration, but also class fractionation can be achieved simultaneously by a single sorbent cartridge. Compared to the  $\text{C}_{18}$  cartridge, additional advantages of using a Carbo-pack cartridge are that the extraction procedure is about 7 times shorter, no pH adjustment of the environmental sample is necessary for trapping of the acidic compounds, and one cartridge instead of two suffices to extract base-neutral and acidic pesticides, making the Carbo-pack cartridge more adaptable than the  $\text{C}_{18}$  one for field use. The detection limit by this method for all 35 pesticides considered was between 0.003 and  $0.07 \mu\text{g}/\text{l}$ . The European Community (EC) Drinking Water Directive states that individual pesticides must not exceed



Table 7

Comparison of recovery of pesticides (Di Corcia and Marchetti [133]) from drinking water with Carbopack B and C<sub>18</sub> cartridges; sampling volume 2 l

Compound	Pesticide class	Recovery (%)	
		Carbopack	C <sub>18</sub>
	<i>Base-neutrals</i>		
Oxamyl	Carbamate	89	4
Methomyl	Carbamate	98	3.7
Chloridazon	Phenylpyridazinone	98	18
Metoxuron	Phenylurea	97	64
Bromacil	Uracil	94	53
Monuron	Phenylurea	100	49
Cyanazine	Triazine	96	95
Metribuzin	Triazine	94	60
Carbofuran	Carbamate	98	64
Atrazine	Triazine	97	96
Carbaryl	Carbamate	96	78
Monolinuron	Phenylurea	100	92
Paraoxon	Organophosphate	97	92
Propachlor	Acetanilide	95	92
Propham	Carbamate	98	80
Propanil	Propioanilide	97	97
Linuron	Phenylurea	98	99
Chloroxuron	Phenylurea	95	97
Chloroprotham	Carbamate	97	97
Fenitrothion	Phosphorothioate	95	98
Azinphos ethyl	Phosphorodithioate	98	98
Parthion ethyl	Phosphorothioate	96	97
Coumaphos	Phosphorothioate	98	100
Phoxim	Phosphorothioate	90	90
	<i>Acids</i>		
Bentazon	Benzothiadiazin	97	75
Bromoxynil	Phenol	96	33
Dinitro- <i>o</i> -cresol	Phenol	97	10
2,4-D	Phenoxyacid	93	41
Mecoprop	Phenoxyacid	92	92
2,4,5-T	Phenoxyacid	95	85
2,4-DB	Phenoxyacid	96	100
MCPB	Phenoxyacid	100	99
2,4,5-TP	Phenoxyacid	95	85
Dinoseb	Phenol	96	99
Dinoterb	Phenol	101	96
Grand mean		96	75

Abbreviations: 2,4-D = (2,4-dichlorophenoxy)acetic acid; 2,4,5-T = (2,4,5-trichlorophenoxy)acetic acid; 2,4-DB = (2,4-dichlorophenoxy)butyric acid; 2,4,5-TP = (2,4,5-trichlorophenoxy)propionic acid.

Water was spiked with 0.25–1.5 µg/l of each pesticide; mean values calculated from three determination.

0.1 µg/l in any sample of drinking water. Di Corcia et al. in a recent systematic study [35] devoted to the characterisation of GCB as an

anion exchanger examined the effects of the pH of the aqueous matrix, its ionic strength and the presence of fulvic acids and acidic surfactants on

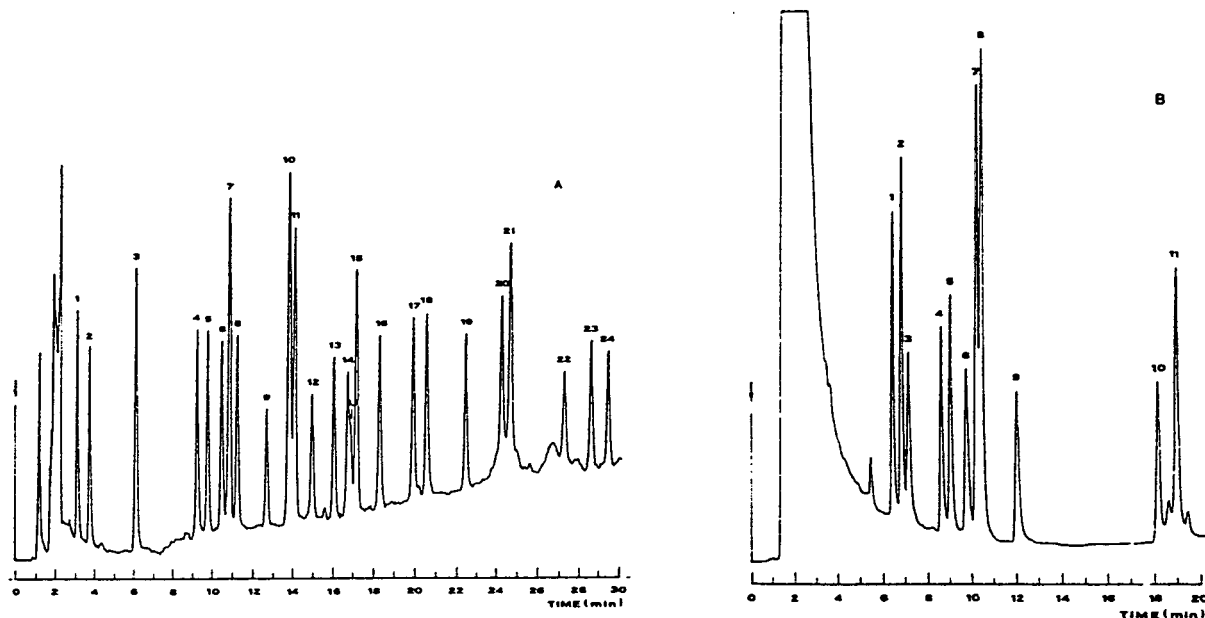


Fig. 9. HPLC chromatograms obtained on sampling the extracts from 2 l of tap water containing 0.4 g/l of sodium sulfite and spiked with base-neutral (A) and acid pesticides (B). Peaks, (A): 1 = oxamyl, 2 = methomyl, 3 = chloridazon, 4 = metoxuron, 5 = bromacil, 6 = monuron, 7 = gyanazine, 8 = metribuzin, 9 = carbofuran, 10 = atrazine, 11 = carbaryl, 12 = monolinuron, 13 = paraoxon, 14 = propachlor, 15 = propham, 16 = propanil, 17 = linuron, 18 = chloroxuron, 19 = chloroprotham, 20 = fenitrothion, 21 = azinphos ethyl, 22 = parathion ethyl, 23 = coumaphos, 24 = phoxim; (B) 1 = bentazone, 2 = bromoxyl, 3 = dinitro-*o*-cresol, 4 = (2,4-dichlorophenoxy)acetic acid, 5 = mecoprop, 6 = (2,4,5-trichlorophenoxy)acetic acid, 7 = MCPB, 8 = (2,4-dichlorophenoxy)butyric acid, 9 = (2,4,5-trichlorophenoxy)propionic acid, 10 = dinoseb, 11 = dinoterb; U = unknown compound contaminating the water specimen. The individual concentrations of the pesticides ranged between 0.125 and 0.750  $\mu\text{g/l}$ . (Reproduced from Ref. [133]).

the capability of a GCB cartridge to extract quantitatively sixteen selected acidic model compounds and on their separation from base-neutral species. The possibility of subfractionating co-extracted acidic compounds on the basis of their acid strength by stepwise desorption was also investigated.

The key parameter in SPE is the sample volume that can be handled without any breakthrough. In general,  $\text{C}_{18}$  silicas are convenient for the trace determination of apolar compounds. Nevertheless, the capacity factors of moderately polar analytes are too low with  $\text{C}_{18}$  silica to allow the handling of a sufficiently large volume. Apolar copolymers cannot be used for on-line preconcentration of more polar compounds, because small-sized precolumns are required [137].

It was shown, that the retention of some polar compounds can be very high using porous graphitic carbon (PGC), available recently as HPLC stationary phase [138]. PGC shows a highly ordered crystalline structure with large bands of delocalized electrons, so that the retention mechanism is a mixture of hydrophobic and electronic interactions and is very different from that observed with  $\text{C}_{18}$  silicas and apolar copolymers [139,140]. PGC is a reversed-phase sorbent and it is observed that the retention of compounds decreases when the organic content of the mobile phase increases. On-line coupling of SPE to LC has several advantages compared to off-line procedures, particularly there is no risk of loss and contamination as there is no sample manipulation between preconcentration and analysis; more precise and reproducible

quantitative data are expected. The size of the precolumn is an important parameter in the coupling because the profile of concentrated species transferred from the precolumn to the analytical column should ideally be as narrow as possible at the beginning of the separation. Consequently precolumn dimensions should be as small as possible and adapted to those of the analytical column. An on-line technique coupling preconcentration via a precolumn packed with PGC (stainless-steel precolumn 1 cm × 0.46 cm I.D. prepacked with 10–15 μm Hypercarb PGC, Shandon, Runcorn, UK) and LC with a PGC analytical column (Hypercarb PGC, Shandon, UK) was published [137] recently. The system was found to be very efficient for the trace-level determination of some polar and water-soluble organic pollutants from environmental waters (low ppb range). As these analytes are much more retained by PGC than they are by C<sub>18</sub> silica, preconcentration on a PGC precolumn cannot be coupled on-line with the widely used and more efficient C<sub>18</sub> silica analytical columns, but with a PGC column. Applications were presented for the determination of some organic compounds included in the EC environmental priority pollutant list such as 2-chloro-4-aminophenol, chloroanilines, aminophenols and 2,4,6-trihydroxy-1,3,5-triazine. The influence of the sample matrix was investigated with drinking and river water samples.

### 6.3.2. Sorption from the gaseous phase—desorption into liquid phase

With regard to the high sorption capacity of activated charcoal this kind of sorbent has been often used in the closed stripping loop according to Grob [141]. For efficient component trapping from the gas phase (after stripping components from the water matrix by a stream of inert gas possibly at elevated temperature) a few mg of sorbent (1.5–5.0 mg) in the form of miniaturised disks is sufficient; off-line liquid desorption is performed by organic solvents, most frequently CS<sub>2</sub> and dichloromethane [142]. This method has the advantage that several portions of eluent, with an overall volume of 8–20 μl, are sufficient to achieve acceptable recoveries [143], where it

is recommended to allow the solvent to go back and forth through the filter. Good recoveries were obtained for hydrocarbons, oxygen-containing compounds and chlorinated pesticides in ppm concentration [144]; at lower concentrations artefact formation was observed. A large number of compounds can be analysed per run, making closed-loop stripping analysis a very cost-effective technique [126].

### 6.3.3. Sorption from the gaseous phase—desorption into gaseous phase

Several reported purge-and-trap methods rely on the solvent desorption of organics adsorbed onto a charcoal filter bed [145]. However, this method has limitations which must be taken into account. Problems include a strong affinity for water, which is frequently found in head-space vapour samples and which affects the adsorption properties, an excessive surface activity or the presence of large numbers of active sites for polar compounds. Additional problems include masking of highly volatile compounds by the solvent peak.

Application of organic polymeric sorbents as alternative trapping media for head-space volatiles combined with thermodesorption has increased significantly during the eighties. In recent years carbon sorbents have been applied in purge-and-trap techniques in single-bed or in multi-bed arrangement (various carbonaceous sorbent types and/or in combination with other types of sorbents). The unconventional porous carbon sorbent Carb I, prepared by controlled pyrolysis of saccharose in a silica gel matrix, was tested as a suitable material for enrichment of multicomponent mixtures of analytes (particularly hydrocarbons in the gasoline range, Fig. 10.) in the ppm–ppb concentration range from various water matrices by the purge-and-trap method with subsequent liquid desorption and on-column capillary GC analysis [146–148];

Most applications of purge-and-trap systems are combined on-line with thermodesorption and capillary GC. A survey of the used multi-bed applications for trapping volatile and semi-volatile compounds is presented in Table 8. The results of various experiments showed that tem-

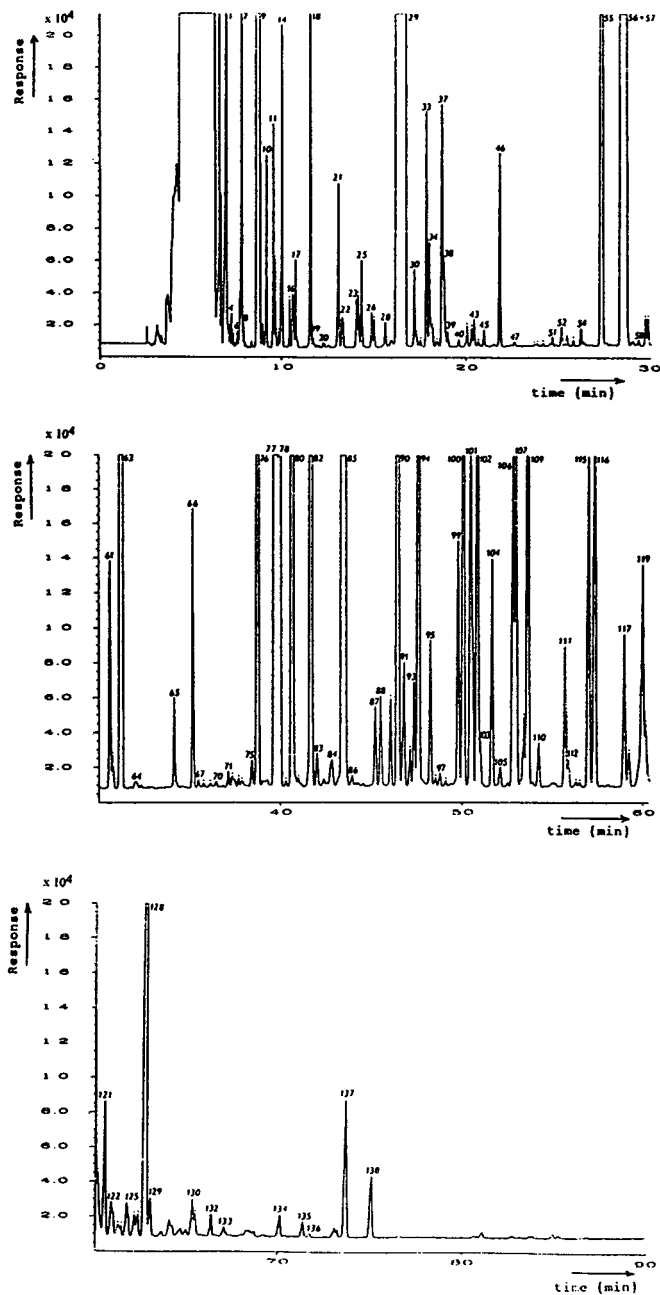


Fig. 10. Chromatogram of the separation of organic compounds (HP-PONA column) stripped from gasoline-contaminated water (30 ml) and trapped on a porous carbon sorbent;  $\text{CS}_2$  desorption; on-column injection; flame ionisation detection. Peaks: 1,18,46,65,89,115,119,133,  $n\text{C}_6$ - $n\text{C}_{12}$ ; 2,3,5,6,8,11,12,14,16,19,20,22,24,25,27,31,32,33,34,35,37,38,44,48,50,51,54,58,59,60,61,62, 68,70,71,72,75,81,83,84,86,93,95,97,105,110,  $\text{C}_4$ - $\text{C}_{10}$  branched alkanes; 4,7,10,13,15,16,17,21,22,23,26,28,30,36,39,40,41,42, 43,45,47,49,52,53,64,67,68,69,73,74,79,86,95,98,  $\text{C}_5$ - $\text{C}_{10}$  cycloalkanes; 9,29,55,56,57,63,66,76,77,78,80,82,85,87,88,90,91,92,94, 96,99,100,101,102,103,104,106,107,108,109,111,112, 113,114,115,116,117, 118,119,120,121, 122,123, 124,125,126,127,128,129,130, 131,132,134,135,136,137,138,  $\text{C}_6$ - $\text{C}_{12}$  aromatics; The individual concentrations of hydrocarbons ranged between 7 ppb–3.5 ppm. (Reproduced from Ref. [146]).

Table 8

Application of sorbents in multi-bed arrangement for trapping volatile and semi-volatile compounds from aqueous samples in purge-and-trap systems with subsequent GC determination

Multi-bed sorbent	Analysed compounds	Volatility range b.p. (°C)	Sample amount (ml)	Detector	Concentration level ( $\mu\text{g/l}$ ) MLD <sup>b</sup>	Reference
Tenax/silica gel/charcoal	Aromatic hydrocarbons	80–217.7	5	ITD	0.2–2; <sup>b</sup> 0.1	149
	Halocarbons	–14–246				
Tenax GC/silica gel/charcoal Carbopack B/Carbosieve S-III	Halocarbons	–29.8–180	5	PID EICD	4; <sup>b</sup> 0.001–0.08 4; <sup>b</sup> 0.5–0.001	150
Carbopack B/Carbosieve S-III	Aromatic hydrocarbons	80–136		FID EICD		151
	Halocarbons	–29–180				
Carbopack B/Carbosieve S-III	Aromatic hydrocarbons	80–145	5	MSD	10–100	152
	Aromatic halocarbons	132–180				
Tenax TA/Chromosorb 106/ Spherocharb	C <sub>4</sub> –C <sub>20</sub> compounds n-Alkanes Branched, unsat. hydrocarbons Aromatic hydrocarbons Organochlorines Oxygenated compounds Sulphides	–4.5–302 35–302 –4.5–104 79–267 40–179 46–179 38–118	1000	ITD,FID	0.005–5	145
Carbotrap 150 <sup>a</sup>	PCB					153
	PAH					154
	Alkybenzenes					
VOCARB 3000	Aromatic hydrocarbons	80–266	5	EICD/PID	5	155
	Halocarbons	–28.9–219				
BTEXTRAP <sup>a</sup>	Aromatic hydrocarbons	80–145	10	PID/FID	18	155
Carbotrap 400	Hydrocarbons	80–266	20	FID	10–100	156
VOCARB 3000 <sup>a</sup> ,4000	Aromatic hydrocarbons	168–217.7	5 25	MS	20–200; <sup>b</sup> 0.05	157
	Halocarbons	–28.9–214				
VOCARB 4000	Oxygenated and polar VOCs	78–127	5	MS	40	158

ITD = ion-trap detector; PID = photo ionisation detector; FID = flame ionization detector; EICD = electrolytic conductivity detector; MSD = mass-selective detector; MS = mass spectrometer.

<sup>a</sup> Also solid waste.

<sup>b</sup> MLD = method detection limit.

perature, stripping time and purge flow-rates all influence the recovery of organic compounds [145]. It was also shown that there is a dependence of the recovery data on the boiling point

of the analysed compounds, particularly for high boilers, and also on their polarity.

The developed carbonaceous adsorbents (GCBs in combinations with carbon molecular

sieves, e.g. VOCARB 3000, 4000) provide several advantages compared to conventional adsorbents such as Tenax TA/silica gel/charcoal combination used in US EPA methods 502.2, 524.2, 624 and 8260, which are the following: the ability to trap small molecules, to minimise water retention and the possibility to use higher desorption temperatures [157]. The higher thermal stability of these adsorbents also ensures faster, more effective baking (thermal cleaning) of a contaminated trap. Peaks are well resolved with only slight tailing on thick-film columns, without cryogenics. The higher desorption temperature releases the analytes more rapidly, providing a more focused plug and allowing the use of lower column flow-rates [157,159].

A higher temperature can create some disadvantages. Carbonaceous adsorbents can induce thermal and catalytic breakdown of some compounds. Also, because the adsorption is stronger, some of the heavier analytes are more difficult to desorb. For highboilers the Tenax TA/silica gel/charcoal combination provides better recovery. The pores in the carbon molecular sieve also trap carbon dioxide which, when desorbed, might interfere with some early eluting, trace-level compounds [157].

## 7. Conclusions

The development of carbon sorbents for the preconcentration of analytes utilizes the results of the long-term research and development of stationary phases for HPLC and GSC. Recent developments in the production of thermally modified carbon blacks, carbon molecular sieves and porous carbons for quantitatively trapping of organic components are reflected in their superior performance over "traditional" sorbents such as activated charcoal and porous polymers which tend to lack uniform sorbent characteristics for the adsorption and retention of the different compounds encountered in different environments. The application of such adsorbents has minimized the problems of contamination and artefact formation, and hence they are suitable for the sampling of VOCs in quite

different environments and preconcentration and isolation of semi-volatile and non-volatile compounds from various matrices.

In spite of the broad application of sorbents in trace analysis for several tens of years, the results of tests of new sorbents, synthesis of tailored sorbents, or combination of sorbents with various physico-chemical properties with the aim of special and very broad application, research on the influence of various factors on the efficiency of preconcentration, show that the developments in this field with the aim to obtain an inert sorbent for ultra-trace analysis will continue.

## References

- [1] J.H. Knox, K.K. Unger and H. Mueller, *J. Liq. Chromatogr.*, 6 (1983) 1.
- [2] J.S. Mattson and H.B. Mark, Jr., *Activated Carbon*, M. Dekker, New York, 1971, p. 1.
- [3] J.C. Bokros, in Walker (Editor), *Chemistry and Physics of Carbon*, M. Dekker, New York, 1969, Vol. 5, p. 1.
- [4] J.H. Knox, B. Kaur and G.R. Millward, *J. Chromatogr.*, 352 (1986) 3.
- [5] J.D. Bernal, *Proc. Roy. Soc. London Ser. A*, 100 (1924) 749.
- [6] H. Lipson and A.R. Stokes, *Proc. Roy. Soc. London Ser. A*, 181 (1942) 93.
- [7] B.E. Warren, *Phys. Rev.*, 59 (1941) 693.
- [8] T.V. Barmakova, A.V. Kiselev and N.V. Kovaleva, *Kolloid Zh.*, 36 (1974) 133.
- [9] M. Smišek and S. Černý, *Aktivné uhlie*, SNTL, Prague, 1964.
- [10] A.V. Kiselev and J.P. Yashin, *Gas Adsorption Chromatography*, Plenum Publishing, New York, 1969.
- [11] I.D. Belyakova and A.V. Kiselev, *Anal. Chem.*, 36 (1964) 1517.
- [12] A.V. Kiselev, N.V. Kovaleva and Yu.S. Nikitin, *J. Chromatogr.*, 58 (1971) 19.
- [13] F. Brunner, P. Ciccioli, G. Crescentini and M.T. Pistolesi, *Anal. Chem.*, 45 (1973) 1851.
- [14] F. Brunner, G. Bertoni and P. Ciccioli, *J. Chromatogr.*, 120 (1976) 307.
- [15] V. Patzelova, J. Jansta and F.P. Dousek, *J. Chromatogr.*, 148 (1978) 53.
- [16] T.A. Zwier and M.F. Burke, *Anal. Chem.*, 53 (1981) 812.
- [17] K.K. Unger, *Anal. Chem.*, 55 (1983) 361A.
- [18] M.T. Gilbert, J.H. Knox and B. Kaur, *Chromatographia*, 16 (1982) 138.

- [19] F. Derby Shire and B. McEnaney, *Energeia*, 2 (1991) 1.
- [20] J. Wilson, *Fuel*, 60 (1981) 823.
- [21] C. Pierce, R.N. Smith, J.W. Wiley and H. Cordes, *J. Am. Chem. Soc.*, 75 (1951) 4551.
- [22] I.A. Dolova, A.V. Kiselev and Ja.I. Jašin, *Zh. Fiz. Chim.*, 48 (1974) 1285.
- [23] S.P. Nandi and P.L. Walker, *Sep. Sci.*, 11 (1976) 441.
- [24] I. Halasz and G. Horvath, *Anal. Chem.*, 34 (1969) 409.
- [25] C. Vidal Madjar, G. Granasia and G. Guichon, in R. Stock (Editor), *Gas Chromatography 1970*, Institute of Petroleum, London, 1971, p. 20.
- [26] F. Brunner, G. Crescentini and F. Mangani, *Chromatographia*, 30 (1990) 565.
- [27] W. Engewald, J. Porschmann and T. Welsh, *Chromatographia*, 30 (1990) 537.
- [28] W.R. Betz and W.R. Supina, *J. Chromatogr.*, 471 (1989) 105.
- [29] N.V. Kovaleva and K.D. Scherbakova, *J. Chromatogr.*, 520 (1990) 55.
- [30] A. Di Corcia and A. Liberti, *Adv. Chromatogr.*, 14 (1976) 305.
- [31] F.L. Lopez-Garzon, I. Fernandez-Morales and M. Domingo-Garcia, *Chromatographia*, 23 (1987) 97.
- [32] G. Crescentini, F. Managani, A.R. Mastrogiamco and P. Palma, *J. Chromatogr.*, 392 (1987) 83.
- [33] A. Di Corcia, R. Samperi, E. Sebestiani, C. Sererini, *Chromatographia*, 14 (1981) 86.
- [34] L. Campanella, A. Di Corcia, R. Samperi and A. Gambacorta, *Mater. Chem.*, 7 (1982) 429.
- [35] A. Di Corcia, S. Marchese and R. Samperi, *J. Chromatogr.*, 642 (1993) 163.
- [36] K.S.W. Sing, *Extended Abstracts of the The Second International Conference on Carbon Black*, Mulhouse, September 1993, p. 53.
- [37] I. Novák, D. Berek and J. Lipták, in D. Kaniansky (Editor), *Abstracts of Papers of the 9th International Symposium Advances and Applications of Chromatography in Industry*, Bratislava, 1993, p. 164.
- [38] D. Berek and I. Novák, *Chromatographia*, 30 (1990) 582.
- [39] B.J. Bassler and R.A. Hartwick, *J. Chromatogr. Sci.*, 27 (1989) 162.
- [40] O. Chiantore, I. Novák and D. Berek, *Anal. Chem.*, 60 (1988) 638.
- [41] E. Škuchtanová, L. Felzl and E. Smolková-Keulemansová, *J. Chromatogr.*, 292 (1984) 233.
- [42] I. Novák and J. Lipták, in *Zborník súhrnov príspevkov 2. konferencia Extrakcia sorbentami*, Bratislava, 1992, p. 36.
- [43] W.R. Betz, S.A. Hazard and E.M. Yearick, *International Labmate*, XV (1990).
- [44] M. Domingo Garcia, I. Fernandez Moralez, F.J. Lopez Garzon and M. Pyda, *Chromatographia*, 34 (1992) 568.
- [45] W.R. Betz and S.J. Lambiase, *J. Chromatogr.*, 556 (1991) 433.
- [46] N.A. Eltekova, *Chromatographia*, 34 (1992) 178.
- [47] J. Jagiello, T.J. Badosz and J.A. Schwarz, *Chromatographia*, 30 (1992) 441.
- [48] M.B. Martin-Hopkins, R.K. Gilpin and M. Jaroniec, *J. Chromatogr. Sci.*, 29 (1991) 147.
- [49] M.J.D. Low and C. Morterra, *Carbon*, 21 (1983) 275.
- [50] C. Morterra and M.J.D. Low, *Carbon*, 21 (1983) 283.
- [51] C. Morterra, M.J.D. Low and A.G. Severdia, *Carbon*, 22 (1984) 5.
- [52] C. Morterra and M.J.D. Low, *Langmuir*, 1 (1985) 320.
- [53] C. Morterra and M.J.D. Low, *Mater. Chem. Phys.*, 12 (1985) 207.
- [54] W.M. Hess and C.R. Herd, in *Extended Abstracts of the The Second International Conference on Carbon Black*, Mulhouse, September, 1993, p. 251.
- [55] J.-B. Donnet and E. Custodero, in *Extended Abstracts of the The Second International Conference on Carbon Black*, Mulhouse, September, 1993, p. 177.
- [56] R. Dobrowolski, Staszczuk and M. Jaroniec, in *Extended Abstracts of the The Second International Conference on Carbon Black*, Mulhouse, September, 1993, p. 87.
- [57] W.R. Betz, S.G. Maroldo, G.D. Wachob and M.C. Firth, *Am. Ind. Hyg. Assoc. J.*, 50 (1989) 181.
- [58] K. Figge, W. Rabel and A. Wieck, *Fres. Z. Anal. Chem.*, 327 (1987) 261.
- [59] Xu-Liang Cao, *J. Chromatogr.*, 586 (1991) 161.
- [60] J.Y.K. Lai, E. Matisová, D. He, E. Singer and H. Niki, *J. Chromatogr.*, 643 (1993) 77.
- [61] *NIOSH Manual of Analytical Methods*, HEW Publication No. (NIOSH) 75.
- [62] *Annual Book of ASTM Standards*, 11.03 Atmospheric Analysis, Occupational Health and Safety, D 3686-89, Philadelphia, USA, 1991.
- [63] V.G. Berezkin and Y.S. Drugov, *Gas Chromatography in Air Pollution Analysis (J. Chromatogr., Library Vol. 49)*, Elsevier, Amsterdam, 1991.
- [64] *Annual Book of ASTM Standards*, 11.03 Atmospheric Analysis, Occupational Health and Safety, D 3687-89, Philadelphia, USA, 1991.
- [65] O. Einarsson, J. Gorczak, B. Ovelundmark and U. Palmquist, *J. Chromatogr.*, 498 (1990) 381.
- [66] E. Matisová, F. Halmo, J. Lehotay and M. Onderová, *Ropa a Uhlie*, 34 (1992) 408.
- [67] E. Matisová, J. Lehotay, M. Onderová and F. Halmo, *Chemický průmysl*, 43/68 (1993) 116.
- [68] C. Lefevre, P. Ferrari, J.P. Guenier and J. Müller, *Chromatographia*, 27 (1989) 37.
- [69] E. Atlas and S. Schauffler, *Environ. Sci. Technol.*, 25 (1991) 61.
- [70] E. Atlas, S.M. Schauffler, J.T. Merrill, C.J. Hahn, B. Ridley, J. Walega, J. Greenberg, L. Heidt and P. Zimmerman, *J. Geoph. Res.*, 97 (1992) 10 331.
- [71] K. Grob, *J. Chromatogr.*, 321 (1985) 45.
- [72] B.V. Burger and Z. Munro, *J. Chromatogr.*, 394 (1987) 443.
- [73] B.V. Burger and Z. Munro, *J. Chromatogr.*, 370 (1986) 449.

- [74] B.V. Burger and Z. Munro, *J. Chromatogr.*, 402 (1987) 95.
- [75] K. Grob, A. Artho, Ch. Frauenfelder and I. Roth, *J. High Resolut. Chromatogr.*, 13(1990) 257.
- [76] G.P. Cobb, R.S. Braman and K.M. Hua, *Anal. Chem.*, 58 (1986) 2213.
- [77] C. Bicchi, A. D'Amato, F. David and P. Sandra, *J. High Resolut. Chromatogr.*, 12 (1989) 316.
- [78] J. Roerade and S. Blomberg, *J. High Resolut. Chromatogr.*, 12 (1989) 138.
- [79] S. Blomberg and J. Roerade, *J. High Resolut. Chromatogr.*, 13 (1990) 509.
- [80] B.V. Burger, M. LeRoux, Z.M. Munro and M.E. Wilken, *J. Chromatogr.*, 552 (1991) 137.
- [81] S. Škrabáková, E. Matisová, M. Onderová, I. Novák and D. Berek, *Chem. Papers*, 48 (1994) 169.
- [82] S. Škrabáková, E. Matisová, M. Onderová, I. Novák, in P. Sandra and G. Devos (Editors), *Proceedings of the 15th Int. Symposium on Capillary Chromatography*, Riva del Garda, May, 1993, Huethig, Heidelberg, 1993, p. 622.
- [83] E. Matisová and S. Škrabáková, *Anal. Chem. Acta*, in press.
- [84] E. Matisová and S. Škrabáková, in M.B. Evans and A.F. Feell (Editors), *The Chromatography Year Book*, 20th International Symposium on Chromatography, Bornemouth, The Chromatographic Society, 1994, OR3.3.
- [85] J.M. Wong, N.Y. Kado, P.A. Kuzmicky, H.-S. Ning, J.E. Woodrow, D.P.H. Hsieh and J.N. Seiber, *Anal. Chem.*, 63 (1991) 1644.
- [86] N. Schmidbauer, M. Oehme, *Fresenius Z. Anal. Chem.*, 331 (1988) 14.
- [87] P. Ciccio, E. Brancaleoni, A. Cecinato, C. DiPalo, A. Brachetti and A. Liberti, *J. Chromatogr.*, 351 (1986) 433.
- [88] P. Ciccio, A. Cecinato, E. Brancaleoni, M. Frattoni and A. Liberti, *J. High. Resolut. Chromatogr.*, 15 (1992) 75.
- [89] P. Ciccio, E. Brancaleoni, A. Cecinato and M. Frattoni, *Fresenius Environ. Bull.*, 1 (1992) 73.
- [90] P. Ciccio, E. Brancaleoni, A. Cecinato, R. Sparapani and M. Frattoni, *J. Chromatogr.*, 643 (1993) 55.
- [91] P. Ciccio, in P. Sandra and G. Devos (Editors), *Proceedings of the 15th Int. Symposium on Capillary Chromatography*, Riva del Garda, May, 1993, Huethig, Heidelberg, 1993, p. 483.
- [92] P. Sandra (Editor), *Sample Introduction in Capillary Gas Chromatography*, Vol. 1, Huethig, Heidelberg, 1985.
- [93] L. Senf, F. Stapf and B. Düsédau, *Fresenius Z. Anal. Chem.*, 333 (1989) 47.
- [94] L. Senf, F. Stapf, B. Düsédau and H. Frank, *J. Thermal Anal.*, 33 (1988) 371.
- [95] L. Senf and H. Frank, *J. Chromatogr.*, 520 (1990) 131.
- [96] V. Cocheo, G.G. Bombi and R. Silvestri, *Am. Ind. Hyg. Assoc. J.*, 48 (1987) 189.
- [97] E.D. Pelizzari and K.J. Krost, *Anal. Chem.*, 56 (1984) 1813.
- [98] A. Betti, S. Coppi, C. Bigli, *J. Chromatogr.*, 349 (1985) 181.
- [99] G. Macleod and J.M. Ames, *J. Chromatogr.*, 355 (1986) 393.
- [100] *Supelco GC Bull.*, 846A (1986).
- [101] K.J. Krost, E.D. Pellizzari, S.G. Walburn and S.A. Hubbard, *Anal. Chem.*, 54 (1982) 810.
- [102] H. Rothweiler, P.A. Wäger and Ch. Schlatter, *Atmospheric Environment*, 25B (1991) 231.
- [103] M. De Bortoli, H. Knoppel, E. Pecchio and H. Visser, in B. Seifert, H. Esdorn., M. Fischer and J. Wegner (Editors), *Indoor Air 87*, Institute for Water, Soil and Air Hygiene, Berlin, 1987, pp. 139–143.
- [104] *Supelco GC Bull.*, 846C (1986).
- [105] R.W. Bishop and R.J. Valis, *J. Chromatogr. Sci.*, 28 (1990) 589.
- [106] W.R. Betz, G.D. Wachob and M.C. Firth, *Proceedings of EPA/APCA Symposium, Measurement of Toxic and Related Air Pollutants*, Raleigh, NC, 1987, pp. 761–770.
- [107] D.L., Heavner, M.W. Ogden and P.R. Nelson, *Environ. Sci. Technol.*, 26 (1992) 1737.
- [108] W.R. Betz and W.R. Supina, *Pure Appl. Chem.*, 61 (1989) 2147.
- [109] S.A. Hazard, J.L. Brown and W.R. Betz, *LC·GC*, 9(1) 1991.
- [110] Ch. Lancesdorfer and H. Puxbaum, *Water Air Soil Pollut.*, 51 (1990) 345.
- [111] A.J. Pollack, M.W. Holdren and W.A. McClenny, *J. Air Waste Manage. Assoc.*, 41 (1991) 1213.
- [112] L. Löfgren, P.M. Berglund, R. Nordlinder, G. Petersson and O. Ramnäs, *Intern. J. Environ. Anal. Chem.*, 45 (1991) 39.
- [113] G. Barrefors and G. Peterson, *J. Chromatogr.*, 643 (1993) 71.
- [114] You-Zhi Tang, Guang Tran, P. Fellin, W.K. Cheng and I. Drummond, *Anal. Chem.*, 65 (1993) 1932.
- [115] A.P. Bianchi and M.S. Varney, *J. Chromatogr.*, 643 (1992) 11.
- [116] T. Knobloch and W. Engewald, *Proceedings of the 16th Int. Symposium on Capillary Chromatography*, Riva del Garda, September 1994, p. 472.
- [117] R.G. Melcher, *ASTM Special Technical Publication 957*, Baltimore, MD, 1987, pp. 149–165.
- [118] *Sample Handling Bulletin 850A*, Supelco, 1991.
- [119] W. Frank and H. Frank, *Chromatographia*, 29 (1990) 571.
- [120] S. Mitra and Ch. Yun, *J. Chromatogr.*, 648 (1993) 415.
- [121] H. Frank, W. Frank, H.J.C. Neves and R. Englert, *Fresenius J. Anal. Chem.*, 340 (1991) 678.
- [122] H. Frank, W. Frank and M. Gey, *Z. Umweltchem. Ökotox.*, 3 (1991) 167.
- [123] S.J. O'Doherty, P.G. Simmonds and G. Nickless, *J. Chromatogr. A*, 657 (1993) 123.
- [124] S.J. O'Doherty, P.G. Simmonds, G. Nickless and W.R. Betz, *J. Chromatogr.*, 630 (1993) 265.



- [125] F.I. Onuška, J. High Resolut. Chromatogr., 12 (1989) 4.
- [126] J. Namiestnik, T. Gorecki and M. Biziuk, Anal. Chim. Acta, 237 (1990) 1.
- [127] S.K. Poole, T.A. Dean, J.W. Oudsema and C.F. Poole, Anal. Chim. Acta, 236 (1990) 3.
- [128] I. Liška, J. Krupčík and P.A. Leclercq, J. High. Resolut. Chromatogr., 12 (1989) 577.
- [129] J.W. Neely and E.G. Isacoff, Carbonaceous Adsorbents for the Treatment of Ground and Surface Waters, Marcel Dekker, New York, 1982.
- [130] M.W.F. Nielen, R.W. Frei and U.A. Th. Brinkman, in R.W. Frei and K. Zech (Editors), Selective Sample Handling and Detection in High-Performance Liquid Chromatography, Part A (J. Chromatogr., Library Vol. 39A), Elsevier, Amsterdam, 1989, pp. 5–78.
- [131] Supelco Environmental Notes, T411076 (1991).
- [132] M. Battista, A. DiCorcia and M. Marchetti, Anal. Chem., 61 (1989) 935.
- [133] A. DiCorcia and M. Marchetti, Anal. Chem., 63 (1991) 580.
- [134] A. DiCorcia, M. Marchetti and R. Samperi, Anal. Chem., 58, (1986) 2048.
- [135] A. DiCorcia and R. Samperi, Anal. Chem., 62 (1990) 1490.
- [136] A. Di Corcia and M. Marchetti, Environ. Sci. Technol., 26 (1992) 66.
- [137] S. Guenu and M.-C. Hennion, J. Chromatogr. A, 665 (1994) 243.
- [138] M.-C. Hennion and V. Coquart, J. Chromatogr., 642 (1993) 211.
- [139] V. Coquart and M.-C. Hennion, J. Chromatogr., 600 (1992) 195.
- [140] J.H. Knox and B. Kaur, in P.R. Brown and R.A. Hardwick (Editors), High-Performance Liquid Chromatography (Chemical Analysis, Vol. 98), Wiley, New York, 1989, pp. 189–222.
- [141] K. Grob, J. Chromatogr., 84 (1973) 225.
- [142] J. Curvers, T. Noij, C. Cramers and J. Rijks, J. Chromatogr., 289 (1984) 171.
- [143] J.I. Gómez-Belinchón and J. Albaigéz, Int. J. Environ. Anal. Chem., 30 (1987) 183.
- [144] B.A. Colenutt and S. Thorburn, Int. J. Environ. Anal. Chem., 7 (1980) 231.
- [145] A. Bianchi, M.S. Varney and J. Phillips, J. Chromatogr., 467 (1989) 111.
- [146] S. Škrabáková, E. Matisová, E. Benická, I. Novák and D. Berek, J. Chromatogr. A, 665 (1994) 27.
- [147] S. Škrabáková, E. Matisová, I. Novák and D. Berek, in D. Kaniansky (Editor), Abstract of Papers of the 9th Int. Symposium Advances and Application of Chromatography in Industry, Bratislava, 1993, p. 94.
- [148] E. Matisová and S. Škrabáková, in W. Günter, W. Hempel and G. Wulf (Editors), InCom'94, International Symposium on Instrumentalized Analytical Chemistry and Computer Technology, Tagungsband, March 1994, Düsseldorf, 1994, p. 259.
- [149] J.W. Eichelberger, T.A. Bellar, J.P. Donnelly, W.L. Budge, J. Chromatogr. Sci., 28 (1990) 460.
- [150] M.F. Mehran, M.G. Nickelsen, N. Golkar and W.J. Cooper, J. High. Resolut. Chromatogr., 13 (1990) 429.
- [151] N.H. Mosesman, L.M. Sidisky and S.D. Corman, J. Chromatogr. Sci., 25 (1987) 351.
- [152] S. Liu, J. Kang, D.L. Strother, R.J. Carley and J.D. Stuart, J. High. Resolut. Chromatogr., 12 (1989) 779.
- [153] The Supelco Reporter, VI (3) (1986) 4.
- [154] The Supelco Reporter, VIII (4) (1989) 12.
- [155] S.A. Hazard, The Supelco Reporter, XIII (1) (1993) 22.
- [156] S.A. Hazard, J.L. Brown and W.R. Betz, The New Expanded Supelco Reporter, XI (5) (1992) 3.
- [157] R.E. Shirey and S.B. Cole, The New Expanded Supelco Reporter, XII (1) (1993) 21.
- [158] The Supelco Reporter, XI (3) (1992) 7.
- [159] The Supelco Reporter, X (4) (1991) 5.





ELSEVIER

Journal of Chromatography A, 707 (1995) 181–187

JOURNAL OF  
CHROMATOGRAPHY A

# Study of aroma compound–natural polymer interactions by dynamic coupled column liquid chromatography

Sylvie Langourieux, Jean Crouzet\*

*Laboratoire de Génie Biologique et Sciences des Aliments, Unité de Microbiologie et Biochimie Industrielles Associée à l'INRA, Université de Montpellier II, F 34095 Montpellier Cedex 05, France*

First received 9 November 1994; revised manuscript received 18 January 1995; accepted 6 March 1995

## Abstract

Dynamic coupled column liquid chromatography (DCCLC) was used to study the interactions between the model aroma compounds  $\beta$ -ionone and limonene and the model food components dextrin and soya bean trypsin inhibitor. Solutions saturated with aroma compound can be obtained by a dynamic and reversible process. Interactions between the two categories of molecules were evidenced using exponential dilution and DCCLC, and the reversibility of the complex formation between limonene and trypsin inhibitor was established. The association constants  $K_a$  calculated for the complexes dextrin–limonene and trypsin inhibitor–limonene were  $13\,650 \pm 250$  and  $2\,944 \pm 784\ M^{-1}$ , respectively. The decrease of the calculated  $K_a$  values when  $\beta$ -ionone and dextrin are used is indicative of an irreversible adsorption of  $\beta$ -ionone on dextrin whereas a weak interaction,  $K_a = 385 \pm 105\ M^{-1}$  is obtained in the presence of trypsin inhibitor.

## 1. Introduction

Interactions between aroma compounds and macromolecules in aqueous solution are generally studied using equilibrium methods: liquid–liquid partitioning [1–3], gas–liquid partitioning [4] or equilibrium dialysis [5–9]. These methods, however, have several drawbacks: difficulty in determining the equilibrium which is reached after varying lengths of time, non-specific binding and volatilization of aroma compounds occurring particularly during equilibrium dialysis [10]. It is, moreover, generally difficult to obtain a quantitative extraction of aroma compounds. The use of dynamic methods based on gas

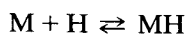
chromatography, such as exponential dilution [11,12] or liquid chromatography have therefore been investigated for the study of these interactions [13–15].

The decrease and increase of the infinite dilution activity coefficient of volatile components in the presence of macromolecules, as a result of the interactions occurring between these categories of molecules [16–18], can be determined by exponential dilution. This method is particularly well adapted for molecule screening.

DCCLC, initially introduced to study the aqueous solubility of polycyclic aromatic hydrocarbons (PAHs) [19,20] is derived from the Hummel and Dreyer gel-filtration techniques [13]. According to this method, a saturated solution of an hydrophobic compound is gener-

\* Corresponding author.

ated by pumping water through a generator column containing glassbeads coated with the hydrophobic compound. The concentration of this compound, which corresponds to the solubility of the compound in water, is determined by HPLC using a reversed phase contained in the analytical column. A short  $C_{18}$  reversed-phase column, the extractor column, can be placed between the generator and the analytical columns. When a macromolecule (M) aqueous solution is used instead of water for the generator column flow, an increase in the solubility of the hydrophobic compound (H), resulting from complex formation, is detected by HPLC. The association constant ( $K_a$ ) corresponding to the equilibrium:



$$K_a = \frac{[MH]}{[M][H]}$$

may be calculated, assuming that the hydrophobic compound concentration in the generator column is not depleted due to extensive complex formation, according to:

$$k_a = \frac{S_t - S_0}{[M]_t S_0}$$

where  $S_0$  is the solubility of the hydrophobic compound in water,  $S_t$  its solubility in macromolecular solution and  $[M]_t$  the initial macromolecular concentration.

The objective of the present study is to adapt DCCLC in order to determine the intensity of the interactions between food constituents such as aroma compounds and natural polymers previously detected by exponential dilution. Limonene and  $\beta$ -ionone and dextrin and soya bean trypsin inhibitor were chosen as models compounds for these two categories of components.

## 2. Experimental

### 2.1. Material

Corn starch dextrin Tackidex J060K was kindly donated by Roquette Frères (62136 Lestrem). Soya bean trypsin inhibitor, typeII-S, limonene

and  $\beta$ -ionone were from Sigma (St. Louis, MO, USA).

### 2.2. Dynamic coupled column liquid chromatography (DCCLC)

DCCLC equipment, similar to that used by May et al. [19,20] was used. The stainless steel generator column ( $25 \times 0.46$  cm I.D.) was fitted with glass beads 80–120 mesh coated with aroma compounds (1% w/w).

For the determination of aroma compound solubility this column was eluted with distilled water at 25°C at a flow-rate varying from 2.0 to 4.7 ml/min using a Milton Roy pump. The saturated aqueous solutions were introduced through the sample loop (20  $\mu$ l) of a 6-port switching valve (Rheodyne) onto the HPLC column.

For the determination of aroma compound solubility in the presence of macromolecules the distilled water was replaced by an aqueous solution of the macromolecule under study.

The extraction column, when used, located between the generator and analytical column in the place of the sample loop, was a Bondapack  $C_{18}$ , 300 Å, 37–55  $\mu$ m,  $6 \times 0.46$  cm I.D. column (Waters).

### 2.3. High-performance liquid chromatography

A Shimadzu LC 9A pumping system fitted with a Spheri 5 RP<sub>18</sub>, 5  $\mu$ m,  $25 \times 0.46$  cm I.D. (Applied Biosystem, San José, CA, USA), a Varian 2550 UV detector and a Shimadzu CR 6A integrator was used. The column was eluted with acetonitrile–water (80:20, v/v) at a flow rate of 1 ml/min. Detection was performed at 294 nm for  $\beta$ -ionone and 210 nm for limonene, the aroma compound concentrations were calculated from the peak areas using response coefficients determined for each compound from solutions of known concentration.

### 2.4. Exponential dilution

The exponential dilution equipment as previously described [17] was used. Dilute solutions of

volatile compounds contained in an equilibrium cell, maintained at  $25 \pm 0.1^\circ\text{C}$ , were stripped by nitrogen at a flow-rate between 30 and 100 ml/min according to the nature of the volatile compound under study. The gas leaving the cell was automatically sampled every 1 to 3 min through a 6-way electropneumatic valve VICI thermostated at  $150^\circ\text{C}$ . This valve was operated by the chromatograph relay.

A Varian Model 3300 chromatograph, fitted with an FID detector and a CP-Sil 5 CB 5 (methyl silicone) (Chrompack, Middelburg, Netherlands) silica capillary column (50 m  $\times$  0.32 mm I.D.) and a Shimadzu CR 3A integrator, isothermally operated at  $150^\circ\text{C}$ , was used for dynamic head space analysis.

An all-glass closed diffusion cell as described by Duhem and Vidal [12] for non-foaming materials was used, the gas flow was dispersed into small-diameter bubbles through a glass frit disk (No. 4).

A 0.5- $\mu\text{l}$  volume of limonene or 50  $\mu\text{l}$  of  $\beta$ -ionone were added with a chromatographic syringe fitted with a long needle to 30 g of water contained in the diffusion cell. The infinite dilution activity coefficient in water,  $\gamma_{iw}^\infty$ , was calculated from the exponential decrease of the volatile compound concentration determined by GLC.

For the determination of the infinite dilution activity coefficient in the presence of a macromolecular system,  $\gamma_{im}^\infty$ , the same quantities of aroma compounds were introduced in 30 g of water containing 0–5% (w/w) dextrin, 0–2% (w/w) of trypsin inhibitor. The mixture was incubated for 2 h at  $25^\circ\text{C}$  under magnetic stirring prior to measurement.

The reduced activity coefficient  $\gamma_{ir}^\infty$ , defined by the ratio  $\gamma_{im}^\infty/\gamma_{iw}^\infty$ , gives a good indication of the extent of these interactions [16,17].

## 2.5. Statistical treatment of data

The population standard deviation indicated in Table 3 has been calculated with the equation:

$$\sqrt{\frac{n\sum x^2 - (\sum x)^2}{n^2}}$$

The mean difference test (two-sided) accounts for a significant difference between two means  $\mu_1$  and  $\mu_2$  in two normal distributions  $N(\mu_1, \sigma^2)$  and  $N(\mu_2, \sigma^2)$ .

From a  $n_1$ -size sample ( $x_{11}, x_{12}, \dots, x_{1n_1}$ ) and a  $n_2$ -size sample ( $x_{21}, x_{22}, \dots, x_{2n_2}$ ), the hypothesis, to be tested is  $H_0: \mu_1 = \mu_2$  against the alternative hypothesis  $H_1: \mu_1 \neq \mu_2$ . The test is performed using the t-distribution of degree of freedom ( $n_1 + n_2 - 2$ ):

$$\frac{|\bar{X}_1 - \bar{X}_2|}{\sqrt{\left(\frac{1}{n_1} + \frac{1}{n_2}\right)\left(\frac{S_1 + S_2}{n_1 + n_2 - 2}\right)}} > t\left(\frac{\alpha}{2}, n_1 + n_2 - 2\right)$$

$\mu_1$ : population mean 1;  $\mu_2$ : population mean 2

$\bar{X}_1$ : sample mean 1;  $\bar{X}_2$ : sample mean 2

$S_1$ : sum of square 1;  $S_2$ : sum of square 2

$\sigma^2$ : population variance;  $\alpha$ : significance level (5%)

$$S = \sum(x - \bar{X})^2$$

## 3. Results and discussion

### 3.1. Preliminary study

When DCCLC is used, the first step in the calculation of the association constant is the determination of the solubility of the aroma compound in water. It was necessary to check the constancy of the aroma compound concentration at the exit of the generator column for sufficiently large eluent volumes.

The results given in Figs. 1 and 2 for  $\beta$ -ionone and limonene show that solutions with a constant concentration may be obtained after a short purge period. It was also shown, using limonene, that a modification (increase or decrease) of the flow-rate of water through the generator column when the equilibrium is reached slightly alters the concentration. The fact that the equilibrium is rapidly restored is indicative of the dynamic and reversible nature of the transfer process.

Solubility, which is the mean concentration calculated for a flow-rate of 2 ml/min in the generator column, was determined from the data of Figs. 1 and 2 for  $\beta$ -ionone and limonene, the

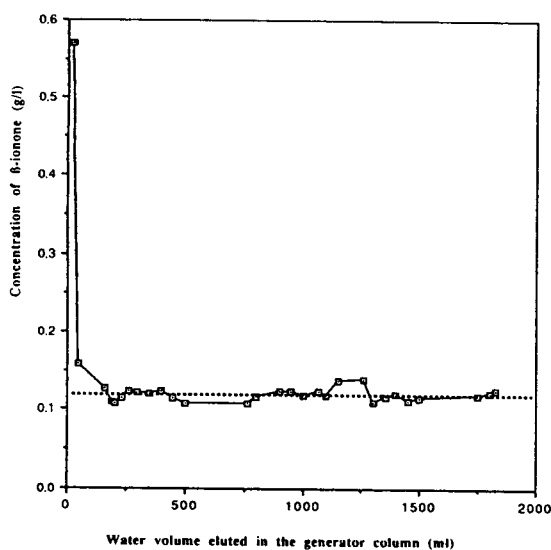


Fig. 1. Variation of the concentration of  $\beta$ -ionone aqueous solution (g/l) eluted from the generator column as a function of the water volume (ml) passed through the generator column. ( $\square$ )  $\beta$ -Ionone concentration, ( $\cdots$ ) mean  $\beta$ -ionone concentration.

values obtained being  $119.6 \pm 7.9$  mg/l and  $12.7 \pm 1.9$  mg/l, respectively.

A major problem in determining the solubility of hydrophobic compounds is that adsorption on the vessel walls generally leads to underestimated values. This problem is largely avoided using DCCLC, although adsorption may occur in the sample loop which alternately contains saturated solutions of aroma compound and solvent used for elution of the HPLC column.

The adsorption of limonene, the most hydrophobic compound used in this study, was evaluated with different volumes of the saturated solution pumped through the sample loop before injection. The increase in limonene concentration detected by HPLC when the volume of the limonene saturated solution passed through the sample loop was more than 2 ml (Table 1) is indicative of adsorption of limonene on the sample loop walls. According to this result a volume of saturated solution less than 2 ml should have been used for the determination of the solubility of limonene or  $\beta$ -ionone.

It was found that the concentration column

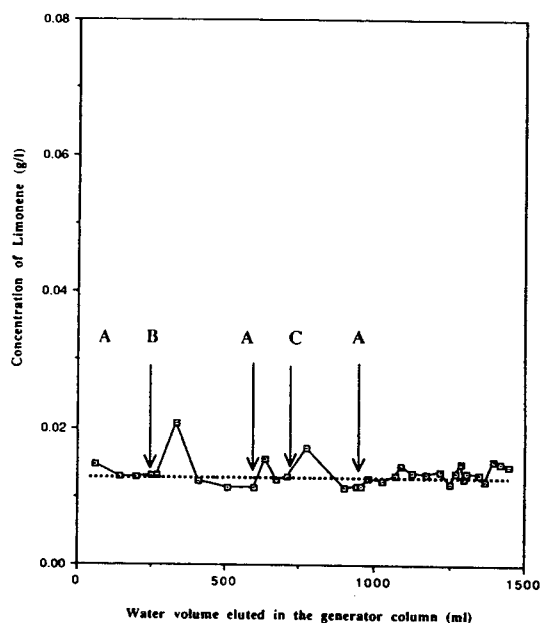


Fig. 2. Variation of the concentration of limonene aqueous solution (g/l) eluted from the generator column as a function of the water volume (ml) passed through the generator column at several flow-rates; (A) 2.0 ml/min, (B) 3.7 ml/min, (C) 4.7 ml/min. ( $\square$ ) Limonene concentration, ( $\cdots$ ) mean limonene concentration.

used for PAH studies [19,20] was not needed when  $\beta$ -ionone and limonene were used as the hydrophobic compounds.

### 3.2. Evidence for interactions between aroma compounds and polymers

A decrease in  $\gamma_{ir}^{\infty}$  is observed when limonene is added to an aqueous solution of dextrin or of soya bean trypsin inhibitor (Fig. 3). As a consequence of the interactions occurring between the aroma compounds and the macromolecular systems in aqueous solutions, the reduced infinite dilution activity coefficient  $\gamma_{ir}^{\infty}$  varies with the polysaccharide or peptide concentration. A decrease indicates the retention of the aroma compound by the macromolecule whereas an increase indicates an increase of the vapor pressure of the volatile compound in the vapor phase known as "salting-out effect" [3,16-18]. The

Table 1  
Adsorption from a saturated solution of limonene on the sample loop walls

Volume of limonene saturated solution passed through the sample loop (ml)	Limonene concentration (mg/l)	Adsorption (%)
1	13.00	0
2	12.72	0
3	14.32	11
5	16.26	22
10	19.54	35

Water flow-rate (generator column): 2 ml/min. Limonene concentration is determined by HPLC, Spheri 5 RP 18 (5  $\mu\text{m}$ , 25  $\times$  0.46 cm I.D.) column, eluted with acetonitrile–water (80:20, v/v) at a flow-rate of 1 ml/min. Detection at 210 nm.

observed decrease of the limonene  $\gamma_{ir}^{\infty}$  is the result of the retention of this compound by the two polymers.

This retention is confirmed using DCCLC. When the generator column coated with  $\beta$ -ionone or limonene is eluted with a solvent containing dextrin or soya bean trypsin inhibitor, an increase of the peak area of the compound–

limonene or  $\beta$ -ionone–in the HPLC chromatogram is observed (Fig. 4). This increase, corresponding to an increase in the solubility of the aroma compound, is the result of the formation of a complex between the aroma compound and the polysaccharide or the peptide [21].

### 3.3. Complex reversibility

The reversibility of the complex formation between limonene and dextrin or soya bean trypsin inhibitor was established from the results obtained with alternate elution with water and with the macromolecular system solutions from the generator column coated with limonene. As indicated in Table 2 the limonene concentration rapidly increased from ca. 13 mg/l, corresponding to the water solubility of this compound, to ca. 21 mg/l when 0.5% (w/w) of trypsin inhibitor is substituted for water. When this solvent is used again, the limonene solubility again decreases to its original value. Analogous results were obtained in the presence of dextrin. The rate of the increase and decrease of the limonene concentration is a strong argument for the reversibility of the complex formation [22].

### 3.4. Determination of association constants

The values of the association constants for limonene and dextrin and soya bean trypsin inhibitor, calculated according to the equation

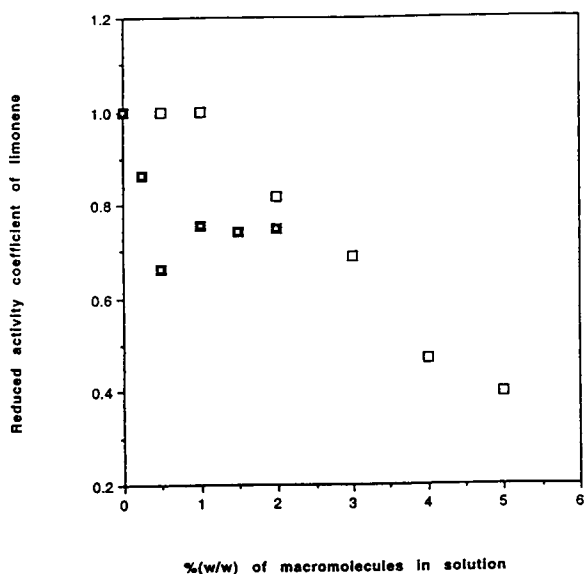


Fig. 3. Variations of limonene reduced infinite dilution activity coefficient as a function of: (□) dextrin Tackidex J060K, (■) soya bean trypsin inhibitor percent (w/w) in water.

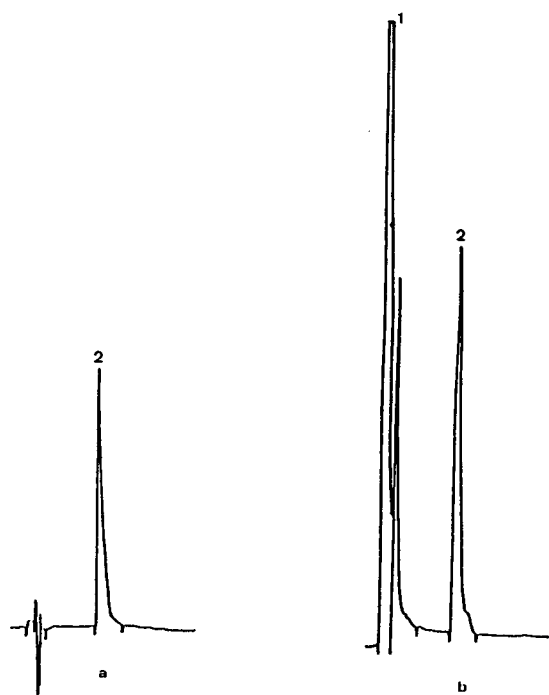


Fig. 4. HPLC chromatogram of limonene eluted at a flow-rate of 2 ml/min from the generator column, (a) with water, (b) with a soya bean trypsin inhibitor aqueous solution (10 g/l). Spheri 5 RP 18 ( $5 \mu\text{m}$ ,  $25 \times 0.46 \text{ cm}$  I.D.) column; elution solvent, acetonitrile–water (80:20, v/v) at a flow-rate of 1 ml/min; detection at 210 nm. Peaks: 1 = trypsin inhibitor, 2 = limonene.

given in the Introduction, are given in Table 3. A 1:1 stoichiometry for the complexes is assumed, and the values reported are means of the values obtained for different generator column eluent volumes. A mean difference test reveals no significant differences at the 95% confidence level for the values obtained for different macromolecule concentrations in the eluent, 0.5–5% for dextrin and 0.25–1% for soya bean trypsin inhibitor. Since the association constants of the complexes formed between limonene and dextrin and soya bean trypsin inhibitor are independent of the macromolecule concentration it can be concluded that neither the macromolecule concentration nor the limonene concentration are limiting.

Under the same experimental conditions, when elution of the generator column coated

Table 2

Reversibility of limonene–soya bean trypsin inhibitor complex: solubility of limonene as a function of the nature and the volume of eluent used

Eluent	Eluent volume (ml)	Limonene concentration (mg/l)
Water	60	14.68
	200	12.99
	600	15.53
	1000	12.41
Soya bean trypsin inhibitor (0.5% w/w)	50	21.86
	100	31.04
	150	20.74
	175	20.80
Water	20	14.53
	100	13.26
	200	13.51

Solvent flow-rate (generator column): 2 ml/min. Limonene concentration is determined by HPLC, Spheri 5 RP 18 ( $5 \mu\text{m}$ ,  $25 \times 0.46 \text{ cm}$  I.D.) column, eluted with acetonitrile–water (80:20, v/v) at a flow-rate of 1 ml/min. Detection at 210 nm.

with  $\beta$ -ionone is performed with dextrin solutions (1 and 2.5% w/w), a steady decrease of the calculated value for the association constant is observed when the elution volume is increased (Table 4). According to Blyshak et al. [21] this phenomenon is indicative of an irreversible adsorption of  $\beta$ -ionone to dextrin.

When a  $\beta$ -ionone generator column is eluted using a 0.5% soya bean trypsin inhibitor solution the  $\beta$ -ionone solubility is unchanged relative to pure water. In contrast, the  $\beta$ -ionone solubility is increased and the association constant  $K_a = 385 \pm 105 \text{ M}^{-1}$  can be calculated when the trypsin inhibitor concentration is increased to 1% (w/w). The  $K_a$  value obtained is indicative of a weak interaction between the two components.

#### Acknowledgements

This work was supported by the Ministère de la Recherche et de la Technologie, grant no. 90 G 0325, "Interactions entre les biopolymères d'origine levurienne et les composés d'arôme du



Table 3

Association constants ( $M^{-1}$ ) for dextrin–limonene and soya bean trypsin inhibitor–limonene complexes as a function of the macromolecule percent

Macromolecule (%)	$K_a$ ( $M^{-1}$ )	
	Dextrin	Soya bean trypsin inhibitor
0.25	–	2929 ± 207
0.50	15 607 ± 2094	2932 ± 1124
1.00	16 122 ± 2573	2978 ± 220
2.50	12 801 ± 1008	–
5.00	11 963 ± 603	–
Mean	13 650 ± 250	2944 ± 784

Solvent flow-rate (generator column): 2 ml/min. Limonene concentration is determined by HPLC, Spheri 5 RP 18 (5  $\mu$ m, 25 × 0.46 cm I.D.) column, eluted with acetonitrile–water (80:20, v/v) at a flow-rate of 1 ml/min. Detection at 210 nm.

Table 4

Variation of the calculated values for the association constant of the dextrin– $\beta$ -ionone complex as a function of the dextrin solution elution volume for two dextrin concentrations

Elution volume (ml)	$K_a$ ( $M^{-1}$ )	
	Dextrin 1%	Dextrin 2.5%
40	3960	3580
60	3360	3247
120	3028	3207
160	2762	3114
200	2728	3021
250	2495	2875
280	2395	2821

Solvent flow-rate (generator column): 2 ml/min.  $\beta$ -Ionone concentration is determined by HPLC, Spheri 5 RP 18 (5  $\mu$ m, 25 × 0.46 cm I.D.) column, eluted with acetonitrile–water (80:20, v/v) at a flow-rate of 1 ml/min. Detection at 294 nm.

vin”, and one of the author (S.L.) received financial support of the same Ministère.

## References

- [1] A.A. Spector, J. Kathryn and J.E. Flechte, *J. Lipid Res.*, 10 (1969) 56.
- [2] S. Damadoran and J.E. Kinsella, *J. Agric. Food Chem.*, 28 (1980) 567.
- [3] A. Sadafian and J. Crouzet, in D. Joulain (Editor), *Progress in Terpene Chemistry*, Frontières, Gif sur Yvette, 1987, p. 165.
- [4] A. Voilley, D. Simatos and M. Loncin, *Lebensm. Wiss. u. Technol.*, 10 (1977) 45.
- [5] M. Beyeler and J. Solms, *Lebensm. Wiss. u. Technol.*, 7 (1974) 217.
- [6] S. Damadoran and J.E. Kinsella, *J. Agric. Food Chem.*, 29 (1981) 1249.
- [7] S. Damadoran and J.E. Kinsella, *J. Agric. Food Chem.*, 29 (1981) 1253.
- [8] T.E. O'Neill and J.E. Kinsella, *J. Agric. Food Chem.*, 35 (1987) 770.
- [9] T.E. O'Neill and J.E. Kinsella, *J. Food Sci.*, 53 (1988) 906.
- [10] L.A. Wilson, in M.R. Okos (Editor), *Physical and Chemical Properties of Food*, Am. Soc. Agricultural Engineers, St. Joseph, 1986, p. 382.
- [11] J.C. Leroi, J.C. Masson, H. Renon, J.F. Fabries and H. Sannier, *Ind. Eng. Chem. Proc. Des. Dev.*, 16 (1977) 139.
- [12] P. Duhem and J. Vidal, *Fluid Phase Equilib.*, 2 (1978) 231.
- [13] J.P. Hummel and W.J. Dreyer, *Biochem. Biophys. Acta*, 63 (1962) 530.
- [14] B. Seville, N. Thuaud, J.P. Tillement, *J. Chromatogr.*, 167 (1978) 159.
- [15] S.F. Sun, S.W. Kuo and R.A. Nash, *J. Chromatogr.*, 288 (1984) 377.
- [16] A. Lebert and D. Richon, *J. Agric. Food Chem.*, 32 (1984) 1151.
- [17] S. Langourieux and J. Crouzet, *Lebensm. Wiss. u. Technol.*, 27 (1994), in press.
- [18] D. Richon, F. Sorrentino and A. Voilley, *Ind. Eng. Chem. Pros. Des. Dev.*, 24 (1985) 1160.
- [19] W.E. May, S.P. Wasik and D.H. Freeman, *Anal. Chem.*, 50 (1978) 175.
- [20] W.E. May, S.P. Wasik and D.H. Freeman, *Anal. Chem.*, 50 (1978) 997.
- [21] L.A. Blyshak, K.Y. Dodson, G. Patonay, I.M. Warner and W.E. May, *Anal. Chem.*, 61 (1989) 955.
- [22] W.E. May, Ph.D. Thesis, University of Maryland, MD, 1977.





ELSEVIER

Journal of Chromatography A, 707 (1995) 189–197

JOURNAL OF  
CHROMATOGRAPHY A

## Analysis of colloids

# VIII. Concentration- and memory effects in size exclusion chromatography of colloidal inorganic nanometer-particles<sup>☆</sup>

Christian-Herbert Fischer\*, Thore Siebrands

*Hahn-Meitner Institut Berlin, Abt. Kleinteilchenforschung, Glienicker Str. 100, D-14109 Berlin, Germany*

First received 1 December 1994; revised manuscript received 31 December 1994; accepted 8 March 1995

### Abstract

Colloidal cadmium sulfide with diameters of ca. 17 nm was used as a model substance to study the effects of sample concentration on elution time and peak area in size exclusion chromatography (SEC) of colloidal inorganic particles in the low nm-size regime. A clear distinction had to be made between the pure particle concentration and that of the accompanying electrolytes. The effects were astonishingly high taking into account that particles and small electrolytes are separated immediately in SEC. The reasons for these phenomena are discussed. The electrical double layer was found to play an important role. The results obtained for solid particles were compared with those for organic polymers in SEC. A memory effect of the column was observed due to temporarily adsorbed particles.

### 1. Introduction

Colloidal inorganic particles of metals as well as of semiconductors present a very exciting and rapidly growing topic in physical chemistry because of their extraordinary properties [4]. After size exclusion chromatography (SEC) had been applied to the characterization of organic polymer latex samples down to a size of 100 nm [5], it has been shown that this method is also a powerful tool for the research on particles with a diameter ranging between 2 nm and 20 nm. It not only provides rapid information about the

size distribution [3,6], but also about the size depending properties, when appropriate detectors are used, e.g. UV-Vis spectra with a diode-array detector [7]. Colloidal silica [8], cadmium sulfide [3,6,9], zinc sulfide [3] and gold [10] have been investigated. From the differences between the particular calibration curves the relative thickness of the electrical double layer could be estimated [3]. The study of rigid solid particles, which do not swell or shrink as polymer coils do, could also be helpful in understanding the mechanism of SEC of organic polymers. Preparative SEC is useful when very monodisperse colloids have to be prepared from polydisperse ones [2]. During the studies carried out for the optimization of the conditions of the preparative separations, anomalies were found. The present work

\* Corresponding author.

\* For part VII see Ref. [1], for part VI see Ref. [2] and for part V see Ref. [3].

was performed on an analytical scale in order to elucidate and explain these effects in detail. In SEC of organic polymers strong effects of the concentration on the recovery and the elution time were found [11]. It was also the aim of this work to compare the inorganic particles with the polymers in this respect.

## 2. Experimental

The equipment consisted of a Merck-Hitachi L 6000 pump (Merck, Darmstadt, Germany), and a Merck Hitachi L4200 UV-Vis detector operating at 250 nm or a Waters 990 diode-array detector (Milford, MA, USA) and a Merck-Hitachi autosampler using a 20- $\mu$ l sample loop. Under standard conditions a set of two 125  $\times$  4 mm I.D. Knauer columns (Berlin, Germany) were used in most cases, the first packed with Nucleosil 500 C<sub>4</sub> (7  $\mu$ m) and the second with Nucleosil 1000 C<sub>4</sub> (7  $\mu$ m) from Macherey and Nagel (Düren, Germany). For the estimation of the adsorption a 250  $\times$  4 mm I.D. column packed with Nucleosil 120 C<sub>4</sub> (5  $\mu$ m) was applied. The mobile phase was an aqueous solution of 6 mM sodium polyphosphate (the molarity refers to the phosphate units) (Riedel de Haen, Seelze, Germany) and 1 mM cadmium perchlorate (Ventron, Karlsruhe, Germany). In some experiments these concentrations were higher or sodium chloride (Merck) was added. The flow-rate was 0.5 ml/min. Data were collected either with a Bruker Chromstar system or with a 990 Waters system.

Colloidal cadmium sulfide was prepared from 12 mM cadmium perchlorate, 72 mM polyphosphate and 12 mM hydrogen sulfide gas (Messer Griesheim, Düsseldorf, Germany). The details were described in the previous papers [1–3].

## 3. Results and discussion

Studies on the effect of concentration were carried out with aqueous cadmium sulfide sols, because they belong to the best known inorganic colloids. In general, colloids have to be stabilized

in order to prevent coagulation and even precipitation. In this case polyphosphate was used. It covers the surface of the particles, forming complex bonds [12].

When in preparative SEC sample concentration and sample volume were varied in such a complementary way that the injected sample mass was kept constant, large differences in the resulting chromatograms were found (Fig. 1). The higher the concentration the smaller the eluting peak. This result led to the conclusion that larger sample volumes and low concentrations should be used rather than the opposite, when high yields are required [2]. The following experiments were carried out on an analytical scale with a combination of two C<sub>4</sub> modified-silica columns with 50 nm and 100 nm pore size. The eluent consisted of an aqueous solution of 1 mM cadmium perchlorate and 6 mM polyphosphate (referring to phosphate units) as described previously [7]. The colloidal CdS samples had a relatively large particle size of ca. 17 nm. The reason was that a wide concentration range had

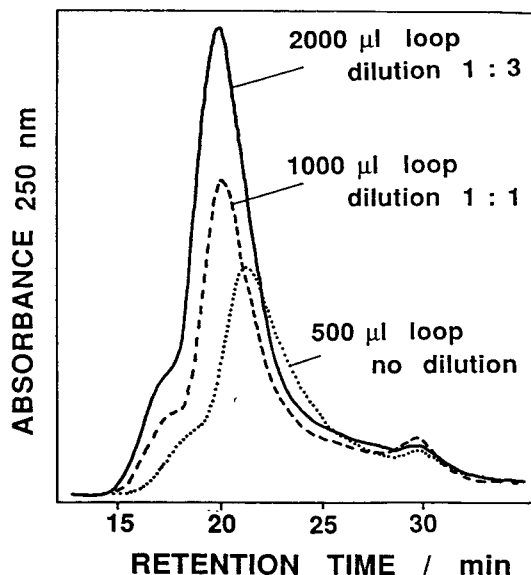


Fig. 1. Preparative chromatograms of a CdS sol (standard conditions as in the present work except for an 8-fold column diameter). The same sample amount was injected three times using different concentrations and correspondingly different volumes as indicated. Compare [2].

to be investigated and smaller particles could not be obtained in high concentrations.

### 3.1. Peak area recovery

A very concentrated cadmium sulfide sol (12 mM CdS) was diluted stepwise with water and injected. Fig. 2 shows three normalised chromatograms of this series. With increasing concentration the peak width increased dramatically and also the elution time. The small peak at 4.3 min was due to polyphosphate. Its extinction coefficient is very low at 250 nm and it can not be detected when its concentration is the same as in the eluent.

In this section, the area and shape of the CdS peak will be discussed. In Fig. 3 peak width and area were plotted versus the CdS concentration. Astonishingly the latter function had a pronounced maximum at 10 mM CdS and decreased thereafter. It is necessary to stress that in this low nm-range the colloidal particles do not show any significant scattering [4]. Moreover the extinctions were quite low and in the range of Lambert–Beer's law. So the measured extinctions were proportional to the CdS concentration. Therefore it must be concluded that with increasing concentration an increasing amount of colloidal particles was lost in the column. If the

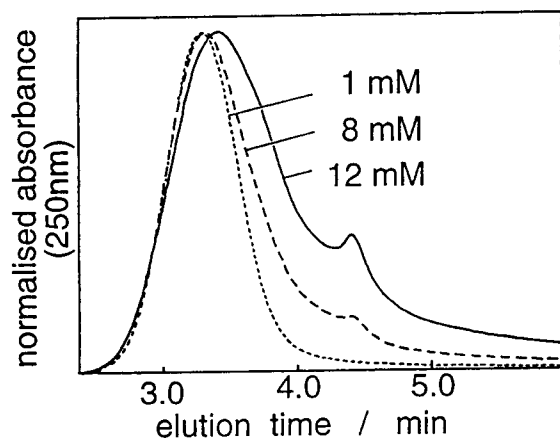


Fig. 2. Normalised chromatograms of a CdS sol of different concentrations as indicated (standard conditions; dilution medium: water).

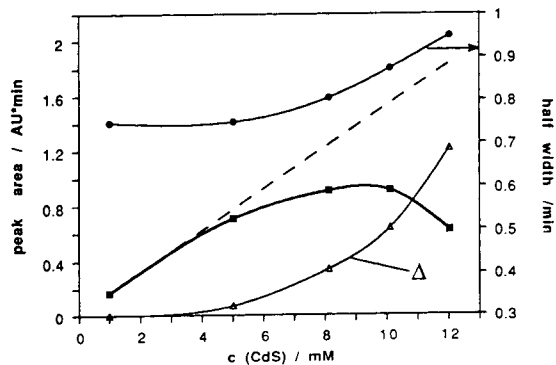
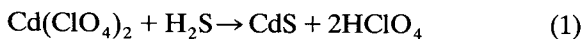


Fig. 3. SEC of a 12 mM CdS sol stepwise diluted with water (standard conditions). Area (■) and half width (●) of the CdS peak as a function of the CdS concentration.  $\Delta$  Area ( $\Delta$ ) is the loss of CdS calculated as the difference between the area curve and its extrapolated initial slope.

loss is assumed to be negligible in the lowest concentration range, the lost amount at higher concentration can be estimated from the difference  $\Delta A$  between the measured peak area and the linear extrapolation of the initial slope (Fig. 3). The only explanation for this effect can be an irreversible adsorption of the CdS particles on the surface of the stationary phase. A strong adsorption at high concentration was also indicated by increased tailing (see half peak width, Fig. 3) and finally by the fact that after many CdS injections (after several months) the first part of the column was turning yellow. The effect of electrolyte concentration on adsorption, aggregation and flocculation is well known [13]. Examples for such an exponentially increasing adsorption are described in the literature [14] for multilayer adsorption when the first layer is complete. Taking the small sample volume of 20  $\mu$ l and the low particle concentration (not molar CdS concentration, *vide infra*) into consideration, such a multilayer adsorption is very unlikely. Moreover, in the section dealing with the memory effect, it will be shown that the adsorption activity of a CdS covered surface was lower than that of a clean surface. Nevertheless, some change in the system has to occur. The eluent composition and the stationary phase remained the same. Therefore the reason for this anomaly has to be found in the sample itself. A

similar effect was observed in SEC of organic polyelectrolytes, e.g. proteins in an ionised form. Potschka [15] and Hearn et al. [16] described the lower recovery at high concentrations in these cases. Solid particles carrying surface charges might be considered as a special case of a polyelectrolyte. Now it should be noted that in the preparation of the CdS sols, hydrogen sulfide gas was added to a cadmium perchlorate/polyphosphate solution. According to Eq. 1



two molecules of perchloric acid per molecule cadmium sulfide are formed. When the dilution was carried out with water, of course all of the electrolytes present were also diluted. It is well known in colloid chemistry that electrolytes decrease the stability of sols. The surface charges of the colloidal particles cause a repulsion from each other. Oppositely charged ions from the solution are adsorbed onto the particles, thereby diminishing the net charge and thus the repelling forces. Consequently, adsorption among the particles (= coagulation) and enhanced adsorption on other surfaces occurs.

If this assumption is right, it is clear that electrolytes in the eluent should have an even worse effect, because particles are in contact with the eluent during the whole passage through the column. In the experiments of Fig. 4 a concentration series (dilution medium: water) was injected onto the HPLC system using different eluent compositions: (a) 1 mM cadmium perchlorate–6 mM polyphosphate (standard condition); (b) 1 mM cadmium perchlorate–6 mM polyphosphate–10 mM sodium chloride; (c) 8 mM cadmium perchlorate–48 mM polyphosphate.

An addition of 10 mM sodium chloride to the normal eluent reduced the CdS peak area by roughly 25%, whereas an eight-fold increase of the normal cadmium perchlorate/polyphosphate concentration led to a loss of about 80% cadmium sulfide. The reason for this was that the multiple-charged electrolytes destabilise colloids more than single-charged electrolytes (see also electrical double layer in the next paragraph).

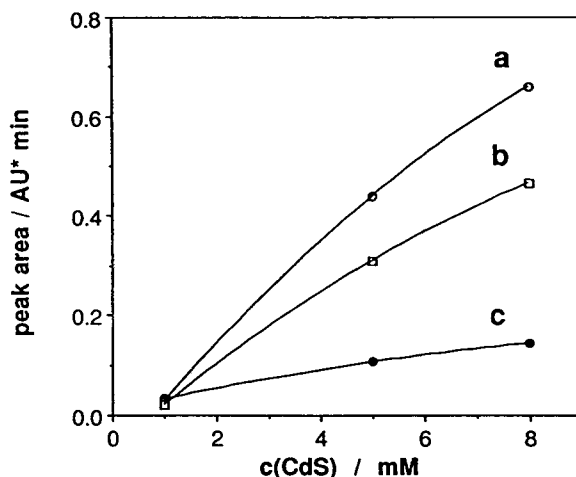


Fig. 4. SEC of a CdS sol using three different eluent compositions: (a) 1 mM cadmium perchlorate–6 mM polyphosphate (standard condition); (b) 1 mM cadmium perchlorate–6 mM polyphosphate–10 mM sodium chloride; (c) 8 mM cadmium perchlorate–48 mM polyphosphate. CdS peak area as a function of the CdS concentration (dilution medium: water).

These latter experiments show the strong effect of electrolytes and explain also the change in the recovery in one series in terms of electrolyte content.

In order to study the effect of the particle concentration, further dilution series with different dilution media were performed: (a) water, i.e. the electrolytes were diluted by a factor of up to twelve; (b) 72 mM polyphosphate, i.e. the polyphosphate concentration of the most concentrated CdS sol was kept constant in all diluted samples; (c) 72 mM polyphosphate–24 mM perchloric acid, i.e. the electrolyte concentration of the most concentrated CdS sol is kept constant in all diluted samples.

The results under standard chromatographic conditions are shown in Fig. 5. Compared to series (a) with a change of all concentrations, the constant polyphosphate content (curve b) did not essentially change the situation, because polyphosphate forms complexes with the particles and thus stabilises them [12]. However, the constant perchloric acid concentration led to an increased adsorption of colloidal CdS. The al-

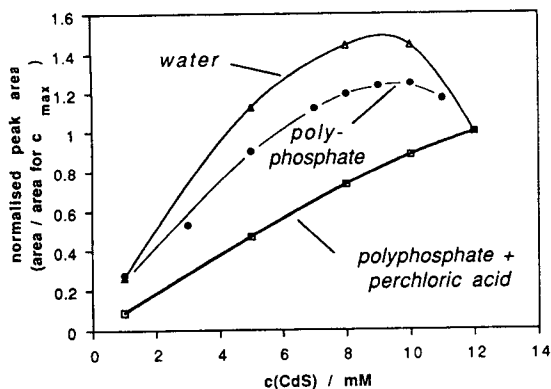


Fig. 5. SEC of a 12 mM CdS sol stepwise diluted with (a) water ( $\Delta$ ), (b) 72 mM polyphosphate ( $\bullet$ ), or (c) 72 mM polyphosphate–24 mM perchloric acid ( $\square$ ) solutions. Normalised CdS peak area (referring to the peak area of the undiluted original sample).

most linear curve c indicates an adsorption proportional to the particle concentration. This result was in accordance with previous stationary experiments studying the adsorption of ferric oxide or arsenic trisulfide sols on silica. Also Freundlich et al. [17] and Buzágh et al. [18] described the independence of adsorption on particle concentration as long as the electrolyte content was constant. It is worth mentioning that all CdS peaks of series c had the same retention time and very broad half widths just as the highest of series a. Obviously the electrolytes, in the present case especially the perchloric acid, were responsible for the loss of CdS particles. The concentration of the particles themselves had only a relatively small effect on the adsorption. Anyhow, the astonishing point about the chromatography was that the electrolytes in the sample had such a strong effect, although they were separated immediately from the particles by the SEC mechanism because these ions are comparatively very small. The adsorption can only take place in the very first part of the column. It should be stressed that all injected solutions were clear without any flocculation. However, it seems reasonable that the colloid in the sample has already been (at least partially) destabilized by the electrolyte environment.

### 3.2. Elution times

In SEC of organic polymers concentration effects are well studied. Several reasons for these effects have been discussed [11,19–22]: hydrodynamic volume contraction, frictional forces, viscosity phenomena and secondary exclusion, i.e. the analyte itself consumes space in the pores and thus reduces the accessible volume. Janca [20] found a relative increase of the elution volumes of about 5% for polystyrenes with a molar mass of 498 000 and 867 000, when the concentration was varied between 0.005% and 0.1% (w/v). In the consideration of inorganic colloids again the two cases have to be distinguished:

(A) When both the particle and the electrolyte concentration varied in parallel (upon dilution in water), the elution times  $t_e$  were constant at 3.16 min below a concentration of 5 mM CdS and increased up to 3.31 min at a concentration of 12.5 mM, i.e. an increase of ca. 5%, (Fig. 6, left, curve b; please note the expanded time scale!). The calibration on this column combination was established by electron microscopy with CdS concentrations not higher than 1 mM (compare [3]). After conversion of the equation for the calibration line (Eq. 2) to the exponential form (Eq. 3) diameters could be calculated.

$$\log d = -0.734t_e + 3.558 \quad (2)$$

$$d = 3612 \cdot 10^{-0.734t_e} \quad (3)$$

Thus the two above mentioned elution times of the different sample concentrations correspond to diameters,  $d$ , between 17.26 nm and 13.40 nm (Fig. 6, right part). The difference  $\Delta d$  was 3.86 nm.

Within the possible concentration range no differences in viscosity between the sols and pure water could be measured with an Ubbelohde viscosimeter. Therefore changes in viscosity can be neglected for inorganic colloids. One could argue that the shift was only due to the enhanced adsorption discussed in the previous section. That could be proofed by using a Nucleosil 120 C<sub>4</sub> column (5  $\mu$ m, 250  $\times$  4 mm I.D.) instead of the Nucleosil 500 C<sub>4</sub> and 1000 C<sub>4</sub> (7  $\mu$ m, 120  $\times$  4

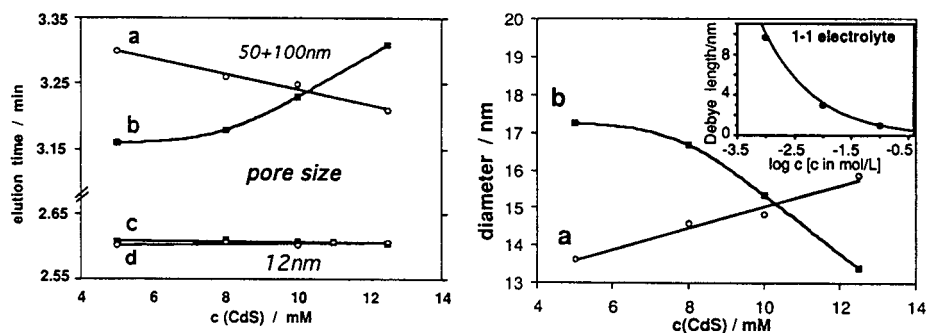


Fig. 6. SEC of a 12 mM CdS sol stepwise diluted with water (■) or 72 mM polyphosphate–24 mM perchloric acid (○) solution, respectively. Left part: Elution time as a function of the CdS concentration. Curves a and b: chromatographic standard conditions. For comparison all samples were also injected on a Nucleosil 120 C<sub>4</sub> column, 250 × 4 mm I.D. (curves c and d). Right part: Average particle diameters corresponding to curves a and b in the left part calculated from the calibration Eq. 3 as a function of the CdS concentration. Inset: Debye length as a function of the concentration of an 1–1 electrolyte according to the Debye–Hückel model.

mm I.D. each), i.e. the same material with small pore size, where adsorption should be dominant and any SEC mechanism negligible in this size regime (Fig. 6, left, curves c and d). Only 5- $\mu$ m material was available here; however, the larger specific surface was a compensation for the inaccessible surface inside the pores. Indeed no shift in elution time was observed, indicating that adsorption was not responsible at all for this concentration effect on elution time. However, it is important with respect to the SEC method to stress that generally no preferential adsorption of larger particles was found, which would also explain such a shift. This was shown by the reinjection of collected effluate as well as by sequential injection (see next section).

However, there is another, and probably the most important reason for the shift in elution time in question. An electrical double layer is formed at any charged interface between a solid and a liquid containing electrolytes by attraction of oppositely charged ions towards the surface. The thickness of this layer is dependent on the electrolyte concentration in the solution. The double layer is quite rigid and cannot easily be penetrated, neither by charged nor by neutral species [15]. For coiled, charged organic polymers, such as proteins, Potschka found a similar behaviour of the elution times [15]; thus again there is a parallel with colloidal inorganic par-

ticles, where the interface is really obvious. Therefore the thickness of the double layer has to be taken into account when the effective diameter of a colloidal particle is considered in SEC. However, this thickness depends strongly on the bulk electrolyte valency and concentration, because at higher electrolyte density the potential drops down much faster. The Debye–Hückel model for the diffuse double layer describes the potential  $\Psi$  as a function of the distance  $x$ . In the case of the CdS sols we mainly have to consider perchloric acid as electrolyte, i.e. a 1–1 electrolyte, because the complex formation between polyphosphate and the particles has only minute effects as shown in the previous section. The Debye length  $\kappa^{-1}$  represents that distance  $x$  from the interface, at which the double layer potential  $\Psi$  has dropped down to the value  $\Psi_0/e$ , where  $\Psi_0$  is the potential directly at the interface. The insert in the right part of Fig. 6 shows the Debye length  $\kappa^{-1}$  versus the logarithm of the concentration for a 1–1 electrolyte according to the Debye–Hückel approximation (modified from the data of Hiemenz [23]). In SEC, the shift in elution time took place between 5 mM and 12 mM CdS. This corresponded to 10 mM and 24 mM perchloric acid according to Eq. 1. In that range  $\kappa^{-1}$  decreases from 3 nm to 2 nm, i.e. by a difference  $\Delta(\kappa^{-1}) = 1.0$  nm. This was approximately a quarter of the



measured  $\Delta d$ . However, these calculations can present no more than an estimation because in chromatography we have a steady dilution of the sample and thus varying concentrations. Thus one should expect no more than the right order of magnitude.

(B) When only the concentration of the particles was varied and that of the electrolytes was kept constant, the effect on elution time was opposite (Fig. 6, left, curve b). Here the elution time decreased somewhat with increasing concentration. For the discussion of secondary exclusion the particle concentration  $c_p$  has to be considered. From the elution time  $t_e = 3.16$  min a weight average diameter  $d_w = 17.3$  nm was obtained by means of the calibration. Assuming the particles to be spherical, the volume of one particle was  $V_p = 2711$  nm<sup>3</sup>. With the volume of a CdS unit cell  $V_u = 0.049$  nm<sup>3</sup> a number of unit cells per particle  $n = 55\,300$  was calculated. In the case of the highest used CdS concentration  $c(\text{CdS}) = 12$  mM the CdS particle concentration was  $c_p = 1.3 \cdot 10^{18}$  l<sup>-1</sup>, or in other words one particle in a volume  $V = 7.5 \cdot 10^5$  nm<sup>3</sup>, i.e. 277-fold its own volume. If two Debye lengths of 2 nm are added to  $d_w$ , the effective diameter would be  $d_{\text{eff}} = 17.3$  nm + 4 nm = 21.3 nm and the effective particle volume  $V_{p,\text{eff}} = 5060$  nm<sup>3</sup>, i.e. still one particle in 148-fold its own effective volume. Under these circumstances secondary exclusion should not be very pronounced. Therefore decrease in elution time at high concentration must be explained in terms of partial, weak and reversible agglomeration. Due to dilution during the run through the separation column later disintegration takes place. That is why the decrease in elution time does not correlate to a dimer diameter.

### 3.3. Memory effect

In this section an effect is described which is generally referred to as conditioning. Because in particle chromatography this effect is extraordinarily pronounced and because it is closely related to the previously discussed recovery problem, it should be briefly demonstrated. When the chromatographic signal was greatly

amplified, it was observed that the “baseline” after the colloidal peak was somewhat higher than the initial one. This led to the conclusion that at least a certain portion of the adsorbed CdS was not completely irreversibly adsorbed on the surface of the stationary phase and that it desorbed only very slowly. Injections of pure methanol–water mixtures after several CdS separations wetted the  $C_4$ -phase and led to enhanced desorption, as indicated by the peak, which showed a typical CdS spectrum in the diode-array detector. The area of this “CdS peak” decreased exponentially with the number of methanol injections. After these observations it remained to be investigated whether a stationary phase which was “modified” by adsorbed particles had a different adsorptivity than uncovered fresh material. For this purpose the same 10 mM CdS sol was injected five times after exactly the same intervals (10 min) by an autosampler. Indeed the peak area increased with the number of injections by ca. 10% and reached a plateau after the fifth injection (Fig. 7, inset). Two points were evident:

- (1) The adsorption activity of a stationary phase already covered by CdS was lower than that of an uncovered one.
- (2) The desorption of CdS from the silica

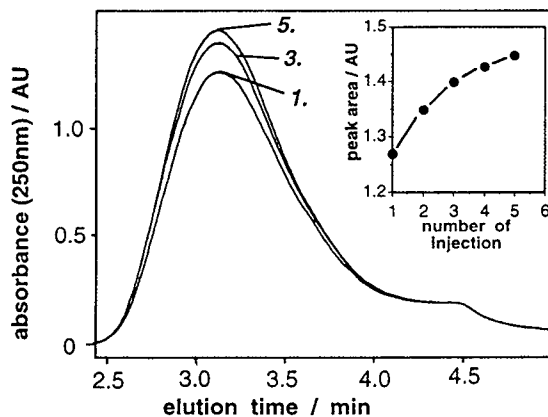


Fig. 7. Memory effect of the column. The same 10 mM CdS sol was injected five times in a 10 min interval (standard condition). Overlay plot of the 1st, 3rd and 5th chromatograms. Inset: CdS peak area as function of the number of injection. (Details in the text).

surface was much slower than the time of one run (5 min).

After five 20- $\mu$ l injections the small initial part of the column bed was covered by CdS, and in this section of the column particles and electrolytes of the sample were not yet completely separated. It can be said that for a certain time the column has a memory of the previous runs, which was lost after careful purging. Fig. 7 shows also that the elution time was constant during the whole series, which excluded any preferential adsorption of particles of one particular size.

The memory effect could also be demonstrated by the experiments shown in Fig. 8. A dilution series of CdS colloids with constant electrolyte content was injected twice, once in increasing order of concentration, and once in decreasing order of concentration. Between both series the column was purged extensively. It is obvious that a sample showed a smaller peak when it was injected on a rather fresh, uncovered clean column surface "with no mem-

ory". At the end of a series the peak was clearly larger. This effect was most pronounced for the most diluted sample, because the loss (ca. 50%) was high compared with the absolute amount of sample.

#### 4. Conclusions

The concentration range for proper SEC of colloidal cadmium sulfide particles has been defined. It has been shown that in the normal concentration range of inorganic sols up to 5 mM the chromatographic behaviour of colloidal cadmium sulfide is quite normal. Above that concentration a dramatic increase of absorption takes place which is mainly caused by the accompanying, and also more concentrated, electrolytes. A remarkably decreased recovery as well as an increase in elution times were found. The changing thickness of the electrical double layer was the main reason for these phenomena. Generally, attention should be paid to the large influence of the electrolytes in the sample, and even more so, in the eluent. Retardation and peak broadening could result in incorrect size distributions. Therefore sol concentrations above 5 mM should be diluted with pure solvent. Increasing particle concentrations with constant electrolyte content gave almost proportional peak areas, but slightly shorter elution times, which is interpreted as weak aggregation.

With respect to concentration effects colloidal inorganic particles behave completely different from neutral organic polymers, but resemble charged polymers such as proteins.

The memory effect of the column was due to a layer of particles on the surface of the stationary phase. If there is a necessity to obtain exact results for particle concentration, one has to work with an already saturated column. However, when SEC is used, generally the main interest is the size distribution, i.e. only the relative amounts of species with different sizes, and fortunately no preferential loss of particular particle sizes was observed here. Therefore the results were not affected by a memory effect.

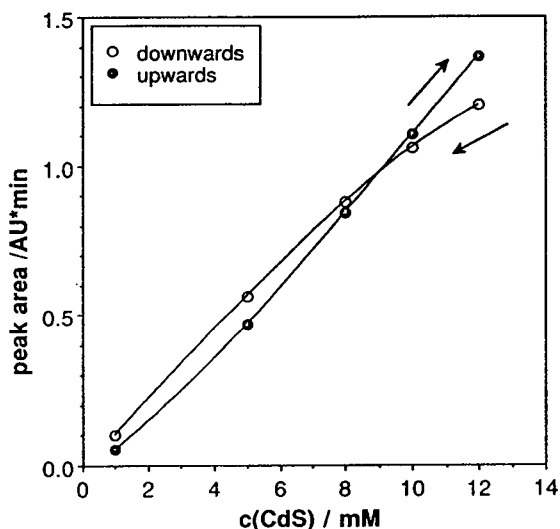


Fig. 8. Memory effect of the column. SEC of a 12 mM CdS sol stepwise diluted with a 2 mM polyphosphate–24 mM perchloric acid solution (standard condition). Order of injection: increasing concentration (●); decreasing concentration (○). Between both series the column was purged extensively. Peak area as a function of CdS concentration.

## Acknowledgement

The authors wish to thank Ms. M. Michalczik for the help with the laboratory work.

## References

- [1] Ch.-H. Fischer, *J. Chromatogr. A*, 688 (1994) 97.
- [2] Ch.-H. Fischer, *J. Liq. Chromatogr.*, 17 (1994) 1593.
- [3] Ch.-H. Fischer, M. Giersig, T. Siebrands, *J. Chromatogr. A*, 670 (1994) 89.
- [4] A. Henglein, *Top. Curr. Chem.*, 143 (1988) 115.
- [5] S. Singh, A.E. Hamielec, *J. Liq. Chromatogr.*, 1 (1978) 187.
- [6] Ch.-H. Fischer, J. Lilie, H. Weller, L. Katsikas, A. Henglein, *Ber. Bunsenges. Phys. Chem.*, 93 (1989) 61.
- [7] Ch.-H. Fischer, H. Weller, L. Katsikas, A. Henglein, *Langmuir*, 5 (1989) 429.
- [8] J.J. Kirkland, *J. Chromatogr.*, 185 (1979) 273.
- [9] Ch.-H. Fischer and M. Giersig, *Langmuir*, 8 (1992) 1475.
- [10] T. Siebrands, M. Giersig, P. Mulvaney, Ch.-H. Fischer, *Langmuir*, 9 (1993) 2297.
- [11] J. Janca, *J. Liq. Chromatogr.*, 3 (1980) 953.
- [12] A. Fojtik, H. Weller, U. Koch, A. Henglein, *Ber. Bunsenges. Phys. Chem.*, 88 (1984) 969.
- [13] D.H. Everett, *Basic Principles of Colloid Science*, Royal Society of Chemistry, Letchworth, UK, 1988.
- [14] A.W. Adamson, *Physical Chemistry of Surfaces*, Wiley and Sons, New York, NY, 1976.
- [15] M. Potschka, *J. Chromatogr.*, 441 (1988) 239.
- [16] M.T.W. Hearn, B. Grego, C.A. Bishop, W.S. Hancock, *J. Liq. Chromatogr.*, 3 (1980) 1549.
- [17] H. Freundlich, A. Poser, *Kolloid-Beihefte*, 6 (1934) 297.
- [18] A. v. Buzágh, E. Kneppó, *Kolloid-Zeitschrift*, 82 (1938) 150.
- [19] J. Janca, S. Pokorny, *J. Liq. Chromatogr.*, 170 (1979) 319.
- [20] J. Janca, *Polymer J.*, 12 (1980) 405.
- [21] J. Janca, S. Pokorny, M. Bleha, O. Chiantore, *J. Liq. Chromatogr.*, 3 (1980) 953.
- [22] O. Chiantore, M. Guaita, *J. Chromatogr.*, 353 (1986) 285.
- [23] P.C. Hiemenz, *Principles of Colloid and Surface Chemistry*, 2nd ed., Marcel Dekker, New York 1986.





ELSEVIER

Journal of Chromatography A, 707 (1995) 199–203

JOURNAL OF  
CHROMATOGRAPHY A

# Molecular imprinting of acetylated carbohydrate derivatives into methacrylic polymers<sup>☆</sup>

Kurt G.I. Nilsson<sup>a,\*</sup>, Kenji Sakaguchi<sup>b</sup>, Peter Gemeiner<sup>c</sup>, Klaus Mosbach<sup>a</sup>

<sup>a</sup>Department of Pure and Applied Biochemistry, Chemical Center, University of Lund, P.O. Box 124, S-221 00 Lund, Sweden

<sup>b</sup>Nihon Shokuhin Kako Co., 4-1, Maruno-ichi, 3-Chome Chiyoda Ku, Tokyo, Japan

<sup>c</sup>Institute of Chemistry, Slovak Academy of Sciences, Dubravská cesta 9, 842 SK 38 Bratislava, Slovak Republic

First received 18 May 1994; revised manuscript received 20 February 1995; accepted 27 February 1995

## Abstract

The non-covalent imprinting procedure was used for the preparation of polymers selective for various carbohydrate derivatives, i.e. peracetylated phenyl  $\alpha$ - and  $\beta$ -D-glycosides of galactose. The selectivities of the resulting polymers were tested in a HPLC procedure. The selectivity was influenced by the anomeric configuration of the glycoside ( $\alpha$ - or  $\beta$ -configuration). Thus, a polymer prepared with *p*-aminophenyl  $\beta$ -galactoside as print molecule, gave a relatively high selectivity ( $\alpha = 1.27$ ) for the  $\beta$ -galactoside over the  $\alpha$ -galactoside, whereas a polymer prepared with the corresponding  $\alpha$ -galactoside showed no or low selectivity towards the  $\alpha$ -glycoside ( $\alpha = 1.02$ ). Moreover, the structure of the aglycon was important. Thus, the use of aminophenyl glycosides as print molecules resulted in polymers with induced selectivity, whereas the use of the corresponding nitrophenyl- and acetaminophenyl-galactosides gave no induced selectivity.

## 1. Introduction

The method of preparing polymers with different selectivities, named molecular imprinting, has recently been demonstrated to be a powerful technique to prepare chromatographic adsorbents suitable for the chiral separation of biologically active compounds [1]. Thus, results from our laboratory have shown that polymers with high selectivity ( $\alpha$ -values of 3 or higher when tested in the HPLC mode) for either L- or D-amino acid derivatives can be obtained by

polymerising methacrylic acid as functional monomer and ethylene glycol dimethacrylate (EDMA) as crosslinker together with either the L- or D-amino acid derivative (the “print molecule”), respectively [2,3]. In an alternative and also successful approach, covalent interactions between monomer and print molecule have been used to prepare selective polymers [4].

In the present study, the non-covalent imprinting procedure for the preparation of polymers selective for various carbohydrate derivatives, i.e. peracetylated phenyl  $\alpha$ - and  $\beta$ -D-glycosides of D-galactose, was investigated. Previously, a covalent imprinting procedure for unprotected sugar glycosides, which require unprotected vicinal hydroxyl groups for the formation of boronate esters between sugar hydroxyl groups and

\* Corresponding author. Present address: Glycorex AB, Sölveg. 41, S-223 70 Lund, Sweden.

\* Presented at the 18th International Symposium on Column Liquid Chromatography, Minneapolis, MN, 8–13 May 1994.

phenyl boronic acid groups on the polymer, has been described [5]. However, in general, protected mono- or oligosaccharides are of importance as they are widely used as intermediates in the chemical synthesis of biologically active carbohydrates found in glycoproteins and glycolipids [6].

The phenyl and amino-groups of print molecules, governing non-covalent and ionic interactions with functional monomers (methacrylic acid), have been shown previously to promote a high enantiomeric selectivity or specificity of recognition of imprinted polymers against derivatized amino acids [3,7]. Thus, in this investigation we were interested to compare the selectivity of polymers prepared by imprinting of aminophenyl, nitrophenyl and acetamidophenyl groups as aglycons of acetylated glycosides.

## 2. Experimental

### 2.1. Materials

The *p*- and *o*-nitrophenyl  $\alpha$ -D- and  $\beta$ -D-galactopyranosides were obtained from Sigma (St. Louis, MO, USA), ethylene glycol dimethacrylate (EDMA) was obtained from Polysciences (Warrington, FL, USA), methacrylic acid (MAA) and 2,2'-azobis (2-methyl-propionitrile) (AIBN) were from Janssen Chimica (Beerse, Belgium). Solvents and other reagents were of either HPLC grade or analytical reagent grade.

### 2.2. Preparation of print molecules

Peracetylation of D-galactoside anomers was performed by treatment with pyridine and acetic anhydride and the nitrophenyl group was converted to the aminophenyl group with  $H_2/Pd$ , active carbon [8]. The structures and purity of the corresponding print molecules (Table 1) were confirmed by means of TLC (ethylacetate–isooctane; Kieselgel 60 F 254; Merck), UV–Vis (Hitachi, Model 3200) and NMR spectra ( $^1H$ ,  $^{13}C$ , XL-300 MHz, Varian).

Table 1

Polymers prepared employing different carbohydrate derivatives as template molecules

Polymer <sup>a</sup>	Structure of template molecule
I	<i>p</i> -aminophenyl tetraacetyl $\alpha$ -D-galactoside
II	<i>p</i> -aminophenyl tetraacetyl $\beta$ -D-galactoside
III	<i>p</i> -nitrophenyl tetraacetyl $\alpha$ -D-galactoside
IV	<i>p</i> -nitrophenyl tetraacetyl $\beta$ -D-galactoside
V	<i>p</i> -acetamidophenyl tetraacetyl $\alpha$ -D-galactoside
VI	<i>p</i> -acetamidophenyl tetraacetyl $\beta$ -D-galactoside
VII	<i>o</i> -aminophenyl tetraacetyl $\alpha$ -D-galactoside
VIII	<i>o</i> -aminophenyl tetraacetyl $\beta$ -D-galactoside

<sup>a</sup> All polymers were prepared using EDMA (52.4 mmol) as crosslinking monomer, chloroform (16 ml) as solvent and AIBN (0.76 mmol) as the initiator at 0°C as described in Section 2.

### 2.3. Polymer preparation

Methacrylic polymers were prepared according to a slightly modified standard method [7] using methacrylic acid (MAA) as functional monomer and ethylene glycol dimethacrylate (EDMA) as crosslinker. The molar ratio of crosslinker to functional monomer to print molecule was within the range of 44:8.8:1–38.4:7.7:1 employing peracetylated galactosides as print molecules. The bulk polymers were ground to particles, size-separated (25–50  $\mu$ m) and packed into 250  $\times$  5.0 mm I.D. stainless-steel columns with acetonitrile as solvent at 150 bar using an air-driven fluid pump (Haskel Engineering Supply, Burbank, CA, USA).

### 2.4. HPLC analyses

The column was washed on-line with methanol–acetic acid (9:1, v/v) until a stable baseline was obtained. The print molecule was quantitatively removed from the polymer by this treatment as judged from the elution profiles. HPLC analyses (LKB 2150, Bromma, Sweden) were performed with the solvent compositions and flow-rates indicated in Table 2 and Fig. 2. Detection was at either 290 or 300 nm. An amount of 20–40  $\mu$ g of each of the anomers/isomers of a given compound, prepared in the

Table 2  
Capacity factors for the different *ortho*- and *para*-amino-phenyl galactoside derivatives on different polymers<sup>a</sup>

Polymer	Capacity factor $k'$		$\alpha_{12}$
	$\alpha$ -anomer	$\beta$ -anomer	
I	1.34	1.32	1.02
II	1.09	1.38	1.27
VII	1.61	1.61	1.00
VIII	1.88	2.00	1.06

<sup>a</sup> Each of the anomers of the galactoside derivatives was injected (20–40  $\mu\text{g}$ ) onto the polymer-containing columns in a total volume of 20  $\mu\text{l}$  of aqueous acetonitrile and eluted at room temperature using the mixture of acetonitrile–water (50:50); the void volume was measured with acetone.

mobile phases, was injected for analysis in a total volume of 20  $\mu\text{l}$ . The void volumes of the columns were determined by injection of acetone. Capacity factors ( $k'$ ) and separation factors ( $\alpha$ ), were calculated according to standard chromatographic theory [3].

### 3. Results and discussion

In this study, the acetylated carbohydrate moiety of the print molecules was kept constant, i.e. the galactose structure was used throughout the experiments, whereas the anomeric configuration and aglycon structure were varied (cf. Fig. 1 and Table 1).

As mentioned above, previous data obtained with amino acid derivatives show the importance of the amino group as well as of the phenyl group for the induction of specificity in this type

of polymers. Therefore, in this study, we investigated the *o*- and *p*-aminophenyl glycoside structures shown in Fig. 1 as template molecules. Control polymers were also prepared, employing template molecules which did not contain the amino function, i.e. *p*-acetamidophenyl glycosides and nitrophenyl glycosides (Table 1).

Moreover, all polymerizations were performed under equivalent conditions to ensure that the physical properties of the polymers were as equivalent as possible, exhibiting comparable pore volumes (0.04–0.05  $\text{cm}^3/\text{g}$ ) to the previously reported for other polymers (0.08  $\text{cm}^3/\text{g}$ ) [5]. The molar ratio of crosslinker (EDMA) to functional monomer (MAA) was 5:1. The ratio of functional monomer to print molecule, was in the range of 7.7–8.8:1 as determined by the solubility of the print molecule.

#### 3.1. Chromatography and specificity of recognition

Polymers were evaluated in the HPLC mode using isocratic elution. The composition of the eluent (acetonitrile–water) was chosen to give a capacity factor,  $k'$ , for the  $\beta$ -form of the print molecule of ca. 1 (data shown in Table 2).

Table 2 summarizes the results obtained with polymers I, II, VII and VIII, which were prepared using the various aminophenyl tetraacetyl galactosides shown in Fig. 1 as print molecules. The use of *p*- or *o*-aminophenyl  $\beta$ -galactosides as print molecules resulted in polymers II and VIII which exhibited higher selectivity than polymers I and VII prepared from the corresponding  $\alpha$ -glycosides. Thus, polymer II, prepared with *p*-aminophenyl  $\beta$ -galactoside (struc-

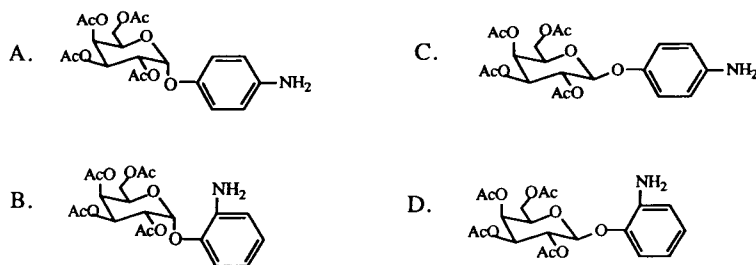


Fig. 1. Structure of the carbohydrate derivatives employed as print molecules in this study.

ture C in Fig. 1) as print molecule, gave a relatively high selectivity ( $\alpha = 1.27$ ) for the  $\beta$ -glycoside over the  $\alpha$ -glycoside, whereas polymer I prepared with *p*-aminophenyl  $\alpha$ -galactoside (structure A in Fig. 1), showed no or low selectivity towards the  $\alpha$ -glycoside ( $\alpha = 1.02$ ).

Similar results were obtained using the *ortho*-substituted aminophenyl  $\alpha$ - and  $\beta$ -galactosides as print molecules (polymer VII and VIII, respectively). Thus, polymer VIII prepared with the  $\beta$ -galactoside (structure D in Fig. 1) exhibited an  $\alpha$ -value of 1.06, whereas polymer VII prepared with the  $\alpha$ -galactoside did not show discrimination. Interestingly, polymer VIII also showed selectivity towards the *para*-amino substituted phenyl  $\beta$ -galactoside (i.e. as compared with the corresponding *para*-amino substituted  $\alpha$ -galactoside).

Importantly, none of the above polymers, including polymer II, exhibited selectivity against the galactosides which did not contain an amino group, i.e. the *p*-acetamido or nitrophenyl tetraacetyl galactosides. Moreover, none of the four different control polymers (polymers III, IV, V, and VI in Table 1) prepared with the latter galactosides as print molecules, showed any induced selectivity and the capacity factors ( $k'$ -values) for these columns were practically zero for the compounds tested in this study.

The chromatographic performance of the imprinted polymers is illustrated in Fig. 2, which shows a chromatogram obtained upon injection of the positional isomers *o*- and *p*-aminophenyl tetraacetyl  $\beta$ -galactoside on a column containing polymer VIII (prepared with the *o*-aminophenyl tetraacetyl  $\beta$ -galactoside as the print molecule). As can be seen, a complete separation was obtained ( $\alpha = 1.51$ ). No separation of these two compounds was obtained with the polymers prepared with the corresponding amino-phenyl  $\alpha$ -galactosides (polymers I and VII; Table 1), nor with the polymers prepared with the nitrophenyl or acetamidophenyl glycosides as print molecules (polymers III–VI).

From the data it is obvious that the amino function is required both for the preparation of polymers with induced selectivity as well as for the recognition of the injected carbohydrate

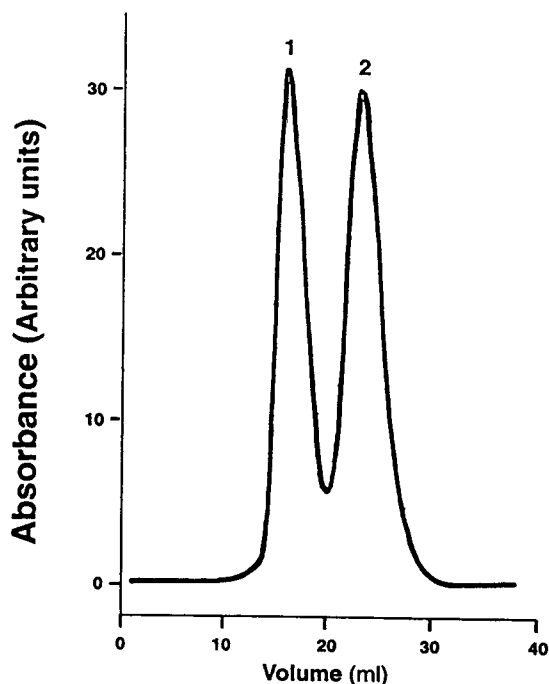


Fig. 2. Separation of (1) *para*- and (2) *ortho*-aminophenyl tetraacetyl  $\beta$ -D-galactoside, on a polymer prepared with the *o*-aminophenyl  $\beta$ -galactoside derivative as the template molecule. Analysis was performed isocratically using acetonitrile–water (2:3, v/v) as the eluent (0.5 ml/min) at room temperature. Detection was at 290 nm. A mixture containing 30  $\mu$ g of each of the isomers was injected.

derivative. This is in line with previous findings in our laboratory, which show that the amino group is important for the selectivity of imprinted polymers towards enantiomers of amino acid derivatives [1]. A schematic illustration of the proposed cavities that might be formed when the aminophenyl  $\beta$ -galactoside is used as print molecule, is given in Fig. 3. From this model, it can be assumed that if the amino function is

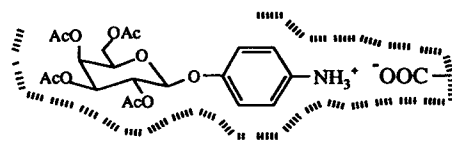


Fig. 3. Schematic illustration of the proposed interaction between the *p*-aminophenyl  $\beta$ -galactoside acetate and the polymer.



missing in the print molecule, induction of polymer cavities with specifically oriented carboxyl groups is not expected. This is in line with the observation that polymers III–VI, obtained with the *p*-nitro- or *p*-acetamido galactosides did not show induced selectivity.

The illustration in Fig. 3 might be used to rationalize the less pronounced selectivities obtained with the *o*-aminophenyl  $\beta$ -galactoside as the print molecule. Thus, comparing the molecular structures of the *p*- and *o*-aminophenyl galactosides, rotation of the *o*-aminophenyl group in the latter type of print molecule leads to a much larger movement of the amino group than in the *p*-aminophenyl  $\beta$ -galactoside, and therefore a much less pronounced chiral recognition might be expected.

In conclusion, the separation of carbohydrates is a challenge because of their complex structures and their potential as pharmaceutically active compounds. The results obtained in this study clearly show induced selectivity in polymers prepared by non-covalent imprinting and the method may be extended to preparation of

separation materials which are selective towards other protected carbohydrate derivatives as well as towards materials for the separation of partially protected or non-protected carbohydrates employing other polymerisation conditions.

## References

- [1] B. Ekberg and K. Mosbach, TIBTECH, 7 (1989) 92–96.
- [2] D.J. O'Shanessy, L.I. Andersson and K. Mosbach, J. Mol. Recogn., 2 (1989) 1–5.
- [3] L.I. Andersson and K. Mosbach, J. Chromatogr., 513 (1990) 167–179.
- [4] G. Wulff and S. Schauhoff, J. Org. Chem., 56 (1991) 395–400.
- [5] G. Wulff and J. Haarer, Makromol. Chem., 192 (1991) 1329–1338.
- [6] K.G.I. Nilsson, TIBTECH, 6 (1988) 256–264.
- [7] L.I. Andersson and K. Mosbach, J. Chromatogr., 516 (1990) 313–322.
- [8] M.L. Wolfrom and A. Thompson, in R.L. Whistler, M.L. Wolfrom and J.N. BeMiller (Editors), Methods in Carbohydrate Chemistry, Vol. II, Academic Press, New York, NY, 1963, pp. 211–215.





ELSEVIER

Journal of Chromatography A, 707 (1995) 205–216

JOURNAL OF  
CHROMATOGRAPHY A

# Capability of a polymeric C<sub>30</sub> stationary phase to resolve *cis*–*trans* carotenoid isomers in reversed-phase liquid chromatography

Curt Emenhiser<sup>a</sup>, Lane C. Sander<sup>b</sup>, Steven J. Schwartz<sup>a,\*</sup>

<sup>a</sup>Department of Food Science, Box 7624, North Carolina, State University, Raleigh, NC 27695-7624, USA

<sup>b</sup>Analytical Chemistry Division, Chemical Science and Technology Laboratory, National Institute of Standards and Technology, Gaithersburg, MD 20899, USA

First received 14 February 1995; revised manuscript received 6 March 1995; accepted 7 March 1995

## Abstract

A novel polymeric C<sub>30</sub> stationary phase was tested for its ability to separate geometric isomers of six common carotenoids (lutein, zeaxanthin,  $\beta$ -cryptoxanthin,  $\alpha$ -carotene,  $\beta$ -carotene, and lycopene) prepared by photoisomerization of all-*trans* standards. Resolution and tentative identification of asymmetrical carotenoid isomers yielded the 13-*cis*, 13'-*cis*, all-*trans*, 9-*cis*, and 9'-*cis* isomers of both lutein and  $\alpha$ -carotene, and the 15-*cis*, 13-*cis*/13'-*cis*, all-*trans*, 9-*cis*, and 9'-*cis* isomers of  $\beta$ -cryptoxanthin. Among symmetrical carotenoids, the 15-*cis*, 13-*cis*, all-*trans*, and 9-*cis* isomers of both zeaxanthin and  $\beta$ -carotene were resolved and tentatively identified, and nineteen geometric isomers of lycopene were separated. Separations were carried out using Vydac 201TP54 and Suplex pkb-100 stationary phases for comparison; in all cases, the C<sub>30</sub> stationary phase gave superior resolution and produced unique separations.

## 1. Introduction

Certain carotenoids are metabolic precursors to vitamin A. Other forms of biological activity (e.g., singlet oxygen quenching) have also been demonstrated *in vitro* for some carotenoids, apparently independent of provitamin A activity [1–5]. This activity is believed to occur *in vivo*, and has been postulated to manifest itself in the significant inverse association between dietary intake of carotenoids and the incidence of certain types of cancer [6,7]. Among dietary sources of carotenoids, various geometric (*cis* and all-

*trans*) isomers of carotenoids either occur naturally, or are formed during thermal processing [8–10]. With provitamin A carotenoids, the *cis*-isomeric forms are less efficiently converted to vitamin A than are their all-*trans* counterparts [11,12]. The presence and distribution of *cis*-carotenoids in biological tissues also varies [11,13,14]. Accurate nutritional assessment of foods, blood, and tissues is, therefore, dependent upon resolving and quantifying the geometric isomers of these provitamin A carotenoids. With respect to nutritional and other health-related aspects of carotenoid metabolism, the possibility that unique or altered physiological roles could be associated with *cis* versus

\* Corresponding author.

all-*trans* carotenoids has not yet been rigorously addressed. To this end, the ability to accurately determine *cis-trans* carotenoid profiles of biological tissues is a prerequisite to acquiring a better understanding of the biological significance of *cis*-carotenoids.

Existing reversed-phase (RP) liquid chromatography (LC) methods are well suited for separating major carotenoids, but their ability to separate *cis-trans* isomers of a particular carotenoid is seldom adequate. In this regard, polymeric C<sub>18</sub> stationary phases generally possess greater shape selectivity towards geometric carotenoid isomers than do monomeric C<sub>18</sub> stationary phases [15], resulting in better performance for these separations. Traditionally, normal-phase liquid chromatography (NPLC) using a calcium hydroxide stationary phase has produced excellent separations of *cis-trans* carotenoid isomers, including sets of  $\beta$ -carotene [16–18],  $\alpha$ -carotene [17], and several other carotenoids [19–21], but its use has been severely limited because these columns are not commercially available and their preparation is highly irreproducible. Other successful applications of NPLC to separations of carotenoid isomers include the use of an alumina stationary phase to separate  $\beta$ -carotene isomers [22] and a silica-based nitrile-bonded stationary phase for the separation of geometric isomers of lutein and zeaxanthin [23,24]. Argentation chromatography, where silver ions are incorporated into either the stationary phase or mobile phase, has been demonstrated to aid in LC separations of methyl ester derivatives of *cis* and *trans* fatty acids [25]; however, this approach has not yet been successfully applied to separations involving carotenoids or their geometric isomers.

The polymeric C<sub>30</sub> stationary phase used in the present study was developed at NIST to optimize RPLC separations of carotenoids [26]. It was successfully demonstrated that this C<sub>30</sub> stationary phase provides excellent resolution of all-*trans* carotenoids and possesses outstanding shape selectivity toward the predominant geometric isomers in a  $\beta$ -carotene sample prepared from *Dunaliella* algae (Betatene, Melbourne, Australia). In a separate report, the same type of

stationary phase was used to separate the major carotenoids in an extract of human serum [27]. Our present objectives were: (1) to assess shape selectivity of the polymeric C<sub>30</sub> stationary phase by determining its ability to separate geometric isomers of common carotenoids; and (2) to obtain comparative separations of the same isomer mixtures using RP stationary phases that are commercially available and commonly used for carotenoid chromatography.

## 2. Experimental<sup>1</sup>

### 2.1. Chemicals

The following all-*trans* carotenoid standards were used in this study: lutein (Kemin, Des Moines, IA, USA); zeaxanthin (Indofine, Belle Mead, NJ, USA);  $\beta$ -cryptoxanthin (Hoffmann-La Roche, Nutley, NJ, USA); lycopene (Sigma, St. Louis, MO, USA);  $\alpha$ -carotene (Sigma); and  $\beta$ -carotene (Sigma). For the convenience of the reader, structures of these carotenoids are given in Fig. 1. HPLC solvents were methanol (certified ACS; Fisher Chemical, Fairlawn, NJ, USA) and methyl-*tert*-butyl ether (MTBE) (HPLC grade; Fisher).

### 2.2. Stationary phases

Four RPLC stationary phases were tested using analytical scale (250 × 4.6 mm I.D.) columns. Of these stationary phases, two were prepared at NIST by polymeric synthesis of a C<sub>30</sub> alkyl-bonded phase onto silica supports, without subsequent endcapping, according to the report on its development [26]. These polymeric C<sub>30</sub> stationary phases were prepared using the same synthetic procedure, but with different diameter

<sup>1</sup>Certain commercial equipment, instruments, or materials are identified in this report to specify adequately the experimental procedure. Such identification does not imply recommendation or endorsement by North Carolina State University or the National Institute of Standards and Technology, nor does it imply that the materials or equipment identified are necessarily the best available for the purpose.

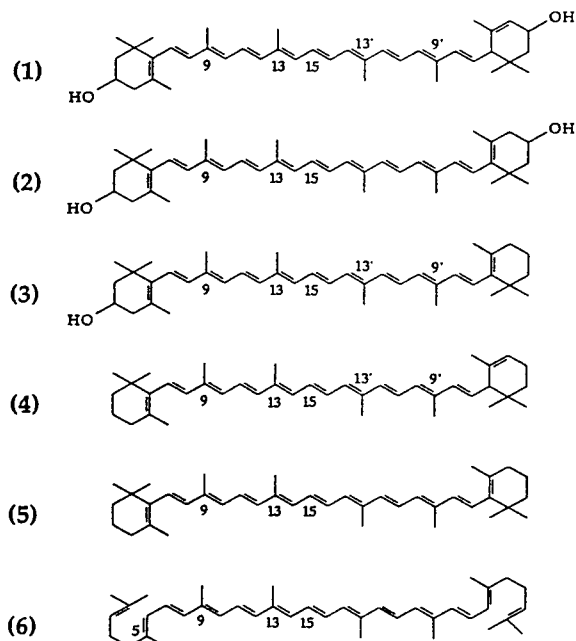


Fig. 1. Structures of the carotenoids analyzed in this report, shown in their all-*trans* configurations: 1 = lutein; 2 = zeaxanthin; 3 =  $\beta$ -cryptoxanthin; 4 =  $\alpha$ -carotene; 5 =  $\alpha$ -carotene; 6 = lycopene. Carbon numbers indicate positions where formation of *cis*-bonds is sterically unhindered.

silica particles (5  $\mu\text{m}$  and 3  $\mu\text{m}$ ). The stationary phase containing 5- $\mu\text{m}$  silica particles was used for most of the research presented here, and unless the particle size of the silica is otherwise indicated as 3  $\mu\text{m}$  in diameter, the 5- $\mu\text{m}$  stationary phase was used. The other two stationary phases were obtained in commercially manufactured columns: Suplex pkb-100 (Supelco, Bellefonte, PA, USA); and Vydac 201TP54 (Separations Group, Hesperia, CA, USA). These stationary phases were chosen from the many commercially available  $\text{C}_{18}$  columns because they are commonly used for carotenoid analyses and are known to exhibit selectivity toward geometric carotenoid isomers. Pertinent available data on the four stationary phases are given in Table 1. Guard columns were not used to preclude any possible pre-column effects on the resultant separations.

### 2.3. Instrumentation

The HPLC system used in this work consisted of a Waters (Milford, MA, USA) Model 501 solvent delivery system, a Waters Model U6K

Table 1  
Physical properties of the stationary phases tested

Stationary phase	5- $\text{C}_{30}^a$	Suplex pkb-100	Vydac 201TP54	3- $\text{C}_{30}^a$
Bonded phase	$\text{C}_{30}$	– <sup>b</sup>	$\text{C}_{18}$	$\text{C}_{30}$
Synthesis	polymeric	– <sup>b</sup>	polymeric	polymeric
Endcapping	no	yes <sup>c</sup>	no	no
Silica				
–type	YMC S5-SIL200	– <sup>b</sup>	Vydac TP	YMC S3-SIL200
–particle shape	spherical	spherical	spherical	spherical
–particle diam. ( $\mu\text{m}$ )	5	5	5	3
–pore diam. ( $\text{\AA}$ ) <sup>d</sup>	200	100	300	200
–surface area ( $\text{m}^2/\text{g}$ ) <sup>d</sup>	200	– <sup>b</sup>	90	200
Percent carbon	19.41	– <sup>b</sup>	8 <sup>d</sup>	– <sup>b</sup>
Coverage ( $\mu\text{mol}/\text{m}^2$ )	3.64	– <sup>b</sup>	4.16	– <sup>b</sup>

<sup>a</sup> Ref. [26].

<sup>b</sup> Information is proprietary or unavailable.

<sup>c</sup> Reagent used for endcapping is proprietary.

<sup>d</sup> Nominal values provided by the purveyors.

injector, and an Anspec UV-Vis detector (Model SM 95; Linear Instruments, Reno, NV, USA). The detector was linked to a Dramen personal computer (Dramen, Raleigh, NC, USA) via a Dionex advanced computer interface (Model ACI-1; Dionex, Sunnyvale, CA, USA). Dionex AI-450 chromatography software (release 3.30; Dionex) was used to integrate the chromatograms. Electronic absorption spectra were obtained for some chromatographic peaks using a Waters Model 996 photodiode-array detector interfaced with a Gateway 2000 personal computer (Model 4DX2-66V; North Sioux City, SD, USA) equipped with Millennium 2010 chromatography software (LC Version 2.00; Millipore, Milford, MA, USA).

#### 2.4. Sample preparation

All-*trans* carotenoid standards were purified of any oxidized carotenoid contaminants that may have formed during manufacture and storage of the standards using open alumina columns and acetone-hexane eluents. Briefly, acetone concentrations were adjusted to elute only the all-*trans* carotenoid, thereby removing any oxidized carotenoid contaminants which are preferentially retained on alumina. Purity of the all-*trans* carotenoids was assessed using the polymeric C<sub>30</sub> column. Mobile phases of MTBE in methanol flowing at a rate of 1 ml/min were used for this assessment. Lutein, zeaxanthin,  $\beta$ -cryptoxanthin, and lycopene were of sufficient purity ( $\geq 97\%$  all-*trans*) to obviate further preparative chromatography. Additional purification was necessary, however, to achieve adequate purity of the  $\alpha$ -carotene and  $\beta$ -carotene standards. Removal of contaminating  $\beta$ -carotene and  $\alpha$ -carotene, respectively, was achieved using a Vydac 201TP510 semi-preparatory column (250  $\times$  10 mm I.D.; Separations Group, Hesperia, CA, USA), a mobile phase of 8% tetrahydrofuran and 0.05% triethylamine in methanol, and a flow-rate of 1.5 ml/min. This procedure gave  $\alpha$ -carotene and  $\beta$ -carotene of high purity ( $\geq 97\%$  all-*trans*). Each standard was photoisomerized into an equilibrium mixture of various geometric isomers by iodine catalysis accord-

ing to the general procedure reported by Zechmeister [12]. Briefly, after dissolving each all-*trans* carotenoid in a suitable solvent (hexane when possible) and diluting it with hexane, iodine was added at a concentration of about 1% by weight of the carotenoid weight (determined spectrophotometrically using published extinction coefficients), and the solution was then exposed to ambient laboratory light for 1 h. After isomerization, each sample was dried over sodium sulfate, dried under a stream of nitrogen gas, and stored at  $-20^{\circ}\text{C}$  until further use.

#### 2.5. Chromatography

All separations on the polymeric C<sub>30</sub> stationary phases were achieved isocratically using a binary mobile phase of MTBE in methanol, flowing at 1 ml/min. The concentration of MTBE in the mobile phase was adjusted to give optimal resolution of analytes under the other conditions of chromatography. Mobile-phase compositions for separations on the Suplex pkb-100 and Vydac 201TP54 stationary phases were selected to give optimal or near optimal resolution of each isomer set on the stationary phase being tested [28–30]. This approach was believed to provide a better comparison of column separation efficiency than would be possible using the same mobile phase, or same mobile-phase components, when testing different stationary phases and analytes. For all separations, the specific composition of the mobile phase used is given in the appropriate figure legend. When several stationary phases were tested comparatively for their ability to resolve a particular set of carotenoid isomers, the same isomer mixture was used for all chromatographic analyses, including photodiode-array detection.

All columns were used at ambient laboratory temperature (ca. 23°C). Injection solvents were MTBE in methanol mixtures for application to all four stationary phases. Injection volumes ranged from 2 to 25  $\mu\text{l}$ . Column effluent was monitored at 453 nm during all separations, except for that of isomerized lycopene (460 nm), using a sensitivity setting absorbance units full

scale (AUFS) of 0.008. Electronic absorption spectra were obtained from 250 to 550 nm.

## 2.6. Peak identifications

For each set of geometric carotenoid isomers, all-*trans* configurations and *cis*-bond positions were tentatively assigned to chromatographic peaks according to characteristics of their electronic absorption spectra [12] and relative patterns of chromatographic retention [26].

## 3. Results and discussion

### 3.1. Asymmetrical carotenoids

With asymmetrical carotenoids (e.g., lutein,  $\beta$ -cryptoxanthin, and  $\alpha$ -carotene), the number of theoretically possible geometric isomers is approximately two-fold greater than with those carotenoids having a plane of symmetry (e.g., zeaxanthin, lycopene, and  $\beta$ -carotene) [12]. We were interested in determining how well the  $C_{30}$  stationary phase could resolve the potentially complex isomerized mixtures of common asymmetrical carotenoids, and more specifically, whether mono-*cis* geometric isomers of asymmetrical carotenoids could be resolved where the *cis*-bonds are present at the same carbon number but at opposite ends of the molecule (e.g., 9-*cis* and 9'-*cis*). For these de-

terminations, carotenoids were selected according to structural features that preclude a plane of symmetry as well as prevalence in human and food tissues. Isomeric mixtures of lutein,  $\beta$ -cryptoxanthin, and  $\alpha$ -carotene were believed to serve adequately as probes for ascertaining shape selectivity of the polymeric  $C_{30}$  stationary phase.

### Lutein

The separation of geometric lutein isomers on the  $C_{30}$  stationary phase is given in Fig. 2A. The  $C_{30}$  stationary phase completely resolved nine *cis-trans* lutein peaks. The 13-*cis*, 13'-*cis*, all-*trans*, 9-*cis*, and 9'-*cis* geometric forms of lutein were tentatively identified (Table 2), and the remaining four resolved peaks are unidentified *cis*-isomers of lutein. Unambiguous assignment of individual peak identities, including the 13-*cis* or 13'-*cis* and 9-*cis* or 9'-*cis* isomers, was not possible because NMR spectroscopy has not yet been applied to any peaks resolved on the  $C_{30}$  column. In Fig. 3, the absorption spectra for the 13-*cis* and 13'-*cis* isomers of lutein are given. When normalized and superimposed, these spectra are nearly indistinguishable, as are the absorption spectra for the 9-*cis* and 9'-*cis* isomers of lutein (not shown). The wavelengths of maximal absorbance and relative abundances of some of the resolved lutein peaks are given in Table 2. The 15-*cis* isomer of lutein was not resolved on the  $C_{30}$  stationary phase under the chromatographic conditions employed, but was believed

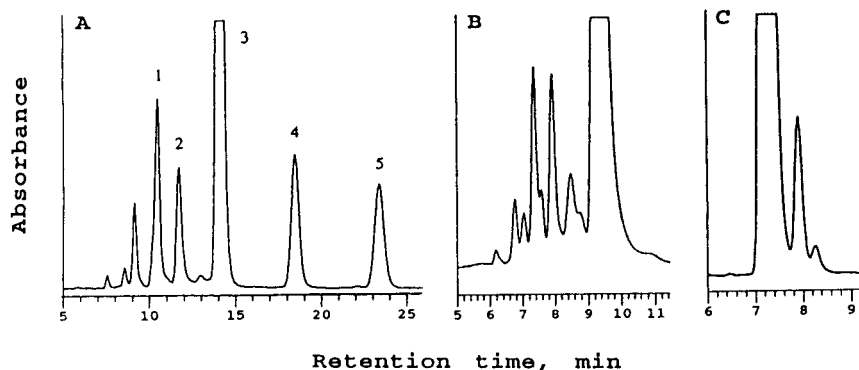


Fig. 2. RPLC separations of isomerized lutein. (A)  $C_{30}$  stationary phase; MTBE-methanol (5:95, v/v) mobile phase. (B) Vydac 201TP54; methanol mobile phase, 0.7 ml/min. (C) Suplex pkb-100; methanol mobile phase, 0.7 ml/min. Tentative peak identifications for (A) are given in Table 2.

Table 2

Wavelengths of maximum absorbance and relative abundances of certain geometric carotenoid isomers separated from iodine-isomerized mixtures on the C<sub>30</sub> stationary phase

Carotenoid	Peak number <sup>a</sup>	Tentative identification	$\lambda_{\max}^b$ (nm)	Relative abundance <sup>c</sup> (%)
Lutein	1	13- or 13'- <i>cis</i>	435	10.2
	2	13- or 13'- <i>cis</i>	436	7.6
	3	all- <i>trans</i>	442	56.3
	4	9- or 9'- <i>cis</i>	438	10.3
	5	9- or 9'- <i>cis</i>	439	10.0
$\beta$ -Cryptoxanthin	1	15- <i>cis</i>	444	3.6
	2	13- & 13'- <i>cis</i>	442	8.5
	3	all- <i>trans</i>	449	60.5
	4	9- or 9'- <i>cis</i>	444	13.0
	5	9- or 9'- <i>cis</i>	444	11.5
$\alpha$ -Carotene	1	13- or 13'- <i>cis</i>	438	9.4
	2	13- or 13'- <i>cis</i>	438	9.4
	3	all- <i>trans</i>	444	53.8
	4	9- or 9'- <i>cis</i>	441	11.0
	5	9- or 9'- <i>cis</i>	441	10.0
$\beta$ -Carotene	1	15- <i>cis</i>	447	1.2
	2	13- <i>cis</i>	443	16.7
	3	all- <i>trans</i>	450	47.3
	4	9- <i>cis</i>	444	22.1
Zeaxanthin	1	15- <i>cis</i>	446	1.4
	2	13- <i>cis</i>	443	14.2
	3	all- <i>trans</i>	450	53.9
	4	9- <i>cis</i>	446	21.0
Lycopene	1	15- <i>cis</i>	466	1.9
	2	13- <i>cis</i>	465	7.8
	3	all- <i>trans</i>	472	13.3
	4	unidentified <i>cis</i>	472	23.2

<sup>a</sup> Numbers correspond to those given in Figs. 2A, 4A, 5A, 6A, 7, and 8.

<sup>b</sup> Obtained for the main absorption peak using photodiode-array spectrophotometry in the mobile phase (5–38% MTBE in methanol). Relative differences in  $\lambda_{\max}$  of ca. 3 nm or less are generally insignificant when considered for assigning double bond geometries.

<sup>c</sup> Peak-area percent relative to total area of all peaks detected at the  $\lambda_{\max}$  reported here for the all-*trans* forms, except for lycopene, which was monitored at 460 nm and integrated only for peaks eluting after 14 min. Measurements are based upon the assumption that absorptivities ( $\epsilon$ ) for geometrical isomers of each carotenoid are equal or nearly equal.

to elute in peak 1. This observation is based on the measured increase in the *cis*-peak effect (absorbance at ca. 330 nm) on a shoulder of peak 1 when multiple absorption spectra were obtained in this peak. Since absorbance in the *cis*-peak region is greatest with centrally located *cis*-bonds [12], the presence of the 15-*cis* isomer is suggested. In addition, when the same lutein mixture was separated on the 3- $\mu$ m C<sub>30</sub> stationary phase (not shown), a peak that could correspond to the 15-*cis* isomer was partially resolved

at the same relative position in the chromatogram.

Using the Vydac 201TP54 column, nine geometric isomers of lutein were partially separated, but with poor resolution (Fig. 2B). On the Suplex pkb-100 stationary phase, only three peaks were separated from the same luteins mixture (Fig. 2C), and these peaks were not baseline-resolved. Neither the Vydac 201TP54 nor the Suplex pkb-100 stationary phase provide adequate retention of isomers of lutein, a rela-



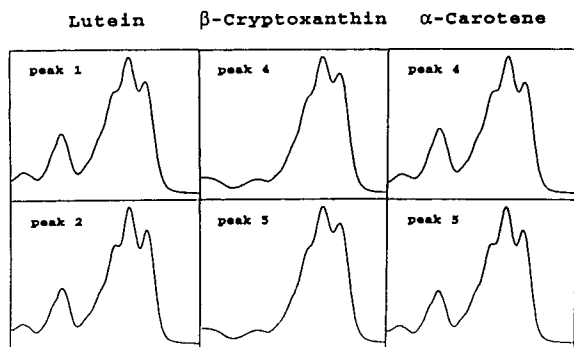


Fig. 3. UV-Vis absorption spectra for selected geometric carotenoid isomers: 13-*cis* and 13'-*cis* luteins (Fig. 2, peaks 1 and 2); 9-*cis* and 9'-*cis*  $\beta$ -cryptoxanthins (Fig. 4, peaks 4 and 5); and 9-*cis* and 9'-*cis*  $\alpha$ -carotenes (Fig. 5, peaks 4 and 5).

tively polar carotenoid. Both the  $C_{30}$  and Vydac stationary phases, however, possess good selectivity toward these isomers, and this may be attributable to the presence of silanol activity, i.e., lack of endcapping (Table 1). Certain separations of oxygenated carotenoids have been shown to be aided by silanol activity in the stationary phase [26,31], but this has been recognized only for structural xanthophyll isomers (i.e., lutein and zeaxanthin; neoxanthin and antheraxanthin) and epimers (i.e., auroxanthins 2 and 3) and not for separations involving geometric carotenoid isomers. The advantage of using the  $C_{30}$  stationary phase for separations of lutein isomers is that this column combines a high degree of shape selectivity with adequate

retention to a greater extent than either the Vydac 201TP54 or Suplex pkb-100 stationary phases.

There are several published reports of HPLC separations of geometric lutein isomers that compare favorably [32–35]. Five geometric isomers of lutein have been separated from an isomerized mixture using NPLC [32]. Similar results have been obtained using a  $C_{18}$  column in RPLC, by which four *cis-trans* luteins were resolved from an isomerized mixture and tentatively identified [35]. Excellent separations of lutein isomers have also been achieved using nitrile-bonded columns in NPLC [23,24]. Isomers of lutein were isolated from extracts of human plasma and unambiguously identified as all-*trans*, 9-*cis*, 9'-*cis*, and 13-*cis*/13'-*cis*.

#### $\beta$ -Cryptoxanthin

Separations of geometric  $\beta$ -cryptoxanthin isomers obtained on the tested stationary phases are presented in Fig. 4. Using the  $C_{30}$  stationary phase and MTBE-methanol (8:92 v/v) as mobile phase, excellent resolution was achieved for most of the predominant  $\beta$ -cryptoxanthin isomers (Fig. 4A). The 15-*cis* and all-*trans* isomers were completely resolved, and the 9-*cis* and 9'-*cis* isomers were separated, but not fully resolved. Electronic absorption spectra for the 9-*cis* and 9'-*cis* isomeric pair are virtually identical (Fig. 3). Interestingly, the 13-*cis* and 13'-*cis* isomeric pair was resolved from all other major

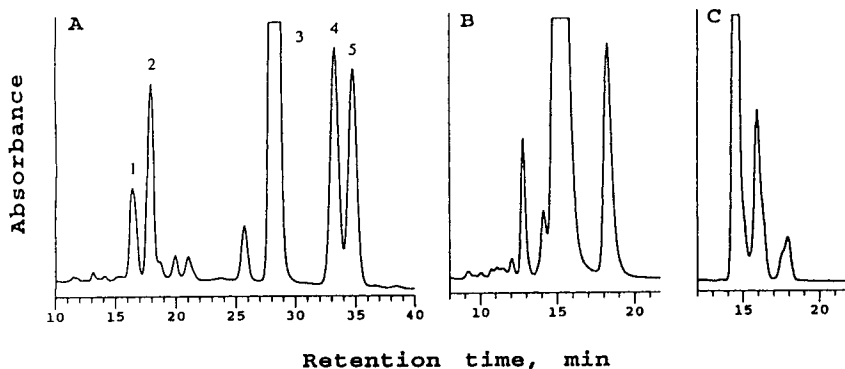


Fig. 4. RPLC separations of isomerized  $\beta$ -cryptoxanthin. (A)  $C_{30}$  stationary phase; MTBE-methanol (8:92, v/v) mobile phase. (B) Vydac 201TP54; acetonitrile-methanol (5:95, v/v) mobile phase, 1 ml/min. (C) Suplex pkb-100; methanol-acetonitrile-isopropanol-water (10:40:40:10, v/v) mobile phase, 0.7 ml/min. Tentative peak identifications for (A) are given in Table 2.

isomers, but these individual isomers were not separated from one another. Evidence for this observation includes analysis of absorption spectra for the resolved peaks, and a chromatogram of the same  $\beta$ -cryptoxanthins mixture developed on the 3- $\mu$ m  $C_{30}$  stationary phase (not shown), where the 13-*cis*/13'-*cis* peak is partially separated into two peaks of almost equal abundance. In Table 2, wavelengths of maximal absorbance and percent composition of major peaks are provided. Several other, unidentified  $\beta$ -cryptoxanthin isomers were also separated. Other LC separations of geometrical  $\beta$ -cryptoxanthin isomers of this kind were not found in the literature for comparison.

Chromatography of the same isomerized mixture of  $\beta$ -cryptoxanthins on the Vydac 201TP54 stationary phase yielded separation of four *cis*-isomers from the predominant peak containing the all-*trans* form (Fig. 4B). When the  $\beta$ -cryptoxanthins mixture was applied to the Suplex pkb-100 stationary phase (Fig. 4C), three distinct peaks were separated, with the predominant peak containing the all-*trans* isomer and the other two peaks, each having a shoulder, containing *cis*-isomers.

#### $\alpha$ -Carotene

Comparative separations of an isomerized mixture of *cis-trans*  $\alpha$ -carotenes are presented in Fig. 5. When  $\alpha$ -carotene isomers were applied to

the  $C_{30}$  column, the 13-*cis*, 13'-*cis*, all-*trans*, 9-*cis*, and 9'-*cis* isomers were at least partially resolved and are tentatively identified (Fig. 5A; Table 2). The absorption spectra for the 13-*cis*/13'-*cis* and 9-*cis*/9'-*cis* isomeric pairs are quite similar as can be seen in Fig. 3 for the latter pair. The remaining  $\alpha$ -carotenes peaks separated are unidentified.

Six  $\alpha$ -carotene isomers were separated on the Vydac 201TP54 stationary phase, but these peaks were poorly resolved (Fig. 5B). Fig. 5C is the chromatogram obtained for the same  $\alpha$ -carotenes mixture when applied to the Suplex pkb-100 stationary phase. Under the chromatographic conditions employed, three *cis*-peaks and the all-*trans* isomer were nearly baseline-resolved.

Few HPLC separations of  $\alpha$ -carotene isomers exist in the literature [17,35–37]. However, resolution of all-*trans*, 15-*cis*, 13-*cis*, 13'-*cis*, 9-*cis*, and 9'-*cis*  $\alpha$ -carotenes from an iodine-isomerized mixture was recently achieved in our laboratory using a calcium hydroxide stationary phase [17].

It is interesting to note that, for the  $\beta,\epsilon$ -carotenoids (lutein and  $\alpha$ -carotene), the 15-*cis* isomers were unresolved on the  $C_{30}$  phase, while the 13-*cis*/13'-*cis* and 9-*cis*/9'-*cis* isomeric pairs were well separated. This is in contrast to the  $\beta,\beta$ -carotenoid ( $\beta$ -cryptoxanthin), for which the  $C_{30}$  separation resolved the 15-*cis* isomer but not the 13-*cis*/13'-*cis* isomeric pair.

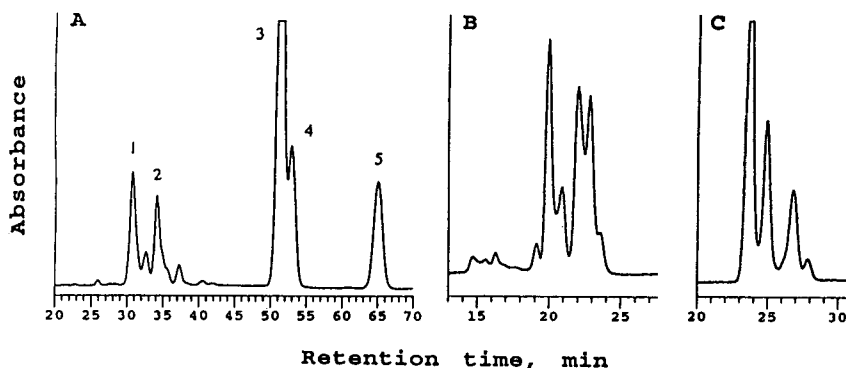


Fig. 5. RPLC separations of isomerized  $\alpha$ -carotene. (A)  $C_{30}$  stationary phase; MTBE-methanol (9:91, v/v) mobile phase. (B) Vydac 201TP54; acetonitrile-methanol (10:90, v/v) mobile phase, 1 ml/min. (C) Suplex pkb-100; methanol-acetonitrile-isopropanol-water (10:40:40:10, v/v) mobile phase, 1 ml/min. Tentative peak identifications for (A) are given in Table 2.

### 3.2. Symmetrical carotenoids

Although isomerized mixtures of symmetrical carotenoids are generally less complex than are those of asymmetrical carotenoids, LC separations of either type of mixture are equally challenging.  $\beta$ -Carotene, lycopene, and zeaxanthin were selected for this study among the many known symmetrical carotenoids because of their prevalence in biological tissues and their structural features.

#### $\beta$ -Carotene

Chromatographic separations of isomerized  $\beta$ -carotene on the  $C_{30}$ , Vydac 201TP54, and Suplex pkb-100 stationary phases are illustrated in Fig. 6. When chromatographed on the  $C_{30}$  stationary phase, excellent resolution of the tentatively identified 15-*cis*, 13-*cis*, all-*trans*, and 9-*cis* isomers was achieved (Fig. 6A). The wavelengths of maximal absorbance and relative abundances of these isomers are given in Table 2. Several other *cis*-isomers of unknown geometrical configuration were also separated from this mixture. The Vydac 201TP54 stationary phase was also tested for its ability to resolve the same geometric isomers of  $\beta$ -carotene (Fig. 6B). As with all isomer sets chromatographed on the Vydac stationary phase, several peaks containing *cis*-isomers were separated from all-*trans*  $\beta$ -carotene, but the resolution was not comparable

to that achieved when using the  $C_{30}$  stationary phase. On the Suplex pkb-100 stationary phase, four peaks containing *cis*-isomers of  $\beta$ -carotene were nearly baseline-resolved from the predominant all-*trans* peak (Fig. 6C).

There have been numerous other separations of  $\beta$ -carotene isomers, and these have been recently reviewed [38]. Several normal-phase separations of geometric  $\beta$ -carotene isomers [16–18,22] have given comparable or favorable resolution with that which we achieved; however, no RP stationary phase has shown shape selectivity towards geometric isomers of  $\beta$ -carotene to the extent of the  $C_{30}$  phase used here. Interestingly, retention characteristics and elution order of  $\beta$ -carotene isomers are strikingly similar on calcium hydroxide and  $C_{30}$  stationary phases, despite the fundamental differences between their mechanisms of retention and selectivity. The same observation can be made for the  $\alpha$ -carotene set [17], and perhaps for other sets of geometric carotenoid isomers as well. On calcium hydroxide, adsorption affinity of carotenoids is dependent upon the number and types of conjugated double bonds present, giving rise to stronger adsorption: (a) when conjugation is increased; (b) with acyclic versus cyclic carotenoids; and (c) with  $\beta,\beta$ -carotenoids as compared to  $\beta,\epsilon$ -carotenoids [39]. The same general retention patterns are observed for carotenoids on the  $C_{30}$  stationary phase, although a different

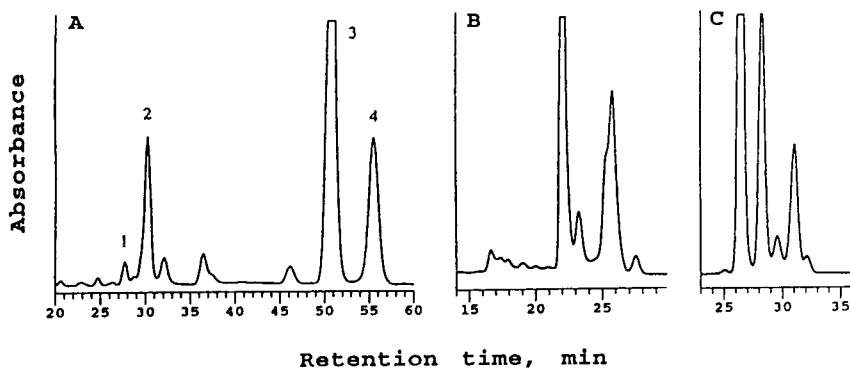


Fig. 6. RPLC separations of isomerized  $\beta$ -carotene. (A)  $C_{30}$  stationary phase; MTBE–methanol (11:89, v/v) mobile phase. (B) Vydac 201TP54; acetonitrile–methanol (10:90, v/v) mobile phase, 0.7 ml/min. (C) Suplex pkb-100; methanol–acetonitrile–isopropanol–water (10:40:40:10, v/v) mobile phase, 1 ml/min. Tentative peak identifications for (A) are given in Table 2.

retention mechanism has been proposed. Unlike the primary retention mechanism on  $C_{18}$  stationary phases (i.e., solvophobic interactions), the "slot model" was introduced, where solutes interact within "slots" of the  $C_{30}$ -bonded phase surface during retention [40]. This model could account for the excellent shape selectivity of the  $C_{30}$  polymeric phase toward geometric carotenoid isomers as well as the preferential retention of the acyclic lycopene, in a fashion similar to that observed for polyaromatic hydrocarbons of differing shapes [40]. Further insight into possible retention mechanisms can be gained through comparison of the relative dimensions of carotenoids and bonded-phase thicknesses. The length of all-*trans*  $\beta$ -carotene (as determined by molecular modeling) is ca. 29 Å, and the thickness of a  $C_{30}$  stationary phase estimated from small-angle neutron-scattering measurements is 25–30 Å [26]. By contrast,  $C_{18}$  stationary phases range in thickness from 17 to 21 Å. The enhanced selectivity exhibited by the  $C_{30}$  polymeric phase toward geometric carotenoid isomers has been attributed in part to the greater thickness of the stationary phase. More complete interaction of carotenoids is thought to be possible with a stationary phase with thickness comparable to the dimensions of the solute. By similar reasoning, it is hypothesized that because  $C_{18}$  stationary phases possess insufficient thickness to permit full penetration of carotenoid molecules, solute-bonded phase interactions do not occur at all points along the molecule, and poorer isomer separations result.

### Zeaxanthin

An isomeric mixture of geometric zeaxanthins was chromatographed only on the  $C_{30}$  stationary phase (Fig. 7). Among the predominant geometric isomers separated and tentatively identified are 15-*cis*, 13-*cis*, all-*trans*, and 9-*cis* zeaxanthins (Table 2). Several other unidentified zeaxanthin isomers were also separated.

There are few reports of HPLC separations of zeaxanthin isomers, and all deal with extracts of human plasma [23,24,33,34]. All-*trans* and 13-*cis* zeaxanthin were resolved using an Adsorbo-

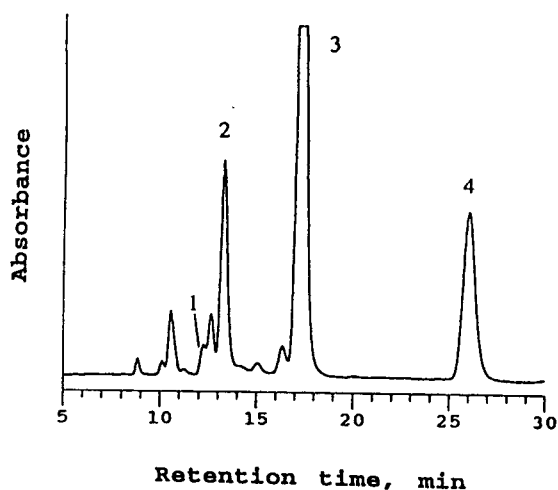


Fig. 7.  $C_{30}$  chromatogram of isomerized zeaxanthin, MTBE-methanol (5:95, v/v) mobile phase. Tentative peak identifications are given in Table 2.

sphere-HS  $C_{18}$  column, and the 9-*cis* isomer was additionally separated from a corn meal extract [34]. A better separation of zeaxanthin isomers was obtained using NPLC with a nitrile-bonded silica-based column, on which the all-*trans*, 9-*cis*, 13-*cis*, and 15-*cis* geometric forms of zeaxanthin were resolved [23,24]. The geometrical configurations of these isomers were unambiguously identified using  $^1\text{H}$  NMR.

### Lycopene

An isomerized mixture of geometric lycopene isomers was also applied to the  $C_{30}$  stationary phase. The resultant chromatogram (Fig. 8) contains peaks of at least 18 *cis*-lycopene isomers plus the all-*trans* form. Peaks eluting before 14 min are presumed to be degradation (oxidation) products of lycopene formed during sample handling and chromatography. Because the absorption spectra of the two latest eluting peaks were indistinguishable, co-chromatography of a biological extract that contained numerous lycopene isomers and added all-*trans* lycopene was used to identify the all-*trans* isomer. Among the *cis*-lycopene isomers, only the 15-*cis* and 13-*cis* forms could be tentatively identified on the basis of electronic absorption spectra, because of

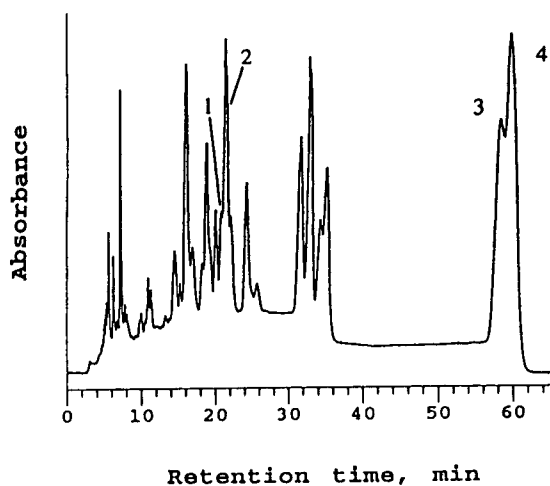


Fig. 8.  $C_{30}$  Chromatogram of isomerized lycopene, MTBE-methanol (38:62, v/v) mobile phase. All peaks eluting after 14 min are *cis*-lycopenes. Tentative peak identifications are given in Table 2.

remarkable similarities among these spectra for nearly all of the other *cis*-lycopene peaks. The wavelengths of maximal absorbance and relative abundances of several lycopene isomers are given in Table 2.

To our knowledge, separation of lycopene isomers has not been investigated using NPLC. There have been several reports in which a number of isomers of lycopene have been partially resolved from the all-*trans* configuration [14,34,35]. Six *cis-trans* lycopenes were separated from an isomerized standard using a  $C_{18}$  column [35], and four peaks containing *cis*-lycopenes were separated from all-*trans* lycopene in extracts of human plasma using a  $C_{18}$  column [34]. A Suplex pkb-100 column has previously given peaks corresponding to the all-*trans*, 15-*cis*, 13-*cis*, and 9-*cis* isomers of lycopene in human serum extracts [14]. Thus, many of the *cis*-lycopene peaks in Fig. 8 have not been previously observed, although numerous geometric lycopene isomers have been previously isolated using extensive open column chromatography [12]. Nonetheless,  $C_{30}$  column selectivity towards geometric isomers of lycopene is clearly unique in comparison to that of any other existing stationary phase.

### 3.3. $C_{30}$ stationary phase prepared from 3- $\mu\text{m}$ silica particles

Isomerized mixtures of all of the carotenoids included in this study were chromatographed on the 3- $\mu\text{m}$   $C_{30}$  stationary phase, in addition to the 5- $\mu\text{m}$   $C_{30}$  column. For isomerized lutein, the 3- $\mu\text{m}$   $C_{30}$  phase separated two peaks in addition to those resolved on the 5- $\mu\text{m}$   $C_{30}$  column, one eluting before peak 1 and the other after peak 3 of Fig. 2A. The 3- $\mu\text{m}$   $C_{30}$  separation of isomerized  $\beta$ -cryptoxanthin included partial separation of the 13-*cis* and 13'-*cis* isomers (peak 2 of Fig. 4A) as well as baseline resolution of the 9-*cis* and 9'-*cis* isomers (peaks 4 and 5 of Fig. 4A) as improvements over the corresponding 5- $\mu\text{m}$   $C_{30}$  separation. Similar improvements in resolution were also observed for the other carotenoid isomer sets.

## 4. Conclusions

The polymeric  $C_{30}$  RPLC stationary phase possesses outstanding shape selectivity toward geometric isomers of lutein, zeaxanthin,  $\beta$ -cryptoxanthin,  $\alpha$ -carotene,  $\beta$ -carotene, and lycopene. This stationary phase also gives adequate retention for resolution of polar carotenoids. For all of the carotenoid isomer sets included in this work, *cis*-isomers were separated on the  $C_{30}$  phase that have not been previously separated on RP stationary phases. Assignment of peak identities using  $^1\text{H}$  NMR spectroscopy is currently in progress for certain predominant geometric isomers of the carotenoids reported herein. As expected, the resolution of each isomer set was slightly enhanced when using the 3- $\mu\text{m}$   $C_{30}$  stationary phase as compared to that achieved with the 5- $\mu\text{m}$  column. Shape discrimination and peak retention of *cis-trans* carotenoid isomers on the  $C_{30}$  stationary phases are superior to that available with existing, commercially available RPLC columns routinely used for carotenoid analysis.

The polymeric  $C_{30}$  stationary phase can be successfully applied to: (a) more accurate determinations of the provitamin A content and

geometric carotenoid isomer profiles of biological tissues; (b) analysis of *cis* versus all-*trans* carotenoids in studies of their comparative metabolic or physiological roles; and (c) purification and purity assessment of carotenoids.

### Acknowledgements

The authors thank Hoffmann-La Roche (Nutley, NJ, USA) for generously furnishing all-*trans*  $\beta$ -cryptoxanthin. Technical assistance provided by Nada Simunovic and Ruth Watkins is acknowledged with gratitude.

### References

- [1] G.W. Burton and K.U. Ingold, *Science*, 224 (1984) 569–573.
- [2] P.F. Conn, W. Schalch and T.G. Truscott, *J. Photochem. Photobiol. (B) Biol.*, 11 (1991) 41–47.
- [3] P.F. Conn, C. Lambert, E.J. Land, W. Schalch and T.G. Truscott, *Free Rad. Res. Commun.*, 16 (1992) 401–408.
- [4] P. Di Mascio, S. Kaiser and H. Sies, *Arch. Biochem. Biophys.*, 274 (1989) 532–538.
- [5] N.I. Krinsky, *Free Rad. Biol. Med.*, 7 (1989) 617–635.
- [6] R. Peto, R. Doll, J.D. Buckley and M.B. Sporn, *Nature*, 290 (1981) 201–208.
- [7] N.J. Temple and T.K. Basu, *Nutr. Res.*, 8 (1988) 685–701.
- [8] A. Ben-Amotz, A. Lers and M. Avron, *Plant Physiol.*, 86 (1988) 1286–1291.
- [9] L.A. Chandler and S.J. Schwartz, *J. Agric. Food Chem.*, 36 (1988) 129–133.
- [10] J.P. Sweeney and A.C. Marsh, *J. Assoc. Off. Anal. Chem.*, 53 (1970) 937–940.
- [11] J.P. Sweeney and A.C. Marsh, *J. Am. Diet. Assoc.*, 59 (1971) 238–243.
- [12] L. Zechmeister, *cis-trans* Isomeric Carotenoids, Vitamins A and Arylpolyenes, Academic Press, New York, 1962.
- [13] S. Mokady, M. Avron and A. Ben-Amotz, *J. Nutr.*, 120 (1990) 889–892.
- [14] W. Stahl, W. Schwarz, A.R. Sundquist and H. Sies, *Arch. Biochem. Biophys.*, 294 (1992) 173–177.
- [15] K.S. Epler, L.C. Sander, R.G. Ziegler, S.A. Wise and N.E. Craft, *J. Chromatogr.*, 595 (1992) 89–101.
- [16] Y. Koyama, M. Hosomi, A. Miyata, H. Hashimoto, S.A. Reames, K. Nagayama, T. Kato-Jippo and T. Shimamura, *J. Chromatogr.*, 439 (1988) 417–422.
- [17] H.H. Schmitz, C. Emenhiser and S.J. Schwartz, *J. Agric. Food Chem.*, in press.
- [18] K. Tsukida, K. Saiki, T. Takii and Y. Koyama, *J. Chromatogr.*, 245 (1982) 359–364.
- [19] H. Hashimoto, Y. Koyama and T. Shimamura, *J. Chromatogr.*, 448 (1988) 182–187.
- [20] N. Katayama, H. Hiashimoto, Y. Koyama and T. Shimamura, *J. Chromatogr.*, 519 (1990) 221–227.
- [21] Y. Koyama, I. Takatsuka, M. Kanaji, K. Tomimoto, M. Kito, T. Shimamura, J. Yamashita, K. Saiki and K. Tsukida, *Photochem. Photobiol.*, 51 (1990) 119–128.
- [22] M. Vecchi, G. Englert, R. Maurer and V. Meduna, *Helv. Chim. Acta*, 64 (1981) 2746–2758.
- [23] F. Khachik, G.R. Beecher, M.B. Goli, W.R. Lusby and J.C. Smith, Jr., *Anal. Chem.*, 64 (1992) 2111–2122.
- [24] F. Khachik, G. Englert, C.E. Daitch, G.R. Beecher, L.H. Tonucci and W.R. Lusby, *J. Chromatogr.*, 582 (1992) 153–166.
- [25] W.W. Christie, *High-performance Liquid Chromatography and Lipids: A Practical Guide*, Pergamon Press, Oxford, 1987.
- [26] L.C. Sander, K.E. Sharpless, N.E. Craft and S.A. Wise, *Anal. Chem.*, 66 (1994) 1667–1674.
- [27] N.E. Craft, *Meth. Enzymol.*, 213 (1992) 185–205.
- [28] N.E. Craft, S.A. Wise and J.H. Soares, Jr., *J. Chromatogr.*, 589 (1992) 171–176.
- [29] C.A. O'Neil, S.J. Schwartz and G.L. Catignani, *J. Assoc. Off. Anal. Chem.*, 74 (1991) 36–42.
- [30] W. Stahl, A.R. Sundquist, M. Hanusch, W. Schwarz and H. Sies, *Clin. Chem.*, 39 (1993) 810–814.
- [31] Z. Matus and R. Ohmacht, *Chromatographia*, 30 (1990) 318–322.
- [32] A. Fiksdahl, J.T. Mortensen and S. Liaaen-Jensen, *J. Chromatogr.*, 157 (1978) 111–117.
- [33] G.J. Handelman, B. Shen and N.I. Krinsky, *Methods Enzymol.*, 213 (1992) 336–346.
- [34] N.I. Krinsky, M.D. Russett, G.J. Handelman and D.M. Snodderly, *J. Nutr.*, 120 (1990) 1654–1662.
- [35] F.W. Quackenbush, *J. Liq. Chromatogr.*, 10 (1987) 643–653.
- [36] L.A. Chandler and S.J. Schwartz, *J. Food Sci.*, 52 (1987) 669–672.
- [37] A. Pettersson and L. Jonsson, *J. Micronutr. Anal.*, 8 (1990) 23–41.
- [38] C.A. O'Neil and S.J. Schwartz, *J. Chromatogr.*, 624 (1992) 235–252.
- [39] G. Britton, *Methods Enzymol.*, 111 (1985) 113–149.
- [40] L.C. Sander and S.A. Wise, *Anal. Chem.*, 59 (1987) 2309–2313.



ELSEVIER

Journal of Chromatography A, 707 (1995) 217–224

JOURNAL OF  
CHROMATOGRAPHY A

# Normal-phase high-performance liquid chromatography using enhanced-fluidity liquid mobile phases

Stephen T. Lee, Susan V. Olesik\*

*Department of Chemistry, The Ohio State University, 120 West 18th Avenue, Columbus, OH 43210-1173, USA*

First received 22 July 1994; revised manuscript received 8 February 1995; accepted 21 February 1995

## Abstract

The application of an enhanced-fluidity liquid mixture (*n*-hexane–CO<sub>2</sub>) as a mobile phase in normal-phase HPLC using a 3-cyanopropyl polysiloxane stationary phase was evaluated. Decreased pressure drop across the chromatographic column was observed with increasing proportions of added CO<sub>2</sub> to the mixtures. For selected mixture conditions, increased efficiency and decreased peak asymmetry were obtained in comparison to that for separations with 100% *n*-hexane. A limiting amount of CO<sub>2</sub> that could be added to hexane was found. If more CO<sub>2</sub> was added past that limit, serious peak asymmetry lowered the measured column efficiency.

## 1. Introduction

High-performance liquid chromatography (HPLC) is presently the most widely used separation technique for nonvolatile compounds. However, HPLC is not without limitations. HPLC typically has larger pressure drops across the chromatographic column, longer analysis times, and lower efficiencies than supercritical fluid chromatography (SFC) or gas chromatography (GC). These deficiencies can be attributed to higher viscosities and lower solute diffusion rates in liquids compared to supercritical fluids or gases. GC and SFC also have limitations: GC is limited to the separation of volatile compounds, while SFC is limited in its ability to chromatograph polar molecules.

Enhanced-fluidity liquid mobile phases provide HPLC some of the advantages of SFC.

Enhanced-fluidity mobile phases are prepared by dissolving large proportions of low-viscosity liquids, such as CO<sub>2</sub>, in commonly used solvents. It was previously demonstrated in our laboratory that the use of enhanced-fluidity liquids provided mobile phases with low viscosities. In addition, chromatographic advantages such as increased diffusion, lower pressure drops, and decreased analysis times without loss of solvent strength were demonstrated for reversed-phase HPLC [1–3] and for HPLC using a glassy carbon stationary phase [4].

In this paper, we report initial studies of enhanced-fluidity mobile phases in normal-phase HPLC with a hexane–CO<sub>2</sub> mobile phase. Mobile phases in normal-phase chromatography are typically mixtures of a nonpolar solvent, such as hexane, and one or more polar solvents. The polar solvents are added to control the selectivity of the separation. The addition of CO<sub>2</sub> to normal-phase mobile phases should be viewed as

\* Corresponding author.

a fluidity modifier. Especially for the separation of polar solutes, the addition of CO<sub>2</sub> will not affect markedly the selectivity of the separation. As a benchmark characterization, we have concentrated on an evaluation of the hexane–CO<sub>2</sub> mixture with the full understanding that more polar modifiers must be added to this mixture for the separation of polar solutes. An attractive feature of the use of liquid carbon dioxide as a co-solvent in normal-phase HPLC is that when carbon dioxide is included in mixtures, it functions as a homogenizing agent and often allows complete miscibility of solvent pairs with substantially different polarity. [5]

## 2. Experimental

### 2.1. Instrumentation

The chromatographic system was previously described [2]. Briefly, it consists of an ISCO LC-2600 syringe pump (ISCO, Lincoln, NE, USA), a Valco W-series high-pressure injection valve with an injection volume of 60 nl (Valco Instruments, Houston, TX, USA), a Deltabond Cyano (3-cyanopropyl polysiloxane stationary phase), 250 × 1 mm I.D. column packed with 5-μm diameter particles containing 300 Å pores with stationary-phase loading of ca. 4% carbon (Keystone Scientific, Bellefonte, PA, USA) and a Spectra-Physics UV2000 UV–Vis absorbance detector equipped with a capillary flow cell mounting (Model 9550-0155). A piece of 50 μm I.D. fused-silica tubing (Polymicro Technologies, Phoenix, AZ, USA) was connected to the end of the column with a zero dead volume fitting; a flow cell was created by removing the polyamide coating from a 5-mm length of the tubing and centering it in the capillary flow cell mounting. The detector excitation wavelength was 210 nm. A Setra 204 series pressure transducer (Setra Systems, Acton, MA, USA) was placed in-line after the detector and before the post-detection restrictor. The outlet pressure was monitored because the column pressure must be maintained above a minimum pressure to prevent the hexane–CO<sub>2</sub> mobile-phase mixture from

separating into two phases (liquid/gas). For example, at 25°C and a CO<sub>2</sub> mole fraction of 0.6, the hexane–CO<sub>2</sub> separates into two phases at pressures lower than 4.36 MPa [6]. All experiments in this study were performed under conditions in which the hexane–CO<sub>2</sub> mixture was in a single liquid phase. The flow control for the chromatographic system was maintained by an appropriate length of 8, 15, or 20 μm I.D. fused-silica tubing. The column inlet pressure was maintained at 13.8 MPa throughout this study except when hexane was the mobile phase. When *n*-hexane was used as the mobile-phase higher pressures were necessary to obtain linear velocities above 0.22 cm/s. Data were collected on a strip chart recorder (Linear Instruments, Reno, NV, USA).

Column efficiency, *N*, was calculated manually via the method developed by Foley and Dorsey [7] (Eq. 1):

$$N = \frac{41.7(t_r/W_{0.1})^2}{B/A + 1.25} \quad (1)$$

where *t<sub>r</sub>* is retention time, *W*<sub>0.1</sub> is the width of the chromatographic band at 10% of the peak's height and *B/A* is an empirical asymmetry factor. *A* and *B* are referenced to the peak maximum with *A* + *B* = *W*<sub>0.1</sub> [8]. This calculation is based on the exponentially modified Gaussian model (Eq. 2):

$$N = \frac{t_r^2}{\sigma_G^2 + \tau^2} \quad (2)$$

where *σ* is the standard deviation of the Gaussian function and *τ* is the time constant of the exponential. Two independent studies recently showed that Foley and Dorsey's method is the most accurate means to manually determine chromatographic column efficiency [9,10].

The solvent strength was characterized by measuring the Kamlet–Taft *π*\* parameter for the hexane–CO<sub>2</sub> mixtures. To determine the *π*\* parameter the solvatochromic shift of the ortho-nitroanisole UV–Vis spectrum was measured [11]. A DMS-100 UV–Vis (Varian, Sunnyvale, CA, USA) was used in these studies. The *π*\* parameter was calculated using Eq. 5 [11]:



$$\pi^* = \frac{\nu_{\max} - \nu_0}{s} \quad (3)$$

where  $\nu_{\max}$  is the frequency of the absorbance maximum of *o*-nitroanisole, when dissolved in the solvent of interest,  $\nu_0$  is the frequency of the absorbance maximum for the molecular probe in a reference solvent (typically cyclohexane), and  $s$  is a proportionality constant that limits the values of  $\pi^*$  to a range of 0 to 1 for common solvents. The literature value of  $s$  for *o*-nitroanisole,  $-2.428 \pm 0.195$  kK, was used to calculate  $\pi^*$  in these experiments [12]. Cyclohexane was used as the reference solvent. The absorption spectrum was obtained using a home-made, stainless-steel, high-pressure, optical flow cell with an internal volume of 10 ml and an optical path-length of 3.5 cm. The optical path was terminated on each end with cylindrical quartz windows that were 2.86 cm diam. by 1.75 cm thick (ESCO Prod., Oak Ridge, NJ, USA). The optical cell was sealed with Teflon O-rings. The concentration of *o*-nitroanisole used in these studies was approximately  $1 \cdot 10^{-4}$  M.

## 2.2. Materials

The test analytes used in this study were phenetole, methyl benzoate, nitrobenzene, and dimethyl phthalate. The concentrations of the analytes were 4830 ppm phenetole, 5470 ppm methyl benzoate, 5950 ppm dimethyl phthalate, and 3590 ppm nitrobenzene in pentane. Pentane was unretained. Supercritical fluid grade CO<sub>2</sub> from Scott Specialty Gases (Plumsteadville, PA, USA) and 99 + % hexane from Aldrich Chemical (Milwaukee, WI, USA) were used as purchased. Hexane–CO<sub>2</sub> mixtures were prepared using two high-pressure syringe pumps. A known volume of hexane was placed in one pump. Liquid CO<sub>2</sub> at 13.8 MPa and 25°C was held in another pump. Using the known density of CO<sub>2</sub> at these conditions the appropriate volume of CO<sub>2</sub> was calculated and then delivered to the pump holding the hexane to make a given hexane–CO<sub>2</sub> mixture. The mixture was then pressurized to 13.8 MPa and allowed to equilibrate at 25°C for at least 12 h to ensure complete

mixing of the solution. This waiting period was not necessary for these mixtures because they are highly miscible. However this is standard procedure for all mixtures that we make in a syringe pump by this means. The completeness of mixing was then checked by monitoring the reproducibility of the solute capacity factors for a given composition.

## 3. Results and discussion

### 3.1. Viscosity and pressure drop

The viscosity of the mobile-phase mixtures (Fig. 1) was estimated using the estimation methods of Teja and Rice, and Grunberg and Nissan [13]. The mixture viscosity decreases substantially with increasing proportions of CO<sub>2</sub>. As expected when the viscosity of the mobile phase decreases, the pressure drop across the column also decreases for the same linear velocity. Table 1 shows the pressure drop measured across the system for comparable linear velocities with different mobile-phase compositions. The pressure drop across the column decreased by a factor of approximately 6.5 when the mobile-phase mixture was varied from 100% *n*-hexane to 100% CO<sub>2</sub>.

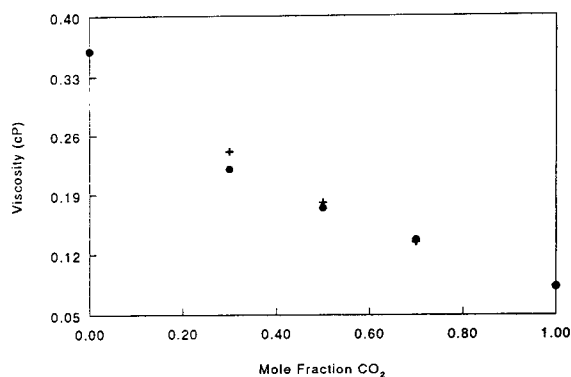


Fig. 1. Estimated viscosity of mobile phases at 25°C and 13.8 MPa: the Grunberg and Nissan method [13] (+); the Teja and Rice method [13] (●).

Table 1  
Variation in pressure drop across the chromatographic column with mobile-phase conditions

Mole fraction CO <sub>2</sub>	Linear velocity (cm/s)	Pressure drop (MPa)
0.0	0.121	6.18
0.33	0.118	5.40
0.5	0.121	4.18
0.7	0.121	1.53
1.0	0.116	0.95

### 3.2. Diffusion coefficients

Various empirical expressions have been used to describe the relationship between the viscosity of a solvent and solute diffusivity. Eq. 1 has proven to be the most accurate relationship for predicting diffusion coefficients from solvent viscosities for nonaqueous and mixed solvents over a wide range of temperatures and viscosities [13,14].

$$D_m = A\eta^p \quad (4)$$

where  $D_m$  is the diffusion coefficient of a given solute,  $\eta$  is the viscosity of the solvent and  $A$  and  $p$  are parameters that are characteristic of the solute.  $A$  and  $p$  can be readily determined from the radius of the solute [15]. Using Bondi radii [16] for the studied solutes, the  $p$  parameter is approximately 0.9. Therefore from Eq. 1, the diffusion coefficients for the studied solutes are expected to vary approximately inversely with the viscosity of the mobile-phase mixture (Fig. 1).

### 3.3. Retention

Fig. 2 shows the variation in capacity factor with mobile-phase composition. The capacity factors of nitrobenzene and dimethyl phthalate decreased with increasing proportions of liquid carbon dioxide added to the mobile phase. Minimum capacity factor values were reached at a CO<sub>2</sub> mole fraction of 0.70. Also as the mole fraction of CO<sub>2</sub> is increased the selectivity of the separation decreases. Fig. 3A is a chromatogram

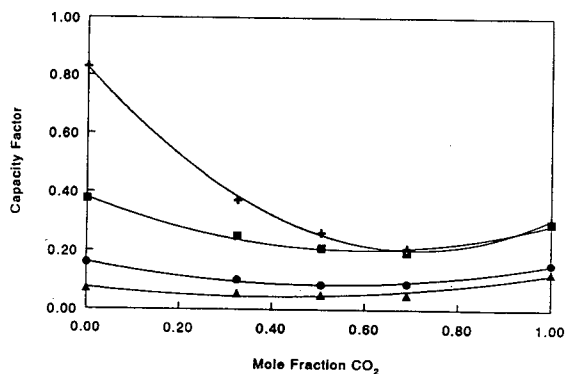


Fig. 2. Variation in capacity factor with mobile-phase composition: phenetole (Δ); methyl benzoate (○); nitrobenzene (□); dimethyl phthalate (+). 95% confidence intervals are within the size of the marker. Lines are added as a guide to the eye.

of the test solutes with *n*-hexane as the mobile phase, while Fig. 3B is a chromatogram of the test solutes with 0.50:0.50 mole fraction of *n*-hexane–CO<sub>2</sub> as the mobile phase at the same linear velocity. This comparison illustrates the reduction in retention and selectivity with a 0.50:0.50 mole fraction of *n*-hexane–CO<sub>2</sub> mobile phase.

From the data in Figs. 2 and 3, the addition of CO<sub>2</sub> to hexane clearly increases the mobile-phase solvent strength. Retention of solutes is expected to decrease as the polarity of the solvent increases. The Kamlet–Taft  $\pi^*$  parameter was measured for the hexane–CO<sub>2</sub> mixtures.  $\pi^*$  is a measure of solvent polarizability and dipolarity. Fig. 4 shows that as more CO<sub>2</sub> is added to the mixture, the  $\pi^*$  of the mixture also increases. Interestingly, the  $\pi^*$  parameter of the mixture begins to reach an asymptote near a CO<sub>2</sub> mole fraction of 0.70 which is where the capacity factor levels off as well. Electron donor–acceptor complexing of CO<sub>2</sub> with unsaturated compounds, such as alkenes and benzene [17,18] is well documented. Therefore another possible reason for the diminished retention with the addition of CO<sub>2</sub> is that similar complexation with the cyano-functionality of the stationary phase might occur. More studies are required to understand better the exact reason for the retention variation.

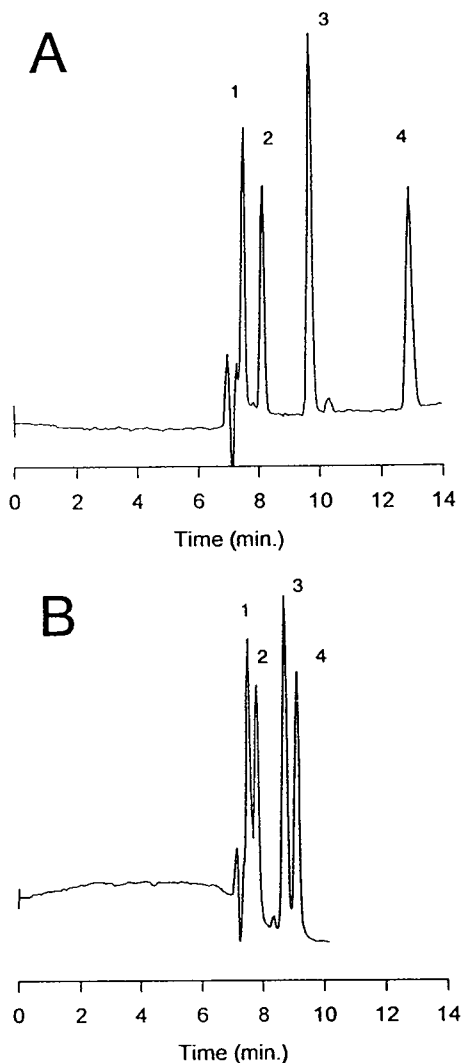


Fig. 3. Chromatograms at 13.8 MPa and 25°C: (A) with *n*-hexane as the mobile phase, and (B) with 0.50 mole fraction of CO<sub>2</sub> in hexane as the mobile phase. Peaks: 1 = phenetole, 2 = methyl benzoate, 3 = nitrobenzene, and 4 = dimethyl phthalate.

### 3.4. Band dispersion and efficiency

The non-coupled Van Deemter equation shows the relationship between the column band dispersion or plate height,  $H$ , and linear velocity of the mobile phase,  $u$ :

$$H = A + \frac{B}{u} + Cu \quad (5)$$

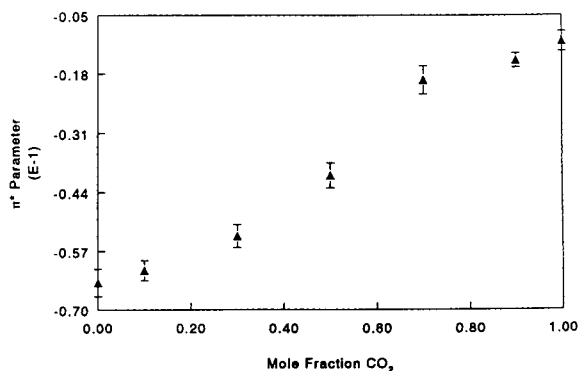


Fig. 4. Variation in the Kamlet-Taft  $\pi^*$  parameter as a function of mobile-phase composition. Error bars indicate 95% confidence intervals.

where  $A$  and  $B$  are measures of the band dispersion from multiple flow paths and longitudinal diffusion, respectively, and  $C$  is a measure of the summation of band dispersion caused by the combined resistance to mass transfer in the mobile phase, the stagnant mobile phase that is present in the pores of the particles, and the stationary phase. In packed columns,  $B = \gamma D_m$ , where  $\gamma$  is an obstruction factor and  $D_m$  is the diffusion coefficient of the solute in the mobile phase. The resistance to mass transfer in the mobile and stagnant mobile phases in the particle pores can be expressed as  $C_{m,sm} = f(k')/D_m$ , where  $k'$  is the capacity factor.

In most HPLC separations, the linear velocity used is such that the  $C$  terms are the major cause of band dispersion in the column. Also, when microporous particles are used, the  $C_{sm}$  term (due to dispersion in the stagnant mobile phase in the pores) often predominates [19]. If the packing particles are spherical, the following expression describes the variables that control the  $C_{sm}$  term:

$$C_{sm} = \frac{(1 - \phi + k')^2 d_p^2 u}{30(1 - \phi)(1 + k')^2 \gamma D_m} \quad (6)$$

where  $\phi$  is the fraction of total mobile phase in the intraparticle space, and  $\gamma$  is the tortuosity factor. Since the diffusion coefficient of the solute is inversely related to solvent viscosity,

from Eq. 6, the  $C_{sm}$  term is expected to decrease with decreasing mobile-phase viscosity. Over the limited range of viscosities possible with common liquid mobile phases in normal-phase liquid chromatography using bonded phases, this is clearly the experimentally observed trend [20]. Therefore if diffusion in the stagnant mobile phase controls band dispersion in the present system, then from Eq. 6, the addition of  $\text{CO}_2$  to hexane should cause decreased band dispersion due to increased solute diffusion coefficients as long as the capacity factors do not increase with the addition of  $\text{CO}_2$ .

Also when the first derivative of the van Deemter equation is taken with respect to  $u$ , set equal to zero, and the definitions of  $B$  and  $C$  are substituted, we obtain the following expression:

$$u_{\text{opt}} \propto \frac{D_m}{\sqrt{f(k')}} \quad (7)$$

This relationship predicts that if diffusion is the rate-limiting step in the mass transfer process, then as the diffusion coefficient of a solute increases, a corresponding shift in the optimum linear velocity should occur when all other factors remain the same.

To evaluate the effect of mobile-phase composition on band dispersion, the variation of plate height with linear velocity was determined for nitrobenzene and dimethyl phthalate for mobile-phase compositions of 0.0, 0.33, 0.50, 0.70, and 1.0 mole fractions of  $\text{CO}_2$  in  $n$ -hexane at  $26^\circ\text{C}$  and 13.8 MPa. Eq. 1 was used to calculate the plate heights from the experimental peak shapes.

Figs. 5A and 5B show the reduced plate height versus linear velocity (0.00–0.40 cm/s) for nitrobenzene and dimethyl phthalate, respectively. For both analytes, there is no observable shift in the optimum velocity as a function of added  $\text{CO}_2$  to the mobile phase. For high linear velocities, the slope of the reduced plate height versus linear velocity plots for dimethyl phthalate decreased when  $\text{CO}_2$  was added to hexane for the following mixtures: 0.00 mole fraction of  $\text{CO}_2$ , 0.33 mole fraction of  $\text{CO}_2$ , 0.50 mole fraction of  $\text{CO}_2$ . For nitrobenzene, the slopes of these curves for the same mobile-phase compositions

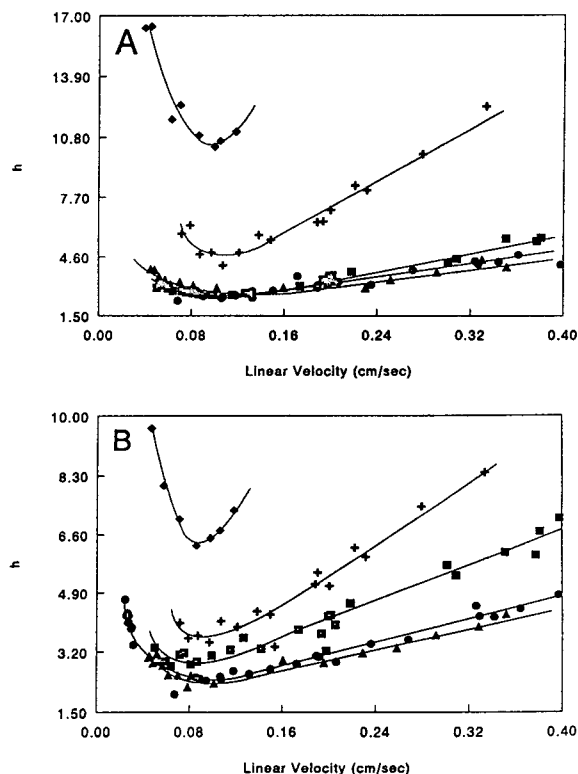


Fig. 5. Variation of reduced plate height of (A) nitrobenzene and (B) dimethyl phthalate as a function of mobile-phase linear velocity at 13.8 MPa for different mobile-phase compositions:  $n$ -hexane ( $\square$ ); 0.33 mole fraction of  $\text{CO}_2$  in hexane ( $\circ$ ); 0.50 mole fraction of  $\text{CO}_2$  in hexane ( $\triangle$ ); 0.70 mole fraction of  $\text{CO}_2$  in hexane ( $+$ );  $\text{CO}_2$  ( $\diamond$ ). Average relative standard deviation of the data was 5%.

were statistically the same. By comparing Fig. 5A and Fig. 5B and knowing that the capacity factor of dimethyl phthalate decreased significantly with increased  $\text{CO}_2$  while that of nitrobenzene decreased minimally (see Fig. 2), it is clear that the decrease in plate height with added  $\text{CO}_2$  for dimethyl phthalate was primarily due to the capacity factor change, and not to a decrease in diffusion coefficient. Also interestingly, instead of seeing a further enhancement in efficiency when the added  $\text{CO}_2$  was greater than the 0.50 mole fraction, the reduced plate height dramatically increases for mobile-phase compositions of 0.70 and 1.00 mole fractions of  $\text{CO}_2$  in  $n$ -hexane.

Fig. 6 shows the variation in asymmetry factor,

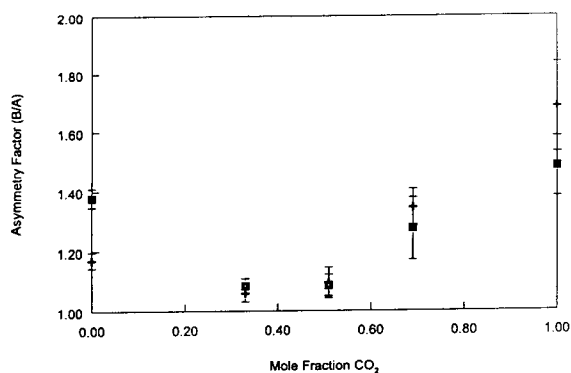


Fig. 6. Variation in peak asymmetry ( $B/A$ ) with mobile-phase composition: nitrobenzene (+); dimethyl phthalate (■). Error bars indicate 95% confidence intervals.

$B/A$ , with mobile-phase composition over the linear velocity range 0.00–0.12 cm/s. The observed trend in the plate height measurements correlates closely with the variation in the peak asymmetry factor over the same mobile-phase compositions. Peak tailing is lowest for nitrobenzene and dimethyl phthalate with mobile-phase compositions of 0.33 and 0.50 mole fractions of  $\text{CO}_2$  in *n*-hexane and increases markedly for 0.70 and 1.00 mole fractions of  $\text{CO}_2$  in neat *n*-hexane. The asymmetry factor was also measured for the two solutes over the 0.16–0.24 cm/s linear velocity range. The shape of the curve of  $B/A$  versus  $\text{CO}_2$  mole fraction was the same as that observed in Fig. 6 for the lower flow-rate conditions. The major difference between the measured asymmetry factors for the two linear velocities ranges is that the magnitude of the asymmetry factor is greater for the higher linear velocity conditions. For example, the asymmetry factor for 0.70 mole fraction of  $\text{CO}_2$  in *n*-hexane at the higher linear velocities was 1.82 and 1.67 for nitrobenzene and dimethyl phthalate, respectively, which is substantially higher than the  $B/A$  values observed at the lower linear velocities. The asymmetry factor for the 0, 0.33, and 0.50 mole fractions of  $\text{CO}_2$  in *n*-hexane mobile-phase compositions did not vary substantially with linear velocity. The measured peak asymmetry did not vary with solute concentration. From a comparison of the band

dispersion data in Fig. 5 with the peak asymmetry data in Fig. 6 and a careful look at the data used to calculate plate heights, it is clear that the peak asymmetry caused the variation in the measured plate height.

Many possible causes for the observed variations in plate height and peak asymmetry exist [21]. The surfaces of chemically bonded stationary phases are often heterogeneous. For moderately polar compounds, such as those used in this study, the 3-cyanopropylpolysiloxane bonded phases have been found to behave chromatographically like a deactivated silica gel column [22,23]. Residual surface silanols were believed to substantially control the retention under those conditions. From the present data and our prior experience with supercritical  $\text{CO}_2$  as an eluent, we speculate that the addition of liquid  $\text{CO}_2$  to the mobile phase initially lowers the asymmetry of the chromatographic band because it is more polar than *n*-hexane. However, when more than 0.50 mole fraction of  $\text{CO}_2$  is added to hexane, the stationary phase may begin to expand slightly (as is often the case with supercritical  $\text{CO}_2$ ) and then more surface silanols are exposed on the support which causes the increased band broadening with mixture compositions of 0.7 and 1.0 mole fractions of  $\text{CO}_2$ .

Because of the mixed retention mode (combined interaction of silanols and cyano groups with solutes) of the cyano phase, amines are often added to the mobile phase for complexing with the surface silanol groups. Additional studies to develop and further understand enhanced-fluidity normal-phase separations are presently underway. The addition of a more polar modifier to the eluent should provide better capping of the surface silanols; then the expected increase in efficiency should be more readily apparent when  $\text{CO}_2$  is added to the mixture.

#### 4. Conclusions

In previous published work on reversed-phase separations we illustrated that by using enhanced-fluidity liquid mixtures as eluents the pressure

drop across a chromatographic column was diminished, as well as that the efficiency and speed of separation increased. This study was an initial step to analyze the attributes of enhanced-fluidity liquid mixtures for normal-phase chromatography. The viscosity of the eluent was lowered by adding CO<sub>2</sub> to *n*-hexane which resulted in substantially decreased pressure drop across the chromatographic column and increased solute diffusion in the eluent. The linear velocity range and the length of the chromatographic column in HPLC is often limited by the viscosity of the mobile phases employed and the unreasonable head pressures needed to achieve fast linear velocities. The low viscosities and pressure drops attained by using enhanced-fluidity mixtures as mobile phase for HPLC will extend the operable linear velocity range and/or the length of the chromatographic column in HPLC. Extending the linear velocity range will lead to faster separations, while the use of longer columns will provide more total theoretical plates for resolution of complex samples.

However, gains in efficiency were only observed for specific mixtures of hexane–CO<sub>2</sub>. This trend correlates closely with the observed trend in peak asymmetry, where enhanced-fluidity mixtures of 0.33 and 0.50 mole fractions of CO<sub>2</sub> in *n*-hexane provided chromatograms with the most symmetric peaks. Variations in solute interactions in the bulk mobile phase or the stationary phase when CO<sub>2</sub> was added, probably caused changes in peak asymmetry and also controlled the measured efficiency. Resistance to mass transfer in the bulk mobile phase or in the stagnant mobile phase of the pores was not the controlling force that caused the chromatographic band shape for some of the hexane–CO<sub>2</sub> mixtures. More studies are necessary to determine whether small proportions of polar cosolvent can stop the variation of peak asymmetry with added CO<sub>2</sub>. Only then will the lowered solvent viscosity have a measurable effect on the chromatographic efficiency. These experiments are presently underway.

### Acknowledgements

We thank Qin Chen for measuring the polarity of the mixtures. We gratefully acknowledge the

support for this work by the National Science Foundation under Grant CHE-9118913.

### References

- [1] Y. Cui, Ph.D. Dissertation, The Ohio State University, Columbus, OH, 1992.
- [2] S.T. Lee and S.V. Olesik, *Anal. Chem.*, 66 (1994) 4498.
- [3] Y. Cui and S.V. Olesik, *J. Chromatogr. A*, 691 (1994) 151.
- [4] Y. Cui and S. Olesik, *Anal. Chem.*, 63 (1991) 1812.
- [5] A.W. Francis, *J. Am. Chem. Soc.*, 58 (1954) 1099.
- [6] K. Ohgagaki and T. Katayama, *J. Chem. Eng. Data*, 21 (1976) 53.
- [7] J.P. Foley and J.G. Dorsey, *Anal. Chem.*, 55 (1983) 730.
- [8] J.J. Kirkland, W.W. Yau, H.J. Stoklosa and C.H. Dilks Jr., *J. Chromatogr. Sci.*, 15 (1977) 303.
- [9] B.A. Bidlingmeyer and F.V. Warren Jr., *Anal. Chem.*, 56 (1984) 1583A.
- [10] A. Berthod, *J. Liq. Chromatogr.*, 12 (1989) 1187.
- [11] P.C. Sadek, P.W. Carr, R.M. Doherty, M.J. Kamlet, R.W. Taft and M.H. Abraham, *Anal. Chem.*, 57 (1985) 2971.
- [12] M.J. Kamlet, J.L. Abboud and J.L. Taft, *J. Am. Chem. Soc.*, 99 (1977) 6027.
- [13] A.S. Teja and P. Rice, in R.C. Reid, J.M. Prausnitz and B.E. Poling (Editors), *The Properties of Gases and Liquids*, 4th ed., McGraw-Hill, New York, NY, 1987, Ch. 9.  
L. Grunberg and A.H. Nissan, in R.C. Reid, J.M. Prausnitz and B.E. Poling (Editors), *The Properties of Gases and Liquids*, 4th ed., McGraw-Hill, New York, NY, 1987, Ch. 11.
- [14] W. Hayduk and S.C. Cheng, *Chem. Eng. Sci.*, 26 (1971) 635.
- [15] S.H. Chen, H.T. Davis and D.F. Evans, *J. Chem. Phys.*, 77 (1982) 2540.
- [16] A. Bondi, *J. Phys. Chem.*, 68 (1964) 441.
- [17] A.L. Meyers and J.M. Prausnitz, *Ind. Eng. Chem. Fund.*, 4 (1965) 209.
- [18] J.H. Hildebrand and R.L. Scott, *Regular Solutions*, Prentice-Hall, New York, NY, 1962.
- [19] C. Horváth and H.-J. Lin, *J. Chromatogr.*, 149 (1978) 43.
- [20] J.J. Kirkland, *J. Chromatogr. Sci.*, 9 (1971) 206.
- [21] L.R. Snyder and J.J. Kirkland, *Introduction to Modern Liquid Chromatography*, 2nd ed., John Wiley, New York, NY, 1979, p. 791.
- [22] P.L. Smith and W.T. Cooper, *J. Chromatogr.*, 410 (1987) 249.
- [23] E.L. Weiser, A.W. Salotto, S.M. Flach and L.R. Snyder, *J. Chromatogr.*, 303 (1984) 1.



ELSEVIER

Journal of Chromatography A, 707 (1995) 225–231

JOURNAL OF  
CHROMATOGRAPHY A

## Purification of antibody Fab fragments by cation-exchange chromatography and pH gradient elution

R. Mhatre\*, W. Nashabeh, D. Schmalzing, X. Yao, M. Fuchs, D. Whitney,  
F. Regnier

*PerSeptive Biosystems, 500 Old Connecticut Path, Framingham, MA 01701, USA*

First received 10 November 1994; revised manuscript received 27 February 1995; accepted 7 March 1995

### Abstract

The use of a pH gradient as opposed to conventional salt gradient for elution in cation-exchange chromatography was explored. pH gradients were found to be very effective in separating Fab fragments and other proteins with differences in isoelectric point as low as 0.1. To determine the efficiency of purification, the separated peaks were collected and further analyzed by capillary electrophoresis.

### 1. Introduction

With the increasing use of immunoaffinity chromatography, the separation and purification of antibodies has been an ongoing challenge. In addition, the recent work on capillary electrophoresis (CE)-based immunoassays have stretched the need for highly purified antibodies or antibody fragments [1–4]. To improve sensitivity and specificity in CE, either the antibody or the antigen is labeled with a dye. Prior to labeling, it is desirable that the antibody be purified since the various isoforms that recognize the antigen will generally all be labeled. The micro heterogeneity of an antibody complicates the purification and in most cases, the various isoforms of the antibody are only partially resolved. Purification of an antibody therefore requires extremely powerful separation techniques. Preparative isoelectric focusing (IEF)

has been shown to resolve the isoforms of monoclonal antibodies [5,6]. However, the low product yield and the laborious extraction of sample from the gel pose a major limitation.

Chromatofocusing is an alternative to IEF [7–9]. In chromatofocusing a weak ion-exchanger is titrated with an amphoteric buffer (mobile phase). Upon titration, a pH gradient that is established in the column focuses the proteins into sharp bands. Proteins with minor differences in isoelectric point (*pI*) are easily resolved and the separations are comparable to preparative IEF. Chromatofocusing is ideal for preparative-scale purification of components with closely related *pI* values. However, in cases where chromatofocusing is used in a semi-preparative or analytical format [10,11], pH gradient separation may be more appropriate since the separation time is significantly reduced.

Ion-exchange chromatography has been proven to be a more practical approach for purification of biomolecules [12,13]. Though the

\* Corresponding author.

product throughput/yield is high, the resolution in ion-exchange is generally lower than with IEF, especially when salts gradients are used. More recently, ion-exchange chromatography using pH gradients has been demonstrated to effectively resolve isoforms of an antibody [6]. Though the isoforms were only partially resolved by the pH gradient, sufficient purified material could be obtained by collection of the fractions.

This report explores the use of pH gradients for resolution of Fab fragments and other proteins having closely related *pI* values. The advantage of using a pH gradient vs. a conventional salt gradient is that the collected fractions contain very low levels of salt (10–20 mM) thereby eliminating the necessity of desalting. Also, the resolution can be far superior to salt gradient elution because the separation is based on relative differences in *pI* of the protein (see Results and discussion).

## 2. Experimental

### 2.1. Apparatus

A gradient HPLC system (BioCAD, PerSeptive Biosystems, Framingham, MA, USA) equipped with a UV detector operating at 280 nm was used. The CE system was assembled in the laboratory and consisted of a Spellman 1000 R power supply (Plainview, NY, USA) and a PerSeptive Biosystems UV/VIS-250 detector operating at 214 nm.

### 2.2. Chemicals and reagents

All chemicals used for preparation of HPLC buffers were of analytical grade. 2-(N-Morpholino)ethanesulfonic acid (MES), 2-amino-2-methyl-1,3-propanediol (AMPD) and N-tris(hydroxymethyl)-3-aminopropanesulfonic acid (TAPS) and the  $\beta$ -lactoglobulin were from Sigma (St. Louis, MO, USA). Reagents used for digestion of the antibody were from Pierce (Rockford, IL) and the Fab fragments were produced as described in the Immunopure kit from Pierce. The mouse monoclonal anticortisol anti-

body (subclass IgG<sub>2</sub>b) was purchased from Fitzgerald (Concord, MA, USA).

### 2.3. Cation-exchange HPLC

A strong cation-exchange (100 × 4.6 mm, 20  $\mu$ m particle size, sulfonic acid, catalog No. P021M526), POROS S/M column was used for the separation (PerSeptive Biosystems). The column was equilibrated with 10 mM, MES, pH 4.5. After injecting the sample, a linear gradient of increasing pH (10 mM, MES, pH 7.5) was used for elution of the proteins. The eluted peaks were collected and further analyzed by CE to determine their purity.

### 2.4. CE of the collected fractions

The collected fractions were analyzed by CE using a siloxanediol/polyacrylamide (27 cm × 50  $\mu$ m) capillary coated in the laboratory. The running buffer was 20 mM TAPS/AMPD, pH 8.8. The applied field strength was 1100 V/cm. Samples were loaded hydrodynamically for 10 s using a 10 cm differential height between the ends of the capillary.

## 3. Results and discussion

The principle for separation of proteins using pH gradients is quite straightforward. At the start of a cation-exchange run (loading step), pH of the mobile phase must be below the *pI* of the protein so that the protein has a net positive charge. The protein is therefore adsorbed on the cation-exchange surface. To elute a protein, the pH is gradually increased above the *pI* of the protein. At this point the protein acquires a negative charge and elutes from the column. Since elution is dependent on the *pI* of the protein, proteins with minor differences in *pI* can be very efficiently separated. A similar procedure could be used for elution from an anion-exchange surface except that the pH would have to be above the *pI* during loading and should be



gradually decreased below the *pI* of the protein for elution.

A strong cation-exchange column was used for separation to maintain a constant charge on the column surface throughout the pH gradient while changing the surface charge on only the protein. If the surface charge density on the column decreases during elution, it is possible that the resolution would be compromised. It is desirable that column charge density be high to maintain maximum resolution.

The Fab fragments were generated by digestion of an anti-cortisol IgG<sub>2</sub>b with papain. Papain cleaves one or more peptide bonds in the hinge region of the antibody producing two identical Fab and one Fc fragment. After removal of the Fc portion, three Fab isoforms were observed by gel IEF (not shown). The origin of heterogeneity in the Fab fragments is unclear. However, others have also reported on the heterogeneity obtained after papain digestion of IgG [14,15]. The three isoforms had *pI* values of 5.4, 5.5 and 5.8.

### 3.1. HPLC purification of Fab isoforms

During optimization of the pH gradient, it was found that slight variations in the gradient resulted in a significant change in resolution. Fig. 1 shows the separation of the various isoforms of the Fab using a pH gradient from 4.5 to 6.4 in 20 column volumes at a flow-rate of 1 ml/min. Approximately 100 µg of sample were injected and the various isoforms were easily separated within 20 mins. The fractions were collected and later analyzed by CE to determine the purity. Despite incomplete resolution of the isoforms, fractions could be collected from each peak devoid of impurities from other partially resolved peaks. The electropherograms for the individual fractions (Fig. 2) show that a single peak was obtained for each fraction. Recovery of the material was about 90%. The recovery was determined by collecting fractions off the HPLC column and measuring the UV absorbance at 280 nm vs. the absorbance of the original Fab mixture. An electropherogram of the Fab mixture is also shown at the bottom of Fig. 2. It is seen that

the resolution of CE is superior to that of HPLC in this case.

In most purifications, one of the goals is to maintain the biological activity of the protein. Harsh elution conditions such as salt, organic or extremes in pH can affect the biological activity of a protein. The mild loading and elution conditions used during pH gradient elution are therefore ideal for purification of the Fab fragments. All three isoforms were shown to be active by their ability to recognize the specific antigen [4]. Any one of the three purified isoforms could therefore be used to perform immunoassays.

### 3.2. Separation of β-lactoglobulin A and B

To further evaluate the resolution obtained with pH gradients, a mixture of β-lactoglobulins A and B was injected. The two forms differ in *pI* by approximately 0.1 unit (*pI* of β-lactoglobulin A is 5.13 and that of B is 5.23) [16]. The difference in *pI* stems from the differences in the amino acid composition. Asparagine (64) and valine (118) in A are replaced by glycine and alanine respectively in B [17]. A gradient from pH 5 to 6.6 was run over 15 min at a flow-rate of 0.5 ml/min. The separation of β-lactoglobulin A and B by pH gradients is shown in Fig. 3. In spite of a difference in *pI* of approximately 0.1 between the two species, a reasonably good separation was obtained. Separation of β-lactoglobulin A and B using a salt gradient (0–0.5 M NaCl) was unsuccessful. Resolution of the peaks could not be obtained using any of the salt gradients attempted.

## 4. Conclusions

It may be concluded that pH gradient elution cation-exchange chromatography can be a valuable tool for preparation of a single Fab isoform of a monoclonal antibody. Although CE is of superior resolution, it has inadequate loading capacity for the preparation of sufficient antibody to be used for immunological assays.

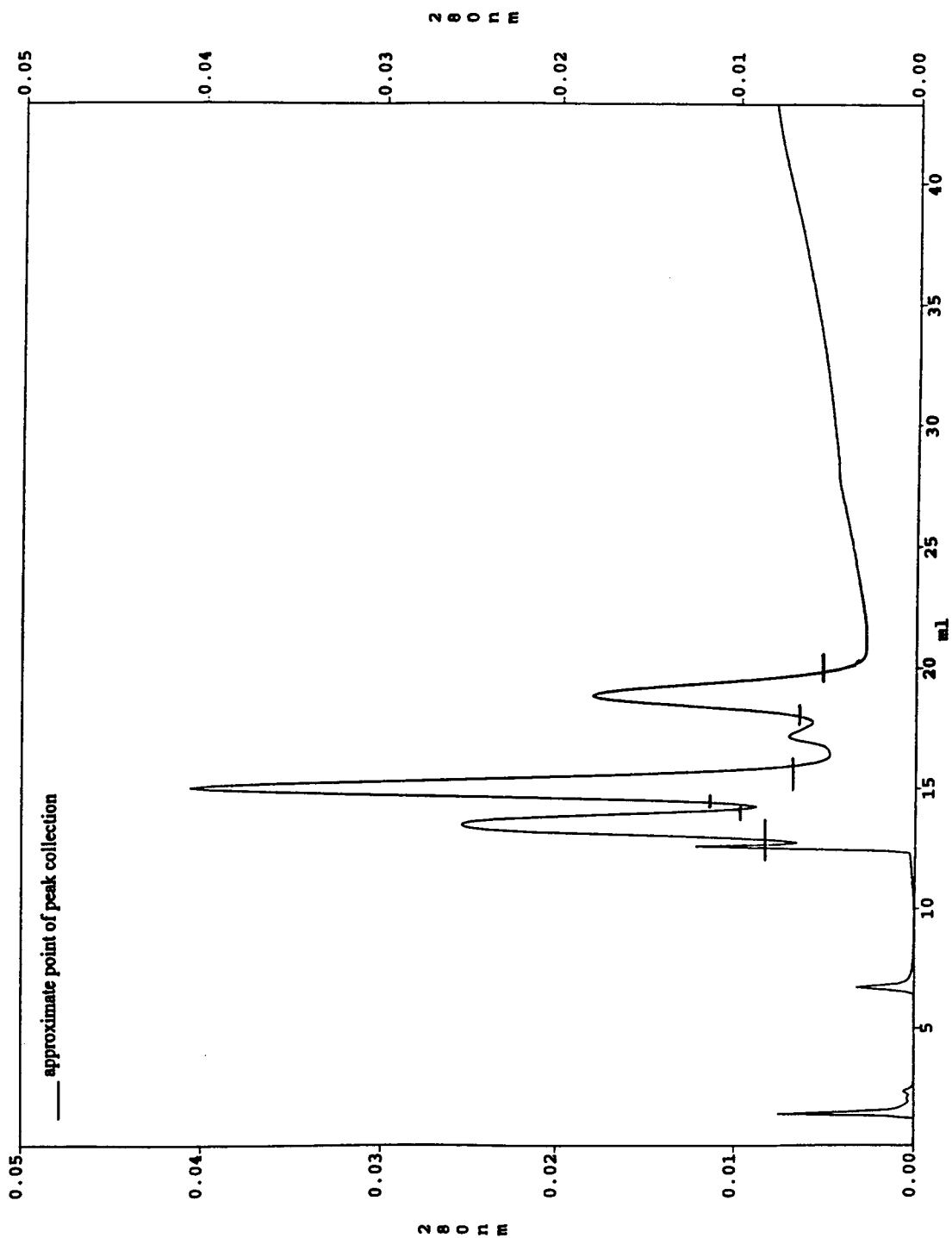


Fig. 1. Fab fragments separated by HPLC. HPLC conditions:  $100 \times 4.6$  mm strong cation-exchange column (sulfonic acid); mobile phase A: 10 mM MES, pH 4.5; B: 10 mM MES, pH 7.5; gradient 0–40% B in 20 column volumes at 1 ml/min. UV: 280 nm.

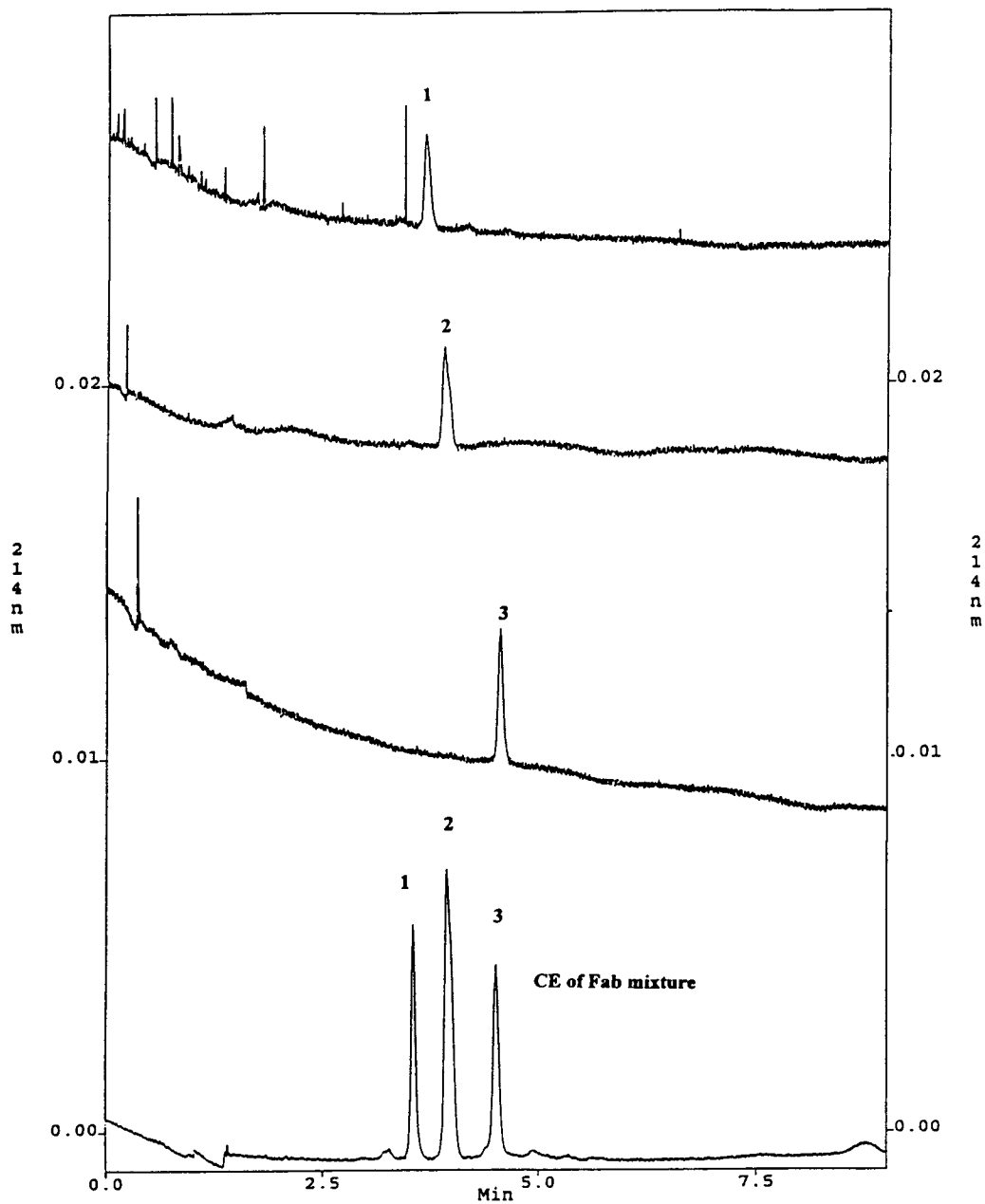


Fig. 2. CE of the collected fractions. Coated fused silica, 30 cm  $\times$  50  $\mu$ m at 30 kV; buffer 20 mM TAPS, pH 8.8; UV detection at 214 nm.

Our initial results using pH gradients clearly demonstrate that ion-exchange chromatography with pH gradient elution is capable of separating

proteins and their isoforms that differ by 0.1 pI unit. Separations can be achieved in less than 30 min. In spite of incomplete resolution of the Fab

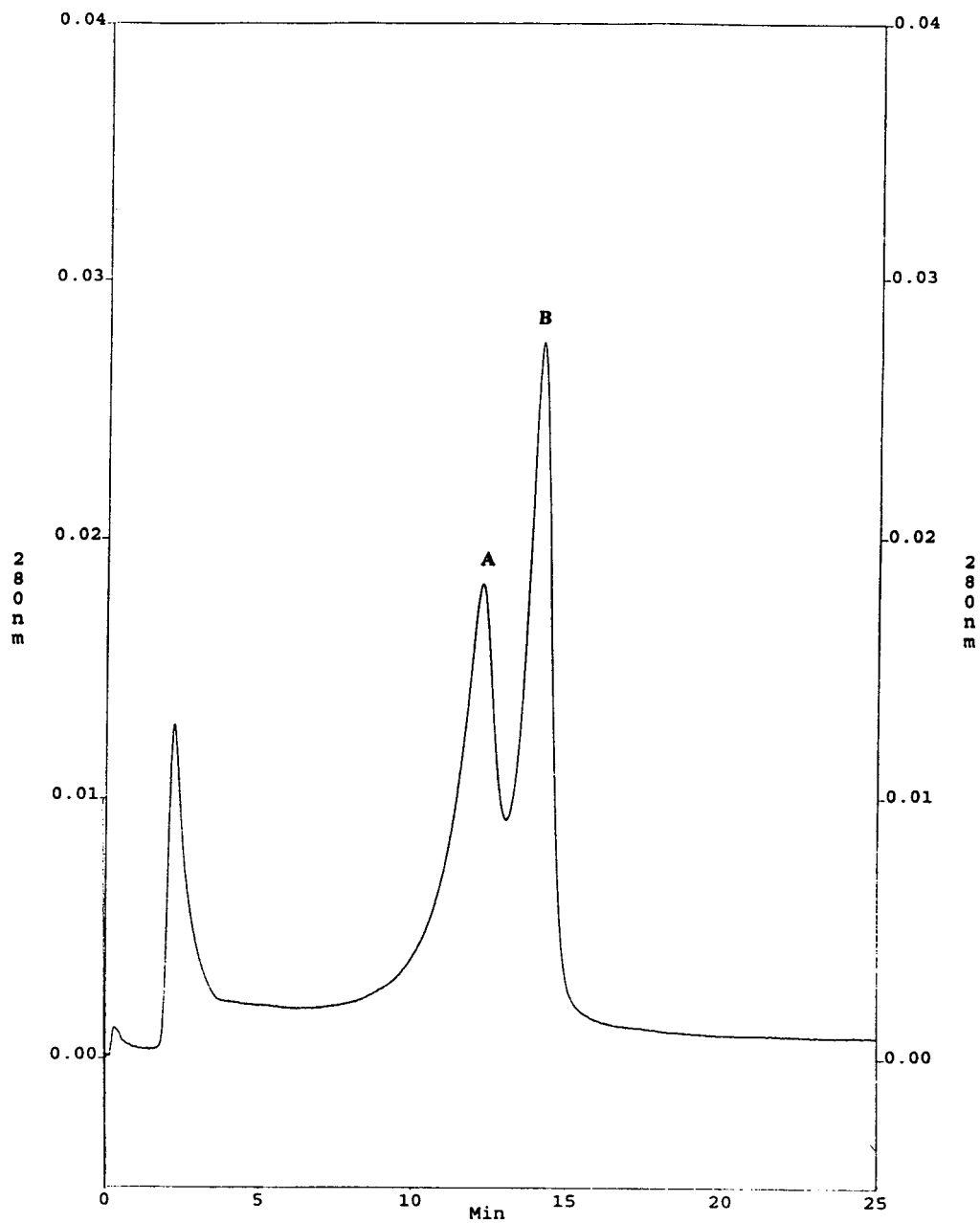


Fig. 3. Separation of  $\beta$ -lactoglobulins A and B using pH gradients. HPLC conditions as in Fig. 2, except a gradient of pH 5-6.6 was run over 15 min at 0.5 ml/min.

fragments, sufficient amount of purified material could be collected from the fractions.

## References

- [1] N.M. Schultz and R.T. Kennedy, *Anal. Chem.*, 65 (1993) 3161.
- [2] K. Shimura, B.L. Karger, *Anal. Chem.*, 66 (1994) 9.
- [3] F.-T.A. Chen and R.A. Evangelista, *Clin. Chem.*, 40 (1994) 1819.
- [4] D. Schmalzing, W. Nashabeh, X. Yao, R. Mhatre, F. Regnier, N. Afeyan and M. Fuchs, *Anal. Chem.*, 67 (1995) 606.
- [5] E. Wenisch, A. Jungbauer, C. Tauer, M. Rieter, G. Gruber, F. Steindl and H. Katinger, *J. Biochem. Biophys. Methods*, 18 (1989) 309.
- [6] C. Silverman, M. Komar, K. Shields, G. Diegan and J. Adamovics, *J. Liq. Chromatogr.*, 15 (1992) 207.
- [7] L.A.Æ. Sluyterman and O. Eggersma, *J. Chromatogr.*, 150 (1978) 17.
- [8] L.A.Æ. Sluyterman and J. Wijdenes, *J. Chromatogr.*, 150 (1978) 31.
- [9] P. Gallo, O. Olson and Å. Sidén, *J. Chromatogr.*, 375 (1986) 277.
- [10] A. Jungbauer, C. Tauer, E. Wenisch, K. Uhl, J. Brunner, M. Purtscher, F. Steindl and A. Buchacher, *J. Chromatogr.*, 512 (1990) 157.
- [11] R. Vincentelli and N. Bihoreau, *J. Chromatogr.*, 641 (1993) 383.
- [12] F.E. Regnier and K.M. Gooding, *Anal. Biochem.*, 103 (1980) 1.
- [13] L. Varady, N. Mu, Y.-B. Yang, C.E. Cook, N. Afeyan and F.E. Regnier, *J. Chromatogr.*, 631 (1993) 107.
- [14] A. Fresht, *Enzyme Structure and Mechanism*, W.H. Freeman, New York, 1985, pp. 413–416.
- [15] E. Harlow and D. Lane (Editors), *Antibodies*, Cold Spring Harbor Laboratory Press, Cold Spring Harbor, NY, 1988, pp. 626–628.
- [16] S. Fredrickson, *Anal. Biochem.*, 50 (1972) 575.
- [17] K.A. Piez, E.W. Davie, J.E. Folk and J.A. Gladner, *J. Biol. Chem.*, 236 (1961) 2912.





ELSEVIER

Journal of Chromatography A, 707 (1995) 233–244

JOURNAL OF  
CHROMATOGRAPHY A

# Peptide chiral purity determination: hydrolysis in deuterated acid, derivatization with Marfey's reagent and analysis using high-performance liquid chromatography–electrospray ionization–mass spectrometry

David R. Goodlett<sup>1</sup>, Perlette A. Abuaf, Peter A. Savage, Kevin A. Kowalski, Tarit K. Mukherjee, John W. Tolan<sup>2</sup>, Nancy Corkum, Gideon Goldstein, Jonathan B. Crowther<sup>2</sup>

*Immunobiology Research Institute, Annandale, NJ 08801, USA*

First received 23 December 1994; revised manuscript received 28 February 1995; accepted 13 March 1995

## Abstract

A high-performance liquid chromatography–electrospray ionization–mass spectrometric (LC–ESI–MS) method is presented that allows rapid and accurate determination of amino acid chiral purity in a peptide. Peptides are hydrolyzed in hydrochloric acid- $d_1$ /acetic acid- $d_4$  and then converted to diastereomers by derivatization with 1-fluoro-2,4-dinitrophenyl-5-L-alanine amide (FDAA, Marfey's reagent). Mixtures of D- and L-amino acid diastereomeric pairs are resolved in one chromatographic separation using conventional reversed-phase high-performance liquid chromatography. Hydrolysis in a deuterated solvent is necessary because the original ratio of D-/L-amino acids present in a peptide changes during acid hydrolysis due to racemization. Peptide hydrolysis in deuterated acids circumvents this problem by labeling each amino acid that racemizes with one deuterium at the  $\alpha$ -carbon. An increase in molecular mass of one atomic mass unit allows racemized amino acids to be distinguished from non-racemized amino acids by mass spectrometry. This procedure was used to determine the chiral purity of each amino acid in a purified, hexapeptide by-product (Arg-Lys-Lys-Asp-Val-Tyr) present in a kilogram batch of the synthetic pentapeptide, thymopentin (Arg-Lys-Asp-Val-Tyr).

## 1. Introduction

The chiral purity of an amino acid in a peptide is usually determined by acid hydrolysis of the

peptide and resolution of the amino acid mixture using either direct or indirect chromatographic schemes [1]. Unfortunately, racemization of amino acids occurs concomitant with acid hydrolysis [2] causing a change in the enantiomeric conformation of each amino acid in the peptide. In order to determine the chiral purity of amino acids in a peptide, racemization must be corrected for or circumvented. Correcting for racemization can be carried out by co-hydrolysis

\* Corresponding author.

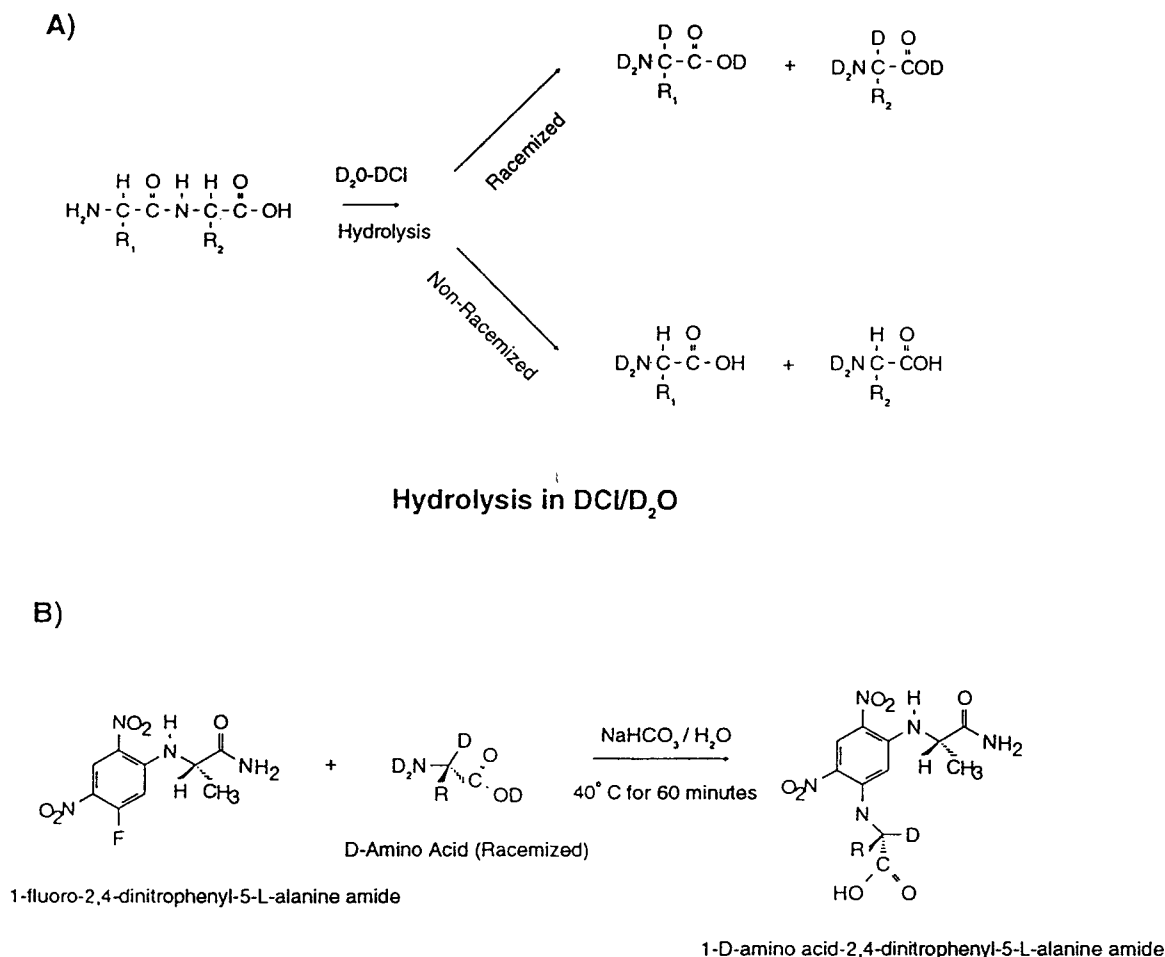
<sup>1</sup> Current address: Bristol-Myers Squibb, 3005 First Avenue, Seattle, WA 98121, USA.

<sup>2</sup> Current address: Affymax Pharmaceuticals, 3410 Central Expressway, Santa Clara, CA 95051, USA.

of a peptide that is nearly identical to the unknown or by combinations of acidic and enzymatic hydrolysis [3]. However, accurate correction factors are difficult to obtain because racemization rates depend on the location of an amino acid in a peptide and differ between individual free amino acids [4].

Methods that label amino acids as racemization occurs are preferred over correction factors

because they offer an in situ control. Liardon et al. [5] demonstrated that hydrolysis of peptides in  $D_2O$  labeled each amino acid that racemized with one deuterium at the  $\alpha$ -carbon as shown in Fig. 1A. A subsequent derivatization to increase the volatility of the amino acids was done in the absence of deuterium. This produced a volatile amino acid and removed all excess deuterium except for the deuterium at the  $\alpha$ -carbon which



### Diastereomer Formation Using Marfey's Reagent

Fig. 1. (A) Amino acid racemization during peptide hydrolysis in a deuterated, acidic solution results in loss of one proton from the  $\alpha$ -carbon and is followed by formation of an  $\alpha$ -carbon-deuterium bond. (B) Formation of a diastereomer by derivatization of a chiral amino acid with 1-fluoro-2,4-dinitrophenyl-5-L-alanine amide (FDAA).



is not exchanged under the experimental conditions. Analysis of the hydrolysate by gas chromatography–mass spectrometry (GC–MS) on a chiral column provided a means for selective detection of non-racemized amino acids. This GC–MS method allowed the original chiral content of a peptide to be determined, but it had two disadvantages which limited broad applicability. Electron ionization (EI) caused fragmentation of amino acids requiring more than one ion be monitored for each amino acid to ensure proper identification. Furthermore, an optically active stationary phase was required for the direct separation of amino acid enantiomers.

Indirect chromatographic schemes for resolution of racemic mixtures allow conventional achiral columns to be used. Indirect methods separate diastereomers of amino acids prepared by derivatizing amino acids with a chiral reagent. Conformational differences between amino acid diastereomers provide chromatographic resolution. Separation is achieved by either high-performance liquid chromatography (HPLC) or gas chromatography (GC). However, the difficulty of preparing volatile amino acid diastereomers by a two-step derivatization procedure for GC separation has made HPLC the preferred method. Of the many methods for preparing amino acid diastereomers for HPLC separation, diastereomers formed with 1-fluoro-2,4-dinitrophenyl-5-L-alanine amide (FDAA, Marfey's reagent) have proven very successful for analyzing complex mixtures of amino acids [6–9].

A liquid chromatographic–electrospray ionization–mass spectrometry (LC–ESI–MS) method for determining the chiral purity of each amino acid in a peptide is presented. Racemization was circumvented by hydrolyzing peptides in  $^2\text{HCl}/[^2\text{H}_4]\text{acetic acid}$  (1:1). Amino acids were then derivatized with FDAA according to the scheme in Fig. 1B and analyzed by LC–ESI–MS on a reversed-phase column. This method allows the original chiral purity of each amino acid in a peptide to be determined using common achiral reversed-phase HPLC columns. Data are presented showing that chromatographic resolution of a mixture of 39 FDAA labeled amino acids can be achieved in a single analysis. Use of ESI

instead of EI prevents fragmentation during ionization and allows the protonated molecular ion to be monitored for each amino acid.

The pentapeptide thymopentin (Arg-Lys-Asp-Val-Tyr) is presently being studied in the treatment of asymptomatic human immunodeficiency virus (HIV) infected subjects [10]. The LC–ESI–MS method was applied to a peptide isolated from a kilogram-scale batch of synthetic Arg-Lys-Asp-Val-Tyr. The chiral purity of a series of synthetic standards: Arg-Lys-Lys-Asp-Val-Tyr, Arg-Lys-Lys-Asp-*D*-Val-Tyr, Arg-Lys-Lys-*D*-Asp-Val-Tyr and the isolated peptide were determined using the method described above.

## 2. Experimental

### 2.1. Sample preparation

Peptides (0.1 mg) were hydrolyzed in 10-ml Pierce Reacti-vials that had been purged with nitrogen. After 18 h at 130°C in 1:1 hydrochloric acid–acetic acid (HCl–HOAc) or DCl/ $[\text{}^2\text{H}_4]\text{acetic acid}$  (DCl/DOAc), 400  $\mu\text{l}$  of  $\text{H}_2\text{O}$  was added and the sample lyophilized. To this was added 100  $\mu\text{l}$  of 1 M  $\text{NaHCO}_3$  and then 200  $\mu\text{l}$  of 38.7 mM 1-fluoro-2,4-dinitrophenyl-5-L-alanine amide (FDAA) in acetone. The solution was vortexed and incubated at 40°C for 60 min. Reactions were quenched by addition of 50  $\mu\text{l}$  of 2 M HCl. Samples were diluted 1:10 with mobile phase A (below) and 80  $\mu\text{l}$  of this solution analyzed by high-performance liquid chromatography–mass spectrometry (LC–MS) or HPLC with UV detection at 340 nm.

### 2.2. Materials, reagents and peptides

HPLC grade acetonitrile and methanol were obtained from Burdick and Jackson (Muskegon, MI, USA). Trifluoroacetic acid (HPLC spectra grade) and 1-fluoro-2,4-dinitrophenyl-5-L-alanine amide (FDAA) were obtained from Pierce Chemical Company (Rockford, IL, USA). ACS grade ammonium formate and formic acid were purchased from Eastman Kodak (Rochester, NY, USA). ACS grade hydrochloric acid was

purchased from Fisher Scientific (Pittsburgh, PA, USA). Water was purified for HPLC using a Millipore (Super 2) water purification system (Milford, MA, USA). Individual D- and L-amino acids were purchased from Sigma (St. Louis, MO, USA). Twenty percent  $^2\text{HCl}$  (99.96% deuterium) in deuterium oxide (w/w), [ $^2\text{H}_4$ ]acetic acid (99.5% deuterium) and deuterium oxide (99.9% deuterium) were purchased from Cambridge Isotope Laboratories (Woburn, MA, USA). Except for thymopentin (Cilag AG, Switzerland) and related substances therein, all peptides used in this study were synthesized, purified and characterized at Immunobiology Research Institute. Synthetic peptides and isolated peptides were characterized by amino acid analysis, Edman sequence analysis and mass spectrometric analysis. Isolated peptides were further analyzed by multidimensional NMR. Purity was assessed by reversed-phase high-performance liquid chromatography and thin layer chromatography.

The chiral purity of synthetic peptide standards used in these studies was confirmed by reversed-phase HPLC. Five thymopentin diastereomers containing a single D-amino acid substitution were chromatographically resolved from each other and from thymopentin. Limit of detection for any of the five D-amino acid analogs spiked into thymopentin was 0.1% (w/w).

### 2.3. Instrumentation

#### *High-performance liquid chromatography*

A Perkin-Elmer (Norwalk, CT, USA) system was used for analytical scale method development and consisted of an ISS-100 autosampler, series 410 LC pump and a Waters (Milford, MA, USA) 484 tunable absorbance detector. Separations were carried out on a YMC (Wilmington, NC, USA) Basic B-03-5 250 × 4.6 mm I.D. column. The ammonium formate mobile phase consisted of 1% methanol in both A and B with 5% acetonitrile in A and 60% acetonitrile in B. Mobile phases A and B were each brought to volume with 10 mM ammonium formate, pH 5.2. Linear gradients started with 0% B and finished with 100% B in 45 min. The system was

allowed to equilibrate for 15 min at 0% B prior to the next analysis. Flow-rate was 1 ml/min with UV detection at an absorbance of 340 nm. For liquid chromatography–electrospray ionization–mass spectrometry (LC–ESI–MS) separations a Waters (Milford, MA, USA) system comprised of a 717 autosampler, a 600-MS system controller/pump, a 484 detector, and a YMC Basic MCB-03-5 250 × 2.0 mm I.D. column with post-column split flow was used. Using a linear restrictor and a tee, two-thirds of the flow was split for UV detection at 340 nm and one-third for mass spectrometric detection. Flow-rate at the pump was 0.25 ml/min and in 20 min the linear gradient went from 20% B to 80% B. A trifluoroacetic acid (TFA, 0.05%) mobile phase system was used for most LC–ESI–MS analyses. Methanol and acetonitrile concentrations in the TFA mobile phases were the same as used in the ammonium formate mobile phases.

#### *Mass spectrometry*

A FinniganMAT TSQ 700 equipped with a Finnigan electrospray ionization source was used for LC–ESI–MS. Modifications to the standard instrument were limited but included the two following changes. (1) Rough pumping capacity was increased to decrease the time necessary for reaching operating pressure in the manifold after changing the heated capillary. An Alcatel 2012A (310 l/min) that backed up the manifold was replaced with an Edwards EM2-30 (570 l/min) and the ESI roughing pump was changed from an Edwards EM2-30 to a Galileo D045 (35 cfm). (2) A Shimadzu LC-10AD (Columbia, MD, USA) was used to provide co-axial sheath flow. To prevent current from the ESI source from damaging electronics in the sheath pump the methanol coaxial sheath liquid (0.1 ml/min) was grounded using a 1/16 inch metal union attached to the mass spectrometer chassis.

After the post-column split, flow entered the ESI source at 0.083 ml/min. Total liquid flow out of the ESI source was 0.183 ml/min (column + sheath). A typical ESI voltage was +3.0 kV with the auxiliary and sheath gas nitrogen pressures set at 103.4 and 179.3 MPa,

respectively. Prior to analysis of DNPA-amino acids, a mixture of L-L-glutamic acid-DNPA and L-L-glutamine-DNPA was analyzed by LC-ESI-MS to confirm that the mass spectrometer was set to resolve differences of one atomic mass unit.

### 3. Results and discussion

#### 3.1. HPLC separation of 2,4-dinitrophenyl-5-L-alanine amide amino acids

Derivatization of an amino acid with 1-fluoro-2,4-dinitrophenyl-5-L-alanine amide (FDAA) produces a diastereomer with a highly sensitive and specific UV label ( $\epsilon = 3 \times 10^4$  at 340 nm) on the  $\alpha$ -amino group. Such diastereomers are referred to as 2,4-dinitrophenyl-5-L-alanine amide (DNPA) amino acids or simply DNPA-amino acids. All amino acids including the imino acid proline and the achiral amino acid glycine are easily derivatized with FDAA. In the original report on the use of FDAA, Marfey [6] demonstrated that a select set of five DNPA-amino acids (Ala, Asp, Glu, Met and Phe) could be separated on a conventional reversed-phase column without the addition of chiral modifiers to the mobile phase. Kochhbar and Christen [9] were able to separate a mixture of 19 DNPA-L-amino acids by reversed-phase HPLC. Data in Tables 1 and 2 show that even more complex mixtures consisting of both D- and L-DNPA-amino acids can be resolved by conventional reversed-phase HPLC.

Data in Tables 1 and 2 were acquired by reversed-phase HPLC separation of individual DNPA-amino acid diastereomeric pairs with UV detection at 340 nm. As exhibited by the  $\alpha$ -values in Tables 1 and 2, ammonium formate and trifluoroacetic acid mobile phases were capable of separating most diastereomeric pairs. Table 1 shows that each of the 39 DNPA-D- and DNPA-L-amino acids may be resolved using an ammonium formate mobile phase. Excellent resolution was achieved between individual D- and L-amino acid diastereomeric pairs and between all 39 components. Alternatively, the

Table 1  
HPLC separation using the ammonium formate mobile phase of all 19 common D- and L-amino acid pairs and glycine derivatized with 1-fluoro-2,4-dinitrophenyl-5-L-alanine amide

Amino acid	Ammonium formate			AA-DNPA $R_F$ ratio (D/L)
	Retention time (min)			
	L	D	$\alpha$	
Ala	10.93	13.66	1.356	1.25
Arg	10.29	11.17	1.124	1.27
Asn	7.88	9.63	1.375	1.13
Asp	7.98	9.85	1.394	1.16
Cys	10.89	12.56	1.218	1.22
Glu	9.42	11.35	1.313	1.40
Gln	8.97	10.03	1.186	1.31
Gly	11.03		N.A.	N.A.
His	9.08	9.23	1.026	N.D.
Ile	17.01	20.94	1.286	1.24
Leu	17.58	21.28	1.257	1.19
Lys	9.67	10.57	1.140	1.24
Met	14.54	17.98	1.304	1.22
Phe	18.33	21.23	1.192	1.32
Pro	11.57	13.82	1.270	1.02
Ser	8.48	9.93	1.277	1.19
Thr	9.01	12.28	1.566	1.32
Trp	18.37	20.52	1.142	1.24
Tyr	13.34	15.67	1.230	1.28
Val	14.29	18.22	1.355	1.27

N.A. = not applicable and RF ratio = UV response factor ratio at 340 nm.

N.D. = not determined.

trifluoroacetic acid mobile phase (Table 2) permitted better resolution of the histidine diastereomeric pair, but the individual diastereomeric pairs of glutamine, proline and serine were not resolved. As expected the C<sub>8</sub> YMC-basic column separated hydrophobic diastereomers better than polar DNPA-amino acid diastereomeric pairs. In all cases, DNPA-L-amino acids eluted prior to DNPA-D-amino acids possibly due to greater intramolecular hydrogen bonding in the DNPA-D-amino acids [6].

While very good resolution of all DNPA-amino acid diastereomeric pairs can be achieved, differences in absorption between diastereomeric pairs have been observed. If absorbance at 340 nm is the sole method of detection, then integrated areas must be corrected for quantitative

Table 2

HPLC separation using the trifluoroacetic acid mobile phase of all 19 common D- and L-amino acid pairs and glycine derivatized with 1-fluoro-2,4-dinitrophenyl-5-L-alanine amide

Amino acid	Trifluoroacetic acid		$\alpha$
	Retention time (min)		
	L	D	
Ala	18.34	19.98	1.108
Arg	14.45	15.38	1.083
Asn	13.93	14.21	1.026
Asp	15.88	16.33	1.035
Cys	11.66	13.08	1.167
Glu	17.11	17.77	1.047
Gln	14.99	14.99	1.00
Gly	17.21		N.A.
His	11.85	13.37	1.175
Ile	25.36	28.03	1.121
Leu	25.64	28.10	1.109
Lys	13.98	15.03	1.098
Met	22.38	24.62	1.117
Phe	25.95	27.85	1.083
Pro	19.12	19.12	1.00
Ser	14.80	14.80	1.00
Thr	15.54	17.57	1.164
Trp	25.20	26.52	1.060
Tyr	18.05	20.73	1.180
Val	22.88	25.49	1.133

N.A. = not applicable.

analysis. Prior to beginning work with ESI-MS detection, the UV response factors for all DNPA-amino acid diastereomeric pairs at 340 nm were determined (Table 1). The ammonium formate mobile phase was used because of the better resolution achieved for all DNPA-amino acids. Each diastereomeric pair was analyzed as a mixture of 0% D, 5% D, 15% D and 25% D. Graphical analysis of the observed DNPA-D-amino acid area percent versus the actual DNPA-D-amino acid percent yielded a line the slope of which represents the DNPA-D-amino acid to DNPA-L-amino acid response factor ratio. Laboratories with access to LC-ESI-MS will not require such corrections because all 19 response factors were found to have a value of one by mass spectrometry. However, as described in detail below, mass spectrometry can also be used to unequivocally distinguish racemized from non-racemized amino acids. Racemization of amino acids during peptide hydrolysis has been a more perplexing problem to solve than separation of amino acids.

### 3.2. Racemization during peptide hydrolysis

Fig. 2 illustrates one of the challenges presented in attempting to use single amino acids as

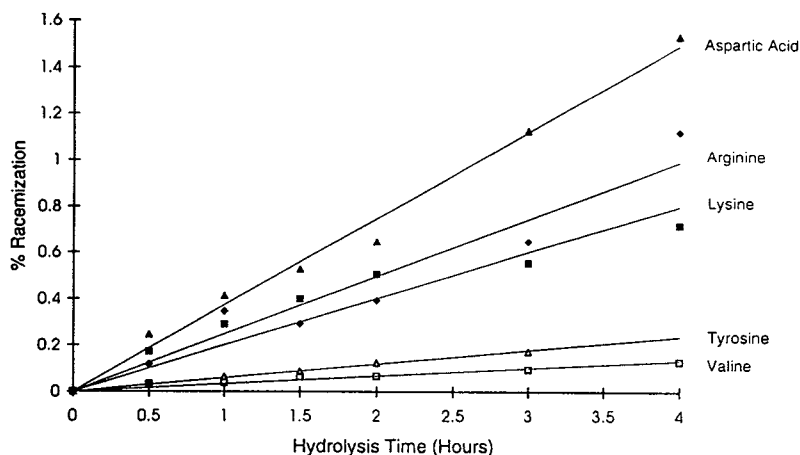


Fig. 2. Example of the variability in racemization between free amino acids during conditions of acid hydrolysis. Individual amino acids were incubated for various times at 130°C in HCl-HOAc (1:1).

controls for racemization. The five amino acids found in thymopentin were incubated in HCl–HOAc at 130°C for varying lengths of time (Fig. 2). Degree of racemization differed between amino acids and increased over time for all amino acids tested. The observed difference in racemization between aspartic acid and valine at each time point is expected based on the mechanism of racemization [11]. The carbanion intermediate formed during amino acid racemization is stabilized by the carboxyl side chain of aspartic acid and destabilized by the alkyl side chain of valine. A further complication during the hydrolysis of thymopentin and other peptides arises from the location of a given amino acid residue within the primary sequence [4]. A given amino acid will exhibit rates of racemization that are specific to the amino acid sequence in which it is located. Differences in racemization between amino acids and the dependence of amino acid location within a peptide preclude the use of free amino acids or related peptides as controls for racemization.

Fig. 3 shows HPLC separations for a mixture of five DNPA-amino acid standards for the amino acids found in thymopentin (Fig. 3A) and a mixture of the same DNPA-amino acids produced by hydrolysis of thymopentin (Fig. 3B) in HCl–HOAc. Fig. 3A illustrates the excellent resolution that can be achieved with DNPA-amino acids. More than the expected ten responses are observed in Fig. 3A,B, because FDAA reacts with water (DNPA-OH), at the  $\epsilon$ -amino group of lysine (*R*-Lys) and at the  $p$ -hydroxyl group of tyrosine (*R*-Tyr) [12]. Formation of bis-DNPA-amino acids was minimal under the derivatization conditions used. At higher concentrations of FDAA bis-DNPA-amino acid products may be significant [12].

Prior to the work with the DNPA-amino acids, the chiral purity of each residue in thymopentin was determined to be greater than 99.9% (see Experimental). The observation of DNPA-D-amino acids in Fig. 3B indicates that racemization occurred during hydrolysis. This conclusion is based on separate experiments, where very little racemization (<0.06%) of the five amino acids in thymopentin occurred as a result of

FDAA derivatization. One way to circumvent the racemization observed in Fig. 3B is to carry out hydrolysis in deuterated acids being careful to exclude any source of protons. Any amino acid that racemizes will be labeled with one deuterium at the  $\alpha$ -carbon. This allows racemized amino acids to be distinguished from non-racemized amino acids by an increase of one atomic mass unit using mass spectrometry [5].

In the original GC–MS method [5] peptides were hydrolyzed in  $^2\text{HCl}$ , derivatized for increased volatility and ionized by EI. Fragmentation of the molecular ion during EI forced multiple ions to be monitored for each derivatized amino acid. Recently, thermospray ionization has also been shown to cause fragmentation of DNPA-amino acids [13]. Using ESI–MS prevents fragmentation of DNPA-amino acids during ionization and allows only the protonated molecular ion to be monitored for identification of each DNPA-amino acid. This is an advantage over the GC–MS method because more amino acids can be monitored per separation. While chiral analysis of free amino acids not subjected to hydrolysis can be carried out as in Fig. 3, analysis of the chirality of amino acids originating in a peptide require hydrolysis in deuterated acids followed by selected-ion monitoring (SIM) mass spectrometric analysis to distinguish non-racemized amino acids.

### 3.3. Detection of non-racemized amino acids by LC–ESI–MS

Amino acids undergoing racemization during hydrolysis in a deuterated medium increase in molecular mass by one atomic mass unit. At unit resolution a quadrupole mass spectrometer can distinguish between two ions that differ by only one  $m/z$  value. This allows non-racemized amino acids to be distinguished from amino acids that racemize in an environment of deuterium (>99.99%). In a typical LC–ESI–MS experiment multiple protonated molecular ions ( $[M + H]^+$ ) are monitored for each expected  $m/z$  value corresponding to a non-racemized amino acid. The total-ion chromatogram for such an experiment will indicate the D- and L-amino acids

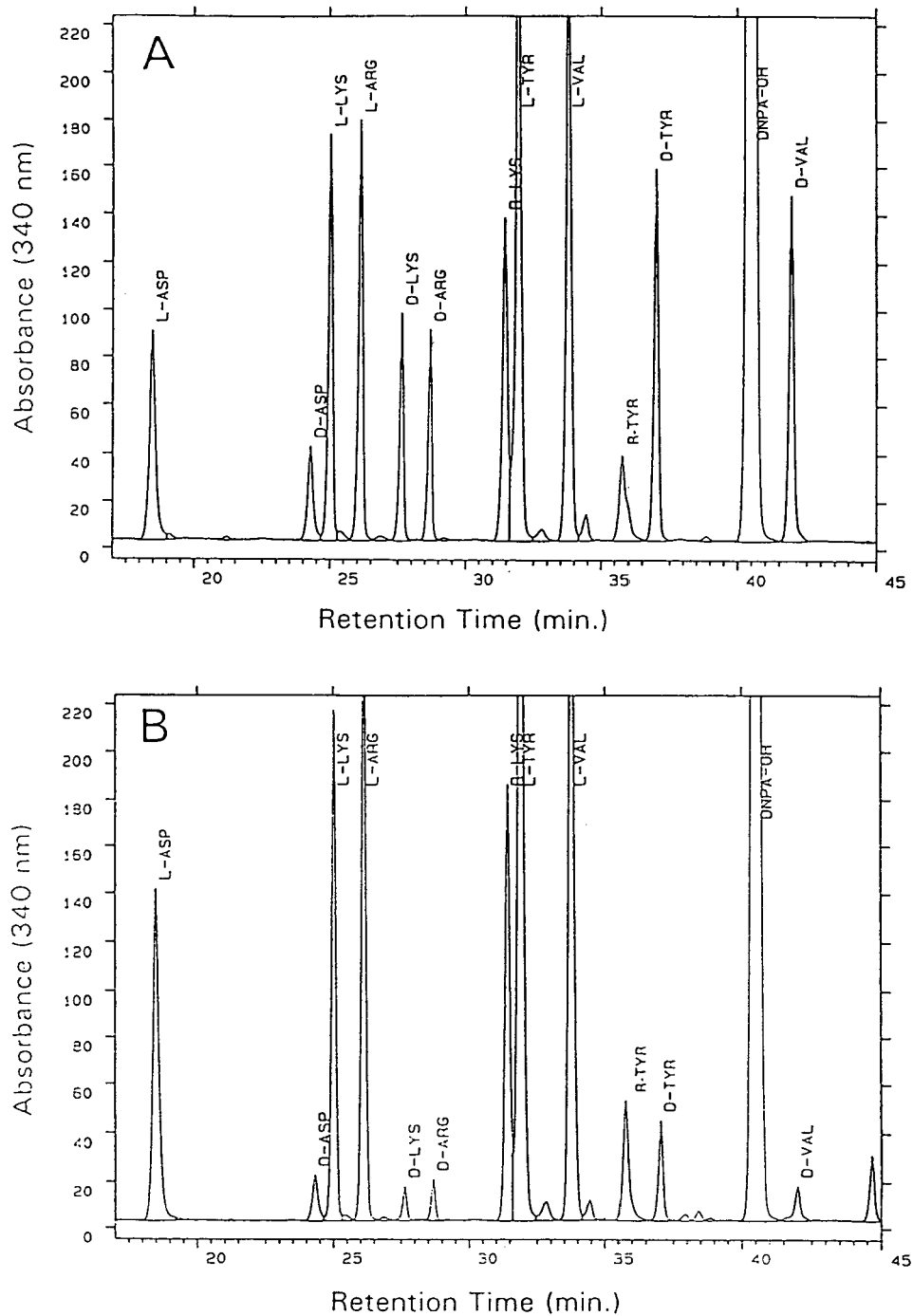


Fig. 3. Reversed-phase separations of 2,4-dinitrophenyl-5-L-alanine amide (DNPA) amino acids: (A) from a mixture of the D- and L-DNPA-diastereomers of arginine, lysine, aspartic acid, valine, and tyrosine, and (B) after hydrolysis of thymopentin in HCl-HOA (1:1). Separation was carried out using the ammonium formate mobile phase and detection was at 340 nm. DNPA-OH is hydrolyzed FDAA, *R*-Lys is  $\epsilon$ -DNPA-lysine and *R*-TYR is  $\rho$ -DNPA-tyrosine.

present in the peptide prior to hydrolysis. Any racemized amino acids are excluded from consideration because of an increase in molecular mass of one atomic mass unit. For a peptide with five different amino acids, all five DNPA-amino acids can be examined in a single LC-ESI-MS experiment by monitoring only five ions. Alternately, if only one amino acid in a peptide is suspected of being a D-isomer, then the mass spectrometer can be scanned over a narrow range to detect that isomer. This concept is presented in Figs. 4 and 5 by comparing the results of peptide hydrolysis in HCl-HOAc against hydrolysis in DCI-DOAc.

Thymopentin was hydrolyzed overnight in HCl-HOAc (Fig. 4A,B). Hydrolysates were subjected to derivatization with FDAA and analyzed by LC-ESI-MS. In Figs. 4 and 5 lysine is used as an example of how one amino acid in a peptide can be checked for enantiomeric configuration. Data in Fig. 4 was acquired by scanning over a narrow range around the protonated

molecular ion for DNPA-lysine ( $m/z$  399). Extracted ion chromatograms displayed for [DNPA-lysine + H]<sup>+</sup> ( $m/z$  399) (Fig. 4A) and [DNPA-lysine-d<sub>1</sub> + H]<sup>+</sup> ( $m/z$  400) (Fig. 4B) each show three peaks. The three species were identified as: [ $\alpha$ -DNPA-L-lysine + H]<sup>+</sup> (1), [ $\alpha$ -DNPA-D-lysine + H]<sup>+</sup> (2) and [ $\epsilon$ -DNPA-L-lysine + H]<sup>+</sup> (3). Peak 2 was due to racemization of L-lysine to D-lysine during hydrolysis. This assignment was based on findings that none of the five amino acids in thymopentin underwent racemization during FDAA derivatization alone. The three responses in Fig. 4B represent the same species as in Fig. 4A, but are due to the natural abundance of deuterium.

When thymopentin was hydrolyzed in DCI-DOAc under conditions similar to those used with HCl-HOAc, then only two responses were observed for the extracted ion chromatogram of [DPNA-lysine + H]<sup>+</sup> ( $m/z$  399) (Fig. 5A). Responses 1 and 3 are the same as those identified in Fig. 4A. In Fig. 5B the extracted ion chro-

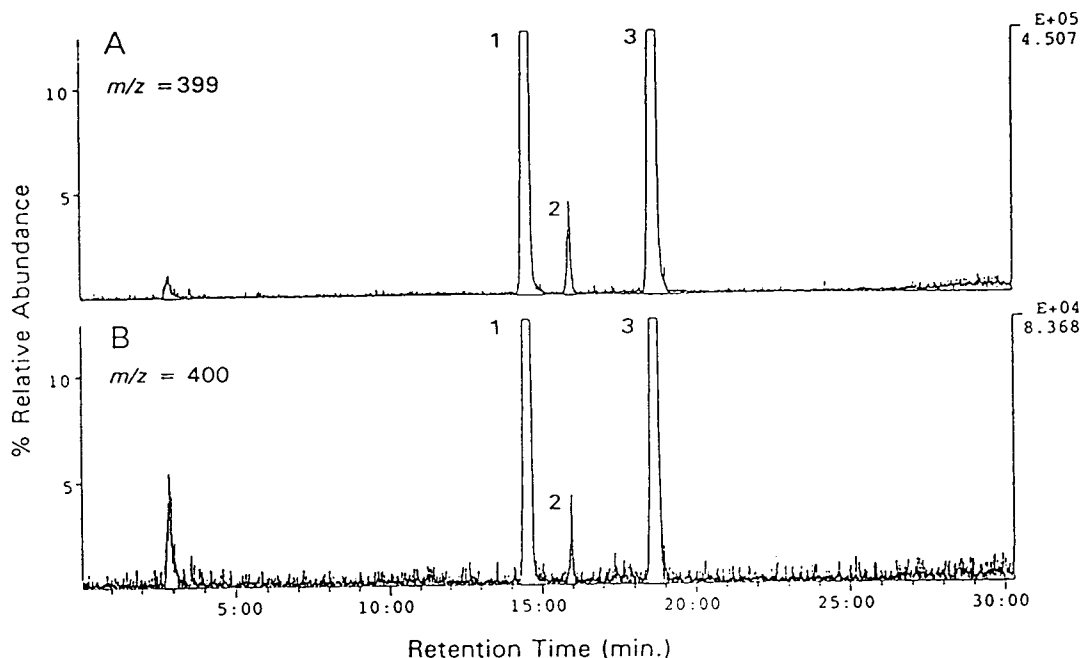


Fig. 4. Scanning LC-ESI-MS analysis ( $m/z$  394–404 in 1.0 s) of DNPA-lysine from thymopentin hydrolyzed in HCl-HOAc. Extracted single ion chromatograms are shown for (A) [DNPA-lysine + H]<sup>+</sup> ( $m/z$  399.1) and for (B) [DNPA-lysine-d<sub>1</sub> + H]<sup>+</sup> ( $m/z$  400.1). The three annotated peaks were identified as: [ $\alpha$ -DNPA-L-lysine + H]<sup>+</sup> (1), [ $\alpha$ -DNPA-D-lysine + H]<sup>+</sup> (2) and [ $\epsilon$ -DNPA-L-lysine + H]<sup>+</sup> (3).

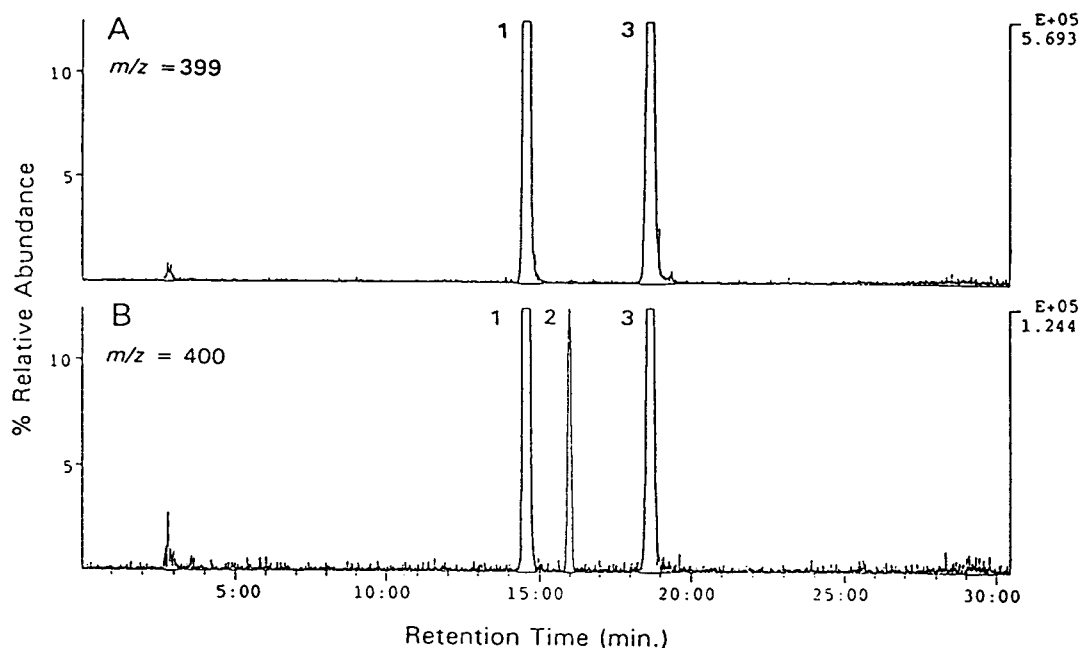


Fig. 5. Scanning LC-ESI-MS analysis ( $m/z$  394–404 in 1.0 s) of DNPA-lysine from thymopentin hydrolyzed in DCI-DOAc. Extracted single ion chromatograms are shown for (A)  $[\text{DNPA-lysine} + \text{H}]^+$  ( $m/z$  399.1) and for (B)  $[\text{DNPA-lysine-}d_1 + \text{H}]^+$  ( $m/z$  400.1). The three annotated peaks were identified as:  $[\alpha\text{-DNPA-L-lysine} + \text{H}]^+$  (1),  $[\alpha\text{-DNPA-D-lysine} + \text{H}]^+$  (2) and  $[\epsilon\text{-DNPA-L-lysine} + \text{H}]^+$  (3).

matogram for the protonated molecular ion of DNPA-lysine- $d_1$  ( $m/z$  400) is shown. In Fig. 5A response 2, identified in Fig. 4A as  $[\alpha\text{-DNPA-D-lysine-}d_1 + \text{H}]^+$ , is absent. Any D-lysine present in thymopentin prior to hydrolysis would elute at 16.0 min in Fig. 5A. Figs. 4 and 5 illustrate the power of this LC-ESI-MS method to determine the enantiomeric configuration of amino acids present in a peptide prior to hydrolysis. Any amino acids that racemize during hydrolysis can be effectively circumvented so that only non-racemized amino acids are observed.

### 3.4. Application of the LC-ESI-MS method

This LC-ESI-MS method was used to establish the chiral purity of a thymopentin related substance. An unknown peptide, originally present at less than 0.1% relative to thymopentin, was isolated by reversed-phase HPLC and characterized. Tandem mass spectrometry and Edman chemistry identified the sequence as Arg-

Lys-Lys-Asp-Val-Tyr. From heteronuclear NMR data the peptide was suspected of containing either all L-amino acids, a D-aspartic acid substitution for L-aspartic acid or a D-valine substitution for L-valine. Three standards were synthesized for comparison to the unknown and to validate the LC-ESI-MS method: Arg-Lys-Lys-Asp-Val-Tyr, Arg-Lys-Lys-D-Asp-Val-Tyr and Arg-Lys-Lys-Asp-D-Val-Tyr. The unknown and standards were separately hydrolyzed in DCI-DOAc, derivatized with FDAA and analyzed by LC-ESI-MS as shown in Fig. 6.

Results for the three control peptides Arg-Lys-Lys-Asp-Val-Tyr, Arg-Lys-Lys-D-Asp-Val-Tyr and Arg-Lys-Lys-Asp-D-Val-Tyr are shown in Fig. 6. Data was acquired in three experiments by continuously monitoring the same five ions during each LC-ESI-MS experiment. Chromatographic resolution of all DNPA-amino acids allowed the original chiral purity to be determined quickly from the total ion chromatogram for each peptide. The method accurately pre-



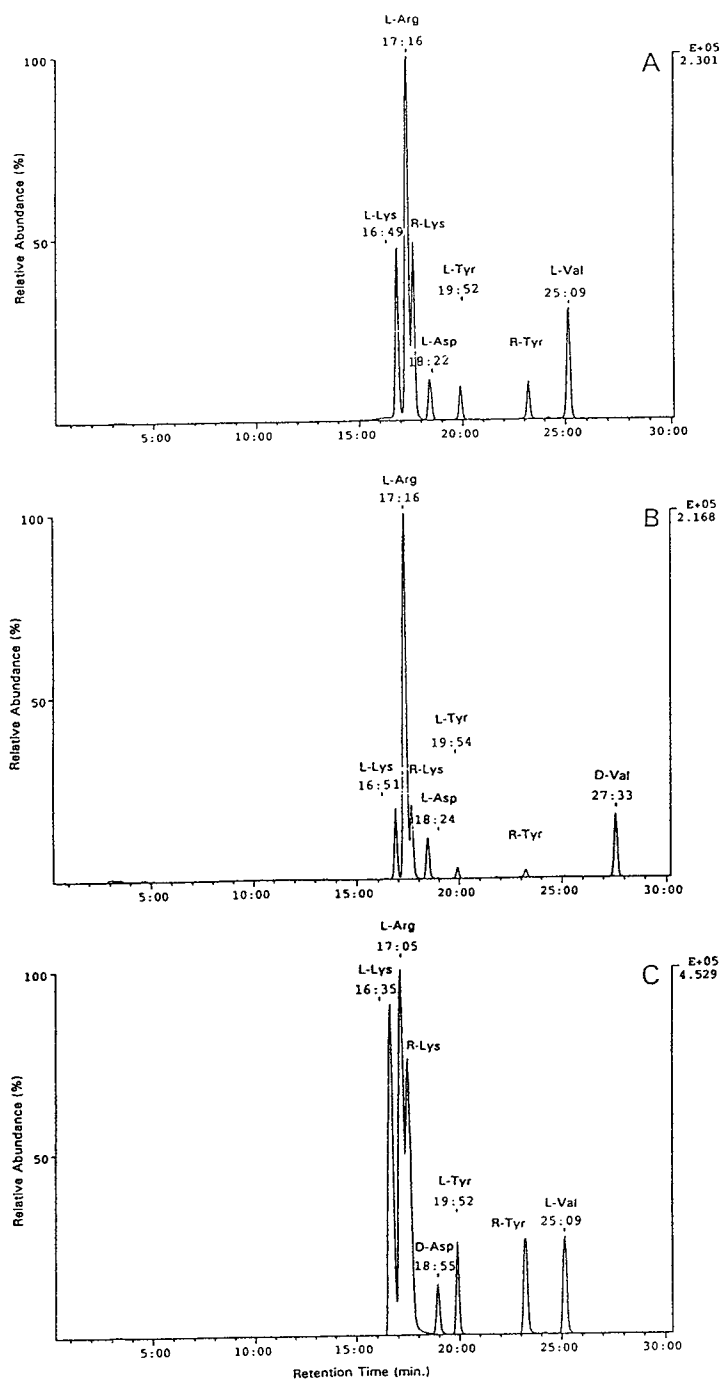


Fig. 6. Analysis by LC-ESI-MS of (A) Arg-Lys-Lys-Asp-Val-Tyr, (B) Arg-Lys-Lys-Asp-*D*-Val-Tyr and (C) Arg-Lys-Lys-*D*-Asp-Val-Tyr hydrolyzed in DCI-DOAc for 12 h at 130°C. One ion was monitored for each of the five anticipated DNPA-amino acids (e.g. for  $[\text{DNPA-L-lysine} + \text{H}]^+$   $m/z$   $399.1 \pm 0.1$  amu in 0.3 s) and the summed ion chromatograms displayed. *R*-Lys is  $[\epsilon\text{-DNPA-lysine} + \text{H}]^+$  and *R*-Tyr is  $[\rho\text{-DNPA-tyrosine} + \text{H}]^+$ .

dicted the chiral purity of the three standards. Results for the unknown identified it as being identical to the all L-isomer Arg-Lys-Lys-Asp-Val-Tyr in Fig. 6A. The LC-ESI-MS results were corroborated in separate HPLC experiments where the unknown peptide co-eluted with Arg-Lys-Lys-Asp-Val-Tyr.

#### 4. Conclusions

We have extended the advances in reversed-phase separation of DNPA-amino acid diastereomers to resolution of 39 DNPA-amino acids. By combining this advance with peptide hydrolysis in deuterated acids to circumvent racemization, ESI-MS detection was used to unambiguously detect non-racemized amino acids in peptide hydrolysates. Simple, volatile mobile phases allowed DNPA-amino acids to be resolved and detected by ESI-MS analysis. By varying the gradient conditions complex mixtures were readily resolved. Isomers such as DNPA-isoleucine and DNPA-leucine were distinguishable because of the high chromatographic resolution that was achieved. Use of ESI-MS to analyze DNPA-amino acids prevented the fragmentation of amino acid derivatives common with electron ionization [4] and thermospray ionization [13]. This advantage over the GC-EI-MS method can be used to monitor a greater number of ions per LC-ESI-MS analysis or to monitor fewer ions at a lower limit of detection. A second advantage of ESI over EI is that amino acids need not be derivatized to increase volatility and this decreases sample preparation time. The LC-ESI-MS method as described provides a rapid and accurate determination of the enantiomeric purity of each amino acid in a given peptide. We are now applying the method to larger peptides and proteins.

#### Acknowledgements

The authors wish to thank the Peptide Synthesis Group at Immunobiology Research Insti-

tute for preparation of the peptide standards used in these studies. We thank Dr. Peter Marfey in the Department of Biological Sciences at the University at Albany, SUNY, for helpful discussions on the derivatization of amino acids. A preliminary report of this work was presented at the 42<sup>nd</sup> American Society for Mass Spectrometry and Allied Topics meeting in Chicago, IL, USA.

#### References

- [1] V.A. Davankov, A.A. Kurganov, A.S. Bochkov, *Advances in Chromatography*, 22 (1983) 71–116.
- [2] A. Neuberger, *Adv. in Protein Chem.*, 4 (1948) 297–383.
- [3] A. D'Aniello, L. Petrucelli, C. Gardner, G. Fisher, *Anal. Biochem.*, 213 (1993) 290–295.
- [4] J.M. Manning, *J. Am. Chem. Soc.*, 92 (1970) 7449–7454.
- [5] R. Liardon, S. Ledermann, U. Ott, *J. Chromatogr.*, 203 (1981) 385–395.
- [6] P. Marfey, *Carlsberg Res. Commun.*, 49 (1984) 591–596.
- [7] G. Szókán, G. Mezö, F. Hudecz, *J. Chromatogr.*, 444 (1988) 115–122.
- [8] G. Szókán, G. Mezö, F. Hudecz, Z. Majer, I. Schön, O. Nyéki, T. Szirtes, R. Dölling, *J. Liq. Chromatogr.*, 12 (1989) 2855–2875.
- [9] S. Kochhar, P. Christen, *Anal. Biochem.*, 178 (1989) 17–21.
- [10] G. Goldstein, M.A. Conant, G. Beall, H.A. Grossman, J.E. Galpin, G. Blick, L.H. Calabrese, R.L. Hirsch, A. Fisher, P. Stampone, L.A. Meyerson, *J. Acquir. Immune Defec. Syndr.*, (1995) in press.
- [11] J.L. Bada, *Ann. Rev. Earth Planet. Sci.*, 13 (1985) 241–268.
- [12] H. Bruckner, C. Keller-Hoehl, *Chromatographia*, 30 (1990) 621–629.
- [13] T. Krishnamurthy, *J. Am. Soc. Mass Spectrom.*, 5 (1994) 724–730.



ELSEVIER

Journal of Chromatography A, 707 (1995) 245-254

JOURNAL OF  
CHROMATOGRAPHY A

# Simultaneous determination of enalapril, felodipine and their degradation products in the dosage formulation by reversed-phase high-performance liquid chromatography using a Spherisorb C<sub>8</sub> column

Xue-Zhi Qin\*, Joe DeMarco, Dominic P. Ip

Pharmaceutical Research and Development, WP78-210, Merck Research Laboratories, West Point, PA 19486, USA

First received 22 December 1994; revised manuscript received 10 March 1995; accepted 10 March 1995

## Abstract

A reversed-phase high-performance liquid chromatographic (RP-HPLC) method was developed and validated for the simultaneous determination of enalapril and its two degradation products, enalaprilat (diacid, hydrolytic degradation product of enalapril) and enalapril-DKP (cyclization of enalapril); and felodipine and its degradation product, H152/37 (oxidation of felodipine) in the combined enalapril/felodipine (5 mg/5 mg) formulation. Using a Spherisorb C<sub>8</sub> column with a CH<sub>3</sub>CN-0.001 M KH<sub>2</sub>PO<sub>4</sub> (pH 2) (35:65, v/v) mobile phase, these compounds were well separated from each other, and also from maleic acid and the excipients in the formulation. The method was demonstrated to be precise, accurate, specific and robust. Optimization of the separation in terms of mobile phase composition is crucial to the method development, which is discussed in detail. It is proposed that under the experimental conditions used, the retention of felodipine, DKP and H152/37 is governed by the reversed-phase partitioning process whereas that of enalapril and diacid is governed by both the partitioning and the cation-exchange process with residual silanols.

## 1. Introduction

Development of combination drugs has become a routine practice in pharmaceutical industry. An example is the development of the enalapril (1)/felodipine (4) (5 mg enalapril maleate/5 mg felodipine) combination formulation (see Fig. 1 for structures of the compounds). Enalapril is a pro-drug, which is hydrolyzed to enalaprilat (diacid) in vivo. The diacid acts as an angiotensin-converting enzyme inhibitor [1]. Felodipine is a calcium blocker [2]. Both are

effective drugs for treating hypertension [1,2]. The antihypertensive effect and tolerance of the combined low doses of enalapril maleate and felodipine (5 mg/5 mg daily) have been evaluated and shown to be improved [3,4].

There are two general approaches in the methods development for combination drugs. One is to develop separate analytical methods for each of the active substances and their degradation products, and the other is to develop a single method for the simultaneous determination of all the active substances and their degradation products. Since the first approach is very time-consuming, the second ap-

\* Corresponding author.

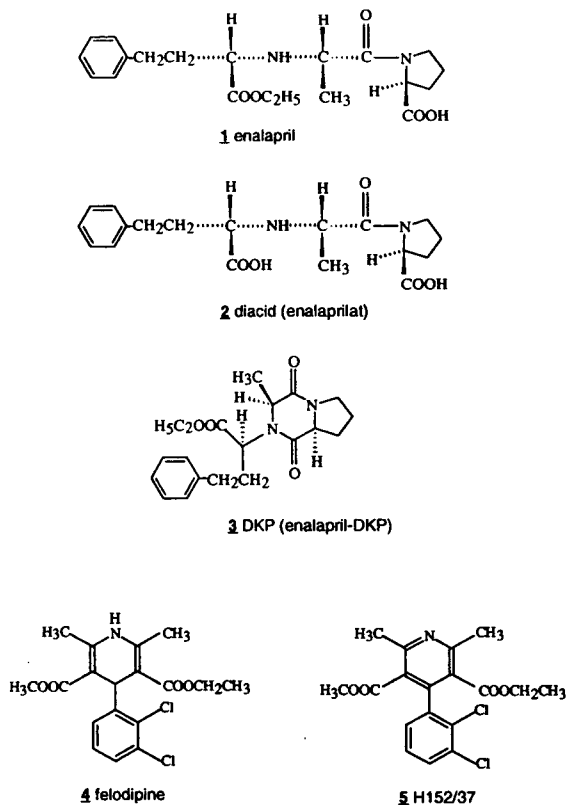


Fig. 1. Structures of the compounds of interest.

proach was attempted in the present study. This is challenging, since, during stability testing of tablets exposed to high temperature and/or high humidity, it was observed that enalapril formed two degradation products, diacid (enalaprilat, 2, hydrolysis degradation product) and enalapril-DKP (3, cyclization degradation product) [5]; and felodipine formed one degradation product, H152/37 (5, photo- or thermal oxidation degradation product) [6]. This approach has been accomplished by an isocratic, reversed-phase high-performance liquid chromatographic (RP-HPLC) method, which uses a Spherisorb C<sub>8</sub> column (5 μm particle size, 250 × 4.6 mm I.D.) with a CH<sub>3</sub>CN–0.001 M KH<sub>2</sub>PO<sub>4</sub> (pH 2) (35:65, v/v) mobile phase. The method can simultaneously determine both active substances and the three degradation products by separating them from each other and from maleic acid and the excipients of the formulation. The method was

validated according to the USP validation guidelines, and was demonstrated to be precise, accurate, specific and robust.

The mechanistic aspects of the method have been investigated. The retention of enalapril-DKP, felodipine and H152/37 is governed by the reversed-phase partitioning process, while that of enalapril and diacid is governed by both the reversed-phase mechanism and the cation-exchange mechanism. The latter is associated with the type of the amino acids, the pH-dependent protolytic equilibria, and other secondary equilibria such as solvation. As demonstrated in detail below, the success of the method should be attributed to the selectivity due to the distinct separation mechanisms of these compounds.

## 2. Experimental

### 2.1. Chemicals and reagent

Enalapril/felodipine (5 mg/5 mg) combination tablets and placebo tablets were manufactured by Merck Research Laboratories (West Point, PA, USA). The standards of enalapril maleate (1, MK-0421), felodipine (4, MK-0218), and their degradation products, diacid (enalaprilat 2), enalapril-DKP (3) and H152/37 (5) of pharmaceutical grade were manufactured by Merck Research Laboratories (Rahway, NJ, USA). Potassium phosphate monobasic (99.8%, certified A.C.S.) and acetonitrile (Optima) were purchased from Fisher Scientific (Philadelphia, PA, USA). All solvents and reagents were used as received without further purification. Deionized water with at least 18 MOhm purified by a Milli-Q system was used for the mobile phase, and the sample and standard preparations.

### 2.2. Equipment

The development and validation work was performed on a Hewlett-Packard (HP) 1090 system equipped with a Spectra Physics (SP) 100 variable-wavelength UV detector. The column used is Spherisorb C<sub>8</sub> column (5 μm particle size, 250 × 4.6 mm I.D.) purchased from Phase

Separations. The column temperature is 40°C. The packing material has the following characteristics: pore size, 80 Å; pore volume, 0.5 ml/g; surface area, 220 m<sup>2</sup>/g; carbon load, 6%, monomeric; and bonded phase coverage, 2.51 μmole/m<sup>2</sup>.

### 2.3. Mobile phase, standard, and sample preparations

The mobile phase was prepared by first preparing a solution of 0.001 M KH<sub>2</sub>PO<sub>4</sub>, then adjusting its pH to 2 with phosphoric acid, and finally mixing the solution with acetonitrile in a volume ratio of 65:35 (v/v), respectively. Mobile phases of other concentrations were made by the same procedure. The diluent (50% CH<sub>3</sub>CN and 50% 0.001 M KH<sub>2</sub>PO<sub>4</sub> (pH 2)) was also prepared by this procedure. The standard solution was prepared by dissolving an appropriate amount of reference standard in the diluent to yield the desired assay concentration (0.1 mg/ml for enalapril maleate and felodipine (100% standard), and 0.001 mg/ml for the three degradation products diacid, DKP and H152/37 (1% standard). Tablet samples of enalapril/felodipine (5 mg/5 mg) formulation were prepared in an appropriate volume of the diluent by stirring until tablet(s) was completely dissolved. A portion of the resulting solution was centrifuged in a microcentrifuger for 3 min and the clear supernatant was transferred to an HPLC vial for analysis.

### 2.4. Assay conditions and procedure

The HPLC system (including column) was equilibrated with the mobile phase at a flow-rate of 2.5 ml/min (pressure ca. 3000 psi) by injecting the standard solution until reproducible injections (R.S.D. <2%) were observed prior to the sample analysis. Standard and sample solutions (injection volume, 50 μl) were injected directly. The detection was by UV absorption at 215 nm. Chromatograms were recorded by the Multichrom 2.0 program (Fisons Instruments, Danvers, MA, USA) using a VG computer.

## 3. Results and discussion

### 3.1. Optimization of the method

The HPLC conditions were developed on the basis of the existing method for the determination of enalapril maleate drugs, in which a Lichrosorb RP-8 column (10 μm particle size, 300 × 4.6 mm I.D., E.S. Industries or Phenomenex using RP-8 packing material made by E. Merck) was used with a CH<sub>3</sub>CN–0.02 M potassium phosphate (pH 2.25) (45:55, v/v) mobile phase [5,7]. Under these conditions, enalapril and its degradation products eluted in the first half of the chromatogram, while felodipine and its degradation product eluted in the second half of the chromatogram, which formed a good base for further optimization. However, recently, E. Merck has changed the manufacturing process of the packing material. The Lichrosorb columns with the new “RP-8” material showed chromatographic difficulties in the separation of enalapril and its two degradation products in the combination drug. Thus, several other C<sub>8</sub> columns were evaluated. Among them, Spherisorb C<sub>8</sub> columns were found to give similar and more rugged separation conditions with better column-to-column reproducibility.

As shown in Fig. 2, good resolutions between maleic acid, diacid, enalapril-DKP, enalapril, H152/37, felodipine, and an UV-absorbing excipient are achieved using the conditions described in the Experimental section.

The mobile phase CH<sub>3</sub>CN–0.001 M KH<sub>2</sub>PO<sub>4</sub> (pH 2) (35:65, v/v), characterized by the low concentration and the low pH of the phosphate solution, was obtained from an optimization process based on several considerations.

The low pH is critical to the determination of enalapril and diacid. Enalapril is a dipeptide with a proline peptide bond, which has *trans* and *cis* conformations due to its partial double bond character. The enalapril peak could be distorted or even splitted into two peaks at high pH. At low pH, it gives a sharper, single peak shape because the proline peptide bond is partially protonated, which decreases its partially double bond character, and increases the relaxation rate

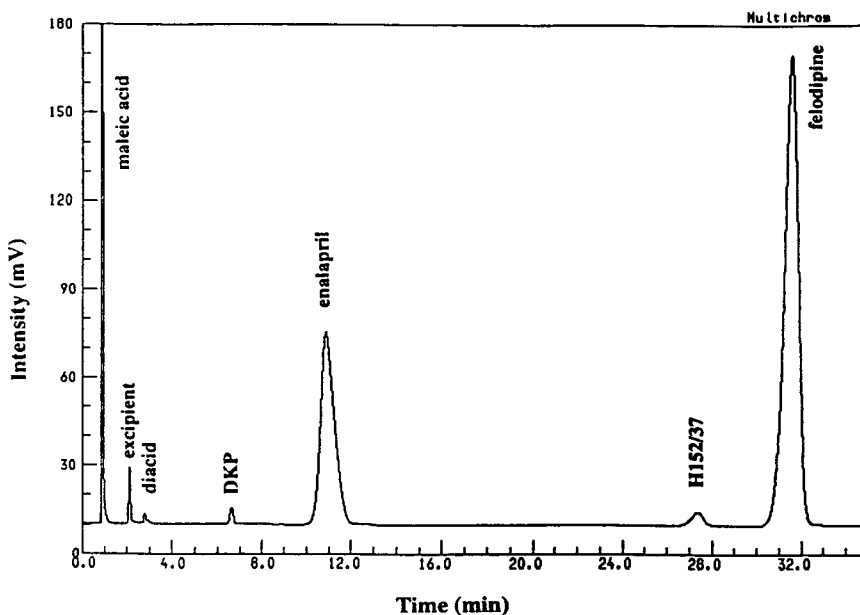


Fig. 2. Typical chromatogram showing the separation of enalapril, felodipine, their degradates and an UV-absorbing excipient by the use of the HPLC conditions listed in the text.

of the *cis* and *trans* isomerization [8]. Similarly, diacid has a much sharper peak shape at lower pH.

In addition to peak shape, the retention of enalapril and diacid is greatly influenced by pH. Since the  $pK_a$  values of enalapril are 2.97 (the carboxyl group) and 5.35 (the amine group) at 25°C [5], enalapril possesses a net positive charge at pH 2. Diacid also has a net positive charge at pH 2 because its two carboxyl groups have  $pK_a$  values between 2 and 3, and its amine group has a  $pK_a$  value between 5 and 6 [5]. As is well known, there are unreacted silanol groups in the bonded  $C_8$  phase, which can have a density as high as 8  $\mu\text{mole}/\text{m}^2$ , higher than that of the bond phase of the Spherisorb column (2.51  $\mu\text{mole}/\text{m}^2$ ). Most of these silanols are acidic with  $pK_a$  values between 5 and 7. However, some silanols can have lower  $pK_a$  values. At pH 2, although most of the silanol groups are protonated, some silanols could be deprotonated. These deprotonated silanols can interact with the positively charged enalapril and diacid through hydrogen-bonding and cation-exchange interactions [9–11]. When pH is increased from pH 2,

the cation-exchange process will be influenced due to the change in the ionization status of the silanols, enalapril and diacid. In turn, the retention of enalapril and diacid will be influenced. Clearly, the pH is a good means to control the retention of enalapril and diacid.

The control of the retention of enalapril by adjusting the pH is important in achieving good resolution between enalapril and H152/37 and between diacid and the UV-absorbing excipient. As shown in Fig. 3a, when the pH increases from 1.8 to 3, the  $k'$  of enalapril increases much faster than that of H152/37. At about pH 3, it becomes overlapping with H152/37. Also, as shown in Fig. 3b, when the pH increases from 1.8 to 3, the  $k'$  of the excipient remains relatively unchanged; the  $k'$  of diacid first increases, which results in better separation between diacid and the excipient, and then decreases, which results in partial overlapping of the two species at pH 3.

Besides pH, the salt concentration is another parameter controlling the retention of enalapril and diacid. The salt concentration was varied with the pH of its solution always adjusted to 2. The low concentration (0.001 M  $\text{KH}_2\text{PO}_4$ ) was

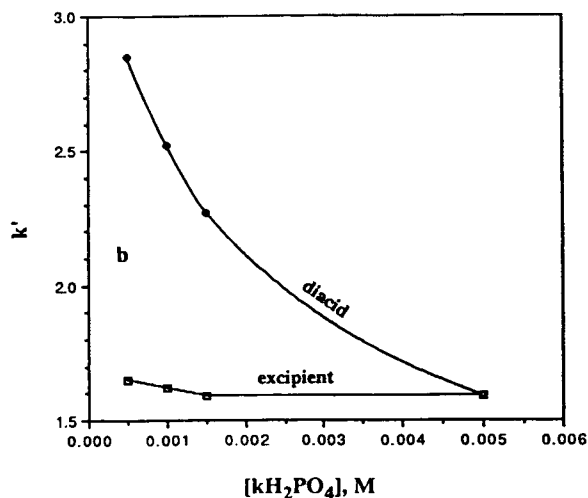
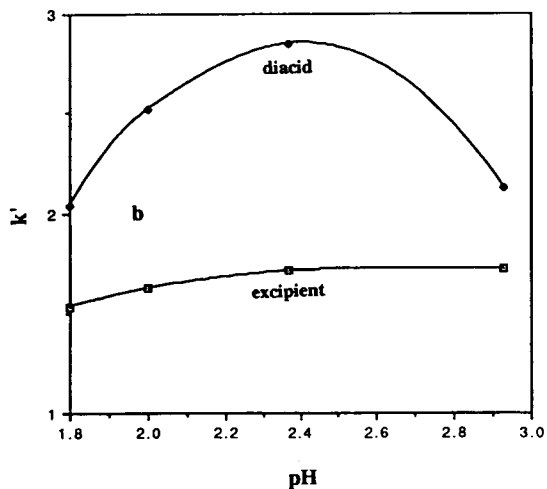
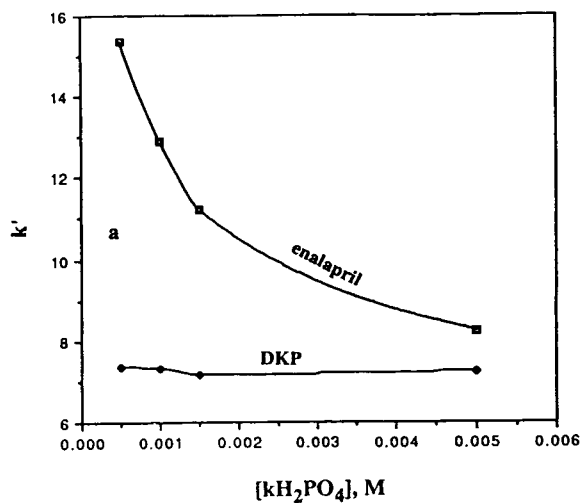
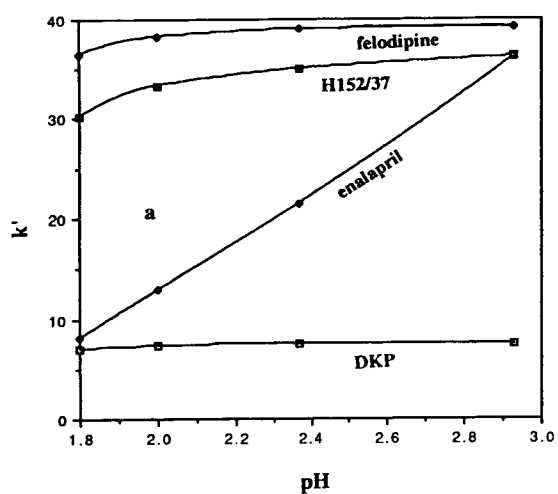


Fig. 3. Plots of  $k'$  as a function of pH of phosphate solution in the mobile phase.

found to be important for the rugged separation of enalapril and DKP. The  $k'$  of enalapril decreases while that of DKP remains relatively unchanged as the salt concentration increases (Fig. 4a). This can be attributed to the ionic strength effect of added potassium cations, which can shield the deprotonated silanols. Another explanation is the ion-pair formation between the enalapril cation and phosphate, which increases as the salt concentration increases. Since the ion-pair does not participate in the cation exchange with silanol groups, the  $k'$  of enalapril

Fig. 4. Plots of  $k'$  as a function of  $[\text{KH}_2\text{PO}_4]$  in the mobile phase.

decreases. However, since phosphate is very hydrophilic, and its ion-pairing with an amine cation in aqueous solutions has never been reported, this is very unlikely. Since the  $k'$  of enalapril is affected, whereas the  $k'$  of DKP is not affected by the salt concentration, enalapril moves closer to DKP at higher salt concentrations, and starts overlapping with DKP at concentrations above 0.005 M  $\text{KH}_2\text{PO}_4$ . When the salt concentration further increases, the

elution order of enalapril and DKP will be reversed. Low salt concentration is also crucial for the separation of diacid from the excipient. It was observed that the  $k'$  of diacid decreases as the salt concentration increases (see Fig. 4b), probably due to a similar mechanism as for enalapril. At higher concentrations (0.005 M  $\text{KH}_2\text{PO}_4$  and above), diacid co-elutes with the excipient.

DKP, felodipine and H152/37 are neutral in the pH range 1.8–3, and thus their retentions are not significantly affected by the salt concentration or pH. The controlling factor for these compounds is the percentage of acetonitrile, which has a significant effect on their  $k'$ . As demonstrated in Fig. 5a, the  $k'$  of these compounds decreases as the percentage of acetonitrile increases. It can be seen that felodipine and H152/37 have very similar  $k'$  values. They co-elute at higher percentages of organic modifier (> 40% acetonitrile). A solvent strength of 35% acetonitrile is used in the mobile phase to separate them. Although their separation is better using a low percentage of organic modifier (< 35% acetonitrile), the total run time will become unfavorably longer. The retention of enalapril and diacid is also affected by the percentage of acetonitrile, but to a much smaller extent (see Fig. 5b).

In summary, by variation of the salt concentration, pH and organic modifier in the mobile phase, the resolution of the compounds of interest is optimized on the Spherisorb column.

### 3.2. Validation of the method

The method was validated according to the USP guidelines [12]. The results are all satisfactory.

#### Accuracy

The accuracy of the method was determined by investigating the recovery of enalapril maleate and felodipine in duplicate at 5 levels ranging from 50% to 150% of the method concentration (0.1 mg/ml) from solid spiked placebo tablets. The results indicate recoveries ranging from 98.6% to 102.1% with a mean of 100.7%

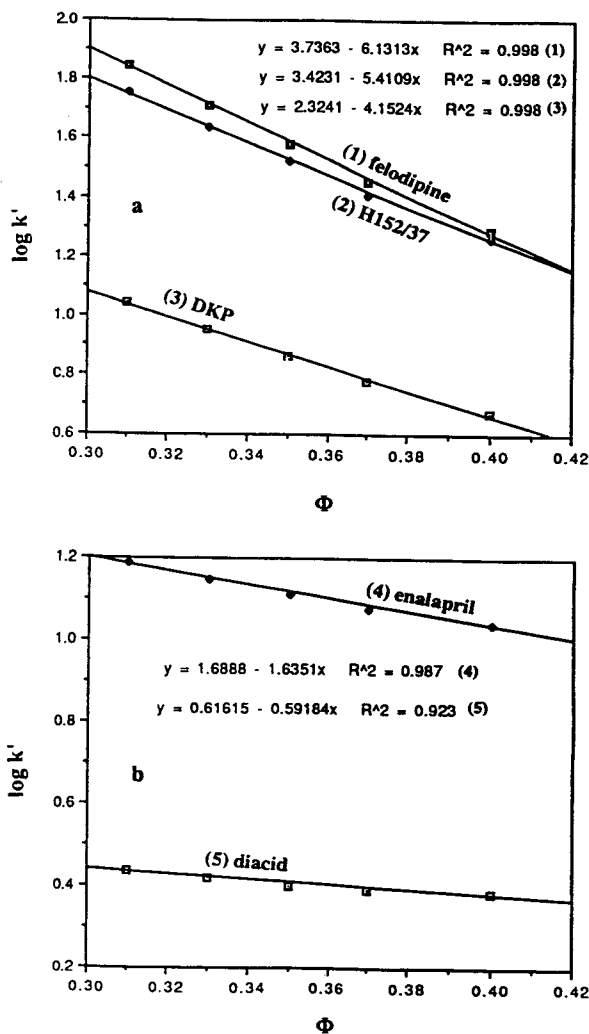


Fig. 5. Plots of  $\log k'$  vs. percentage of acetonitrile ( $\Phi$ ) in the mobile phase.

(R.S.D. = 1.3%,  $n = 10$ ) for enalapril maleate, and ranging from 99.7% to 102.0% with a mean of 100.2% (R.S.D. = 1.7%,  $n = 10$ ) for felodipine. The accuracy was also measured for the degradation products by investigating the recovery of diacid, DKP and H152/37 in duplicate at 6 levels ranging from 0.1% to 3% from solution spiked placebo tablets. The results indicate acceptable recoveries ranging from 88.1% to 116.9% with a mean of 101.0% (R.S.D. = 8.1%,  $n = 12$ ) for diacid, from 83.6 to 97.5%



with a mean of 93.0% (R.S.D. = 5.3%,  $n = 12$ ) for DKP, and from 83.6 to 97.5% with a mean of 93.0% (R.S.D. = 5.3%,  $n = 12$ ) for H152/37, respectively.

### Precision

The measurement precision was determined by performing ten replicate injections of standard solution containing enalapril maleate, felodipine, diacid, DKP, and H152/37 [0.1 mg/ml for enalapril maleate and felodipine (the method concentration), and 1  $\mu$ g/ml for diacid, DKP and H152/37 (1% of the method concentration)]. The measurement precision of all species was excellent with R.S.D. < 1% ( $n = 10$ ) by either peak area or peak height measurement.

The method precision was determined by the analysis of 10 replicate samples. The R.S.D.s (4.2% for enalapril maleate and 1.3% for felodipine) are satisfactory.

### Linearity

The detector responses were found to be linear for enalapril and felodipine both in the absence and in the presence of placebo over a concentration range of 50% to 150% of the method concentration (0.1 mg/ml) by peak area measurement. The correlation coefficients ( $r^2$ ) were all 1.000. The bias contributed by placebo interference is negligible. The detector responses were also linear for diacid, DKP and H152/37 in the presence of placebo over a concentration range of 0.1% to 3%. The correlation coefficients ( $r^2$ ) were all greater than 0.998.

### Limit of detection and limit of quantitation

The limits of detection (LOD) were determined to be 0.02%, 0.01% and 0.02% for diacid, DKP and H152/37, respectively, based on a signal-to-noise ratio of 3. The limit of quantitation was determined to be 0.1% for the three degradation products. As shown above, recovery of these degradation products from 3.0% down to 0.1% was acceptable and the detector response was linear from 3.0% to the 0.1% level. In addition, measurement precision of the three

degradation products at the 0.1% level was also acceptable (R.S.D. < 10%,  $n = 10$ ).

### Robustness

The method conditions are robust. Good resolutions (>1.3) of the seven compounds of interest are obtained on small changes in the mobile phase (ranges: pH, from 1.8 to 2.4;  $\text{KH}_2\text{PO}_4$  concentration, from 0.0005 to 0.0015 M; and percentage of acetonitrile, from 33% to 37%), and on small changes in temperature (range: 30°C to 50°C). The diacid, enalapril-DKP and H152/37 are the frequently observed degradation products during long term stability testing (25°C/60% rh or 30°C/60% rh for a long period of time), and thus they were used in the method validation. However, under certain accelerated stability and severe stress testing, some other degradation products, such as diastereoisomers of enalapril, diastereoisomers of diacid, and diacid-DKP could be formed. Since the method conditions are robust, they can be easily adjusted to separate these degradation products. Other possible impurities, such as the two symmetrical esters of felodipine formed in the synthesis process, can also be easily separated.

### 3.3. Further elucidation of separation mechanisms

Despite the many studies on the reversed-phase separation theory, there still seems to be considerable uncertainty as to the mechanism of the overall process. It appears that under the conditions used in the present method, the retention of enalapril-DKP, felodipine and H152/37 is governed by the reversed-phase partitioning process, while that of enalapril and diacid is governed by both the reversed-phase partitioning and the cation-exchange mechanism with residual silanols. The latter is associated with the type of the amino acids, the pH-dependent protolytic equilibria, and other secondary equilibria such as solvation, as briefly discussed in the optimization process.

It is observed that the elution of DKP, felodipine, and H152/37 follows quite well the regular reversed-phase behavior with increasing

content of the organic modifier, i.e.  $k'$  decreases inversely proportional with increasing volume fraction of acetonitrile ( $\Phi$ ) while the other conditions remained unchanged. A number of useful empirical relationships between  $k'$  and the solvent strength (percentage of organic modifier) can be found in the literature, the simplest equation being [13]:

$$\log k' = \log k'_w - S\Phi \quad (2)$$

where  $S$  is the slope of the curve, and  $k'_w$  is the value of  $k'$  in pure water. By plotting  $\log k'$  vs.  $\Phi$ , as shown in Fig. 5, the values of  $\log k'_w$  and  $S$  are obtained (see Table 1). The fitting for DKP, felodipine and H152/37 in the plots is excellent ( $r^2 = 0.998$ ), while some curvature was observed for the fitting of enalapril ( $r^2 = 0.987$ ) and diacid ( $r^2 = 0.923$ ). The deviation from linearity for these two compounds is attributed to the silanol interactions, i.e. the cations of these compounds interact with accessible silanols present in the packing via a cation-exchange mechanism in addition to the reversed-phase mechanism [14] (see below).

The slope  $S$  is an important parameter from both the practical and the theoretical point of view. Practically,  $S$  for two adjacent peaks (for example, the felodipine and H152/37 peaks) determines the selectivity as a function of a change in the percentage of organic modifier. Theoretically,  $S$  gives insight into the retention process. The parameter  $S$  is not merely a solvent-stationary phase parameter. It varies with solute structure. It increases with molecular size, and also with increasing hydrophobicity, which,

in the present study, follows the order: felodipine > H152/37 > DKP > z.Gt;enalapril > diacid. The values of  $k'_w$  are estimated by the extrapolated intercept, which are also important. The value of  $k'_w$  is also dependent on the solute's structure and is suggested to be the best hydrophobic parameter [15]. As shown, the  $k'_w$  values follow the same order as the  $S$  values, confirming the hydrophobicity order of these compounds under the conditions employed.

To further explore the cation-exchange mechanism of the retention of enalapril and diacid, the relationship between the  $k'$  values of these compounds and the concentration of  $K^+H_2PO_4^-$  is examined by the equation developed by Regnier et al., which is based on a non-mechanistic model to investigate charge-charge and other interactions between solutes and the surfaces of ion-exchange packing materials [16]:

$$\log k' = 2Z \log (1/[X^+Y^-]) + \log K_Z \quad (3)$$

where the parameter  $Z$  measures the number of charges interacting between the surface of the ion exchanger (e.g., residual silanol groups) and the solute ion (e.g., the enalapril and diacid cation), and  $[X^+Y^-]$  is the concentration of the salt used as a displacing agent (e.g.,  $K^+H_2PO_4^-$ ) and  $\log K_Z$  is a constant. The equation shows that if obeying the ion-exchange mechanism, the  $k'$  of enalapril (or diacid) should be a function of the concentration of  $K^+H_2PO_4^-$ , which decreases with the increasing of the concentration of  $K^+H_2PO_4^-$ . This is in good agreement with the experimental observations shown in Fig. 4, where the  $k'$  is plotted against  $[K^+H_2PO_4^-]$ . Using these experimental data and the data for felodipine and H152/37, the values of  $Z$  ( $Z = \text{slope}/2$ ) (see Table 2) are derived by plotting  $\log k'$  against  $\log 1/[K^+H_2PO_4^-]$  in Fig. 6. The fittings of the plots for DKP, felodipine and H152/37 are very poor, indicating that their retention does not follow the ion-exchange process. On the other hand, the fittings of the plots for enalapril ( $r^2 = 0.998$ ) and diacid ( $r^2 = 0.986$ ) are fairly good, in consistency with the suggestion that their retention follows cation-exchange mechanism with silanol groups. The

Table 1  
Log  $k'_w$ ,  $S$ , and  $r^2$  values

Species	$\log k'_w$	$S$	$r^2$
Felodipine	3.74	6.13	0.998
H152/37	3.42	5.41	0.998
DKP	2.32	4.15	0.998
Enalapril	1.69	1.64	0.987
Diacid	0.62	0.59	0.923

Table 2  
Log  $k'_z$ ,  $Z$ , and  $r^2$  values

Species	log $k'_z$	$Z$	$r^2$
Felodipine	1.56	0.0031	0.256
H152/37	1.45	0.012	0.799
DKP	0.839	0.0039	0.364
Enalapril	0.289	0.14	0.998
Diacid	-0.385	0.13	0.986

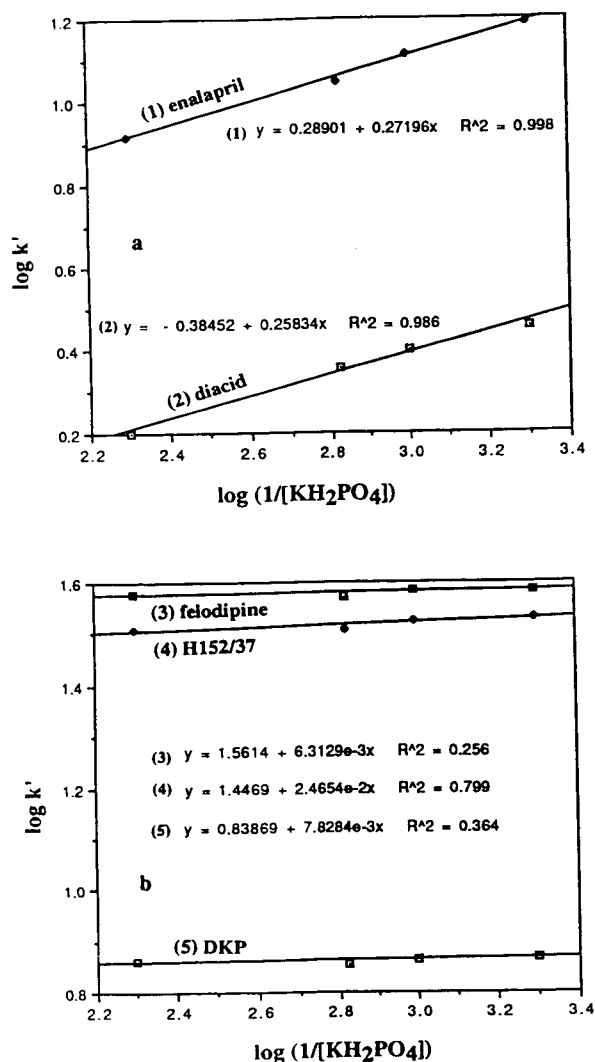


Fig. 6. Plots of  $\log k'$  vs.  $\log (1/[\text{KH}_2\text{PO}_4])$ .

exceedingly small  $Z$  values for DKP, felodipine and H152/37 also indicate no charge–charge interaction of these species with residual silanol groups. The  $Z$  values for enalapril and diacid are derived to be 0.14 and 0.13, respectively, which represents the charge of these species in the interaction with silanol groups according to the Regnier model. The charges deviated from the “net charge”, which indicates that only a fraction of the enalapril or diacid surface interacts with the silanol groups like proteins [16], probably due to the charge asymmetry of these species, the counter-ion effect and solvation of ions. From the above discussion, it is clear that the separation mechanisms of enalapril and diacid and that of enalapril-DKP, felodipine and H152/37 are distinct, which induces selectivity, and facilitates the simultaneous determination of these compounds.

#### 4. Conclusions

Simultaneous determination of enalapril, felodipine and their degradation products in the enalapril/felodipine (5 mg/5 mg) formulation has been accomplished by reversed-phase HPLC using a Spherisorb  $C_8$  column. The retention of felodipine, DKP and H152/37 follows the reversed-phase partitioning process whereas that of enalapril and diacid follows both the partitioning and the cation-exchange process with residual silanols. The selectivity induced by the distinct separation mechanisms facilitates the simultaneous determination of these compounds. This study gives an example of a contribution of silanol interaction in the reversed-phase mode.

#### Acknowledgements

The authors thank Drs. M.A. Brooks and P. deMontigny for critical review and helpful discussions. The authors also thank Dr. T.S. Chen for supplying the enalapril/felodipine tablets and placebo tablets.

**References**

- [1] A.A. Patchett, E. Harris, E.W. Tristram, M.J. Wyvratt, M.T. Wu, D. Taub, E.R. Peterson, T.J. Ikeler, J. ten Broecke, L.G. Payne, D.L. Ondeyka, E.D. Thorsett, W.J. Greenlee, N.S. Lohr, R.D. Hoffsommer, H. Joshua, W.V. Ruyle, J.W. Rothrock, S.D. Aster, A.L. Maycock, F.M. Robinson and R. Hirschmann, *Nature (London)*, 288 (1980) 280.
- [2] S. Takka and F. Acarturk, *Fabad Farm. Bilimler Derg.*, 17 (1992) 307.
- [3] T.O. Morgan, A. Anderson, E. Jones, *Am. J. Hypertens.*, 5 (1992) 238.
- [4] P.H.J.M. Dunselman, T.W. Van Der Mark, C.E.E. Kuntze, A. Van Bruggen, J.P.M. Hamer, A.H.J. Scaf, H. Wesseling, K.I. Lie, *Eur. Heart J.*, 11 (1990) 200.
- [5] D.P. Ip and G.S. Brenner, in K. Florey (Editor), *Analytical Profiles of Drug Substances*, Vol. 16, Academic Press, London, 1987, pp. 207–243.
- [6] M. Ahnoff, *J. Pharm. Biomed. Anal.*, 2 (1984) 519.
- [7] J. DeMarco, Merck Research Lab., unpublished results.
- [8] W.R. Melander, J. Jacobson and C. Horvath, *J. Chromatogr.*, 234 (1982) 269.
- [9] K.K. Unger, *Porous Silica*, Elsevier, Amsterdam, 1979, pp. 130–141.
- [10] S.G. Weber and G. Tramposch, *Anal. Chem.*, 55 (1983) 1771.
- [11] J. Salamoun and K. Slais, *J. Chromatogr.*, 537 (1991) 249.
- [12] *The United States Pharmacopeia 23, 1982–1983*, United States Pharmacopeial Convention, Rockville, MD, 1995.
- [13] L.R. Snyder, J.W. Dolan and J.R. Gant, *J. Chromatogr.*, 165 (1979) 31.
- [14] K.E. Bij, C. Horvath, W.R. Melander and A. Nahum, *J. Chromatogr.*, 203 (1981) 65.
- [15] K. Valko, L.R. Snyder and J.L. Glajch, *J. Chromatogr. A*, 656 (1993) 501.
- [16] W. Kopaciewicz, M.A. Rounds, J. Fausnaugh and F.E. Regnier, *J. Chromatogr.*, 266 (1983) 3.



ELSEVIER

Journal of Chromatography A, 707 (1995) 255–265

JOURNAL OF  
CHROMATOGRAPHY A

# Investigation of the use of oxygen doping of the electron-capture detection for determination of atmospheric halocarbons

G.A. Sturrock, P.G. Simmonds, G. Nickless\*

*Biogeochemistry Centre, University of Bristol, Cantock's Close, Bristol BS8 1TS, UK*

First received 15 November 1994; revised manuscript received 9 January 1995; accepted 9 January 1995

## Abstract

The development of a GC–electron-capture detection instrument to determine accurately certain important trace  $C_1$  halocarbons in a single analytical procedure from ambient air is reported. The procedure utilizes preconcentration at room temperature on an efficient microtrap filled with a commercially available adsorbent, Carboxen, followed by direct thermal desorption in a single stage on to a high-resolution capillary column. Detection is achieved with dual electron-capture detectors in series; the second being oxygen doped to dramatically enhance the sensitivity of the detector towards those halocarbons (hydrofluorochlorocarbon 22,  $CH_3Cl$ ) which normally react feebly with thermal electrons.

## 1. Introduction

Recent studies [1–3] have provided clear evidence of the significant reduction in fluorochlorocarbon (CFC) 11 and 12 concentrations in Europe over the period 1987–1990 following the phase-out in CFC use. In addition to the principal CFCs, HCFCs (hydrofluorochlorocarbons) and the replacement HFCs (hydrofluorocarbons), there are a number of other trace halogenated gases which are of environmental concern for which no continuous monitoring programmes exist. The present study concentrated on the group of halogenated methane compounds of both natural and anthropogenic origin; HCFC 22 ( $CHClF_2$ ), the primary interim

replacement compound, already in widespread use, was included in this group. Due to the single chlorine and partial removal in the troposphere by hydroxyl radicals, HCFC 22 was excluded from the controls under the Montreal Protocol while the search was initiated for safer, chlorine-free chemicals. Its rapidly increasing use [4] suggests a need for careful atmospheric monitoring, due to an uncertain atmospheric lifetime of between 12 and 40 years [5] and because HCFC 22 is a significant absorber of infrared radiation. The first measurements of HCFC 22 in the atmosphere were made in 1979 by GC–MS and GC–electron-capture detection (ECD) techniques [6]. Long-term, high-frequency atmospheric measurements are relatively sparse and improved techniques are therefore required.

The first measurements of  $CH_3Cl$ , a major

\* Corresponding author.

contributor to the total chlorine budget of the atmosphere, were reported by Grimsrud and Rasmussen [7] and by Lovelock [8]. Both indicated that the primary source was from natural emissions from the oceans, however, a significant contribution also arises from biomass burning [9].  $\text{CHCl}_3$  has approximately equal natural and anthropogenic sources with a substantial seasonal ocean flux [10]. Although  $\text{CHCl}_3$  can be determined by existing GC-ECD techniques, the precision is poor due to the proximity of the limit of detection to its atmospheric concentration. Similarly,  $\text{CH}_2\text{Cl}_2$  has limited data, and will contribute chlorine to the atmosphere. There are almost no reliable estimates for the relative emissions from their different natural sources. To understand fully the role of  $\text{CH}_3\text{Cl}$ ,  $\text{CH}_2\text{Cl}_2$  and  $\text{CHCl}_3$  in the global environment, there is a need for contiguous measurements to establish accurate trends and atmospheric lifetimes.

The atmospheric chemistry of bromine containing compounds plays an important role in the stratosphere — with synergistic interactions of chlorine and bromine in the lower stratosphere [11,12]. Brominated compounds have up to 60 times the ozone depletion potential of the CFCs, although bromine is in the atmosphere at a hundredth of the concentration of chlorine species. The large uncertainties in  $\text{CH}_3\text{Br}$  atmospheric abundance, which range from 10 to 20 ppt [12], is due to difficulties of absolute calibration and poor understanding of relative sources (natural versus anthropogenic), although studies are increasing, as this compound is implicated as an important player in stratospheric ozone depletion [13,14]. The two Halons, 13B1 ( $\text{CF}_3\text{Br}$ ) and 12B1 ( $\text{CF}_2\text{ClBr}$ ), are entirely manmade and used almost exclusively as fire extinguishers. Before implementation of the Montreal Protocol, the use of the Halons was increasing (ca. 15–20%/year) [15]; now, recent results indicate this rate of increase has substantially decreased [16] although they may induce significant ozone depletion in the short term [11]. There are at present no long-term observational records of sufficient frequency and duration to determine accurate trends in these brominated species.

The special challenge comes for the group of

compounds, 13B1, 12B1, HCFC 22,  $\text{CH}_3\text{Cl}$ ,  $\text{CH}_3\text{Br}$ ,  $\text{CH}_2\text{Cl}_2$  and  $\text{CHCl}_3$ , from the low concentrations and/or low ECD response which prevent their direct measurement. Although determination of halocarbons down to the ppt level has been achieved by concentration from ambient air cryogenically [17], the associated problem of collection of large quantities of water during sampling is an inherent drawback — presenting a problem in the subsequent chromatographic analysis. The method used here is based on a single microtrap developed in earlier work in these laboratories [18]. A small ambient air sample is trapped at room temperature, thereby avoiding the use of cryogenics which is expensive, time consuming and technically demanding in field analysis or automated operation. A single desorption stage directly onto the column suffices, due to the small design of the microtrap with near capillary dimensions, thereby avoiding the need for a second cryofocusing stage, while maintaining suitable chromatography. This eliminates additive errors obtained in each stage of desorbing when using several trapping and desorbing stages.

Grimsrud and co-workers [19–21] demonstrated that the response of the ECD to certain compounds which normally produce very low signals can be considerably enhanced by addition of oxygen as a dopant of the carrier gas. It has, therefore, become apparent that the presence of certain electron-attaching molecules as part of the carrier gas produced both interesting and analytically useful effects [20], increasing the ECD response to many compounds by reactions of the additional  $\text{O}_2^-$  negative ions which are then present. Specific applications of the oxygen doped ECD to atmospheric analysis have been shown [9,21,22]. As yet, the number of research groups working in this area is limited and the ultimate importance of the method to the broad scope of chemical analysis has yet to be determined. The fact that oxygen can alter the response characteristics of the ECD leads to the improved sensitivity desired for detection of the ultra low concentrations of the target species.

The basis of this work was the development of a single GC-ECD instrument using two elec-

tron-capture detectors in series, the second ECD apparatus sensitized with oxygen, and the use of a microadsorption trap to concentrate trace atmospheric contaminants. The Halons, despite their low atmospheric concentrations, are strong electron absorbers, and do not need oxygen doping provided there is a reasonable preconcentration ratio and, in fact, show no response enhancement with oxygen doping. A similar situation pertains to  $\text{CHCl}_3$ , which only shows a minor response enhancement with an oxygen doped ECD. The method will allow construction of a near real-time/field portable GC instrument to determine these trace halocarbons accurately in a single analysis of air samples, ultimately for use in a remote field station.

## 2. Experimental

### 2.1. Preconcentration

The microtrap was constructed from thin-walled type 304 [0.023 in. I.D.  $\times$  0.035 in. O.D. (1 in. = 2.54 cm)] stainless-steel tubing (Coopers Needle Works, Birmingham, UK) and filled with Carboxen 1003 and Carboxen 1000 (Supelco, Bellefonte, PA, USA), which were held in by end plugs of stainless-steel wire (0.017 in. O.D.) with flattened ends. The adsorbents were select-

ed from studies of the breakthrough volume of the halocarbons, on a variety of materials, by a procedure which is reported in an earlier paper [23]. Desorption was facilitated with direct ohmic heating to 200°C by application of 90 V a.c. from a Variac transformer for 3 s to the microtrap. The dimensions of the microtrap and gas flows were equivalent to those of the capillary column (1–2 ml/min) allowing flow path uniformity and preventing possible pressure differentials in the system and turbulence in the flowing gas stream, which may alter sample residence time. The method of measuring the volume of a sample passing through the microtrap involved a three-way valve (Hamilton, HVP 3-3) connected to an appropriate sized syringe (100 ml). Fig. 1 shows the entire system configuration for the preconcentration and detection of atmospheric halocarbons.

Two Valco valves (Valco Instruments, Houston, TX, USA) were incorporated in the system: the first (a four-port valve) enabled the system to be purged to this point with either sample or nitrogen; the second (a six-port switching valve) allowed sample or nitrogen to be passed through the trap in one mode, while column nitrogen carrier gas flowed through the trap in the other mode. Pressurized air samples, contained in 3.5-l passivated stainless-steel canisters (SUMMA polished), were connected via a three-way valve

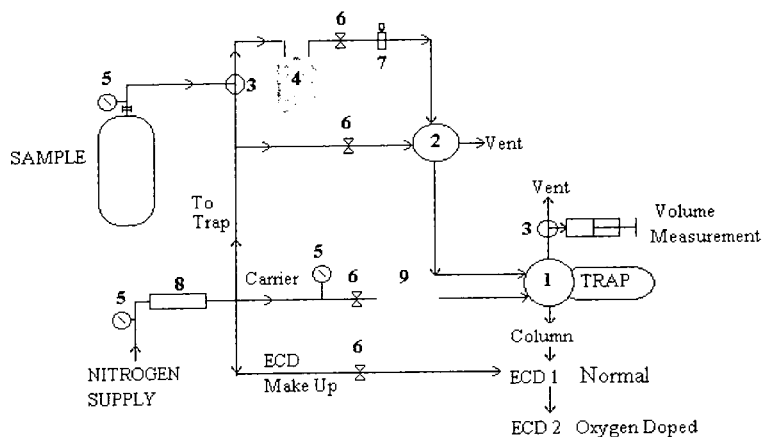


Fig. 1. Apparatus for halocarbon preconcentration and detection. 1 = 6-Port Valco valve, 2 = 4-port Valco valve, 3 = 3-way valve, 4 = Nafion drier, 5 = pressure regulator, 6 = needle valve, 7 = toggle valve, 8 = molecular sieve/charcoal trap, 9 = particle filter.

(Whitey ss-41 xs2) to permit either sample or nitrogen purge gas to be passed through a Nafion Permeation Drier to reduce sample moisture content reaching the trap. Consequently, the microtrap was always under an atmosphere of pure nitrogen when not sampling and during any pre-conditioning thermal desorption cycles. Flow-rates were controlled by Nupro fine metering valves (Bristol Valve and Fitting, Bristol, UK). The optimum flow-rate for air sampling was 10 ml/min to avoid the possibility of component breakthrough and incomplete trapping.

## 2.2. Chromatography

Studies, detailed in an earlier paper [24], concentrated on optimizing the chromatographic separation on a variety of high-resolution capillary columns including PoraPLOT, Alumina PLOT and WCOT columns, of the target halocarbons, as well as other components of atmospheric air, e.g. CFCs, HFCs, other HCFCs and the ubiquitous hydrocarbons, which could complicate the interpretation of results. However, in such a complex matrix (air), it is unlikely that a single chromatographic column will resolve all the individual compounds. The similar physical properties of HCFC 22 to CFC 12 which it replaces makes their complete chromatographic separation difficult. Table 1 gives details of the halocarbons identified in this study. GC-MS studies [25] confirmed the identities of the other compounds eluting in this important region, with propene and propane eluting after HCFC 22 and propyne eluting on the shoulder of the CFC 12 peak. These hydrocarbons are fortunately less susceptible to response enhancement and therefore unlikely to cause any interference with HCFC 22 determination in the second detector, which is oxygen doped.

Separation was carried out on the WCOT CP Sil 5 CB column (Chrompack, Middelburg, Netherlands) (50 m × 0.32 mm I.D.) with a temperature programme of 30°C (8 min) to 80°C at a rate of 10°C/min. This column and temperature programme gave the best resolution of the problematic HCFC 22/CFC 12 peak pair. Connection of the capillary column to the six-port

Table 1  
Major atmospheric halocarbons

Chemical formula	Trade name or abbreviation	Boiling point/°C
CF <sub>3</sub> H	HFC 23	-82.2
CF <sub>3</sub> Cl	CFC 13	-81.4
CF <sub>3</sub> Br	13B1	-57.8
CHClF <sub>2</sub>	HCFC 22	-40.8
CF <sub>2</sub> CICF <sub>3</sub>	CFC 115	-38.7
CF <sub>2</sub> Cl <sub>2</sub>	CFC 12	-29.8
CH <sub>3</sub> Cl	-	-24.2
CF <sub>2</sub> CIBr	12B1	-4.0
CH <sub>3</sub> Br	-	3.6
CF <sub>2</sub> CICF <sub>2</sub> Cl	CFC 114	3.7
CFCl <sub>3</sub>	CFC 11	23.8
CH <sub>2</sub> Cl <sub>2</sub>	-	40.0
CH <sub>3</sub> I	-	42.4
CF <sub>2</sub> CICFCI <sub>2</sub>	CFC 113	47.4
CHCl <sub>3</sub>	-	61.2
CH <sub>3</sub> CCl <sub>3</sub>	-	74.0
CCl <sub>4</sub>	-	76.3
CCl <sub>3</sub> CHCl	TCE	87.0
CCl <sub>2</sub> CCl <sub>2</sub>	PCE	121.0

injection/microtrap valve was achieved via a short length (25 cm) of deactivated fused-silica (0.32 mm I.D.) capillary tubing. Nitrogen was used as the column carrier gas (BOC Gases) and was purified by passage through a molecular sieve 5Å and activated charcoal filter.

## 2.3. Instrumentation

The GC used was a Varian 3700 Aerograph with a constant current, pulse-modulated 8 mCi <sup>63</sup>Ni detector. The detector cell had displaced coaxial cylinder geometry, 0.3 ml internal volume and was polarised with a negative voltage pulse of 50 V amplitude and 0.64 μs width, and a pulse frequency output range of 1.57 kHz to 1.4 MHz. The output signals were recorded with both a standard potentiometric recorder and a 3390A Hewlett Packard integrator. The final instrument involved the simultaneous use of normal and oxygen doped detection. The procedure is achievable via two electron-capture



detectors coupled in series with the first, the Varian ECD apparatus, in normal mode, using 20 ml/min of nitrogen gas as make up. The second ECD apparatus, a Shimadzu constant-current Ni<sup>63</sup> ECD instrument, combined the effluent from the first ECD apparatus with a make up of 2% oxygen in nitrogen (20 000 ppm) (BOC Special Gases) at ca. 2 ml/min to give a concentration of nominally 2000 ppm oxygen in nitrogen in the detector.

#### 2.4. Procedure

Preliminary studies on a standard mixture of HCFC 22, CH<sub>3</sub>Cl, CH<sub>2</sub>Cl<sub>2</sub> and CHCl<sub>3</sub>, via sample loop injection, were performed to observe response enhancement and allow selection of the oxygen doped ECD conditions. A standard mixture was prepared by static dilution with nitrogen from pure samples to give concentrations at the 100 ppb level. The ECD response was observed over the temperature range 250 to 350°C, since electron capturing compounds are known to have widely varying responses as a function of detector temperature [21] and will have a similar influence on oxygen doped detection. Various oxygen concentrations in the ECD apparatus were investigated to confirm Grimsrud and Miller's finding [19] that 2000 ppm oxygen in nitrogen in the ECD apparatus was the most suitable concentration for the response enhancement of these halocarbons. Detector cell current was varied to determine the effect on signal response for specifically HCFC 22 and CH<sub>3</sub>Cl.

The linearity of the entire system was tested by trapping increasing volumes of an air sample over the range of 20 to 120 ml on the microtrap at room temperature and desorbing each time under the same conditions. Extensive checks of system blanks were run to estimate interferences from other sources due to the ubiquitous nature of halocarbons. A blank analysis involved passing the same amount of nitrogen as used in the air sampling procedure, from either the carrier line or the purge and trap line, through the trap using the normal thermal desorption procedures on to the capillary column.

### 3. Results and discussion

The variation in ECD baseline frequency as a function of detector temperature and oxygen doping is represented in Fig. 2. The baseline frequency increases dramatically at lowest temperatures as the concentration of oxygen in the ECD apparatus is increased, while the lowest frequencies, i.e. "cleanest", are observed at high temperature, because the instantaneous O<sub>2</sub><sup>-</sup> concentration (the reagent thought to be responsible for response enhancement [19,21]) is reduced at elevated temperatures. Further results in Table 2, for the standard mixture, show that for the susceptible target halocarbons, response enhancement by oxygen doping of the ECD is least at the highest ECD temperatures.

The increase in response enhancement is most impressive on reducing the ECD temperature from 350 to 300°C, particularly for HCFC 22, but was less marked for CHCl<sub>3</sub> due to its higher normal ECD response. For example, from the peak area data for HCFC 22, the ECD response was increased by a factor of 2.4 on reducing the ECD temperature from 350 to 300°C, while reducing the ECD temperature to 250°C only increased the response by a further factor of 0.4. Overall, higher ECD temperatures are preferable with respect to providing minimum baseline noise with oxygen doping, but provide lower response enhancement. Therefore, a fine balance between the two (i.e. least noise gave the least response enhancement) has to be achieved. Signal-to-noise ratios allowed selection of the optimum ECD operating temperature of 300°C. This temperature provides maximum response for the weakest electron capturing compounds, HCFC 22 and CH<sub>3</sub>Cl, with adequate, although not the greatest, signal-to-noise ratio for CH<sub>2</sub>Cl<sub>2</sub>. CHCl<sub>3</sub> is most sensitively determined by operating the ECD apparatus in the normal mode with modest sample preconcentration.

A detrimental side effect is that the oxygen enhancement process will also increase the instrument's sensitivity to column bleed molecules as well as to the analytes of interest. It is therefore important to select the optimum detector standing current since with oxygen doping,

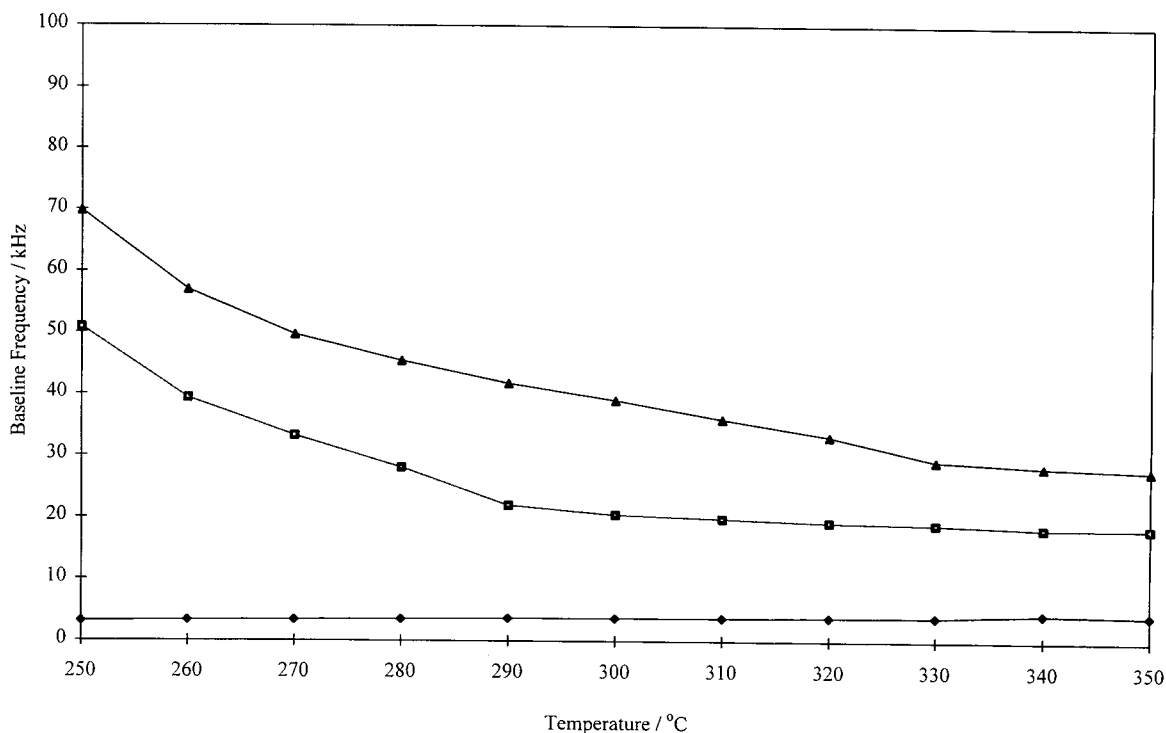


Fig. 2. Effect of oxygen on the baseline frequency at various ECD temperatures.  $\blacktriangle$  = 2000 ppm O<sub>2</sub>,  $\blacksquare$  = 1000 ppm O<sub>2</sub>,  $\blacklozenge$  = normal.

unavoidably column bleed results in a high baseline frequency. The present work showed that a detector current of 0.5 nA current should be used for both the Varian and the Shimadzu ECD systems in the oxygen doped mode. With the Varian ECD apparatus in the normal mode, a detector current of 0.5 nA causes the baseline

frequency to fall below the minimum operating frequency of the system of 1.57 kHz, and is unusable without a minimum current of 1 nA. Similarly, for the Shimadzu ECD apparatus in the oxygen doped mode, satisfactory responses were achieved at 0.5 nA and 1 nA, with only the 2-nA current being unsuitable, while the normal mode required a detector current of 1 nA. Signal-to-noise ratios are shown for HCFC 22 and CH<sub>3</sub>Cl, from a trapped air sample (80 ml), using the Shimadzu system in Table 3, which illustrates the favoured conditions for an oxygen doped detector at 2000 ppm and 300°C for these specific target compounds.

Table 2  
Effect of ECD temperature on compound response with 2000 ppm O<sub>2</sub> in the ECD apparatus

ECD temp (°C)	HCFC 22	CH <sub>3</sub> Cl	CH <sub>2</sub> Cl <sub>2</sub>	CHCl <sub>3</sub>
<i>Peak area/counts</i>				
250	245703	129240	351440	55591
300	207997	109517	152183	49607
350	87512	47291	62768	44324
<i>Signal-to-noise ratio</i>				
250	196	103	280	44
300	295	155	216	70
350	175	95	126	89

The following conditions were found to be the optimal for the target halocarbons on this particular GC system: (i) 2000 ppm oxygen in nitrogen to give sufficient compound response enhancement in the second ECD; (ii) 300°C for optimum detector operating temperature for the oxygen doped mode and 330°C for the normal

Table 3  
Signal-to-noise ratios for HCFC 22 and CH<sub>3</sub>Cl at different ECD currents

ECD current (nA)	Signal-to-noise ratio	
	HCFC 22	CH <sub>3</sub> Cl
0.5	104	440
1.0	39	165
2.0	25	16

mode; (iii) ECD cell current of 0.5 nA in oxygendoped mode, and 1 nA for normal ECD operation.

The efficacy of the analytical procedure was explored by analysis of samples of rural air in SUMMA-polished stainless-steel canisters, collected from the west coast of Ireland and from the Mendip Hills. A wide range of air volumes trapped have been quantitatively retained, and have shown to provide linearity in the range required for determination of the target compounds (Fig. 3). The precision from replicate Irish air samples adsorbed and desorbed from the microtrap are given in Table 4. Precisions are presented as peak areas relative to CFC 12 from the ECD mode which gives the highest signal-to-noise ratio for each target halocarbon. The precisions levels are very acceptable for this type of analytical procedure.

From the examination of the Mendip Hills air sample, the necessity of the concentration procedure is illustrated in Fig. 4, from a sample loop of air (5 ml) compared with a trapped air sample (80 ml). The CFCs, known to be in the air at trace levels, could easily be detected in rural air samples of <20 ml sample volume. Overall results demonstrated clearly that sufficient sensitivity had been achieved via the trapping system for trace gas analysis: even CH<sub>3</sub>I, at an atmospheric concentration of 2–3 ppt, could be detected routinely from 80 ml air samples by the normal ECD mode. Chromatograms of blank analyses are shown in Fig. 5 indicating adequate clean up procedures have been used within the system, preventing interference from contaminants.

The advantage of this technique over earlier methods [6,9] is that the major contaminant peaks (e.g. CFC 12, CFC 11) will be reduced in their passage through the first ECD apparatus, thereby, reducing their response in the second, highly sensitized detector, selectively revealing the remainder of the target compounds by response enhancement. The percentage reductions of the major chlorinated compounds and target halocarbons, from an air sample from Ireland, via passage through the first ECD apparatus are shown in Fig. 6. All the target compounds can be accomplished in a single analytical procedure, significantly reducing analysis time and allowing higher frequency routine analysis.

The additional sensitization of the second ECD with oxygen extends the range of the ECD to the weak electron adsorbers, HCFC 22, CH<sub>3</sub>Cl and CH<sub>2</sub>Cl<sub>2</sub>. Further compounds shown to be responsive in the present work were: SO<sub>2</sub>, COS, CS<sub>2</sub>, CFC 1113 (CClFCCl<sub>2</sub>), HFC 134a (CF<sub>3</sub>CH<sub>2</sub>F) and the HFCs 141b (CH<sub>3</sub>CFCl<sub>2</sub>), 124 (CF<sub>3</sub>CFHCl) and 142b (CH<sub>3</sub>CF<sub>2</sub>Cl). Other workers have also recently demonstrated the potential application of oxygen doping for certain HCFCs and HFCs [26]. It is important to be aware of their possible interference with and response to oxygen doping of the ECD. Some are of particular concern due to the predicted increase in usage and therefore atmospheric release as they replace the CFCs. Therefore, the potential exists for the analysis of a much wider range of halocarbons [25], subject to judicious capillary column choice. Additionally, atmospheric hydrocarbons would be suitably determined by this preconcentration procedure with separation using an Alumina/KCl PLOT column, which is specifically made for the analysis of such compounds, followed by flame ionization detection.

#### 4. Conclusions

This work has demonstrated the development of a practical GC–ECD instrument to determine accurately seven important trace atmospheric-halocarbons with a combination of adsorption on

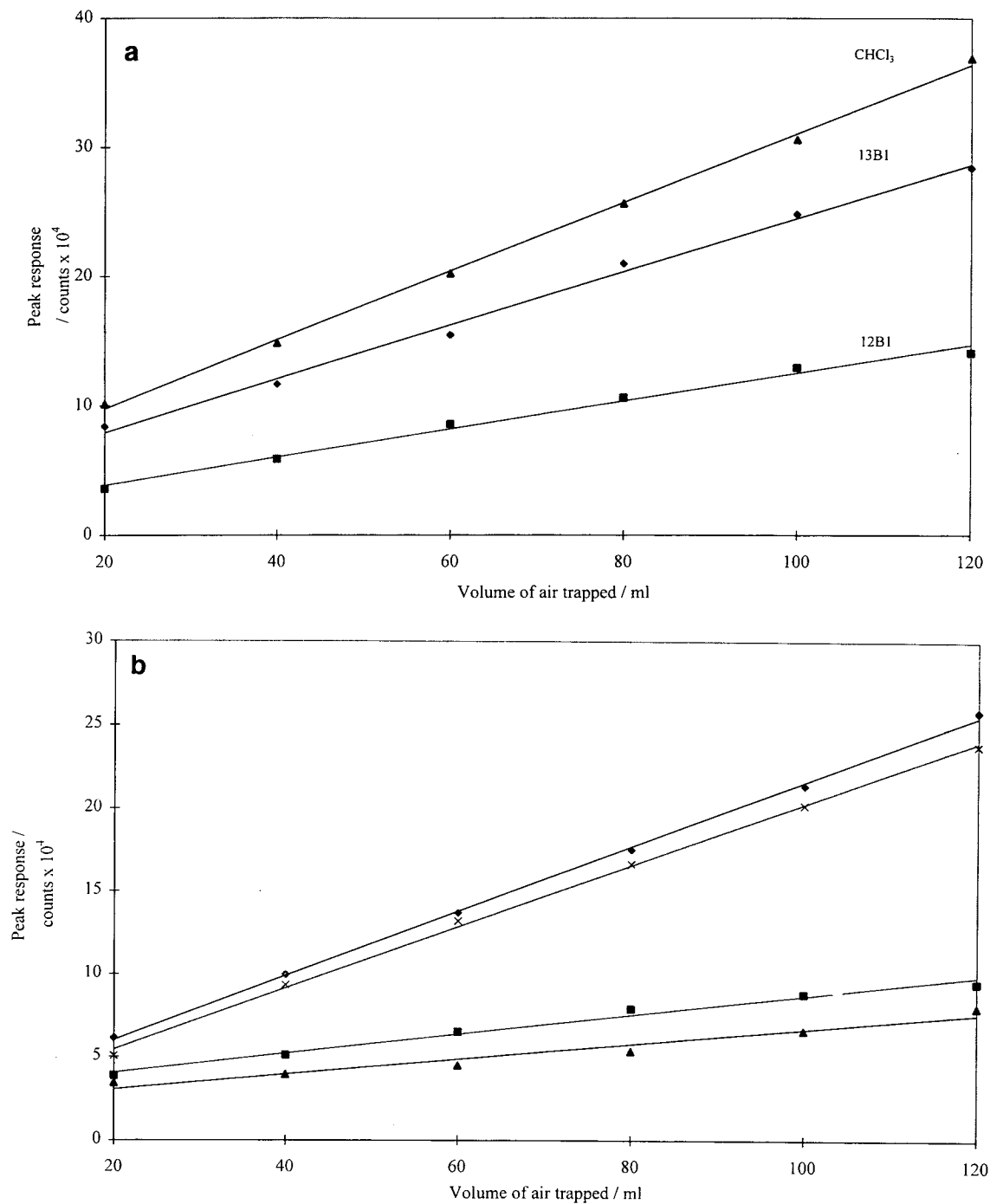


Fig. 3. Linearity of the ECD for trapping increasing volumes of air. (a)  $\blacktriangle$  = CHCl<sub>3</sub> ( $r = 0.999$ ),  $\blacklozenge$  = 13B1 ( $r = 0.995$ ),  $\blacksquare$  = 12B1 ( $r = 0.989$ ). (b)  $\blacklozenge$  = HCFC 22 ( $r = 0.999$ ),  $\times$  = CH<sub>2</sub>Cl<sub>2</sub> ( $r = 0.998$ ),  $\blacksquare$  = CH<sub>3</sub>Cl ( $r = 0.985$ ),  $\blacktriangle$  = CH<sub>3</sub>Br ( $r = 0.956$ ).

Table 4  
Precision levels for the analytical procedure for  $n = 10$

Compound	Peak area ratio %R.S.D.	
	Normal ECD	Oxygen doped ECD
13B1	0.8	–
HCFC 22	–	1.3
CH <sub>3</sub> Cl	–	3.6
12B1	1.7	–
CH <sub>3</sub> Br	–	3.9
CH <sub>2</sub> Cl <sub>2</sub>	–	1.8
CHCl <sub>3</sub>	1.6	–

a microtrap and detection with an oxygen doped ECD, due to their low concentration and low ECD response. It was directed towards the continuous long-term monitoring of specifically HCFC 22, 13B1, 12B1, CH<sub>3</sub>Cl, CH<sub>3</sub>Br, CH<sub>2</sub>Cl<sub>2</sub> and CHCl<sub>3</sub> from ambient air at near real time in a single analysis with high-frequency, high-precision measurements.

Complete trapping efficiency at ambient temperatures and efficient band-focusing (without the need for cryogenics) was achieved with a microtrap of near capillary dimensions packed with a small amount of the adsorbent, Carboxen.

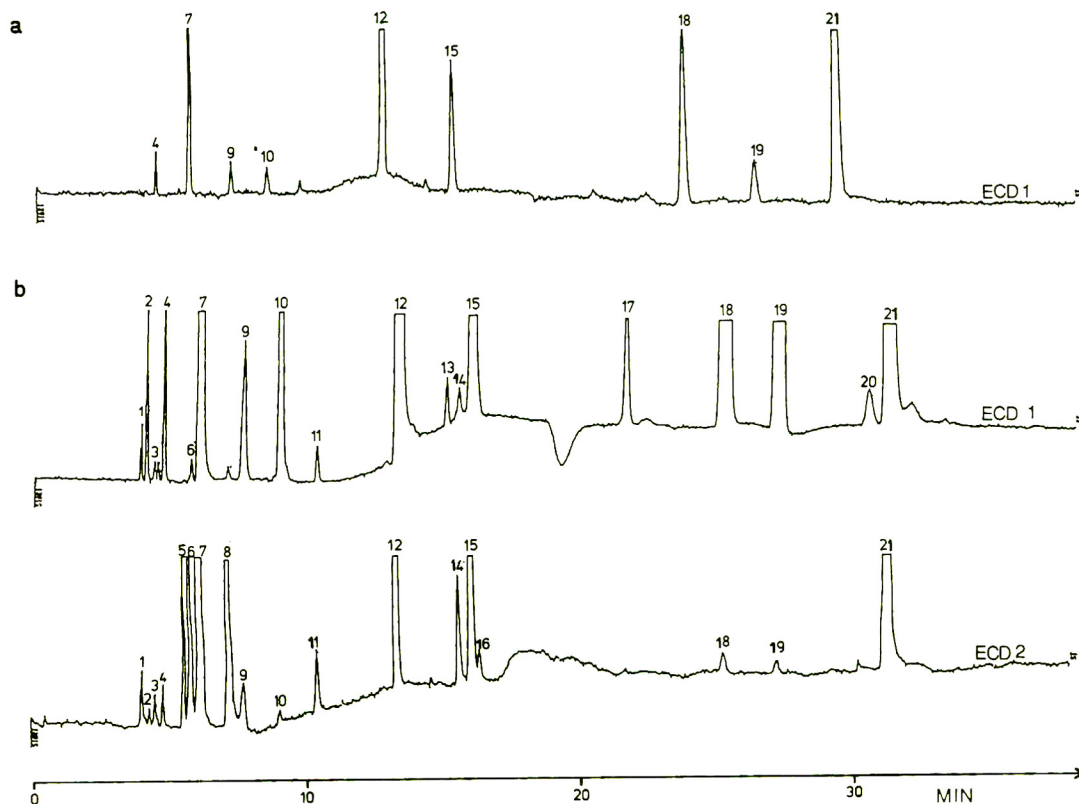


Fig. 4. Chromatograms of (a) a 5-ml and (b) an 80-ml Mendip Hills air sample on the WCOT CP Sil 5 CB column with nitrogen carrier gas flow-rate of (a) 1.8 ml/min and (b) 1.6 ml/min, with ECD 1 in normal and ECD 2 in oxygen doped mode. Peak identification: 1 = CFC 13, 2 = CFC 23, 3 = CFC 115, 4 = 13B1, 5 = HCFC 22, 6 = COS, 7 = CFC 12, 8 = CH<sub>3</sub>Cl, 9 = CFC 114, 10 = 12B1, 11 = CH<sub>3</sub>Br, 12 = CFC 11, 13 = CH<sub>3</sub>I, 14 = CH<sub>2</sub>Cl<sub>2</sub>, 15 = CFC 113, 16 = CS<sub>2</sub>, 17 = CHCl<sub>3</sub>, 18 = CH<sub>3</sub>CCl<sub>3</sub>, 19 = CCl<sub>4</sub>, 20 = TCE, 21 = PCE.

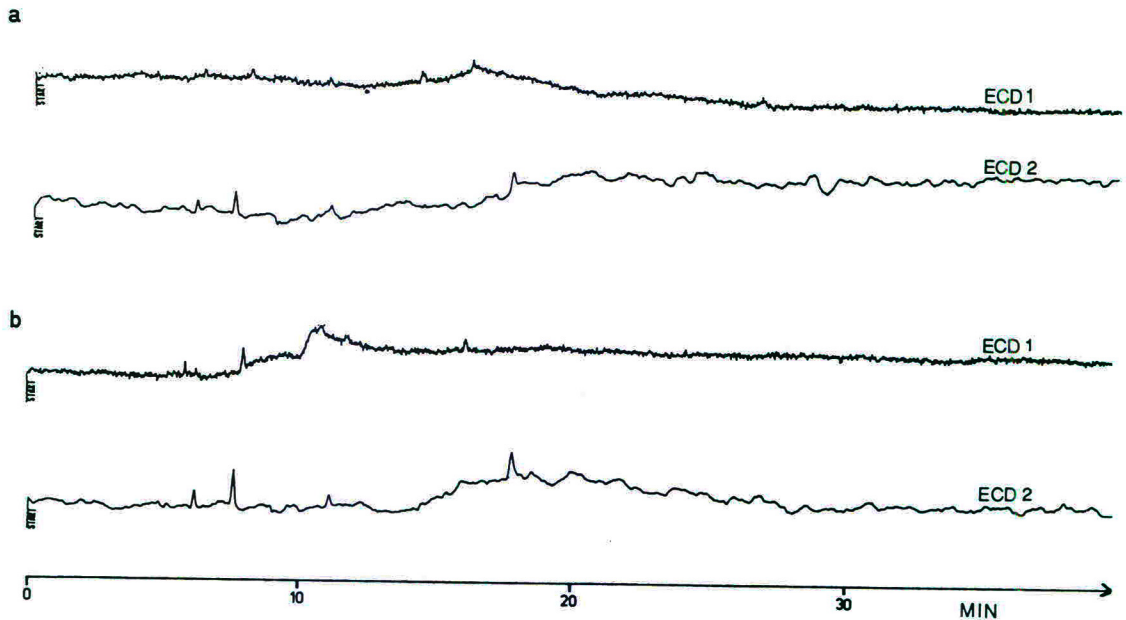


Fig. 5. System blanks: (a) 100 ml nitrogen carrier gas and (b) 100 ml nitrogen purge gas, with the same conditions as for Fig. 4.

Maintenance of the trap at ambient temperature during the concentration procedure was a key requirement for this work, thereby avoiding the need for expensive liquid nitrogen supply. Desorption on to the capillary column from the one-stage multibed trap was facilitated, under

carrier gas flow reversion, using direct ohmic heating. Subambient temperature programming for the GC was also unnecessary. Investigations using oxygen doped ECD to enhance the response of certain halocarbons, which react feebly with thermal electrons, were successfully made

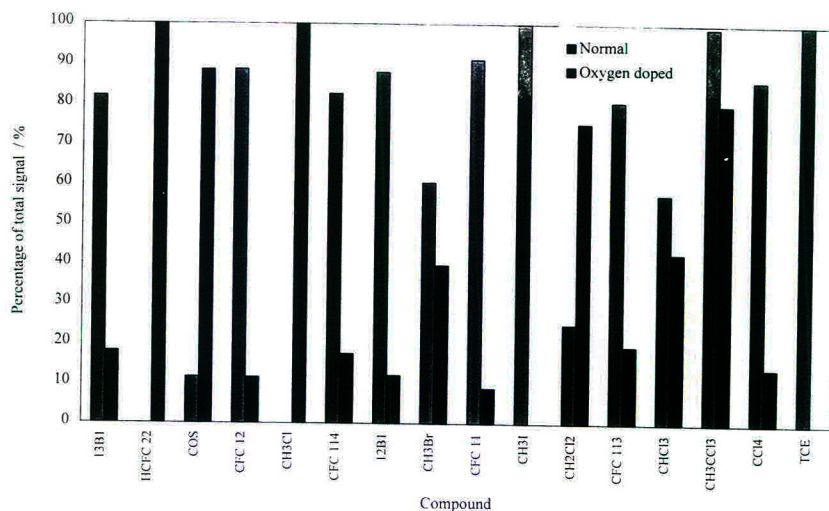


Fig. 6. Percentage compound response for the normal ECD and oxygen doped ECD in series.

with selection of operating parameters such as the required oxygen concentration for sufficient compound response enhancement, detector temperature and cell current. The use of two ECD instruments in series allowed simultaneous determination of the CFCs and oxygen-enhanced compounds from an air sample in a single analysis. The method has wider application, in addition to the group of compounds in this study, to atmospheric analysis.

## References

- [1] D.M. Cunnold, P.J. Fraser, R.F. Weiss, P.G. Simmonds, B.R. Miller, F.N. Alyea and A.J. Crawford, *J. Geophys. Res.*, 99 (1994) 1107–1126.
- [2] D.A. Fisher and P.M. Midgley, *Atmos. Environ.*, 27 (1993) 271–276.
- [3] J.W. Elkins, T.M. Thompson, T.H. Swanson, J.H. Butler, B.D. Hall, S.O. Cummings, D.A. Fisher and A.G. Raffo, *Nature*, 364 (1993) 780–783.
- [4] S.A. Montzka, R.C. Myers, J.H. Butler, J.W. Elkins and S.O. Cummings, *Geophys. Res. Lett.*, 20 (1993) 703–706.
- [5] P.M. Midgley and D.A. Fisher, *Atmos. Environ.*, 27 (1993) 2215–2223.
- [6] R.A. Rasmussen, M.A.K. Khalil, S.A. Penkett and N.J.D. Prosser, *Geophys. Res. Lett.*, 7 (1980) 809–812.
- [7] E.P. Grimsrud and R.A. Rasmussen, *Atmos. Environ.*, 9 (1975) 1010–1014.
- [8] J.E. Lovelock, *Nature*, 256 (1975) 193–194.
- [9] R.A. Rasmussen, I.E. Rasmussen, M.A.K. Khalil and R.W. Dalluge, *J. Geophys. Res.*, (1980) 7350–7356.
- [10] M.A.K. Khalil, R.A. Rasmussen and S.D. Hoyt, *Tellus*, 35 (1983) 266–274.
- [11] S. Solomon and D.L. Albritton, *Nature*, 357 (1992) 33–37.
- [12] K.K. Tung, M.K.W. Ko, J.M. Rodriguez and N. Dak Sze, *Nature*, 322 (1986) 811–814.
- [13] S. Mario and M.O. Andreae, *Science*, 263 (1994) 1255–1257.
- [14] J.H. Butler, *Geophys. Res. Lett.*, 21 (1994) 185–188.
- [15] S. Lal, R. Borchers, P. Fabian and B.C. Krüger, *Nature*, 316 (1985) 135–136.
- [16] J.H. Butler, J.W. Elkins, B.D. Hall, S.O. Cummings and S.A. Montzka, *Nature*, 359 (1992) 403–405.
- [17] L.E. Heidt, R. Lueb, W. Pollock and D.H. Enhalt, *Geophys. Res. Lett.*, 2 (1975) 445–454.
- [18] S.J. O'Doherty, P.G. Simmonds, G. Nickless, *J. Chromatogr.*, 657 (1993) 123–129.
- [19] E.P. Grimsrud and D.A. Miller, *Anal. Chem.*, 50 (1978) 1141–1145.
- [20] J.A. Campbell and E.P. Grimsrud, *J. Chromatogr.*, 243 (1982) 1–8.
- [21] E.P. Grimsrud and R.G. Stebbins, *J. Chromatogr.*, 155 (1978) 19–34.
- [22] P.G. Simmonds, *J. Chromatogr.*, 166 (1978) 593–598.
- [23] S.J. O'Doherty, P.G. Simmonds, G. Nickless and W.R. Betz, *J. Chromatogr.*, 630 (1993) 265–274.
- [24] G.A. Sturrock, P.G. Simmonds, G. Nickless and D. Zwiép, *J. Chromatogr.*, 648 (1993) 423–431.
- [25] P.G. Simmonds, S.J. O'Doherty, G. Nickless, G.A. Sturrock, R. Swaby, P. Knight, J. Ricketts, G. Woffendin and R. Smith, *Anal. Chem.*, (1995) in press.
- [26] W.T. Sturges and J.W. Elkins, *J. Chromatogr.*, 642 (1993) 123–134.







ELSEVIER

Journal of Chromatography A, 707 (1995) 267–281

JOURNAL OF  
CHROMATOGRAPHY A

# Endogenous alkaloids in man XXI.<sup>☆</sup> Analysis of glyoxylate-derived 1,3-thiazolidines and their precursors after trimethylsilylation by gas chromatography–mass spectrometry

Gerhard Bringmann\*, Christiana Hesselmann, Doris Feineis

*Institute of Organic Chemistry, University of Würzburg, Am Hubland, D-97074 Würzburg, Germany*

First received 23 November 1995; revised manuscript received 3 March 1995; accepted 7 March 1995

## Abstract

A gas chromatographic procedure was developed for the simultaneous analysis of glyoxylate-derived 1,3-thiazolidines and their precursors, such as L-cysteine, cysteamine, and D-(–)-penicillamine as well as the toxic glyoxylic acid. The assay involves conversion of these highly polar compounds to volatile trimethylsilyl (TMS) derivatives, chromatography on a polar fused-silica capillary column, and determination using flame-ionization detection or electron-impact ionization mass spectrometry. On the base of this analytical device, the resolution of the diastereomeric pairs of 1,3-thiazolidine-2,4-dicarboxylic acids was achieved. Based upon the observation that no epimerization occurs during the silylation procedure, for the first time a reliable method was established for the determination of the diastereomeric ratio of such alkaloid-type heterocycles on a trace scale. Furthermore, studies concerning thiazolidine formation under derivatization conditions in the presence of the precursors glyoxylic acid and D-(–)-penicillamine are described.

## 1. Introduction

Primary hyperoxaluria (HOU) type I is a rare, but severe and hitherto incurable inherited disease [2,3]. Its toxic principle, an overproduction of oxalic acid, followed by an accumulation of calcium oxalate, is the result of an enzymatic block in the degradation pathway of glyoxylic acid (**1**). This highly reactive aldehyde is the most important metabolic precursor to oxalic acid, which itself cannot be detoxified further in humans [4]. Due to the low solubility of calcium

oxalate, hyperoxaluria is characterized by serious pathological symptoms, such as urolithiasis, nephrocalcinosis, and, in severe cases, systemic as well as cerebral oxalosis. Most of the patients die from chronic renal failure in early adulthood [2,3]. But also exogenous factors, such as ethylene glycol intoxications by accident or suicide [5,6] as well as medicinally indicated therapies [7–9] cause an extreme increase in glyoxylate or oxalate concentration in the living organism. The consequences thereof are atrocious: severe central nervous system dysfunctions were observed upon treatment with glycine during transurethral surgery [7] or after post-operative administration of xylitol as an intravenous nutrient [8,9].

\* Corresponding author.

<sup>☆</sup> For part XX, see Ref. [1].

Chemical deactivation of the toxin glyoxylic acid (**1**) by therapeutical administration of sulphur-containing binucleophilic amino acids or biogenic amines, leading to thiazolidine formation (see Fig. 1), is the key step of a therapeutical concept for the treatment of glyoxylate-induced oxalurias recently developed [10–14]. The realization of such a novel, still speculative approach requires the study of the metabolic “fate” of such chemical detoxication products, and thus the elaboration of an efficient analytical procedure.

This becomes evident from apparently contradictory results described in the literature for two possible glyoxylate scavengers. Thus, studies by Hamilton et al. [15–17] show that L-cysteine (**2**) and cysteamine (**3**) indeed spontaneously condense in vivo, leading to the thiazolidines **5a**, **5b** and **6**, respectively (see Fig. 1). These heterocycles, however, are subsequently metabolized by the organism, ultimately resulting in the undesired formation of oxalic acid as final product. By contrast, an Australian group [18,19] treated rats with daily doses of L-cysteine i.p., with a simultaneous addition of ethylene glycol

to the drinking water, and found a distinct decrease in the excretion of oxalic acid. This reduction, which was explained by a possible formation of the thiazolidine **5**, was significant compared with control animals without a cysteine treatment.

Our concept [10–14] favours the non-natural amino acid D-(–)-penicillamine (**4**) as a scavenger for glyoxylic acid (**1**), since it does not undergo an extensive metabolism [20], and thus stays available for an in vivo cyclocondensation with **1** for a longer time. Meanwhile, we could demonstrate that the 1,3-thiazolidine-2,4-dicarboxylic acids **7a** and **7b** as resulting from this rapid and spontaneous condensation reaction (see Fig. 1), are extremely hydrophilic. First animals studies revealed their excellent physiological compatibility. Furthermore, the calcium thiazolidine dicarboxylate **Ca-7a** exhibits a high solubility,  $1.8 \cdot 10^4$  times larger than that of calcium oxalate [12].

From the above-mentioned results it becomes evident that with respect to a possible therapeutic application of such scavenging reactions as presented in Fig. 1, a detailed knowledge of

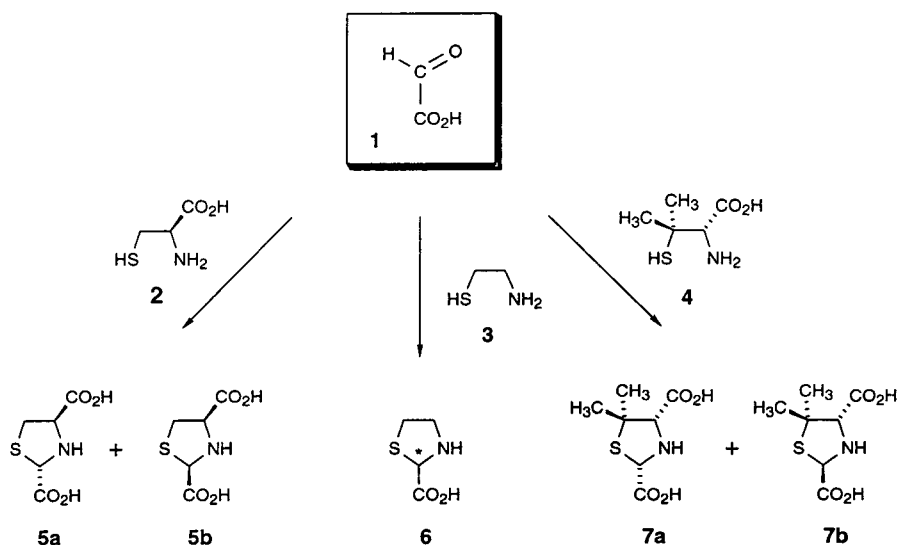


Fig. 1. Formation of the glyoxylate-derived 1,3-thiazolidines **5a/5b**, **6**, and **7a/7b** by condensation with L-cysteine (**2**), cysteamine (**3**), and D-(–)-penicillamine (**4**), respectively.

optimum condensation conditions, of the reaction course, and the epimerization behaviour of the thiazolidines **5a** and **5b** as well as **7a** and **7b** is indispensable. In this connection, especially investigations concerning the *in vivo* fate of these heterocycles are of great importance, too. This, however, requires the availability of appropriate analytical procedures that allow the unambiguous identification of these compounds even in low, biologically relevant concentrations.

TLC [21] and HPLC [22] analytical as well as spectroscopic [23] methods, as well as our own investigations [24] aiming at a direct detection of carboxy-substituted 1,3-thiazolidines show that, apparently because of their highly hydrophilic and their amphoteric character, these compounds are not easily accessible to a direct analysis. On the base of ion-pair assisted reversed-phase chromatography, we have developed an analytical device that allows, for the first time, the resolution of the highly functionalized diastereomeric 1,3-thiazolidine-2,4-dicarboxylic acids **5a** and **5b**, respectively **7a** and **7b**. Due to the absence of a characteristic UV chromophore and the low-intensity UV maximum, which is located almost exactly at the UV cut-off of the utilized solvents, application of this HPLC method is restricted to samples containing amounts of **5**, **6**, and **7** that are significantly above the trace range [24,25]. By contrast, derivatization of the thiazolidines with fluorescence reagents, e.g. dansyl chloride or 9-fluorenylmethyl chloroformate, leads to an enhanced sensitivity, allowing the separation and detection of the heterocycles **5**, **6**, and **7** by HPLC even from biological matrices. With respect to the required diastereomeric analysis, however, these reactions are most disappointing, because, probably due to steric reasons, only the *cis*-thiazolidines **5a** and **7a** react [25,26].

In this paper, we present a gas chromatographic analytic device, which, after trimethylsilylation, allows the separation of all the starting materials (**1**, **2**, **3**, and **4**) and products (**5a**, **5b**, **6**, and **7a**, **7b**) of the scavenging reactions as relevant for our therapeutical concept. Furthermore, it permits a direct physical identification on the base of mass spectrometry.

## 2. Experimental

### 2.1. Chemicals

Glyoxylic acid monohydrate was purchased from Merck (Darmstadt, Germany). Cysteamine hydrochloride and L-cysteine were obtained from Fluka (Buchs, Switzerland), whereas D-(–)-penicillamine was a generous gift from Degussa (Hanau, Germany). The derivatizing reagent *N*-methyl-trimethylsilyl-trifluoroacetamide (MSTFA) was supplied from Macherey and Nagel (Düren, Germany). All reagents and solvents used were of analytical grade quality. High-purity Milli-Q water (Millipore, Bedford, MA, USA) was used throughout.

### 2.2. Syntheses

The thiazolidines **5**, **6**, and **7** were synthesized according to procedures already published [27–30], and described in a previous paper [24]. The structures of the diastereomeric products **7a** and **7b** were unequivocally established by spectroscopic [31] and by X-ray crystallographic methods [31–33].

### 2.3. Gas chromatography

Gas chromatography was performed on a Model HRGC 5160 Mega gas chromatograph equipped with a split-splitless injector and a flame-ionization detector (FID) (Carlo Erba Instruments, Milan, Italy). The analyses were carried out on a DB 225 fused-silica capillary column (J&W Scientific, Folsom, CA, USA) with 0.25  $\mu\text{m}$  film thickness (30 m  $\times$  0.32 mm I.D.). Helium was used as the carrier gas at a column head pressure of 80 kPa. The samples were introduced into the capillary column using the split injection mode at a split ratio of 1:60. The injection port and the detector were both maintained at 220°C. The column oven temperature was initially set at 100°C for 3 min, then programmed at 10°C/min to 220°C, then held for 5 min. The chromatograms were recorded and processed by computer-aided methods using Maxima evaluation software 820 (Millipore, Ven-

tura, CA, USA) in combination with a Maxima system Interface I-200.

#### 2.4. Mass spectrometry

For mass spectral identification of TMS derivatives of the amino thiols, glyoxylic acid, and the glyoxylate-derived thiazolidines, a Varian Model 3700 gas chromatograph (Varian Instruments, Sunnyvale, CA, USA) coupled with a Finnigan MAT Model 8200 mass spectrometer (Finnigan MAT, San Jose, CA, USA) was used. All experimental work was done on a DB 17 fused-silica capillary column (J&W Scientific, Folsom, CA, USA) with 0.25  $\mu\text{m}$  film thickness (30 m  $\times$  0.32 mm I.D.) using helium as the carrier gas. For the separation, the same temperature program as described above was applied. Electron-impact (EI) mass spectra were recorded at 70 eV and a helium carrier gas head pressure of 80 kPa. Operations in the chemical ionization (CI) mode were performed with isobutane as the reagent gas at a similar carrier gas head pressure, but the ion source pressure was increased by admitting isobutane via a separate capillary inlet (reagent gas pressure 0.3 mbar). The temperature of the transfer line was maintained at 250°C. The ion source temperature was set at 220°C in the EI mode (respectively 140°C in the CI mode). The emission current was 1 mA in the EI mode and 0.05 mA in the CI mode, respectively. The electron multiplier voltage was set at 3000 V. Full mass spectra (EI mode 35–550 amu, CI mode 60–600 amu) were recorded every 0.7 s over the entire elution profile.

#### 2.5. Derivatization

##### *Dimethylester derivatives*

For esterification the thiazolidine **7** (**7a/7b** = 28:72) was dissolved in an ether solution of diazomethane [33] and stirred at room temperature for 12 h. After removal of the solvent in vacuo, the residue was chromatographed on silica gel with ether–petroleum ether (1:1) as an eluent to give the diastereomeric esters **8a** and **8b** as well as the *N*-methylated compounds **9a** and **9b**, respectively [31]. For GC analysis, the

isolated pure dimethylester derivatives as well as aliquots of the reaction mixture were used. From a series of experiments with pure **7a** or mixtures **7a/7b** of different diastereomeric ratios, it could be deduced that **7a** gives rise to **8a** and **9a**, exclusively, whereas **7b** specifically delivers the esters **8b** and **9b**.

##### *Trimethylsilyl (TMS) ester derivatives*

The thiazolidines **5a**, **5b**, **6**, **7a** and **7b** as well as their precursors **1**, **2**, **3** and **4** can be derivatized by silylation reagents. Derivatives are formed by the exchange of the active hydrogens of amino or acid functions by trimethylsilyl groups. For the formation of TMS ester derivatives, the reaction procedure was as follows. An aliquot of a standard solution was placed in a screw-cap vial and evaporated to dryness. The dry residue was dissolved in 100  $\mu\text{l}$  of MSTFA and the derivatization reaction was allowed to proceed at 80°C for 10 min. A 2- $\mu\text{l}$  volume of this solution was directly injected onto the gas chromatograph.

#### 2.6. Calibration graphs, reproducibility and linearity

For an examination of the reproducibility and linearity of the described silylation technique with MSTFA, as obtained by gas chromatographic analysis of the resulting TMS derivatives with flame-ionization detection, analysis functions  $m = f(R)$ , where  $m$  is the mass of the analyte and  $R$  is the detector response, were determined for the thiazolidines **5a/5b**, **6**, **7a/7b** and for the precursors **1** and **4**.

Stock solutions of the thiazolidines **5**, **6**, and **7** were prepared by dissolving 10.04 mg of **5** (**5a/5b** = 46:54) in 1 ml of 2 M HCl, 5.27 mg of **6** in 1 ml of methanol, and 20.34 mg of **7** (**7a/7b** = 37:63) in 2 ml of Milli-Q-water. Various aliquots of the undiluted (for **5** and **6**: 20, 40, 60  $\mu\text{l}$ ; for **7**: 30  $\mu\text{l}$ ) and of the ten-fold diluted stock solution (for **5** and **6**: 20, 40, 60, 80, 100  $\mu\text{l}$ ; for **7**: 20, 40, 70, 100  $\mu\text{l}$ ), respectively, were pipetted into Wheaton-V vials and evaporated to dryness. For the generation of data for calibration graphs, 2  $\mu\text{l}$  of these solutions were injected onto the GC

system mentioned above, after derivatization with 100  $\mu\text{l}$  of MSTFA.

For the aldehyde carboxylic acid **1** and the amino thiol **4**, respectively, six-point calibration graphs were generated by analyzing standard solutions silylated in the same way as described above. Stock solutions of **1** and **4** were prepared in Milli-Q water at concentrations of 5.3 mg/ml (solution of **1**) and 5.05 mg/ml (solution of **4**). For the calibration of the two substances, aliquots of the undiluted (30 and 50  $\mu\text{l}$ ) and of the ten-fold diluted stock solutions (20, 40, 70, and 100  $\mu\text{l}$ ) were used.

In each instance, calibration curves were constructed by plotting the integrated peak area against the corresponding standard concentration of the compounds **1**, **4**, **5a**, **5b**, **6**, **7a**, and **7b**. For all these substances, a linear correlation between the injected mass and the detector response was stated over the whole concentration range, with correlation coefficient  $r > 0.98$ .

### 2.7. Determination of the diastereomeric ratio of **7a/7b**

In order to compare the diastereomeric ratio of **7a/7b**, as determined by  $^1\text{H}$  NMR spectroscopy with those obtained by gas chromatography of the TMS derivatives **10a/10b**, samples containing only the *cis*-thiazolidine **7a** as well as mixtures of **7a** and **7b** were analyzed. For all measurements ( $^1\text{H}$  NMR, GC), pyridine was used as the solvent to guarantee epimerization-free conditions.

For the determination of the *cis/trans* ratio of mixtures of **7a** and **7b**, two series of tests were carried out. Stock solutions of the thiazolidine **7** were prepared by dissolving 10.04 mg (**7a/7b** = 50:50; solution A) and 6.43 mg (**7a/7b** = 29:71; solution B) in 1 ml of pyridine. Aliquots of the undiluted [60  $\mu\text{l}$  (S 1), 40  $\mu\text{l}$  (S 2), and 20  $\mu\text{l}$  (S 3)] and of the ten-fold diluted stock solution A [100  $\mu\text{l}$  (S 4), 60  $\mu\text{l}$  (S 5), and 40  $\mu\text{l}$  (S 6)] were evaporated to dryness. After derivatization with 100  $\mu\text{l}$  of MSTFA, the diastereomeric ratio was determined by GC analysis. Volumes of 100  $\mu\text{l}$  (S 7), 80  $\mu\text{l}$  (S 8), and 60  $\mu\text{l}$  (S 9) of the stock

solution B were treated in the same way as described above.

Silylation of the pure *cis*-thiazolidine **7a** yielded only one peak for the corresponding TMS derivative **10a**. Samples containing an aliquot of 100  $\mu\text{l}$  (S 10) and 50  $\mu\text{l}$  (S 11) of a solution of 4.46 mg of **7a** in 1 ml of pyridine were used for GC analysis (see Table 3).

### 2.8. Condensation reaction of glyoxylic acid (**1**) and *D*-(-)-penicillamine (**4**) under silylation conditions

In order to determine the reliability of the derivatization procedure of **7** in the presence of the thiazolidine precursors **1** and **4**, we analyzed six samples concerning the formation of the heterocycles **7a** and **7b** under silylation conditions. The samples were prepared as follows. A volume of 20  $\mu\text{l}$  of a solution of 10.12 mg of glyoxylic acid (**1**) in 2 ml of Milli-Q water was pipetted into a Wheaton-V vial and cooled down to  $-196^\circ\text{C}$ . To this frozen sample an aliquot of 20  $\mu\text{l}$  of a solution of 10.10 mg of *D*-(-)-penicillamine (**4**) in 2 ml of Milli-Q water was added and immediately frozen at  $-196^\circ\text{C}$ . After lyophilization, the dry residue was dissolved in 100  $\mu\text{l}$  of MSTFA. For derivatization, the sample solution was heated at  $80^\circ\text{C}$  for 10 min and the reaction mixture was subsequently analyzed by GC-FID and GC-MS, respectively.

In the chromatograms of these samples a hitherto not detected reaction product appeared, besides the well known bis-trimethylsilyl esters **10a**, **10b** as well as the additionally *N*-derivatized TMS compound **11**. Based upon GC-MS analysis, this new peak was interpreted as the silylated thiazolidine derivatives **20/21** (see Fig. 5) because of the following mass fragmentation pattern: GC-MS (70 ev):  $m/z$  (%) = 496 (3.9)  $[\text{M} - \text{CH}_3]^+$ , 468 (0.6)  $[\text{M} - \text{CO} - \text{CH}_3]^+$ , 421 (0.8)  $[\text{M} - \text{HOSi}(\text{CH}_3)_3]^+$ , 406 (2.5)  $[\text{M} - \text{HOSi}(\text{CH}_3)_3 - \text{Si}(\text{CH}_3)_3]^+$ , 394 (6.4)  $[\text{M} - \text{CO}_2\text{Si}(\text{CH}_3)_3]^+$ , 350 (2)  $[\text{M} - \text{CO}_2\text{Si}(\text{CH}_3)_3 - \text{CO}_2]^+$ , 292 (43)  $[\text{C}_{11}\text{H}_{26}\text{NO}_2\text{SSi}_2]^+$ , 219 (100)  $[\text{C}_{11}\text{H}_{26}\text{NO}_2\text{SSi} - \text{Si}(\text{CH}_3)_3]^+$ , 147 (32) (see also Section 3.7).

Quantitation of the amounts of starting material (**1** and **4**, respectively) and resulting products (**7a** and **7b**, respectively) was achieved by external calibration (for calibration graphs see Section 2.6). Estimation of the amount of the compounds **20/21** detected in these experiments in addition to the usually formed thiazolidine TMS derivatives **10a/10b** and **11** was done by use of the calibration graph of the *cis*-thiazolidine **7a** (see Fig. 6).

### 3. Results and discussion

For the investigation of each of the condensation reactions of glyoxylic acid (**1**) as presented in Fig. 1, the elaboration of a GC analytical device for the identification of all the starting materials and products was the first crucial task to be fulfilled. Thus, we aimed at the development of a derivatization procedure simultaneously suited for the aldehyde **1** and for the binucleophiles **2**, **3**, and **4** as well as for the thiazolidines **5a/5b**, **6**, and **7a/7b**. For this purpose, we primarily tested conventional methods like methylation with diazomethane [35,36], and silylation with commercially available reagents, such as *N*-methyl-trimethylsilyl-trifluoroacetamide (MSTFA) or bis-trimethylsilyl-trifluoroacetamide (BSTFA) [37–40].

#### 3.1. Methylation

From the point of view of such a required uniform derivatization procedure for all the compounds to be analyzed, the methylation turned out to be unsatisfying: upon attempted esterification of the thiazolidines **7a** and **7b** with diazomethane, in each case two reaction products per thiazolidine were formed, namely the desired thiazolidine dicarboxylic esters **8a** and **8b**, giving yields of 60–70%, yet along with the *N*-methyl-thiazolidines **9a** and **9b** (ca. 30–40%) [31]. Although the methyl esters **8a**, **8b**, **9a**, and **9b** can efficiently be separated by gas chromatography on a polar DB 225 capillary column (see Fig. 2), a further use of this derivatization reaction did not seem rewarding, all the more as

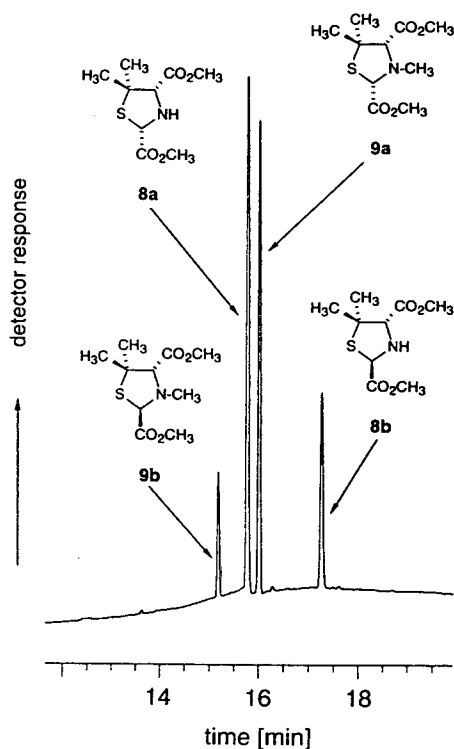


Fig. 2. Gas chromatographic analysis of the dimethyl ester derivatives **8a**, **8b**, **9a** and **9b** resulting from esterification of the penicillamine-derived thiazolidines **7a** and **7b** (*cis/trans* ratio 28:72) with diazomethane. GC separation was done on a DB 225 capillary column. For determination flame-ionization detection was used. Detailed synthetic procedures and chromatographic conditions are described in Section 2.

it is known from the literature [41] that also glyoxylic acid (**1**), on reaction with diazomethane, gives up to four reaction products.

#### 3.2. Trimethylsilylation

By contrast, the goal of a generally applicable analysis should be the unambiguous derivatization to give only one single product, thus allowing a maximum of sensitivity. For this purpose, the transformation of the thiazolidines and their precursors into volatile trimethylsilyl (TMS) derivatives, using *N*-methyl-trimethylsilyl-trifluoroacetamide (MSTFA), seemed much more promising.

Of predominant interest was the analysis of the heterocycles **5a/5b**, **6**, and **7a/7b**. Thus, using a large excess of MSTFA, the dicarboxy-substituted thiazolidines **5** and **7** can each be reproducibly transformed at 80°C and a reaction time of 10 min, into a single volatile derivative. After significantly longer reaction times or in the case of retarded analysis, two additional peaks were observed in the chromatogram for the penicillamine-derived thiazolidines **7**, and one further product for the cysteine-derived heterocycles **5**, albeit to a small degree (<3%) in both cases.

For the cysteamine-derived thiazolidine **6**, which was treated with MSTFA under identical conditions, an immediate analysis frequently showed the presence of still two reaction products, one of which, however, was further converted in favour of the second one in course of the time.

### 3.3. Identification of the TMS derivatives by mass spectrometry

Mass spectroscopic investigations concerning the derivatization reaction of the penicillamine-derived heterocycles **7a/7b** as well as the cysteine-derived compounds **5a/b** with MSTFA revealed the main products of these two-fold carboxy-substituted thiazolidines to be the bis-trimethylsilyl esters **10a/10b** respectively **13a/13b**, whereas the side-products turned out to be the additionally *N*-derivatized trimethylsilyl esters **11** respectively **14** (see Fig. 3). In the case of the cysteamine-derived thiazolidine carboxylic acid **6**, the *N,O*-bis-derivatized compound **16** was the main product of the silylation reaction (see Fig. 3). The initially formed side-product (see Section 3.2) could not be elucidated by mass spectrometry.

Apparently, the high steric demand of the bulky trimethylsilyl group is responsible for the observed product selectivity in the trimethylsilylation of the 2,4-dicarboxy-substituted thiazolidines, compared with the introduction of the distinctly smaller methyl group using diazomethane.

Fortunately, the mass spectrometric analysis

using the electron-impact (EI) ionization mode showed a characteristic fragmentation pattern for the TMS derivatives **10a/10b**, **13a/13b**, and **16** (see Table 1). Thus, in all cases, the base peak (100%) of the obtained mass spectra was the  $[M - \text{COOSi}(\text{CH}_3)_3]^{++}$  peak, which can be used as leading fragment for the compound, even in a complex environment. As an indicator for the entire molecular mass, the  $[M - 15]^{++}$  and the  $[M - 43]^{++}$  peaks have to be used, since the  $[M]^{++}$  peak itself could be identified only in one single case. Characteristic for the thiazolidine system and thus independent from the silylation degree are those peaks that result from a loss of the whole functionality, i.e. signals at  $m/z$  114 for the penicillamine-derived heterocycles **7a/7b**, and  $m/z$  86 for the cysteine- as well as the cysteamine-derived thiazolidines **5a/5b** and **6**.

With the chemical ionization (CI) as a mild ionization technique, the  $[\text{MH}]^+$  ion is obtained as the base peak, thus delivering unambiguous information on the molecular mass. As already described above for the EI spectra of the TMS derivatives **10a/10b**, **13a/13b**, and **16**, also in the CI mode mass fragments were observed hinting at the loss of a methyl group  $[\text{MH}^+ - 16]$  respectively originating from a formal elimination of a trimethylsilylated carboxyl function  $[\text{MH}^+ - 118]$  (see also Table 2).

In Fig. 4 the EI and CI mass spectra, respectively, of the TMS derivative **10a** are given with the fragmentation pattern as typical for silylated thiazolidine ring systems. Table 1 (EI) and Table 2 (CI) show the characteristic mass spectroscopic data of all the glyoxylate-derived thiazolidines investigated here.

Similarly unambiguous and already described in the literature [42] is the trimethylsilylation of the amino acids L-cysteine (**2**) and D-(–)-penicillamine (**4**). This led to the formation of only one derivative each, which were identified to be the *N,O,S*-tris-trimethylsilylated compounds **15** and **12** (see Fig. 3) according to electron-impact mass spectrometric analysis. Again, the characteristic  $[M - \text{COOSi}(\text{CH}_3)_3]^{++}$  signals were used for the identification.

By contrast, the detection of the biogenic amine cysteamine (**3**) required further optimi-

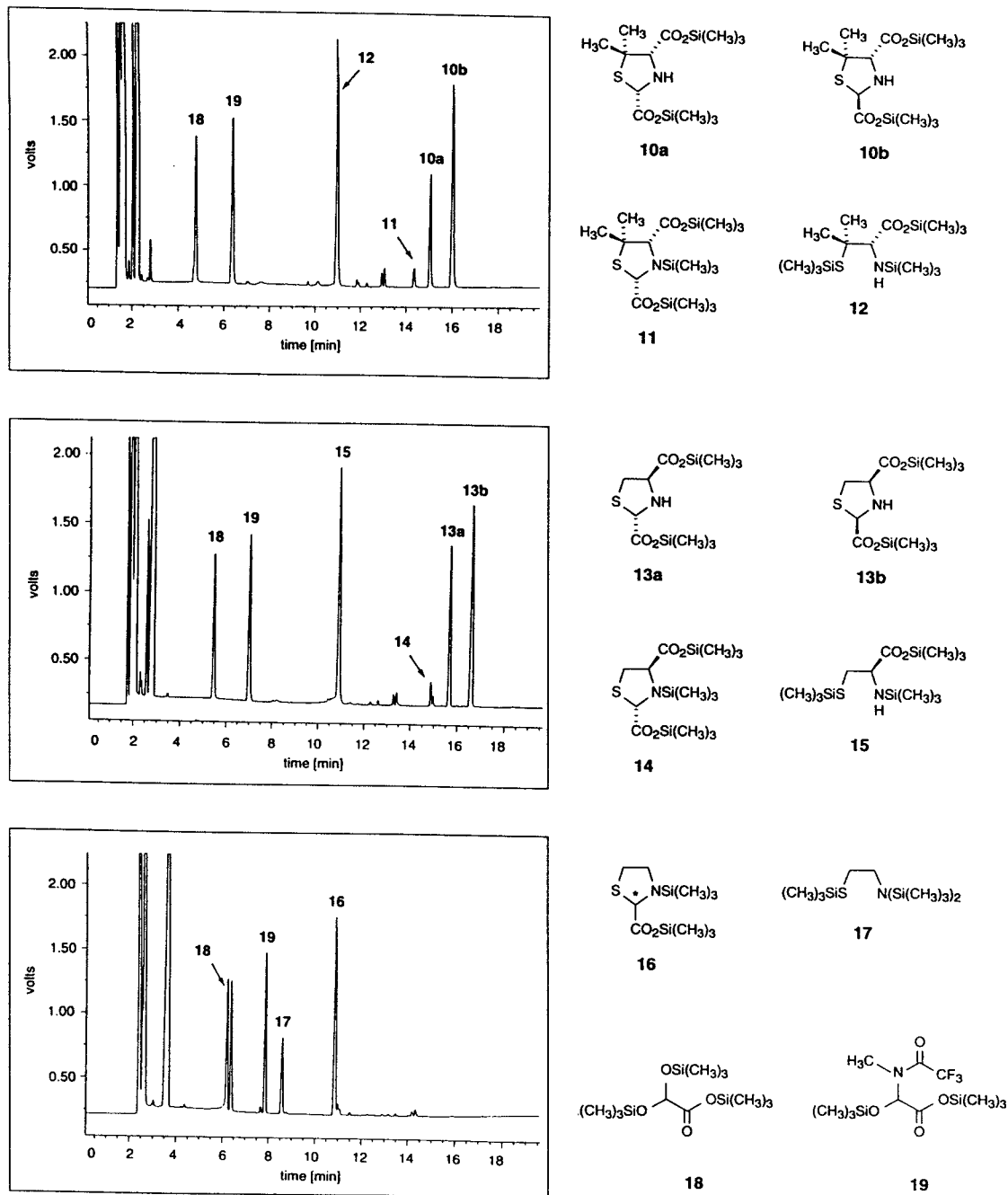


Fig. 3. Gas chromatographic analysis of the glyoxylate-derived thiazolidines **5a/5b**, **6** and **7a/7b** as well as their precursors **1**, **2**, **3** and **4**, after trimethylsilylation with MSTFA. GC separation of the resulting TMS derivatives (the inset formulas show their structures) was done on a DB 225 capillary column using flame-ionization detection for determination. For detailed derivatization and chromatographic conditions see Section 2.



Table 1

Electron-impact (70 eV) mass fragmentation pattern of the TMS derivatives **10a**, **10b**, **11**, **13a**, **13b**, **14** and **16** of glyoxylate-derived thiazolidines

Compound	[M] <sup>++</sup>	[M - 15] <sup>++</sup>	[M - 43] <sup>++</sup>	[M - 117] <sup>++</sup>	[M - 234] <sup>++</sup>	[M - 307] <sup>++</sup>
<b>10a</b>	–	334 (10)	–	232 (100)	114 (25)	–
<b>10b</b>	–	334 (5)	–	232 (100)	114 (41)	–
<b>11</b>	421 (1)	406 (2)	378 (4)	304 (100)	–	114 (18)
<b>13a</b>	–	306 (4)	278 (1)	204 (100)	86 (52)	–
<b>13b</b>	–	306 (6)	278 (1)	204 (100)	86 (27)	–
<b>14</b>	–	378 (3)	350 (4)	276 (100)	–	86 (3)
<b>16</b>	–	262 (2)	234 (2)	160 (100)	–	–

Formal fragments: 117 = COOSi(CH<sub>3</sub>)<sub>3</sub>; 234 = 2COOSi(CH<sub>3</sub>)<sub>3</sub>; 307 = 2COOSi(CH<sub>3</sub>)<sub>3</sub> + Si(CH<sub>3</sub>)<sub>3</sub>. Numbers in parenthesis represent relative intensities.

zation. As for the glyoxylate-derived compound **6**, also in this case initially two silylation products were found. In the presence of active silylation reagent, one of these products, probably an incompletely silylated compound, which could not fully be elucidated structurally, was transformed into the other derivative, identified as **17** by mass spectrometry (EI mode). The molecular mass of the TMS compound **17** was deduced from the mass peak *m/z* 278 [M - 15]<sup>+</sup> resulting from the loss of a methyl group of a TMS unit, a decomposition process typical for TMS derivatives [43].

For the reaction of aldehydes with MSTFA the formation of addition products has been described [44]. Thus, for the trimethylsilylation of the aldehyde glyoxylic acid (**1**), the formation of two products had to be taken into account that

should not be further convertible: **18**, the silylated hydrate of the aldehyde function, and **19**, the silylated product of an addition of the *N*-nucleophile *N*-methyl-trifluoroacetamide to the carbonyl group.

In the GC and MS analysis of silylation reactions of glyoxylic acid (**1**), indeed both the completely silylated product **18** and the substitution product **19** could be identified (see Fig. 3).

### 3.4. Gas chromatographic separation

Due to the formation of two different TMS derivatives, the detection sensitivity for glyoxylic acid (**1**) was diminished down to a factor of approximately 50%. With respect to the uniform derivatization procedure that is also easy to handle for all the precursors and products of the

Table 2

Chemical ionization (reagent gas: isobutane) mass fragmentation pattern of the TMS derivatives **10a**, **10b**, **11**, **13a**, **13b**, **14** and **16** of glyoxylate-derived thiazolidines

Compound	[M + 57] <sup>+</sup>	[M + 43] <sup>+</sup>	MH <sup>+</sup>	MH <sup>+</sup> - 16	MH <sup>+</sup> - 74	MH <sup>+</sup> - 118	MH <sup>+</sup> - 190	MH <sup>+</sup> - 235
<b>10a</b>	406 (5)	392 (7)	350 (100)	334 (4)	276 (2)	232 (38)	–	114 (6)
<b>10b</b>	406 (3)	392 (5)	350 (100)	334 (3)	276 (2)	232 (36)	–	114 (5)
<b>11</b>	–	–	422 (100)	406 (5)	348 (39)	304 (58)	232 (22)	–
<b>13a</b>	378 (8)	364 (5)	322 (100)	306 (10)	248 (4)	204 (45)	–	87 (7)
<b>13b</b>	378 (8)	364 (6)	322 (100)	306 (9)	248 (3)	204 (40)	–	87 (5)
<b>14</b>	–	–	394 (100)	378 (6)	320 (46)	276 (63)	204 (18)	–
<b>16</b>	334 (9)	320 (6)	278 (100)	262 (5)	–	160 (49)	–	–

Formal fragments: 74 = Si(CH<sub>3</sub>)<sub>3</sub> + H; 118 = COOSi(CH<sub>3</sub>)<sub>3</sub> + H; 235 = 2COOSi(CH<sub>3</sub>)<sub>3</sub> + H; 190 = COOSi(CH<sub>3</sub>)<sub>3</sub> + Si(CH<sub>3</sub>)<sub>3</sub>. Numbers in parenthesis represent relative intensities.

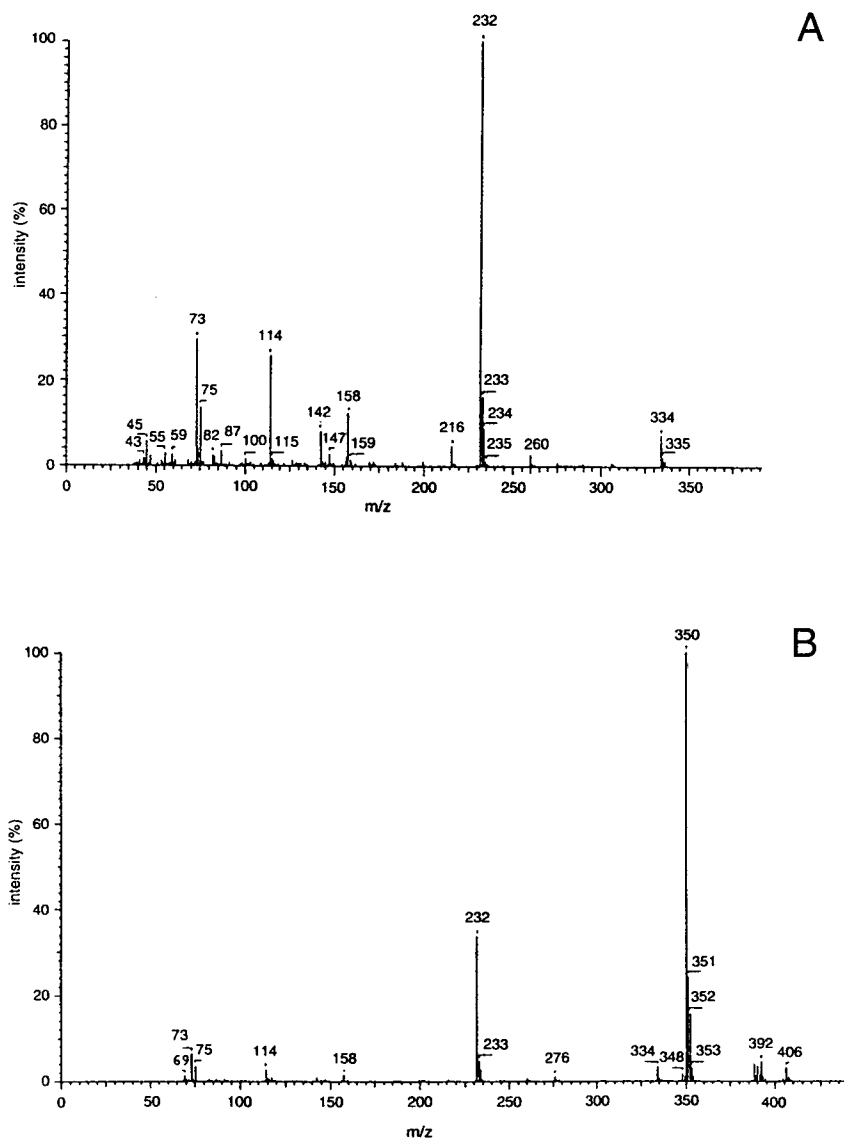


Fig. 4. GC-MS analysis of the trimethylsilylated derivative of the thiazolidine **7a**. The figure shows the EI (A) and CI (B) mass spectra of the TMS derivative **10a** yielded from silylation of **7a** with MSTFA. The identities of the characteristic ion fragments are described in Tables 1 and 2. For detailed GC-MS conditions see Section 2.

relevant condensation reactions, the application and further elaboration of this analytical concept was justified. Furthermore, separation of all the respective starting materials and thiazolidines on

a fused-silica capillary column DB 255 or DB 17 within 20 min, using a special temperature program (see Section 2), proved to be greatly advantageous for a rapid and reliable identifica-

tion of these compounds by mass spectrometry in the same analytical run (see Fig. 3).

### 3.5. Investigations on the formation and epimerization of the thiazolidine **7** under silylation conditions

With respect to the planned *in vivo* experiments, exemplary for the penicillamine-derived compounds **7a** and **7b**, two important questions concerning the analytical concept had to be investigated based upon this derivatization procedure. Thus, it was necessary to study whether under silylation conditions, epimerization of the 2,4-disubstituted thiazolidine dicarboxylic acids takes place. Another important question was whether D-(–)-penicillamine (**4**) and glyoxylic acid (**1**) condense during the derivatization reaction with MSTFA.

### 3.6. Determination of the diastereomeric ratio

Especially the first of the two questions was relevant for an evaluation and interpretation of the results of the planned *in vivo* experiments

concerning an enzymatic assistance in the endogenous condensation reaction. Furthermore, a chromatographic investigation on the epimerization behaviour was of most general interest since unambiguous information on diastereomeric ratios of thiazolidine mixtures could be obtained exclusively by NMR spectroscopy so far [12].

Thus, mixtures of **7a** and **7b** with stereoisomeric **7a/7b** ratios of 50:50, 25:75, and 100:0 as determined by NMR, were silylated under the conditions described above, and were then investigated by gas chromatography. In an impressive agreement, the given stereoisomeric ratios of **7a** vs. **7b** were reproduced by GC analysis of the silyl derivatives **10a** and **10b**, as illustrated in Table 3.

Thus, for the first time a chromatographic method was available that, like a snapshot, allowed a determination of the actual diastereomeric ratio and thus was clearly superior to the direction-pair assisted reversed-phase chromatography of **7a** and **7b** [24]. For the latter method, due to solubility problems, an epimerization had to be taken into account already while dissolving the compounds.

Table 3

Gas chromatographic studies on the stereochemically defined transformation of **7a** to **10a**, and **7b** to **10b** under silylation conditions

Sample <sup>a</sup>	<i>cis/trans</i> ratio of <b>7a/7b</b> determined by <sup>1</sup> H NMR	<i>cis/trans</i> ratio of <b>7a/7b</b> determined by GC as <b>10a/10b</b>	Calculated ratio <i>cis/trans</i> <b>7a/7b</b>
1	50:50	50:50	
2	50:50	51:49	
3	50:50	48:52	
4	50:50	47:53	51:49
5	50:50	51:49	
6	50:50	51:49	
7	25:75	24:76	
8	25:75	25:75	5:75
9	25:75	23:77	
10	100:0	100:0	
11	100:0	100:0	0:0

<sup>a</sup> For description of the preparation and treatment of sample solutions see Section

### 3.7. Condensation of glyoxylic acid (**1**) and D-(–)-penicillamine (**4**) during silylation

The question whether silylating conditions are condensation conditions, is of crucial importance for all further investigations concerning the elaboration of a GC-suited workup procedure: if, during silylation of glyoxylic acid (**1**) and D-(–)-penicillamine (**4**), condensation to the heterocycles **7a** and **7b** takes place, the subsequent GC analysis can no longer distinguish between the substance genuinely present and the material that is formed de novo, during the silylation process in the sense of an artifact. In that case the analytical procedure would be invalid unless either a corresponding further workup procedure would prevent the non-desired condensation reaction or if this additional cyclocondensation reaction could be shown to convert reproducible percentages of the precursors into the thiazolidines. Thus, for these questions, qualitative as well as quantitative aspects have to be taken into consideration.

Consequently, the procedure was performed with a mixture of the condensation partners **1** and **4** in a realistic concentration range that also reflects the ratios of the silylating reagent and starting materials given in a normal analysis. Due to the impossibility of a direct weighing of the solid material in that order of magnitude, aqueous standard solutions of **1** and **4** were subsequently shock-frozen down to  $-196^{\circ}\text{C}$  in the silylating vessels and then lyophilized. By this way, condensation of **1** and **4** upon mixing of the standard solutions was excluded. The solids of **1** and **4** as present after lyophilization were silylated without problems in the usual way. Subsequent GC–MS investigation of the reaction mixtures showed that the condensation between glyoxylic acid (**1**) and D-(–)-penicillamine (**4**) indeed occurred during the silylation reaction since both **7a** and **7b** were unambiguously identified as their silylation products **10a** respectively **10b** according to their retention times and mass spectra (see Fig. 5).

Interestingly, under these conditions, a third reaction product in the polarity range of the thiazolidines **10a** and **10b** was registered that had

never been observed before. It seemed probable that a possible intermediate product resulting from the initial addition reaction of glyoxylic acid (**1**) and D-(–)-penicillamine (**4**) might have been trapped by the very active reagent MSTFA before the ring closure had been taken place to give a chromatographically stable product. Mass spectrometrical investigations revealed evidence for the formation of the silylated compounds **20** or **21** (see Fig. 5). Also in this case, as for the thiazolidines previously described, a characteristic  $[M - 15]^{+}$  peak, a valuable indicator for the molecular mass, was again registered besides several other signals from known decomposition processes (see Section 2). Yet, a definite structure elucidation, exclusively based upon the mass spectrum, did not succeed.

Because of this additional reaction product, it was not possible to quantitate the condensation reaction by a simple comparison of the calibration curves of the TMS derivatives **10a** and **10b** corresponding to the thiazolidines **7a** and **7b**, as initially assumed. For this reason, the amounts (in mol) of the reaction products **10a**, **10b**, and **20/21** originating in the different experiments were estimated by using the calibration curve of **10a** (derivative of **7a**) for **20/21**. For a further confirmation, this result was compared with the molar turnovers of the precursors **1** and **4** as likewise determined by calibration curves within the margins of error. A really good agreement between the quantities of the starting materials used and the products formed could be attained as seen in the bar graph (see Fig. 6), a hint that the applied procedure indeed allows a quantitative evaluation. Simultaneously, it becomes clear that, on the other hand, no reliable correlation between the experimental parameters and the degree of the condensation reaction can be stated.

## 4. Conclusions and outlook

Summarizing, the sulphur-containing compounds **2**, **3** and **4** as well as their condensation products **5a**, **5b**, **6**, **7a** and **7b** (see Fig. 1) can unambiguously be trimethylsilylated to give one

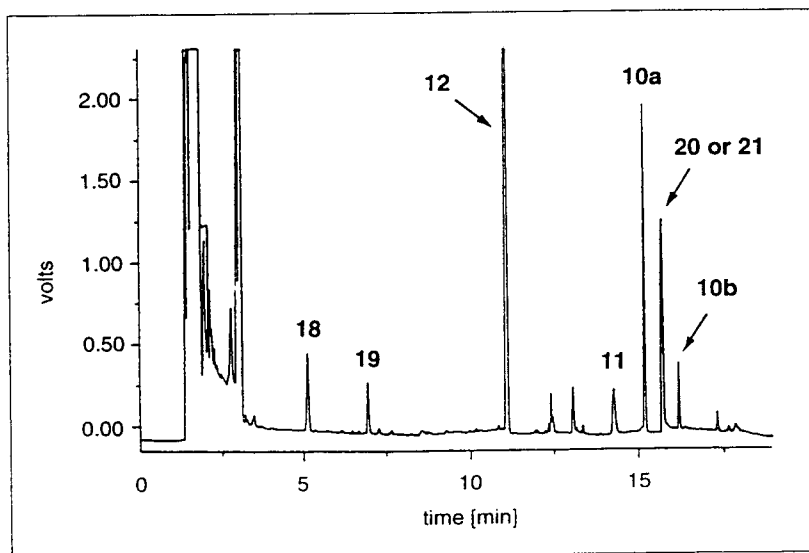
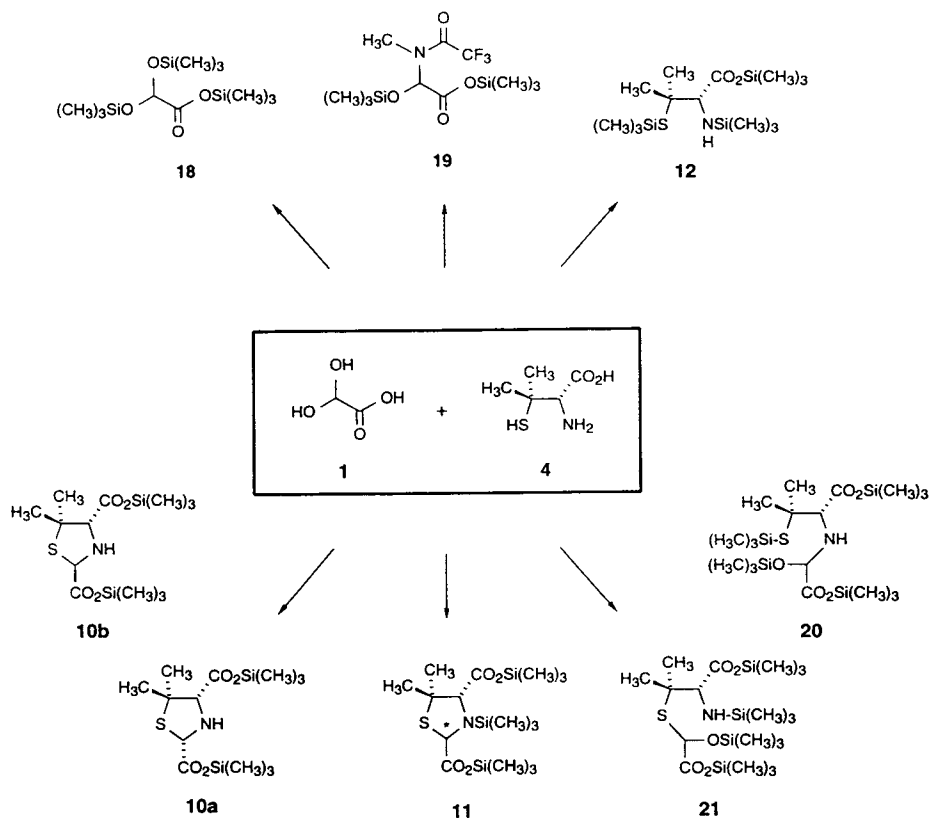


Fig. 5. Thiazolidine formation during trimethylsilylation. The figure shows a typical GC-FID chromatogram obtained from a mixture of glyoxylic acid (**1**) and D-(-)-penicillamine (**4**) after trimethylsilylation with MSTFA. The scheme above illustrates the formation of all the TMS derivatives detected and identified in the sample solution by GC-MS analysis. For detailed experimental conditions see Section 2.

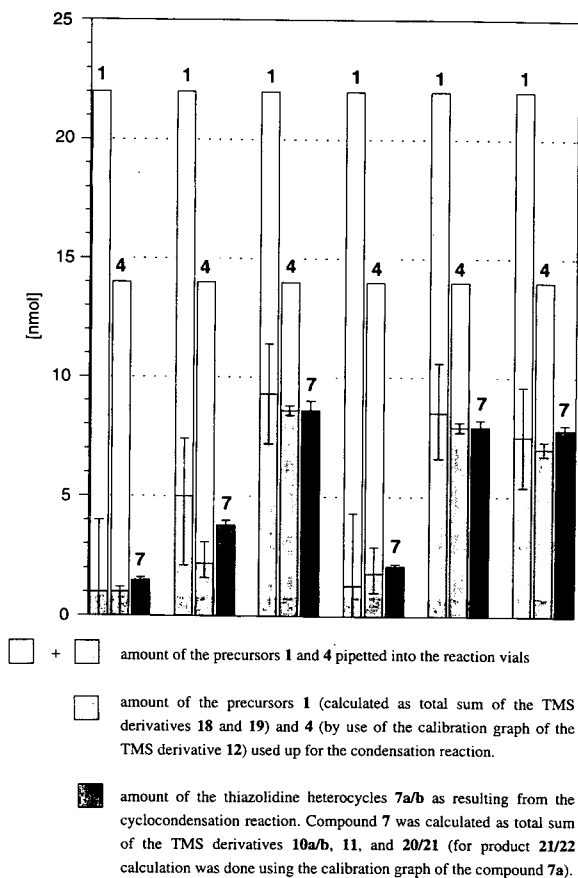


Fig. 6. Quantitation of the extent of thiazolidine formation caused by the condensation of glyoxylic acid (1) and D-(–)-penicillamine (4) under silylation conditions. For detailed experimental and chromatographic conditions see Section 2.

gas chromatographically analyzable main product each (see Fig. 3), although a time-dependence in the product ratio has to be taken into account. Thus, in combination with mass spectrometry, for the first time a method has become available that allows a sensitive and unequivocal identification of glyoxylate-derived thiazolidines. Still, the very rapid spontaneous condensation of glyoxylic acid (1) with binucleophilic amino acids to give alkaloid-type heterocycles, as essential for the presented therapeutic concept, constitutes a particular challenge to an analytical method for the quantitation of the thiazolidines in the presence of their precursors. Thus, the gas chromatographic procedure developed by us can

be applied only if the non-desired condensation step during the silylating process can be excluded by a preceding workup step. It should be possible to prevent a spontaneous reaction of the starting material if at least one of the two reaction partners – glyoxylic acid or the amino acid – is immediately eliminated from the reaction mixture. Such a pre-separation to avoid artifact formation must be considered as the key step of the entire analytical device for the scheduled investigation program. Consequently, the present work aims at the elaboration of appropriate sample workup steps also suited for the analysis of these compounds from a complex biological matrix such as urine. Detailed investigations based upon ion chromatography are in progress.

#### Acknowledgements

This work was supported by the Fonds der Chemischen Industrie. A generous gift of larger quantities of D-(–)-penicillamine by the Degussa AG is gratefully acknowledged.

#### References

- [1] P. Riederer, G. Bringmann, K. Jellinger, W.D. Rausch, H. Reichmann, K.-H. Sontag and W. Wesemann, in Projektträger des BMBF Forschung im Dienste der Gesundheit (Editor), Materialien zur Gesundheitsforschung, Schriftenreihe zum Programm der Bundesregierung "Gesundheitsforschung 2000", Morbus Parkinson und andere Basalganglienerkrankungen Wirtschaftsverlag NM, Verlag für Neue Wissenschaft GmbH, Bremerhaven, 1995, Vol. 27, pp. 139–157.
- [2] H.E. Williams and L.H. Smith Jr., in J.B. Stanbury, J.B. Wyngaarden, D.S. Fredrickson, J.L. Goldstein and M.S. Brown (Editors), The Metabolic Basis of Inherited Disease, McGraw-Hill, New York, NY, 5th ed., 1983, pp. 204–228.
- [3] C.J. Danpure, J. Inher. Metab. Dis., 12 (1989) 210.
- [4] W. Berg, Z. Urol. Nephrol., 83 (1990) 481.
- [5] M.F. Parry and R. Wallach, Am. J. Med., 57 (1974) 143.
- [6] C.L. Winek, D.P. Shingleton and S.P. Shanor, Clin. Toxicol., 13 (1978) 297.
- [7] C. Perier, J. Frey, C. Auboyer, A. Richard, G. Aulagnier, P. Heritier and A. Gilloz, Clin. Chem., 34 (1988) 1471.

- [8] R. Schröder, *Dtsch. Med. Wochenschr.*, 105 (1980) 997.
- [9] R.A.J. Conyers, A.M. Rofo, R. Bais, H.M. James, J.B. Edwards, D.W. Thomas and R.G. Edwards, *Int. J. Vitam. Res., Suppl.*, 28 (1985) 9.
- [10] G. Bringmann, S. Schneider and A. Hille, *Nachr. Chem. Tech. Lab.*, 34 (1986) 222.
- [11] G. Bringmann, D. Feineis, H. Friedrich and A. Hille, *Planta Med.*, 57 (Suppl. 1) (1991) 73.
- [12] G. Bringmann, D. Feineis, C. Hesselmann, S. Schneider, M. Koob and D. Henschler, *Life Sci.*, 50 (1992) 1597.
- [13] A. Brossi, in G.A. Cordell (Editor), *The Alkaloids*, Academic Press, New York, NY, 1993, Vol. 43, pp. 119–183.
- [14] G. Bringmann and D. Feineis, *Nachr. Chem. Tech. Lab.*, 41 (1993) 419.
- [15] N. Naberl, P. Prasanna, P. Venkatesan and G.A. Hamilton, *Biochem. Biophys. Res. Commun.*, 107 (1982) 374.
- [16] C.L. Burns, D.E. Main, D.J. Buckthal and G.A. Hamilton, *Biochem. Biophys. Res. Commun.*, 125 (1984) 1039.
- [17] G.A. Hamilton, *Adv. Enzymol.*, 57 (1985) 85.
- [18] R. Bais, A.M. Rofo and R.A.J. Conyers, *J. Urol.*, 145 (1991) 1302.
- [19] R. Bais, A.M. Rofo and R.A.J. Conyers, *Nephron*, 57 (1991) 460.
- [20] D. Perrett, *J. Rheumatol., Suppl.* 7 (1981) 41.
- [21] A.J.L. Cooper, M.T. Haber and A. Meister, *J. Biol. Chem.*, 257 (1981) 816.
- [22] J. Alary, G. Carrera, G. de Saint Blanquat, F. Anglade and C. Escrieut, *J. Chromatogr.*, 496 (1989) 485.
- [23] J. Alary, G. Carrera, C. Escrieut and A. Periquet, *J. Pharm. Biomed. Anal.*, 7 (1989) 715.
- [24] G. Bringmann, C. Hesselmann and D. Feineis, *J. Chromatogr.*, 595 (1992) 351.
- [25] D. Feineis, G. Bringmann and C. Hesselmann, in 11. *Königsteiner Chromatographietage 1991*, GIT-Verlag, Darmstadt, 1991, pp. 204–213.
- [26] G. Bringmann, D. Feineis and C. Hesselmann, *Anal. Lett.*, 25 (1992) 497.
- [27] J.C. Fourneau, O. Efimovsky, J.C. Gagnault, R. Jacquier and C. LeRidant, *C.R. Acad. Sci. Ser. C*, 272 (1971) 1515.
- [28] C. De Marco, C. Cini, R. Coccia and C. Blarmino, *Ital. J. Biochem.*, 28 (1979) 104.
- [29] R. Bentley, A.H. Cook and J.A. Elvidge, *J. Chem. Soc.*, (1949) 3216.
- [30] I. McMillian and R.J. Stoodley, *Chem. Commun.*, (1968) 11.
- [31] G. Bringmann, C. Hesselmann and D. Leimkötter, unpublished results.
- [32] K. Peters, E.-M. Peters, H.-G. von Schnering, G. Bringmann, C. Hesselmann and D. Leimkötter, *Z. Kristallogr.*, 206 (1993) 267.
- [33] K. Peters, E.-M. Peters, H.-G. von Schnering, G. Bringmann and D. Leimkötter, *Z. Kristallogr.*, 208 (1993) 223.
- [34] M. Hudlicky, *J. Org. Chem.*, 45 (1980) 5377.
- [35] M. Spittler and G. Spittler, *J. Chromatogr.*, 164 (1978) 253.
- [36] H.M. Liebich, A. Pickert, U. Stierle and J. Wöll, *J. Chromatogr.*, 199 (1980) 181.
- [37] D.L. Stalling, C.W. Gehrke and R.W. Zumwalt, *Biochem. Biophys. Res. Commun.*, 31 (1968) 616.
- [38] L. Birkhofer and M. Donike, *J. Chromatogr.*, 26 (1967) 270.
- [39] M. Donike, *J. Chromatogr.*, 42 (1969) 103.
- [40] J.F. Klebe, H. Finkbeiner and D.M. White, *J. Am. Chem. Soc.*, 88 (1966) 3390.
- [41] C.A. Atkins and D.T. Canvin, *Can. J. Biochem.*, 49 (1971) 949.
- [42] H. Iwase, Y. Takeuchi and A. Murai, *Chem. Pharm. Bull.*, 27 (1979) 1307.
- [43] R.A. Chalmers and A.M. Lawson, in *Organic Acids in Man*, Chapman and Hall, London, New York, 1982, pp. 113–115.
- [44] M. Ende and H. Luftmann, *Tetrahedron*, 40 (1984) 5167.





# Multi-residue pesticide analysis in environmental water samples using solid-phase extraction discs and gas chromatography with flame thermionic and mass-selective detection

Triantafyllos A. Albanis\*, Dimitra G. Hela

*Department of Chemistry University of Ioannina, Ioannina 45110, Greece*

First received 19 December 1994; revised manuscript received 6 March 1995; accepted 6 March 1995

## Abstract

A multi-residue analysis for 25 pesticides was developed as a rapid screening method for organic contaminants in river, lake and sea water samples. Gas chromatography with flame thermionic detection (GC–FTD) and mass selective detection (GC–MSD) using two different capillary columns, DB-1 and HP-5, was employed for the identification of 25 selected pesticides belonging to triazines, organophosphorus compounds and substituted ureas, carbamates, anilides, anilines and amides. The extraction of various natural waters spiked with pesticide mixtures was effected with C<sub>18</sub> Empore solid-phase extraction discs and filter-aid glass beads. The triazine compounds (atrazine, simazine, propazine, prometryne and cyanazine) were recovered from distilled and underground water samples at relative high levels (73.5–105%) compared with the river waters (39.9–80.5%), lake water (54.6–81.8%) and marine water (38.6–79.9%). The organophosphorus compounds studied (monocrotophos, terbufos, diazinon, methyl parathion, ethyl parathion, malathion and ethion) were also recovered from distilled and underground water samples at relatively high levels (62.4–118%) compared with river waters (27.3–98.9%), lake water (41.0–85.2%) and marine water (33.4–81.3%). The substituted ureas (monuron, diuron and linuron), substituted anilines and anilides (trifluralin, propanil, propachlor and alachor), carbamates (EPTC and carbofuran) and other compounds (molinate, picloram, captan and MCPA isooctyl ester) were recovered at the same level as triazines. Confirmation of pesticide identity was performed by using GC–MS in the selected-ion monitoring mode.

## 1. Introduction

Pesticides of different chemical nature are widely used for agricultural and non-agricultural purposes throughout the World. Some of the modern pesticides have replaced the organochlorine pesticides, which were banned after evidence of their toxicity, persistence and bioaccumulation in the environment [1]. Because of their widespread use, pesticides are currently

detected by determination of their residues in various environmental matrices, such as soil, water and air [2,3].

The determination of pesticide residues in water samples is necessary for solving various environmental and biological problems [3]. The chromatographic techniques used for pesticide analysis require efficient isolation and concentration procedures such as liquid–liquid supercritical fluid and solid-phase extraction [4–6]. Although single-residue methods are often used in the analyses required by legislation or in

\* Corresponding author.

results confirmations, in the case of environmental water sample analysis where nothing is known about the nature of possible contaminants, universal and reliable analytical methods are required. These methods enable one to analyse in a single run and within the shortest possible time as many pesticides as possible from the bulk of those which may occur in a sample of unknown origin. It is then an advantage to use methods that permit the determination of pesticide residues of different chemical classes in the same extract.

The chromatographic stage of a method for pesticides determination at low levels in drinking and surface waters requires previous efficient solvent extraction and concentration procedures [5,6], which can make pesticide determination a time-consuming and laborious process involving consumption of organic solvents in large volumes. To overcome these problems, solid-phase extraction has been extensively applied to the extraction of pesticides present in water samples. The adsorbed compounds are then eluted from the solid phase with an organic solvent [7].

C<sub>8</sub>- and C<sub>18</sub>-bonded-phase cartridges [8,9], XAD resins [10–12], activated charcoal [13,14], graphitized carbon blank and Tenax GC [15,16] have all been employed for the analysis of a variety of pesticides. In the last 3 years, solid-phase extraction discs have been employed as an alternative method for the trace enrichment of organic compounds, including pesticides, in water. The solid-phase extraction discs are available in a diameter of 47 and 90 mm, similar to LC solvent filters. Such discs have been tested for different groups of compounds, including pesticides, organotins and phthalates [17]. The system has also been applied on-line with LC for the concentration of triazine herbicides and chlorophenols from river and sea-water [18].

The purpose of this work was to carry out a systematic study to select certain of the most commonly used and important pesticides in the European Community [19] and especially in the Mediterranean region [20], belonging to triazines, organophosphorus compounds and substituted ureas, carbamates, anilides anilines and amides, and study their retention times in two

different columns, DB-1 and HP-5, to characterize these compounds by the use of GC–MS, to develop an extraction method for various environmental waters by the use of solid-phase extraction with Empore C<sub>18</sub> discs and to apply the analytical methodology developed to analyse spiked and natural water samples of different origin (underground water of Ioannina, Louros river, Pamvotis lake and Ionian sea in N.W. Greece and Nestos river and Thermaikos gulf in N. Greece).

## 2. Experimental

### 2.1. Chemicals

HPLC-grade water, methanol, dichloromethane from Pestiscan (Labscan, Dublin, Ireland) were passed through a 0.45- $\mu$ m filter before use. Alachlor, atrazine, captan, carbofuran, cyanazine, diazinon, diuron, EPTC, ethion, linuron, malathion, MCPA is. ester, molinate, monocrotophos, monuron, parathion ethyl, parathion methyl, picloram, prometryne, propachlor, propanil, propazine, simazine, terbufos and trifluralin were purchased from Promochem (Wesel, Germany). Empore extraction discs were manufactured by 3M and distributed by Varian (Harbor City, CA, USA). The discs used were 47 mm in diameter and 0.5 mm thick. Each disc contained about 500 mg of C<sub>18</sub>-bonded silica (92  $\pm$  2%) and 10  $\pm$  2% PTFE. The particle characteristics were particle size 8  $\mu$ m, pore size 60 Å and shape irregular. Empore (St. Paul, MN, USA) filter-aid 400 glass beads were used as a filtration aid when extracting samples with high particulate content using extraction discs.

### 2.2. Waters used

Water samples were collected, in summer 1993, from Louros and Nestos rivers, Pamvotis lake (Ioannina) Amvrakikos gulf and Ionian sea; underground water from the Ioannina area and distilled water were also used. Their characteristics are given in Table 1.

Table 1  
Characteristics of selected environmental waters

Origin of water sample	pH	Conductivity ( $\mu\text{s}/\text{cm}$ )	Total suspended matter ( $\text{mg}/\text{l}$ ) <sup>a</sup>	TOC <sup>b</sup> ( $\text{mg}/\text{l}$ )	Salinity (%)
Distilled water	5.95	5	–	b.d.l. <sup>c</sup>	– <sup>d</sup>
Underground water	7.93	450	15	0.03	– <sup>d</sup>
Pamvotis lake	8.25	350	385	9.65	0.55
Louros river	8.72	350	115	4.16	0.36
Nestos river	7.76	300	56	3.20	0.21
Thermaikos gulf	8.01	15,240	310	5.25	16.54
Ionian sea	8.02	14,400	240	1.32	34.40

<sup>a</sup> TSM (total suspended matter) was measured by filtration through a 0.45- $\mu\text{m}$  PTFE filter (Millipore).

<sup>b</sup> TOC = total organic carbon.

<sup>c</sup> b.d.l. = below detection limit (0.01  $\text{mg}/\text{l}$ ).

<sup>d</sup> Not determined.

### 2.3. Sample extraction and concentration

Empore extraction discs were conditioned with 10 ml of acetone for 3 h. Environmental water samples ( $n = 3$ ) of 1 l each were spiked with a mixture of the 25 selected pesticides at final concentrations of 0.1, 0.25, 1.0, 2.5, 5, 10, 20 and 50  $\mu\text{g}/\text{l}$ . Methanol modifier (5 ml) was added to 1-l water samples to allow a better extraction [21,22]. The sample pH was adjusted to  $<3$  with 1:1 (v/v) sulfuric acid.

Twelve grams (1 cm) of glass beads were poured on the disc already placed in the conventional Millipore apparatus, and both were washed with 10 ml of dichloromethane with the vacuum on and with 10 ml of methanol for 3 min with the vacuum off. The disc was not allowed to become dry, as recommended [23,24]. The sample was mixed well and allowed to percolate through the discs at a flow-rate of 50 ml/min under vacuum. After sample extraction, the pesticides trapped in the disc were collected by using 2  $\times$  5 ml of solvent mixture [dichloromethane–ethyl acetate (1:1, v/v)] as eluting solvent. The fractions were evaporated to 4 ml on a rotary evaporator (35°C). After careful evaporation of the solvent to 0.5 ml in a gentle stream of nitrogen, the residue was dissolved in 2 ml of *n*-hexane and the solution was evaporated to a final volume of 1 ml for GC injection.

### 2.4. Chromatographic conditions

#### GC–FTD

Single pesticide standards and 1.5  $\mu\text{l}$  of extracts from the Empore disc preconcentration step were injected in the splitless mode into a Shimadzu 14A capillary gas chromatograph equipped with an instrument for flame thermionic detection (FTD) at 250°C. The DB-1 column (30 m  $\times$  0.32 mm I.D.) used contained 5% methylsilicone (J&W Scientific, Folsom, CA, USA). The column was programmed from 55°C (2 min) to 210°C (20 min) at 5°C/min and to 270°C (4 min) at 20°C/min. The injection temperature was 220°C.

Helium was used as the carrier and nitrogen as make-up gas. The detector gases were hydrogen and air, and their flow-rates were regulated according to results obtained through simplex optimization of the analytical variables, in this instance air and hydrogen flow-rates in the detector. The FTD ion source was an alkali metal salt ( $\text{Rb}_2\text{SO}_4$ ) bonded to a 0.2-mm spiral of platinum wire.

#### GC–MS

A Hewlett-Packard (Palo Alto, CA, USA) Model 5890B instrument with an HP autosampler model and 5971A mass-selective detector interfaced to a Model 59970C instrument for

data acquisition and processing were used. A HP-5 fused-silica capillary column coated with 5% phenyl–95% methyl-polysiloxane (25 m × 0.25 mm I.D.) (Hewlett-Packard) was used. Helium was used as the carrier gas at 83 kPa. The injection temperature was 240°C. The column was programmed from 55°C (2 min) to 210°C at 5°C/min and to 270°C at 20°C/min (4 min). The ion source were maintained at 200°C and electron impact (EI) mass spectra were obtained at 70 eV. The spitless mode was used for injection of 1.5- $\mu$ l volumes with the valve opened for 30 s.

Two ions for each pesticide were chosen for screening analysis in selected-ion monitoring (SIM). The ion traces were divided into five groups that were recorded sequentially during the injection, on the basis of the retention times of the single substances; the first group was from 17.1 to 27.2 min, the second from 27.2 to 29.0 min, the third from 29.0 to 31.3 min, the fourth from 31.3 to 34.0 min and the fifth from 34.0 to 50.2 min.

### 3. Results and discussion

#### 3.1. General considerations

The main advantage of using Empore extraction discs over liquid–solid extraction cartridges is the increased productivity resulting from the high extraction flow-rate, which facilitates sampling in the field water. In this study, only a 20-min extraction time was needed for the trace enrichment of 1-l water samples. These results are in good agreement with those of other studies [17,25,26]. Generally, prefiltration of (sea and lake) surface water samples through 0.45- $\mu$ m PTFE filters has been recommended when Empore discs [17,25,27] are used and it would not affect the determination of the polar pesticides used in this study. The polar pesticides (Table 2) exhibit a  $\log K_{oc}$  (partition coefficient between organic carbon and water) of 2 and consequently are widely distributed in the dissolved (>99%) and not in the suspended phase of water [17,28] (Table 2). In contrast, for non

polar pesticides,  $\log K_{oc} > 3$ , prefiltration would yield much lower recoveries. Therefore, for our multi-residue analytical method in this study, which included compounds with a wide level of  $\log K_{oc}$ , we decided to use Empore filter aid 400. Filter aid 400 is a high-density glass bead product intended for use as a filtration aid when Empore discs are used for the extraction of samples with high particulate content. The non-polar compounds adsorbed strongly on particulate matter are eluted simultaneously by the extraction solvent along with the compounds trapped in the extraction discs.

The eluent volume effect (1–15 ml) was investigated. The maximum recovery was obtained with 8 ml for all the pesticides; 2 × 5 ml was adopted because it was found that the relative standard deviation was slightly lower.

#### 3.2. Gas chromatographic techniques

Table 3 gives the retention times and the detection limits obtained for the 25 selected pesticides by GC–FTD using a DB-1 column and by GC–MS using an HP-5 column. Figs. 1 and 2 show the simultaneous determination of typical chromatograms, obtained after extraction of 1 l of Nestos river and Amvrakikos gulf water samples spiked with pesticides at the 0.25–5  $\mu$ g/l level. Owing to the selectivity of the detector, no interferences were noticed in the GC–FTD retention time data of these compounds. When comparing the elution order obtained with the two columns used, the elution order is the same for both the DB-1 and HP-5 columns with different stationary phases for seventeen of the selected compounds. Monuron, monocrotophos and carbofuran do not elute from the HP-5, similarly to their retention order on DB-1, and four compounds, picloram, diuron, prometryne and cyanazine, cannot be determined by GC–MS under conditions described for the HP-5 column. Finally, the resolution by column DB-1 permits, in two cases, overlappings between carbofuran and simazine and between atrazine and diuron to be observed. Similar problems appearing with the HP-5 column in GC–MS could be attributed to overlapping between

Table 2  
Molecular mass solubility in water and log  $K_{oc}$  (ml/g) of selected pesticides

No.	Compound	Activity <sup>a</sup>	Molecular mass	Solubility in water (mg/l)	Log $K_{oc}$ [19,29]
1	EPTC	H	189.4	370–375	2.44
2	Monuron	H	198.7	230	2.25
3	Molinate	H	187.3	800–912	2.62
4	Propachlor	H	211.7	700	2.62
5	Monocrotophos	I	223.2	1 (kg/l)	–
6	Trifluralin	H	335.3	0.05	3.86
7	Picloram	H	241.5	430	1.68
8	Carbofuran	I	221.3	700	1.44
9	Simazine	H	201.7	5	2.10
10	Atrazine	H	215.7	35	2.20
11	Diuron	H	233.1	42	2.50
12	Propazine	H	230.0	4.8	2.20
13	Terbufos	I	288.4	4.5	3.60
14	Diazinon	I	304.4	40	1.92
15	Propanil	H	218.1	500	2.15
16	Methyl parathion	I	263.2	50	3.70
17	Prometryne	H	241.4	40	2.78
18	Alachlor	H	269.8	148	2.07
19	Cyanazine	H	240.7	171	2.20
20	Linuron	H	249.1	75	2.93
21	Malathion	I	330.4	145	3.25
22	Ethyl parathion	I	291.3	24	4.04
23	Captan	F	300.6	3.3	2.50
24	MCPA is. ester	H	312.8	550	1.69
25	Ethion	I	384.5	1	3.64

<sup>a</sup> I = insecticide; H = herbicide; F = fungicide.

prometryne and alachlor and between cyanazine and linuron. In this last case the problem seems also to come from the lower detector sensitivity for propachlor, picloram, diuron, prometryne and cyanazine.

In Table 3 the selected typical fragment ions of the selected pesticides studied are listed. It is possible that two compounds have an ion with the same  $m/z$  value but with different structures and belonging to different retention time groups.

### 3.3. Recovery studies

The mean recoveries of three analyses, obtained for the 25 selected pesticides spiked into seven different types of water (see Table 1), are given in Table 4. It should be noted that the recoveries obtained for distilled and underground water samples were higher than 80% for

twenty and fifteen compounds, respectively, indicating that the use of the disc does not pose any problem to the analysis of such a type of water.

The recoveries of all the pesticides were higher in distilled and underground water than those from surface waters (rivers, lake and marine waters). The main differences among the studied surface waters are the high salinity and conductivity of Thermaikos gulf and Ionian sea water and the higher concentration of the total organic carbon in Pamvotis lake water samples. Chromatograms for two types of spiked samples of Nestos river and Amvrakikos gulf water are shown in Figs. 1 and 2. It is clearly seen that the lake and marine waters pose more problems to the analysis, with high interferences. All the studied pesticides show lower levels of recovery in marine waters (Themaikos gulf and Ionian sea

Table 3  
Analysed pesticides, retention times and selected ions

No.	Compound	DB-1 and FTD			HP-5 and GC-MS		
		$t_R$ (min)	RRF <sup>a</sup> (diazinon)	LOD <sup>b</sup> ( $\mu\text{g/l}$ )	$t_R$ (min)	Selected ions ( $m/z$ )	LOD ( $\mu\text{g/l}$ )
1	EPTC	23.04	5.41	0.005	18.30	190, 192	0.0008
2	Monuron	27.64	338.1	0.08	23.13	198, 200	0.010
3	Molinate	27.77	5.79	0.003	22.94	187, 189	0.001
4	Propachlor	29.65	10.94	0.005	24.88	211, 213	0.010
5	Monocrotophos	30.56	1.77	0.001	26.82	223, 225	0.010
6	Trifluralin	31.61	8.41	0.001	26.56	335, 337	0.005
7	Picloram	32.13	166.6	0.05			
8	Carbofuran	32.32	0.92	0.001	28.02	221, 223	0.010
9	Simazine	32.44	4.29	0.005	27.35	201, 203	0.010
10	Atrazine	32.75	3.27	0.002	28.22	215, 217	0.005
11	Diuron	32.77	36.79	0.05			
12	Propazine	33.05	3.23	0.002	28.44	229, 231	0.004
13	Terbufos	33.93	1.59	0.001	28.66	231, 233	0.010
14	Diazinon	34.40	1.00	0.001	29.28	304, 306	0.015
15	Propanil	35.96	20.28	0.010	30.97	217, 219	0.010
16	Methyl parathion	36.80	1.04	0.0005	31.16	263, 265	0.015
17	Prometryne	37.76	62.49	0.005			
18	Alachlor	37.84	3.87	0.002	31.52	269, 271	0.010
19	Cyanazine	39.19	5.24	0.005			
20	Linuron	39.30	1.98	0.002	32.47	248, 250	0.005
21	Malathion	39.54	1.16	0.001	32.79	127, 173	0.010
22	Ethyl parathion	40.74	0.68	0.0005	33.20	291, 293	0.005
23	Captan	43.57	135.2	0.05	34.97	264, 266	0.020
24	MCPA is. ester				36.43	312, 314	0.0005
25	Ethion	60.06	0.58	0.0008	41.61	384, 386	0.008

FTD with DB-1 capillary column (30 m  $\times$  0.32 mm I.D.) and temperature programme 55°C (2 min), increased at 5°C/min to 210°C (30 min). GC-MS with HP-5 column (25 m  $\times$  0.25 mm I.D.) and temperature programme 55°C (2 min), 55–210°C at 5°C/min, 210°C (20 min), 210–270°C at 20°C/min, 270°C (4 min).

<sup>a</sup> RRF = relative response factor.

<sup>b</sup> LOD = limit of detection.

waters) with higher salinity values and, consequently, the interferences in the GC-FTD and GC-MS traces are higher when analysing samples of high salinity [18]. This negative influence of salinity on the pesticide levels obtained is stronger for monocrotophos, picloram, terbufos, prometryne and MCPA, where the recoveries are below 50% in marine water samples. The influence of salinity is greater for more polar compounds. This behaviour in the case of atrazine and simazine agrees with that reported in Chakespeare Bay and Ebro river estuaries [18,30]. In contrast, a positive salting-out effect

on adsorption on  $C_{18}$  silica has been observed for some herbicides and organophosphorus insecticides [31,32]. It is possible that the influence of negative salinity is stronger than the increase in extraction efficiency due to the ionic strength of aqueous samples.

The more hydrophobic compounds of the 25 pesticides studied ( $\log K_{oc} > 3$ : trifluralin, methyl and ethyl parathion and malathion) seem to show no significant decrease in their recoveries from lake and gulf water due to the higher organic carbon content. In the same way, experiments with hydrophobic organochlorine pesti-

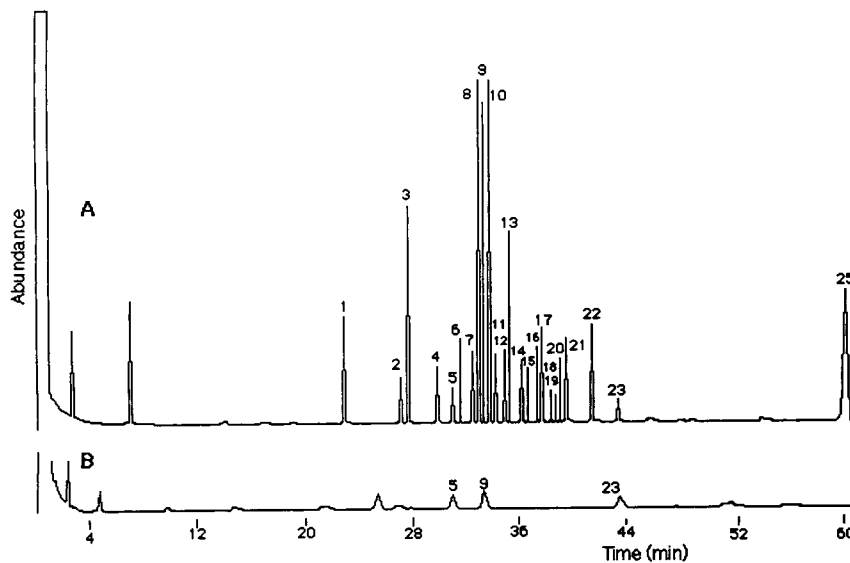


Fig. 1. GC-FTD for (A) ca. 0.25–5  $\mu\text{g/l}$  of 24 selected pesticides in spiked water and (B) water sample from Nestos river under the same conditions. A DB-1 column 30 m long containing 5% methylsilicone was programmed as follows: 55°C (2 min) to 215°C (20 min) at 5°C/min and from 210 to 270°C at 20°C/min, 270°C (4 min). For peak numbers, see Table 2.

cides ( $\log K_{oc} \approx 6$ ) have shown a strong tendency to adsorb on the particulate matter on the filter [18,33] and pre-filtration would give much lower recoveries.

The triazine compounds (atrazine, simazine, propazine, prometryne and cyanazine) were re-

covered from distilled and underground water samples at relative high levels (73.5–105%) compared with river waters (39.9–80.5%), lake water (54.6–81.8%) and marine water (38.6–79.9%). The decreased recoveries of prometryne from marine and lake waters is the main problem

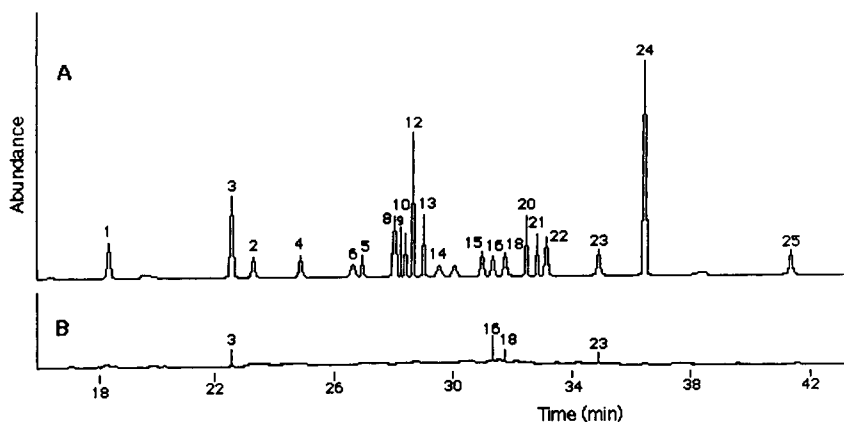


Fig. 2. GC-MS for (A) ca. 0.25–5  $\mu\text{g/l}$  of 19 selected pesticides in spiked water and (B) water sample from Thermaikos gulf under the same experimental conditions. A HP-5 column 25 m long containing 5% phenyl–95% methyl-polysiloxane was programmed as follows: 55°C (2 min) to 210°C at 5°C/min and 270°C at 20°C/min (4 min). For peak numbers, see Table 2.

Table 4  
Mean recoveries of 25 selected pesticides in environmental water samples by using C<sub>18</sub> Empore extraction discs

No.	Compound	Mean recovery (%)						
		Distilled water	Underground water	Pamvotis lake	Louros river	Nestos river	Thermaikos gulf	Ionian sea
1	EPTC	98.3	89.8	81.4	64.7	98.4	99.2	62.4
2	Monuron	87.6	80.3	76.2	92.7	64.3	50.7	48.3
3	Molinate	98.8	93.5	65.8	56.1	76.6	78.8	51.5
4	Propachlor	96.2	73.8	60.5	61.1	84.1	50.6	63.9
5	Monocrotophos	75.3	62.4	41.0	54.9	57.3	43.4	37.7
6	Trifluralin	106	96.7	48.9	82.8	76.5	55.7	61.8
7	Picloram	52.4	49.7	40.6	27.3	18.8	19.5	16.9
8	Carbofuran	85.4	80.1	87.4	60.7	49.8	54.3	54.8
9	Simazine	89.2	73.5	81.8	60.2	72.8	58.4	64.0
10	Atrazine	88.5	80.6	54.6	74.8	65.1	68.	58.4
11	Diuron	76.2	66.4	72.5	60.3	56.8	68.6	59.3
12	Propazine	105	87.7	62.2	78.1	78.6	79.8	72.2
13	Terbufos	81.6	87.8	53.4	27.3	48.7	33.4	40.2
14	Diazinon	112	104	84.1	77.8	76.1	81.4	70.1
15	Propanil	92.9	94.5	83.8	60.7	71.5	69.3	54.1
16	Methyl parathion	118	109	85.2	61.3	79.7	65.3	61.5
17	Prometryne	87.0	80.5	61.4	39.9	52.4	38.6	47.5
18	Alachlor	68.7	63.7	53.4	60.5	79.2	86.2	50.0
19	Cyanazine	82.3	78.6	61.3	70.4	80.5	61.8	59.4
20	Linuron	92.7	91.6	65.8	71.4	86.8	52.4	72.9
21	Malathion	89.6	95.4	64.3	75.3	70.4	55.2	67.5
22	Ethyl parathion	106	101	76.8	81.7	98.9	56.3	59.2
23	Captan	82.5	80.3	67.5	75.4	79.6	71.6	89.5
24	MCPA is. ester	56.3	62.6	57.3	58.2	65.2	43.2	34.8
25	Ethion	66	76.8	63.2	72.3	78.4	56.8	50.3

Spiking levels 0.1, 0.25, 1.0, 5, 10, 20 and 50  $\mu\text{g/l}$  ( $n = 3$ ).

with the studied triazines. The organophosphorus compounds (monocrotophos, terbufos, diazinon, methyl parathion, ethyl parathion, malathion and ethion) were also recovered from distilled and underground water samples at relative high levels (62.4–118%) compared with river waters (27.3–98.9%), lake water (41.0–85.2%) and marine water (33.4–81.3%). The substituted ureas (monuron, diuron and linuron), substituted anilines and anilides (trifluralin, propanil, propachlor and alachlor), carbamates (EPTC and carbofuran) and the other compounds studied (molinate, picloram, captan and MCPA is. ester) were recovered at the same level as triazines.

### 3.4. Environmental levels

The water samples analysed were collected in Northern Greece during 1993–94 during periods of pesticide spraying. Screening analysis by GC–FTD showed the presence of monocrotophos, molinate, atrazine, simazine, methyl parathion, ethyl parathion alaclor and captan at low levels. Confirmatory analyses were made with GC–EI–MS. The first sampling was done in August 1993 and the second in June 1994. The concentrations of pesticides are given in Table 5. The levels of monocrotophos, captan and methyl parthion deleted are below the the limits set for drinking water (0.1  $\mu\text{g/l}$ ). The concentrations of moli-



Table 5  
Concentrations of pesticides found in natural waters of Northern Greece (GC-FTD)

Origin of water sample	Compound	Level ( $\mu\text{g/l}$ )	
		August 1993	June 1994
Underground water (Ioannina)	Atrazine	0.009	b.d.l. <sup>a</sup>
	Monocrotophos	0.024	0.015
Pamvotis lake (Ioannina)	Atarazine	0.140	0.085
	Molinate	0.055	0.050
Louros river	Monocrotophos	0.016	b.d.l.
	Simazine	0.135	0.070
	Monocrotophos	0.082	– <sup>b</sup>
Nestos river	Simazine	0.120	– <sup>b</sup>
	Captan	0.080	– <sup>b</sup>
	Molinate	0.150	0.126
Thermaikos gulf	Methyl parathion	0.021	0.034
	Alachlor	0.043	0.065
	Captan	b.d.l.	0.060

<sup>a</sup> b.d.l. = below detection limit.

<sup>b</sup> No sampling.

nate, atrazine and simazine were at the same levels as reported for surface waters in the Mediterranean region [20].

#### 4. Conclusions

In conclusion, the use of Empore extraction discs of  $C_{18}$ -bonded silica provides a rapid, efficient and reproducible method for the simultaneous determination of various pesticides in waters. The identification of 25 selected and first priority pesticides for the Mediterranean region was achieved by their retention times obtained with two GC columns, DB-1 and HP-5, using GC-FTD and from complementary structural information achieved by GC-MS. The use of  $C_{18}$  Empore discs was found to be an effective means for the trace determination of these pesticides in natural waters at detection limit at least ten times below the drinking water limit ( $0.1 \mu\text{g/l}$ ) for individual pesticides. GC-FTD is the best choice for the confirmation of organophosphorus pesticides from natural water samples, being a very selective means of detecting

levels as low as  $0.001 \mu\text{g/l}$ . All the pesticides studied showed lower recoveries from surface natural waters (rivers, lake and sea) than distilled and underground water. The salinity and the total organic compound content increase the interferences in the GC-FTD and GC-MS traces, reaching higher values when analysing surface water samples.

The combination of solid-phase extraction with GC-FTD and GC-MS permits the application of the method to the detection of compounds belonging to different chemical classes. This method can be easily extended to additional compounds, while simpler temperature and SIM programs could be developed for larger numbers of pesticides.

#### Acknowledgements

This work was supported by GGET (General Secretariat of Research and Technology, Athens, Greece), programme PENED/91-ED-601, and was completed in the Department of Physiology, University of Kuopio, Finland.

Professor Osmo Hanninen is thanked for support in the frame of European Science Foundation (ESF) Programme of Research Fellowships in Toxicology, Ref. SVF/94/16/E. J. Tarhanen (Department of Environmental Sciences, University of Kuopio) is thanked for laboratory assistance with the GC–MS instrument.

## References

- [1] D. Barcelo, *J. Chromatogr.*, 643 (1993) 117–143.
- [2] C.D. Watts, L. Clark, S. Hennings, K. Moore and C. Parker, in: B. Crathorne and G. Angeletti (Editors), *Pesticides: Analytical Requirements for Compliance With EC Directives*, Water Pollution Research Report 11, Commission of the European Communities, Brussels, 1989, pp. 16–34.
- [3] D. Barcelo, *Analyst*, 116 (1991) 681.
- [4] G. Font, J. Manes, C.J. Molto and Y. Pico, *J. Chromatogr.*, 642 (1993) 135.
- [5] J. Manes, Y. Pico, C.J. Molto and G. Font, *J. High Resol. Chromatogr.*, 13 (1990) 843.
- [6] A. Ambrus, J. Lantos, E. Visi, I. Csaltos and L. Sarvari, *J. Assoc. Off. Anal. Chem.*, 64 (1981) 733.
- [7] J.S. Andrews and T.J. Good, *Am. Lab.*, 14 (1982) 70.
- [8] T.A. Bellar and W.L. Budde, *Anal. Chem.*, 60 (1988) 2076.
- [9] P.A. Greve and C.E. Goewie, *Int. J. Environ. Anal. Chem.*, 20 (1985) 29.
- [10] G.A. Junk and J.J. Richard, *J. Res. Natl. Bur. Stand. (U.S.)*, 93 (1988) 274.
- [11] J.I. Gomez-Belichon, J.O. Grimalt and J. Albaiges, *Environ. Sci. Technol.*, 22 (1988) 143.
- [12] Z. Frobe, V. Drevenkar, B. Stengl and Z. Stefanac, *Anal. Chim. Acta*, 206 (1988) 299.
- [13] A. Di Corcia and M. Marchetti, *Environ. Sci. Technol.*, 26 (1992) 66.
- [14] V.D. Chmil, T.N. Burushnika and V.K. Pogorelyi, *Zh. Anal. Khim.*, 40 (1988) 1876.
- [15] C. Leuenberger and J.F. Pankow, *Anal. Chem.*, 56 (1984) 2518.
- [16] A. Agostiano, M. Caselli and M.R. Provenzano, *Water Air Soil Pollut.*, 19 (1983) 309.
- [17] D. Barcelo, G. Durand, V. Bounvot and M. Nielen, *Environ. Sci. Technol.*, 27 (1993) 271.
- [18] G. Durand and D. Barcelo, *Talanta*, 40 (1993) 1665.
- [19] M. Fielding, D. Barcelo, A. Helweg, S. Galassi, L. Torstensson, P. Van Zoonen, R. Wolter and G. Angletti, *Pesticides in Ground and Drinking Water*. Water Pollution Research Report 27, Commission of the European Communities, Brussels, 1992, pp. 1–136.
- [20] J.W. Readman, T.A. Albanis, D. Barcelo, S. Galassi, J. Tronczynski and G.P. Gabrielides, *Mar. Pollut.*, 26 (1993) 613.
- [21] M.J.M. Wells and J.L. Michael, *J. Chromatogr. Sci.*, 25 (1987) 345.
- [22] E.R. Brouwer, H. Lingeman and U.A.Th. Brinkman, *Chromatographia*, 29 (1990) 415.
- [23] D. Barcelo, G. Durand, R.J. Vreeken, G.J. de Jong and U.A.Th. Brinkman, *Anal. Chem.*, 62 (1991) 1696.
- [24] S. Lacorte, C. Molina and D. Barcelo, *Anal. Chim. Acta*, 281 (1993) 71.
- [25] D.F. Hagen, C.G. Markell, G.A. Schmitt and D. Blevins, *Anal. Chim. Acta*, 236 (1990) 157.
- [26] A. Kraut-Vass and J. Thoma, *J. Chromatogr.*, 538 (1991) 233.
- [27] O. Evans, B.J. Jacobs and A.L. Cohen, *Analyst*, 116 (1991) 15.
- [28] W.E. Pereira and C.E. Rostad, *Environ. Sci. Technol.*, 24 (1990) 1400.
- [29] W.A. Jury, D.D. Focht and W.J. Farmer, *J. Environ. Qual.*, 16 (1987) 422.
- [30] J.C. Stevenson, T.W. Jones, W.M. Kemp, W.R. Boyton and J.C. Means, in *Proceedings of Workshop on Agrochemicals and Estuarine Productivity*, US Department of Commerce, National Technical Information Service, Washington, DC, 1982, pp. 71–94.
- [31] W. Dedek, K.D. Wencel, F. Luft, H. Overländer and B. Mothes, *Fresenius' J. Anal. Chem.*, 328 (1987) 484.
- [32] J. Akerblom, *J. Chromatogr.*, 319 (1985) 427.
- [33] M. Valls, J.M. Bayona and J. Albaiges, *Int. J. Environ. Anal. Chem.*, 39 (1990) 329.



ELSEVIER

Journal of Chromatography A, 707 (1995) 293–302

JOURNAL OF  
CHROMATOGRAPHY A

# Determination of permethrin and cyfluthrin in water and sediment by gas chromatography–mass spectrometry operated in the negative chemical ionization mode

G.A. Bonwick<sup>a</sup>, C. Sun<sup>b</sup>, P. Abdul-Latif<sup>b</sup>, P.J. Baugh<sup>b,\*</sup>, C.J. Smith<sup>c</sup>,  
R. Armitage<sup>d</sup>, D.H. Davies<sup>a</sup>

<sup>a</sup>Department of Biological Sciences, University of Salford, Salford M5 4WT, UK

<sup>b</sup>Department of Chemistry and Applied Chemistry, University of Salford, Salford M5 4WT, UK

<sup>c</sup>Cortex Diagnostics Ltd., Techbase 1, Newtech Square, Deeside Industrial Park, Deeside, Clwyd. CH5 2NT, UK

<sup>d</sup>National Rivers Authority (Yorkshire Region), Rivers House, 21 Park Square South, Leeds LS1 2QG, UK

First received 27 June 1994; revised manuscript received 13 March 1995; accepted 13 March 1995

## Abstract

Gas chromatography–mass spectrometry operated in the negative chemical ionization mode (GC–NCI–MS) with selected-ion monitoring (SIM) showed both high sensitivity and excellent specificity for permethrin and cyfluthrin. The detection limit for both permethrin and cyfluthrin was 50 fg, whilst a linear response was observed from 50 fg to 80 pg. A sample extraction method using an ultrasonic bath was developed enabling simultaneous processing of multiple samples. Good percentage recoveries of both permethrin and cyfluthrin from spiked sediments were obtained ( $97.3 \pm 4.8\%$  and  $93.9 \pm 5.3\%$ , respectively) and sample clean-up was avoided. These methods were also successfully applied to samples obtained from a contaminated ecosystem, the highest concentrations recorded in water and sediment samples were  $0.048 \mu\text{g l}^{-1}$  and  $305 \mu\text{g kg}^{-1}$ , respectively.

## 1. Introduction

Permethrin and cyfluthrin are both synthetic pyrethroid insecticides. One of the major uses for these pyrethroids is as mothproofing agents for wool and wool-based fabrics by the textile industry. These compounds can enter aquatic ecosystems either by direct discharge, or indirectly within the effluents of sewage treatment works. The toxicity of both permethrin and cyfluthrin to aquatic invertebrates and fish is reflected by the corresponding environmental

quality standards (EQS) of  $0.01 \mu\text{g l}^{-1}$  and  $0.001 \mu\text{g l}^{-1}$ , respectively [1,2]. Thus, there is a need for continuous and accurate monitoring of these pollutants in both effluents and receiving waters if member states are to comply with European Community legislation (76/434/EEC).

Several methods have been previously reported for the determination of permethrin and cyfluthrin residues [3–11]. Most of these are based on either high-performance liquid chromatography (HPLC) or gas–liquid chromatography with electron-capture detection (GC–ECD). These methods are either inefficient or meet with some difficulty when dealing with trace pesticide

\* Corresponding author.

residues in field samples, due to the poor detection limits of the instruments, the presence of background contamination and non-specific chemical interference.

The potential sensitivity of gas chromatography–mass spectrometry operated in the negative chemical ionization mode (GC–NCI–MS) was demonstrated by Hunt et al. [12]. A 10–100 fold increase in sensitivity was obtained over that typically achieved by GC–ECD. A further advantage of GC–NCI–MS is the capability to conduct selected-ion monitoring (SIM), where the instrument is adjusted to collect only ions of one defined mass. Siegel et al. [13] demonstrated a detection limit of 50 pg for permethrin when using GC–SIM–MS. Mattern et al. [14,15] recognized the unique advantage of GC–MS in positive chemical ionization (GC–PCI–MS) and SIM mode. This technique was used successfully for the detection and quantification of pesticides, including permethrin. However, the limits of detection reported for permethrin residues from crop plants ( $0.10\text{--}0.50\ \mu\text{g g}^{-1}$ ) indicated that GC–PCI–MS, even when operated in the SIM mode, would not be suitable for the detection of permethrin and cyfluthrin at, or below, the EQS levels.

In this paper, a GC–NCI–MS method is reported which enabled quantitation of both permethrin and cyfluthrin in water at concentrations which ranged from  $50\ \text{pg l}^{-1}$  to  $500\ \text{ng l}^{-1}$ . In conjunction with an extraction procedure based on the use of an ultrasonic bath, both permethrin and cyfluthrin were successfully detected in spiked stream sediments at concentrations which ranged from  $5\ \text{ng kg}^{-1}$  to  $200\ \mu\text{g kg}^{-1}$ . In comparison to traditional methods such as Soxhlet extraction, the ultrasonic extraction method was more rapid. Simultaneous processing of multiple samples was also performed whilst the problem of cross-contamination, inherent in methods where an ultrasonic probe tip is inserted directly into the sample, was avoided. Good analyte recoveries and detection levels were achieved following 90 min of sonication. In addition, the analyses of permethrin and cyfluthrin in both water and sediments were achieved without recourse to prior sample clean-

up. Through use of the methods reported in this paper, samples obtained from a contaminated aquatic ecosystem were also successfully analysed for both permethrin and cyfluthrin.

## 2. Experimental

### 2.1. Materials

Permethrin [3-phenoxybenzyl-3-(2,2-dichlorovinyl) - 2,2 - dimethylcyclopropanecarboxylate], cyfluthrin [ $\alpha$ -cyano - 3- phenoxy - 4 - fluorobenzyl - 3 - (2,2-dichlorovinyl) - 2,2 - dimethylcyclopropanecarboxylate] and decachlorobiphenyl (DCBP) were of certified purity (British Greyhound, Birkenhead, Merseyside, UK). HPLC grade hexane, analytical reagent grade acetone, dichloromethane, sodium chloride and anhydrous sodium sulphate were obtained from Chem Service (Merck, Lutterworth, Leicestershire, UK).

Clean materials used for recovery and sensitivity studies were previously determined to be free of any of the pesticides in the study. Uncontaminated stream sediments for spiked recovery experiments were obtained from a tributary of the River Tame, Uppermill, Lancashire, UK. Contaminated water and sediment samples were collected from the catchment of the River Calder located at Meltham, Yorkshire, UK. Water samples were collected such that a head space was avoided. Sediment samples were obtained manually as the rocky substrate prevented use of standard sampling apparatus. Glass sample bottles and jars fitted with PTFE-lined caps were used throughout. After collection, samples were transported rapidly to the laboratory where they were stored at  $4^\circ\text{C}$ . Extraction of the samples was performed within 48 h of collection.

### 2.2. Instrumentation

An HP5890 gas chromatograph with a split/splitless injector for capillary columns (Hewlett-Packard, Cheadle Heath, Greater Manchester, UK), combined with a VG TRIO 1000 quadrupole mass spectrometer with EI and PCI/NCI

capability (Fisons Instruments, Wythenshaw, Greater Manchester, UK) was employed.

### 2.3. Gas chromatography and conditions

A fused-silica column, 20 m × 0.32 mm I.D. DBS-MS (Jones Chromatography, Hengoed, UK) was used with helium (CP grade, purity 99.9995%) as the carrier gas (BOC, Eccles, Greater Manchester, UK). Temperature programme: 1.5 min at 100°C, 12°C/min to 300°C, held for 2 min. A 1- $\mu$ l volume of sample was injected manually, applying the hot splitless injection technique with the purge off for 1.5 min.

### 2.4. Mass spectrometric acquisition parameters

Temperature settings: ion source, 250°C; interface line, 250°C. Electron voltage, 70 eV. Scan parameters: scanned mass range, 50–650 a.m.u.; scan rate, 600 a.m.u. in 0.9 s for full scan, 0.2 a.m.u. in 0.08 s for SIM. Solvent delay, 1.5 min. The voltages of the ion repeller, ion focus, ion and electron energies, and the parameters for the quadrupole mass filter were optimised using the negative ion at  $m/z$  452 generated from the calibration compound perfluorotributylamine (PFTBA). Methane (CP grade) was used as the reagent gas (BOC, Eccles, Greater Manchester) at a nominal source pressure of 66.7–133.3 Pa.

### 2.5. Calibration

For long term storage stock solutions of the reference compounds and the volumetric standard, DCBP, were prepared at concentrations of 100 mg l<sup>-1</sup>. Short term storage stock solutions containing reference compounds (1 mg l<sup>-1</sup>) were serially diluted to prepare working standards in the required concentration ranges (0.05  $\mu$ g l<sup>-1</sup> to 80  $\mu$ g l<sup>-1</sup>) which were dispensed daily or as required for use in calibration.

An appropriate amount of volumetric standard stock solution (0.4–4 mg l<sup>-1</sup>) was then added to each to give a final DCBP concentration of 4 and 40  $\mu$ g l<sup>-1</sup>. The standard solutions were subsequently analyzed by GC–NCI–MS operated in

the SIM mode. The ion selected for the detection/quantification of both permethrin and cyfluthrin was  $m/z$  209, whilst for DCBP  $m/z$  498 was chosen. Peak areas were obtained from the mass chromatograms generated for the ions selected for the quantitation of each analyte. For both permethrin and cyfluthrin, calibration curves were obtained from plots of response factor (pesticide peak area/DCBP peak area) against analyte concentration.

Note: The use of DCBP as a volumetric standard is an extension of its use as an external/volumetric standard for analysis by GC–ECD. It is useful in that it elutes at a retention time close to the pyrethroids (narrow retention time window as recommended – US-EPA) and does not interfere chemically – important for pyrethroid specificity and extracts used for ELISA validation. It is also suitably electron affinic and gives therefore a highly reliable and sensitive response (low noise at  $m/z$  498) to MS in NCI-mode operation as with GC–ECD.

DCBP is used for the purpose of correcting for any variation in the sensitivity of the MS instrument and obtaining valid relative response factors.

### 2.6. Preparation of field samples

Water (1 l) was filtered into a separating funnel. Sodium chloride (20 g) was added and the sample acidified (pH 4.0) by the addition of sulphuric acid. Dichloromethane (50 ml) was added and the funnel shaken vigorously for 3 min. The phases were allowed to separate and the lower fraction transferred into a 250-ml conical flask containing anhydrous sodium sulphate (5 g). This extraction procedure was repeated twice and the extracts combined. The extract was evaporated to dryness using a Kuderna–Danish concentrator and the residue redissolved in hexane. After addition of DCBP, the final extract volume was adjusted to 1.0 ml.

Sediment samples from the field were air dried in the laboratory. After drying, the sediment samples were ground and graded through a metal sieve (20 mesh). Dried sediment (10 g) was placed in a 200-ml glass bottle and dichloro-

methane (20 ml) added. The sample was then sonicated (30 min) in Dawe Sonicleaner Type 644 sonic bath (Dawe Instruments, UK). The solvent was passed through a glass sinter (porosity 4) as a filter containing anhydrous sodium sulphate (5 g) into a 250-ml conical flask. The extraction was repeated twice and the extracts combined. Subsequent concentration of the extract was performed as for the water samples (above).

### 2.7. Sample analyses

Samples were analyzed by GC–NCI–MS in the SIM mode. At low pesticide concentration, the  $m/z$  209 and 498 ions were selected for use, due to the lower ion background observed for the  $m/z$  209 ion, than for  $m/z$  207. Peak areas were determined manually using the manufacturer software (LabBase). At high concentration of the pesticides the  $m/z$  207 and 498 ions were selected and peak areas were measured by the software automatically. The threshold for manual intervention in peak area determination is considered below. Because of the nature of the detection, NICI, and the consequent large ion background above which the chromatographic peak for the ion selected for quantitation is observed it is not easy to define the instrument detection limit (DL) in terms of the peak response for which the signal-to-noise ( $S/N$ ) ratio is 2/1. Based on the total ion background valid quantitation can be conducted at signal-to-total ion background ratios considerably less than 2/1 ignoring detector noise which is insignificant for this mode of detection. Here, the DL can be taken as the signal intensity to total ion background intensity ratio in SIM mode obtained for a peak characterised by  $m/z$  207 (cyfluthrin) for a concentration of 50–100 ng l<sup>-1</sup> (equivalent to 50–100 fg μl<sup>-1</sup> injected).

Conventionally area determinations are not carried out at the lowest peak responses near to the DL but at a quantitation limit (QL) about 10 × DL. An assumption could be made that the response for a concentration of 50–100 ng l<sup>-1</sup> at the DL is 3 × S.D. of the background noise ( $S/N = 2/1$ ). Then making a background correc-

tion using the mean of the background response an estimate of the instrument QL could be obtained using the following expression:

$$QL = 10 \times \frac{3S.D. + \text{Mean background}}{\text{Mean response} - \text{mean background}} \\ \times (\text{analyte}) \approx 500 \text{ ng l}^{-1} \text{ (fg } \mu\text{l}^{-1}\text{)}$$

Alternatively, the DL could be based on peak precision favoured by the EPA/FDA. However, we favour considering correlation coefficients obtained by linear regression analysis of the calibration data to validate or invalidate quantitative determination and consequently the threshold for manual intervention in peak area determination (see section 3 for the additional linear regression data included for the lowest concentration range).

Note that the analytical method detection limit depends on the concentration factor possible with the matrix, water or sediment, concerned.

For SIM the collection of ions by the MS was set to 30 s before and after the retention time of the analyte. The diagnostic ions used for permethrin and cyfluthrin were  $m/z$  207, 209, 211, 173, and 171 and for DCBP were  $m/z$  496, 498 and 500.

### 2.8. Recovery studies

Known concentrations of permethrin and cyfluthrin in acetone (0.05–500 ng l<sup>-1</sup>) were spiked into clean water matrices. Spiked water samples were prepared by adding pesticide solution (1 ml) to distilled water (1 l), and then shaking the samples vigorously to ensure mixing. Sediment samples (10 g) were fortified by the addition of pesticide solution (1 ml), followed by shaking for 10 h with protection from light. Sediment samples were kept in the dark for two days prior to extraction. Extraction and analysis of spiked samples was performed as described for the field samples (above).

## 3. Results

Representative mass spectra obtained from the GC–NCI–MS analysis of permethrin and cyflu-

thrin are shown in Fig. 1A,B. A chromatogram of permethrin, cyfluthrin and DCBP is shown in Fig. 1C. A total separation of permethrin into the *cis* and *trans* isomers can be observed as well as four isomers of cyfluthrin. Although the molecular ions of permethrin and cyfluthrin were not observed in the NCI mass spectra, the stabilized carboxylate anions at  $m/z$  207 (209, 211) were detected. This suggested that the pyrethroids in the MS chemical ionization source form stabilized anions by loss of the ester substituent as a neutral fragment.

For both analytes the calibration range extended from  $0.05 \mu\text{g l}^{-1}$  to  $80 \mu\text{g l}^{-1}$ . Peak areas were linearly related to permethrin concentration ( $a = 5.14 \cdot 10^3 \pm 3.65 \cdot 10^{-2}$ ,  $b = 1.27 \cdot 10^4 \pm$

$1.18 \cdot 10^{-3}$ ,  $n = 9$ ) and cyfluthrin concentrations ( $a = 2.09 \cdot 10^4 \pm 4.9 \cdot 10^{-2}$ ,  $b = 5.0 \cdot 10^4 \pm 1.59 \cdot 10^3$ ,  $n = 9$ ). The correlations recorded for both analytes ( $r = 0.999$ ) were significant ( $p < 0.05$ ). We have determined correlation coefficients close to unity for concentrations of both target compounds approaching the detection limit ( $0.05 \mu\text{g l}^{-1} = 0.05 \text{ pg } \mu\text{l}^{-1}$  injected). The linear regression data for the concentration range,  $0.1$ – $0.5 \mu\text{g l}^{-1}$  for the two analytes is as follows: (i) permethrin  $r^2 = 0.977$ ,  $n = 5$ ,  $F = 0.0001$ ,  $A = 3.026 \cdot 10^3 \pm 1.033 \cdot 10^3$ ,  $B = 1.438 \cdot 10^4 \pm 4.191 \cdot 10^2$ ; (ii) cyfluthrin  $r^2 = 1.000$ ,  $n = 5$ ,  $F = 0$ ,  $A = 5.143 \cdot 10^3 \pm 2.07 \cdot 10^{-1}$ ,  $B = 1.272 \cdot 10^5 \pm 8.45 \cdot 10^{-2}$ .

These results demonstrate the validity of linear

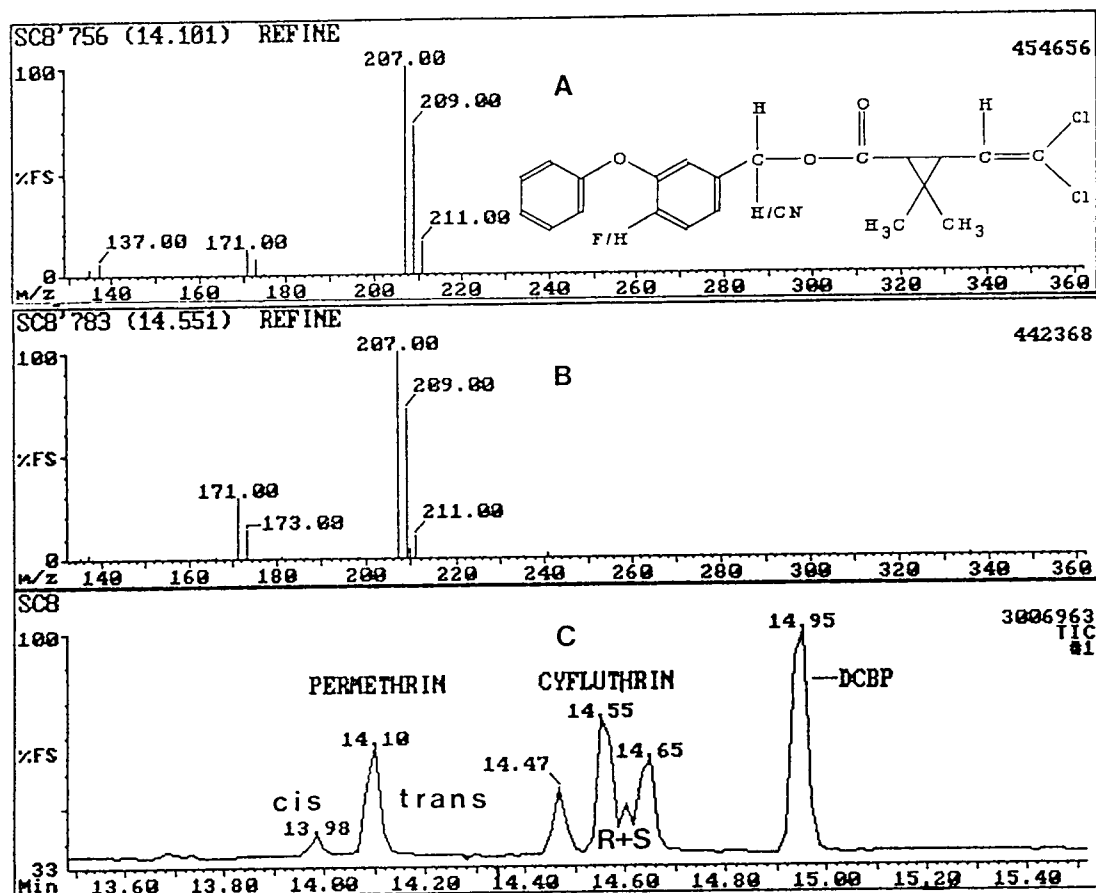


Fig. 1. GC-NCI-MS mass spectra for permethrin (A) and cyfluthrin (B) and the total ion chromatogram (C) of permethrin, cyfluthrin and DCBP indicating *cis/trans* isomers, 2 for permethrin, *R/S* isomers, 4 for cyfluthrin, respectively.

Table 1  
Percentage recoveries of permethrin and cyfluthrin from spiked water samples

Concentration range (ng l <sup>-1</sup> )	Permethrin recovery (%)	Cyfluthrin recovery (%)
0.05–0.5	115.5 ± 7.3 (6)	97.0 ± 10.4 (7)
1.0–5.0	98.4 ± 13.1 (5)	98.4 ± 21.6 (5)
10–50	104.1 ± 16.5 (6)	99.5 ± 6.6 (6)
100–500	101.5 ± 17.5 (6)	101.2 ± 14.0 (5)

Values are expressed as mean percentage recovery ± standard deviation. Values in parentheses denote number of observations,  $n - 1$  used in computation.

regression analysis of the calibration data over an extremely wide dynamic range and importantly when the data at the low end of the concentration range in particular is focused on.

The percentage recoveries of permethrin and cyfluthrin from water are summarised in Table 1. The concentration range of the pesticides fortified was from 50 pg l<sup>-1</sup> to 500 ng l<sup>-1</sup>, a dynamic range over 4 orders of magnitude. The percentage recoveries of permethrin varied from 98.4 ± 13.1% to 115.5 ± 7.3%, and those of cyfluthrin from 97.0 ± 10.4% to 101.2 ± 14.0%.

Table 2 illustrates the percentage recoveries of the pesticides from sediment. The concentration spiked in sediment was from 5 ng kg<sup>-1</sup> to 200 µg kg<sup>-1</sup>, a dynamic range of nearly 5 orders of magnitude. The percentage recoveries of per-

Table 2  
Percentage recoveries of permethrin and cyfluthrin from spiked sediment samples

Concentration range (µg kg <sup>-1</sup> )	Permethrin recovery (%)	Cyfluthrin recovery (%)
0.005–0.05	88.4 ± 21.5 (5)	94.6 ± 7.3 (4)
0.01–0.5	91.5 ± 14.4 (9)	96.3 ± 13.0 (9)
1–5	94.7 ± 15.8 (10)	98.4 ± 12.4 (10)
10–200	82.3 ± 9.7 (10)	90.5 ± 21.4 (10)

Values are expressed as mean percentage recovery ± standard deviation. Values in parentheses denote number of observations. Spiking concentrations expressed in terms of sample dry weights.

methrin ranged from 88.4 ± 21.5% to 94.7 ± 15.8%, whilst those of cyfluthrin ranged from 90.5 ± 21.4% to 98.4 ± 12.4%.

These results are an impressive demonstration of the capabilities of this method for the determination of both permethrin and cyfluthrin in water and stream sediments. Overall, the analysis procedure was considered to be effective for these pesticides when present in such environmental matrices. Although the determination of recoveries in this study has been carried out with reference to authentic compounds analysed in the presence of a volumetric or external standard DCBP (NB internal in the sense that it is present at the analysis stage in the extract examined and as such it can be termed a volumetric standard) other closely associated work of the group has employed a combination of internal and external/volumetric standards for QA/QC purposes [16].

To summarise, mirex was employed as the internal (surrogate) standard and deltamethrin as an external/volumetric standard. %R has been determined for spiked samples of water and sediment. Using ultrasonic extraction several extraction solvent systems have been compared giving comparable results. As examples, the results for sediment spiked at 0.1 and 0.05 mg kg<sup>-1</sup> are included. The %R for permethrin, cyfluthrin and mirex are 124.4 ± 19.6 and 93.7 ± 11.5; 106.5 ± 12.6, 69.8 ± 4.8; 105.2 ± 8.7 and 117.4 ± 8.5, respectively for  $n = 4$  using the relative retention factor (RRF) calculated from calibration curves derived using deltamethrin (50 µg l<sup>-1</sup>) as the external/volumetric standard. These results confirm that the recoveries of permethrin and cyfluthrin are consistent and reliable in satisfactory agreement with the recovery of the internal standard, mirex. It is worth noting that the role of mirex and deltamethrin as standards can be reversed with equivalent results.

Mirex was selected in that study as an internal standard because of its elution in close proximity to the target analytes, the low probability of its environmental occurrence, optimal high mass response ( $m/z$  368) and wide dynamic range.

The utilisation of deltamethrin as an external/



volumetric standard has however been discontinued because of its possible interference in extracts made available for the development and assessment of ELISA for which chemical analysis methods are being employed in data correlation and as a monitor. In addition, it is not the most appropriate standard for NCI-MS in SIM mode in spite of its similar pyrethroid structure because of its prominent response in the low mass region resulting from a favoured fragmentation to yield  $\text{Br}^-$  where the ion background interference is greatest.

This requirement led to the subsequent selection of DCBP as an external/volumetric standard (retention time similar to that of deltamethrin) because of its wide employment and high reliability for sample analysis using ECD, the equivalent conventional GC detection system to NCI-MS. Furthermore, it elutes in a narrow retention window adjacent to the targets, slightly later than cyfluthrin, has maximum response in a high mass region ( $m/z$  498) making it eminently suitable for use in SIM and exhibits a wide linear dynamic range in response. Its use as an external standard has been correlated with that of deltamethrin.

Given the confidence in the %R obtained in the QC work using mirex and deltamethrin in combination and the fact that control sediment had an integrity compatible with that of environmental sediment it was considered valid to use only an external (volumetric standard) in the current work. It is worth noting that the %R for spiked sediment demonstrates a low variance and high reliability comparable with those using mirex and deltamethrin in combination.

An additional problem experienced initially was a persistent low-level contamination by permethrin which affected the validity of %R at low spiking levels. The source of contamination was ultimately traced to the filter paper used for sample preparation. Typically, a single 9-cm diameter filter paper was found to contain approximately 2 ng of permethrin. The use of paper filters during sample preparation was consequently discontinued.

Chemical ionization mass spectrometry often produces only a limited number of ions for each

analyte and is important for obtaining the desired sensitivity. Of even greater importance, selected-ion monitoring offers both qualitative and quantitative methods for several targets in the presence of considerable amounts of interference. The analytical method detection limit for GC-MS in both the SIM and NCI mode for water was  $50 \text{ pg l}^{-1}$  (concentration factor of 1000), whilst for sediment it is thought to be less than  $2 \text{ ng kg}^{-1}$ . Figs. 2A,B shows chromatograms of the same sample under near identical GC-MS conditions, the only difference being that the former was conducted in the full scan mode whilst the latter was performed in the SIM mode. In the full scan mode the individual analytes are not readily discernible without processing to obtain mass chromatograms for  $m/z$  207 and 209 (211). Conversely, the application of SIM (see Fig. 2B highlighting the retention time region 14.0–14.5 min) enables diagnostic detection of the analyte, both from the TIC and mass chromatograms for  $m/z$  207 and 209. From quantitation in the SIM mode the concentration of permethrin was determined to be  $335 \text{ } \mu\text{g kg}^{-1}$ .

Field samples from a contaminated freshwater ecosystem were analysed to assess the performance of these methods when extended to real environmental samples. Field samples were collected from three sites; site A (downstream of an active textile mill), site B (downstream of the effluent discharge from a sewage treatment works) and site C (upstream of the textile mill). These were processed and analysed in an identical fashion to the spiked materials and the concentrations of permethrin and cyfluthrin in both water and sediment samples are recorded in Table 3.

Permethrin was detected in both water and sediment samples from sites A and B. This was expected as both sites were known to have received either direct or indirect inputs of mothproofing agents. Cyfluthrin was not detected at these sites, however this is considered to reflect the pattern of mothproofing agent usage by the local industry rather than a failure of the sampling strategy or quantitative technique employed. The failure to detect either of

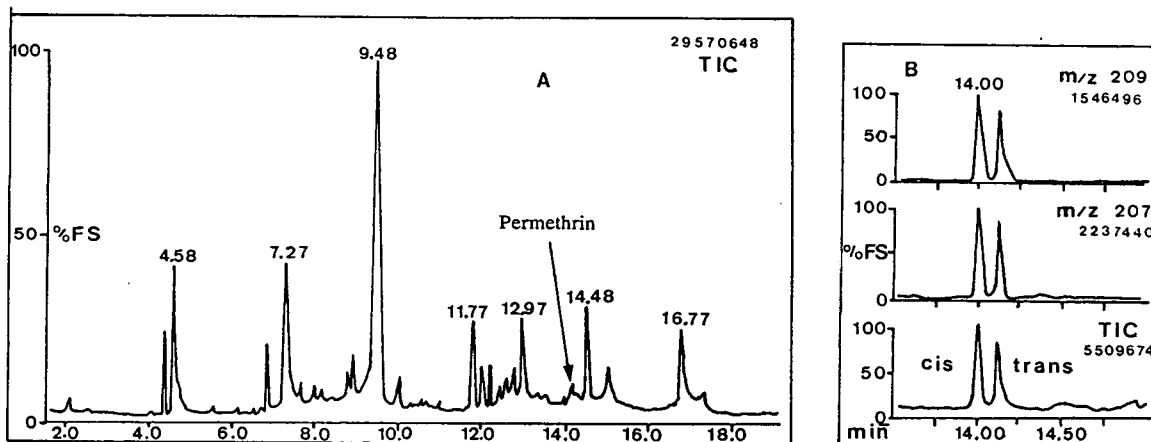


Fig. 2. GC-NCI-MS mass chromatograms of a permethrin contaminated stream sediment. A full scan mode total ion chromatogram (A) fails to show permethrin, the expected position of which is arrowed. Permethrin *cis* and *trans* isomers are revealed in both the total ion chromatogram and mass chromatograms for *m/z* 207 and 209 during operation in the SIM mode (B).

the target analytes at site C was anticipated as this site is not known to have a history of contamination and was therefore expected to be a clean site. This result helped to confirm that the analytical method was not subject to interference and that the prior clean-up of these matrices was unnecessary. Since clean-up can be problematic with losses of analyte it is desirable not to use the extra steps involved in clean-up. The specific quality of the real samples involved allowed us to eliminate clean-up from the procedure. It could be argued that some clean-up is provided by the drying agent anhydrous sodium sulphate which, in addition to removal of water, will remove polar materials which may affect the chromatography. The QC work with spiked samples enables determination of the quality of

the results including the chromatography (efficiency reproducibility) and reliability of the response and tuning of the mass spectrometer.

The concentration of permethrin in the water at both sites A and B was in excess of the EQS value ( $0.01 \mu\text{g l}^{-1}$ ). Sediment values were considerably higher than those recorded for the water samples and indicated that accumulation within the sediment had occurred. Concentration factors for the sediment relative to water at the time of sampling are approximately 10 700 and 7000 for sites A and B, respectively. Although the accumulation of pyrethroids within sediments has been previously demonstrated [17], the concentrations recorded in this study are some of the highest reported for a freshwater ecosystem. EQS values have not been established for

Table 3  
Permethrin and cyfluthrin levels in water and sediment samples from the River Calder catchment

Site	Water samples ( $\mu\text{g l}^{-1}$ )		Sediment samples ( $\mu\text{g kg}^{-1}$ )	
	Permethrin	Cyfluthrin	Permethrin	Cyfluthrin
A	0.020	ND	214.0	ND
B	0.048	ND	335.0	ND
C	ND <sup>a</sup>	ND	ND	ND

Concentrations recorded for sediments expressed in terms of sample dry weights. ND = not detected (lower than the analytical method quantitation limit  $\sim 500 \mu\text{g l}^{-1}$ ,  $5 \text{ ng kg}^{-1}$ ).

aquatic sediments, however it is thought likely that the occurrence of permethrin at such high concentrations will be hazardous to the indigenous benthophagic aquatic organisms.

The ratios of the abundance of the *cis*- and *trans*-permethrin isomers in the sediment samples from sites A and B were different from those observed for the standard material: *cis/trans* ratios of 34:66 and 53:47 were seen in the sediment samples from sites A and B, respectively, whilst in the analytical standard the ratio was generally 25:75. Both photoisomerisation of *cis*-permethrin to *trans*-permethrin and the preferential biodegradation of *trans*-permethrin isomer have been reported [18,19]. It is thought that both mechanisms will have contributed to the increased abundance of the *cis* isomer relative to the *trans* isomer within the environmental samples. This would appear to be supported by the ratio for the site B sediment, where the analyte would have passed through the treatment works and would thus have experienced a much greater biodegradation influence prior to discharge into the aquatic environment.

#### 4. Discussion and conclusions

It has been shown that GC–NCI–MS in the SIM mode is capable of monitoring at or below the EQS level for both permethrin and cyfluthrin in water. These analytes can also be detected in more complex matrices such as stream sediments at levels below the EQS for water. Preliminary studies have shown that this method is also applicable to other complex matrices such as fish tissues and plants, however clean-up procedures are required to remove extracted fats and pigments (data not shown). The performance of this method in relation to aquatic sediments with a higher clay or humic content is also being studied, whilst an extension to the monitoring of sewage sludges is also under consideration. Although EQS levels have not been set for aquatic sediments, recent EEC legislation (93/57/EEC and 93/58/EEC) has defined maximum residue levels (MRLs) for a range of foods and in most cases an MRL of  $0.05 \mu\text{g kg}^{-1}$  has been set. It is

therefore considered that GC–NCI–MS will also prove suitable for monitoring pyrethroids such as permethrin and cyfluthrin when present at, or below, the MRL in such matrices.

Ultrasonic extraction of stream sediments was not only effective and inexpensive, but also simple and rapid. In particular, the time required to extract the pesticides from sediment was less than two hours when an ultrasonic bath was used. Use of the bath was considered advantageous in comparison to an ultrasonic probe method as eight or more samples could be simultaneously extracted, the final number influenced by bath size and container dimensions. An added advantage of the bath over the sonic probe was that cross-contamination of samples was not possible. It is thought that extraction times can be further reduced and an assessment of this parameter is in progress.

During this study, clean sediments were spiked with pesticide in order to examine the effectiveness of the extraction procedure. Clean stream sediments were used because standard materials were not available. Although it may be argued that pesticide spiking and extraction should have been conducted using a standard soil, the relevance of such material to that of the matrix of interest in terms of pesticide-retaining properties and extractibility is doubtful. It is considered that the use of a material which more closely simulates the properties of the target matrix, as in this study, ultimately provides for greater accuracy.

Immunoassay methods such as the enzyme-linked immunosorbent assay (ELISA) have been reported for pyrethroid insecticides such as permethrin [20–23]. Chemical methods are required to validate ELISA performance and the GC–NCI–MS method reported in this paper has been used successfully to assess the performance of a permethrin ELISA [24]. Although ELISA methods offer considerable advantages for environmental monitoring, such as increased sample throughput and on-site testing, they are less sensitive and less specific than methods such as GC–NCI–MS. Despite the higher costs and operative skills required, GC methods will not be superseded but rather supplemented by

ELISA techniques. GC–NCI-MS would appear to provide a useful means of confirming the identity of analytes within samples testing positive during ELISA screening procedures.

Overall, it has been clearly demonstrated that the methods developed during this study for the analysis of spiked samples are also applicable to environmental samples with similar matrix compositions. The SIM method is specific for retention time as well as for characteristic ions ( $m/z$ ). This is not only useful as a tool to confirm the analyses, but also increases the sensitivity of the MS, due to the short scan time. GC–NCI-MS in SIM mode could be widely applied to trace organic analysis, especially for the detection of pesticide residues in complex, ill-defined environmental matrices. GC–NCI-MS in SIM mode should provide a useful tool for the monitoring of toxic haloorganics in the environment. However, it is considered that the GC–NCI-MS method requires further study. In particular, generation of a negative chemical ionisation library would be useful for the rapid identification of pesticides in sample extracts.

### Acknowledgements

This study was conducted as part of an United Kingdom National Rivers Authority (Yorkshire Region) Research Contract (Mothproofing Agents and Water Quality Management, R & D Project Number 319). The authors would like to thank the NRA for permission to reproduce this data.

### References

- [1] T.E. Tooby, Ecotoxicological aspects of water pollution by certain mothproofing agents with reference to Eulan, Mitin and permethrin, Report prepared for the Commission of the European Communities – Environment and Consumer Protection Service, 1981.
- [2] T.F. Zabel, J. Seager and S.D. Oakley, Proposed Environmental Quality Standards for List II Substances in Water, WRC, Marlowe, Buckinghamshire, UK, 1988.
- [3] R.A. Chapman, *J. Chromatogr.*, 258 (1983) 175.
- [4] N. Oi, H. Kithara and R. Kira, *J. Chromatogr.*, 515 (1990) 441.
- [5] Y. Nakamura, Y. Tonogai, Y. Tsumara and Y. Ito, *J. Assoc. Off. Anal. Chem. Int.*, 76 (1993) 1348.
- [6] Y. Nishikawa, *Anal. Sci.*, 9 (1993) 39.
- [7] W.L. Reichel, E. Kolbe and C.J. Stafford, *J. Assoc. Off. Anal. Chem.*, 64 (1981) 1196.
- [8] K.M.S. Sundaram, *Pestic. Sci.*, 31 (1991) 281.
- [9] U. Preiss, P.R. Wallnofer and G. Engelhardt, *Pestic. Sci.*, 23 (1988) 13.
- [10] G.P. Rawn, G.R.B. Webster and D.C.G. Muir, *J. Environ. Sci. Health B*, 17 (1982) 463.
- [11] E. Papadopoulou-Mourkidou and T. Tomazou, *J. Stored Prod. Res.*, 27 (1991) 249.
- [12] D.F. Hunt, G.C. Stafford, Jr., F.W. Crow and J.W. Russell, *Anal. Chem.*, 48 (1976) 2098.
- [13] M.M. Siegel, B.E. Hildebrand and D.R. Hall, *Int. J. Environ. Anal. Chem.*, 8 (1980) 107.
- [14] G.C. Mattern, G.M. Singer, J. Louis, M. Robson and J.D. Rosen, *J. Agric. Food Chem.*, 38 (1990) 402.
- [15] G.C. Mattern, C.H. Liu, J.B. Louis and J.D. Rosen, *J. Agric. Food Chem.*, 39 (1991) 700.
- [16] P. Abdul-Latif, Ph.D. Thesis, University of Salford, 1994.
- [17] C.M. Cooper, *J. Freshwater Ecol.*, 6 (1991) 237.
- [18] G.P. Rawn, G.R.B. Webster and D.C.G. Muir, *J. Environ. Sci. Health B*, 17 (1982) 463.
- [19] M.S. Sharom and K.R. Solomon, *J. Agric. Food Chem.*, 29 (1981) 1122.
- [20] L.H. Stanker, C. Bigbee, J. Van Emon, B. Watkins, R.H. Jensen, C. Morris and M. Vanderlaan, *J. Agric. Food Chem.*, 37 (1989) 834.
- [21] J.H. Skerritt, A.S. Hill, D.P. McAdam and L.H. Stanker, *J. Agric. Food Chem.*, 40 (1992) 1287.
- [22] A.S. Hill, D.P. McAdam, S.L. Edward and J.H. Skerritt, *J. Agric. Food Chem.*, 41 (1993) 2011.
- [23] G.A. Bonwick, M. Putman, P.J. Baugh, C.J. Smith, R. Armitage and D.H. Davies, 2nd International Conference and Industrial Exhibition on Food Safety and Quality Assurance: Use of Antibody Methods, 9–12 September 1993, El Escorial, Spain, *Food & Agricultural Immunology*, 6 (1994) 341.
- [24] G.A. Bonwick, P. Abdul-Latif, C. Sun, P.J. Baugh, C.J. Smith, R. Armitage and D.H. Davies, 2nd International Conference and Industrial Exhibition on Food Safety and Quality Assurance: Use of Antibody Methods, 9–12 September 1993, El Escorial, Spain, *Food & Agricultural Immunology*, 6 (1994) 276.



ELSEVIER

Journal of Chromatography A, 707 (1995) 303-310

JOURNAL OF  
CHROMATOGRAPHY A

# Packed capillary column supercritical fluid chromatography using SE-54 polymer encapsulated silica

Yufeng Shen, Abdul Malik, Wenbao Li, Milton L. Lee\*

*Department of Chemistry, Brigham Young University, Provo, UT 84602, USA*

First received 22 November 1994; revised manuscript received 7 March 1995; accepted 7 March 1995

## Abstract

A new method of preparing stationary phases for packed capillary column supercritical fluid chromatography (SFC) is presented. Surface deactivation of silica particles was carried out by dehydrocondensation of the silicon hydride groups in polymethylhydrosiloxane with the silanol groups on the silica surface. The deactivated particles were then coated with a thin film of SE-54 stationary phase. The coated layer was immobilized by a crosslinking reaction between the methyl groups of the surface-bonded polymethylhydrosiloxane and the SE-54 stationary phase using dicumyl peroxide as a free radical initiator. With these two reactions, the polar groups on the silica surface were more completely capped than with bonding only a monomolecular polymeric layer on the silica surface. The SFC performance of the newly developed packing materials was evaluated using a standard polarity mixture, a series of fatty acid methyl esters, a peppermint oil, and several high-molecular-mass and complex polymers.

## 1. Introduction

Packed capillary column supercritical fluid chromatography (SFC) has the advantages of larger sample capacity and higher plate number per unit time than open tubular column SFC [1,2]. The packing materials used in packed capillary column SFC are the key to obtaining the desirable separation performance. Currently, the most widely used packing materials are silica-based particles. This is because silica particles have good mechanical strength and a narrow size distribution. However, two factors should be considered when choosing particles for columns

in SFC: the polarity and the porosity of the surface of the particles.

The adsorption activity of the silica surface due to silanol groups is a major concern in SFC. Various approaches have been followed to deactivate the packing materials. Using polar organic solvents as modifiers in the supercritical fluid mobile phase can reduce the polarity of the silica packing materials by interaction with the silanol groups. However, this method does not allow the use of flame ionization detection (FID) which is the most desirable detection method for quantitative analysis. A few selected polar compounds such as water or formic acid can be added to the carbon dioxide mobile phase to achieve SFC separation of polar analytes and still retain the use of FID [3,4].

\* Corresponding author.

Deactivation of the silica surface is a common method to obtain less polar packing materials used for the separation of polar analytes. Deactivation can be carried out with a variety of monomeric or polymeric silylation reagents. Using small mono- or multifunctional silylation reagents, it is impossible to completely react with all silanol groups on the silica surface because of steric hindrance [5,6]. A number of reviews have described this in detail [7–9]. The residual silanol groups on the silica surface strongly interact with polar solutes and negatively affect the separation efficiency in SFC [10–12].

A polymer coating and crosslinking method was introduced by Figge et al. [13] for the preparation of packing materials used in reversed-phase high-performance liquid chromatography (LC). The coating was formed by crosslinking of the deposited polymers and by bonding the coating to the presilanized (trimethylsilylated or “pre-capped”) silica particles via free radicals formed from the Si-CH<sub>3</sub> groups which were fixed to the silica surface. With this method, the silanol groups may be either partly eliminated by precapping, or remain unchanged on the surface underneath the coated layer. Schoenmakers et al. [14] and Ashraf-Khorassani et al. [15] compared the polymer-coated particles with other types of packings, and found that the polymer-coated packings had low activity and produced high efficiency in SFC.

Simultaneous deactivation and coating of the porous silica particles for micropacked column SFC was developed by Payne et al. [16]. This method was based on a dehydrocondensation reaction between a home-made polymeric silicon hydride reagent and the silanol groups on the silica surface. The results showed that the procedure generated a less active particle surface than that of a C<sub>18</sub>-bonded stationary phase.

High particle porosity is detrimental in SFC because pores in the silica packing result in significant solute retention, and lead to long analysis times. Partially filling the pores with the polymer coating is a method to decrease the porosity. Recently, an excellent review on the reduction of the porosity of silica particles using

polymers was published [17].

In this paper, we report a new method for the preparation of packing materials used for packed column SFC. Simultaneous deactivation and coating of porous silica particles were carried out by dehydrocondensation of hydride groups on a commercial methylhydrosiloxane polymer and silanol groups on the silica surface. Then, a commercial polysiloxane stationary phase used in gas chromatography, SE-54 (5% diphenyl–94% dimethyl–1% vinyl siloxane), was coated and immobilized on the polymethylhydrosiloxane-deactivated silica surface via a free radical reaction. The effects of the polymer coating and surface deactivation on the polarity and porosity of the packing materials were examined by chromatographic measurements under SFC conditions. Efficient SFC separations of peppermint oil and various commercial high-molecular-mass and complex samples were obtained.

## 2. Experimental

### 2.1. Materials and instrumentation

Porous silica particles (10 μm diameter, 300 Å pore size) and SE-54 stationary phase were purchased from Alltech Associates (Deerfield, IL, USA). C<sub>18</sub>-bonded particles (10 μm diameter, 300 Å pore size) were purchased from Phenomenex (Torrance, CA, USA). Polymeric silicon hydride reagents (polymethylhydrosiloxane and other methylhydrosiloxane polymer and copolymer samples) were purchased from Hüle (Bristol, PA, USA). Polydimethylsiloxane with a molecular mass of 3900 was purchased from Polysciences (Warrington, PA, USA). Fused-silica tubing was purchased from Poly-micro Technologies (Phoenix, AZ, USA). Column connections were made using Valco ZU.T zero dead volume unions (Valco Instruments, Houston, TX, USA). Packing of the capillary columns and the SFC separations were performed using a Lee Scientific Model 600 SFC instrument (Dionex, Salt Lake City, UT, USA).

Peppermint oil was purchased from Berje (Bloomfield, NJ, USA). All other chemicals were purchased from Aldrich (Milwaukee, WI, USA).

### 2.2. Deactivation of porous silica particles

A previously reported reaction vessel [16] was used for the deactivation reaction. Silica particles (0.5 g) were transferred into the reaction vessel and washed with 50 ml of HPLC grade water. The particles were dried with a vacuum pump connected to the vessel. The vessel was placed in a chromatographic oven and connected to an argon gas source (70 ml min<sup>-1</sup>). The oven temperature was increased from ambient to 300°C at 5°C min<sup>-1</sup>, and held at 300°C for 10 h. After cooling, 0.1 g of polymethylhydrosiloxane dissolved in 50 ml of HPLC grade CH<sub>2</sub>Cl<sub>2</sub> was transferred into the reaction vessel. The particles were fluidized in the methylene chloride–polymethylhydrosiloxane solution with bubbling argon (70 ml min<sup>-1</sup>) at ambient temperature. This facilitated uniform coating of the polymethylhydrosiloxane on the silica surface and filling of the pores in the silica particles with the polymer. After evaporating the methylene chloride, the temperature was increased from ambient to 270°C at 5°C min<sup>-1</sup>, and held at 270°C for 20 h to carry out the dehydrocondensation reaction. After cooling, the particles were washed with 50 ml of HPLC grade CH<sub>2</sub>Cl<sub>2</sub> and then dried in argon gas at ambient temperature.

### 2.3. Crosslinking reaction

SE-54 stationary phase (0.075 g) and 0.002 g of dicumyl peroxide were dissolved in 10 ml of HPLC grade CH<sub>2</sub>Cl<sub>2</sub>. The solution and the deactivated particles were introduced into the reaction vessel and fluidized with argon gas (70 ml min<sup>-1</sup>) at ambient temperature. Evaporation of the solvent further covered the silica surface and filled the pores with polymer. The temperature was increased from ambient to 250°C at 2°C min<sup>-1</sup> and held at 250°C for 10 h to carry out the crosslinking reaction, still under an argon gas

purge (70 ml min<sup>-1</sup>). After cooling, the product was washed with 50 ml of HPLC grade CH<sub>2</sub>Cl<sub>2</sub> and dried with argon gas at ambient temperature.

### 2.4. Packing of capillary columns

Fused-silica capillary columns (40 cm × 320 μm I.D.) were packed according to the procedure described in Ref. [18].

## 3. Results and discussion

The conditions of the dehydrocondensation reaction were discussed in detail in Ref. [16]. The reaction temperature selected was 270°C. Free-radical crosslinking is widely used in the preparation of open tubular columns for gas chromatography and SFC [19,20]. Typical conditions were used in this study, and 250°C was selected as the highest temperature for crosslinking.

Chromatographic measurements were made using a test mixture containing four compounds of wide polarity. The polar compounds used were acetophenone, naphthol, benzo(f)-quinoline, and cholesterol. Chromatograms of the polar mixture are shown in Fig. 1. All four polar compounds could be eluted, and relatively good peak shapes were obtained using the column packed with SE-54-coated particles (Fig. 1A). Under the same experimental conditions, only acetophenone could be eluted using the column packed with untreated porous silica particles (Fig. 1C). This illustrates that there is very strong interaction between the polar groups on the silica surface and the -OH or -N= groups in the test solutes. From Figs. 1A and 1B, it can be seen that coating the SE-54 stationary phase on the surface of the polymethylhydrosiloxane-deactivated particles encapsulated the surface further and provided better peak shapes than could be obtained with only polymethylhydrosiloxane-deactivated particles. The different relative peak areas seen in Figs. 1A and 1B could result from irreversible adsorption or differences

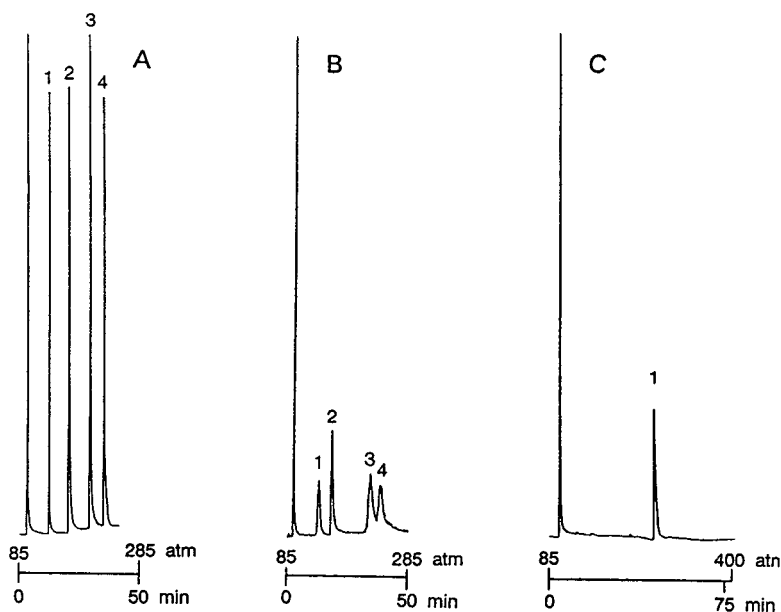


Fig. 1. SFC chromatograms of a mixture of four polar test compounds. Conditions: 40 cm  $\times$  320  $\mu$ m I.D. fused-silica capillary columns packed with (A) silica particles deactivated with polymethylhydrosiloxane and coated and crosslinked with SE-54, (B) silica particles deactivated with polymethylhydrosiloxane only, and (C) untreated porous silica particles; neat CO<sub>2</sub>; 90°C; linear pressure program from 85 atm to 285 atm at 4 atm min<sup>-1</sup>. Peak identifications: 1 = acetophenone, 2 = naphthol, 3 = benzo[*f*]quinoline, 4 = cholesterol.

in split injection when the two columns were investigated.

Fig. 2 shows a chromatogram of weakly polar fatty acid methylesters (FAMEs). Even though the FAMEs are polar, the retention times and pressures needed for their elution can be reduced, and better peak shapes can be obtained, using the column packed with particles that were both polymethylhydrosiloxane-deactivated and SE-54-coated. An apolar sample was used to investigate the effect of porosity on chromatographic performance. The sample used in this test was a polydimethylsiloxane with mean molecular mass of 3900. Fig. 3 shows chromatograms obtained using columns packed with untreated porous silica particles and those encapsulated with SE-54 stationary phase. It can be seen that longer time and higher pressure is needed to elute the sample when the untreated porous silica particles are used. The porous silica particles have a certain range of pore size distribution and a large specific surface area which

produce long retention of the sample. The polymethylhydrosiloxane deactivation reagent and SE-54 stationary phase fill and partially seal the small and deep pores in the silica particles, resulting in reduction of the specific surface area and the solute retention.

The deactivated and coated particles have reduced polarity as well as reduced porosity. A column packed with this packing material can be used to separate polar as well as high-molecular-mass, complex, nonpolar polymers using neat CO<sub>2</sub> as mobile phase. Fig. 4 shows the separation of peppermint oil using columns packed with both untreated porous silica particles and coated particles. A number of peaks seriously tail and few peaks can be obtained using the untreated silica particles as stationary phase. The separation can be greatly improved, leading to reduced analysis time and pressure, using the column packed with polymer-deactivated, SE-54-coated particles. Figs. 5 and 6 demonstrate the separation of a polymethylhydrosiloxane oligo-



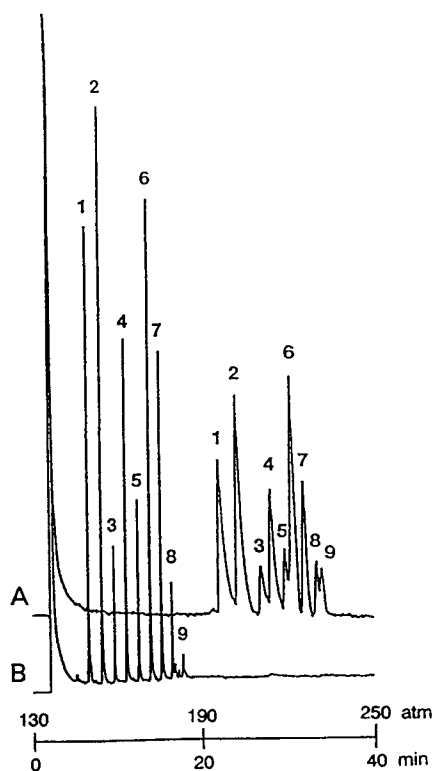


Fig. 2. SFC chromatograms of FAMES. Conditions: 40 cm  $\times$  320  $\mu$ m I.D. fused-silica capillary columns packed with (A) untreated porous silica particles and (B) silica particles deactivated with polymethylhydrosiloxane and coated and crosslinked with SE-54; neat CO<sub>2</sub>; 85°C; linear pressure program from 130 atm to 280 atm at 3 atm min<sup>-1</sup>. Peak identifications: 1 = capric acid methylester, 2 = lauric acid methylester, 3 = myristic acid methylester, 4 = palmitic acid methylester, 5 = stearic acid methylester, 6 = arachidic acid methylester, 7 = behenic acid methylester, 8 = lignoceric acid methylester, 9 = unknown.

mer mixture. With increasing molecular mass, the composition of this polymer becomes very complicated. Fig. 7 shows the separation of a copolymer sample. Using the capillary column packed with the polymer-deactivated, SE-54-coated particles, impressive separations of these high-molecular-mass and complex nonpolar polymers were obtained using neat supercritical CO<sub>2</sub> as mobile phase at pressures lower than 300 atm.

C<sub>18</sub>-bonded phases (ODS) are the most widely used packing materials in packed column SFC. Fig. 8 shows SFC chromatograms of different

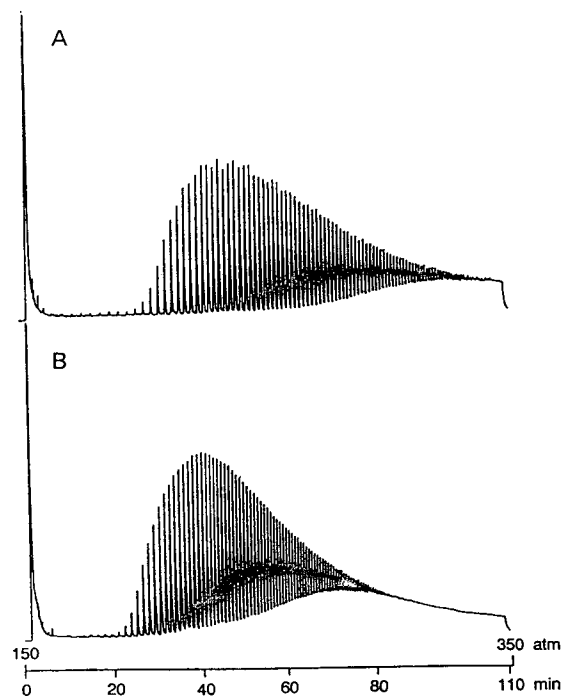


Fig. 3. SFC chromatograms of a polydimethylsiloxane sample (molecular mass 3900). Conditions: 40 cm  $\times$  320  $\mu$ m I.D. fused-silica capillary columns packed with (A) untreated porous silica particles and (B) silica particles deactivated with polymethylhydrosiloxane and coated and crosslinked with SE-54; neat CO<sub>2</sub>; 75°C; linear pressure program from 150 atm to 300 at 1.8 atm min<sup>-1</sup>.

polar compounds on a capillary column packed with ODS particles. Comparing Fig. 8A with Fig. 1, it is clear that ODS particles have stronger polarity than either polymethylhydrosiloxane-deactivated or polymethylhydrosiloxane-deactivated and SE-54-coated particles. Comparing Figs. 8B and 8C with Figs. 2 and 3, it can be seen that for the separation of weakly polar esters and nonpolar polydimethylsiloxanes, there is no significant difference between the columns packed with ODS and SE-54-encapsulated particles except for the longer analysis time needed on the ODS column. These results suggest that ODS particles are suitable for the separation of non- or weakly polar compounds when neat supercritical CO<sub>2</sub> is used as mobile phase. Fig. 8D shows the separation of peppermint oil on a column packed with ODS particles.

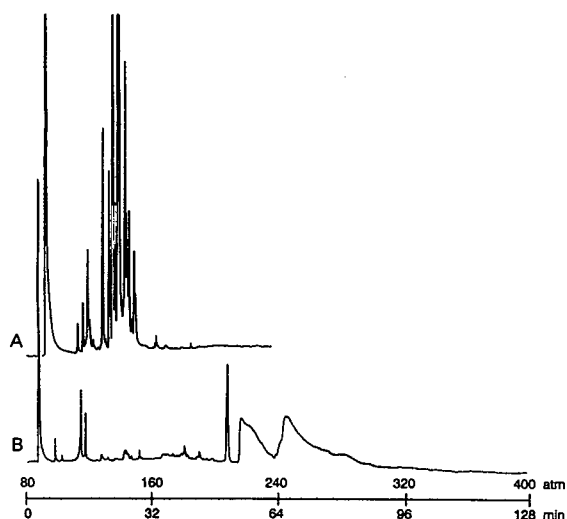


Fig. 4. SFC chromatograms of a peppermint oil. Conditions: 40 cm  $\times$  320  $\mu$ m I.D. fused-silica capillary columns packed with (A) particles deactivated with polymethylhydrosiloxane and coated and crosslinked with SE-54 and (B) untreated porous silica particles; neat CO<sub>2</sub>; 85°C; linear pressure program from 80 atm to 400 atm at 2.5 atm min<sup>-1</sup>.

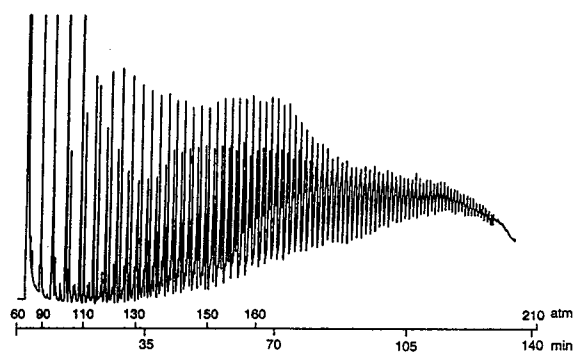


Fig. 6. SFC chromatogram of a polymethylhydrosiloxane sample (molecular mass 2270, PS120). Conditions: pressure program from 60 to 90 atm at 4 atm min<sup>-1</sup>, 90 to 110 atm at 2 atm min<sup>-1</sup>, 110 to 130 atm at 1.6 atm min<sup>-1</sup>, 130 to 150 atm at 1.2 atm min<sup>-1</sup>, and 150 to 300 atm at 1.0 atm min<sup>-1</sup>. Other conditions are the same as in Fig. 5.

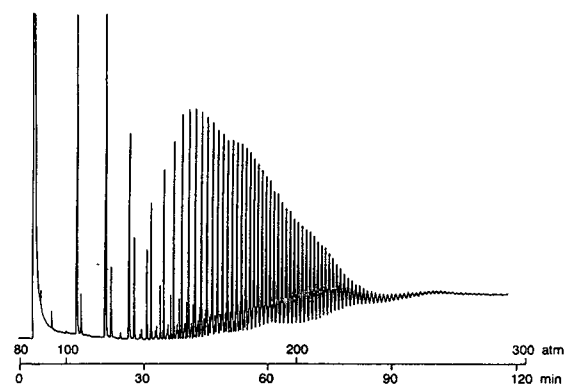


Fig. 5. SFC chromatogram of a polymethylhydrosiloxane sample (molecular mass 1500, PS119). Conditions: 40 cm  $\times$  320  $\mu$ m I.D. fused-silica capillary column packed with particles deactivated with polymethylhydrosiloxane and coated and crosslinked with SE-54; neat CO<sub>2</sub>; 75°C; linear pressure program from 80 atm to 300 atm at 1.8 atm min<sup>-1</sup>.

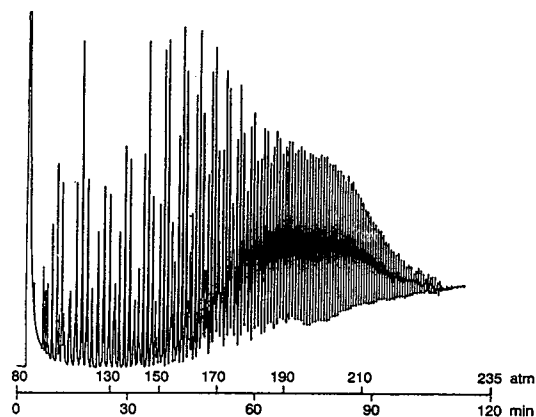


Fig. 7. SFC chromatogram of (30–50%)-methylhydro-(65–70%)-dimethylsiloxane copolymer (molecular mass 2000–2100, PS123). Conditions: 100°C; pressure program from 80 to 130 atm at 2 atm min<sup>-1</sup>, 130 to 170 atm at 1.7 atm min<sup>-1</sup>, 170 to 200 atm at 1.3 atm min<sup>-1</sup>, and 200 to 300 atm at 1.0 atm min<sup>-1</sup>. Other conditions are the same as in Fig. 5.

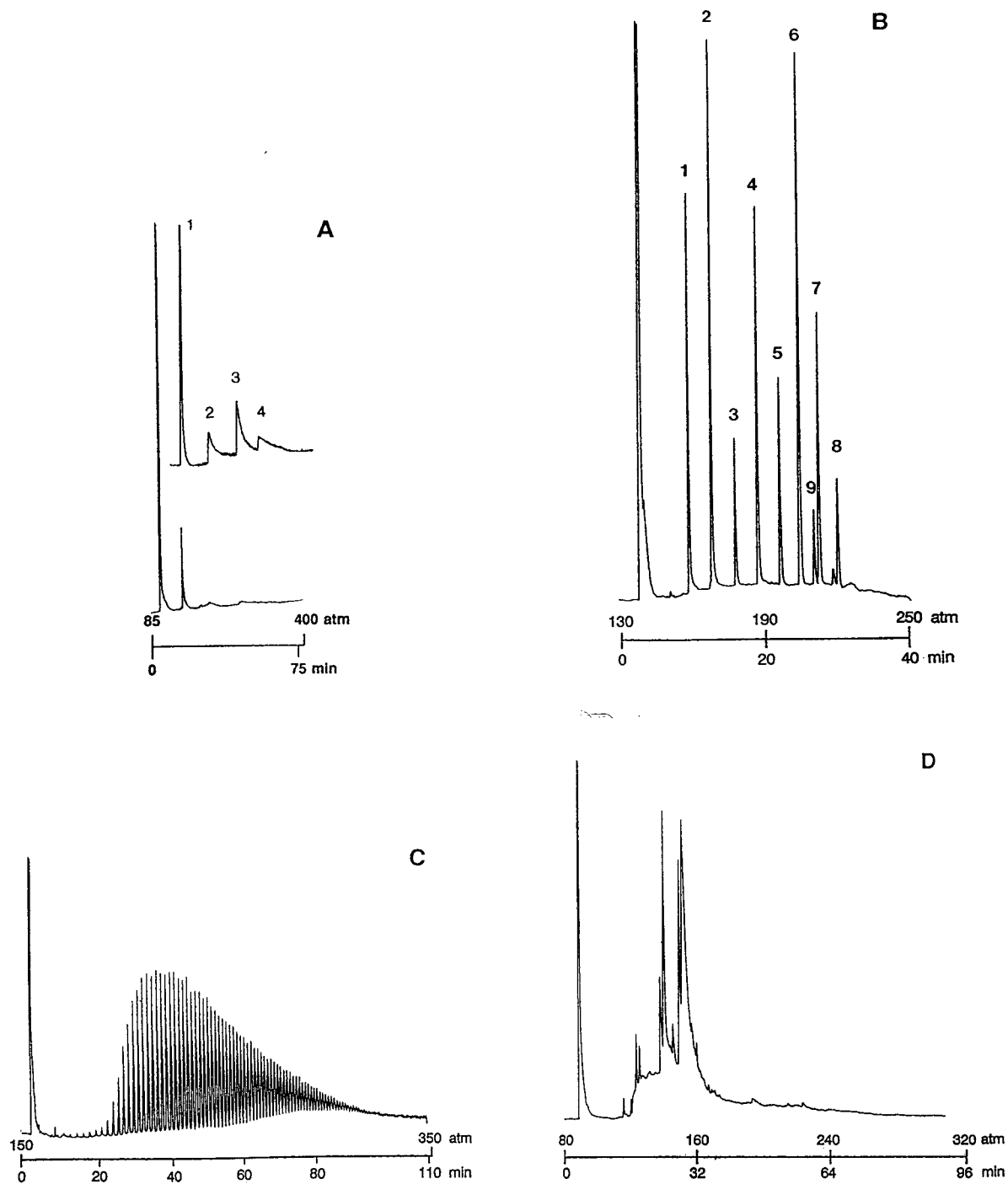


Fig. 8. SFC chromatograms of different polar compounds on a capillary column packed with commercial ODS particles. Conditions: 40 cm  $\times$  320  $\mu$ m fused-silica capillary column packed with ODS particles. Other conditions and peak identifications for (A)–(D) are the same as those in Figs. 1–4, respectively.

Comparing Fig. 4 with Fig. 8D, it can be seen that the column packed with SE-54-encapsulated particles can give much better separation than when packed with ODS particles.

## References

- [1] M.L. Lee and K.E. Markides, Analytical Supercritical Fluid Chromatography and Extraction, Chromatography Conferences, Provo, UT, 1990.
- [2] M.L. Lee and K.E. Markides, *Science*, 235 (1987) 1342.
- [3] F.O. Geiser, S.G. Yocklovich, S.M. Lurcott, J.W. Guthrie and E.J. Levy, *J. Chromatogr.*, 459 (1988) 173.
- [4] J.M. Levy and W.M. Ritchey, *J. Chromatogr. Sci.*, 24 (1986) 242.
- [5] L.C. Sander and S.A. Wise, *CRC Crit. Rev. Anal. Chem.*, 18 (1987) 299.
- [6] K. Jinno and H. Mae, *J. High Resolut. Chromatogr.*, 13 (1990) 512.
- [7] J. Nawrocki and B. Buszewski, *J. Chromatogr.*, 449 (1988) 1.
- [8] B.W. Sands, Y.S. Kim and J.L. Bass, *J. Chromatogr.*, 360 (1986) 353.
- [9] B. Buszewski, D. Berek, J. Garaj, I. Novak and Z. Suprynowicz, *J. Chromatogr.*, 446 (1988) 191.
- [10] T.A. Dean and C.F. Poole, *J. Chromatogr.*, 468 (1989) 127.
- [11] J. Nawrocki, *Chromatographia*, 31 (1991) 177,193.
- [12] A. Nomura, J. Yamada and K.I. Tsunoda, *J. Chromatogr.*, 448 (1988) 87.
- [13] H. Figge, A. Deege, J. Köhler and G. Schomburg, *J. Chromatogr.*, 351 (1986) 393.
- [14] P.J. Schoenmakers, L.G.M. Uunk and H.G. Janssen, *J. Chromatogr.*, 506 (1990) 563.
- [15] M. Ashraf-Khorassani, L.T. Taylor and R.A. Henry, *Chromatographia*, 28 (1989) 569.
- [16] K.M. Payne, B.J. Tarbet, J.S. Bradshaw, K.E. Markides and M.L. Lee, *Anal. Chem.*, 62 (1990) 1379.
- [17] M. Petro and D. Berek, *Chromatographia*, 37 (1993) 549.
- [18] A. Malik, W. Li and M.L. Lee, *J. Microcol. Sep.*, 5 (1993) 365.
- [19] B.W. Wright, P.A. Peaden, M.L. Lee and T.J. Stark, *J. Chromatogr.*, 248 (1982) 17.
- [20] J.C. Fjeldsted and M.L. Lee, *Anal. Chem.*, 56 (1984) 619A.



ELSEVIER

Journal of Chromatography A, 707 (1995) 311–326

JOURNAL OF  
CHROMATOGRAPHY A

# Determination of $\beta$ -cyclodextrin inclusion complex constants for 3,4-dihydro-2-*H*-1-benzopyran enantiomers by capillary electrophoresis

Ph. Baomy, Ph. Morin\*, M. Dreux, M.C. Viaud, S. Boye, G. Guillaumet

Laboratoire de Chimie Bioorganique et Analytique (LCBA), URA CNRS 499, B.P. 6759, Université d'Orléans, 45067 Orléans Cedex 2, France

First received 26 July 1994; revised manuscript received 6 March 1995; accepted 6 March 1995

## Abstract

Chiral separation of 3,4-dihydro-2*H*-1-benzopyran derivatives by capillary zone electrophoresis was achieved by employing  $\beta$ -cyclodextrin ( $\beta$ -CD) as chiral selector. The effects of electrolyte composition ( $\beta$ -cyclodextrin concentration, ionic strength and pH of the buffer) on the migration time, enantioselectivity, peak efficiency and resolution were investigated. As expected, there was an optimum  $\beta$ -CD concentration ( $C_{opt}$ ) which gave maximum enantioselectivity. The stability constant for the  $\beta$ -CD inclusion complex was determined for each enantiomer of two 3,4-dihydro-2*H*-1-benzopyran derivatives. For each solute, the experimental value of  $C_{opt}$  agreed well with the value calculated from the equation  $[C]_{opt} = 1/(K_R K_S)^{1/2}$ , where we used experimental values for the inclusion complex constants ( $K_R, K_S$ ). The enantiomeric separation of three 3,4-dihydro-2*H*-1-benzopyran derivatives was achieved using this optimization method, and baseline separation was obtained in less than 15 min with an efficiency of between 300 000 and 600 000 theoretical plates.

## 1. Introduction

Molecular recognition is a major concept in the understanding of many important chemical interactions such as drug–receptor interactions or enzyme–substrate interactions. For example, many compounds synthesized as potential drugs contain one or several chiral centres; the resulting enantiomers often having different biological activities and different pharmacological effects. Hence it is important to develop chiral separation methods, particularly in the pharma-

ceutical and medicinal areas, for the determination of the optical purity of drugs.

Chiral separation by capillary zone electrophoresis (CZE) or micellar electrokinetic capillary chromatography (MEKC) is a rapidly developing area owing to the high efficiency and resolution that can be achieved and the option of adding molecular recognition agents to the electrolyte [1–8].

This paper describes the chiral separation of several 3,4-dihydro-2*H*-1-benzopyran derivatives by CZE using  $\beta$ -cyclodextrin ( $\beta$ -CD) as a chiral selector, which is added to the running electrolyte. In CZE, the basic thermodynamic dif-

\* Corresponding author.

ferentiation of enantiomers in many chiral systems is poor, which means that the enantioselectivity value is very close to unity, and consequently the need for a high column efficiency is very important.

In this work, we studied the influence of electrolyte properties ( $\beta$ -CD concentration, ionic strength, pH value) and run voltage on the peak efficiency ( $N$ ), enantioselectivity ( $\alpha$ ) and resolution ( $R_S$ ) between two enantiomers. The main objective was to confirm the capability of a capillary electrophoresis technique to determine the  $\beta$ -CD inclusion complex constant of each enantiomer.

## 2. Experimental

### 2.1. Apparatus

All open-tube electrokinetic capillary chromatographic separations were performed with a Spectra-Physics (San Jose, CA, USA) Spectrophoresis 1000 instrument using a 70 cm  $\times$  50  $\mu$ m I.D. silica capillary column. The separations were performed at 25°C at a voltage of +18 kV. The capillaries were conditioned by washing first with 1 M sodium hydroxide (5 min) at 60°C, followed by 0.1 M sodium hydroxide (5 min) at 40°C, water at 40°C and finally with the electrophoretic buffer (60 min). Between consecutive analyses, the capillary tube was flushed with the electrophoretic buffer (5 min) in order to improve the migration time and the peak-shape reproducibility. Analytes were injected on-column using hydrodynamic injection for 1 s. Data were processed with an IBM PS/2 Model 70 386 computer. Software, operating under IBM OS/2, was supplied by Spectra-Physics. The migrating solutes were detected by on-column measurement of UV absorption at 210 nm.

### 2.2. Reagents

All chemicals were of analytical-reagent grade. Disodium hydrogenphosphate (Fluka, Buchs, Switzerland), sodium tetraborate (Fluka), 1 M sodium hydroxide (Fluka), urea (Merck, Darm-

stadt, Germany) and orthophosphoric acid (Sigma, St. Louis, MO, USA) were used. Water used for dilutions and in buffer solutions was on HPLC grade (Carlo Erba, Milan, Italy). The pH was adjusted with orthophosphoric acid.

The  $\beta$ -CD solutions were prepared by dissolving  $\beta$ -CD in 50 mM phosphate–borate buffer containing 8 M urea. Finally, the electrophoretic buffer was filtered prior to use through a polypropylene filter (0.22- $\mu$ m pore size, 25 mm diameter) (Whatman, Maidstone, UK).

Stock standard solutions (100 ppm) were prepared first by dissolving a small amount of each racemic solute in methanol and second by dilution of this methanolic solution in 50 mM phosphate–borate solution (pH 7.0).

The effects of  $\beta$ -CD concentration on the migration time and chiral resolution were observed with three different 3,4-dihydro-2H-1-benzopyran derivatives, 3-(di-*n*-propylamino)chroman (DPAC), 5-methoxy-3-(di-*n*-

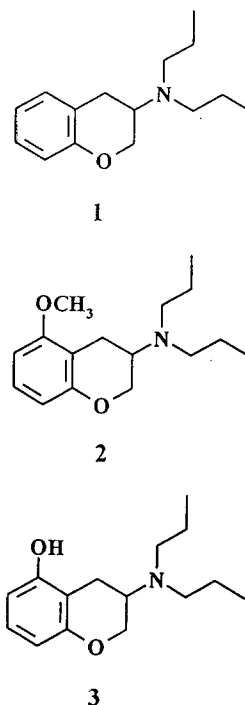


Fig. 1. Structures of the solutes: 1 = DPAC; 2 = 5-MeO-DPAC; 3 = 5-OH-DPAC.

propylamino)chroman (5-MeO-DPAC) and 5-hydroxy-3-(di-*n*-propylamino)chroman (5-OH-DPAC) (Fig. 1). DPAC and 5-MeO-DPAC were prepared in four steps from salicylaldehyde and 2-hydroxy-6-methoxybenzaldehyde, respectively [9,10]. The O-demethylation of 5-MeO-DPAC by refluxing bromhydric acid in acetic acid produced 5-OH-DPAC with a very good yield [9,10]. Investigations on the pharmacological properties of these products indicated that 5-MeO-DPAC and 5-OH-DPAC act in the nM range on 5-HT<sub>1A</sub> sites but are recognized very poorly on other 5-HT sites. Conversely, the non-5-substituted compound DPAC shows a low affinity for all 5-HT sites [10,11].

The resolution ( $R_S$ ) between the two enantiomers has been calculated using the equation  $R_S = 2(t_{m_R} - t_{m_S}) / (w_{b_R} + w_{b_S})$ , where  $t_{m_R}$  and  $t_{m_S}$  are the migration times and  $w_{b_R}$ ,  $w_{b_S}$  the base peak widths of the *R* and *S* enantiomer, respectively. The enantioselectivity ( $\alpha$ ) was calculated using the equation  $\alpha = t_{m_R} / t_{m_S}$  [12,13].

### 3. Results and discussion

#### 3.1. Theoretical model

Formation of inclusion complexes with a chiral selector is a convenient method to resolve enantiomers by CZE. Cyclodextrins and their alkylated derivatives have been successfully used in CE as chiral selectors added to the electrophoretic buffer [1–8]. For example,  $\beta$ -CD is a well known, commercially available cyclic non-reducing oligosaccharide with seven glucopyranose units and is toroidal with a hydrophobic interior cavity. Several workers have developed theoretical models to describe the variation of electrophoretic mobility versus chiral selector concentration [14–19].

According to the cyclodextrin inclusion complex model, developed by Wren and Rowe [14–16], a pair of cationic enantiomers,  $R^+$  and  $S^+$ , interact with the neutral cyclodextrin *C* producing rapid and dynamic chemical equilibria:



where  $m_{R^+}$  is the electrophoretic mobility of the free enantiomer  $R^+$  and  $m_{RC^+}$  is the electrophoretic mobility of the inclusion complex  $RC^+$  between the enantiomer  $R^+$  and the chiral selector *C*.  $K_R$  and  $K_S$  are the inclusion complex stability constants of  $RC^+$  and  $SC^+$  complexes. The model assumes that the electrophoretic mobilities of the complex  $RC^+$  and  $SC^+$  are equal.

If the kinetics of complex formation are rapid enough, the electrophoretic mobility [ $m_{(R)^+}$ ] of enantiomer  $R^+$  (in our study a benzopyran derivative) was determined as the weighted average of the electrophoretic mobility of the free enantiomer ( $m_{R^+}$ ) and the complexed enantiomer ( $m_{RC^+}$ ) with the cyclodextrin *C*, as expressed by the following equation:

$$m_{(R)^+} = \frac{[R^+]}{[R^+] + [RC^+]} \cdot m_{R^+} + \frac{[RC^+]}{[R^+] + [RC^+]} \cdot m_{RC^+} \quad (3)$$

where  $[R^+]$  and  $[RC^+]$  represent the concentration at equilibrium of the free and complexed enantiomers,  $R^+$  and  $RC^+$ , respectively. The apparent mobility of the enantiomer is determined by the proportion of time between when the analyte is free and when it is part of the inclusion complex. The following expression was derived for the calculation of  $m_{(R)^+}$ :

$$m_{(R)^+} = \frac{1}{1 + K_R[C]} \cdot m_{R^+} + \frac{K_R[C]}{1 + K_R[C]} \cdot m_{RC^+} \quad (4)$$

where  $K_R$  is the stability constant of the inclusion complex  $RC^+$  and  $[C]$  is the  $\beta$ -CD concentration at equilibrium. Consequently, the variation of electrophoretic mobility [ $m_{(R)^+}$ ] versus the negative logarithm of the  $\beta$ -CD concentration ( $pC = -\log[C]$ ) allows us to determine the stability constant  $K_R$ . This plot has a similar shape to an

acid–base titration curve where the abscissa of the inflection point is equal to  $\log K_R$  [18].

Penn et al. [17] recently proposed a relationship to calculate the equilibrium constant from electrophoretic mobility measurements at different chiral selector concentrations. Rearrangement of Eq. 4 gives the following relationship:

$$K_R = \frac{m_{R^+} - m_{(R)^+}}{(m_{(R)^+} - m_{RC^+})[C]} \quad (5)$$

The difference between the electrophoretic mobilities of the two enantiomers,  $\Delta m^+ = m_{(S)^+} - m_{(R)^+}$ , can be calculated from the following relationship:

$$\Delta m^+ = \frac{(m_{R^+} - m_{RC^+})(K_S - K_R)}{1 + [C](K_S + K_R) + K_R K_S [C]^2} \cdot [C] \quad (6)$$

Thus, chiral recognition will depend on the difference between the electrophoretic mobilities of each free and complexed enantiomer. The separation cannot be achieved if the difference in the mobilities of the free and the complexed solute is too small. Chiral resolution may be achieved if the two enantiomers have different affinities with the chiral selector and if the exchange between free and complexed forms is very rapid and does not give rise to band broadening [14]. Wren and Rowe [14] showed that maximum separation is achieved for a  $\beta$ -CD concentration  $[C]_{opt}$  of

$$[C]_{opt} = \frac{1}{(K_R K_S)^{1/2}} \quad (7)$$

From experimental data, the electrophoretic

Table 1

Electrophoretic mobilities of the two enantiomers of 3,4-dihydro-2H-1-benzopyran derivatives versus  $\beta$ -CD concentration in the range 1  $\mu$ M–100 mM (not corrected for viscosity)

[ $\beta$ -CD] ( $\mu$ M)	-log[ $\beta$ -CD]	DPAC		5-MeO-DPAC		5-OH-DPAC	
		$m_{epR} \times 10^5$ ( $\text{cm}^2 \text{V}^{-1} \text{s}^{-1}$ )	$m_{epS} \times 10^5$ ( $\text{cm}^2 \text{V}^{-1} \text{s}^{-1}$ )	$m_{epR} \times 10^5$ ( $\text{cm}^2 \text{V}^{-1} \text{s}^{-1}$ )	$m_{epS} \times 10^5$ ( $\text{cm}^2 \text{V}^{-1} \text{s}^{-1}$ )	$m_{epR} \times 10^5$ ( $\text{cm}^2 \text{V}^{-1} \text{s}^{-1}$ )	$m_{epS} \times 10^5$ ( $\text{cm}^2 \text{V}^{-1} \text{s}^{-1}$ )
1	6.00	—	—	8.47	8.47	8.93	8.93
2.5	5.60	—	—	8.47	8.47	8.89	8.89
5	5.30	—	—	8.36	8.36	8.82	8.82
10	5.00	—	—	8.35	8.35	8.76	8.76
25	4.60	—	—	8.61	8.61	8.68	8.68
50	4.30	—	—	8.30	8.30	8.62	8.62
100	4.00	—	—	8.20	8.20	8.59	8.59
250	3.60	—	—	8.28	8.28	8.37	8.37
500	3.30	—	—	7.94	7.94	8.06	7.91
1 000	3.00	—	—	7.60	7.60	7.58	7.30
2 500	2.60	—	—	7.06	6.86	6.37	5.91
5 000	2.30	5.80	5.48	6.19	5.88	5.04	4.48
10 000	2.00	3.86	3.49	4.80	4.39	3.40	2.88
20 000	1.70	1.95	1.67	3.82	3.35	2.37	1.96
30 000	1.52	1.11	0.91	3.17	2.75	1.71	1.35
40 000	1.40	0.72	0.55	2.19	1.86	1.11	0.87
50 000	1.30	0.43	0.31	1.59	1.37	0.83	0.67
60 000	1.22	0.46	0.36	1.23	1.04	0.66	0.50
70 000	1.16	0.15	0.07	1.09	0.93	0.48	0.36
80 000	1.10	0.13	0.13	0.86	0.73	—	—
90 000	1.05	—	—	0.66	0.55	—	—
100 000	1.00	—	—	0.72	0.61	0.35	0.29

Fused-silica capillary column, 70 cm  $\times$  50  $\mu$ m I.D.; applied voltage, +18 kV; buffer, 50 mM phosphate–borate (pH 7.0)– $\beta$ -CD–8 M urea; detection at 210 nm; temperature, 25°C.



mobility [ $m_{(R)^+}$ ] of the enantiomer  $R^+$  was determined using the following equation:

$$m_{(R)^+} = \frac{L_d \cdot L_T}{V} \left( \frac{1}{t_m} - \frac{1}{t_0} \right) \quad (8)$$

where  $L_d$  is the length of the capillary from the inlet to the detector,  $L_T$  is the total length of the capillary,  $V$  is the applied voltage,  $t_m$  is the migration time of the enantiomer and  $t_0$  is the migration time of a neutral marker (methanol).

Calculation of binding constants from CE mobility data requires that any change in mobility at higher chiral selector concentration is due to complexation of the analyte to the selector and also to changes in buffer viscosity. Consequently, electrophoretic mobilities have been corrected according to the expression [20]

$$m_{\text{corr.}(R)^+} = m_{(R)^+} \cdot \frac{\eta_C}{\eta_0} \quad (9)$$

where  $\eta_C$  and  $\eta_0$  are the viscosity of electrolyte with and without  $\beta$ -cyclodextrin addition, respectively. The relative viscosity  $\eta_C$  (in cP) of 8 M urea solutions depends on  $\beta$ -CD concentration according to the following equation at 21°C [21]:

$$\eta_C = 1.50 + 9.58[C] \quad (10)$$

where  $[C]$  is the  $\beta$ -CD concentration (in M).

### 3.2. Determination of optimum concentration of $\beta$ -cyclodextrin

These tertiary amine analytes have ionization constants in the 5–8 pK<sub>a</sub> range and consequently their apparent positive charge depends on their pK<sub>a</sub> value and on the pH of the running electrolyte. The pH value of the electrolyte (pH 7.0) was selected in order to cause the solutes to be partially protonated. Under these conditions, cationic species moved towards the cathode with the velocity of electrophoretic migration plus that of electroosmotic flow.

The effects of  $\beta$ -CD concentration on the migration time and on the chiral resolution of 5-MeO-DPAC and 5-OH-DPAC enantiomers were investigated using 50 mM phosphate–borate buffer (pH 7.0) containing both 8 M urea

and  $\beta$ -CD at concentrations varying from 1  $\mu$ M up to 100 mM. Urea was added to the cyclodextrin solutions to increase their solubilities. For each of the 22  $\beta$ -CD concentration values, the separation was performed in triplicate from consecutive injections to obtain an average value for the electrophoretic parameters of each enantiomer (Tables 1 and 2). The influence of the selector concentration on the electrophoretic mobility of each 5-OH-DPAC enantiomer is shown in Fig. 2a. As the  $\beta$ -CD concentration increases, the free enantiomer fraction becomes smaller and consequently the electrophoretic mobility is reduced. At the micromolar level of  $\beta$ -CD concentration (1–100  $\mu$ M), no enantio-separation occurred because the benzopyran derivative enantiomers were not complexed (Fig. 3a and b). The electrophoretic mobilities of free enantiomers were  $8.47 \cdot 10^{-5} \text{ cm}^2 \text{ V}^{-1} \text{ s}^{-1}$  for 5-MeO-DPAC and  $8.93 \cdot 10^{-5} \text{ cm}^2 \text{ V}^{-1} \text{ s}^{-1}$  for 5-OH-DPAC. At the millimolar level of  $\beta$ -CD

Table 2  
Complexation degree of each 5-OH-DPAC enantiomer versus  $\beta$ -CD concentration in the range 1  $\mu$ M–100 mM (not corrected for viscosity)

[ $\beta$ -CD] ( $\mu$ M)	–log[ $\beta$ -CD]	5-OH-DPAC	
		$x_R$	$x_S$
1	6.00	0.00	0.00
2.5	5.60	0.45	0.45
5	5.30	1.23	1.23
10	5.00	1.90	1.90
25	4.60	2.80	2.80
50	4.30	3.47	3.47
100	4.00	3.81	3.81
250	3.60	6.27	6.27
500	3.30	9.74	11.42
1000	3.00	15.12	18.25
2500	2.60	28.67	33.82
5000	2.30	43.56	49.83
10000	2.00	61.93	67.75
20000	1.70	73.46	78.05
30000	1.52	80.85	84.88
40000	1.40	87.57	90.26
50000	1.30	90.71	92.50
60000	1.22	92.61	94.40
70000	1.16	94.62	95.97
100000	1.00	96.00	96.75

Conditions as in Table 1.

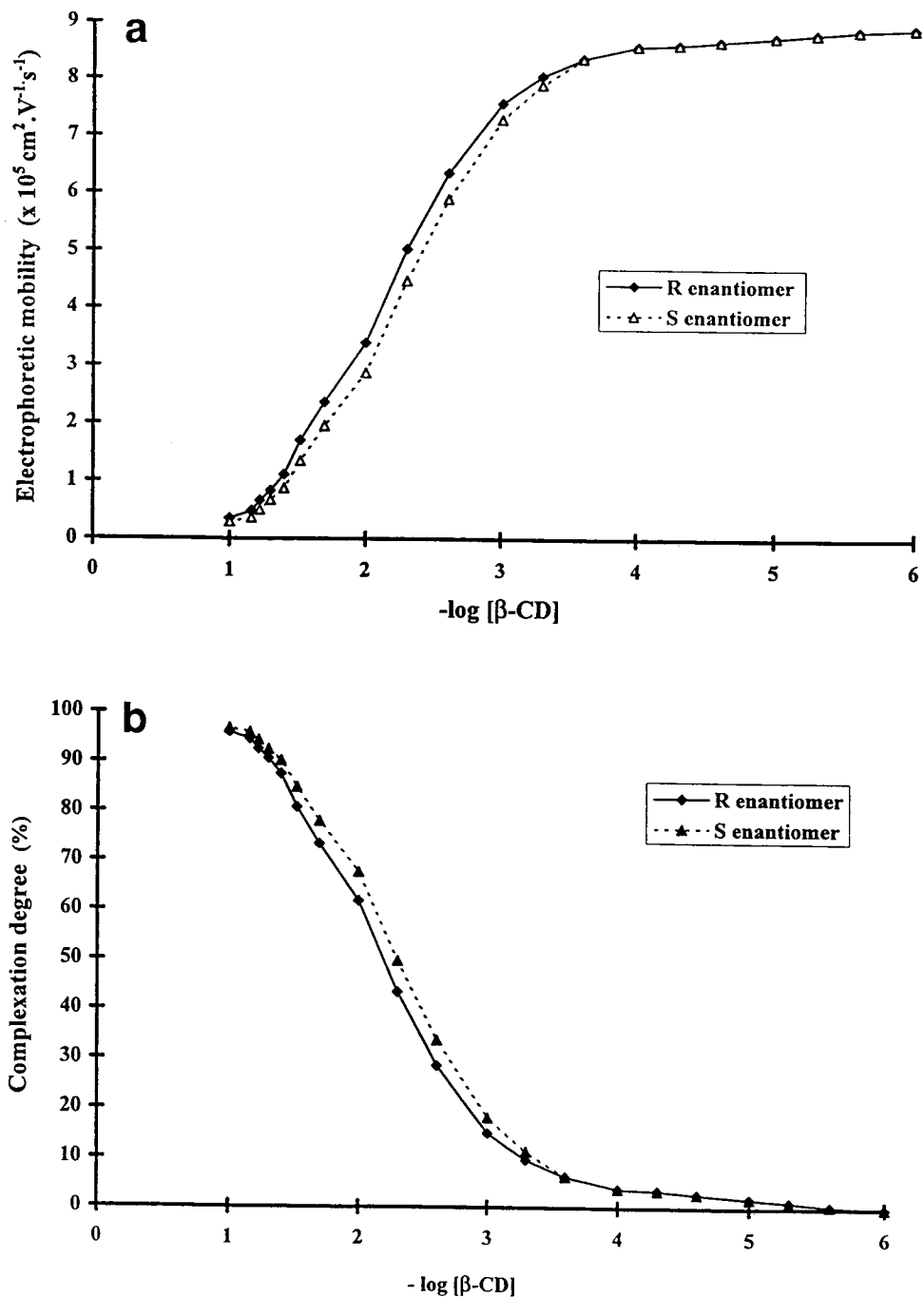


Fig. 2. (a) Variation of the electrophoretic mobility of each the two enantiomers of 5-OH-DPAC versus  $-\log[\beta\text{-CD}]$ . (b) Variation of the degree of complexation ( $x$ ) for each enantiomer of 5-OH-DPAC versus  $-\log[\beta\text{-CD}]$ . Fused-silica capillary column, 70 cm  $\times$  50  $\mu\text{m}$  I.D.; applied voltage, +18 kV; buffer, 50 mM phosphate-borate (pH 7.0)- $\beta$ -CD-8 M urea; detection at 210 nm; temperature, 25°C.

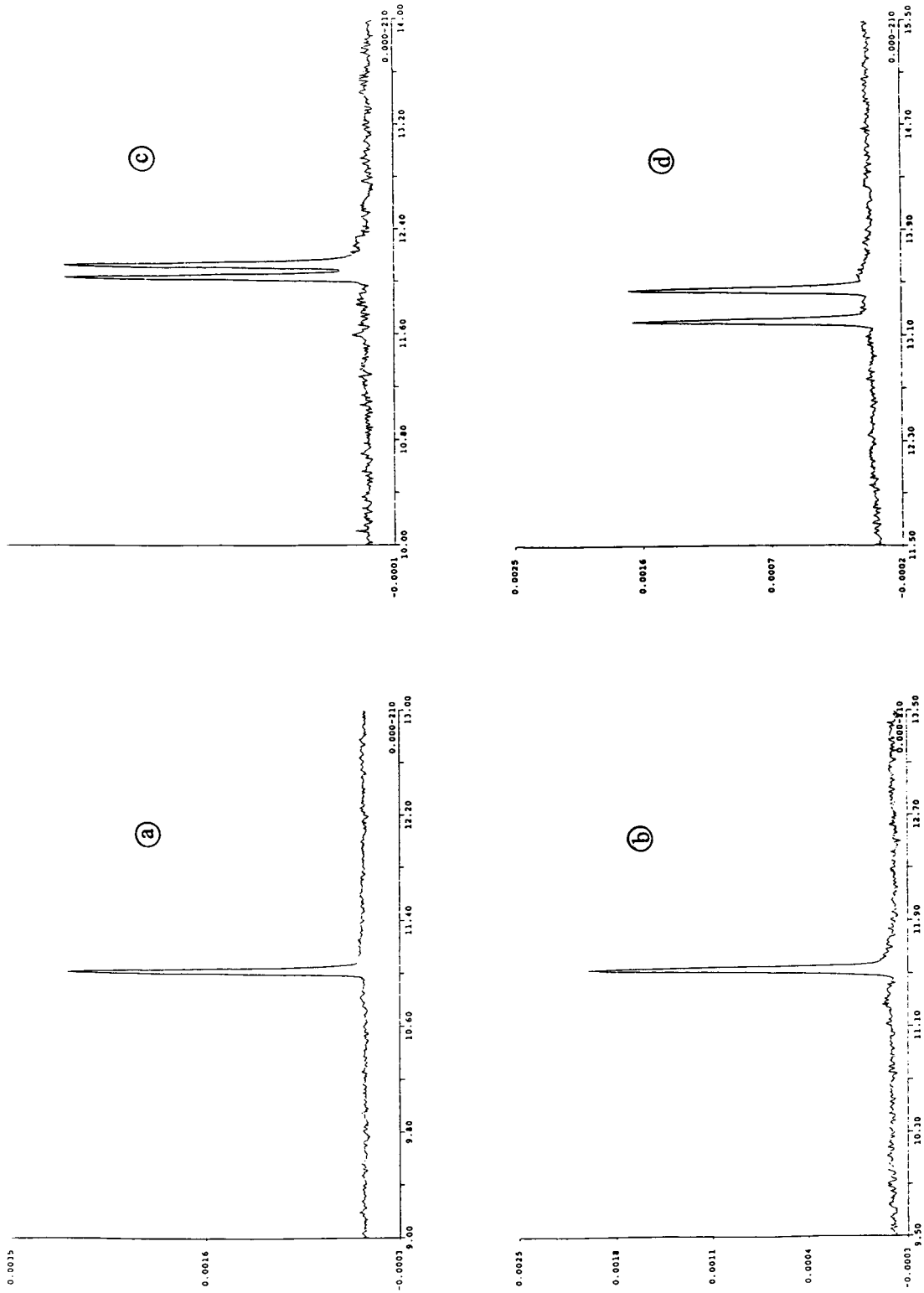


Fig. 3. Effect of  $\beta$ -CD concentration on the enantioseparation of 5-OH-DPAC. Fused-silica capillary column, 70 cm  $\times$  50  $\mu$ m I.D.; applied voltage, +18 kV; buffer, 50 mM phosphate-borate (pH 7.0)- $\beta$ -CD-8 M urea; detection at 210 nm; temperature, 25°C.  $\beta$ -CD concentration: (a) 1  $\mu$ M; (b) 100  $\mu$ M; (c) 1  $\mu$ M; (d) 5 mM.

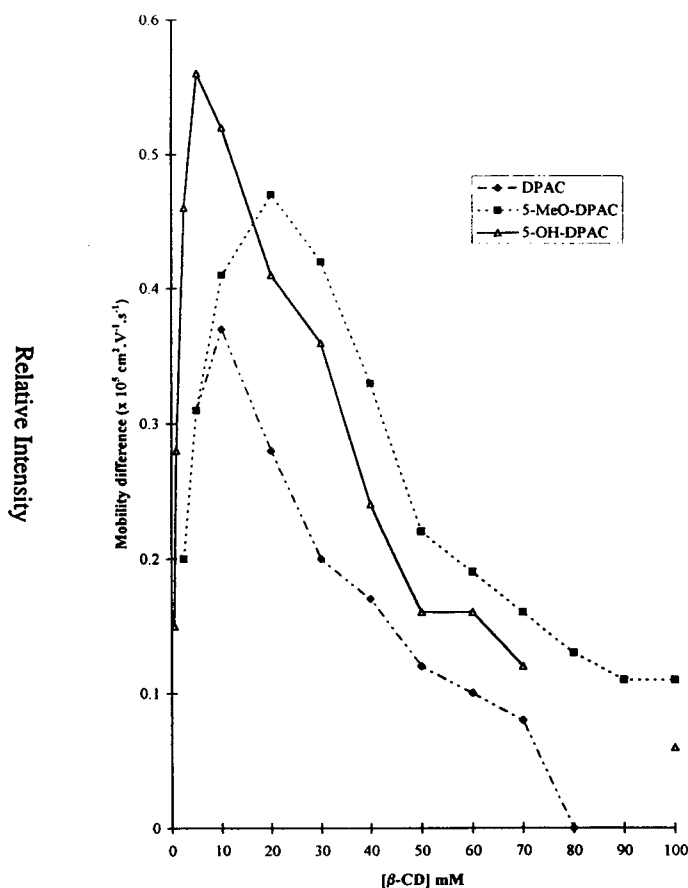


Fig. 4. Determination of the optimum concentration of  $\beta$ -CD for the CZE enantioseparation of three 3,4-dihydro-2H-1-benzopyran derivatives. Fused-silica capillary column, 70 cm  $\times$  50  $\mu$ m I.D.; applied voltage, +18 kV; buffer, 50 mM phosphate-borate (pH 7.0)- $\beta$ -CD-8 M urea; detection at 210 nm; temperature, 25°C.

concentration (1–5 mM), the electrophoretic mobility of each enantiomer decreased with increasing complexation percentage and a baseline resolution of the two enantiomers was achieved (fig. 3c and d). The solubility of  $\beta$ -CD, which is only 16 mM in the aqueous phase, can be considerably increased by the addition of urea at a high molar concentration. Therefore, a 100 mM concentration of  $\beta$ -CD dissolved in the phosphate-borate buffer (pH 7.0) with an 8 M urea concentration was used. Even at this extreme  $\beta$ -CD concentration, the electrophoretic mobility of the two enantiomers of 5-OH-DPAC are not yet equal ( $0.35 \cdot 10^{-5}$  and  $0.29 \cdot 10^{-5}$  cm<sup>2</sup> V<sup>-1</sup> s<sup>-1</sup>). In fact, the lower part of the curves in

Fig. 2a, which corresponds to the complexed form, could be only reached at chiral selector concentrations higher than 100 mM. The complexed forms of 5-OH-DPAC and 5-MeO-DPAC have electrophoretic mobilities of ca. 20 and 12, respectively, times smaller than that of the free form, as a consequence of the smaller effective charge to hydrodynamic radius ratio.

However, the complexation process may be easily followed by the degree of complexation  $x$  of the enantiomer  $R^+$ , defined as

$$x = \frac{[RC^+]}{[R^+] + [RC^+]} = \frac{m_{R^+} - m_{(R)^+}}{m_{R^+} - m_{RC^+}} \quad (11)$$

Table 3  
 $\beta$ -Cyclodextrin inclusion constants ( $K_R$ ,  $K_S$ ) for enantiomers of two 3,4-dihydro-2*H*-1-benzopyran derivatives determined by capillary electrophoresis. Conditions as in Table 1.

Solute	$K_R$ ( $M^{-1}$ )	$K_S$ ( $M^{-1}$ )	$C_{opt}^a$ (mM)	$C_{opt}^b$ (mM)
5-MeO-DPAC	58	72	18.2	15.5
5-OH-DPAC	138	166	6.4	6.6

The electrophoretic mobilities were corrected according to Eqns. 9 and 10.

<sup>a</sup> Experimentally determined from Fig. 4.

<sup>b</sup> Calculated from Eq. 7.

where  $m_{RC^+}$ ,  $m_{R^+}$  and  $m_{(R)^+}$  are the electrophoretic mobilities of the complexed enantiomer, of the free form and of the partially complexed enantiomer  $R^+$  by the  $\beta$ -CD (concentration [C]), respectively. The variation of degree of 5-OH-DPAC complexation versus  $-\log[\beta\text{-CD}]$  is shown in Fig. 2b. If two enantiomers are both complexed at 3.8% at 100  $\mu\text{M}$   $\beta$ -CD concentration, their degrees of complexation become different at 5 mM (44% and 50% for *R*- and *S*-enantiomers, respectively).

The difference between the electrophoretic mobility of each enantiomer ( $\Delta m^+$ ) was plotted against the chiral selector concentration for each of the three 3,4-dihydro-2*H*-1-benzopyran derivatives (Fig. 4). The enantiomeric resolution depends on the concentration of the chiral selector in the electrolyte. As expected, there is an optimum  $\beta$ -CD concentration ( $C_{opt}$ ), which leads to a maximum  $\Delta m^+$  value and, hence, to an optimum enantioselectivity. The experimen-

tally determined optimum  $\beta$ -CD concentrations for DPAC, 5-MeO-DPAC and 5-OH-DPAC were 9.3, 18.2 and 6.4 mM, respectively. Further increases in  $\beta$ -CD concentration resulted in a decrease in resolution (at 100 mM  $\beta$ -CD, the resolution decreased dramatically). This behaviour agrees well with what is predicted by Eq. 7.

From Fig. 2a, the inclusion complex stability constant can be determined from the  $x$ -value of the inflection point, according to Eq. 4. The resulting  $K$  values are summarized in Table 3. Although the interior cavity size of  $\beta$ -CD fits reasonably well with the steric volume of such solutes having a benzopyran moiety, the inclusion complex of these molecules with  $\beta$ -CD appears to be of moderate stability. The magnitude of the equilibrium constant also influences the migration order. For solutes which are positively charged below pH 7.0, the *R*-enantiomer with the lower equilibrium constant will elute first. These values are approximately two orders of magnitude higher than the equilibrium constants calculated by Valko et al. [19] for the complexation of mandelic acid enantiomers and  $\gamma$ -CD (2.8 and 2.4  $M^{-1}$ ). In this particular case, the  $\gamma$ -CD had an interior cavity too large for the mandelic acid enantiomers. A better steric fit was reported by Penn et al. [17] with equilibrium constants for the complexation of tioconazole and hydroxypropyl- $\beta$ -cyclodextrin of 201 and 231  $M^{-1}$ , respectively. The theoretical model predicts that the optimum concentration for the chiral selector ( $C_{opt}$ ) depends on the inclusion constant of each enantiomer ( $K_R$  and  $K_S$ ) as expressed by Eq. 7. The experimentally deter-

Table 4  
 Determination of enantioseparation parameters of three 3,4-dihydro-2*H*-1-benzopyran derivatives at optimum  $\beta$ -CD concentration ( $C_{opt}$ )

Solute	$[\beta\text{-CD}]$ (mM)	$t_{mR}$ (min)	$t_{mS}$ (min)	$N_R$	$N_S$	$\alpha$	$R_s$	$\Delta(m^+) \times 10^5$ ( $\text{cm}^2 \text{V}^{-1} \text{s}^{-1}$ )
DPAC	9.3	12.89	13.04	403 000	322 000	1.012	1.72	0.37
5-MeO-DPAC	18.2	11.72	11.88	423 000	423 000	1.014	2.61	0.47
5-OH-DPAC	6.4	13.20	13.44	640 000	604 000	1.018	3.57	0.55

Migration time ( $t_m$ ), efficiency ( $N$ ), enantioselectivity ( $\alpha$ ), resolution ( $R_s$ ) and the difference in electrophoretic mobilities of two enantiomers ( $\Delta m^+$ ). Conditions as in Table 1.

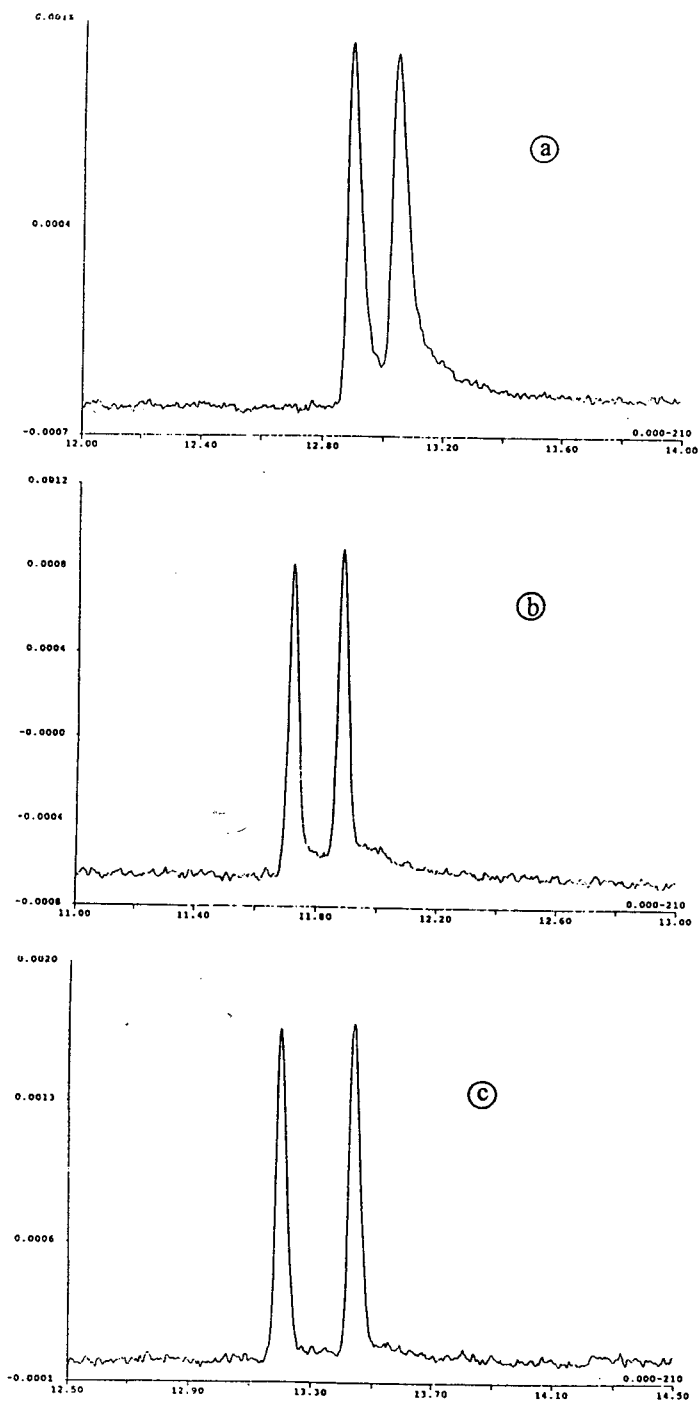


Fig. 5. Enantioseparation of three 3,4-dihydro-2H-1-benzopyran derivatives at the optimum  $\beta$ -CD concentration ( $C_{opt}$ ). Fused-silica capillary column, 70 cm  $\times$  50  $\mu$ m I.D.; applied voltage, +18 kV; buffer, 50 mM phosphate-borate (pH 7.0)- $\beta$ -CD-8 M urea; detection at 210 nm; temperature, 25°C. Solutes: (a) DPAC ( $C_{opt}$  = 10 mM); (b) 5-MeO-DPAC ( $C_{opt}$  = 20 mM); (c) 5-OH-DPAC ( $C_{opt}$  = 6 mM).

mined  $C_{opt}$  value for 5-OH-DPAC agrees well with the calculated value from the previous equation in which we used experimental values for the inclusion constants (Table 3). The two enantiomers of 5-OH-DPAC have higher  $K$  values (138 and 166) than those of 5-MeO-DPAC (58 and 72), which means that for an optimum separation a lower  $\beta$ -CD concentration is required.

The separation parameters, migration time, efficiency, enantioselectivity, resolution and difference in electrophoretic mobilities of the two enantiomers of the three 3,4-dihydro-2*H*-1-benzopyran derivatives, calculated at the optimum  $\beta$ -CD concentration, are given in Table 4. The very high efficiency (320 000–640 000 theoretical plates) of this method allows the separation of these enantiomers (e.g.,  $R_s = 3.57$  between the two enantiomers of 5-OH-DPAC) with even a small enantioselectivity ( $\alpha = 1.018$ ), which is normally the limiting factor in chiral separations.

Under the optimum analytical conditions, the enantioseparation of each of the 3,4-dihydro-2*H*-1-benzopyran derivatives was achieved in less than 15 min (Fig. 5), with peak efficiencies one order or more higher than are usually encountered in HPLC.

### 3.3. Influence of phosphate–borate concentration

The effects of buffer ionic concentration on the migration time and chiral resolution of 5-

OH-DPAC were evaluated with phosphate–borate buffer (pH 7.0) at the optimum  $\beta$ -CD concentration (6 mM). Table 5 shows the variation of migration times, peak efficiency and resolution when the buffer concentration varies from 10 up to 50 mM. As expected, an increasing ionic strength results in a longer migration time owing to a slower electroosmotic flow and a reduced electrophoretic mobility of the ionic solute. The migration time of 5-OH-DPAC increases from 8 to almost 12 min as the phosphate–borate buffer concentration increases from 10 to 50 mM (Fig. 6a–c). Working with a high ionic strength buffer (50 mM) generates a better resolution owing to a large improvement in peak efficiency whilst the enantioselectivity remains approximately constant ( $\alpha = 1.014$ ), as shown in Fig. 6d and e. Using 50 mM rather than 10 mM phosphate–borate buffer, the electrophoretic parameters were 0.3%, 450% and 193% higher for enantioselectivity, efficiency and resolution, respectively. Since the solutions of 3,4-dihydro-2*H*-1-benzopyran derivatives were dissolved in 50 mM phosphate–borate buffer (pH 7.0), no stacking phenomenon occurred as the conductivity of the sample was significantly higher than that of the running buffer. Nevertheless, a buffer of higher ionic strength may perhaps promote the inclusion of the solute hydrophobic moiety into the interior cavity of the  $\beta$ -CD, and hence increase the efficiency.

Further studies are in progress to investigate the effect of the ionic strength of the buffer on the electrophoretic separation performance.

Table 5  
Effect of phosphate–borate buffer concentration on the enantioseparation parameters of 5-OH-DPAC resolved by capillary electrophoresis

Buffer concentration (mM)	$t_{mR}$ (min)	$t_{mS}$ (min)	$t_0$ (min)	$m_{epR} \times 10^5$ (cm <sup>2</sup> V <sup>-1</sup> s <sup>-1</sup> )	$m_{epS} \times 10^5$ (cm <sup>2</sup> V <sup>-1</sup> s <sup>-1</sup> )	$N_R$	$N_S$	$\alpha$	$R_s$
10	7.81	7.92	8.90	6.4	5.7	134 000	110 000	1.014	1.18
25	8.70	8.81	10.31	7.3	6.7	403 000	358 000	1.013	1.94
50	11.44	11.64	13.08	4.5	3.9	681 000	658 000	1.017	3.46

Buffer: phosphate–borate (pH 7.0)–6 mM  $\beta$ -CD–8 M; other conditions as in Table 1.

More information is required for a better understanding of the molecular interactions (hydrophobic or H-bonding types) which influence molecular chiral recognition.

### 3.4. Influence of buffer pH

The influence of buffer pH on the resolution of 5-OH-DPAC enantiomers was studied in the

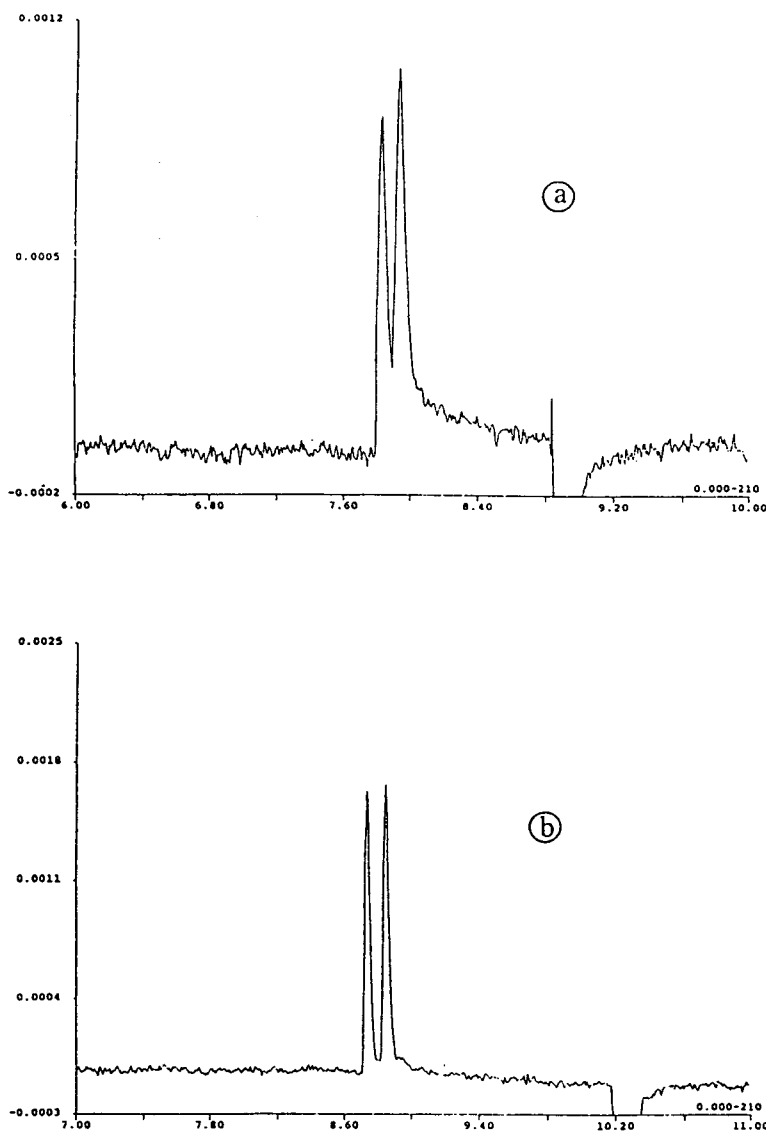


Fig. 6. Effect of phosphate-borate concentration [(a) 10, (b) 25 and (c) 50 mM] on enantioseparation of 5-OH-DPAC by CZE. Effect of phosphate-borate concentration on (d) efficiency and (e) resolution of 5-OH-DPAC by CZE. Fused-silica capillary column 70 cm  $\times$  50  $\mu$ m I.D.; applied voltage, +18 kV; buffer, phosphate-borate (pH 7.0)–6 mM  $\beta$ -CD–8 M urea; detection at 210 nm; temperature, 25°C.



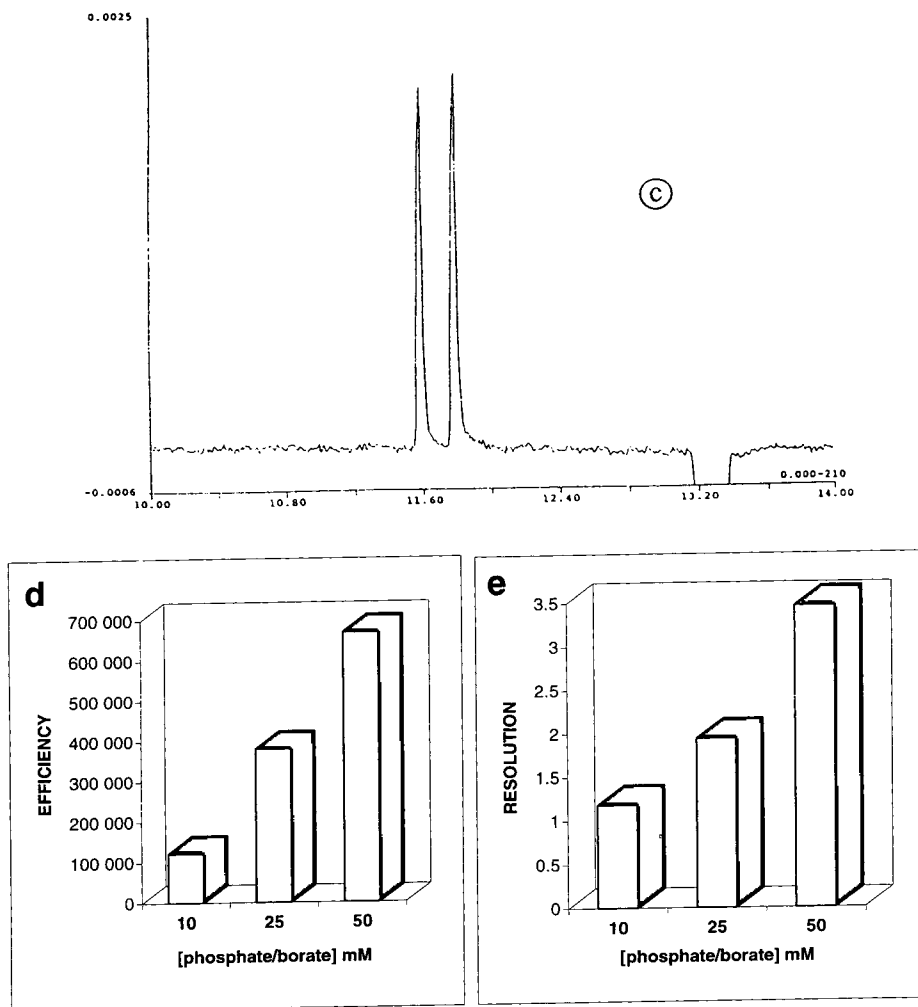


Fig. 6. (continued)

pH range 4.5–12, using 6 mM  $\beta$ -CD and 8 M urea dissolved in 50 mM phosphate–borate buffer (Fig. 7); two optimum resolution values were found at pH 7 and 11.75. Table 6 shows the experimental values for the separation parameters of 5-OH-DPAC using different buffer pH values. We observed migration order reversal of the *R*- and *S*-enantiomers on going from acidic to alkaline pH values (Table 6). Enantioseparation was achieved at either pH 5 or 7 when the two enantiomers were in their cationic form and

migrated from the anode to the cathode (Fig. 8a and b), and also at pH 11.75 when the solutes were in their anionic form (Fig. 8d). Nevertheless, at pH 7, complete baseline separation of 5-OH-DPAC enantiomers was achieved in less than 15 min with a resolution of 4.02; the peak efficiencies were approximately 640 000 theoretical plates for these enantiomers and the enantioselectivity was found to be weak ( $\alpha = 1.021$ ). Fig. 8c shows an unsuccessful chiral separation at pH 9 due to the neutral form of this solute.

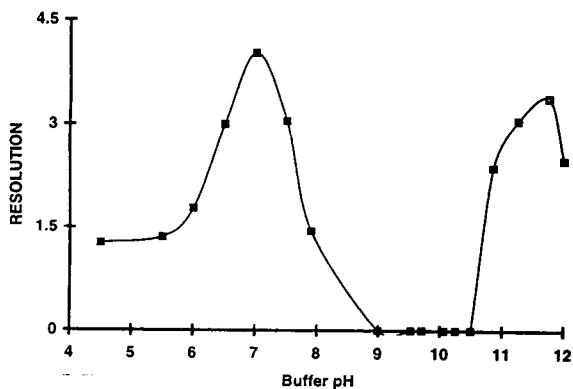


Fig. 7. Variation of the resolution with electrolyte pH during 5-OH-DPAC enantioseparation. Fused-silica capillary column, 70 cm  $\times$  50  $\mu$ m I.D.; applied voltage, +18 kV; buffer, 50 mM phosphate–borate–6 mM  $\beta$ -CD–8 M urea; detection at: 210 nm; temperature, 25°C.

With an acidic background electrolyte, the efficiency for the first peak (*R*-enantiomer) was higher (6%) than that for the second peak (*S*-enantiomer), as expected. However, with the

enantiomers in their anionic form, the efficiency for the *R*-enantiomer (second peak) is always higher (4%) than that for the *S*-enantiomer (first peak), owing to lower complexation, as reported previously [19].

#### 4. Conclusion

Using  $\beta$ -CD as a chiral selector, capillary electrophoresis is an attractive method for the enantioseparation of drugs. The optimum separation conditions depend on the chiral selector concentration, the ionic strength and the pH of the buffer.

The  $\beta$ -CD inclusion complex stability constant of each solute enantiomer can be easily determined by capillary electrophoresis by following the variation of the enantiomer electrophoretic mobility versus the  $\beta$ -CD concentration over a wide range (1  $\mu$ M–100 mM). The theoretical model predicts that the optimum concentration for the chiral selector ( $C_{opt}$ ) depends on the

Table 6  
Effect of electrolyte pH on the enantioseparation parameters of 5-OH-DPAC resolved by capillary electrophoresis

pH	$t_{mR}$ (min)	$t_{mS}$ (min)	$t_0$ (min)	$m_{ePR} \times 10^5$ ( $\text{cm}^2 \text{V}^{-1} \text{s}^{-1}$ )	$m_{ePS} \times 10^5$ ( $\text{cm}^2 \text{V}^{-1} \text{s}^{-1}$ )	$N_R$	$N_S$	$\alpha$	$R_s$
4.5	18.62	18.80	29.35	8.02	7.81	331 400	258 000	1.010	1.27
5.5	15.00	15.12	22.56	9.12	8.91	555 800	475 500	1.008	1.36
6.0	14.36	14.50	20.76	8.77	8.49	533 100	484 500	1.027	1.79
6.5	14.07	14.30	18.72	7.21	6.74	550 750	518 300	1.016	3.00
7.0	14.10	14.41	16.81	4.63	4.05	658 100	618 000	1.021	4.02
7.5	14.89	15.12	16.16	2.16	1.74	658 400	619 600	1.015	3.05
7.9	15.18	15.32	15.65	0.81	0.56	—	—	1.009	1.45
9.0	14.89	—	14.60	−0.54	—	—	—	1.000	0
9.5	14.81	—	14.46	−0.67	—	—	—	1.000	0
9.7	15.02	—	14.47	−1.03	—	—	—	1.000	0
pH	$t_{mS}$ (min)	$t_{mR}$ (min)	$t_0$ (min)	$m_{ePS} \times 10^5$ ( $\text{cm}^2 \text{V}^{-1} \text{s}^{-1}$ )	$m_{ePR} \times 10^5$ ( $\text{cm}^2 \text{V}^{-1} \text{s}^{-1}$ )	$N_S$	$N_R$	$\alpha$	$R_s$
10.1	15.71	15.82	14.87	−1.47	−1.65	—	—	1.007	—
10.3	16.38	16.49	15.26	−1.83	−2.00	—	—	1.007	—
10.9	18.88	19.24	16.35	−3.35	−3.75	545 400	568 000	1.019	2.38
11.3	19.36	19.68	16.79	−3.23	−3.57	526 800	559 250	1.017	3.06
11.8	22.00	22.44	17.98	−4.15	−4.51	451 400	470 500	1.020	3.39
12.0	25.72	26.14	18.79	−5.86	−6.11	385 400	416 250	1.016	2.49

Buffer: 50 mM phosphate–borate–6 mM  $\beta$ -CD–8 M urea; other conditions as in Table 1.

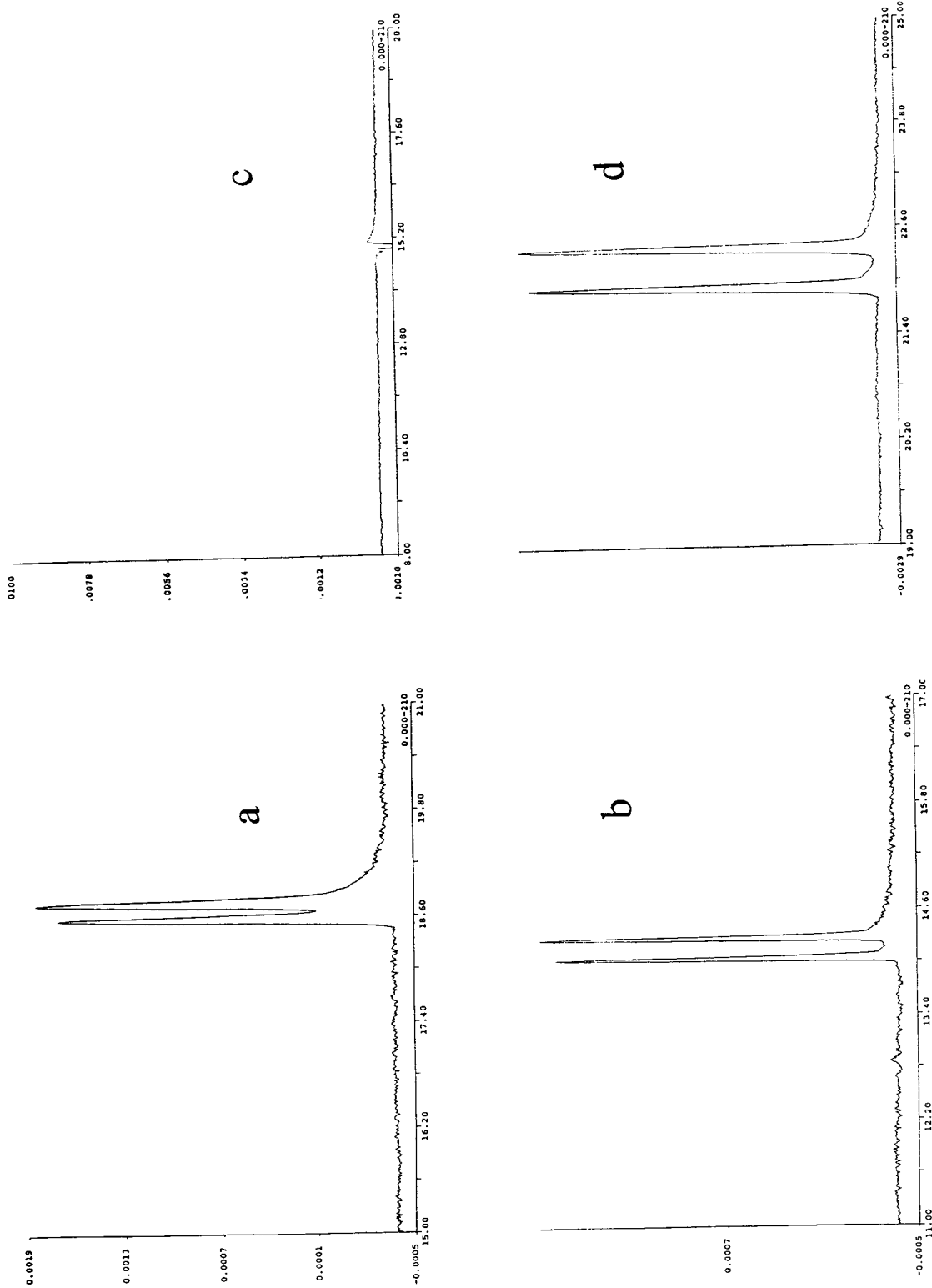


Fig. 8. Electropherogram of 5-OH-DPAC enantiomers at different electrolyte pH values. Fused-silica capillary column, 70 cm  $\times$  50  $\mu$ m I.D.; applied voltage, +18 kV; buffer, 50 mM phosphate–borate–6 mM  $\beta$ -CD–8 M urea; detection at 210 nm; temperature, 25°C. buffer pH: (a) 5; (b) 7; (c) 9; (d) 11.75.

stability constant of each enantiomer ( $K_R, K_S$ ) as expressed by the relationship:  $[C]_{\text{opt}} = 1 / (K_R K_S)^{1/2}$ . The experimentally determined  $C_{\text{opt}}$  value fits well with the calculated value from the previous equation in which we used experimental values for the inclusion complex stability constants. The high efficiencies (400 000–600 000 theoretical plates) of this method allowed the separation of these enantiomers ( $R_S = 4.02$ ) when the enantioselectivity was small ( $\alpha = 1.021$ ), which has been found to be the limiting factor in conventional chiral electrophoretic separations.

## References

- [1] I. Valko, H. Billiet, H. Corstjens and J. Frank, *LC·GC Int.*, 6 (1993) 420.
- [2] T. Bereuter, *LC·GC Int.*, 7 (1994) 78.
- [3] T. Ward, *Anal. Chem.*, 66 (1994) 633A
- [4] S. Terabe, K. Otsuka and H. Nishi, *J. Chromatogr. A*, 666 (1994) 295.
- [5] S. Fanali, *J. Chromatogr.*, 474 (1989) 441.
- [6] H. Nishi, Y. Kokusenya, T. Miyamoto and T. Sato, *J. Chromatogr. A*, 659 (1994) 449.
- [7] M. Heuermann and G. Blaschke, *J. Chromatogr.*, 648 (1993) 267.
- [8] S. Palmarsdottir and L.E. Edholm, *J. Chromatogr. A*, 666 (1996) 337.
- [9] M.Al. Neirabeych, D. Reynaud, T. Podona, L. Ou, C. Perdicakis, G. Coudert, G. Guillaumet, L. Pichat, A. Gharib and N. Sarda, *Eur. J. Chem.*, 26 (1991) 497.
- [10] T. Podona, B. Guardiola-Lemaitre, D.H. Caignard, G. Adam, B. Pfeiffer, P. Renard and G. Guillaumet, *J. Med. Chem.*, submitted for publication.
- [11] J.M. Cossery, H. Golzan, V. Spampinato, C. Perkakis, G. Guillaumet, L. Pichat and M. Hamon, *Eur. J. Pharmacol.*, 140 (1987) 143.
- [12] P. Gareil, *Analisis*, 18 (1990) 221.
- [13] J. Snopek, I. Jelinek and E. Smolkova-Keulemansova, *J. Chromatogr.*, 609 (1992) 1.
- [14] S.A.C. Wren and R.C. Rowe, *J. Chromatogr.*, 603 (1992) 235.
- [15] S.A.C. Wren and R.C. Rowe, *J. Chromatogr.*, 609 (1992) 363.
- [16] S.A.C. Wren, *J. Chromatogr.*, 636 (1993) 57.
- [17] S. Penn, D. Goodall and J. Loran, *J. Chromatogr.*, 636 (1993) 149.
- [18] P. Gareil, D. Pernin, J.P. Gramond and F. Guyon, *J. High. Resolut. Chromatogr.*, 16 (1993) 195.
- [19] I. Valko, H. Billiet, J. Frank and K. Luyben, *Chromatographia*, 38 (1994) 730
- [20] A. Shibukawa, D. Lloyd and I. Wainer, *Chromatographia*, 35 (1993) 419.
- [21] W. Hinze, D. Pharr, Z. Fu and W. Burkert, *Anal. Chem.*, 61 (1989) 422.

# Determination of isoflavones using capillary electrophoresis in combination with electrospray mass spectrometry

M.A. Aramendia\*, I. García, F. Lafont, J.M. Marinas

Department of Organic Chemistry and Mass Spectrometry Service, Faculty of Sciences, University of Córdoba,  
Avda S. Alberto Magno s/n, E-14004 Córdoba, Spain

First received 27 December 1994; revised manuscript received 7 March 1995; accepted 8 March 1995

## Abstract

Various isoflavones were separated on an uncoated fused-silica capillary electrophoresis (CE) column (110 cm  $\times$  75  $\mu$ m I.D.) using 25 mM ammonium acetate buffer and UV and electrospray ionization mass spectrometric (ESI-MS) detection. CE-ESI-MS with negative-ion electrospray ionization has been shown to be a suitable technique for the determination of this type of natural compound. The modest sample loading of the CE technique can be circumvented by coupling it with MS; in addition, the mass-resolving capability and high sensitivity of MS for structural analysis of mixtures can thus be exploited. Furthermore, ESI-MS allows one not only to determine the molecular mass of isoflavones, but also the presence of various functional groups according to observed losses from the  $[M - H]^-$  ion during collision-induced dissociation by adjusting some MS parameters.

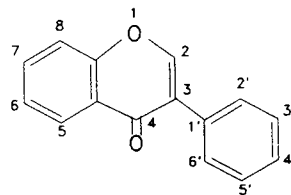
## 1. Introduction

Isoflavonoids make up a large group of naturally occurring substances in plants. In contrast to their near ubiquitous occurrence in higher plants of other flavonoids, isoflavonoids are primarily confined to one group of plants, the sub-family Lotoideae of the Leguminosae [1].

One distinct feature of isoflavonoids is that they possess biological activity. In contrast to other flavonoids, most of which are harmless substances [2], isoflavonoids have oestrogenic, insecticidal, pesticidal and antifungal properties. Isoflavones are by far the most common type of isoflavonoid. Their structures are based on the 3-phenylbenzopyrone group (see formula) and differ in the extent of hydroxylation, methylation

and glycosylation. Isoflavones are weak oestrogens; their presence in forage legumes has been recognized to result in animal infertility. Formononetin, genistein and biochanin A are the principal oestrogenic isoflavones; their degradation products consist mainly of simple phenols such as *p*-ethylphenol [3].

Available analytical techniques for flavonoid determination include HPLC [4], TLC and GC, most of which, however, are laborious and time consuming.



\* Corresponding author.

Electron impact mass spectrometry is a powerful tool for determining isoflavonoid structures. In fact, it has been successfully applied to all types of flavonoid [5]. In contrast, chemical ionization MS using methane as the reactant gas has been applied to only a few flavonoids and produces few diagnostic fragments except for flavonones and dihydroflavonols [6]. Most flavonoids yield intense peaks for the molecular ion  $M^+$  and indeed this is often the base peak. Derivatization is therefore unnecessary unless GC-MS is to be carried out, in which case trimethylsilylation or permethylation [7] provides the required volatility.

Capillary electrophoresis (CE) is a powerful technique that affords rapid, high-resolution separations ( $10^4$ – $10^6$  theoretical plates) while requiring only a few femtomoles of sample. A broad range of compounds, including peptides, nucleotides, surfactants, environmental pollutants and natural products, are amenable to separations by CE. The technique is applicable to a wide range of analytes present in buffered aqueous solution as charged species. The utility of CE, however, is greatly enhanced by MS detection, particularly with electrospray ionization (ESI), a soft ionization technique that can be used to produce ions even from thermally labile, non-volatile, polar compounds [8–11].

In this work, we explored the use of on-line capillary electrophoresis and mass spectrometry with electrospray ionization for the separation and characterization of selected isoflavones. Collision-induced dissociation (CID) reactions in the intermediate pressure region between the ESI source and the single quadrupole mass analyser for this type of compound are described.

## 2. Experimental

### 2.1. Mass spectrometer and electrospray interface

All experiments were performed on a VG Platform single-quadrupole mass spectrometer

(Fisons Instruments) equipped with an electrospray ionization source. A diaxial electrospray probe was used for direct infusion of samples. The instrument was operated in the negative-ion mode at a probe tip voltage of  $-3.5$  kV. The extraction cone voltage was varied from  $-25$  to  $-75$  V. Nitrogen was used as both the electrospray nebulizing gas and the drying gas. The nitrogen pressure was set at 6 bar and the flow-rates of the drying gas and nebulizing gas were set at 200 and  $10 \text{ l h}^{-1}$ , respectively, for maximum sensitivity. The source temperature was maintained at  $70^\circ\text{C}$ . Samples were introduced into the source by direct injection via a Rheodyne Model 7125 injection valve with a  $10\text{-}\mu\text{l}$  loop; the solvent flow ( $10 \mu\text{l min}^{-1}$ ) was delivered by an LKB 2150 HPLC pump. The mass spectrometer was scanned from  $m/z$  90 to 325 at a rate of 2 s per scan.

A triaxial electrospray probe which incorporates a sheath tube (0.005 in. I.D. PEEK tube) allowing additional solvent to be transported to the probe tip and mixed coaxially with the sample flow (at the end of the CE capillary) before spraying, was used in the CE-ESI-MS mode. This make-up fluid performs two functions: (a) to supplement the CE flow by the extent required for electrospray ionization and (b) to make electrical contact between the CE buffer and the probe tip. The probe allows the CE system to be interfaced to a standard electrospray source using the  $375 \mu\text{m}$  O.D. fused-silica column employed in the CE experiment. Approximately 1 cm of the fused-silica external polyamide coating was removed from the outlet side at the probe tip. The source was operated at  $-3.5$  kV (in the negative-ion mode). A coaxial sheath liquid consisting of water–2-propanol (80:20) at a flow-rate of  $10 \mu\text{l min}^{-1}$  was used as the make-up fluid for CE-ESI-MS. Nitrogen was used as both the drying gas ( $50 \text{ l h}^{-1}$ ) and the ES nebulizing gas ( $10 \text{ l h}^{-1}$ ). In this case, mass spectral data were acquired using selected-ion recording (SIR mode; 0.2 s dwell time, 0.2 mass unit span) for the  $[M - H]^-$  ion.

Mass calibration was carried out with a mixture of NaI and CsI in 2-propanol–water (50:50).

## 2.2. Capillary electrophoresis

A P/ACE 5500 CE system (Beckman Instruments) equipped with a P/ACE diode-array detector was used for CE and CE-MS experiments. A 110 cm  $\times$  75  $\mu$ m I.D.  $\times$  375  $\mu$ m O.D. uncoated fused-silica capillary column was used. The polyamide coating was removed 20 cm from the capillary inlet to create a window for UV absorbance measurements. This column was used for CE-UV and CE-UV-ESI-MS analyses. The untreated capillary was washed first with 100 mM NaOH and then with Milli-Q-purified water and the electrolyte. Samples were injected at a low pressure (0.5 bar) for 5 s (injection volume ca. 3 nl). Bulk flow in the CE capillary was minimized by adjusting the height of the inlet (anode) relative to the ES probe. A voltage of 30 kV was applied to the anode; since the electrospray needle acted as the cathode ( $-3.5$  kV), the overall potential difference was 33.5 kV, so samples were electrophoresed at  $305$  V  $\text{cm}^{-1}$ , which resulted in very stable currents of ca. 35  $\mu$ A. UV detection was performed at 260 nm, with scanning between 190 and 400 nm.

## 2.3. Sample preparation

Standards including daidzein (7,4'-dihydroxyisoflavone,  $M_r$  254.2), formononetin (7-hydroxy-4'-methoxyisoflavone,  $M_r$  283), pseudobaptigenin (7-hydroxy-3',4'-dioxomethyleneisoflavone,  $M_r$  282.3), biochanin A (5,7-dihydroxy-4'-methoxyisoflavone,  $M_r$  284.3), genistein (4',5,7-trihydroxyisoflavone,  $M_r$  270.2), isoliquirtigenin (4,2',4-trihydroxychalcone,  $M_r$  256.3) and biochanin A 7-glucoside ( $M_r$  446.4) were all obtained from Sigma. Standard solutions for direct ES experiments were prepared at a 0.1 mM concentration in water-2-propanol (80:20) containing 0.3% ammonia. For CE-ESI-MS, 1 mM standards were dissolved in a buffer solution containing 25 mM aqueous ammonium acetate at pH 9.5 (adjusted with ammonia solution). All organic solvents (HPLC grade) and samples were filtered through 0.2- $\mu$ m pore-size nylon membrane filters (Millipore).

## 3. Results and discussion

### 3.1. Electrospray

Figs. 1–5 show the ESI mass spectra for individual isoflavones dissolved in water-2-propanol containing 0.3% ammonia, recorded at different extraction cone voltages ( $-25$ ,  $-50$  and  $-75$  V). The extraction cone voltages serves primarily to focus ions into the mass analyser. However, above a typical cone voltage of 40 V (absolute value), sample ions can gain sufficient energy to undergo CID reactions with neutral molecules in the intermediate pressure region and thus provide useful information about fragment ions [12–15].

In a basic medium, substances are detected as anions because the acid-base equilibrium is

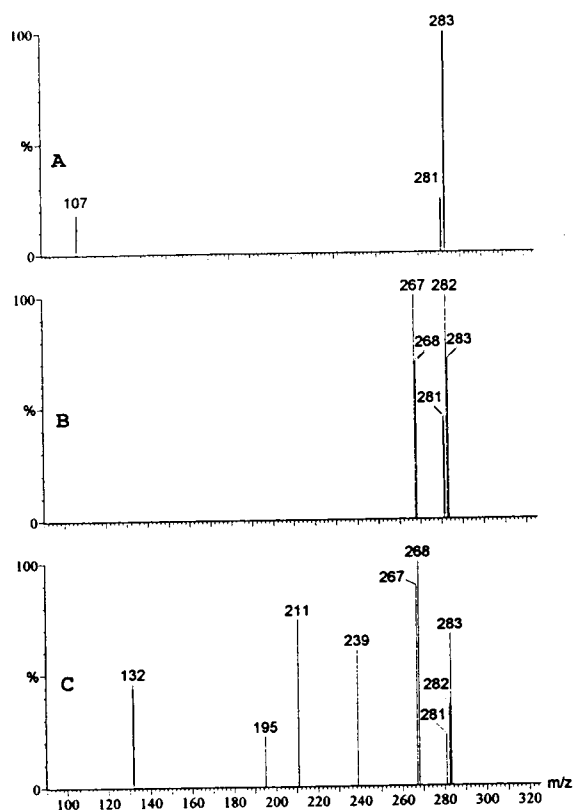


Fig. 1. ESI mass spectra for biochanin A at different extraction cone voltages: (A)  $-25$ ; (B)  $-50$ ; (C)  $-75$  V.

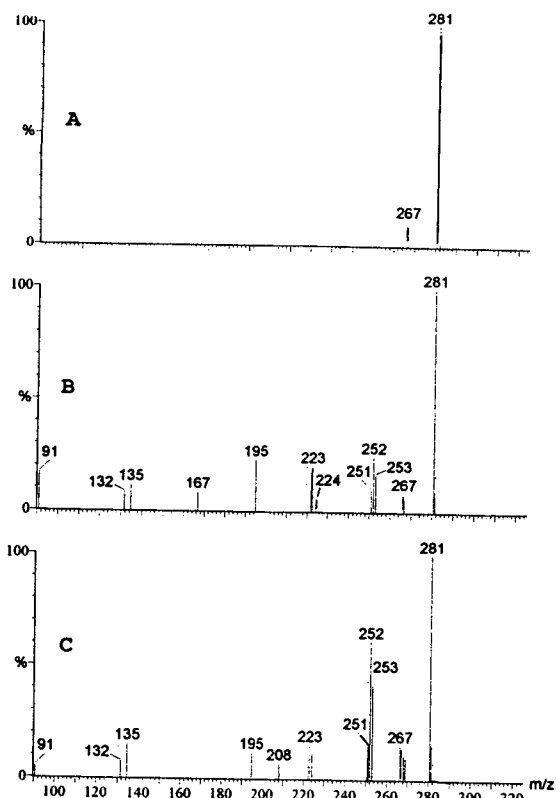


Fig. 2. ESI mass spectra for pseudobaptigenin at different extraction cone voltages: (A)  $-25$ ; (B)  $-50$ ; (C)  $-75$  V.

shifted to the basic form, so the spectrum exhibits the  $[M - H]^-$  peak. At low extraction cone voltages, the mass spectrum of each isoflavone tested consisted exclusively of  $[M - H]^-$  ion as the base peak; fragment peaks from CID reactions appear at high extraction voltages values ( $-50$  and  $-75$  V) and provide structural information about molecules. Biochanin A exhibited an  $[M - H]^-$  ion peak at  $m/z$  283 as the base peak at an extraction cone voltage of  $-25$  V (Fig. 1); however, raising the extraction cone voltage produced new peaks at  $m/z$  268 ( $[M - H - CH_3]^-$ ),  $m/z$  239 ( $[M - H - CH_2 - COH]^-$ ) and  $m/z$  211 ( $[M - H - CH_3 - COH - CO]^-$ ). Pseudobaptigenin (Fig. 2) produced an  $[M - H]^-$  ion at  $m/z$  281 as the base peak and additional peaks at  $m/z$  267 ( $[M - H - CH_2]^-$ ),  $m/z$  252 ( $[M - H - OCH_2]^-$ ),  $m/z$  223 ( $[M - H - OCH_2 - CO]^-$ ) and  $m/z$  195 ( $[M - H -$

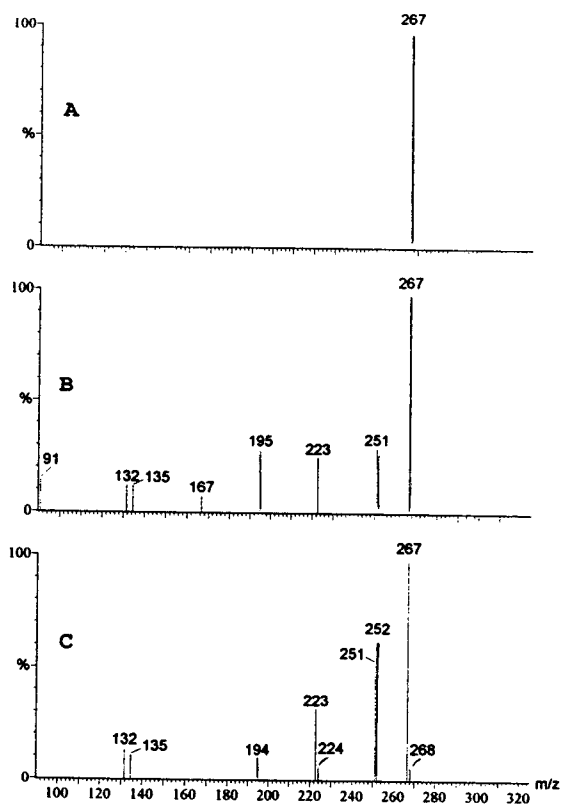


Fig. 3. ESI mass spectra for formononetin at different extraction cone voltages: (A)  $-25$ ; (B)  $-50$ ; (C)  $-75$  V.

$OCH_2 - CO - CO]^-$ ). Formononetin exhibited an  $[M - H]^-$  base peak at  $m/z$  267 (Fig. 3) and other peaks at  $m/z$  252 ( $[M - H - CH_3]^-$ ),  $m/z$  223 ( $[M - H - CH_3 - COH]^-$ ) and  $m/z$  195 ( $[M - H - CH_3 - COH - CO]^-$ ). Biochanin A 7-glucoside (Fig. 4) provided no peak at  $-25$  V; at a higher voltage, however, it produced several peaks, viz., one at  $m/z$  283 (biochanin A) due to glucosidic bond breakdown, another at  $m/z$  255 ( $[M - H - CO]^-$ ) and a very small  $[M - H]^-$  peak at  $m/z$  445. On the other hand, both daidzein and genistein (Fig. 5) gave fewer peaks than the other compounds studied, exhibiting practically the  $[M - H]^-$  peak at extraction cone voltages between  $-25$  and  $-75$  V.

As a general rule, compounds with a methoxy group (biochanin A and formononetin) exhibit one fragment ion at  $m/z$   $[M - H - CH_3]^-$  when a high extraction cone voltages is used.



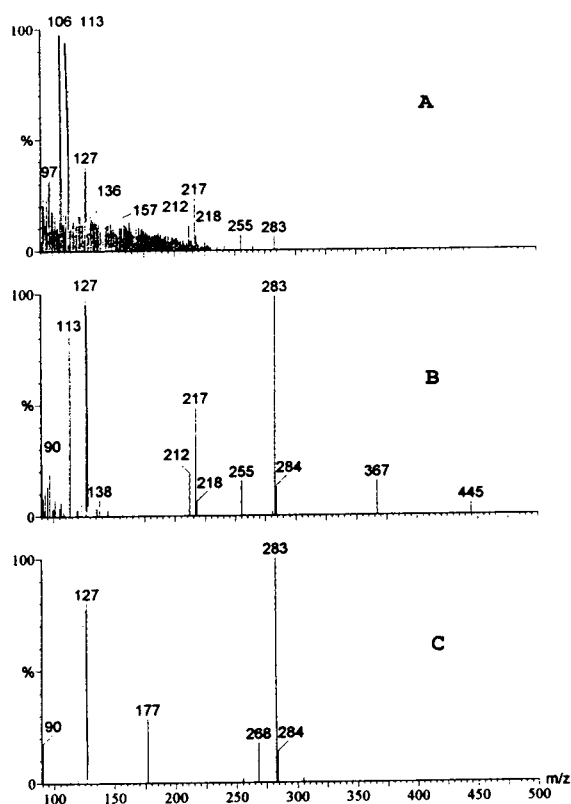


Fig. 4. ESI mass spectra for biochanin A 7-glucoside at different extraction cone voltages: (A)  $-25$ ; (B)  $-50$ ; (C)  $-75$  V.

These results are typical for the negative ES ionization of small molecules, i.e., major ions result from  $[M - H]^-$ , with essentially no fragment ions; also, only under stronger ES conditions no molecular fragments appear.

### 3.2. CE-UV and CE-MS

Figure 6 shows the electropherogram for an isoflavone mixture (1 mM) containing about 3 fmol of each compound after 20 cm of capillary using UV detection at 260 nm. Each analysis was complete within 4 min, although higher resolution could have been achieved by using a longer distance between the capillary inlet and the UV window. On the other hand, biochanin A, formononetin and pseudobaptigenin could not be resolved under these conditions.

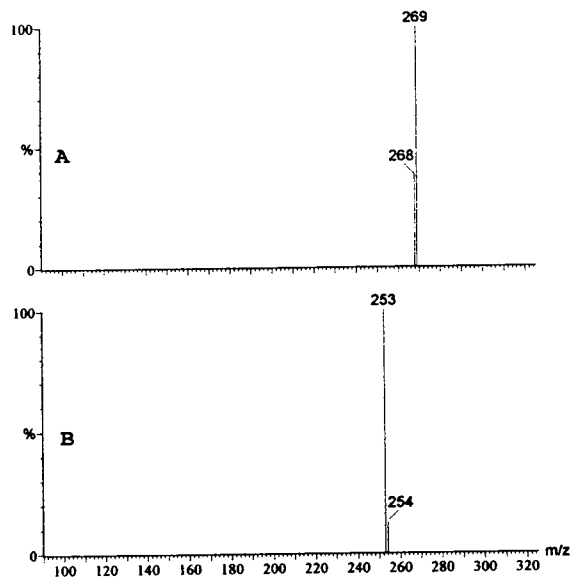


Fig. 5. ESI mass spectra for (A) genistein and (B) daidzein at an extraction cone voltage of  $-75$  V.

The SIR chromatograms in Fig. 7 show the final separation of the mixture achieved after 110 cm of capillary. The elution sequence was established by mass spectral interpretation and the known CE migration behaviour and was found to be (1) genistein, (2) daidzein, (3) formononetin, (4) pseudobaptigenin and biochanin

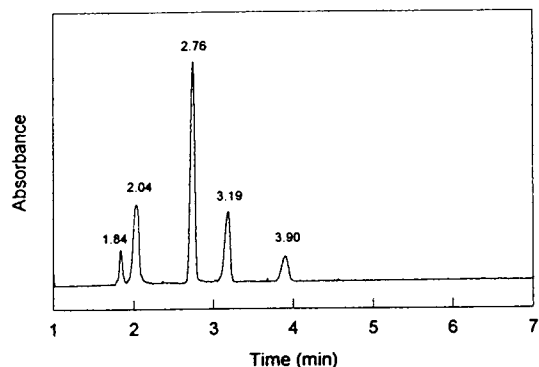


Fig. 6. Electropherogram for an isoflavone mixture with UV detection at 260 nm. Buffer, 25 mM  $\text{NH}_4\text{OAc}$  (pH 9.5); run voltage, 33.5 kV; current, 35  $\mu\text{A}$ ; sample concentration, 0.1 mM; injection, 5 s. Peaks: genistein (1.89 min), daidzein (2.04 min), pseudobaptigenin, formononetin and biochanin A (2.76 min), isoliquirtigenin (3.19 min) and biochanin A 7-glucoside (3.90 min).

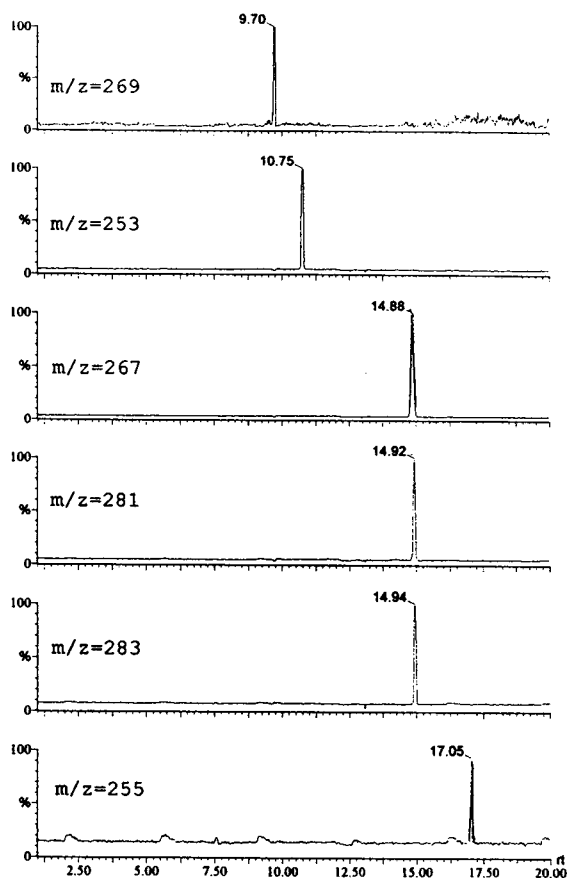


Fig. 7. CE-ESI mass chromatograms for a mixture containing about 3 fmol of each isoflavone.

A and (5) isoliquirtigenin. Biochanin A 7-glucoside did not appear because we used ESI conditions (extraction cone voltage  $-25$  V) where each compound provided a single mass peak  $[M-H]^-$ , so this compound, as noted earlier, gave no signal. Therefore, although this isoflavone mixture cannot be readily resolved using conventional CE with UV detection, it can be resolved by CE-MS. The signal reproducibility was found to be very good (the variation in peak areas was less than 10% for the same sample).

The success of the CE-ESI-MS analysis of isoflavones relies on many factors, including the ESI interface and buffer composition. Analyte detectability and sensitivity vary widely with the buffer concentration, the optimum analytical

signal for CE-ESI-MS being obtained when volatile buffers are utilized at the lowest possible concentration (10–25 mM); in fact, higher concentrations reduce the analyte ionization efficiency in the electrospray process.

#### 4. Conclusions

Combined CE-ESI-MS allows the efficient separation and identification of isoflavones with higher specificity than CE (with UV detection) alone. The reported results demonstrate the utility of this coupled technique for the qualitative analysis of natural compound mixtures such as isoflavones, with high reproducibility and sensitivity. In addition, capillary electrophoresis, with its exceptionally low flow-rate ( $\text{nl min}^{-1}$ ), is easier to interface to MS than is liquid chromatography, since no flow splitting is required. One other advantage of ESI is the ability to induce CID reactions in the intermediate pressure region of the source by increasing the extraction cone voltage; this permits the recognition of certain functional groups in unknown compounds and confirmation of target analytes by using the intensity ratios of several diagnostic fragment ions.

#### Acknowledgements

The authors acknowledge funding of this research by the Consejería de Educación y Ciencia de la Junta de Andalucía and the Dirección General de Investigación Científica y Técnica (DGICYT) in the framework of Project PB92-0816. They also thank Dr. M. Tena for providing the isoflavone standards.

#### References

- [1] M. Jay, P. Lebreton and R. Letoublon, *Boissiera*, 19 (1971) 219.
- [2] W.B. Whalley (Editor), *The Pharmacology of Plant Phenolics*, Academic Press, London, 1959.

- [3] J.B. Harborne, T.J. Mabry and H. Mabry (Editors), *The Flavonoids*, Chapman and Hall, London, 1975.
- [4] S.M. Lunte, *J. Chromatogr.*, 384 (1987) 371.
- [5] A. Weissberger and E.C. Taylor (Editors), *Mass Spectrometry of Heterocyclic Compounds*, Wiley-Interscience, New York, 1971.
- [6] D.G.I. Kingston and H.M. Fales, *Tetrahedron*, 29 (1973) 4083.
- [7] E.D. Pellizzari, C.M. Chuang, J. Kuc and E.B. Williams, *J. Chromatogr.*, 40 (1969) 285.
- [8] T. Braun and S. Zsindely, *Trends Anal. Chem.*, 11 (1992) 307.
- [9] J.A. Loo, H.R. Udseth and R.D. Smith, *Anal. Biochem.*, 179 (1989) 204.
- [10] J.A. Olivares, N.T. Nguyen, C.R. Yonker, and R.D. Smith, *Anal. Chem.*, 59 (1987) 130.
- [11] C.M. Whitehouse, A.N. Dreyer, M. Yamashita and J.B. Fenn, *Anal. Chem.*, 57 (1985) 675.
- [12] D.R. Doerge, S. Bajic and S. Lowes, *Rapid Commun. Mass Spectrom.*, 7 (1993) 462.
- [13] S. Pleasance, P. Blay, M.A. Quilliam and G.J. O'Hara, *J. Chromatogr.*, 558 (1991) 155.
- [14] K.L. Duffin, T. Wachs and J.D. Henion, *Anal. Chem.*, 64 (1992) 61.
- [15] D.R. Doerge, S. Bajic and S. Lowes, *Rapid Commun. Mass Spectrom.*, 7 (1993) 1126.





ELSEVIER

Journal of Chromatography A, 707 (1995) 335–342

JOURNAL OF  
CHROMATOGRAPHY A

# Determination of sugars by capillary electrophoresis with electrochemical detection using cuprous oxide modified electrodes

Xinjian Huang, Wim Th. Kok\*

Laboratory for Analytical Chemistry, University of Amsterdam, Nieuwe Achtergracht 166, 1018 WV Amsterdam, Netherlands

First received 23 December 1994; revised manuscript received 2 March 1995; accepted 7 March 1995

## Abstract

The separation by capillary electrophoresis and off-column amperometric detection of underivatized sugars has been studied. A palladium-metal union was used as grounded cathode to decouple the high separation voltage before detection. With a second piece of capillary the field decoupler was connected to a home-made T-shaped detection cell. Cuprous oxide modified microelectrodes were prepared and evaluated. For the detection of sugars they were operated at a constant potential of +0.60 V. The peak-height reproducibility with these electrodes over a period of 18 h (25 injections) was within 7% absolutely and within 4% when one of the analytes was regarded as internal standard.

To preserve the flat electroosmotic flow profile in the separation capillary, pressure compensation was applied. The contribution of various sources to the system zone variance was studied. Under optimized conditions plate numbers of over 100 000 were obtained.

For the baseline separation of a mixture of sugars 0.10 mol l<sup>-1</sup> sodium hydroxide solutions had to be used as background electrolyte. Detection limits of 1–2 μmol l<sup>-1</sup> were found for various carbohydrates.

## 1. Introduction

Since the inception of capillary electrophoresis (CE) [1] and the clear demonstration of its high separation power by Jorgenson and Lukacs [2], CE has gained popularity over the past decade with an increasing number of publications each year in the field. CE is becoming an alternative separation technique for liquid chromatography on one hand and conventional electrophoresis on the other. Achievements and trends in CE have been reviewed extensively [3–11].

The monitoring of the CE separation process is usually carried out with on-column UV absorption spectrometry or (laser-induced) fluorometry. However, several research groups work on the development of amperometric detectors for CE [12,13]. This interest can be explained by the fact that the sensitivity of amperometric detection is not hampered by the small volumes of the sample zones as encountered in CE, in contrast to most spectrometric techniques. With amperometry, detection limits of 10<sup>-19</sup> mole have already been reported [14].

A prerequisite to perform amperometric detection in CE is to isolate the electrophoretic

\* Corresponding author.

current generated by the high-voltage source used for the separation from the electrochemical detection current. To achieve this, there are basically two approaches: the end-column mode and the off-column mode. In the end-column mode [15,16], the working electrode is placed in the buffer vial with the grounded electrode of the high-voltage source, at a short distance from the capillary end. A compromise must be found between minimum interference of the electric field of the separation on the detection and an acceptable mass sensitivity. Such a set-up is suitable for capillaries with an inside diameter of 25  $\mu\text{m}$  or less, when the electrophoretic currents are small and the detection potential is not biased significantly. Detection limits for end-column amperometric detection have been reported in the range 10–100 amol; due to the extremely low sample volumes in the narrow capillaries, the detection limits in concentration units are less impressive (approximately  $10^{-6} \text{ mol l}^{-1}$ ).

The limitation of the inner capillary diameter is not imposed in the off-column mode [14,17–21]. Here, the separation field is decoupled before the detector through a gap in the capillary system. Electrical contact with the grounded electrode of the high-voltage source, placed in an external electrolyte solution, is made through a sleeve over the gap, made of a porous or semipermeable material. The solution is propelled by the electroosmosis in the separation capillary via a small piece of coupling capillary towards the detector.

A new type of field decoupler for off-column amperometric detection has been developed recently in our laboratory [22]. A union of palladium metal between the separation and the coupling capillary is used as the grounded cathode of the high-voltage source. The hydrogen generated at the inner wall of the union, which constitutes a part of the capillary system, can dissipate through the palladium metal. The main advantages of this decoupler over the previously used types are its robustness and experimental convenience. It was also shown that to preserve the flat electroosmotic flow profile in the separation capillary, pressure compensation can be applied [23]. In this method a

pressure is applied on the front end of the separation capillary, balancing the backpressure of the coupling capillary.

CE has been applied for the determination of a variety of compounds and in most cases a separation efficiency superior to other (chromatographic) methods has been demonstrated. Recently, there is an increasing interest to apply CE methods for the analysis of sugars. For the separation of the many closely related mono- and oligosaccharides the efficiency of CE would be of much value. However, due to their lack of strong chromophore or fluorophore, carbohydrates can not be detected directly with optical methods. To avoid sometimes complicated pre-column derivatization procedures [24–26], on-column complexation with borate and detection at 195 nm [27] or indirect fluorescence [28] or UV detection [29–30] has to be applied. These methods suffer from poor selectivity and high concentration detection limits, which are in the order of  $10^{-4} \text{ mol l}^{-1}$ .

In liquid chromatography pulsed amperometric detection (PAD) with gold or platinum electrodes [31] has become a routine method for the determination of sugars. Recently it has been shown that PAD can also be applied in CE for the detection of sugars [32,33]. A problem here may be that the optimal cycle time in PAD (approximately 1 s) is rather long for the fast separations obtained in CE. Alternatively, constant-potential detection with copper electrodes has been applied [34,35]. The high pH necessary for the separation is also essential for sensitive detection in both cases.

In previous work it has been found that cuprous oxide is an effective electrode modifier for the detection of sugars in flow injection analysis [36,37], giving a high sensitivity and selectivity. We used conductive carbon cement (CCC) as matrix for the modified electrodes, since it provides a better versatility and mechanical stability for use in flowing solutions, compared to for instance carbon paste [38]. In the work presented here, we have studied the possibility to use cuprous oxide modified microelectrodes in a CE system. The electrochemical characteristics of the modified microelec-

trodes have been studied and compared with those of normal-sized electrodes [36,37]. Off-line detection utilizing a palladium decoupler was applied. The importance of pressure compensation on the separation efficiency has been studied. The performance of the system has been assessed using standard mixtures of carbohydrates.

## 2. Experimental

### 2.1. Apparatus

The experimental set-up is depicted in Fig. 1. A Prince programmable injector for capillary electrophoresis, including a high-voltage supply, was obtained from Lauer Labs (Emmen, Netherlands). Samples were injected hydrodynamically at a pressure of 20 mbar for 12 s; the volume of sample loaded was approximately 15 nl. The forced-air thermostat was set at 28°C. Fused-silica capillaries were provided by Polymicro Technologies (Phoenix, AZ, USA). The internal diameter of the separation capillary was 75  $\mu\text{m}$  and that of the coupling capillary 50  $\mu\text{m}$ . Unless stated otherwise, their lengths were 100 and 8 cm, respectively. New separation capillaries were etched with 1 mol l<sup>-1</sup> NaOH for 1 h before use. The field decoupler was made from a palladium cylinder [22,23]. The T-shaped electrochemical

microcell was a modification of the prototype previously described [39], with a three-electrode instead of the two-electrode system. A silver tube functioned as outlet and as in situ Ag/AgCl reference electrode, with the addition of 1 mmol l<sup>-1</sup> NaCl to the background electrolyte to stabilize the potential. A stainless steel tube was used as the auxiliary electrode. PEEK tubes of 6 cm length (1/16 inch O.D., 0.5 mm I.D.) were used to construct Cu<sub>2</sub>O modified carbon working electrodes. The detector cell was located inside a Faraday cage. A Hewlett-Packard (Waldbronn, Germany) 1049A programmable electrochemical detector was used. The signal was registered with a HP 3394A integrator and a strip-chart recorder.

### 2.2. Chemicals and solutions

Carbohydrates, obtained from standard suppliers, were analytical grade and used as received. Concentrated stock solutions (10<sup>-2</sup> mol l<sup>-1</sup>) were kept in the refrigerator (4°C) and diluted to the desired concentration daily. The background electrolytes, NaOH solutions containing 1 mmol l<sup>-1</sup> NaCl, were degassed with helium before use. Subboiled demineralized water was used to prepare solutions.

### 2.3. Working electrode preparation

Cuprous oxide (20% w/w) modified carbon paste [36] and conductive carbon cement [37] were prepared as described previously. To fabricate electrodes suited for the microcell, PEEK tubes were cut into 4-cm long pieces. To make electric contact, a bundle of copper wires was inserted into the PEEK tube and sealed at one end of the tube using fast-drying glue, leaving a chamber of approximately 1 mm depth at the other end of the tube. Thick Cu<sub>2</sub>O/CCC paste was pressed into this chamber and allowed to dry at room temperature for one week. The conductivity of the electrodes was examined with a multimeter, and only those with a resistance of less than 200  $\Omega$  were used. Electrodes were polished using grade 2/0 dry emery paper, a 3- $\mu\text{m}$  imperial micro finishing film sheet and

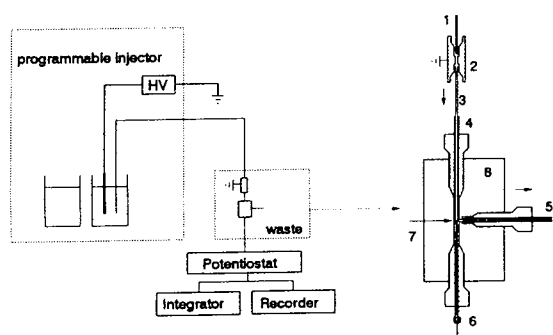


Fig. 1. Scheme of the experimental set-up: 1 = separation capillary; 2 = Pd-decoupler; 3 = coupling capillary; 4 = counter electrode; 5 = reference electrode and outlet; 6 = working electrode; 7 = detection chamber; 8 = T-shaped microcell.

0.05- $\mu\text{m}$  alumina particles on a Buehler pad, successively. The electrode surface was rinsed with water before use.

### 3. Results and discussion

#### 3.1. Electrochemistry

The miniaturized  $\text{Cu}_2\text{O}$  modified CCC electrodes were tested using cyclic voltammetry (CV) in quiescent solution. In a deaerated blank  $0.1 \text{ mol l}^{-1}$  NaOH solution a broad anodic peak at  $+0.15 \text{ V}$  appeared only in the first scan. This peak may be attributed to the oxidation of the surface layer of the cuprous oxide modifier. In subsequent scans no anodic peaks were observed in the potential range up to  $+0.6 \text{ V}$ . After the addition of different sugars to the solution, anodic peaks were observed with peak potentials between  $+0.55$  and  $+0.60 \text{ V}$ . An example is shown in Fig. 2. Since these peaks did not appear with unmodified electrodes, they can be attributed to the electrocatalytic oxidation of the carbohydrates tested. These phenomena are in agreement with the findings with large-area ( $3 \text{ mm}$  diameter) electrodes [36,37].

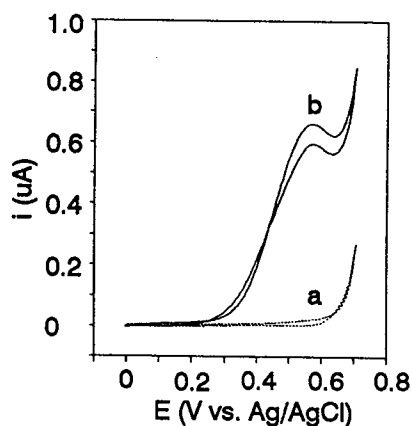


Fig. 2. Cyclic voltammetric responses for a  $\text{Cu}_2\text{O}$  modified CCC electrode in deaerated  $0.1 \text{ mol l}^{-1}$  NaOH: a = blank; b = with  $5 \text{ mmol l}^{-1}$  glucose. Scan rate  $20 \text{ mV s}^{-1}$ .

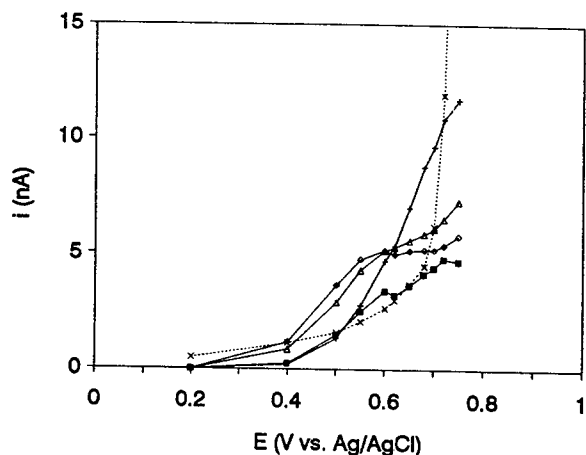


Fig. 3. Hydrodynamic voltammograms with a  $\text{Cu}_2\text{O}$ /CCC electrode in CE. Samples: (□) glycerol; (+) raffinose; (◇) fucose; (△) mannose; (×) background. Conditions:  $L_1 = 100 \text{ cm}$ ;  $L_2 = 8 \text{ cm}$ ;  $0.05 \text{ mol l}^{-1}$  NaOH;  $14 \text{ kV}$  high voltage;  $20 \text{ mbar}$  compensation pressure.

The optimal detection potential for CE was determined by measuring hydrodynamic voltammograms for several sugars in a background electrolyte of  $0.05 \text{ mol l}^{-1}$  NaOH (Fig. 3). For most sugars a limiting current is obtained at  $+0.60 \text{ V}$ , consistent with the CV experiments. Although the signal for raffinose still increased up to  $+0.75 \text{ V}$ , with increasing the applied potential the background current became higher and poorer signal-to-noise ratios were obtained. Therefore, further measurements were carried out with an applied potential of  $+0.60 \text{ V}$ . From the peak areas obtained it was calculated (taking  $2 \text{ eq. mol}^{-1}$  for the number of electrons involved in the oxidation process) that the coulometric efficiency of the microcell ranged from 19% for raffinose to 32% for mannose.

The stability of the modified conductive carbon cement electrode was examined and compared to an electrode with a carbon paste matrix. A standard mixture of four sugars was injected repeatedly during a 18-h period and peak heights were measured (see Fig. 4). The signals obtained with the carbon paste electrode kept decreasing. It is clear that even with the low liquid velocities



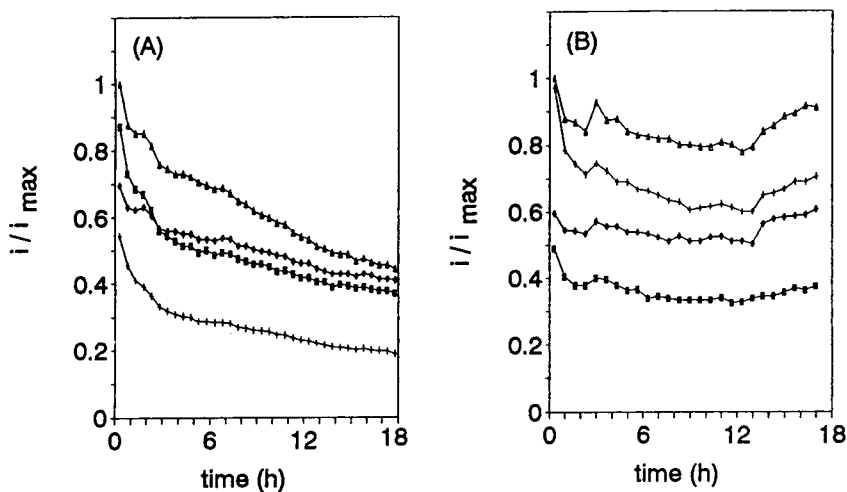


Fig. 4. Stability of Cu<sub>2</sub>O modified (A) carbon paste and (B) conductive carbon cement electrodes at +0.60 V. Conditions as in Fig. 3.

in CE, the leaching of modifier from carbon paste was still problematic. The signals with the CCC electrode became reasonably stable after a short time. The relative standard deviation of the

peak heights after the first hour was from 5.3 to 6.2% for the different compounds ( $n = 25$ ). When the mannose peak was regarded as an internal standard peak, the relative standard

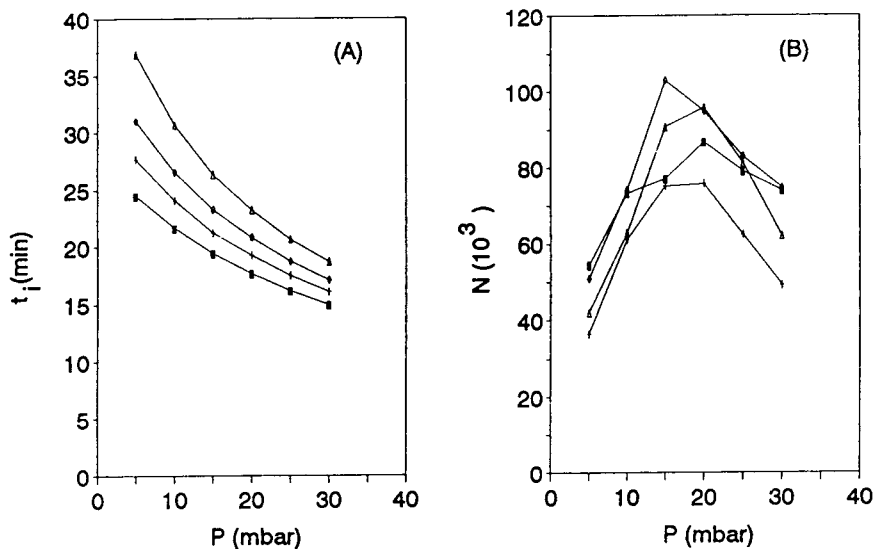


Fig. 5. Influence of the applied pressure on the apparent migration times (A) and the observed plate numbers (B). Sample components: (■) glycerol; (+) raffinose; (◇) fucose; (△) mannose. Conditions as in Fig. 3.

deviation for the other peaks was reduced to 2.2–3.5%.

### 3.2. Pressure compensation optimization

With off-column detection in capillary electrophoresis the flow resistance of the coupling capillary induces a back-pressure against electroosmotic flow in the separation capillary, distorting the uniform flow profile and causing extra zone broadening. The essence of pressure compensation is to provide a suitable driving force on the inlet of the separation capillary, driving the liquid through the coupling capillary with a flow-rate equal to the electroosmotic flow in the separation capillary ( $F_2 = F_{eo}$ ). To obtain a flat-plug flow profile in the separation capillary, this compensation pressure  $P_{comp}$  should be:

$$P_{comp} = 32\eta L_2 \mu_{eo} E \frac{d_1^2}{d_2^4} \quad (1)$$

where  $\eta$  is the solution viscosity,  $L_2$  the length of the coupling capillary,  $\mu_{eo}$  the electroosmotic mobility,  $E$  the electric field strength and  $d_1$  and  $d_2$  are the internal diameter of the separation and the coupling capillary, respectively.

Fig. 5 shows the influence of the applied pressure on apparent migration times and separation efficiencies for four sugars. Deviations from the optimal  $P_{comp}$  resulted in decrease of the separation efficiency, as discussed above. The optimal pressure was found to increase proportional to the coupling capillary length  $L_2$  (varied from 7 to 20 cm) and the field strength  $E$  (from 100 to 160 V cm<sup>-1</sup>), as predicted by Eq. 1. While a compensating pressure of 16 mbar was calculated for the system as used in further experiments (with a 7-cm coupling capillary and a field strength of 140 V cm<sup>-1</sup>), an optimum between 15 and 20 mbar was found experimentally for the different sugars. No obvious influence of  $L_2$  or  $E$  on the maximally obtainable plate numbers was found; these were always in the order of 90 000 to 110 000 when the compensating pressure was optimized. Apparently the dead volume of the decoupler played a major role in the zone broadening under optimized conditions. From

the difference between calculated and experimental values for the plate numbers, this dead volume was estimated as 10–20 nl.

### 3.3. Separation conditions

Since the  $pK_a$  values of most mono- and oligosaccharides are in the order of 12.5, concentrated solutions of sodium hydroxide have to be used as background electrolyte for the electrophoretic separation. Concentrations of 0.01–0.02 mol l<sup>-1</sup>, as have been suggested in the literature [28,29], are insufficient to obtain a satisfactory separation. In accordance to the findings of Colón et al. [34], we found that even with a 0.05 mol l<sup>-1</sup> sodium hydroxide solution the resolution between zones of sugars is low. In Fig. 6, separations of a standard mixture of sugars with 0.05 and 0.10 mol l<sup>-1</sup> NaOH as background electrolyte are compared.

The apparent migration time  $t_i$  of solute  $i$  consists of the migration time  $t_{1,i}$  in the separation capillary and the hold-up time  $t_2$  in the coupling capillary. With the appropriate pressure compensation, these are given by:

$$t_{1,i} = \frac{L_1}{(\mu_{eo} \pm \mu_i)E} \quad (2)$$

$$t_2 = \frac{L_2 d_2^2}{\mu_{eo} E d_1^2} \quad (3)$$

The electroosmotic mobility  $\mu_{eo}$  and effective electrophoretic mobilities of solutes  $\mu_i$  can be calculated from the experimentally available apparent migration times of the osmotic flow marker ( $t_{eo}$ ) and the solutes ( $t_i$ ) with:

$$\mu_{eo} = \frac{L_1 + (d_2/d_1)^2 L_2}{t_{eo} E} \quad (4)$$

$$\mu_i = - \frac{(t_i - t_{eo})[L_1 + (d_2/d_1)^2 L_2]^2}{E t_{eo} [t_i L_1 + (t_i - t_{eo})(d_2/d_1)^2 L_2]} \quad (5)$$

In Table 1 the mobilities of the sugars are given, calculated with Eqs. 4 and 5 from their apparent migration times. The increased ionization of the sugars in 0.10 mol l<sup>-1</sup> NaOH results in an improved resolution. However, the analysis time

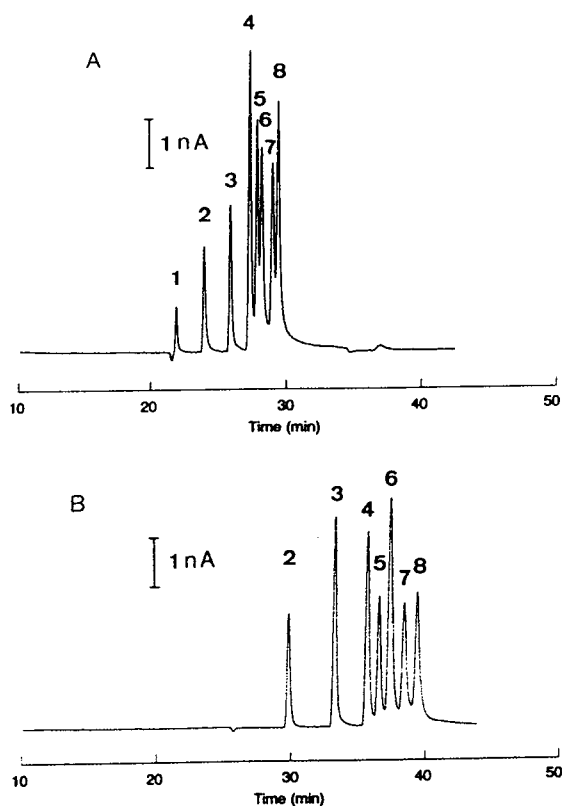


Fig. 6. Electropherograms obtained with (A)  $0.05 \text{ mol l}^{-1}$  and (B)  $0.1 \text{ mol l}^{-1}$  NaOH electrolyte at 12 kV high voltage with optimal compensation pressure. Peaks: 1 = glycerol; 2 = raffinose; 3 = fucose; 4 = galactose; 5 = mannose; 6 = arabinose; 7 = xylose; 8 = glucose ( $20\text{--}240 \text{ } \mu\text{mol l}^{-1}$ ).

is increased with the  $0.10 \text{ mol l}^{-1}$  background electrolyte, partly also by a decrease of the electroosmotic mobility. A relatively low electric field ( $120 \text{ V cm}^{-1}$ ) had to be used to limit the zone broadening by the Joule heating with this high-conductivity electrolyte. The electrophoretic current was  $124 \text{ } \mu\text{A}$  under these conditions.

The sensitivities, linear range and limits of detection (LOD) for the different sugars are listed in Table 2. Detection limits of  $20\text{--}30 \text{ fmol}$  or  $1\text{--}2 \text{ } \mu\text{mol l}^{-1}$  are found based on a signal-to-noise ratio of 3.

The concentration detection limits are at least two orders of magnitude lower than those obtained in CE by indirect UV detection [29–30] or

Table 1  
Effective electroosmotic and electrophoretic mobilities<sup>a</sup>

Peak	$\mu_i$ ( $10^{-8} \text{ m}^2 \text{ V}^{-1} \text{ s}^{-1}$ )	
NaOH concentration ( $\text{mol l}^{-1}$ )	0.05	0.10
Electroosmosis	+7.06	+6.71
Glycerol	-0.09	n.m. <sup>b</sup>
Raffinose	-0.68	-0.79
Fucose	-1.15	-1.32
Galactose	-1.45	-1.65
Mannose	-1.56	-1.74
Arabinose	-1.62	-1.83
Xylose	-1.77	-1.95
Glucose	-1.84	-2.04
Galacturonic acid	-3.51	-3.90

<sup>a</sup> For conditions see Fig. 6.

<sup>b</sup> Not measured.

borate complexation [27]. In comparison to end-column electrochemical detection, an advantage in concentration limits is generated by the larger capillary diameters allowed. Lu and Cassidy [33] found detection limits for sugars, using PAD, of approximately  $1 \text{ fmol}$ . However, with the  $10\text{-}\mu\text{m}$  capillaries they used, this corresponds to sample concentrations of  $2\text{--}3 \text{ } \mu\text{mol l}^{-1}$ . With a copper wire electrode in the end-column mode, Colón et al. [34] found detection limits of less than  $50 \text{ fmol}$ . Together with the sample volume disadvantage in the  $50\text{-}\mu\text{m}$  capillaries used, the concentration limits were almost one order of magnitude higher than in our method.

#### 4. Conclusion

It may be stated that we have shown the feasibility of off-column amperometric detection of sugars in CE using chemically modified electrodes. Our results with respect to separation efficiency and limits of detection are similar to or slightly better than what has been achieved with end-column detection. However, with our system, capillaries and electrodes can be installed and changed easily without the use of a microscope or micromanipulator, so that the detection set-up might be suited for routine analysis.

Table 2  
Linearity and limits of detection<sup>a</sup>

Compound	Sensitivity (nA pmol <sup>-1</sup> )	Injected amount (pmol)	R	LOD (μmol l <sup>-1</sup> )
Raffinose	1.92 ± 0.05	0.37–3.7	0.997	1.9
Fucose	3.17 ± 0.03	0.21–2.1	0.9996	1.4
Mannose	3.44 ± 0.04	0.31–3.1	0.9995	1.3

<sup>a</sup> For conditions see Fig. 6B.

## References

- [1] F.E.P. Mikkers, F.M. Everaerts and Th.P.E.M. Verheggen, *J. Chromatogr.*, 169 (1979) 11.
- [2] J.W. Jorgenson and K.D. Lukacs, *Anal. Chem.*, 53 (1981) 1298.
- [3] B.L. Karger, A.S. Cohen and A. Guttman, *J. Chromatogr.*, 492 (1989) 585.
- [4] H.H. Lauer and J.B. Ooms, *Anal. Chim. Acta*, 250 (1991) 45.
- [5] S.F.Y. Li, *Capillary Electrophoresis: Principles, Practice and Applications*, Elsevier, Amsterdam, 1992.
- [6] P.D. Grossman and J.C. Colburn (Editors), *Capillary Electrophoresis: Theory and Practice*, Academic Press, San Diego, CA, 1992.
- [7] D. Perret and G. Ross, *Trends Anal. Chem.*, 11 (1992) 156.
- [8] P.G. Righetti, in E. Heftmann (Editor), *Fundamentals and Applications of Chromatography and Related Differential Migration Methods, Part A, Fundamentals and Techniques (J. Chromatography Library Series)*, Vol. 51A, Elsevier, Amsterdam, 1992, p. A481.
- [9] T. Wehr, *LC·GC*, 11 (1993) 19.
- [10] Y. Xu, *Anal. Chem.*, 65 (1993) 425.
- [11] C.A. Monnig and R.T. Kennedy, *Anal. Chem.*, 66 (1994) 280.
- [12] A.G. Ewing, R.A. Wallingford and T.M. Olefirowicz, *Anal. Chem.*, 61 (1989) 292.
- [13] Y.F. Yik and S.F.Y. Li, *Trends Anal. Chem.*, 11 (1992) 325.
- [14] T.M. Olefirowicz and A.G. Ewing, *Anal. Chem.*, 62 (1990) 1872.
- [15] X. Huang, R.N. Zare, S. Sloss and A.G. Ewing, *Anal. Chem.*, 63 (1991) 189.
- [16] S. Sloss and A.G. Ewing, *Anal. Chem.*, 65 (1993) 577.
- [17] W. Lu, R.M. Cassidy and A.S. Baranski, *J. Chromatogr.*, 640 (1993) 433.
- [17] R.A. Wallingford and A.G. Ewing, *Anal. Chem.*, 59 (1987) 1762.
- [18] Y.F. Yik, H.K. Lee, S.F.Y. Li and S.B. Khoo, *J. Chromatogr.*, 585 (1991) 139.
- [19] C.W. Whang and I.C. Chen, *Anal. Chem.*, 64 (1992) 2461.
- [20] T.J. O'Shea, R.D. Greenhagen, S.M. Lunte, C.E. Lunte, M.R. Smyth, D.M. Radzik and N. Watanabe, *J. Chromatogr.*, 593 (1992) 305.
- [21] I.C. Chen and C.W. Whang, *J. Chromatogr.*, 644 (1993) 208.
- [22] W.Th. Kok, *Anal. Chem.*, 65 (1993) 1853.
- [23] W.Th. Kok and Y. Sahin, *Anal. Chem.*, 65 (1993) 2497.
- [24] S. Honda, S. Iwase, A. Makino and S. Fujiwara, *Anal. Biochem.*, 176 (1989) 72.
- [25] J. Liu, O. Shirota and M. Novotny, *Anal. Chem.*, 63 (1991) 413.
- [26] J. Liu, O. Shirota and M. Novotny, *Anal. Chem.*, 64 (1992) 973.
- [27] S. Hoffstetter-Kuhn, A. Paulus, E. Gassmann and H.M. Widmer, *Anal. Chem.*, 63 (1991) 1541.
- [28] T.W. Garner and E.S. Yeung, *J. Chromatogr.*, 515 (1990) 639.
- [29] A.E. Vorndran, P.J. Oefner, H. Scherz and G.K. Bonn, *Chromatographia*, 33 (1992) 163.
- [30] A. Klockow, A. Paulus, V. Figueiredo, R. Amadò and H.M. Widmer, *J. Chromatogr. A*, 680 (1994) 187.
- [31] D.C. Johnson and W.R. LaCourse, *Anal. Chem.*, 62 (1990) 589.
- [32] T.J. O'Shea, S.M. Lunte and W.R. LaCourse, *Anal. Chem.*, 65 (1993) 948.
- [33] W. Lu and R.M. Cassidy, *Anal. Chem.*, 65 (1993) 2878.
- [34] L.A. Colón, R. Dadoo and R.N. Zare, *Anal. Chem.*, 65 (1993) 476.
- [35] J. Ye and R.P. Baldwin, *Anal. Chem.*, 65 (1993) 3525.
- [36] Y. Xie and C.O. Huber, *Anal. Chem.*, 63 (1991) 1714.
- [37] X. Huang, J.J. Pot and W.Th. Kok, *Anal. Chim. Acta*, 300 (1995) 5.
- [38] X. Huang and W.Th. Kok, *Anal. Chim. Acta*, 273 (1993) 245.
- [39] A.J. Tudos, M.M.C. van Dyck, H. Poppe and W.Th. Kok, *Chromatographia*, 37 (1993) 79.



ELSEVIER

Journal of Chromatography A, 707 (1995) 343–353

JOURNAL OF  
CHROMATOGRAPHY A

# Migration behaviour of alkali and alkaline-earth metal ion–EDTA complexes and quantitative analysis of magnesium in real samples by capillary electrophoresis with indirect ultraviolet detection

Tianlin Wang, S.F.Y. Li\*

*Department of Chemistry, National University of Singapore, Kent Ridge Crescent, Singapore 0511, Singapore*

First received 10 October 1994; revised manuscript received 28 February 1995; accepted 6 March 1995

## Abstract

A capillary electrophoretic (CE) method was developed for the separation of some common alkali and alkaline-earth metal ions using EDTA as complexing agent and pyridine as UV chromophore for indirect detection at pH 5.00. Effects of pH and concentration of complexing agent on the differences in the effective mobilities between two ions were considered and equations derived were used to deduce the optimum conditions for their separation. Baseline separation of a group of metal ions, including K, Na, Li, Mg, Sr and Ba, was achieved in less than 4 min. The calibration range for magnesium was found to be linear up to 1.00  $\mu\text{g/ml}$  when samples were prepared in the running buffer while a hyperbolic calibration curve was obtained when prepared in water. Application of the method to the analysis of magnesium in river water, urine and a solid sample of calcium carbonate was demonstrated. Magnesium in those samples was determined to be 812  $\mu\text{g/ml}$ , 78.0  $\mu\text{g/ml}$  and 0.023% (w/w), respectively, with reproducibilities between 5–9% R.S.D. in terms of peak height depending on sample matrices.

## 1. Introduction

Capillary electrophoresis (CE) separates components on the basis of their differences in migration velocity in a suitable electrophoretic medium under the influence of an electric field of high strength [1–3]. Applications of CE have been found in many diverse fields, such as large biomolecules [4–6], pharmaceuticals [7], organic compounds [8] and inorganic anions/cations [9–12].

For metal cations there used to be two main

factors which hamper their analysis by CE [10]. One was the poor detectability and the other the insufficient difference in their mobilities. Introducing complexing agents to enlarge the effective mobility differences between the ions and adopting indirect UV or fluorescence detection are common ways to overcome the above problems. The number of applications of capillary electrophoresis to the separation and determination of metal cations has rapidly increased [9–23].

Many of the papers published so far on the separation of metal cations were focused on separation strategies. A few published papers dealt with quantitation of metal ions in real

\* Corresponding author.

samples [10,12,14–16,18,21,22]. In most of the reported CE methods for separation and determination of alkali and alkaline-earth metal ions, the calcium peak appeared before and very close to the magnesium peak in the electropherograms [12,14,15,18–23]. Some difficulties may arise when such methods are applied to the quantification of small amounts of magnesium in the presence of very large amounts of calcium, such as magnesium impurities in a calcium carbonate sample. Thus, there is a need to develop methods for the determination of magnesium in samples where considerable amounts of other cations which are likely to cause interference in the other methods commonly used for determination, such as spectrometric methods [24,25], are expected to be present.

In this paper a CE method was developed for the separation of some alkali and alkaline-earth metal ions using chemicals readily available, i.e. EDTA as a complexing agent, and pyridine as a UV chromophore for indirect detection at pH 5.00. The migration behaviour of alkali and alkaline-earth metal ion–EDTA complexes was studied. Guidelines were worked out for optimization of CE conditions, such as pH and the concentration of complexing agent in buffer, based on theoretical considerations. Effects of pH, concentration of EDTA and sample preparation procedures on separation and quantitation were experimentally investigated. The CE method was successfully applied to the determination of magnesium in real samples with relatively complex matrices.

## 2. Experimental

### 2.1. Chemicals

All metal ion solutions were prepared from nitrate salts. They were prepared as stock solutions of 1000  $\mu\text{g}/\text{ml}$  (metal ion concentration). Metal ion solutions of other concentrations were prepared by appropriately diluting portions of the above stock solutions. Ethylenediaminetetraacetic acid disodium salt (EDTA) was a product

of J.T. Baker (J.T. Baker, Phillipsburg, NJ, USA). Pyridine of analytical grade was purchased from Fluka (Fluka Chemie, Switzerland). Perchloric acid (60%) was also of analytical grade. Benzyl alcohol of analytical grade was used as neutral marker to measure electroosmotic flow (EOF). Deionized water used throughout the experiments was prepared with a Milli-Q system (Millipore, Bedford, MA, USA).

### 2.2. Buffers and pH adjustment

The running buffer contained 10 mM pyridine, which served both as the carrier electrolyte and background absorber for indirect UV detection. The adjustment of pH was accomplished by adding perchloric acid solution. The concentration of the complexing agent, EDTA, was set to 0.8 mM unless otherwise stated.

### 2.3. Sample preparation

Water samples and urine samples were first diluted with deionized water and then mixed with buffer to ensure that the differences in ionic strength, conductivity, and pH between samples and the running buffer were negligible and that peak height was in the linear range of the calibration curve for magnesium. Calcium carbonate (ca. 0.15 g) was accurately weighted into a beaker. A few drops of deionized water were added to wet the sample. Perchloric acid (60%) was added dropwise until calcium carbonate was completely dissolved (N.B., to avoid vigorous or explosive reactions one must be sure there is no oxidizable matter in the samples before adding the perchloric acid). During dissolution the beaker was covered with a watch glass to avoid any loss of the sample. The solution was quantitatively transferred from the beaker into a 10-ml volumetric flask and deionized water was added to the mark. Subsequent procedures for sample preparation were the same as those mentioned above for the liquid samples. Conditions will be specified where appropriate if different from those described above.

## 2.4. Apparatus

CE was performed with a laboratory built capillary electrophoresis system, equipped with a positive power supply (Spellman, Plainview, NY, USA) and a Linear UVIS 200 detector (Linear Instruments Corp., Reno, NV, USA). Electropherograms were recorded with a HP 3394A integrator (Hewlett-Packard, Avondale, PA, USA) connected with a switch for changing the polarity of the input signal. Polyimide-coated fused-silica capillaries (Polymicro Technologies, Phoenix, AZ, USA) used were 39.5 cm long with an inner diameter (I.D.) of 75  $\mu\text{m}$  and an outer diameter (O.D.) of 362  $\mu\text{m}$ . An on-column detection window was created at 30 cm from the injection end and indirect UV detection was conducted at 254 nm. A hydrostatic sample injection mode was employed for sample introduction into the capillary at the anodic side. The field strength applied for separation was 190 V/cm and the voltage was 7500 V. Atomic absorption measurements were performed with an AA-670 atomic absorption/flame emission spectrophotometer (Shimadzu Corp., Kyoto, Japan).

## 3. Theory

In this section, equations for calculating the effective mobility differences between pairs of 1:1 metal ion–ligand complexes are derived. It is assumed that there are two kinds of metal ions, M and N, with identical mobilities  $U_M$  and  $U_N$  in free solution and that both M and N can form 1:1 complexes (ML and NL) with ligand L and the complexes, ML and NL, have identical mobilities  $U_{ML}$  and  $U_{NL}$ . It is also assumed that  $K_{NL} > K_{ML}$ . The effective mobilities of the metal ions will be the weighted sum of the mobilities of the free ions,  $U_f$ , and the mobilities of the complexes,  $U_c$  [26].

$$U_M^{\text{eff}} = (U_f + K_{ML}[L]U_c)(1 + K_{ML}[L])^{-1} \quad (1)$$

$$U_N^{\text{eff}} = (U_f + K_{NL}[L]U_c)(1 + K_{NL}[L])^{-1} \quad (2)$$

Although  $U_M = U_N$  and  $U_{ML} = U_{NL}$ ,  $U_M^{\text{eff}}$  and

$U_N^{\text{eff}}$  can be different from each other due to the difference in their capabilities to form complexes and the difference between  $U_f$  and  $U_c$ .

If the side-reaction of L with  $H^+$  is the only one needed to be taken into account, the apparent stability constants  $K'_{ML}$  and  $K'_{NL}$  [27], can be used instead of  $K_{ML}$  and  $K_{NL}$  and the difference in effective mobilities becomes:

$$U_M^{\text{eff}} - U_N^{\text{eff}} = (K'_{NL} - K'_{ML})(U_f - U_c)[L'] \times \{(1 + K'_{ML}[L'])(1 + K'_{NL}[L'])\}^{-1} \quad (3)$$

and

$$a_{L(H)} = [L']/[L] \quad (4)$$

Rearranging Eq. 3 gives

$$U_M^{\text{eff}} - U_N^{\text{eff}} = (K_{NL} - K_{ML})(U_f - U_c)[L'] \times \{a_{L(H)}(1 + K'_{ML}[L'])(1 + K'_{NL}[L'])\}^{-1} \quad (5)$$

To determine the optimum concentration of the complexing agent for obtaining high resolution, one can differentiate Eq. 3 with respect to  $[L']$  twice to obtain

$$(U_M^{\text{eff}} - U_N^{\text{eff}})_{\text{max}} = (K_{NL}K_{ML})^{1/2}(K_{NL} - K_{ML}) \times (U_f - U_c) \{[(K_{NL}K_{ML})^{1/2} + K_{ML}] \times [(K_{NL}K_{ML})^{1/2} + K_{NL}]\}^{-1} \quad (6)$$

When

$$[L'] = (K'_{ML}K'_{NL})^{-1/2} \quad (7)$$

Eq. 6 indicates the existence of the maximum difference in effective mobilities of ions M and N, which can be theoretically estimated.

It should also be recognized that there are practical limitations, which will be discussed later on, in the use of the concentration of complexing agent as a parameter for the optimization of the separation as calculated on the basis of Eq. 7.

## 4. Results and discussion

### 4.1. Effect of pH on separation and detection

To predict the effect of pH on separation, plots of the terms on the right hand side of Eq. 5

with omission of the factor  $(U_f - U_c)$  (because of the lack of data on  $U_c$ ) vs. pH in a broad range were constructed as shown in Fig. 1. Literature values of  $K'_{CaY}$ ,  $K'_{MgY}$ ,  $K'_{SrY}$ ,  $K'_{BaY}$  and the dissociation constants of EDTA were used [27] and the assumption was made that  $[Y'] = 0.8$  mM. It shows that separation of alkaline-earth metal ions may be achieved within a pH range of 4 to 7, where the values of the term,  $(U_M^{eff} - U_N^{eff})/(U_f - U_c)$ , are  $6.7 \cdot 10^{-4}$  for curve 1 and  $2.1 \cdot 10^{-4}$  for curve 2 at pH 4, and  $1.6 \cdot 10^{-3}$  for curve 2 and  $6.2 \cdot 10^{-3}$  for curve 3 at pH 7, respectively. It also illustrates that the peak pair of Sr–Mg will be the most difficult one of the three peak pairs (Ba–Sr, Sr–Mg and Mg–Ca) to separate in a pH range 4–7.

To examine the effect of pH on separation and detection, all other experimental conditions were kept constant except for the different amounts of

perchloric acid used to adjust the pH of the buffer. At pH 5.00, the peaks for all the ions tested were baseline separated in 4 min with a low noise level and high detectability. Baseline separation of K, Na, Li, Mg, Sr and Ba was achieved. Under the proposed conditions the effective mobility of calcium was so low that the calcium peak eluted much later than the peaks of interest in the electropherogram and hence caused no interference in the analysis of the other cations. Many other metal ions, which form even more stable complexes with EDTA, could also be well resolved from the cations of interest. At pH 4.00, fractions of divalent cations forming complexes were smaller due to the side-reaction of Y with  $H^+$ . Furthermore, divalent cations exhibited effective mobilities which were higher than those at pH 5.00. Differences in the effective mobilities of Ba, Sr and Mg were so

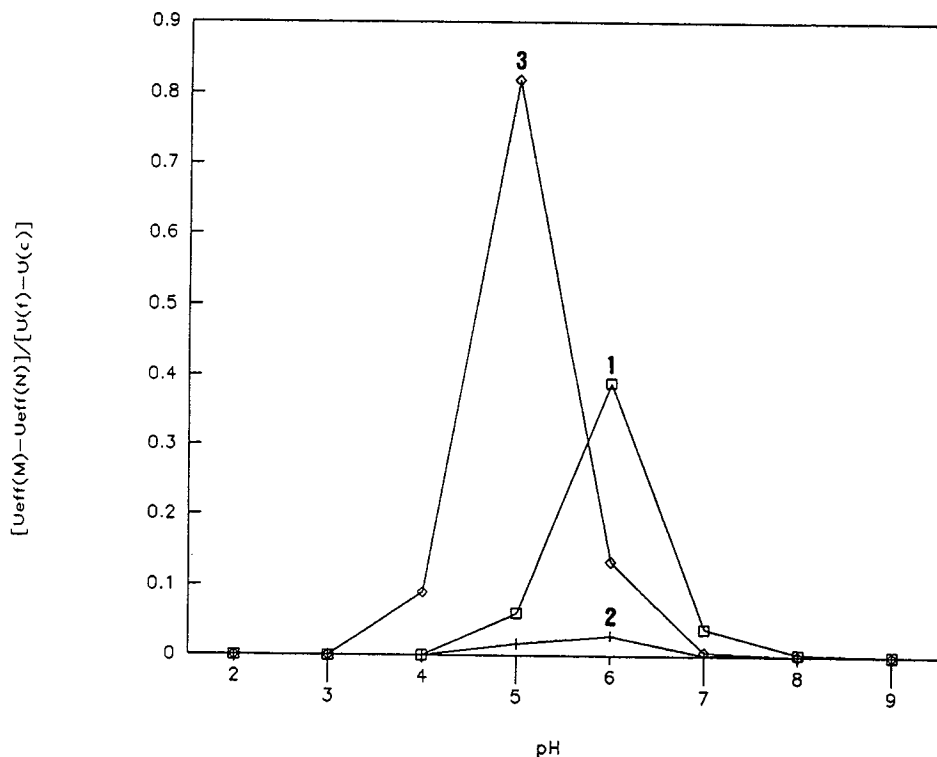


Fig. 1. Theoretical prediction of the effect of pH on the differences in effective mobilities of common alkaline earth metal ions in the presence of 0.8 mM EDTA. Ordinate is value of the terms on right hand side of Eq. 5 with omission of the factor of  $(U_f - U_c)$ . 1 =  $(U_{Ba}^{eff} - U_{Sr}^{eff})$ ; 2 =  $(U_{Sr}^{eff} - U_{Mg}^{eff})$ ; 3 =  $(U_{Mg}^{eff} - U_{Ca}^{eff})$ .



small that separation of those peaks could not be achieved. The current was 11  $\mu\text{A}$ , which is 1.5 times higher than that at pH 5.00. It was observed that a significantly more noisy baseline was obtained under these conditions. Possible reasons for the noisy baseline might be attributable to the effect of Joule heating [28] or the lack of buffering action. At pH 6.00, the migration times of monovalent metal ions, i.e. potassium, sodium, and lithium, were less than 3 min. With a run-time up to 10 min, which was three times longer than the migration time of the neutral marker, no peaks of divalent ions were observed. The reason why no peaks for the divalent metal ions appeared is not clear at present. One possible explanation is that the formation of a large portion of complexes of the divalent cations with EDTA reduced the effective mobilities of the divalent metal ions greatly as the apparent stability constants of the complexes increased with pH and made these ions less detectable. Another possible explanation is that at pH 6.00 pyridine existed mainly as the neutral molecule rather than in the pyridinium ion form since the  $pK_a$  value of the pyridinium ion is 5.2 [29]. This might lower the sensitivity of detection for the divalent metal ions as displacement of pyridinium by the metal ions would be masked by strong background absorbance from neutral pyridine molecules. Thus, although the difference in the effective mobilities of the divalent metal ions was theoretically predicted to be large at pH 6.00, this pH was not a favourable condition for CE analysis of the divalent ions in terms of detectability and separation time. Another observation is that since only a very small amount of perchloric acid was introduced to the buffer to adjust its pH to 6.00, the conductivity and ionic strength of the buffer were rather low. Consequently, a relatively low current of 3  $\mu\text{A}$  was observed at this pH.

At pH 4.00, 5.00 and 6.00, the EOF measured with benzyl alcohol was found to be  $3.1 \cdot 10^{-4} \text{ cm}^2/\text{V s}$ ,  $5.8 \cdot 10^{-4} \text{ cm}^2/\text{V s}$ , and  $8.9 \cdot 10^{-4} \text{ cm}^2/\text{V s}$ , respectively. The EOF increased almost linearly with pH in the pH range 4.00–6.00. Suppression of dissociation of silanol groups on the capillary wall lead to lowering of the charge

density in the double layer. Consequently, a lower EOF was observed at lower pH [28]. Since both the EOF and complexation were affected by pH changes, resolution depended on the combined effects of the two parameters. Increase in the differences in effective mobilities resulting from increasing complexation with increase of pH resulted in enhanced resolution, but the large EOF at high pH had an adverse effect on resolution in the case of EOF and solutes moving in the same direction [1,2].

A more detailed study was performed on the effect of pH on the effective mobilities of Ba, Sr and Mg over the pH range 4.50–5.10. This pH range was chosen based on the facts that a lower pH led to merging of the peaks of Ba, Sr and Mg and that a higher pH caused the Mg peak to migrate slower than the water peak and hence became difficult to detect. In Fig. 2a, curves 1, 2 and 3 are plots of the experimental effective mobilities of Ba, Sr and Mg, i.e.  $U_{\text{Ba}}^{\text{eff}}$ ,  $U_{\text{Sr}}^{\text{eff}}$  and  $U_{\text{Mg}}^{\text{eff}}$ , respectively. Effective mobilities were calculated by

$$U_{\text{M}}^{\text{eff}} = (L_{\text{t}}L_{\text{e}}/V)[(1/t_{\text{M}}) - (1/t_{\text{B}})] \quad (8)$$

where  $L_{\text{t}}$  and  $L_{\text{e}}$  are the total length of the capillary and the effective length of the capillary, i.e., from the injection end of the capillary to the detection window, respectively;  $V$  is the applied voltage for separation;  $t_{\text{M}}$  and  $t_{\text{B}}$  are the migration times of metal ions and the neutral marker benzyl alcohol, respectively. Curves 4 and 5 are their differences, i.e.  $U_{\text{Ba}}^{\text{eff}} - U_{\text{Sr}}^{\text{eff}}$  and  $U_{\text{Ba}}^{\text{eff}} - U_{\text{Mg}}^{\text{eff}}$ . Good agreement was obtained for the trend exhibited by the experimentally obtained curves 4 and 5 in Fig. 2a and the theoretically predicted curves 1 and 2 based on Eq. 5 as shown in Fig. 2b, although an exact comparison was not possible due to a lack of data for  $U_{\text{c}}^{\text{eff}}$ . In the examined pH range of 4.50 to 5.10,  $U_{\text{Ba}}^{\text{eff}} - U_{\text{Sr}}^{\text{eff}}$  increased much faster than  $U_{\text{Sr}}^{\text{eff}} - U_{\text{Mg}}^{\text{eff}}$  with the increase of pH.

The UV chromophore, as a co-ion in the CE buffer, should have both a strong absorption at the detection wavelength and an ionic mobility similar to that of the solutes being detected [16,30]. Imidazole and pyridine were shown to

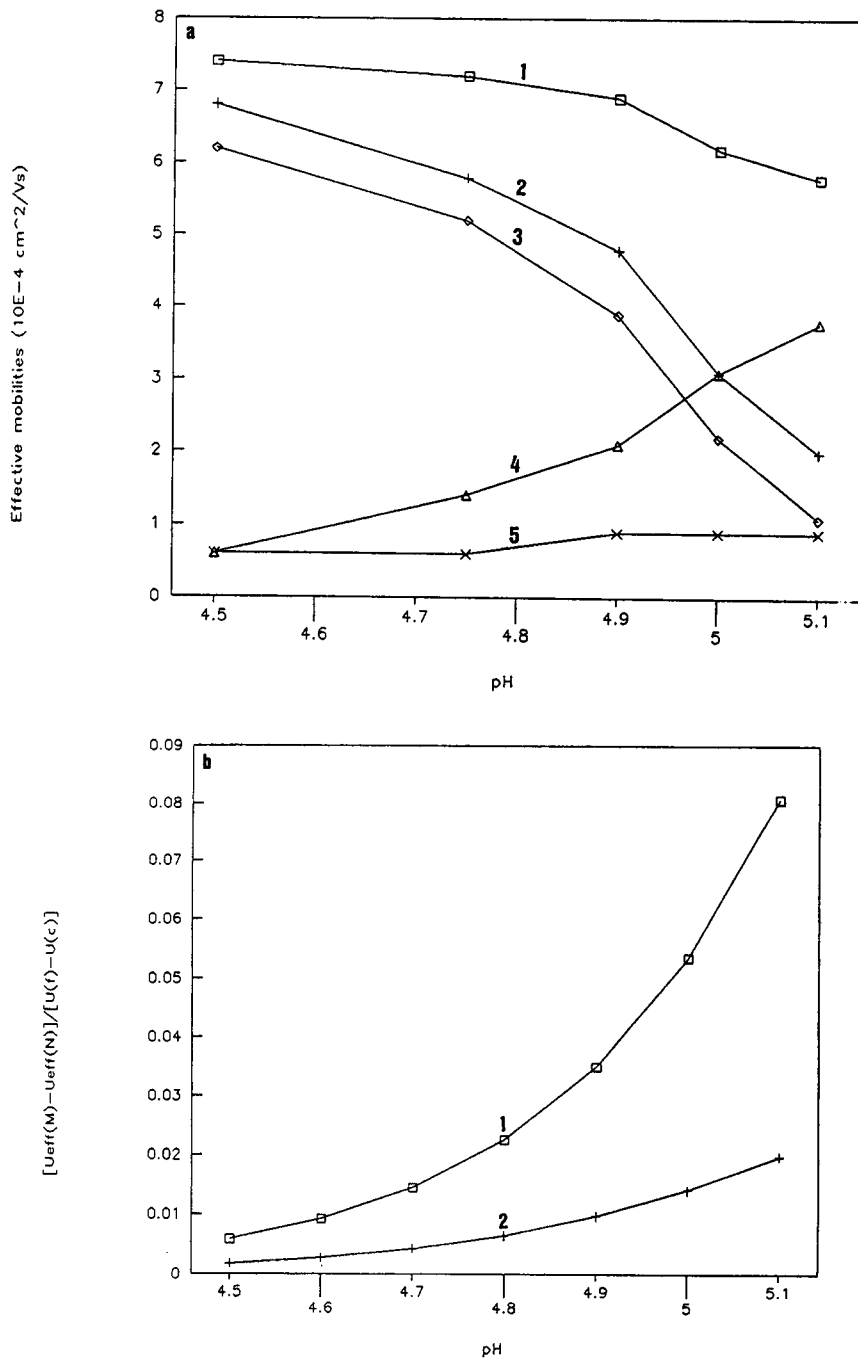


Fig. 2. Effect of pH on the effective mobilities of Ba, Sr and Mg in buffers containing 0.8 mM EDTA. (a) Experimental results. Curves 1, 2 and 3 represent the effective mobilities of Ba, Sr and Mg, respectively. Curves 4 and 5 show the differences in effective mobility ( $4 = U_{\text{Ba}}^{\text{eff}} - U_{\text{Sr}}^{\text{eff}}$ ;  $5 = U_{\text{Sr}}^{\text{eff}} - U_{\text{Mg}}^{\text{eff}}$ ). (b) Theoretical prediction of the effective mobility differences in Ba, Sr and Mg with omission of the factor of  $(U_t - U_c)$  ( $1 = U_{\text{Ba}}^{\text{eff}} - U_{\text{Sr}}^{\text{eff}}$ ;  $2 = U_{\text{Sr}}^{\text{eff}} - U_{\text{Mg}}^{\text{eff}}$ ).

be appropriate as UV chromophores for indirect detection of common alkali and alkaline-earth metal ions [16]. The maximum absorption wavelength of imidazole is 214 nm where the complexing agent EDTA has a significant absorption and hence a high background which lowers the sensitivity. Pyridine has a maximum absorption wavelength of 254 nm where EDTA has only negligible absorption. Therefore pyridine was employed as UV chromophore in the present work.

In terms of sensitivity, a buffer of pH higher than 5.2 is unfavourable because in such cases a large fraction of pyridine exists as neutral molecules which can not be displaced by the metal ions of interest and will serve as UV absorbing species resulting in high UV background and low sensitivity.

#### 4.2. Effect of EDTA concentration on separation

The first step in the optimization of the EDTA concentration was to decide on the concentration range of EDTA to be experimentally tested. Several criteria have been considered. The first is that the resolution should be as high as possible. From Eq. 7, it was calculated that at pH 5.00, to achieve the highest resolution between calcium and magnesium, magnesium and strontium, and strontium and barium, concentrations of EDTA should be 0.79 mM, 8.9 mM and 22 mM, respectively. Secondly, excessively high concentrations of EDTA should be avoided. Otherwise migration times of alkaline-earth metal ion peaks would be too long and the limits of detection would be high. Moreover, significant Joule heating may occur. Finally, extremely low concentrations of EDTA should not be used because in that case the migration times of the alkaline-earth metal ions would be highly sensitive to variations in their concentration and the concentrations of other ions in the sample which may also form complexes with EDTA.

Fig. 3 shows electropherograms obtained with different concentrations of EDTA. In all three electropherograms, calcium, magnesium, strontium and barium were well separated as ex-

pected. As a large portion of the calcium ions existed in the negatively charged complex form and the effective mobility of calcium was very low, no calcium peak did appear in the electropherograms. At 0.8 mM EDTA, the barium peak occurred between but well resolved from the sodium peak and the lithium peak. At lower concentration of EDTA, the effective mobility of the barium ions increased and the barium peak shifted forward closer to the sodium peak. At higher concentration of EDTA, the effective mobility of the barium ions decreased and the barium peak shifted backward closer to the lithium peak. Therefore, the subsequent experiments were conducted under the condition of 0.8 mM EDTA and 10 mM pyridine at pH 5.00.

#### 4.3. Effect of sample preparation procedures on detection and quantitation

Sample preparation affected both detectability and linearity. Dissolving samples in water resulted in good detectability and poor linearity, but dissolving samples in running buffer had the opposite effect. With an injection time of 15 s at a height difference of 4.0 cm between the liquid levels of the sample vial and the buffer reservoir at the grounded electrode, the limit of detection (LOD) for magnesium (signal-to-noise ratio >2) was 75 ng/ml when samples were prepared in deionized water and 150 ng/ml when prepared in the running buffer. Such a difference might result from the sample stacking effect [31]. The LOD decreased down to 20 ng/ml when samples were prepared in deionized water and injections were made in 40 s with 6.5 cm difference in height. No further improvement in LOD was obtained when conditions for injection were set to 60 s and 6.5 cm. Although a slightly lower LOD (ca. 10 ng/ml) was obtained [32] with an extended path length capillary, i.e. with an "egg-shaped cell", the present method has the advantage that it uses conventional capillaries and thus would be compatible with most of the commercial detector designs. In addition, the method also has the advantages that it requires only readily available chemicals and that the resolution between the magnesium and calcium peaks

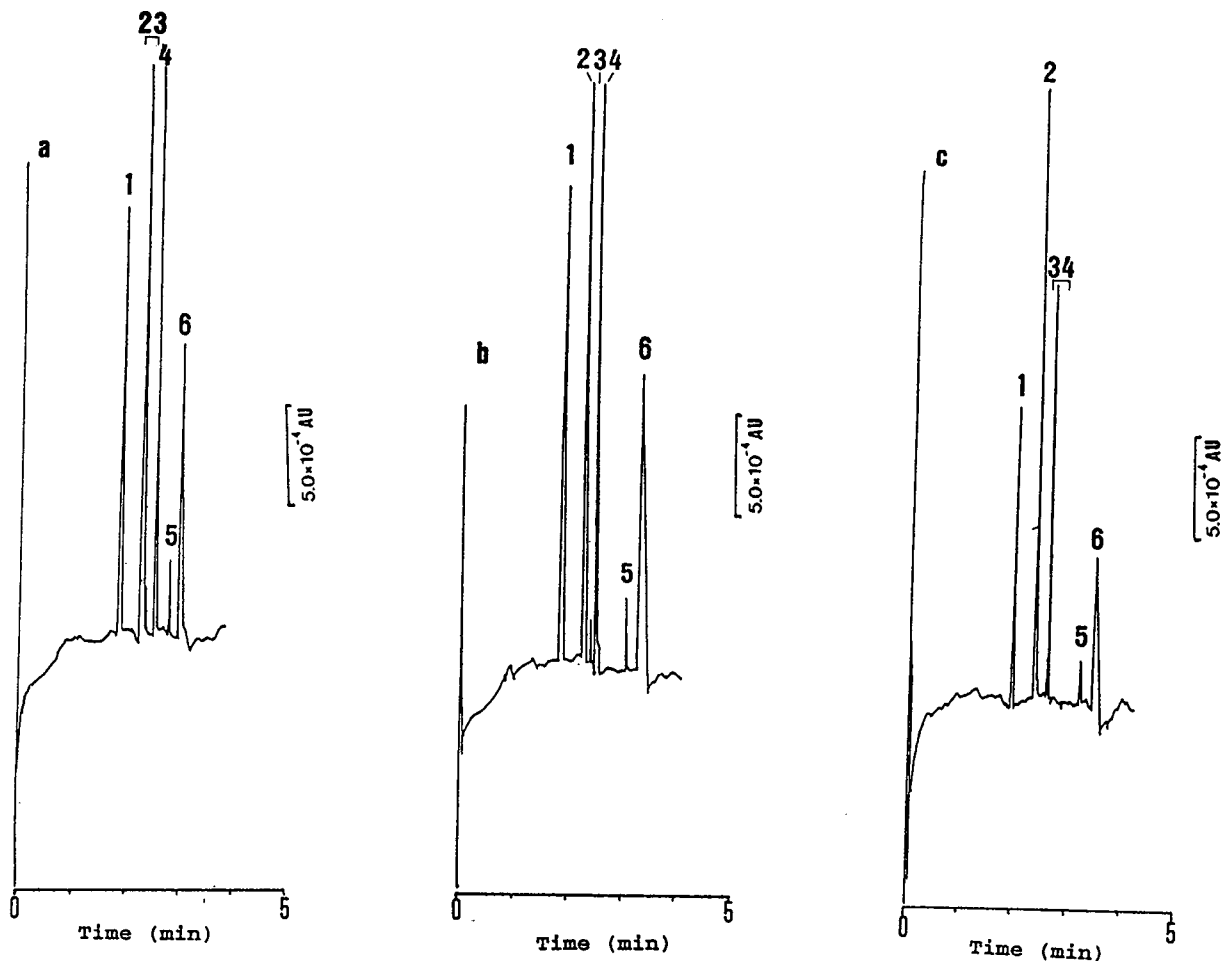


Fig. 3. Effect of concentration of EDTA on the separation of the metal ions. Conditions:  $L_{\text{total}} = 39.5$  cm,  $L_{\text{effective}} = 30.0$  cm; pH 5.00; 10 mM pyridine; hydrostatic injection for 15 s with 4.0 cm height difference. (a) 0.6 mM EDTA; (b) 0.8 mM EDTA; (c) 1.0 mM EDTA. Peaks: 1 = K, 2 = Na, 3 = Ba, 4 = Li, 5 = Sr, 6 = Mg, and 7 = Ca. Sample concentration: K, Na, Ba, Li, Sr, Mg and Ca 1  $\mu\text{g/ml}$  each in deionized water.

is so large that trace amounts of magnesium in the presence of large amounts of calcium can be separated and analyzed.

In order to maximize the dynamic detection range in the indirect UV detection mode, the absorbance of the UV-absorbing species in the running buffer was selected to be close to the upper limit of the detector linearity [10]. The running buffer used in the present experiments had an absorbance of 0.10 AU. The noise level of the baseline was lower than  $2 \cdot 10^{-4}$  AU. Based on these considerations, linearity could be expected over at least two orders of the con-

centration range of the solute. However, the calibration graph for magnesium expressed as peak height vs. concentration in the concentration range of 0.10–1.00  $\mu\text{g/ml}$  showed a hyperbolic curve when standard solutions were prepared in deionized water. Nevertheless, with standard solutions prepared in the running buffer linearity between peak height and concentration was improved although the linear range was still limited. This non-linearity problem was previously reported by other researchers [16,18] in capillary electrophoresis of metal ions in the presence of complexing agents with indirect UV

detection. Full understanding of the reason for the non-linearity of the calibration curves has not yet been achieved.

A calibration graph for magnesium was constructed with the standard solutions prepared in running buffer and was found to be linear up to 1.00  $\mu\text{g/ml}$ . The regression equation for the calibration graph was  $y = 11.2 + 12822.8x$  with  $r^2 = 0.9995$ . Subsequent determinations were based on samples prepared in buffer solution in spite of the fact that the detection limit was lower when the samples were prepared in deionized water.

#### 4.4. Application to the determination of magnesium in real samples

The method developed was applied to the determination of magnesium in river water, urine and a solid calcium carbonate sample. Table 1 gives the CE results for the above samples. Good agreement was obtained between the results obtained by the CE method and those obtained by atomic absorption spectrometry. Fig. 4 shows electropherograms obtained for the above samples. It was noted that even when the concentration of calcium in a sample was 1000 times higher than that of magnesium, these peaks were still well separated (see Fig. 4a). It was noted that the calcium peak was right next to the magnesium peak in Fig. 4a, which was not the case in other electropherograms. This was possibly due to the fact that the concentration of calcium ions was very high in this sample.

Therefore a large portion of the calcium ions was not in the complexed form which had a lower mobility than the free ions. Consequently, a significant increase in the effective mobility of calcium was observed in Fig. 4a. Reproducibility of the CE results was in a range of 5–9% R.S.D. in terms of peak height, depending on sample matrices.

## 5. Conclusions

The migration behaviour of the metal ion–EDTA complexes was investigated. Equations were derived to represent the effects of pH and concentration of complexing agent on the difference in the effective mobilities. The differences in effective mobilities calculated using those equations were used for the optimization of the CE separation of metal ions with similar mobilities. K, Na, Ba, Li, Sr, and Mg could be well separated in less than 4 min by the method described in this paper. Sample preparation affected both linearity and detectability. Dissolving samples in water resulted in good detectability and poor linearity, but dissolving samples in running buffer had the opposite effect. Feasibility of the proposed method for application to real sample separation and quantitation was verified by the determination of magnesium in real samples. The method showed a reproducibility of 5–9% R.S.D. in terms of peak height, depending on sample matrices.

Table 1  
Determination of magnesium in real samples

Sample	Result	
	CE	AA
Calcium carbonate <sup>a</sup> (% w/w)	0.023 (9.0, $n = 5$ ) <sup>d</sup>	0.021 (1.0, $n = 6$ )
River water <sup>b</sup> ( $\mu\text{g/ml}$ )	812 (5.5, $n = 5$ )	773 (1.4, $n = 10$ )
Urine <sup>c</sup> ( $\mu\text{g/ml}$ )	78.0 (6.1, $n = 3$ )	75.4 (0.4, $n = 3$ )

<sup>a</sup> A solution of 1.50 mg sample in 1 ml buffer was injected.

<sup>b</sup> River water was diluted 1000 times with buffer before injection.

<sup>c</sup> Freshly collected urine was diluted 100 times with buffer.

<sup>d</sup> The values in parentheses are the relative standard deviations (%) in terms of peak height and the number of replicates.

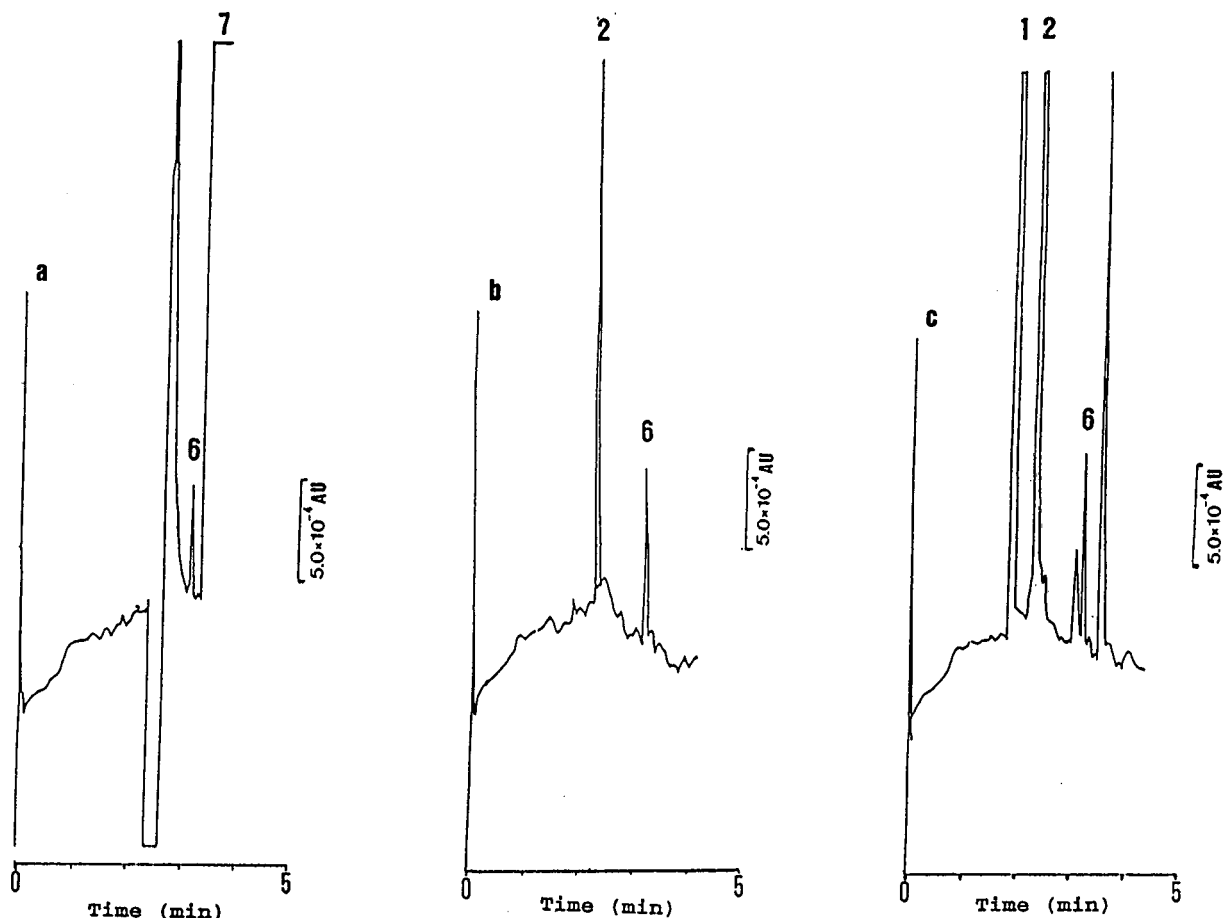


Fig. 4. Electropherograms obtained with some real samples. (a) Calcium carbonate sample, (b) river water, (c) urine. For sample preparation procedures see Table 1. Other conditions and peak identifications are the same as those in Fig. 3b.

### Acknowledgements

The authors thank the National University of Singapore for financial support. The authors also thank Miss Y.J. Yao and Madam Hee for technical assistance.

### References

- [1] J.W. Jorgenson and K.D. Lukacs, *Anal. Chem.*, 53 (1981) 1298.
- [2] J.W. Jorgenson and K.D. Lukacs, *Science*, 222 (1983) 266.
- [3] J.W. Jorgenson and K.D. Lukacs, *J. Chromatogr.*, 218 (1981) 209.
- [4] H.H. Lauer and D. McManigill, *Anal. Chem.*, 58 (1986) 166.
- [5] B.L. Karger, A.S. Cohen, A. Guttman, *J. Chromatogr.*, 492 (1989) 585.
- [6] M. Strega and A. Lagu, *Anal. Chem.*, 63 (1991) 1233.
- [7] H. Nishi, N. Tsumagari, T. Kakimoto and S. Terabe, *J. Chromatogr.*, 477 (1989) 259.
- [8] S. Terabe, K. Otsuka, K. Ichikawa and T. Ando, *Anal. Chem.*, 56 (1984) 113.
- [9] L. Gross and E.S. Yeung, *Anal. Chem.*, 62 (1990) 427.
- [10] F. Foret, S. Fanali, A. Nardi and P. Bocek, *Electrophoresis*, 12 (1990) 780.
- [11] W.R. Jones and P. Jandik, *J. Chromatogr.*, 546 (1991) 445.
- [12] D.F. Swaile and M.J. Sepaniak, *Anal. Chem.*, 63 (1991) 179.
- [13] M. Chen and R.M. Cassidy, *J. Chromatogr.*, 602 (1992) 227.

- [14] A. Weston, P.R. Brown, P. Jandik, W.R. Jones and A.L. Heckenberg, *J. Chromatogr.*, 593 (1992) 289.
- [15] S. Motomizu, M. Oshima, S. Matsuda, Y. Obata and H. Tanaka, *Anal. Sci.*, 8 (1992) 619.
- [16] W. Beck and H. Engelhardt, *Chromatographia*, 33 (1992) 313.
- [17] Y. Shi and J.S. Fritz, *J. Chromatogr.*, 640 (1993) 473.
- [18] T.-I. Lin, Y.-H. Lee and Y.-C. Chen, *J. Chromatogr. A*, 654 (1993) 167.
- [19] R. Zhang, H. Shi and Y. Ma, *J. Microcol. Sep.*, 6 (1994) 217.
- [20] M.J. Wojtusik and M.P. Harrold, *J. Chromatogr. A*, 671 (1994) 411.
- [21] W. Buchberger, K. Winna and M. Turner, *J. Chromatogr. A*, 671 (1994) 375.
- [22] Y. Shi and J.S. Fritz, *J. Chromatogr. A*, 671 (1994) 429.
- [23] Q. Yang, M. Jimider, T.P. Hamoir, J. Smeyers-Verbeke and D.L. Massart, *J. Chromatogr. A*, 673 (1994) 275.
- [24] T. Pal, N.R. Jana and P.K. Das, *Analyst*, 117 (1992) 791.
- [25] S.-J. Tsai and Y.-L. Bae, *Analyst*, 118 (1993) 301.
- [26] A. Guttman, A. Paulus, A.S. Cohen, N. Grinberg and B.L. Karger, *J. Chromatogr.*, 448 (1988) 41.
- [27] R. Pribil, *Applied Complexometry*, Pergamon Press, Oxford, 1982, pp. 4–7.
- [28] S.F.Y. Li, *Capillary Electrophoresis*, Elsevier, Amsterdam, 1992.
- [29] R.M. Smith and A.E. Martell, *Critical Stability Constants*, Vol. 2, Plenum Press, New York, 1975.
- [30] P. Jandik, W.R. Jones, A. Weston and P.R. Brown, *LC·GC*, 9 (1991) 634.
- [31] D.S. Burgi and R.-L. Chien, *J. Microcol. Sep.*, 3 (1991) 199.
- [32] A. Weston, P.R. Brown, P. Jandik, A.L. Heckenberg and W.R. Jones, *J. Chromatogr.*, 608 (1992) 395.





# Free-solution capillary electrophoretic resolution of chiral amino acids via derivatization with homochiral isothiocyanates. Part I

R. Bonfichi\*, C. Dallanocce, S. Lociuoro, A. Spada<sup>1</sup>

Marion Merrell Dow Research Institute, Lepetit Research Center, I-21040 Gerezano (VA), Italy

First received 3 January 1995; revised manuscript received 7 February 1995; accepted 13 March 1995

## Abstract

Within the framework of a more general study aimed at the enantiomeric resolution of non-UV-absorbing chiral amino acids via derivatization with chiral isothiocyanates, we have examined the applicability of two such derivatizing agents, (*S*)-1-(1-naphthyl)ethyl isothiocyanate (SNEIT) and (*S*)-1-phenylethyl isothiocyanate (SAMBI), to the resolution of the enantiomers of alanine, phenylalanine, and valine in free-solution capillary electrophoresis (FSCE). Isothiocyanates have distinct advantages as chiral derivatizing agents in enantiospecific chromatographic analysis, and the two reagents were readily synthesized from commercially available reagents. SNEIT, previously not fully described in the literature, was characterized by rigorous physicochemical and spectroscopic means. The two diastereoisomeric thiourea derivatives of each amino acid were separated by FSCE. Heptakis-2,3,6-tri-*O*-methyl- $\beta$ -cyclodextrin was effective in assuring the solubility of the derivatives in the working buffer and was more efficient than  $\beta$ -cyclodextrin in both dissolving the thioureas and improving the electrophoretic resolution. Enantiomeric pairs migrated in the order *L* before *D*. Under the conditions used SAMBI-derivatized amino acids had longer elution times than the corresponding SNEIT derivatives. The diastereomeric derivatives of valine and of phenylalanine had larger separation factors  $\alpha$  than the corresponding SAMBI derivatives, while the derivatives of alanine had nearly identical  $\alpha$  values with the two derivatizing agents. The two reagents may be advantageous in the enantiospecific analysis of amino acids, and it appears that further exploration of these and other similar reagents is warranted.

## 1. Introduction

Recent studies carried out in our Research Center have been aimed at the enantiomeric separation and identification of chiral amino acids in biological matrices [1] using 2,3,4,6-tetra-*O*-acetyl- $\beta$ -*D*-glucopyranosyl isothiocyanate (TAGIT) as chiral derivatizing agent in conjunc-

tion with HPCE. Isothiocyanates react with primary or secondary amines to produce the corresponding thioureas (Fig. 1).

If the isothiocyanate used in the derivatization of enantiomerically related amines is itself chiral and is used in a single-enantiomeric form, the derivative thioureas will be diastereomeric. This is the basis of the so-called "indirect method" in enantiospecific chromatographic analysis [2]. Because diastereomers are characterized by different electrophoretic mobilities, the indirect

\* Corresponding author.

<sup>1</sup> On leave from the University of Rome.

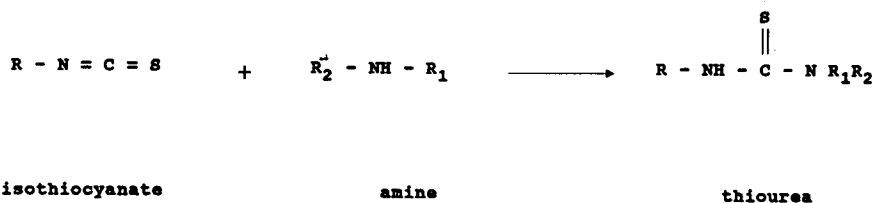


Fig. 1. General reaction scheme for the derivatization of amino groups with isothiocyanates.

method represents an extremely useful tool for the enantiomer separation by HPCE.

A chiral isothiocyanate was chosen for our studies because of the well-documented advantages of this reagent family:

–the reaction with the amino group is rapid and proceeds under mild conditions [2];

–the derivatization reaction can be carried out in aqueous media, a critical advantage in the analysis of amino acids and other polar analytes;

–the derivatization procedure is simpler and more rapid than that with many other chiral derivatizing agents, (see, for instance, Ref. [3] vs. Ref. [4]);

–the diastereomers can often be readily resolved by HPLC [3,5,6] or MEKC [7].

–the thiourea moiety has significant UV absorbing properties, which can enhance detectability;

–chiral isothiocyanates are often less expensive than other commercially available chiral derivatizing agents.

These advantages render chiral isothiocyanates highly useful for enantiospecific analysis and suggested to us that—as an extension and refinement of our above-mentioned work [1] with TAGIT—it would be of interest to investigate the potential applicability of other chiral isothiocyanates to the characterization and chiral separation of amino acids by using HPCE, an analytical technique whose considerable advantages in pharmaceutical/biomedical analysis are very well documented [8].

The state-of-the-art in enantiomeric separations by HPCE has recently been thoroughly discussed by Fanali et al. [9]. From Fanali's review and other technical literature references it emerges that, while several chiral isothiocyanates (in addition to TAGIT) have been used in the HPLC separation of diastereomeric derivatives

of enantiomeric compounds [10], these reagents have been nearly completely ignored in HPCE work. The only exception is represented by Nishi et al. [7] who described recently the resolution of the enantiomers of a series of amino acids via derivatization with TAGIT followed by separation using MEKC. In fact, although several papers have dealt with the indirect resolution method in HPCE [11,12], apart from Nishi's work, it appears that no other studies were published on the application of chiral isothiocyanates in HPCE.

For the present study we chose (*S*)-1-(1-naphthyl)ethyl isothiocyanate (SNEIT, Fig. 2) and (*S*)- $\alpha$ -methylbenzyl isothiocyanate (SAMBI, Fig. 2), primarily because of the presence in these molecules of highly lipophilic organic moieties and UV-absorbing chromophores. Further-

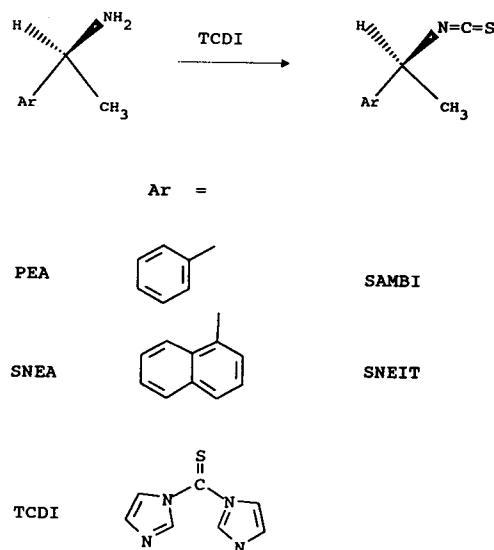


Fig. 2. Reaction scheme for the synthesis of the chiral isothiocyanates SAMBI and SNEIT obtained from the corresponding precursor chiral primary amines.

more, both SNEIT and SAMBI could be readily synthesized in one step from the corresponding precursor primary amines which are commercially available reagents.

In this report we describe our findings on the applicability of the two chiral isothiocyanate reagents to the enantiomeric resolution of selected amino acids by free-solution capillary electrophoresis (FSCE).

## 2. Experimental

### 2.1. Instrumentation

All separations were carried out on a SpectraPhoresis 1000 (Thermo Separation Products, CA, USA) instrument equipped with a programmable, high-speed scanning, multiple-wavelength UV-Vis detector. Data acquisition, handling and reporting were supported by the multi-tasking SpectraPhoresis CE 1000 version 1.05c and by the PC1000 version 2.0 software packages running on a Spectra 386E/25MHz personal computer equipped with a Hewlett-Packard (Avondale, CA, USA) laser jet Model Iip printer.

Elemental analysis was performed on an EA 1106 EAGER 200 instrument (Carlo Erba, Milan, Italy); differential scanning calorimetry was carried out using a DSC 910 TA2000 instrument (DuPont, Wilmington, DE, USA);  $^1\text{H}$  NMR spectra were recorded in  $\text{CDCl}_3$  on an AM 500 NMR spectrometer (Bruker, Karlsruhe, Germany); mass spectra were obtained using an EI-TSQ 700 instrument (Finnigan Mat, San Jose, CA, USA), with a source temperature of  $150^\circ\text{C}$ , electron energy: 70 eV; filament current: 200 mA. IR spectra were recorded in nujol using an IFS 48 FT-IR spectrometer (Bruker, Karlsruhe, Germany); optical rotations were obtained using a Model 241 polarimeter (Perkin-Elmer, Palo Alto, CA, USA).

### 2.2. Reagents and materials

(*S*)-(-)-1-(1-Naphthyl)ethylamine, (*S*)-(-)- $\alpha$ -methylbenzylamine, and  $\text{N,N}'$ -thiocarbonyldiimidazole were obtained from Aldrich

(Milwaukee, WI, USA); all the solvents used were of HPLC grade (Carlo Erba, Milan, Italy); the salts were reagents of analytical grade (Carlo Erba). Water was obtained from a Milli-Q Plus purification system (Millipore, Bedford, MA, USA). Silica gel HPTLC plates, 60  $\text{F}_{254}$ ,  $5 \times 10$  cm, layer thickness 0.25 mm, were from Merck (Darmstadt, Germany).

### 2.3. Synthesis and characterization of (*S*)-1-(1-naphthyl)ethyl isothiocyanate (SNEIT)

To a stirred solution of  $\text{N,N}'$ -thiocarbonyldiimidazole (TCDI, 500 mg, 2.8 mmol) in dichloromethane (20 ml) in a 100-ml round-bottomed flask was added dropwise over 3.5 h a solution of (*S*)-1-(1-naphthyl)ethyl amine (SNEA) (411 mg, 2.4 mmol) in dichloromethane (30 ml) in an argon atmosphere at room temperature [13]. The reaction was monitored by TLC with an eluent of *n*-hexane-methanol (99:1, v/v); SNEIT  $r_F = 0.68$ . After completion of the addition vigorous stirring was continued for an additional hour to assure completion of the reaction. The reaction mixture was then transferred into a separatory funnel and washed with a 5% aqueous solution of sodium bicarbonate ( $3 \times 30$  ml), followed by water ( $3 \times 30$  ml). The organic phase was dried over anhydrous sodium sulfate, filtered and the solvent evaporated in vacuo on a rotary evaporator. The yellow solid obtained was purified by recrystallization from absolute ethanol to obtain the expected product in 85% yield. Found: C: 72.9%; H: 5.2%; N: 6.5%; S: 14.2%; calculated for;  $\text{C}_{13}\text{H}_{11}\text{SN}$ : C: 73.2%; H: 5.2%; N: 6.6%; S 15.0%.

Although SNEIT has been previously used in the HPLC resolution of enantiomeric amines [14,15], a search of the literature produced no published data on its rigorous identification and physicochemical characterization. In order to fully characterize the reagent, therefore, we obtained, in addition to its elemental analysis (see under Experimental), its NMR, IR, and mass spectra, and examined its DSC. The NMR spectrum [ $\delta$ , ppm;  $\delta_{\text{TMS}} = 0$ , 7.95–7.84 (2 H, m), 7.849 (1 H, d), 7.645 (1 H, d), 7.585–7.268 (3

H, m), 5.723 (1 H, q), 1.862 (3 H, d)], the IR spectrum [main absorption bands: 3051 ( $\nu$  arom C–H); 2127 ( $\nu$  S = C = N); 1597, 1512 ( $\nu$  C = C); 805, 798 ( $\gamma$  arom C–H)  $\text{cm}^{-1}$ ], and the mass spectrum [ $m/z$  213 ( $M^+$ );  $m/z$  155 ( $M^+ - \text{SCN}$ )] were in agreement with the structure of SNEIT. DSC analysis confirmed that the sample obtained was highly crystalline and showed a melting peak ( $T_{\text{onset}}$  45.36°C,  $T_{\text{final}}$  46.54°C;  $\Delta H_f = 82.61$  J/g) typical of a compound of high purity. Decomposition occurred above 200°C.

The specific rotation of SNEIT was measured:  $[\alpha]_D^{20} = +114.2$  ( $\text{CHCl}_3$ ; concentration 0.5% w/v). Thus, the starting levorotatory amine of *S* configuration yields the dextrorotatory isothiocyanate of *S* configuration, i.e. the direction of rotation is reversed between starting material and product; the reaction does not affect the actual configuration of the stereogenic center, and there is no change in the Cahn–Ingold–Prelog priority order of substituents at the stereogenic center.

#### 2.4. Synthesis and characterization of (*S*)-(+) $\alpha$ -methylbenzyl isothiocyanate (SAMBI)

The reaction was carried out and worked up as described above for SNEIT and using the same molar ratios, with (*S*)-(–)- $\alpha$ -phenylethyl amine (SPEA) instead of SNEA. The reaction was monitored using the TLC system used in the synthesis of SNEIT; SAMBI  $R_F = 0.74$ . The yellow oil obtained in the reaction was purified by distillation, bp 114–116°C, yielding the title compound as a colourless oil in 51% yield.

SAMBI [(*S*)-(+) -1-phenylethyl isothiocyanate] has been previously characterized [16]. The NMR and IR spectra (data not shown) of our sample of SAMBI were in agreement with the expected structure and with the literature [17,18], and its mass-spectrum [ $m/z$  163 ( $M^+$ );  $m/z$  104 ( $M^+ - \text{SCN}$ )] and elemental analysis was also in agreement with the expected structure. Our specific rotation for SNEIT in chloroform ( $[\alpha]_D^{20} = +14.6$  ( $\text{CHCl}_3$ ; 0.5% w/v)), was different from the specific rotation obtained in toluene ( $[\alpha]_D^{20} = +53.1$ ) [18]. For SAMBI also, the direction of optical rotation is reversed

between the precursor (*S*)-(–)-1-phenylethylamine and the isothiocyanate.

#### 2.5. Background electrolyte (BGE) and working buffer (WB) preparation

The BGE used during this study consisted of a 50 mM  $\text{Na}_2\text{B}_4\text{O}_7$  solution at pH 10.

Within the context of this study, if not otherwise stated, “working buffer” (or WB) is intended to indicate a 20 mM solution of heptakis-2,3,6-tri-*O*-methyl- $\beta$ -cyclodextrin in the BGE.

#### 2.6. Derivatizing solutions

SNEIT or SAMBI (20 mg) was diluted to 1 ml with acetonitrile. The solution was swirl-mixed until complete dissolution and then directly used. Care was taken to protect the vial from light by covering the container with aluminium foil. The reagents in the derivatizing solutions were stable for several weeks provided the vial was tightly closed and protected from light.

#### 2.7. Amino acid reference solutions

For each of the amino acids L-valine, D,L-valine; L-alanine, D,L-alanine; L-phenylalanine, D,L-phenylalanine, a reference solution was prepared by diluting ca. 5 mg of the amino acid to 1 ml with  $\text{H}_2\text{O}-\text{CH}_3\text{CN}$  (50:50, v/v) containing 0.4% (w/v) of triethylamine (TEA).

#### 2.8. Derivatizations with the chiral isothiocyanates

SAMBI: Into a 300- $\mu\text{l}$  glass vial were placed, in order, 50  $\mu\text{l}$  of amino acid standard solution (equivalent to 2.1  $\mu\text{mole}$  of amino acid), and 20  $\mu\text{l}$  of SAMBI solution in  $\text{CH}_3\text{CN}$  (equivalent to 2.4  $\mu\text{mole}$  of SAMBI). After swirl-mixing, the vial was transferred into a Thermoline dry bath (Thermolyne Corp., Dubuque, IA, USA) thermostatted at 60°C and left to stand for 30 min. A 25- $\mu\text{l}$  aliquot of working buffer was then added and the mixture was swirl-mixed for a few seconds. The vial was then transferred into the satellite carousel of the autosampler and the

sample injected according to the method specifications given below.

SNEIT: The procedure described above for SAMBI was also used for SNEIT, with two exceptions: (a) the aliquot of derivatizing agent was 25  $\mu$ l of SNEIT solution (equivalent to ca. 2.3  $\mu$ mole of SNEIT), and (b) in a few cases it was necessary to dilute the final contents of the vial 1:1 with MeOH to dissolve the resulting thioureas.

### 2.9. Operation conditions

Unless otherwise stated, the electropherograms reported in this work were obtained using the following conditions:

–Capillary:  $l = 440$  mm (370 mm from injector to detector), I.D. 50  $\mu$ m

–Applied voltage: 10 kV for 20 min.

–Prefill of the capillary: 1 min with the working buffer.

–Injection: It was performed hydrodynamically for 1 s. By using the Poiseuille equation [19], it can be estimated that, in the assumption of  $\eta = 1$  cP, the amount of sample directly injected into the capillary was ca. 1.8 nl, the total capillary volume being  $\approx 864$  nl.

–Detection: UV at 210 and 254 nm. While both wavelengths were recorded, only 210 nm is plotted in the present report.

### 3. Results and discussion

At the outset of our studies we focused on SNEIT in view of its previously demonstrated utility in chiral chromatographic separations and of its properties [14,15] and its other advantages (see Introduction). Once this choice was made, we also selected SAMBI, a closely related reagent that appeared convenient. It was important to retain the same relative configuration (i.e. *S*) between the two reagents, in light of the additional chiral component in our system which could be a complicating factor (see below). Both SAMBI and its *R*-enantiomer are commercially available (Trans World Chemicals, Rockville, MD, USA), but the quoted purity is only 98–

99%, and we therefore decided to synthesize SAMBI in our laboratory. The *R*-enantiomer of SAMBI has previously been used in the HPLC analysis of the enantiomeric composition of amino compounds [17,18,20,21].

In the preliminary experiments during the development of the analytical method, a poor solubility was observed for some thioureas, formed after derivatization, in the BGE. Among the several additives added to the BGE in order to overcome this problem,  $\beta$ -cyclodextrin seemed, at the first sight, to be the most effective and, therefore, the WB containing  $\beta$ -cyclodextrin was also used to dilute the thioureas obtained from derivatization. However, in spite of the presence of  $\beta$ -cyclodextrin in the WB, the clear derivatization medium still became turbid in 5–10 min. Fig. 3 shows the electropherogram of the SNEIT-derivative of D,L-threonine separated by using a 20 mM solution of  $\beta$ -cyclodextrin in the BGE as working buffer and by applying 20 kV for 10 min, the rest of the operative conditions being unchanged. Under these conditions  $\Delta t_R = 0.05$  min and the resolution,  $R_s$ , was 0.9 as calculated by:

$$R_s = (t_M^2 - t_M^1) / \frac{1}{2}(w_b^2 + w_b^1) \quad (1)$$

where  $t_M^2$  and  $t_M^1$  are the migration times of components 2 and 1, and  $w_b^2$  and  $w_b^1$  are the mean peak base widths relative to components 2 and 1

To improve the solubility of the derivatization mixture in the working buffer and the quality of the separations, experiments were performed with varying concentrations of  $\beta$ -cyclodextrin in the working buffer or by diluting the final derivatization mixture 1:1 with methanol, but none of these attempts lead to any significant change in the separation although the solubility was improved. However, by replacing  $\beta$ -cyclodextrin with heptakis-2,3,6-tri-O-methyl- $\beta$ -cyclodextrin in the working buffer and keeping the concentration unchanged (i.e., 20 mM) the resolution,  $R_s$ , of the enantiomeric pair was improved by a factor  $> 2$ :  $R_s = 2$  (Fig. 4) vs.  $R_s = 0.9$  (Fig. 3). Furthermore, a definite improvement in the solubilization of the reaction product thioureas

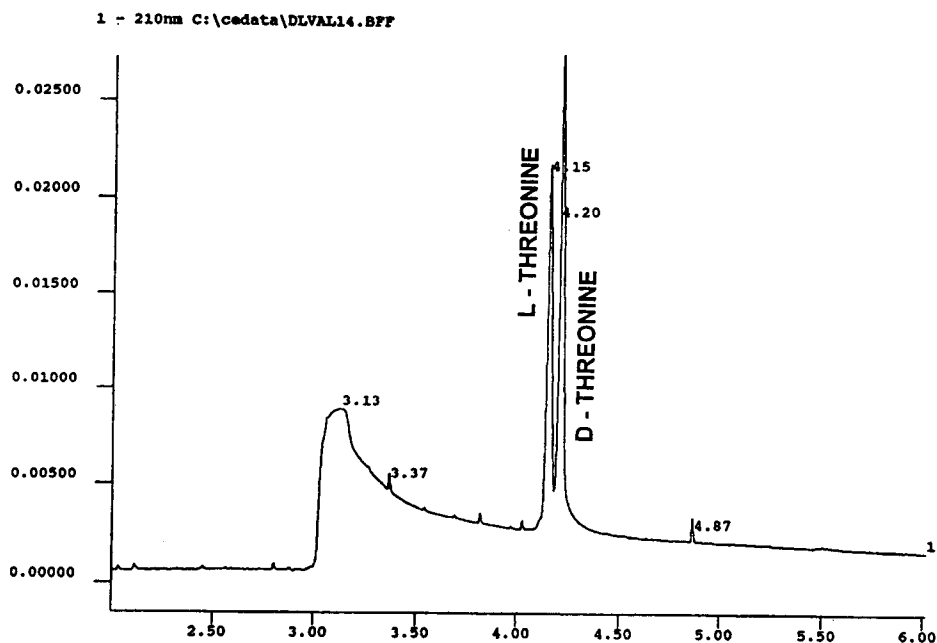


Fig. 3. Electropherogram of the SNEIT-derivatives of D,L-threonine. Sample, 50  $\mu$ l D,L-Thr solution + 25  $\mu$ l SNEIT solution; derivatization, 60°C for 30 min; + 25  $\mu$ l WB; BGE, 50 mM Na<sub>2</sub>B<sub>4</sub>O<sub>7</sub>, pH 10; WB, 20 mM  $\beta$ -CD solution in BGE; voltage, 20 kV for 10 min.

in the working buffer was also achieved in this manner. Indeed, the addition of heptakis-2,3,6-tri-*O*-methyl- $\beta$ -cyclodextrin instead of  $\beta$ -cyclodextrin, to the derivatization mixture led to clear solutions. These findings prompted us to use in all further experiments heptakis-2,3,6-tri-*O*-methyl- $\beta$ -cyclodextrin instead of  $\beta$ -cyclodextrin in the working buffer.

D,L-Alanine, D,L-valine and D,L-phenylalanine were chosen as test compounds, primarily because they are primary protein  $\alpha$ -amino acids and are characterized by a progressively increasing degree of lipophilicity. Furthermore, alanine and valine are non-UV-absorbing amino acids. All the three enantiomeric pairs were tested with both SNEIT and SAMBI. The separations of the diastereoisomeric SAMBI derivatives of alanine and those of phenylalanine are compared in Fig. 5, and the corresponding SNEIT-based separations are shown in Fig. 6. In Table 1 are reported the capacity ratios,  $k'$ , and the separation factors,  $\alpha$ , of the SNEIT- and SAMBI-derivatives of the amino acids studied. Fig. 7

shows the electropherograms that demonstrate the lack of a significant effect of diluting the derivatization mixture of L-alanine and SNEIT 1:1 with methanol. Such dilution was necessary in some cases to assure complete solubility of the derivatives; as seen in the example in Fig. 7, the dilution did not affect significantly the migration times.

The stereoisomeric elution order was assessed by comparing the electropherograms of the isothiocyanate-derivatized D,L-amino acid with that obtained for the corresponding isothiocyanate-derivatized L-amino acids, as reported for L-alanine in Fig. 8. It was thus found that for all the enantiomeric pairs studied and for both chiral derivatizing agents used, the L-enantiomer always migrates first. Interestingly, this stereoisomeric migration order was also found for TAGIT-derivatized amino acids when analyzed by reversed-phase HPLC [6] or by MEKC [7]. In the indirect method of separating enantiomeric analytes the stereoisomeric order of elution can be reversed if the chiral derivatizing agent is

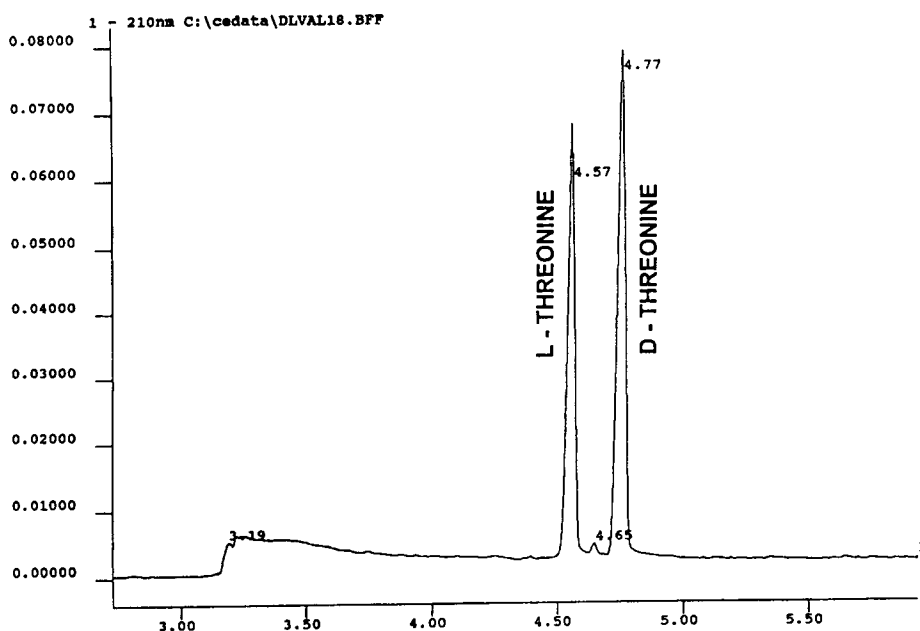


Fig. 4. Electropherogram of the SNEIT-derivatives of D,L-threonine. Sample, 50  $\mu$ l D,L-Thr solution + 25  $\mu$ l SNEIT solution; derivatization, 60°C for 30 min; + 25  $\mu$ l WB; BGE, 50 mM  $\text{Na}_2\text{B}_4\text{O}_7$  pH 10; WB, 20 mM heptakis-2,3,6-tri-O-methyl- $\beta$ -CD solution in BGE; voltage, 20 kV for 10 min.

available in both enantiomeric forms, and such choice in the elution order is a significant advantage if one of the enantiomers in the mixture is present in much higher concentration than the antipode, i.e. it is an advantage to have the lesser component elute before the predominant enantiomer. In this context it is important to note that for both SAMBI and SNEIT the precursor amines are available in both enantiomeric forms and that for SAMBI the *R*-enantiomer itself is also available commercially. It must be pointed out however, that the presence in our system of an additional chiral element, i.e. the cyclodextrin, suggests that without experimental determination of the stereoisomeric elution order as a function of the configuration of the derivatizing agent, caution must be exercised in its prediction. Such predictions may, however, be made with greater confidence if the mechanism of diastereoselectivity in the separation is known in detail.

Fig. 8 also illustrates two other observations: (a) during the derivatization no racemization of

the amino acids or epimerization of the derivative occurs; (b) the enantiomeric purity of the chiral reagents was found to be >99%, inasmuch as a 1% enantiomeric contamination would have been detected under our conditions.

Based on the  $\alpha$ -values given in Table 1 it can be seen that SNEIT gives a better separation of the diastereomeric derivatives, i.e. greater diastereoselectivity, for phenylalanine and valine than does SAMBI. In the case of alanine, however, the two chiral reagents produce nearly identical  $\alpha$  values (Table 1). It is well-known that cyclodextrins can form inclusion complexes with suitable molecules and that such inclusion complexation may play a fundamental role in chromatographic separations mediated by cyclodextrins [9]. The structural features of  $\beta$ -cyclodextrin are such that when inclusion complexations do occur, the naphthalene ring is often well accommodated within the cavity of the cyclodextrin and its presence in the analyte may be crucial for chromatographic separations to occur; it might be attractive to conjecture, there-

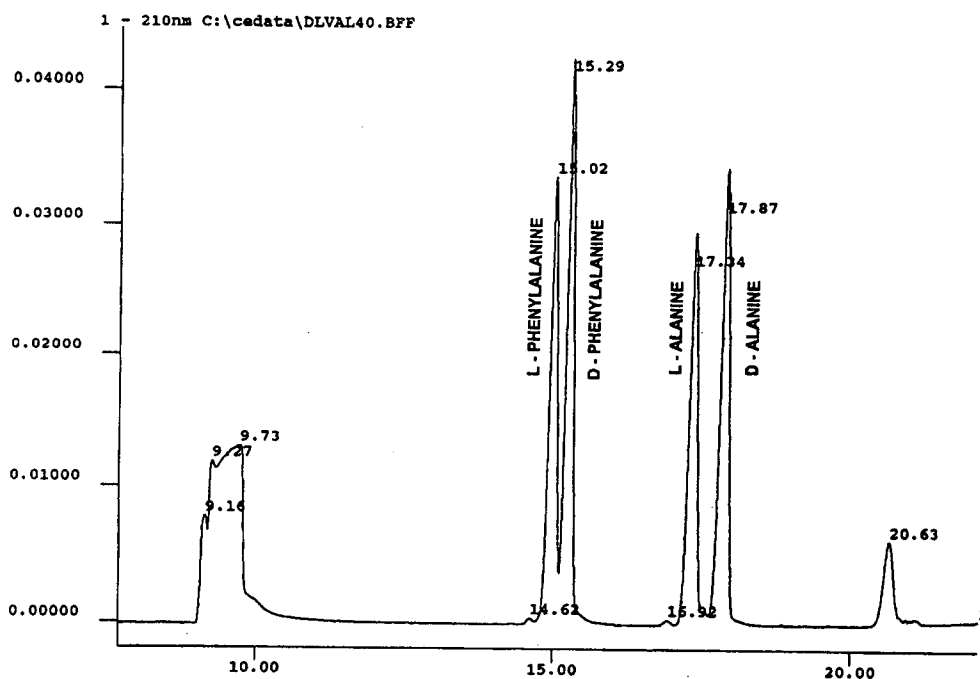


Fig. 5. Electropherogram of the SAMBI-derivatives of D,L-phenylalanine and D,L-alanine. Sample, 50  $\mu$ l D,L-PhAla solution + 50  $\mu$ l D,L-Ala solution + 50  $\mu$ l SAMBI solution; derivatization, 60°C for 30 min; + 50  $\mu$ l WB; BGE, 50 mM  $\text{Na}_2\text{B}_4\text{O}_7$  pH 10; WB, 20 mM heptakis-2,3,6-tri-O-methyl- $\beta$ -CD solution in the BGE; voltage, 10 kV for 20 min; resolution:  $R_s$  (D-PhAla, L-PhAla)  $\approx$  0.9;  $R_s$  (D-Ala, L-Ala)  $\approx$  1.74;  $R_s$  (L-Ala, L-PhAla)  $\approx$  7.6;  $R_s$  (D-Ala, D-PhAla)  $\approx$  8.5.

fore, that the better diastereoselectivity provided by SNEIT, a naphthalene derivative, in two of the three cases could indicate that inclusion complexation is an important contributor to the overall diastereoselectivity. However, the small number of amino acids studied and the failure of the alanine derivatives to follow the pattern suggest that it is premature to draw such conclusions on the role of the cyclodextrin in the separations of the diastereomers obtained in our studies. In this regard it is important to recall that stereoisomer separations by cyclodextrins may also occur by mechanisms other than inclusion complexation [9].

From a practical viewpoint it is of interest to examine the resolution factor  $R_s$  for the separation of the diastereomeric amino acid derivatives. This parameter provides an indication of the extent of overlap of two peaks, and a value of 1.5 corresponds to essentially baseline separation

of two equal-sized peaks [22]. For the separations shown in Fig. 5 (i.e. SAMBI derivatives) the  $R_s$  values for the diastereomeric pairs are as follows (calculated according to Eq. 1): D-PhAla, L-PhAla = 0.9; D-Ala, L-Ala = 1.74; for the separations shown in Fig. 6 (i.e. SNEIT derivatives) the  $R_s$  values are: D-PhAla, L-PhAla = 3.1; D-Ala, L-Ala = 1.72. Thus, under the conditions used the separation of the diastereomeric derivatives of phenylalanine is considerably greater with SNEIT than with SAMBI; since the migration times are not too dissimilar between Figs. 5 and 6 for the phenylalanine derivatives it can be readily concluded that the better separation seen for the SNEIT derivatives is a reflection of the differences between the  $\alpha$ -values (Table 1) for SNEIT vs. SAMBI. Similarly, when alanine is considered, the nearly identical separation factors  $\alpha$  for SAMBI vs. SNEIT (Table 1) coupled with the rather similar



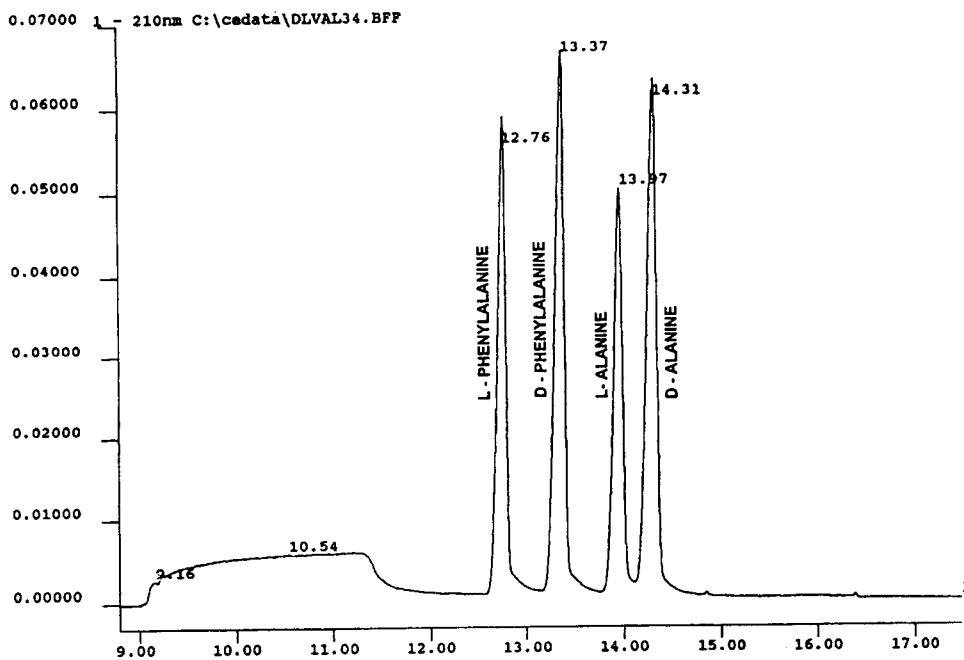


Fig. 6. Electropherogram of the SNEIT-derivatives of D,L-phenylalanine and D,L-alanine. Sample, 50  $\mu$ l D,L-PhAla solution + 50  $\mu$ l D,L-Ala solution + 50  $\mu$ l SNEIT solution; derivatization, 60°C for 30 min; + 50  $\mu$ l WB; BGE, 50 mM  $\text{Na}_2\text{B}_4\text{O}_7$ , pH 10; WB, 20 mM heptakis-2,3,6-tri-O-methyl- $\beta$ -CD solution in the BGE; voltage, 10 kV for 20 min; resolution:  $R_s$  (D-PhAla, L-PhAla)  $\approx$  3.1;  $R_s$  (D-Ala, L-Ala)  $\approx$  1.72;  $R_s$  (L-Ala, L-PhAla)  $\approx$  6.5;  $R_s$  (D-Ala, D-PhAla)  $\approx$  4.5.

Table 1

Capacity ratios,  $k'$ , and separation factors,  $\alpha$ , of the SNEIT- and SAMBI-derivatives of D-, L-phenylalanine; D-, L-valine and D-, L-alanine

Derivatizing agent	SNEIT		SAMBI	
	$k'^a$	$\alpha^b$	$k'$	$\alpha$
L-Phenylalanine	0.37	1.17	0.62	1.03
D-Phenylalanine	0.44	1.01	0.64	1.13
L-Valine	0.46	1.22	0.72	1.07
D-Valine	0.56	0.95	0.77	1.12
L-Alanine	0.50	1.06	0.86	1.07
D-Alanine	0.54		0.92	

<sup>a</sup>  $k'$  = capacity ratio =  $(t_M - t_0)/t_0$ . Acetone was used as neutral marker for  $t_0$  determination ( $t_0 = 9.30$  min).

<sup>b</sup>  $\alpha$  = separation factor =  $k'_2/k'_1$ .

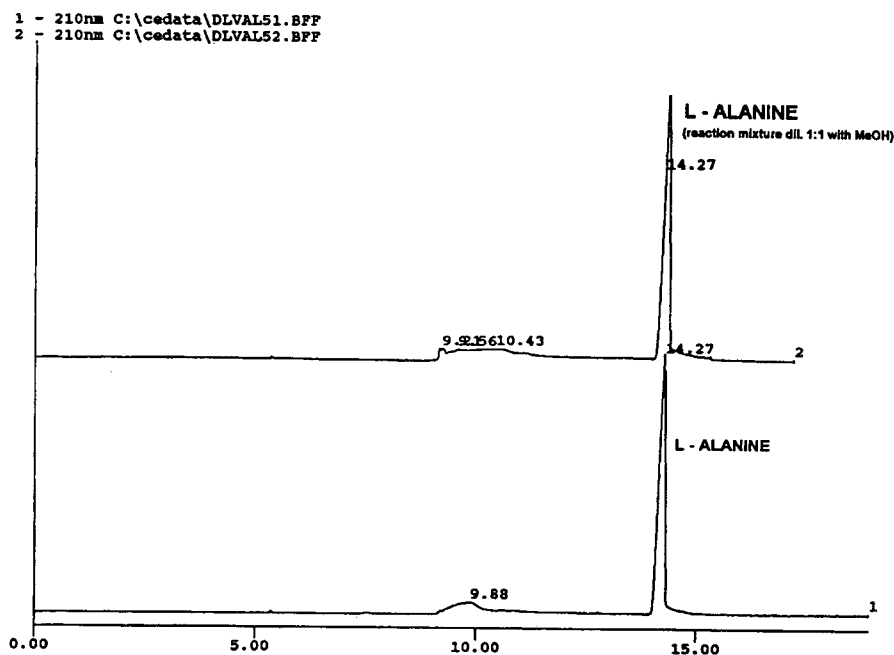


Fig. 7. Comparison between the electropherograms of the SNEIT-derivative of L-alanine when the derivatization mixture (50  $\mu$ l L-Ala solution + 25  $\mu$ l SNEIT solution; derivatization, 60°C for 30 min; + 25  $\mu$ l WB = derivatization mixture) was directly injected or further diluted 1:1 with MeOH; BGE, 50 mM  $\text{Na}_2\text{B}_4\text{O}_7$ , pH 10; WB, 20 mM heptakis-2,3,6-tri-O-methyl- $\beta$ -CD solution in the BGE; voltage, 10 kV for 20 min.

migration times under the two sets of conditions (i.e. Figs. 5 and 6) translate into nearly identical  $R_s$  values (1.72 vs. 1.74).

The order of elution of the individual amino acids was, for both the SNEIT and SAMBI derivatives: phenylalanine, valine, alanine (Table 1). Interestingly, this order is the opposite of that of the corresponding TAGIT derivatives in both HPLC [6] and MEKC [7]. It appears then, that under the conditions used, the migration order of the amino acids is the inverse of their order of lipophilicity.

Enantiospecific analysis of amino acids often involves the simultaneous presence of several amino acids as analytes in a mixture. In such situations there is a requirement not only for the separation of the enantiomers of each amino acid, but also for the separation of each amino acid from all of the others present in the mixture. The limited number of amino acids studied does not permit us to draw extensive conclusions in this regard, but it is noteworthy that the three

amino acids were, in general, better separated via derivatization with SAMBI. It is interesting to note in this context that in a previous study on the separation of amino acid enantiomers as TAGIT derivatives with MEKC the derivatives of D-alanine and L-valine were not separable [7].

In conclusion, it is clear that the chiral isothiocyanates SNEIT and SAMBI may be useful in the enantiospecific analysis of amino acids via FSCE. These reagents are easily prepared (the R-form of SAMBI is commercially available) and have distinct advantages. Additional studies to delineate the scope and mechanisms of such analyses are progress in our laboratory.

#### Acknowledgements

The authors gratefully acknowledge the generous assistance provided by Drs. P. Ferrari, E. Riva, C. Sottani, G. Tamborini, E. Taglietti and P. Zuccolin in the analytical characterization of

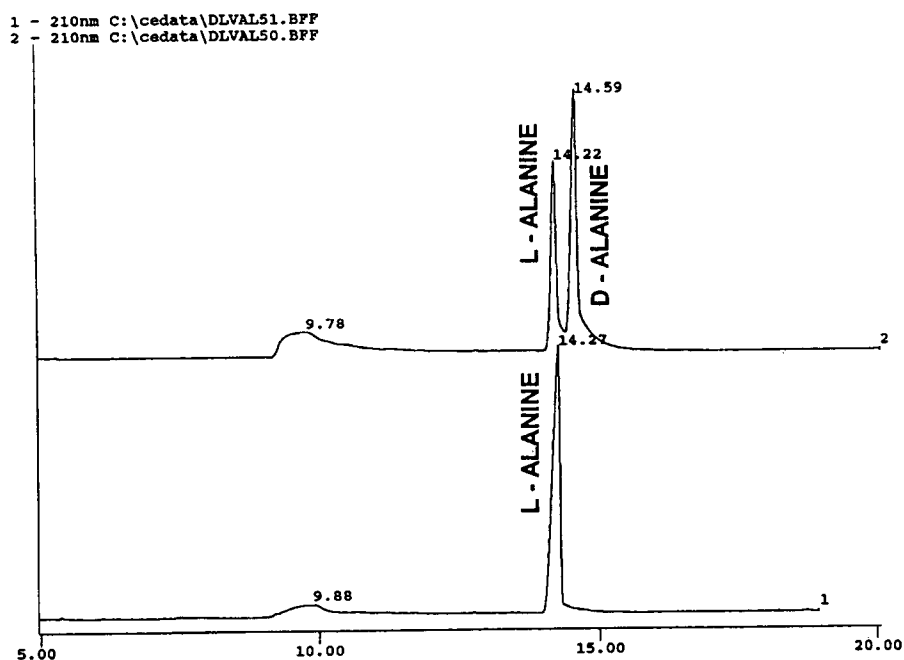


Fig. 8. Comparison between the electropherograms of the SNEIT-derivatives of D,L-alanine (curve 2) and L-alanine (curve 1). Sample, 50  $\mu$ l D,L-Ala (or L-Ala) solution + 25  $\mu$ l SNEIT solution; derivatization, 60°C for 30 min; + 25  $\mu$ l WB; BGE, 50 mM  $\text{Na}_2\text{B}_4\text{O}_7$  pH 10; WB, 20 mM heptakis-2,3,6-tri-O-methyl- $\beta$ -CD solution in the BGE; voltage, 10 kV for 20 min.

SNEIT and SAMBI. The authors are also indebted to Drs. R. Ciabatti and J. Coutant for their support of this project and for their stimulating comments and fruitful discussions. A special thanks is to Prof. J. Gal, University of Colorado, School of Medicine, who has provided many important suggestions.

## References

- [1] R. Bonfichi, E. Riva, unpublished results.
- [2] J. Gal, in I.W. Wainer (Editor), *Drug Stereochemistry: Analytical Methods and Pharmacology*, 2nd ed., Marcel Dekker, New York, 1993, pp. 65–106.
- [3] A.J. Sedman, J. Gal, *J. Chromatogr.*, 278 (1983) 199.
- [4] P. Marfey, *Carlsberg Res. Commun.*, 49, 591.
- [5] J. Gal, *J. Chromatogr.*, 307 (1984) 220.
- [6] T. Kinoshita, Y. Kasahara, N. Nimura, *J. Chromatogr.*, 210 (1981) 77.
- [7] H. Nishi, T. Fukuyama, M. Matsuo, *J. Microcol. Sep.*, 2 (1990) 234.
- [8] S.R. Rabel, J.F. Stobaugh, *Pharmaceut. Res.*, 10 (1993) 171.
- [9] S. Fanali, M. Cristalli, R. Vespalec, P. Boček, in A. Chrambach, M.J. Dunn, B.J. Radola (Editors), *Advances in Electrophoresis*, Vol. 7, VCH, Weinheim, 1994, pp. 1–86.
- [10] S. Gorog, M. Gazdag, *J. Chromatogr. B*, 659 (1994) 51.
- [11] A.D. Tran, T. Blanc, E.J. Leopold, *J. Chromatogr.*, 516 (1990) 241.
- [12] W. Schützner, S. Fanali, A. Rizzi, E. Kenndler, *J. Chromatogr.*, 639 (1993) 375.
- [13] D.M. Desai, J. Gal, *J. Chromatogr.*, 579 (1992) 165.
- [14] J. Gal, D.M. Desai, S. Meyer-Lehnert, *Chirality*, 2 (1990) 43.
- [15] E. Pianezzola, V. Bellotti, E. Fontana, E. Moro, J. Gal, D.M. Desai, *J. Chromatogr.*, 495 (1989) 205.
- [16] U. Kunze, H. Jawad, R. Burghardt, *Z. Naturforsch. B. Anorg. Chem., Org. Chem.*, 41B (1986) 1142.
- [17] J. Boger, L.S. Payne, D.S. Perlow et al., *J. Med. Chem.*, 28 (1985) 1779.
- [18] J. Gal, S. Meyer-Lehnert, *J. Pharm. Sci.*, 77 (1988) 1062.
- [19] P.D. Grossman and J.C. Colburn, *Capillary Electrophoresis*, Academic Press, San Diego, CA, 1992, p. 22.
- [20] J. Gal, A.J. Sedman, *J. Chromatogr.*, 314 (1984) 275.
- [21] J. Gal, *J. Chromatogr.*, 331 (1985) 349.
- [22] L.R. Snyder, J.J. Kirkland, *Introduction to Modern Liquid Chromatography*, 2nd ed., Wiley Interscience, New York, 1979, pp. 34–82.





ELSEVIER

JOURNAL OF  
CHROMATOGRAPHY A

Journal of Chromatography A, 707 (1995) 367–372

Short communication

# Quantitative structure–retention relationships of acyclovir esters using immobilised albumin high-performance liquid chromatography and reversed-phase high-performance liquid chromatography

D.S. Ashton, C. Beddell, A.D. Ray, K. Valkó\*

*Department of Physical Sciences, Wellcome Research Laboratories, Langley Court, Beckenham, Kent BR3 3BS, UK*

First received 27 October 1994; revised manuscript received 7 March 1995; accepted 7 March 1995

## Abstract

Acyclovir and 18 of its esters have been investigated by systematic measurement of their reversed-phase high-performance liquid chromatographic retention using differing mobile phase compositions. The methanol content of the mobile phase was varied between 5 and 95%. By linear least squares regression of the logarithmic retention factor ( $\log k'$ ) against methanol concentration, the slope ( $S$ ) and intercept ( $\log k'_0$ ) of the so obtained straight lines were calculated for each compound. The chromatographic hydrophobicity index ( $\phi_{0,\text{MeOH}}$ ) calculated from the  $S$  and  $\log k'_0$  values ( $\phi_{0,\text{MeOH}} = -\log k'_0/S$ ) showed significant correlation ( $r > 0.96$ ) to the calculated octanol–water partition coefficients ( $\text{cLog } P$ ). The albumin-binding properties of the compounds were characterised by the  $\log k'_{\text{HSA}}$  values obtained by using an immobilised human serum albumin (HSA) HPLC column and 1% propan-2-ol 99% aqueous 10 mM phosphate buffer pH 7.0 as mobile phase. The measured albumin-binding parameters showed significant correlations to the  $\text{cLog } P$ ,  $\phi_{0,\text{MeOH}}$ ,  $S$  and  $\log k'_0$  values, establishing the importance of hydrophobic properties to the interaction of the acyclovir derivatives with HSA.

## 1. Introduction

Acyclovir, 9-(2-hydroxyethoxymethyl) guanine was the first non-toxic drug developed against herpes viral infections [1,2]. It has an acyclic side chain which has been shown to be phosphorylated by the herpes specified thymidine kinase and is converted to the triphosphate in herpes-infected cells to a much greater extent than in uninfected cells. The triphosphate of acyclovir is more inhibitory to the viral DNA polymerase than to the  $\alpha$ -DNA polymerase of

the cell [1]. Pharmacokinetic studies [3,4] have demonstrated that acyclovir has an advantageous kinetic profile and metabolic disposition and it can be administered parenterally as well as orally. However, its penetration through the skin was not ideal [5–7]. To increase skin-penetration efforts have been made to develop prodrugs [8].

Several papers have been published about the use of high-performance liquid chromatography (HPLC) for the analysis of acyclovir in various formulations [9–12] or biological samples [12–16]. Reversed-phase HPLC has been used with a few percent of organic modifier (3–5% methanol [9,15] or 3% acetonitrile [10]). Ion-pair chroma-

\* Corresponding author.

tography has also been used with alkylsulphonates (heptansulphonic acid or octanesulphonic acid) with higher volume percent of organic modifier [11,13,16].

In this paper an investigation of 18 O-carboxylic esters and/or N-carboxamide derivatives of acyclovir, which are potential prodrugs, is presented. Their reversed-phase high-performance liquid chromatographic (RP-HPLC) retention behaviour was studied to reveal their hydrophobic properties. The HSA-binding properties of the compounds were measured by using immobilised HSA on a silica stationary phase in an HPLC column. It has been reported that chromatographic retention data correlate with ultrafiltration measurements of binding to HSA for a series of coumarin derivatives [17]. The applications of biochromatography to the determination of drug-protein interactions were discussed in detail by Aubry and McGann [18]. Excellent correlation was found for a structurally heterogeneous group of compounds between the protein-binding data obtained by HPLC and equilibrium dialysis [19] supporting the applicability of the method for the fast estimation of drug-binding. Kaliszan et al. [20] reported a quantitative structure-retention investigation of benzodiazepines on immobilised HSA, and found that two types of binding sites on HSA have a hydrophobic region with steric restrictions and a cationic region can also interact electrostatically with the compounds.

In this study the correlations between measured albumin-binding data, the chromatographic hydrophobicity data and the  $\text{cLog } P$  values (logarithm of calculated octanol-water partition coefficients) for the acyclovir derivatives were established.

## 2. Experimental

The compounds investigated are listed in Table 1. The compounds were synthesised at Burroughs Wellcome (NC, USA) or at the Wellcome Laboratories (Beckenham and Dartford, Kent, UK). Compounds 6–9 were synthesised by Professor Bundgaard (Royal Danish School of

Pharmacy, Copenhagen, Denmark) with the aim of better skin absorption of the derivatives. All the compounds analysed were checked for purity chromatographically. Solutions of 1 mg/ml of the compounds in methanol-water (50:50, v/v) were used for the analysis. Slow hydrolysis of the esters has been observed during the measurements. Solutions were kept refrigerated (4°C) when not in use to minimise such degradation.

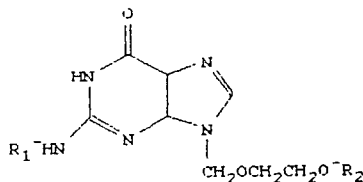
### 2.1. HPLC instrumentation


The HPLC equipment consisted of two Model 510 Waters pumps with automated gradient controller used together with a Waters 712 WISP autosampler and Waters 490E programmable multiwavelength detector (Milford, MA, USA). The column temperature was maintained using an oven unit obtained from Jones Chromatography (Hengoed, Mid Glamorgan, UK). Detection of the compounds was carried out at 254 nm UV with a sensitivity range of 0.05 AUFS. Quantitative evaluations of the chromatograms from the UV absorbance were made using a Multichrom data acquisition and analysis system (VG Data Systems, Altrincham, Cheshire, UK).

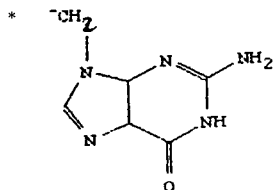
### 2.2. Reversed-phase measurements

A Zorbax  $C_8$  (250 × 4.6 mm I.D.) (DuPont, Wilmington, DE, USA) reversed-phase column was used. The column was maintained at 30°C during the measurements. The mobile-phase flow-rate was 1.0 ml/min. The mobile phase was aqueous methanol with the methanol concentration ranging from 5 to 95%. The HPLC grade methanol was purchased from Rathburn (Loughborough, UK). Water was obtained from a Milli-Q system (Millipore, CA, USA). For compounds 6–9 the mobile phase contained also 10 mM phosphate buffer pH 7.0 (HPLC grade, HiPerSolv, BDH, Poole, UK). The dead time of the system was estimated from the solvent peak. From the retention time and the dead time values the chromatographic retention factor ( $\log k'$ ) was calculated. The  $\log k'$  values were then regressed against the methanol concentration and the slope ( $S$ ) and the intercept ( $\log k'_0$ )

Table 1

The chemical structure of the compounds and their calculated octanol/water partition coefficients (cLog *P*)

Compound	R <sub>1</sub>	R <sub>2</sub>	cLog <i>P</i>
1	CH <sub>3</sub> CO-	H	-2.061
2	H	CH <sub>3</sub> CO-	-1.440
3	CH <sub>3</sub> CO-	CH <sub>3</sub> CO-	-1.194
4	H	C <sub>6</sub> H <sub>5</sub> -CO-	0.288
5	CH <sub>3</sub> CO-	C <sub>6</sub> H <sub>5</sub> -CO-	0.534
6	H	<i>m</i> (C <sub>3</sub> H <sub>7</sub> ) <sub>2</sub> N-CH <sub>2</sub> -C <sub>6</sub> H <sub>5</sub> -CO-	1.898
7	H	<i>p</i> (C <sub>3</sub> H <sub>7</sub> ) <sub>2</sub> N-CH <sub>2</sub> -C <sub>6</sub> H <sub>5</sub> -CO-	1.898
8	H	<i>m</i> (C <sub>4</sub> H <sub>9</sub> ) <sub>2</sub> N-CH <sub>2</sub> -C <sub>6</sub> H <sub>5</sub> -CO-	2.956
9	H	<i>p</i> (CH <sub>3</sub> ) <sub>2</sub> N-CH <sub>2</sub> -C <sub>6</sub> H <sub>5</sub> -CO-	0.102
10	CH <sub>3</sub> CO-	C <sub>2</sub> H <sub>5</sub> CO-	-0.665
11	C <sub>2</sub> H <sub>5</sub> CO-	C <sub>2</sub> H <sub>5</sub> CO-	-0.136
12	H	C <sub>2</sub> H <sub>5</sub> CO-	0.911
13	C <sub>6</sub> H <sub>5</sub> -CO-	C <sub>6</sub> H <sub>5</sub> -CO-	2.023
14	H	*	-3.244
15	H	C <sub>6</sub> H <sub>13</sub> CO-	1.205
16	H	-CO- 	1.150
17	H	C <sub>12</sub> H <sub>25</sub> CO-	4.379
18	H	C <sub>19</sub> H <sub>39</sub> CO-	8.023
19	H	H	-2.307



values of the least squares fitted straight lines were calculated. The chromatographic hydrophobicity index ( $\phi_0$ ) was calculated from the *S* and log  $k'_0$  values ( $-\log k'_0/S$ ) as previously described [19].

### 2.3. Albumin-binding measurements

An immobilised human serum albumin (HSA) column with the dimensions of 50 × 4.6 mm I.D. was obtained from Shandon HPLC (Life Science, Runcorn, UK) and was used for the

measurement of the albumin-binding ability of the derivatives. The column temperature was maintained at 25°C. The mobile phase contained 1% propan-2-ol (HPLC grade, Fisons, Loughborough, UK) and 10 mM phosphate buffer pH 7.0. The flow-rate was 0.5 ml/min. For compounds 6–9 the pH was increased to 7.4 and the propan-2-ol concentration ranged from 4 to 8% in order to obtain shorter retention times and improved peak shapes. The binding properties of the compounds were expressed as the log  $k'_{\text{HSA}}$  values obtained from the retention time and

dead time data. The  $\log k'_{\text{HSA}}$  values for compounds 6–9 were obtained by extrapolation from the data at higher propan-2-ol concentrations to 1% propan-2-ol.

The  $\text{cLog } P$  values (the calculated octanol–water partition coefficients) were obtained by using MedChem Ver. 3.54 (Pomona College, Claremont, CA, USA). The correlation study was carried out by using the DrugIdea program (Chemicro, Budapest, Hungary).

### 3. Results and discussion

The structure and the  $\text{cLog } P$  values of the compounds investigated are shown in Table 1. The reversed-phase retention parameters and the retention factor obtained by the drug-binding column are listed in Table 2.

Acyclovir (compound 19) showed only very weak binding (6%) to HSA which is in agreement with earlier results [9] obtained by ultrafiltration. No data has been reported on the drug-

binding properties of the investigated esters. Compounds 6–9 showed extremely strong binding on the HSA column using 1% propan-2-ol and pH 7.0 buffer in the mobile phase. The propan-2-ol concentration had to be increased to 4% to obtain reasonable retention times. In order to be able to compare the binding parameters to the other compounds the measurements were repeated by using 7% and 8% propan-2-ol in the mobile phase. The  $\log k'_{\text{HSA}}$  values were calculated and plotted as a function of propan-2-ol concentration. Straight lines were obtained which allowed the extrapolation of the  $\log k'_{\text{HSA}}$  values to 1% propan-2-ol. Table 3 shows the slope and the intercept values obtained using these extrapolated parameter values ( $S_{\text{HSA}}$ ,  $\log k'_{0,\text{HSA}}$ ).

Compounds 17 and 18 showed low solubility in methanol–water (50:50, v/v) and they had long retention times on a  $C_8$  column even with a high percentage (99%) of methanol in the mobile phase. Compound 18 showed an extremely long retention time and gave a wide peak on the HSA

Table 2

Parameters from the measured reversed-phase retention data [the slope ( $S$ ) and the intercept ( $\log k'_0$ ) from the  $\log k'$  vs. methanol concentration regression and the correlation coefficient,  $r$ ], the chromatographic hydrophobicity index ( $\phi_0$ ) and the albumin-binding parameter ( $\log k'_{\text{HSA}}$ )

Compound	$S$	$\log k'_0$	$r$	$\phi_0$	$\log k'_{\text{HSA}}$
1	-0.0448	1.098	0.998	24.5	-1.164
2	-0.0379	1.042	0.996	27.5	-0.725
3	-0.0418	1.555	0.999	37.2	-0.752
4	-0.0285	1.579	0.997	55.4	0.224
5	-0.0316	1.877	0.999	59.4	0.134
6	-0.0377	3.144	0.998	83.4	0.499
7	-0.0396	3.326	0.999	84.0	0.581
8	-0.0497	4.323	0.999	87.0	0.842
9	-0.0184	1.161	0.998	63.1	0.302
10	-0.0347	1.639	0.999	47.2	-0.440
11	-0.0240	1.368	0.999	57.0	-0.129
12	-0.0365	1.392	0.999	38.1	-0.461
13	-0.0463	3.336	0.999	72.1	0.230
14	-0.0292	0.290	0.995	9.9	-1.164
15	-0.0422	3.002	0.998	71.1	0.823
16	-0.0414	2.891	0.999	67.9	0.717
17	-0.0589	5.251	0.996	89.2	1.370
18	-0.0819	8.069	0.999	94.8	2.2
19	-0.0351	0.412	0.997	11.7	-1.182

The reversed-phase retention data for compounds 6–9 were obtained by using phosphate buffer pH 7.0 in the mobile phase.



Table 3

The albumin-binding parameters of the four basic compounds obtained by varying the propan-2-ol concentration

Compound	$S_{\text{HSA}}$	$\log k'_{0,\text{HSA}}$	$r$
6	-0.0429	0.542	0.999
7	-0.0432	0.624	0.999
8	-0.0470	0.889	0.997
9	-0.0309	0.333	0.999

$S$  and  $\log k'_0$  are the slope and the intercept of the least squares fitted straight line, and  $r$  is the correlation coefficient; the number of data points was 6.

column using 8% propan-2-ol in the mobile phase. The  $\text{cLog } P$  value of compound 18 is also unrealistically high. The data of compound 18 was often an outlier in the correlation study and therefore its data were omitted from further calculations.

Eq. 1 describes the correlation between the  $\text{cLog } P$  values and the  $\log k'_0$  values.

$$\text{cLog } P = 1.35(\pm 0.13) \log k'_0 - 2.54 \quad (1)$$

$$n = 18, r = 0.935, \text{ and } s = 0.71$$

The correlation coefficients between the slope and the intercept values was small ( $-0.728$ ) showing that the compounds differ from each other significantly with respect to their partition behaviour [23].

The correlation was further studied by using the  $S$  and  $\log k'_0$  values as two independent variables in relation to the  $\text{cLog } P$  and the albumin-binding parameter ( $\log k'_{\text{HSA}}$ ). A highly significant relationship ( $p > 0.95$ ) were obtained and shown in Eq. 2.

$$\text{cLog } P = 72.79(\pm 12.07)S + 1.76(\pm 0.08) \times \log k'_0 - 0.80 \quad (2)$$

$n = 18, r = 0.994, s = 0.33, \text{ and } F_{2,15} = 305.0$  where  $n$  is the number of compounds,  $r$  is the multiple correlation coefficient,  $s$  is the standard error of the estimate,  $F$  is the Fisher-test value. Fig. 1 shows the fit of the predicted  $\text{cLog } P$  vs.  $\text{cLog } P$  values from Eq. 2.

Eq. 3 describes the correlation between the  $\log k'_{\text{HSA}}$  and  $\log k'_0$  values.

$$\log k'_{\text{HSA}} = 0.50(\pm 0.07) \log k'_0 - 1.09 \quad (3)$$

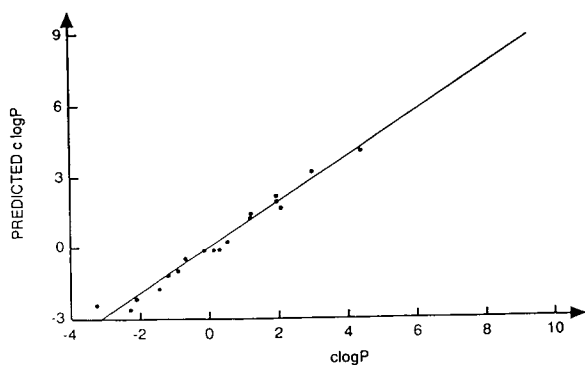


Fig. 1. The plot of the predicted  $\text{cLog } P$  vs.  $\text{cLog } P$  by Eq. 2.

$$n = 18, r = 0.876, \text{ and } s = 0.38$$

Again much better correlation was obtained when the  $S$  values were also introduced as a second independent variable, showing the importance of the contact hydrophobic surface area in the drug-protein binding. Eq. 4 describes the relationship between the reversed-phase retention data and the albumin-binding data of the compounds. The relationships were again highly significant.

$$\log k'_{\text{HSA}} = 48.16(\pm 7.92)S + 0.75(\pm 0.06) \log k'_0 + 0.30 \quad (4)$$

$$n = 18, r = 0.983, s = 0.21, \text{ and } F_{2,15} = 104.2$$

Fig. 2 shows the fit of the predicted  $\log k'_{\text{HSA}}$  vs.  $\log k'_{\text{HSA}}$  values from Eq. 4.

The regression of the albumin-binding data

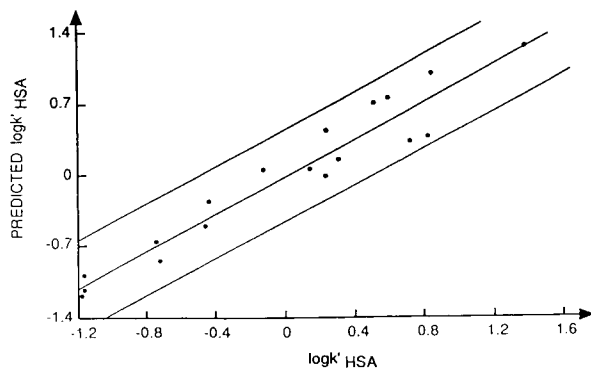


Fig. 2. The plot of the predicted  $\log k'_{\text{HSA}}$  vs.  $\log k'_{\text{HSA}}$  by Eq. 4 together with the 95% confidence interval.

against the  $c\text{Log } P$  values and the chromatographic hydrophobicity index ( $\phi_{0,\text{MeOH}}$ ) values separately is described by Eqs. 5 and 6, respectively.

$$\log k'_{\text{HSA}} = 0.372(\pm 0.031)c\text{Log } P - 0.109 \quad (5)$$

$$n = 18, r = 0.949, s = 0.252, \text{ and } F_{1,16} = 144.4$$

$$\log k'_{\text{HSA}} = 0.029(\pm 0.002)\phi_{0,\text{MeOH}} - 1.1613 \quad (6)$$

$$n = 18, r = 0.953, s = 0.241, \text{ and } F_{1,16} = 158.7$$

Highly significant correlations were found in both cases.

In conclusion, the reversed-phase retention data obtained on the  $C_8$  column by using methanol and pH 7.0 phosphate buffer in the mobile phase showed significant correlation to the calculated octanol–water partition coefficients. The albumin-binding parameters measured on an immobilised HSA column showed high correlation to the calculated octanol–water partition coefficients and the hydrophobicity indices measured by reversed-phase chromatography.

### Acknowledgement

The authors would like to thank Alan Hill and Rachel Siertsema for the calculations of the  $c\text{Log } P$  values.

### References

- [1] G.B. Elion, P.A. Furman, J.A. Fyfe, P. de Miranda, L. Beauchamp and H.J. Schaeffer, *Proc. Natl. Acad. Sci. USA*, 74 (1977) 5716.
- [2] H.J. Schaeffer, L. Beauchamp, P. de Miranda, G.B. Elion, D.J. Bauer and P. Collins, *Nature*, 272 (1978) 583.
- [3] P. de Miranda, R.J. Whitley, M.R. Blum, R.E. Keeney, N. Barton, D.M. Cocchetto, S. Good, G.P. Hemstreet, L.E. Kirk, D.A. Page and G.B. Elion, *Clin. Pharmacol. Ther.*, 26 (1979) 718.
- [4] W.M. Sullender, A.M. Arvin, P.S. Diaz, J.D. Connor, R. Straube, W. Dankner, M.J. Levin, S. Weller, M.R. Blum and S. Chapman, *Antimicrob. Agents Chemother.*, 31 (1987) 1722.
- [5] S.L. Spruance, M.B. McKeough and J.R. Cardinal, *Antimicrob. Agents Chemother.*, 25 (1984) 10.
- [6] E.R. Cooper, E.W. Merritt and R.L. Smith, *J. Pharm. Sci.*, 74 (1985) 688.
- [7] D.J. Freeman, N.V. Sheth and S.L. Spruance, *Antimicrob. Agents Chemother.*, 29 (1986) 730.
- [8] B.G. Petty, R.J. Whitley, S. Liao, H.C. Krasny, L.E. Rocco, L.G. Davis and P.S. Lietman, *Antimicrob. Agents Chemother.*, 31 (1987) 1317.
- [9] G.C. Visor, S.E. Jackson, R.A. Kenley and G. Lee, *J. Liq. Chromatogr.*, 8 (1985) 1475.
- [10] Y. Pramard, V. Das Gupta and T. Zerai, *Drug Dev. Ind. Pharm.*, 16 (1990) 1687.
- [11] D. Marini, G. Pollino and F. Balestrieri, *Boll. Chim. Farm.*, 130 (1991) 101.
- [12] D.S. Ashton and A. Ray, *Anal. Proc.*, 30 (1993) 44.
- [13] S. Bouquet, B. Regnier, S. Quehen, A.M. Brisson, Ph. Courtois and J.B. Fourtillan, *J. Liq. Chromatogr.*, 8 (1985) 1663.
- [14] R.L. Smith and D.D. Walker, *J. Chromatogr.*, 343 (1985) 203.
- [15] J. Cronqvist and I. Nilsson-Ehle, *J. Liq. Chromatogr.*, 11 (1988) 2593.
- [16] A.M. Molokhia, E.M. Niazy, S.A. El-Hoofy and M.E. El-Dardari, *J. Liq. Chromatogr.*, 13 (1990) 981.
- [17] E. Domenici, C. Bertucci, P. Salvadori and I.W. Wainer, *J. Pharm. Sci.*, 80(2) (1991) 164.
- [18] A.-F. Aubry and A. McGann, *LC·GC Int.*, 7 (1994) 389.
- [19] N. Lammers, H. De Bree, C.P. Groen, H.M. Ruijten and B.J. De Jong, *J. Chromatogr.*, 496 (1989) 291.
- [20] R. Kalisz, T.A.G. Noctor and I.W. Wainer, *Mol. Pharmacol.*, 42 (1992) 512.
- [21] D.J.M. Purifoy, L.M. Beauchamp, P. de Miranda, P. Ertl, S. Lacey, G. Roberts, S.G. Rahim, G. Darby, T.A. Krenitsky and K.L. Powell, *J. Mol. Virol., Suppl.* 1 (1993) 139.
- [22] K. Valkó and P. Slegel, *J. Chromatogr.*, 631 (1993) 49.
- [23] K. Valkó, *J. Liq. Chromatogr.*, 10 (1987) 1663.



ELSEVIER

Journal of Chromatography A, 707 (1995) 373–379

JOURNAL OF  
CHROMATOGRAPHY A

Short communication

## Determination of biogenic amines and their precursor amino acids in wines of the Vallée du Rhône by high-performance liquid chromatography with precolumn derivatization and fluorimetric detection

T. Bauza<sup>a,b,\*</sup>, A. Blaise<sup>a</sup>, F. Daumas<sup>b</sup>, J.C. Cabanis<sup>a</sup>

<sup>a</sup>*Centre de formation et de Recherche en Oenologie, Institut Supérieur de la Vigne et du Vin, Faculté de Pharmacie, 15 Avenue Charles Flahault, 34018 Montpellier, France*

<sup>b</sup>*Comité Interprofessionnel des Vins d'A.O.C. de Côtes du Rhône et de la Vallée du Rhône, 6, Rue des trois faucons, 84000 Avignon, France*

First received 1 December 1994; revised manuscript received 2 March 1995; accepted 3 March 1995

### Abstract

The presence of biogenic amines in foods and more particularly in wines is of current interest due to their pharmacological properties and the physiological disorders they may provoke in the human organism. Although at present compounds like histamine or cadaverine can be analyzed with precision in wine, less information is provided on the possible presence of spermine and spermidine. Using fluorenylmethylchloroformate (FMOC) as derivatization reagent we were able to determine these compounds in wines simultaneously with other biogenic amines such as histamine, tyramine, phenylethylamine, putrescine, agmatine, cadaverine, and precursor amino acids of these compounds, in their free state in wine: arginine, ornithine, histidine, phenylalanine, and tyrosine. Samples of 54 red wines, 15 rosé wines and 15 white wines from the Vallée du Rhône (France), all bottled and commercialized, have been analyzed by this method.

The polyamines cadaverine, spermine and spermidine are present in small quantities in these wines. Only agmatine and putrescine appear at levels significantly higher than 1 mg/l. The presence of putrescine is strongly correlated to that of its precursors arginine, ornithine and agmatine, as well as with the presence of tyramine and histamine.

On the other hand, no correlation (threshold of 5%) was found between the levels of phenylethylamine, tyramine and histamine, and those of their free precursor amino acids in the wine, phenylalanine, tyrosine and histidine.

Levels of putrescine, agmatine, histamine, tyramine, spermine, spermidine are higher in red wines than in the other types of wine.

\* Corresponding author.

## 1. Introduction

Since their discovery in 1954 by Tarantola [1], the physiological influence on the human organism of the presence of biogenic amines in wines has been discussed [2,3]. More recently, high-performance liquid chromatography has enabled the development of good reliable analytical methods for the determination of the major biogenic amines in wines [4,5]. However, these methods are not able to detect some of the amines, such as spermidine and spermine. These amines, even though they appear less toxic than other compounds such as histamine or tyramine [6,7], possess nevertheless many functions at the cellular level. By their polycationic long chain structure, they interact with DNA, RNA, proteins and the membrane phospholipides [8,9]. They are also strongly implied in cellular growth phenomena. So, one finds them in great quantities in tumor cells, which possess high growth rates, and in smaller amounts in all living organisms, including viruses. The presence of these polyamines in grape berries, and the role that they may play have been studied for some years [10]. In the vine, potassium deficiency increases the putrescine content in leaves [11–13]. The presence of putrescine and cadaverine in wines is well documented [14,15]. On the other hand, few tests have been realized on spermine, spermidine and agmatine. The classical analytical method [4] for the determination of biogenic amines in wines by HPLC uses a precolumn derivatization with phthaldialdehyde (OPA). This method gives very good results for primary amines, but is not able to derivatize the secondary amines functions of spermine and spermidine. The utilization of fluorenylmethylchloroformate (FMOC) [16–19] allows the direct analysis in wines of the five polyamines putrescine (PU), cadaverine (CA), agmatine (AG), spermine (SM) and spermidine (SD), simultaneously with other biogenic amines, such as histamine (HA), phenylethylamine (PE), tyramine (TA), and their precursor amino acids arginine (AR), ornithine (OR), phenylalanine (PA), histidine (HD) and tyrosine (TS).

In order to measure the biogenic amine and

amino acid precursor concentrations in wine, 84 samples of bottled and commercialized wines (54 red wines, 15 rosé wines and 15 white wines) have been taken from different sites in the region of the Vallée du Rhône, and analyzed with the method described below.

## 2. Experimental

### 2.1. Materials

Analyses were performed with a Hewlett-Packard 1050 series HPLC system consisting of a solvent degasser system, a quaternary pumping module at low pressure mixing, an autosampler, a fluorimetric detector series 1046A with excitation at 263 nm and detection at 313 nm. The system was managed by a Hewlett-Packard Vectra 286-S-20 data analysis station.

The separation column used was an ODS Hypersil column, 200 × 2.1 mm I.D., 5 μm (Hewlett-Packard). The injection volume was 2 μl for all analyses performed.

FMOC, all solvents, as well as the different biogenic amines and amino acids, were furnished by Fluka (Buchs, Switzerland).

### 2.2. Preparation of reagents

A standard solution containing 1 g/l of each compound is prepared in 0.1 M HCl. This solution can be stored for eight weeks in the refrigerator.

Solutions diluted 100- and 200-fold, are prepared daily for calibration. A buffer solution of pH 8.5 is prepared by adjusting the pH of a 0.2 M boric acid solution with 5 M NaOH.

A cleavage solution (0.5 M NH<sub>3</sub>) and a quenching solution (acetonitrile–acetic acid–water, 20:2:3, v/v) are also used.

### 2.3. Derivatization reaction

In a 700-μl amber vial, 20 μl of sample are mixed with 50 μl of borate buffer. An 8-mg amount of FMOC is dissolved in 1 ml of acetonitrile, and 100 μl of this reagent are added to the

Table 1  
Solvent gradient. Flow-rate 0.3 ml/min

Time (min)	A (%)	B (%)
0	15	85
18	15	85
18.1	38	62
25	40	60
30	40	60
67	42	58
103	85	15
110	85	15

vial. After 3 min, 50  $\mu$ l of cleavage solution are added. After 3 min, 300  $\mu$ l of quenching solution are added to the vial, which is then sealed and placed in the autosampler tray.

#### 2.4. Chromatographic conditions

A solvent gradient with a flow-rate of 0.3 ml/min, is realized from two solutions according to Table 1: Eluent A, acetonitrile–2-octanol (1% v/v); Eluent B: acetonitrile 150 ml, phosphoric acid 8.8 ml, dimethylcyclohexylamine 10 ml, bidistilled water QSP 1 l. The pH must be near 2.7.

### 3. Results and discussion

FMOC reacts with primary and secondary amine functions. Optimization of the reaction conditions has been undertaken for the dosage of the polyamines putrescine, cadaverine, spermidine and spermine. The derivatization of spermine and spermidine requires larger quantities of reagent, because of the presence of the secondary functions. An excess of FMOC decreases the reaction efficiency despite the utilization of the cleavage solution. An amount of 6–10 mg/ml appears to be sufficient for derivatizing these compounds in wine. The cleavage solution is used at the end of the reaction to eliminate the excess of reagent, and to break complexes originating from multiple derivatizations of the same

amine function. Its use increases the derivatization yield for spermine and spermidine analyzed directly in the wine, and harmonizes the results obtained with those of the standard solutions. An excess of cleavage solution (higher than 100  $\mu$ l) reduces the efficiency of the derivatization of amines like spermine.

Figs. 1 and 2 show chromatograms obtained with aqueous standard solution and with a red wine.

The repeatability (relative error for six samples in the same analysing sequence) of the method ranges from 1.6% for agmatine to 13.6% for spermine.

When levels are not too high for the sensitivity of the detector, precursor the amino acids, arginine, ornithine, histidine, phenylalanine and tyrosine present in the free state in the wine and susceptible to be metabolized, have also been quantified.

The analysis of the 84 samples shows that wines from the Vallée du Rhône contain small quantities of biogenic amines (Table 2). Only 8% of the samples contain more than 20 mg/l of putrescine, and 1.2% more than 10 mg/l of histamine or tyramine. Phenylethylamine also is present in small quantities, 95% of samples containing less than 5 mg/l. The polyamines cadaverine, spermidine and spermine are rarely present in wine. Their levels were lower than 1 mg/l in 83.3% of the samples for spermidine, 98.9% for spermine and 98.8% for cadaverine. Agmatine, which is an intermediate in the synthesis of putrescine from arginine, appears at higher levels than the other polyamines, exceeding 20 mg/l in one third of the samples. Putrescine shows levels lower than this value in 91.7% of the samples (Table 2). There is a very strong correlation between the presence of putrescine and that of its precursors agmatine, arginine ( $p < 0.001$ ), and ornithine ( $p < 0.01$ ). High concentrations of these latter compounds favor the presence of putrescine in a wine. The presence of this amine is also correlated to the presence of tyramine and histamine ( $p < 0.001$ ). On the other hand, no correlation exists ( $p < 0.05$ ) between histamine and histidine (or the sum of the histidine and histamine contents), phenyl-

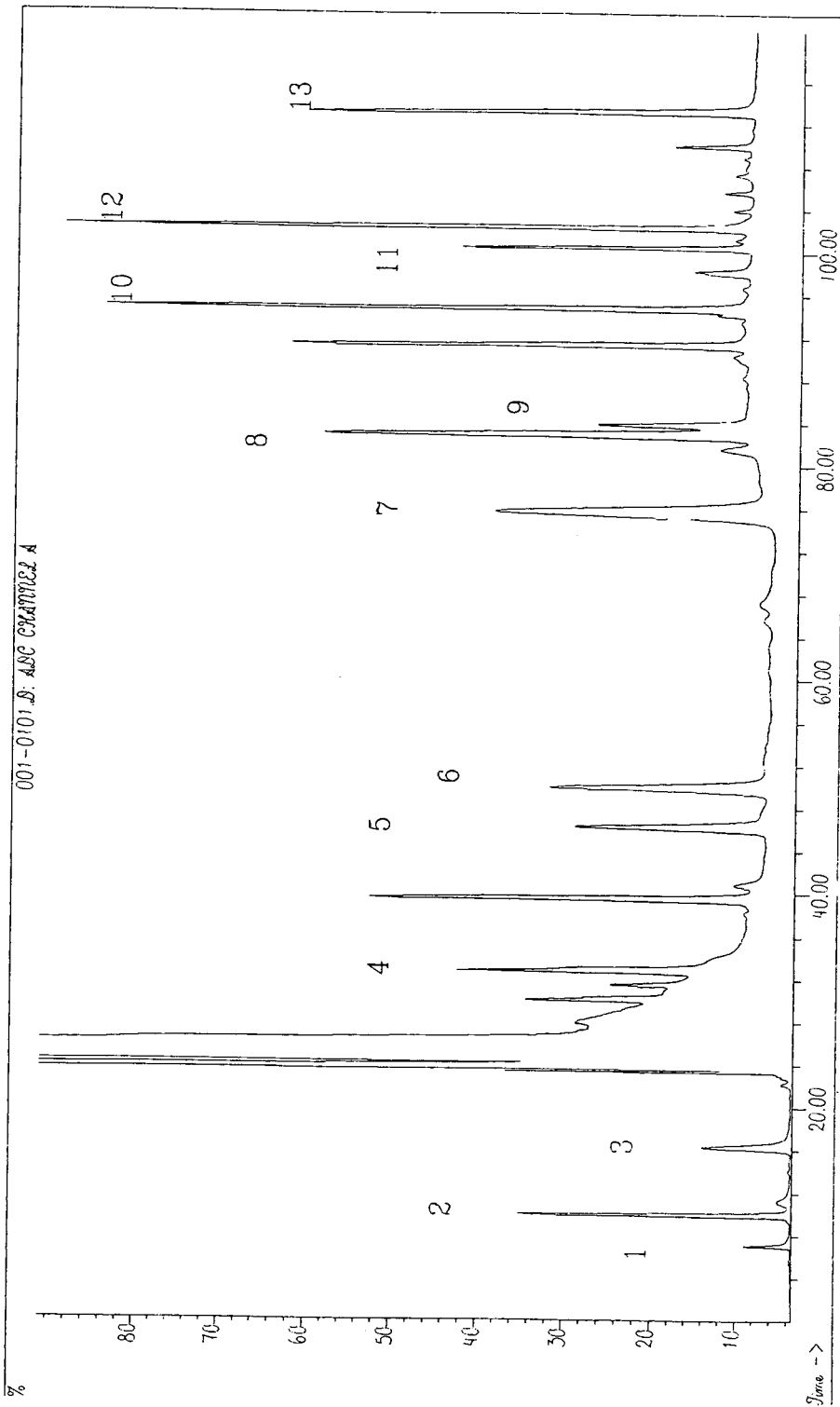


Fig. 1. Chromatogram of a standard solution. Peaks: 1 = histidine, 4.6 mg/l; 2 = arginine, 5.15 mg/l; 3 = agmatine, 4.1 mg/l; 4 = phenylalanine, 4.7 mg/l; 5 = phenylethylamine, 5.2 mg/l; 6 = ornithine, 3.6 mg/l; 7 = putrescine, 4 mg/l; 8 = cadaverine, 4.5 mg/l; 9 = tyrosine, 4.7 mg/l; 10 = tyramine, 6.2 mg/l; 11 = histamine, 4.6 mg/l; 12 = spermidine, 3.9 mg/l; 13 = spermine, 3.9 mg/l.

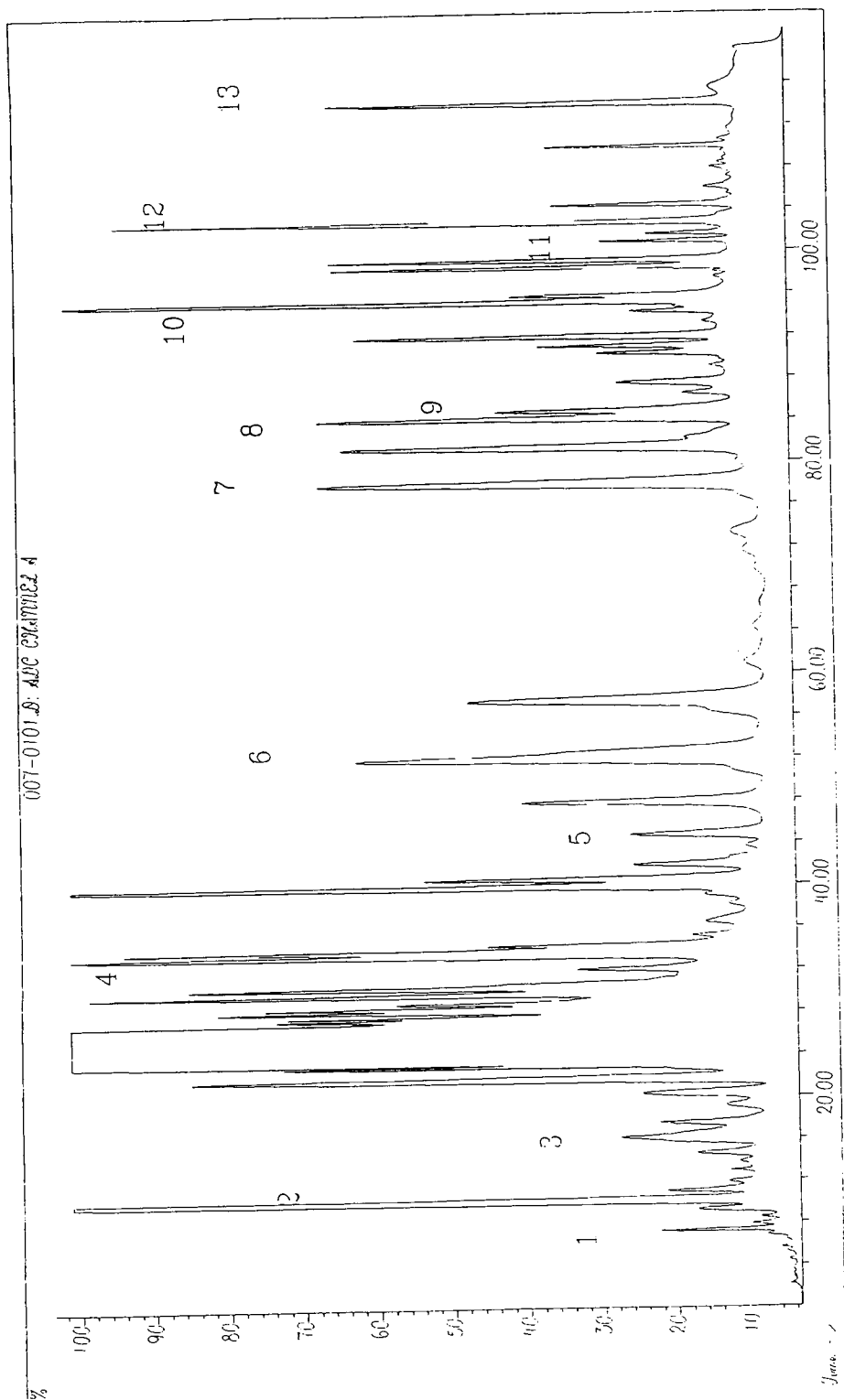


Fig. 2. Chromatogram of a wine sample overlaid with: 1 = histidine, 4.6 mg/l; 2 = arginine, 5.15 mg/l; 3 = agmatine, 4.1 mg/l; 4 = phenylalanine, 4.7 mg/l; 5 = phenylethylamine, 5.2 mg/l; 6 = ornithine, 3.6 mg/l; 7 = putrescine, 4 mg/l; 8 = cadaverine, 4.5 mg/l; 9 = tyrosine, 4.7 mg/l; 10 = tyramine, 6.2 mg/l; 11 = histamine, 4.6 mg/l; 12 = spermidine, 3.9 mg/l; 13 = spermine, 3.9 mg/l.

Table 2

Mean concentration and standard deviation for the different compounds found in wines of the Vallée du Rhône in mg/l

	All samples		Red wines		Rosé wines		White wines	
	Middle	Std. Dev.	Middle	Std. Dev.	Middle	Std. Dev.	Middle	Std. Dev.
AR	22.4	14.8	27.5	14.7	10.5	5.6	16.9	12.7
OR	3.7	4.4	5.0	4.8	1.0	1.2	1.9	2.5
AG	17.3	9.5	21.6	8.4	9.0	3.7	10.3	7.1
PU	7.7	6.8	10.8	6.7	2.5	0.9	1.9	0.7
CA	0.2	0.4	0.2	0.2	0.4	0.9	0.1	0.1
SD	0.5	0.6	0.6	0.6	0.4	0.5	0.3	0.3
SM	0.1	0.2	0.1	0.1	0.2	0.4	0.1	0.2
HI	8.9	10.9	8.2	6.7	13.5	22.0	0.4	0.1
PA	13.0	5.8	13.7	5.9	11.3	7.3	3.7	6.3
TS	3.5	2.3	3.3	2.3	3.3	1.5	4.4	2.6
HA	2.5	2.6	3.7	2.5	0.4	0.6	0.1	0.2
PE	1.7	1.5	1.9	1.6	1.5	1.4	0.9	0.7
TA	3.1	2.1	3.7	2.3	2.3	1.7	2.2	1.4

$n = 84$  samples; red wines = 54, rosés wines = 15, white wines = 15. PU = putrescine, HI = histidine; HA = histamine; OR = ornithine; AR = arginine; AG = agmatine; PA = phenylalanine; PE = phenylethylamine; CA = cadaverine; TS = tyrosine; TA = tyramine; SD = spermidine; SM = spermine.

ethylamine and phenylalanine or between tyramine and tyrosine (or the sum of the tyramine and tyrosine contents).

The Kruskal–Wallis statistical test shows a significant difference between red wines and rosés and white wines with respect to the levels of arginine and ornithine, the precursor amino acids of putrescine, as well as histamine, putrescine, agmatine (1%), spermine, spermidine and tyramine (5%). Red wines are therefore richer in polyamines and their precursors than the other types of wine. Equally, they contain more tyramine and histamine.

#### 4. Conclusions

The use of FMOC as derivatizing reagent seems to be an attractive choice for the determination of biogenic amine analysis in wines. This technique enables a direct analysis with satisfactory sensitivity of this family of compounds in the wine, particularly of spermine and spermidine, which contain secondary amine functions. It also allows the simultaneous de-

termination of some of their precursor amino acids.

Wines of the Vallée du Rhône generally contain small quantities of biogenic amines. However, large differences may occur between different samples. Thus, red wines contain higher levels of histamine, tyramine, agmatine, putrescine, spermine and spermidine than the other types of wine. The levels of spermine, spermidine and cadaverine in wine are nevertheless insignificant from a physiological point of view. The amount of putrescine is linked to the presence of its precursors agmatine, arginine and ornithine, in the free state in the finished wine, as well as to that of the biogenic amines histamine and tyramine. On the other hand, the presence of tyramine and histamine is not linked to the presence of tyrosine and histidine. Similar results are found for phenylethylamine and its precursor phenylalanine.

#### References

- [1] G. Tarantola, *Atti Accad. Ital. Vite Vino*, 6 (1954) 146.
- [2] J.C. Cabanis, *Bull O.I.V.*, 656–657 (1985) 1009.



- [3] J. Aerny, Bull. O.I.V., 656–657 (1990) 1017.
- [4] Ch. Tricard and J.M. Cazabeil, Office International de la Vigne et du Vin, Internal Communication, F.V. No. 850, 1990.
- [5] P.K. Lehtonen, M. Saarinen, M. Vesanto and M.L. Riekkola, Z. Lebensm. Unters. Forsch., 194 (1992) 434.
- [6] R.T. Coutts, G.B. Baker and F.M. Pasutto, Adv. Drug Res., 15 (1986) 169.
- [7] H.M.L.J. Joosten, Neth. Milk Dairy J., 42 (1987) 25.
- [8] C.W. Tabor and H. Tabor, Ann. Rev. Biochem., 53 (1984) 749.
- [9] N. Seiler, Digestion, 46 (1990) 319.
- [10] M. Brodequis, B. Dumery and Bouard, Conn. Vigne Vin, 23 (1989) 1.
- [11] D.O. Adams, K.E. Franke and L.P. Christensen, Am. J. Enol. Vitic., 41 (1990) 121.
- [12] A. Bertrand, M.C. Ingargiola and J. Delas, Rev. Fr. Oenol. (Cah. Sci.), 132 (1991) 7.
- [13] D.O. Adams, D.J. Bates, D.F. Adams and K.E. Franke, Am. J. Enol. Vitic., 43 (1992) 239.
- [14] J. Aerny, Office International de la Vigne et du Vin, Internal Communication, F.V. No. 881, 1990.
- [15] M.C. Ingargiola and A. Bertrand, Office International de la Vigne et du Vin, Internal Communication, F.V. No. 896, 1992.
- [16] S. Einarsson, B. Josefsson and S. Lagerkvist, J. Chromatogr., 282 (1983) 609.
- [17] Z. Harduf, T. Nir and B.J. Juven, J. Chromatogr., 437 (1988) 378.
- [18] P.A. Haynes, D. Sheumack, J. Kibby and J.W. Redmond, J. Chromatogr., 540 (1991) 177.
- [19] H. Godel, P. Seitz and P. Verhoef, LC-GC Intl., 5 (1992) 44.



ELSEVIER

Journal of Chromatography A, 707 (1995) 380–383

JOURNAL OF  
CHROMATOGRAPHY A

Short communication

Direct separation of carboxylic acid and amine enantiomers by high-performance liquid chromatography on reversed-phase silica gels coated with chiral copper(II) complexes

Naobumi Ôi<sup>1</sup>, Hajimu Kitahara, Fumiko Aoki\*

Sumika Chemical Analysis Service, Ltd., 3-1-135, Kasugade-naka, Konohana-ku, Osaka 554, Japan

Received 21 February 1995; accepted 13 March 1995

Abstract

Excellent direct separation of various carboxylic acid and amine enantiomers was accomplished by HPLC on reversed-phase silica gels coated with copper(II) complexes of *N,S*-dioctyl-*D*-penicillamine and (*R,R*)-tartaric acid mono-*(R)*-1-( $\alpha$ -naphthyl)ethylamide. The chiral recognition mechanism is discussed. These copper(II) complexes are promising as chiral stationary phases for the separation of a variety of racemic carboxylic acids and amines in which copper(II) complex formation can be assumed.

1. Introduction

It is well known the chiral ligand-exchange high-performance liquid chromatography (HPLC) using copper(II) complexes of chiral ligands is a powerful tool for the direct separation of various enantiomers [1,2], and this technique is usually applied for the separation of racemic amino acids, hydroxy acids [3] and amino alcohols [4,5]. Recently, it was shown some other racemic compounds, such as pyridonecarboxylic acids [6] and 3-amino- $\epsilon$ -caprolactam [7], were also resolved. These results suggest that chiral ligand-exchange HPLC is suitable for the separation of a wide range of enantiomers in which copper(II) complex formation can be assumed.

In this paper, we report the direct separation of various racemic carboxylic acids and amines by HPLC on reversed-phase silica gels coated with copper(II) complexes of *N,S*-dioctyl-*D*-penicillamine (**1**) [7] and (*R,R*)-tartaric acid mono-*(R)*-1-( $\alpha$ -naphthyl)ethylamide (**2**) [8], developed previously.

2. Experimental

Chiral ligands **1** and **2** were prepared as described previously [7,8]. Commercially available Sumipax ODS columns (150 and 50 mm  $\times$  4.6-mm I.D.) packed with octadecylsilanized silica (5  $\mu$ m) were coated with **1** and **2** and treated with copper(II) ion. These columns are commercially available from Sumika Chemical Analysis Service (Osaka, Japan) as Sumichiral OA-5000 and OA-6000. All chemicals and solvents of analytical-reagent grade were purchased

\* Corresponding author.

<sup>1</sup> Present address: Chiral Chromatography Laboratory, 50-29, Ogura-cho, Kitashirakawa, Sakyo-ku, Kyoto 606, Japan.

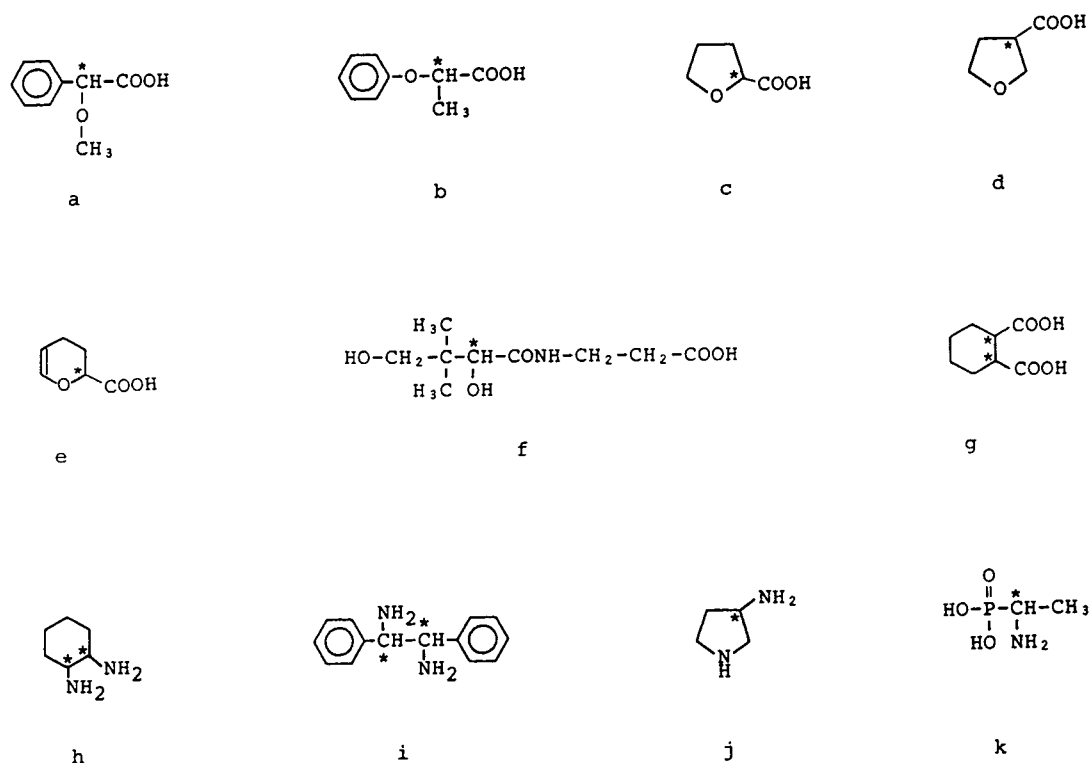


Fig. 1. Structures of racemic compounds.

from Wako (Osaka, Japan). Structures of the racemic carboxylic acids and amines used in this study are shown in Fig. 1.

The experiments were carried out using a Waters Model 510 high-performance liquid chromatograph equipped with a variable-wavelength UV detector (operated at 254 and 280 nm). The chromatographic conditions are given in Table 1.

### 3. Results and discussion

The chromatographic results are summarized in Table 1. Excellent direct separation of various racemic carboxylic acids and amines was accomplished. We can assume the formation of diastereomeric copper(II) complexes with the stationary phases for the chiral recognition of these enantiomers.

The separation of  $\alpha$ -methoxyphenylacetic acid enantiomers (Fig. 2) suggests that the methoxy group attached to the asymmetric carbon atom may contribute to the complexation in place of the hydroxy group in mandelic acid. Similar complexations are assumed with racemic 2-phenoxypropionic acid, tetrahydro-2-furoic acid and tetrahydro-3-furoic acid. The difference in separation factors between tetrahydro-2- and -3-furoic acid shows that the positions of the carboxyl group and the oxygen atom of the ether linkage around the asymmetric carbon atom are important for the formation of the complex.

In the separation of racemic *trans*-1,2-diaminocyclohexane, 1,2-diphenylethylenediamine and 3-aminopyrrolidine (Fig. 3), two amino or imino groups may play an effective cooperative role for the complexation. The phosphoric acid group may contribute to the formation of the complex for the separation of 1-aminoethylphosphonic acid (Fig. 4).

Table 1  
Enantiomer separations by HPLC with copper(II) complexes of chiral ligands

Compound <sup>a</sup>	Name	$k'_1$	$k'_2$	$\alpha$	Chiral ligand	Mobile phase
a	$\alpha$ -Methoxyphenylacetic acid	35.20	37.31	1.06	1	D
b	2-Phenoxypropionic acid	60.78	72.94	1.20	1	E
c	Tetrahydro-2-furoic acid	6.90	12.97	1.88	2	B
d	Tetrahydro-3-furoic acid	13.26	14.59	1.10	2	A
e	3,4-Dihydro-2H-pyran-2-carboxylic acid	9.54	10.97	1.15	2	C
f	Pantothenic acid	7.29(-)	7.95(+)	1.09	2	B
g	<i>trans</i> -1,2-Cyclohexanedicarboxylic acid	91.10	109.32	1.20	1	F(pH 6.4)
h	<i>trans</i> -1,2-Diaminocyclohexane	9.81	11.48	1.17	2	A
i	1,2-Diphenylethylenediamine	3.64	4.00	1.10	1	F(pH 4.5)
j	3-Aminopyrrolidine	0.51	1.33	2.61	2	A
k	1-Aminoethylphosphonic acid	6.67	8.67	1.30	1	B

Mobile phase: A = 1 mM copper(II) sulfate in water; B = 2 mM copper(II) sulfate in water–acetonitrile (95:5); C = 2 mM copper(II) sulfate in water–acetonitrile (90:10); D = 2 mM copper(II) sulfate in water–2-propanol (85:15); E = 2 mM copper(II) sulfate in water–2-propanol (80:20); F = 1 mM copper(II) acetate + 0.1 M ammonium acetate in water–2-propanol (85:15). Column temperature: 25°C (40°C for compound i). A flow-rate of 1.0 ml/min was used for the 150 × 4.6 mm I.D. column. An injection volume of 5  $\mu$ l (2 mg/ml) was typically used.  $k'_1$ ,  $k'_2$  = Capacity factors of first- and second-eluted isomer, respectively  $\alpha$  = separation factor ( $k'_1/k'_2$ ).

<sup>a</sup> See Fig. 1.

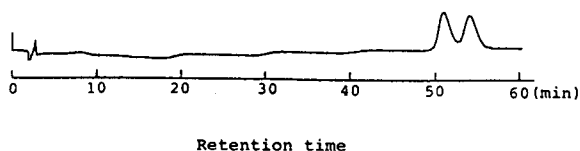


Fig. 2. HPLC separation of racemic  $\alpha$ -methoxyphenylacetic acid with 1. Chromatographic conditions as in Table 1.

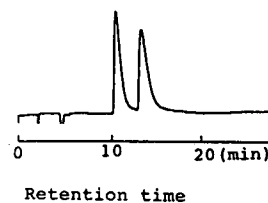


Fig. 4. HPLC separation of racemic 1-aminoethylphosphonic acid with 1. Chromatographic conditions as in Table 1.

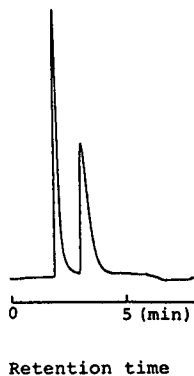


Fig. 3. HPLC separation of racemic 3-aminopyrrolidine with 2. Chromatographic conditions as in Table 1.

#### 4. Conclusion

Excellent direct separation of the enantiomers of various carboxylic acids and amines containing some other polar groups was accomplished on copper(II) complexes of chiral ligands 1 and 2. The results showed that the carboxyl or amino group attached to the asymmetric carbon atom may play the main role and some other polar groups may play a cooperative role in forming the complexes with chiral stationary phases. It is emphasized that the positions of these groups around the asymmetric carbon atom are very

important stereochemically for chiral recognition.

These chiral copper(II) complexes of chiral ligands **1** and **2** are very promising as chiral stationary phases for the direct separation of the enantiomers of a variety of carboxylic acids and amines in which copper(II) complex formation can be assumed.

## References

- [1] V.A. Davankov, *Adv. Chromatogr.*, 18 (1980) 139.
- [2] V.A. Davankov, A.A. Kurganov and A.S. Bochkov, *Adv. Chromatogr.*, 22 (1983) 71.
- [3] H. Katoh, T. Ishida, S. Kuwata and H. Kuniwa, *Chromatographia*, 28 (1989) 481.
- [4] H.G. Kicinski and A. Kettrup, *Fresenius' Z. Anal. Chem.*, 320 (1985) 51.
- [5] S. Yamazaki, T. Takeuchi and T. Tanimura, *J. Liq. Chromatogr.*, 12 (1989) 2239.
- [6] T. Arai, H. Koike, K. Hirota and H. Oizumi, *J. Chromatogr.*, 448 (1988) 439.
- [7] N. Ôi, H. Kitahara and R. Kira, *J. Chromatogr.*, 592 (1992) 291.
- [8] N. Ôi, H. Kitahara and F. Aoki, *J. Liq. Chromatogr.*, 16 (1993) 893.



ELSEVIER

Journal of Chromatography A, 707 (1995) 384–389

JOURNAL OF  
CHROMATOGRAPHY A

Short communication

Use of  $\beta$ -diketonate anions as eluent in non-suppressed ion chromatography: 1,3-cyclohexanedionate as acidic eluent

Naoki Hirayama<sup>1,\*</sup>, Masahiro Maruo<sup>2</sup>, Akinobu Shiota<sup>3</sup>, Tooru Kuwamoto<sup>4</sup>

*Department of Chemistry, Faculty of Science, Kyoto University, Sakyo-ku, Kyoto 606-01, Japan*

First received 3 January 1995; revised manuscript received 7 March 1995; accepted 7 March 1995

**Abstract**

A new low- $pK_a$   $\beta$ -diketonate eluent for non-suppressed ion chromatography was developed for suppressing the dissociation of impurity anions without impairing the separation and determination of fluoride and chloride anions. It was found that 1,3-cyclohexanedionate is the preferred eluent, having a low  $pK_a$  originating from the structural strain of the  $\beta$ -diketonate group.

**1. Introduction**

Non-suppressed ion chromatography (IC) was developed as an effective method for the separation and determination of several anions [1,2]. This method has been improved by the development of new eluent ions [3,4] with superior elution characteristics.

We previously reported the separation and determination of fluoride and chloride anions, which are retained weakly on the anion-exchange resin, by using acetylacetonate as the eluent [5]. This compound is very suitable for the above-mentioned purpose because of its relatively low driving strength and high selectivities of monovalent inorganic anions. However, it is desirable that the pH of the eluent should be relatively low in order to suppress the dissociation of impurity anions, such as carbonate and organic anions. For this purpose, the development of a new  $\beta$ -diketonate eluent having a low  $pK_a$  value and characteristics similar to those of acetylacetonate is needed.

From this standpoint, we investigated two low- $pK_a$   $\beta$ -diketonate eluents: trifluoroacetylacetonate and 1,3-cyclohexanedionate. It was found that 1,3-cyclohexanedionate is the preferred elu-

\* Corresponding author.

<sup>1</sup> Present address: Department of Chemistry, Faculty of Science, Kanazawa University, Kanazawa 920-11, Japan.

<sup>2</sup> Present address: Department of Ecosystem Studies, School of Environmental Science, The University of Shiga Prefecture, Hikone 522, Japan.

<sup>3</sup> Present address: Seian Women's High School, Kamigyo-ku, Kyoto 602, Japan.

<sup>4</sup> Present address: Hiroshima Jogakuin College, Higashi-ku, Hiroshima 732, Japan.

ent anion for the separation and determination of fluoride and chloride anions at relatively low pH in the anion-exchange column used.

## 2. Experimental

### 2.1. Apparatus

A Tosoh Model HLC-601 ion chromatograph system was used, consisting of a computer-controlled pump, a conductivity detector, a sample injector (100  $\mu$ l) and an oven. An anion-exchange column (50 mm  $\times$  4.6 mm I.D.) packed with Tosoh TSKgel IC-Anion-PW (polymethacrylate gel, capacity  $0.03 \pm 0.003$  mequiv./g) was used for the separation of anions. The flow-rate was maintained at 1.0 ml/min under a pressure of 40–60 kg/cm<sup>2</sup>. The separation column and the conductivity detector were placed in an oven regulated at 30°C. The data were recorded with a Shimadzu Chromatopack C-R1A instrument.

### 2.2. Eluents

Acetylacetone (2,4-pentanedione, Hacac;  $pK_a = 8.99$  [6]) was purified by a previously reported method [5,7]. A 100-ml portion of analytical-reagent grade acetylacetone was shaken with 10 ml of dilute ammonia (1 + 10) and shaken with two 10-ml portions of distilled water. This solution was distilled at 136°C.

Trifluoroacetylacetone (1,1,1-trifluoropentane-2,4-dione, H·TFA;  $pK_a = 6.09$  [8]) was purified by the method of Matsubara and Kuwamoto [9] to remove highly acidic impurities. A 10-ml portion of analytical-reagent grade trifluoroacetylacetone was refluxed in the presence of 1 g of disodium hydrogenphosphate and distilled at 107°C.

1,3-Cyclohexanedione (dihydroresorcinol, H·CHD;  $pK_a = 5.26$  [6]) was purified by dissolving analytical-reagent grade 1,3-cyclohexanedione in chloroform and recrystallizing the reagent by adding benzene.

$\beta$ -Diketone–sodium hydroxide solutions as eluents were prepared by dissolving the purified

$\beta$ -diketones in distilled water and adding 1 M sodium hydroxide solution to adjust the eluent pH.

Sodium benzoate ( $pK_a = 4.202$  [6]) and sodium acetate ( $pK_a = 4.757$  [6]) eluents were prepared by dissolving the analytical-reagent grade salts in distilled water. Trifluoroacetic acid ( $pK_a = 0.50$  [8]), resorcinol (*m*-dihydroxybenzene;  $pK_{a_1} = 9.44$ ,  $pK_{a_2} = 12.32$  [8]) and phenol ( $pK_a = 9.98$  [6]) were dissolved in distilled water and used as eluents; the pH of these solutions was adjusted with 1 M sodium hydroxide solution.

All of these eluent solutions were deaerated before use.

### 2.3. Standard sample solutions

Stock standard solutions of 100 mM sodium fluoride ( $pK_a = 3.17$  [6]), sodium chloride, sodium nitrite ( $pK_a = 3.15$  [6]), sodium bromide, sodium nitrate and sodium carbonate ( $pK_{a_1} = 6.35$ ,  $pK_{a_2} = 10.33$  [6]) were prepared by dissolving the analytical-reagent grade salts in water. Working standard solutions were obtained by diluting the stock standard solutions with distilled water.

For the investigation of the effect of counter cations in the sample, several solutions of metal chloride salts (the same as those used in the previous study [5]) were used.

## 3. Results and discussion

### 3.1. Selectivities of monovalent sample anions

Ion chromatography is used to separate many kinds of anions in common sample solutions. Therefore, the selectivities of the sample anions are very important factors for the selection of the eluent anion.

The low  $pK_a$  of TFA<sup>−</sup> originates from the change in the charge distribution in the  $\beta$ -diketone group caused by the substitution of fluorine atoms, which are electron-withdrawing, for the three hydrogen atoms of acac<sup>−</sup>. In contrast, the

low  $pK_a$  of CHD originates from the structural strain of the group caused by cyclization. These structural differences suggested possible differences in the anion selectivities between these two eluents.

Table 1 shows the selectivities of inorganic monovalent anions with several  $\beta$ -diketonates and other organic eluents. These values hardly changed by varying the eluent concentration and pH and, therefore, it is conceivable that these values reflect the characteristics of the eluent anions.

One of the merits of using an  $acac^-$  eluent is the relatively high selectivities of monovalent anions. The values were much better than for those obtained with a benzoate eluent. The selectivities were slightly worse than those observed using an acetate eluent, but the  $acac^-$  eluent is more effective because of the sensitivities [5]. Therefore, for practical use, it is desirable that the low- $pK_a$   $\beta$ -diketonate eluent has similar selectivities to the  $acac^-$  eluent.

From the decrease in the selectivities with a  $TFA^-$  eluent compared with an  $acac^-$ , which was similar to that with a trifluoroacetate eluent compared with an acetate, it was suggested that a design of a new eluent by fluorination is not suitable. On using  $CHD^-$  eluent, in contrast, the selectivities were almost the same as those with

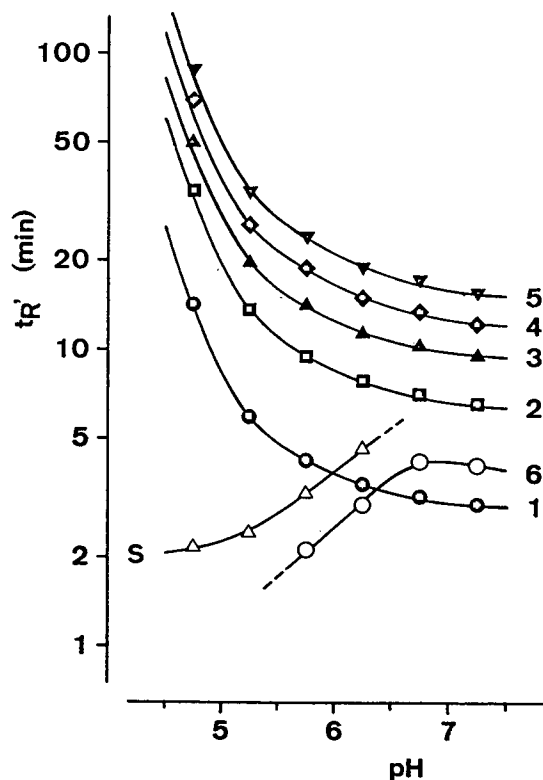


Fig. 1. Relationship between the retention times of anions and the eluent pH. Sample: 1 = fluoride; 2 = chloride; 3 = nitrite; 4 = bromide; 5 = nitrate; 6 = carbonate. S = second system peak. Eluent: 5.0 mM  $H \cdot CHD-NaOH$ .

Table 1  
Selectivities of monovalent anions

Eluent anion	Concentration (mM)	pH	A = $Cl^-$ , B = $F^-$	A = $NO_2^-$ , B = $Cl^-$	A = $Br^-$ , B = $NO_2^-$	A = $NO_3^-$ , B = $Br^-$
$acac^-$	5.0	9.00	2.33	1.45	1.32	1.28
$TFA^-$	5.0	6.09	1.79	1.29	1.23	1.19
$CHD^-$	5.0	5.26	2.32	1.46	1.32	1.30
Benzoate	2.5	6.80	1.81	1.30	1.26	1.20
Acetate	10.0	7.45	2.65	1.63	1.28	1.34
Trifluoroacetate	1.0	5.50	1.90	1.35	1.28	1.21
Resorcinolate	5.0	9.44	1.73	1.31	1.21	1.20
Phenolate	5.0	9.98	1.72	1.29	1.22	1.19

Selectivity:  $\alpha(A, B) = t'_R(A)/t'_R(B) [=k'(A)/k'(B)]$ .



acac<sup>-</sup> eluent and it was found that the design of a low-pH eluent by cyclization is very useful.

In addition, the use of a resorcinolate eluent resulted in very similar selectivities to those with a phenolate eluent rather than CHD<sup>-</sup>. It was also concluded that the characteristic of the  $\beta$ -diketonate as eluent anion is maintained by the existence of the keto-form structure.

From the above, we selected the CHD<sup>-</sup> anion as the preferred eluent for the separation and determination of fluoride, chloride and other monovalent anions in low-pH solutions.

### 3.2. Optimum chromatographic conditions

Fig. 1 shows the relationship between the retention times of sample anions and the eluent pH at a fixed eluent concentration (5.0 mM). With increasing eluent pH, the peaks of monovalent anions were eluted rapidly. However, at high pH, a second system peak [10], which corresponds to the peak of CHD<sup>-</sup> itself, or the peak of monovalent carbonate anion was overlapped with the peak of fluoride by increasing the ratios of charged carbonate species. On the other hand, with decreasing pH, the concentration of CHD<sup>-</sup> as an eluent anion was decreased and the retention times were increased.

Fig. 2 shows the relationship between the retention times and the concentration of H·CHD at a fixed eluent pH (5.26). With decreasing concentration, the retention time was increased. On the other hand, with increasing the concentration, the peak of the fluoride anion overlapped with second system peak.

For convenience, possible interactions between pH and concentration effects were assumed to be negligible; the optimum eluent pH and concentration of H·CHD were chosen as 5.26 and 5.0 mM, respectively. At this optimum condition, the detection limits ( $S/N = 2$ ) of fluoride and chloride were 1.2  $\mu\text{M}$  (23 ng/ml) and 0.8  $\mu\text{M}$  (29 ng/ml), respectively, which were slightly better than those on acac<sup>-</sup> eluent, 1.2  $\mu\text{M}$  (23 ng/ml) and 1.5  $\mu\text{M}$  (55 ng/ml) [5], respectively.

Fig. 3 shows the ion chromatograms of fluoride and chloride anions under the optimum

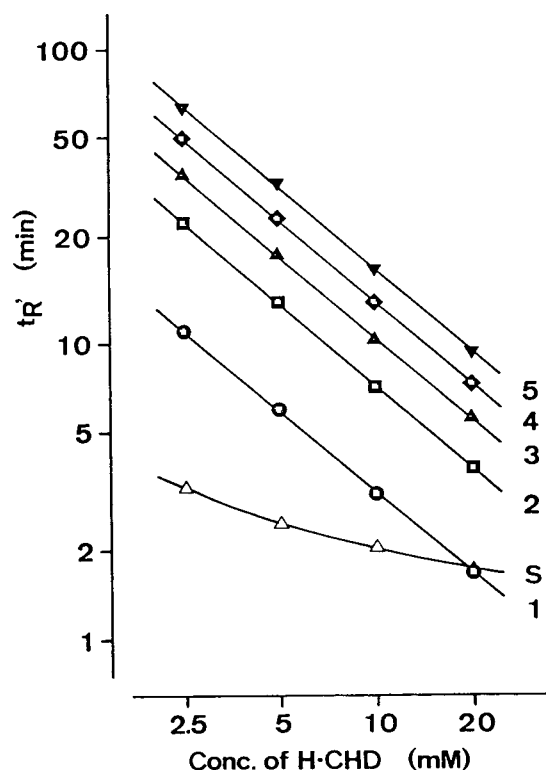


Fig. 2. Relationship between the retention times and the concentration of H·CHD. Sample: 1 = fluoride; 2 = chloride; 3 = nitrite; 4 = bromide; 5 = nitrate. S = second system peak. Eluent: H·CHD–NaOH (pH 5.26).

conditions with the acac<sup>-</sup> and CHD<sup>-</sup> eluents. These elution behaviours were very similar to each other.

### 3.3. Comparison of the influences of metal cations in the sample with acac<sup>-</sup> and CHD<sup>-</sup> eluents

It is well known that  $\beta$ -diketones form chelate compounds with many kinds of metal cations [11]. In a previous study [5], we investigated the elimination of the fluctuation of the baseline level in the chromatogram by metal cations in the sample by calculating the ratio of the deviation at the front of the peak of F<sup>-</sup> (0.5 mM) to the peak height. It was found that an acac<sup>-</sup>

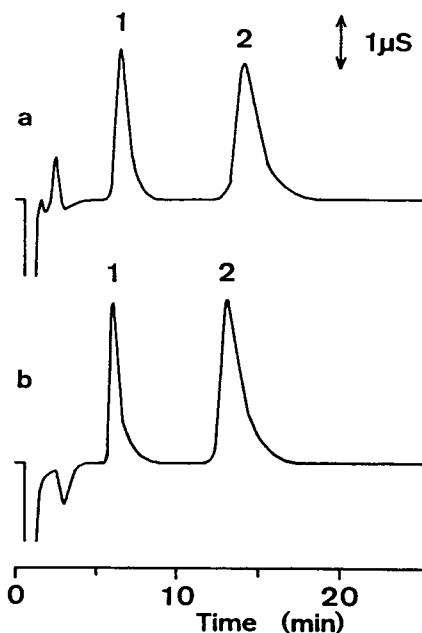


Fig. 3. Ion chromatograms with  $\beta$ -diketonate eluents. Sample: 1 = 0.5 mM (9.5  $\mu$ g/ml) fluoride; 2 = 0.5 mM (17.8  $\mu$ g/ml) chloride. Eluent: (a) 5.0 mM Hacac-NaOH (pH 9.00); (b) 5.0 mM H·CHD-NaOH (pH 5.26).

eluent has this eliminating ability except for the case when  $Mg^{2+}$  or  $Mn^{2+}$  is present.

CHD<sup>-</sup> does not have a chelating strength like acac<sup>-</sup> because of the structural strain in the  $\beta$ -diketonate group caused by the six-membered ring. Therefore, it is considered that the eliminating ability of a CHD<sup>-</sup> eluent is relatively low.

Table 2 shows the influences of fourteen metal cations in a sample on the baselines of the chromatograms using an acetate eluent [5], an acac<sup>-</sup> eluent [5] and a CHD<sup>-</sup> eluent. In general, the values of the deviation on CHD<sup>-</sup> were larger than those on acac<sup>-</sup>. However, the values were all less than 5% except for  $Zn^{2+}$ . In addition, the shapes of first and second system peaks were hardly changed by the co-existence of the metal cations. From this result, it was considered that a CHD<sup>-</sup> eluent can eliminate sufficiently the fluctuation of the baseline level by metal cations, in spite of its relatively weak masking ability. Further, it is remarkable that the values of the deviation for  $Mg^{2+}$  and  $Mn^{2+}$  with the CHD<sup>-</sup> eluent were much smaller than those with the acac<sup>-</sup> eluent.

Table 2

Comparison of the deviation of the baseline on the chromatogram caused by metal cations in the sample with  $\beta$ -diketonate eluents

Cation	Deviation: ratio to peak height of 0.5 mM F <sup>-</sup> (%), <i>n</i> = 3		
	5.0 mM NaOAc <sup>a</sup> (pH 7.70) [5]	5.0 mM Hacac-NaOH (pH 9.00) [5]	5.0 mM H·CHD-NaOH (pH 5.26)
Li <sup>+</sup>	-0.8	0.0	0.0
Na <sup>+</sup>	-0.8	0.0	0.0
Mg <sup>2+</sup>	-4.9	-6.8	0.0
Al <sup>3+</sup>	-0.8	0.0	+0.2
K <sup>+</sup>	-0.8	0.0	0.0
Ca <sup>2+</sup>	-20.3	0.0	+2.8
Cr <sup>3+</sup>	+4.1	0.0	-1.4
Mn <sup>2+</sup>	-13.8	-13.9	+2.2
Fe <sup>2+</sup>	-7.3	0.0	+0.6
Fe <sup>3+</sup>	-7.3	+0.3	0.0
Co <sup>2+</sup>	-17.1	-0.7	+3.0
Ni <sup>2+</sup>	-3.3	-0.7	+4.6
Cu <sup>2+</sup>	0.0	0.0	-0.5
Zn <sup>2+</sup>	-9.8	-1.1	+5.5

Sample: 0.5 mM (9.5  $\mu$ g/ml) fluoride and 0.5 mM (17.8  $\mu$ g/ml) chloride [or 0.25 mM (24.0  $\mu$ g/ml) sulfate]. Cation: 0.5 mM Na<sup>+</sup> and 0.5 mequiv./l metal cation.

<sup>a</sup> Sodium acetate.

#### 4. Conclusions

We investigated the use of a  $\text{CHD}^-$  eluent at relatively low pH for the separation and determination of fluoride and chloride, which are retained very weakly on an anion-exchange resin. A  $\text{CHD}^-$  eluent has very similar characteristics to an  $\text{acac}^-$  eluent. Fluoride and chloride were measured with high sensitivities by using this eluent. Further, the  $\text{CHD}^-$  eluent reduces fluctuations in the baseline of the chromatograms caused by metal cations in the sample.

#### References

- [1] D.T. Gjerde, J.S. Fritz and G. Schmuckler, *J. Chromatogr.*, 186 (1979) 509.
- [2] D.T. Gjerde, G. Schmuckler and J.S. Fritz, *J. Chromatogr.*, 187 (1980) 35.
- [3] J.G. Tarter (Editor), *Ion Chromatography*, Marcel Dekker, New York, 1987.
- [4] D.T. Gjerde and J.S. Fritz, *Ion Chromatography*, Hüthig, Heidelberg, 2nd ed., 1987.
- [5] N. Hirayama, M. Maruo, A. Shiota and T. Kuwamoto, *J. Chromatogr.*, 523 (1990) 257.
- [6] S. Kotrlý and L. Šůcha, *Handbook of Chemical Equilibria in Analytical Chemistry*, Ellis Horwood, Chichester, 1985.
- [7] J.F. Steinbach and H. Freiser, *Anal. Chem.*, 25 (1953) 881.
- [8] J.A. Dean (Editor), *Lange's Handbook of Chemistry*, McGraw-Hill, New York, 13th ed., 1985.
- [9] N. Matsubara and T. Kuwamoto, *Anal. Chim. Acta*, 161 (1984) 101.
- [10] T. Okada and T. Kuwamoto, *Anal. Chem.*, 56 (1984) 2073.
- [11] R.C. Mehrotra, R. Bohra and D.P. Gaur, *Metal  $\beta$ -Diketonates and Allied Derivatives*, Academic Press, London, 1978.

Short communication

# Use of a trio of modified cyclodextrin gas chromatographic phases to provide structural information on some constituents of volatile oils

T.J. Betts

*School of Pharmacy, Curtin University of Technology, GPO Box U1987, Perth, Western Australia 6001, Australia*

First received 22 November 1994; revised manuscript received 1 March 1995; accepted 8 March 1995

## Abstract

A trio of modified cyclodextrin (CD) gas chromatographic phases has been selected to provide structural information on some of the diverse constituents of volatile oils. Trifluoroacetyl-CDs were found to be unstable phases, which probably hydrolyse during use. A stable ester phase chosen is the propionyl-dipentyl-CD, used with an unesterified dipentyl-CD and a hydroxypropyl-dimethyl-CD, picking examples from the three CD ring sizes. They are used in three comparative pairs, when percentage increases in retention times relative to *n*-undecane clearly indicate solute structure such as bicyclic monoterpene, oxygenated aromatic, or non-carbonyl monocyclic. An acyclic monoterpene may not be distinguishable from certain carbonyl monocyclics.

## 1. Introduction

Various modified cyclodextrin (CD) gas-chromatographic phases have previously been used to study how comparative results might indicate the chemical structure of some solutes found in volatile oils [1–4] and hence be of use for unknowns. These may be cyclic or acyclic terpenes, or aromatics. In continuing this work with some hydroxypropyl-(dimethyl)-CDs, when new results were compared with those previously obtained with some esterified-(dipentyl)-CDs, anomalies became apparent. These are reported below. In attempting to select an optimum trio of modified CD phases to obtain structural information, a stable ester-CD is required, along with two other different modifications using the three CD-ring sizes ( $\alpha$ ,  $\beta$  and  $\gamma$ , with six, seven and eight cyclic  $\alpha$ -glucose units, respectively).

The value of such a trio is reported here. The introduction of such CDs as chirally selective phases has been described previously [2], although no work of this type was involved here.

## 2. Experimental

### 2.1. Apparatus

A Hewlett-Packard 5790A gas chromatograph was used, fitted with a capillary control unit and a splitter injection port. The latter, and the flame ionisation detector, were both operated at 215°C.

The various “Chiraldex” modified CD capillaries were obtained from Advanced Separation Technologies (Whippany, NJ, USA) and were all 10 m  $\times$  0.25 mm I.D. with film thickness of

0.125  $\mu\text{m} \pm 10\%$ . Prefixes A, B and G refer to  $\alpha$ ,  $\beta$  and  $\gamma$ -CD, respectively. Suffix PH refers to 2-(*S*)-hydroxypropyl-dimethyl-CDs, DA refers to dipentyl-(3-hydroxyl remaining)-CDs, TA refers to dipentyl-3-trifluoroacetyl-CDs and PN to dipentyl-3-propionyl-CD, which is only available as G-PN. B-PH and B-TA capillaries used here were kindly donated. The others were purchased. All were used at 125°C.

Helium was used as the mobile phase at a flow-rate of ca. 0.9 ml min<sup>-1</sup>, except for B-DA where a faster rate of ca. 1.5 ml min<sup>-1</sup> was used to produce narrower peaks from some solutes.

## 2.2. Methods

The 31 solutes studied are given in Table 1. They represent some of the various constituents found in natural volatile oils. Trace residues from an “emptied” syringe were injected. For the larger ring size CDs, unlike conventional phases, excessive amounts normally cause a typical reduction in retention time. Hold-up times, obtained by extrapolating to the retention times of *n*-heptane and *n*-hexane that of methane on semi-logarithmic graph paper, were deducted from observed retention times. Retention times relative to *n*-undecane were used, and percentage increases in these values on changing CD-phases.

## 3. Results and discussion

New observations (averages of two or more) at 125°C are reported in Table 1 from ChiralDEX B-PH, A-PH and, in part, from B-DA (columns 3, 5 and 8, respectively). They are compared in various pairs, and with G-PN values [3], in columns 4, 6, 7 and 9. Results are usually lowest on B-DA (of the three ChiralDEX phases for which relative retention times are given in Table 1) and always highest on B-PH. Only one-third of the 31 solutes in Table 1 remain in the same descending order of values listed for B-PH, these being particularly non-alcoholic monocyclic monoterpenes. This implies a phase sensitivity to the various other molecular types of solutes.

Comparison of the relative retention times for ChiralDEX B-PH vs. A-PH (column 4, Table 1) should indicate the influence of increasing the ring size of a hydroxypropyl-dimethyl-CD by one glucose unit. Most bicyclic solutes (not 3-carene) show a large increase of 62% or more. In contrast, four of six aromatic solutes (with low polarity) show less than 6% increase, with some having a small decrease – however, this group is “contaminated” by myrcene. Interestingly, all three monocyclic terpenols appear to fall in a narrow group with increases in relative retention times of 40–49%. Previously the B-DA and A-DA phases were compared [1]. Again, the highest increases (74–125%) were found for five bicyclic solutes, with two monocyclic terpenols also falling in this range.

When the results for B-PH were compared with a second set of observations on B-TA, it became apparent that the latter esterified phase had decomposed over a nine-month period. Values of the solute relative retention times had altered to 66–179% of those originally observed [3], with none remaining very close to its initial value. When these repeat results for B-TA were compared with values for B-DA (column 8, Table 1) they were found to be very similar (–4 to +12%), suggesting that the trifluoroacetyl (dipentyl) TA phase had hydrolysed to the hydroxy (dipentyl) phase, equivalent to B-DA. Thus values given previously in Ref. [3] only apply to a relatively new B-TA column. On checking the *c* ratio of  $3(t_{\text{R}} \text{ cuminal})/4(t_{\text{R}} \text{ caryophyllene})$  [5] for B-TA, it was found to have decreased from the original 0.61 down to 0.32, which is practically identical to the *c* ratio of B-DA, itself [3]. The solute overloading responses of B-DA and (hydrolysed) B-TA were also the same—a reduced retention time for most solutes, except for some aromatics—which further confirmed the hydrolysis of B-TA. On B-DA, all aromatic solutes gave varying relative retention times which can only be expressed to one decimal, although their peaks are sharp. This phase gave repeat values deviating no more than +4% from those previously found [3], and was obviously stable.

The instability of B-TA provoked re-examina-



Piperitone	Mco	8.77	15	44	7.60	6	53	4.96	45
4-Terpineol	Mol	7.36			5.10	16		5.26	
Camphor	Bco	6.98			3.24	-46	-3	4.01	-17
Pulegone	Mco	6.63	9	115	6.11	21	-19	3.83	51
Estragole	Aet	5.53	-4		5.76			3.0 <sup>c</sup>	32
Linalol	Nol	4.09	24		3.31	1	47	2.26	7
Menthone	Mco	3.92	24		3.16		37	2.80	11
Thujone <sup>d</sup>	Bco	3.59			2.22	-22	-17	2.69	6
Citronellal	Nco	3.42	14	62	3.01	22		2.26	9
Fenchone	Bco	3.14		68	1.87	-28	-7	2.02	28
Cineole	Bet	1.80		82	0.99	-29	-31	1.43 <sup>c</sup>	
$\gamma$ -Terpinene	Mhc	1.39	8		1.29	13	8	1.19 <sup>c</sup>	
<i>p</i> -Cymene	Ahc	1.26	3		1.22	17		0.95 <sup>c</sup>	9
Limonene	Mhc	1.20	16		1.03	4	-6	1.10 <sup>c</sup>	
Camphene	Bhc	1.15		113	0.54	-34	-40	0.90 <sup>c</sup>	
3-Carene <sup>d</sup>	Bhc	1.11	37		0.81	-11	-21	1.02 <sup>c</sup>	
$\alpha$ -Terpinene	Mhc	1.09	17		0.93	7	6	0.88 <sup>c</sup>	
$\alpha$ -Pinene	Bhc	0.80		82	0.44	-31	-33	0.66 <sup>c</sup>	
Myrcene <sup>d</sup>	Nhc	0.74	4		0.71	6		0.58 <sup>c</sup>	16

<sup>a</sup> Chemical type of solute. A = aromatic; B = bicyclic monoterpene; M = monocyclic; N = acyclic; co = carbonyl; et = ether; hc = hydrocarbon; ol = alcohol.

<sup>b</sup> Previously unpublished relative retention times on Chiraldex G-PN. Other values used are from Ref. [2]. Cinnamal 10.75; safrole 7.68; anethole 6.88.

<sup>c</sup> Newly determined values, not in Ref. [3]. Most aromatics give variable results, and are only averaged to one decimal.

<sup>d</sup> Impure solutes. Main peak used.

tion of the other two trifluoroacetyl (dipentyl) cyclodextrins, A-TA and G-TA. The *c* ratio of A-TA had also fallen, from an originally calculated 0.78 down to 0.59, a value below that of A-DA [2]. Reconsideration of earlier results revealed that 23 of 29 solutes had yielded relative retention times on A-DA which were within  $\pm 5\%$  of those found on (already hydrolysed?) A-TA. The greatest difference was only +13%, so that these phases were behaving very similarly and previous A-TA results should be deleted [2–4]. The *c* ratio of G-TA had also fallen, from an initial 0.53 down to about 0.2, below that of G-DA. On G-TA, after six months, eight of 21 solutes showed large changes in relative retention times, including increases by alcohols. This strongly suggested that the G-TA phase had also hydrolysed back to the alcohol, and confirmed that all three trifluoroacetyl-CD phases are inconsistent in behaviour and unreliable. In contrast, the propionyl ester phase G-PN had a constant *c* ratio of 0.40, and a dozen solutes gave values remaining at 98–104% of those determined nine months previously [4]—this ester had not hydrolysed. It was thus selected as one of a set of three modified CD phases which could provide structural information about solutes, being only available in the largest  $\gamma$ -CD form. To obtain maximum potential from such work, a diversity of CD-derivatives with the three ring-sizes is desirable, and B-DA and A-PH were chosen to give three pairings of optimum value.

An informative pairing of relative retention times is A-PH vs. G-PN in column 6 of Table 1. All 9 bicyclic monoterpenes, with or without oxygen, showed decreases from –11 to –46%, an exclusive set of values. Another valuable pairing is A-PH vs. B-DA (column 7), where six non-carbonyl monocyclics show very little change, and form an exclusive group of –6 to +8% increase. Bicyclics are identified again, exclusively, by considerable decreases (–40 to –7%); and oxygenated aromatics by big increases (209–62%), the only exception being geraniol. The final pairing possible of the three selected modified CDs is G-PN vs. B-DA, which gives no specific groupings in column 9. They all include more than one type of solute. The six

different acyclic monoterpenes are now all grouped together with 2–20% increase in relative time; however, this range also includes some other solute types.

In summary if G-PN vs. B-DA is used first to characterise an unknown solute, an increase greater than 23% could be due to an oxygenated aromatic or a polar bicyclic terpenoid, and such compounds are well distinguished by the other two CD-phase combinations. If not either of these, then the unknown should be a carbonyl-monocyclic monoterpene (See Fig. 1). If there is a negative increase (decrease) using G-PN vs. B-DA, the unknown could be a low-polarity bicyclic or non-carbonyl monocyclic monoterpene. (Monocyclic alcohols could be identified using B-PH vs. A-PH). These substances might also be differentiated by both other phase combinations although they are in adjacent groups. Finally, if the unknown gives a low increase in relative retention time—up to only 23%—it could be an acyclic substance, or possibly an aromatic or carbonyl-cyclic monoterpene. The A-PH vs. B-DA phase combination should then distinguish the aromatics (plus geraniol, unfortunately) and carbonyl bicyclics leaving the acyclics confused only by carbonyl monocyclics and *p*-cymene. An acyclic alcohol can then be confirmed using A-PH vs. G-PN. This procedure is outlined in Fig. 1, and provides good identification of aromatic solutes, and for bicyclic and non-carbonyl monocyclic monoterpenes. The method may also distinguish acyclics from carbonyl-monocyclics, although the latter were previously found to present a problem.

Examples of the use of this method are obtained by re-examining some volatile oils previously studied. Sweet fennel oil has a minor constituent just ahead of the main *trans*-anethole peak [6]. The G-PN vs. B-DA increase for this component is 35%, so that it might be an oxygenated aromatic. The A-PH vs. B-DA increase is 87%, so it clearly belongs to this chemical solute group and it was identified by a mass spectrometry (MS) as *cis*-anethole. The 39% A-PH vs. G-PN increase further complies with an aromatic structure. Dill oil has a minor constituent ahead of the main carvone peak [2].



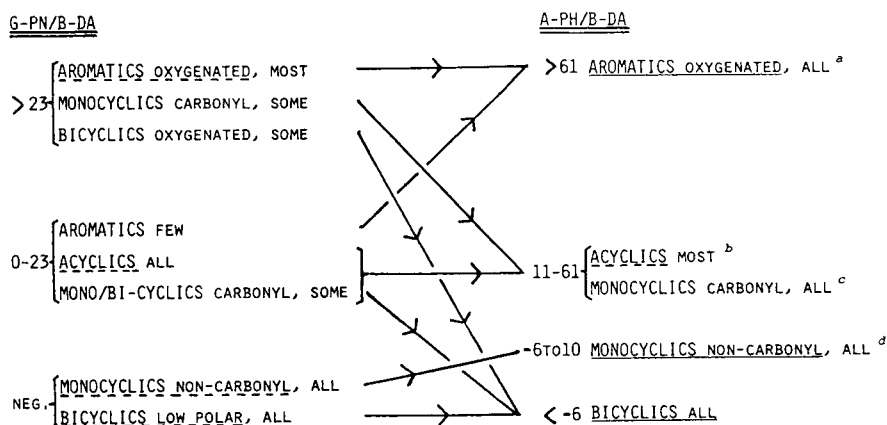


Fig. 1. Solute groupings found for various relative retention time (*n*-undecane = 1.00) percentage increases on changing from ChiralDEX B-DA to the other phase indicated (G-PN or A-PH). <sup>a</sup>Together with acyclic geraniol. <sup>b</sup>Together with aromatic hydrocarbon *p*-cymene. Acyclic alcohols give over 35% increase A-PH/G-PN. <sup>c</sup>Some carbonyl monocyclics have been in a different group before. <sup>d</sup>Monocyclic alcohols can be detected using ChiralDEX B-PH/A-PH, where they give 40–50% increase.

The G-PN vs. B-DA increase for this is 46%, so it could also be an oxygenated aromatic and cannot be acyclic. However, the A-PH vs B-DA increase is only 51% which shows that it cannot be aromatic, and must be a carbonyl monocyclic. The only 4% A-PH vs. G-PN increase agrees with this and MS identified it as dihydrocarvone. Note that it cannot be a carveol with these values. Another slightly bigger peak constitutes ca. 3% of the dill oil. G-PN vs. B-DA gave –5%, as did A-PH vs. B-DA. This indicates (just) a non-carbonyl monocyclic or possibly a low-polarity bicyclic. MS identified it as anethofuran, a bicyclic, non-carbonyl ether terpenoid. Interestingly, this substance eluted after dihydrocarvone from B-DA, unlike the results found for the other two phases. B-DA yields broader peaks for carbonyl compounds than the other phases, suggesting a special interaction.

Some other aromatic volatile oil constituents like eugenol and thymol (phenols), have excessively long retention times at 125°C. They can be studied at 150°C, and still fall in the A-PH vs. B-DA group of greater than 61% increase.

These two compounds give values of over 190% and 165%, respectively, whereas, in contrast, the bicyclic hydrocarbon sesquiterpene caryophyllene gives a decrease of more than –40%.

### Acknowledgements

Some of the ChiralDEX capillaries used in this work were kindly donated by ASTEC. Initial observations on the B-PH phase were made by Siobhan C.L. Andrews, R. Digirolamo and N.M. Norris, and led to the re-evaluation of B-TA.

### References

- [1] T.J. Betts, J. Chromatogr., 639 (1993) 366.
- [2] T.J. Betts, J. Chromatogr. A, 653 (1993) 167
- [3] T.J. Betts, J. Chromatogr. A, 672 (1994) 254.
- [4] T.J. Betts, J. Chromatogr. A, 678 (1994) 370.
- [5] T.J. Betts, J. Chromatogr., 628 (1993) 138.
- [6] T.J. Betts, J. Chromatogr., 626 (1992) 294.



ELSEVIER

Journal of Chromatography A, 707 (1995) 396-400

JOURNAL OF  
CHROMATOGRAPHY A

Short communication

## Analysis of recombinant human growth hormone and its related impurities by capillary electrophoresis

Patrice Dupin, François Galinou, Alain Bayol\*

Sanofi Recherche, Centre de Labège, Labège Innopole Voie 1, B.P. 137, 31676 Labège Cedex France

First received 30 September 1994; revised manuscript received 24 February 1995; accepted 6 March 1995

### Abstract

A convenient free solution capillary electrophoretic method is described for the simultaneous quantitation of human growth hormone (hGH) and its related impurities in pharmaceutical preparations. The separation of the cleaved form, the monodeamidated form and two new compounds which may arise from post-translational modifications in *Escherichia coli*—a succinylated hGH with a blocked amino terminus and a modified hGH having a His to Gln replacement at sequence position 18—is described. The proposed capillary electrophoretic method shows good specificity, linearity and precision. A limit of detection of 0.03% was calculated for the impurities.

### 1. Introduction

Human growth hormone (hGH) is one of the first generation pharmaceutical products made by rDNA technology. Recognition of most of the degradation impurities comes from the study of the native hGH. Deamidated forms, oligomeric aggregates, cleaved and oxidized forms are the major related proteins found in the native [1-3] as well as in the recombinant hGH [4,5].

The assessment of the absence of such impurities by a set of analytical methods is now well established [6]. However, these methods are often not capable to detect traces of new impurities which may arise from the recombinant product during processing. We have found two new isoforms of the recombinant growth hormone expressed in *Escherichia coli*. The first one is a succinylated hGH with a blocked amino

terminus. In the pituitary, on the other hand, only an acetylated form of hGH has been described [7]. The second isoform is growth hormone with a His to Gln replacement at position 18. This variant may originate from an amino acid substitution during translation. Such a variant was also found in the human granulocyte colony stimulating factor produced in *E. coli* [8]. The development of a new analytical method was necessary to demonstrate that these impurities were eliminated during the purification of the hormone.

High-performance capillary electrophoresis (HPCE) had been proved highly efficient for the analysis of complex mixtures, especially in aqueous media, and in recent years some attempts have been made to promote its use in the quality control of pharmaceutical proteins [9,10]. This paper describes the validation of a free solution capillary electrophoretic (FSCE) method for the assessment of the purity of biosynthetic hGH.

\* Corresponding author.

Some reports have described the separation by FSCE of the two deamidated forms originating from the two deamidation sites at Asn 149 and Asn 152 [11,12]; this separation can be performed in a few minutes due to the net charge differences between the proteins. In the present paper, the conditions of the separation were obtained after optimization of the free solution (manuscript in preparation). The validation criteria used were very similar to those applicable to the validation of an HPLC method.

## 2. Experimental

### 2.1. Reagents

All common reagents were of analytical grade. Diammonium hydrogenphosphate was purchased from Riedel-de-Haën (Hannover, Germany) and phosphoric acid from Prolabo (Paris, France). Water, HPLC grade, was obtained from Rathburn (Walkerburn, UK), Acetonitrile was from J.T. Baker (Deventer, Netherlands) and trifluoroacetic acid from SDS (Peypin, France). Recombinant human growth hormone (re-hGH) and related impurities were obtained from Sanofi (Labège, France).

An artificial mixture was made with re-hGH in 50 mM ammonium carbonate (pH 8.3) spiked with small amounts of impurities. The total protein content of this artificial mixture, determined with reversed-phase chromatographic reference method, was 12.8 mg/ml. All FCZE solutions were diluted with water.

### 2.2. High-performance capillary electrophoretic apparatus and conditions

All analyses were carried out on a Model 270 A (Applied Biosystems, San Jose, CA, USA) analytical capillary electrophoretic system used in the normal polarity mode (anode on the injection side). The separations were monitored on-column by measuring the UV absorption at 195 nm. The capillary was thermostated at 30°C. The electrophoregrams were acquired and stored

on a Model C-R4A data collection system (Shimadzu, Kyoto, Japan).

Untreated fused-silica capillaries (50  $\mu\text{m}$  I.D.) were obtained from Applied Biosystems and cut to a total length of 92 cm with the detection window placed at 70 cm.

The running buffer was a solution of 0.1 M diammonium hydrogenphosphate, adjusted to pH 6.0 with phosphoric acid. The solution was filtrated through a disposable filter from Nalge (Rochester, USA) prior to use.

Each new capillary was conditioned by rinsing with 1 M sodium hydroxide for 20 min, then by washing with water for 10 min and filling with the running buffer during 20 min.

Each day, before starting the analysis, the capillary was first purged with 1 M sodium hydroxide for 10 min, followed by water for 10 min. Afterwards it was filled with the running buffer for 20 min. No rinsing sequences were performed between two runs.

Samples were introduced hydrodynamically (vacuum: 12.7 cmHg) with the following sequence: sample injection (3 s), separation buffer injection (1 s) and then analysis with an applied voltage of 20 kV.

### 2.3. Quantitation conditions

All peak areas were normalized with corresponding migration times [13].

According to the high/low sample loading described by Altria [14], each solution to be analyzed was diluted to concentrations of 0.6 mg/ml (low sample loading) and 4.5 mg/ml (high sample loading) prior to injection. The low sample loading was selected to give a main peak which was within the linear range of the detector.

The area of the main peak in the off-scale separation of the high sample loading was estimated by multiplying the main peak area obtained in the on-scale separation of the low sample loading by the factor of the increase in sample loading.

This calculated main peak area was used in the calculation of impurity level as % area/area in the high concentration sample.

The contents of hGH in the solutions to be analyzed were calculated on the nominal electrophoregram (0.6 mg/ml) with reference to an external working standard and corrected for the dilution.

#### 2.4. Reversed-phase chromatography reference method

A 100- $\mu$ g amount of protein sample was applied to a  $C_{18}$ , 300 Å, 250  $\times$  4.6 mm I.D. column (Symchrom, Lafayette, IN, USA) and eluted with a mixture of solvent A (0.1% trifluoroacetic acid in water) and solvent B (0.08% trifluoroacetic acid in acetonitrile) using a linear 25–70% gradient of solvent B over 35 min at a flow-rate of 1 ml/min. Elution was monitored at 220 nm. The accuracy of the protein content expressed in mg ml<sup>-1</sup> was 5%.

### 3. Results and discussion

#### 3.1. Specificity

Fig. 1 shows a typical electrophoregram of an artificial mixture of human growth hormone and its related products. The separation of the deamidated forms and the Gln 18-hGH is remarkable as these compounds differ by only 0.05 pI unit and because there is no calculated charge difference between Gln 18-hGH and hGH (Genetic Computer group, software: Wisconsin package version 8). For these two proteins the separation could probably be correlated to their tertiary structure and the ability of the mutational residue Gln 18 to interact with the eluting solvent and (or) the capillary wall.

The crystal structure of the hGH [15] and the ability of Zn<sup>2+</sup> ions to promote the formation of an hGH dimer in which His 18, His 21 and Glu 174 participate in coordinating the Zn<sup>2+</sup> suggest that the residue in position 18 is effectively pointing out of the structure and therefore could affect the migration.

Moreover, we obtained two peaks for the deamidated forms, as expected from the deami-

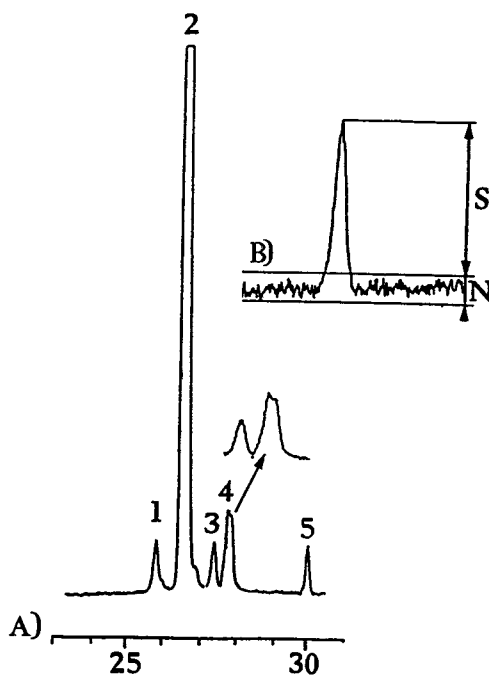


Fig. 1. (A) Typical electrophoregram of an artificial mixture of hGH and its related products. Peaks: 1 = cleaved hGH; 2 = hGH; 3 = Gln 18-hGH; 4 = deamidated-hGH; 5 = N-succinylated hGH. (B) Determination of the detection limit for the N-succinylated hGH obtained with a concentration of 5.2  $\mu$ g/ml (N = 70 mm gave LOD = 1.45  $\mu$ g/ml; S = 13 mm gave LOQ = 4.8  $\mu$ g/ml).

dation mechanism of the protein. If there are interactions between the impurities and the capillary wall—no mobile phase additives were used—they do not affect the migration order according to the isoelectric points measured by isoelectrofocusing on an immobiline gel (Table 1).

Table 1  
Isoelectric points of hGH and its related impurities

Protein	Isoelectric point
Cleaved hGH	5.25
hGH	5.2
Gln18-hGH	5.1
Deamidated-hGH	5.05
Succinylated-hGH	4.9

### 3.2. Repeatability

The repeatability of the peak areas was calculated from the results of seven determinations which were carried out by the same analyst under the same conditions at the nominal concentration. The relative standard deviations (R.S.D.) obtained are shown in Table 2. Acceptable levels of precision for the injection were obtained for the main hGH peak: 1.9%.

### 3.3. Linearity and detection limit

The linear range for hGH was demonstrated from 0 to 1.17 mg/ml. Three replicate injections for each concentration were performed. The correlation between peak area and the concentration of hGH is excellent ( $r^2 = 0.9984$ ) and the regression line obtained passes through the origin (confidence interval of the  $y$ -axis at the origin:  $-953.3$  to  $494.1$  in area units).

In Fig. 1 a signal-to-noise ratio of greater than 3 is shown for the succinylated form, given as an example, at a concentration of  $5.2 \mu\text{g/ml}$ . Finally, a limit of detection of  $1.45 \mu\text{g/ml}$  and a limit of quantitation of  $4.8 \mu\text{g/ml}$  were calculated for this impurity. The detection and quantitation limits were of the same order as for the other

impurities (detection limit 0.25% for a  $0.6 \text{ mg/ml}$  solution of hGH). To improve this detection limit to 0.03% we have used a more concentrated solution ( $4.5 \text{ mg/ml}$ ) in this study (high sample loading).

### 3.4. Quantitation

The precision of the determination of the related impurities and of the hGH protein itself was calculated for the artificial mixture from the results of six determinations carried out over 4 days. All the results obtained (Table 3) show good levels of performance in terms of precision. They illustrate the gain in performance when employing high/low sample loading as described by Altria [14].

It is interesting to compare the hGH content determined for the artificial mixture and corrected for the dilution ( $11.8 \text{ mg/ml}$ ) with the one obtained with the gradient reversed-phase HPLC reference method ( $12.8 \pm 0.6 \text{ mg/ml}$ ). Indeed, if we correct the FCZE value for the content of impurities, which are not separated in the HPLC method, we calculate a value of  $12.5 \text{ mg/ml}$ , which is in good agreement with the value determined with reversed-phase chromatography.

Table 2  
Repeatability of the peak areas

Areas	hGH	Cleaved hGH	Gln 18-hGH	Deam.-hGH	Succ.-hGH
	45835.8	1276.8	992.4	2362.0	645.0
	45006.2	1417.0	1122.1	2530.0	720.9
	45130.5	1278.9	1026.3	2321.9	620.3
	47423.7	1394.6	1163.4	2775.7	735.2
	45982.3	1190.7	929.7	2255.5	632.9
	46898.3	1452.7	1201.1	2330.1	805.1
	46450.4	1315.9	1004.2	2398.3	765.4
Average	46103.9	1332.1	1062.7	2424.8	703.7
Standard deviation	888.1	92.9	100.1	176.6	71.5
R.S.D. (%)	1.9	7.0	9.4	7.3	10.2

Table 3  
Quantitative determinations

Day	hGH (mg/ml)	Cleaved hGH (%)	Gln 18-hGH (%)	Deam.-hGH (%)	Succ.-hGH (%)
1	0.57	1.44	0.99	2.36	0.67
2	0.57	1.52	0.99	2.50	0.63
	0.59	1.73	1.09	2.83	0.67
3	0.59	1.63	0.99	2.59	0.64
	0.60	1.80	1.04	2.62	0.67
4	0.58	1.68	1.01	2.49	0.61
Average	0.58	1.63	1.01	2.56	0.65
Standard deviation	0.01	0.13	0.04	0.16	0.03
R.S.D. (%)	2.1	8.2	4.0	6.2	4.0

#### 4. Conclusions

The validation of the proposed capillary electrophoretic method showed good performance in terms of specificity, linearity and precision.

The results obtained showed that capillary electrophoresis is a convenient, alternative method to HPLC. The ruggedness of this method has now to be demonstrated by an interlaboratory collaborative study.

#### Acknowledgements

We thank M. Laforge for technical assistance in carrying out experiments and J.M. Bras for the determination of the isoelectric points.

#### References

- [1] J. Lewis, E.V. Cheever, W.C. Hopkins, *Bioch. Bioph. Acta*, 214 (1970) 498.
- [2] J. Lewis, *Ann. Rev. Physiol.*, 46 (1984) 33.
- [3] C.H. Li, in *Hormonal proteins and peptides*, Academic Press, NY, 3rd ed., 1975, p. 1.
- [4] W. Becker, R.R. Bowsher, W.C. MacKellar, M.L. Poor, P.M. Tackitt and R.M. Riggan, *Biotechnol. Appl. Biochem.*, 9 (1987) 478.
- [5] W. Becker, P.M. Tackitt, W.W. Bromer, D.S. Lefebvre and R.M. Riggan, *Biotechnol. Appl. Biochem.*, 10 (1988) 478.
- [6] F. Bristow, S.L. Jeffcoate, *Biologicals*, 20 (1992) 221.
- [7] J. Lewis, R.N.P. Singh, L.F. Bonewald, L.J. Lewis and W.P. Vanderlaan, *Endocrinology*, 104 (1979) 1256.
- [8] S. Lu, P.R. Fausset, L.S. Sotos, C.L. Closton, M.F. Rohde, K.S. Stoney and A.C. Herman, *Prot. Expr. Purif.*, 4 (1993) 465.
- [9] A. Guzman, J. Moschera, K. Iqbal and A.W. Malick, *J. Chromatogr.*, 608 (1992) 197.
- [10] R. Rabel and J.F. Stobauch, *Pharm. Res.*, 10 (1993) 171.
- [11] J. Frenz, S.L. Wu and W. Hancock, *J. Chromatogr.*, 480 (1989) 379.
- [12] R.G. Nielsen, G.S. Sittampalam and E.C. Rickard, *Anal. Biochem.*, 177 (1989) 20.
- [13] K.D. Altria, *Chromatographia*, 35 (1993) 177.
- [14] K.D. Altria, *Chromatographia*, 35 (1993) 493.
- [15] M.H. Ultsch, W. Somers, A.A. Kossiakoff and A.M. de Vos, *J. Mol. Biol.*, 236 (1994) 286.
- [16] B.C. Cunningham, M.G. Mulckerrin and J.A. Wells, *Science*, 25 (1991) 545.

# Author Index Vol. 707

- Abdul-Latif, P., see Bonwick, G.A. 707(1995)293  
 Abuaf, P.A., see Goodlett, D.R. 707(1995)233  
 Albanis, T.A. and Hela, D.G.  
 Multi-residue pesticide analysis in environmental water samples using solid-phase extraction discs and gas chromatography with flame thermionic and mass-selective detection 707(1995)283  
 Aoki, F., see Ôi, N. 707(1995)380  
 Aramendia, M.A., García, I., Lafont, F. and Marinas, J.M.  
 Determination of isoflavones using capillary electrophoresis in combination with electrospray mass spectrometry 707(1995)327  
 Armitage, R., see Bonwick, G.A. 707(1995)293  
 Ashton, D.S., Beddell, C., Ray, A.D. and Valkó, K.  
 Quantitative structure-retention relationships of acyclovir esters using immobilised albumin high-performance liquid chromatography and reversed-phase high-performance liquid chromatography 707(1995)367  
 Athalye, A.M., see Lightfoot, E.N. 707(1995)45  
 Basak, S.K., Velayudhan, A., Kohlmann, K. and Ladisch, M.R.  
 Electrochromatographic separation of proteins 707(1995)69  
 Baugh, P.J., see Bonwick, G.A. 707(1995)293  
 Baummy, Ph., Morin, Ph., Dreux, M., Viaud, M.C., Boye, S. and Guillaumet, G.  
 Determination of  $\beta$ -cyclodextrin inclusion complex constants for 3,4-dihydro-2-*H*-1-benzopyran enantiomers by capillary electrophoresis 707(1995)311  
 Bauza, T., Blaise, A., Daumas, F. and Cabanis, J.C.  
 Determination of biogenic amines and their precursor amino acids in wines of the Vallée du Rhône by high-performance liquid chromatography with precolumn derivatization and fluorimetric detection 707(1995)373  
 Bayol, A., see Dupin, P. 707(1995)396  
 Beddell, C., see Ashton, D.S. 707(1995)367  
 Betts, T.J.  
 Use of a trio of modified cyclodextrin gas chromatographic phases to provide structural information on some constituents of volatile oils 707(1995)390  
 Blaise, A., see Bauza, T. 707(1995)373  
 Bonfichi, R., Dallanocce, C., Lociuo, S. and Spada, A.  
 Free-solution capillary electrophoretic resolution of chiral amino acids via derivatization with homochiral isothiocyanates. Part I 707(1995)355  
 Bonwick, G.A., Sun, C., Abdul-Latif, P., Baugh, P.J., Smith, C.J., Armitage, R. and Davies, D.H.  
 Determination of permethrin and cyfluthrin in water and sediment by gas chromatography-mass spectrometry operated in the negative chemical ionization mode 707(1995)293  
 Boye, S., see Baummy, Ph. 707(1995)311  
 Bringmann, G., Hesselmann, C. and Feineis, D.  
 Endogenous alkaloids in man. XXI. Analysis of glyoxylate-derived 1,3-thiazolidines and their precursors after trimethylsilylation by gas chromatography-mass spectrometry 707(1995)267  
 Cabanis, J.C., see Bauza, T. 707(1995)373  
 Cabezas, H., Cole, K.D. and Hubbard, J.B.  
 Foreword 707(1995)1  
 Cabral, J.M.S., see Queiroz, J.A. 707(1995)137  
 Chaiken, I., see Jones, C. 707(1995)3  
 Coffman, J.L., see Lightfoot, E.N. 707(1995)45  
 Cole, K.D., Todd, P., Srinivasan, K. and Dutta, B.K.  
 Free-solution electrophoresis of proteins in an improved density gradient column and by capillary electrophoresis 707(1995)77  
 Cole, K.D., see Cabezas, H. 707(1995)1  
 Corkum, N., see Goodlett, D.R. 707(1995)233  
 Cramer, S.M., see Kundu, A. 707(1995)57  
 Crouzet, J., see Langourieux, S. 707(1995)181  
 Crowther, J.B., see Goodlett, D.R. 707(1995)233  
 Dallanocce, C., see Bonfichi, R. 707(1995)355  
 Daumas, F., see Bauza, T. 707(1995)373  
 Davies, D.H., see Bonwick, G.A. 707(1995)293  
 DeMarco, J., see Qin, X.-Z. 707(1995)245  
 Dreux, M., see Baummy, Ph. 707(1995)311  
 Dupin, P., Galinou, F. and Bayol, A.  
 Analysis of recombinant human growth hormone and its related impurities by capillary electrophoresis 707(1995)396  
 Dutta, B.K., see Cole, K.D. 707(1995)77  
 Elliker, P.R., see Lam, P. 707(1995)29  
 Emehiser, C., Sander, L.C. and Schwartz, S.J.  
 Capability of a polymeric C<sub>30</sub> stationary phase to resolve *cis-trans* carotenoid isomers in reversed-phase liquid chromatography 707(1995)205  
 Feineis, D., see Bringmann, G. 707(1995)267  
 Fischer, C.-H. and Siebrands, T.  
 Analysis of colloids. VIII. Concentration- and memory effects in size exclusion chromatography of colloidal inorganic nanometer-particles 707(1995)189  
 Fuchs, M., see Mhatre, R. 707(1995)225  
 Galinou, F., see Dupin, P. 707(1995)396  
 Garcia, F.A.P., see Queiroz, J.A. 707(1995)137  
 García, I., see Aramendia, M.A. 707(1995)327  
 Gemeiner, P., see Nilsson, K.G.I. 707(1995)199  
 Goldstein, G., see Goodlett, D.R. 707(1995)233  
 Goodlett, D.R., Abuaf, P.A., Savage, P.A., Kowalski, K.A., Mukherjee, T.K., Tolan, J.W., Corkum, N., Goldstein, G. and Crowther, J.B.  
 Peptide chiral purity determination: hydrolysis in deuterated acid, derivatization with Marfey's reagent and analysis using high-performance liquid chromatography-electrospray ionization-mass spectrometry 707(1995)233  
 Griffin, S., see Jones, C. 707(1995)3  
 Guillaumet, G., see Baummy, Ph. 707(1995)311  
 Hela, D.G., see Albanis, T.A. 707(1995)283  
 Hesselmann, C., see Bringmann, G. 707(1995)267  
 Hirayama, N., Maruo, M., Shiota, A. and Kuwamoto, T.  
 Use of  $\beta$ -diketone anions as eluent in non-suppressed ion chromatography: 1,3-cyclohexanedionate as acidic eluent 707(1995)384

- Huang, X. and Kok, W.Th.  
Determination of sugars by capillary electrophoresis with electrochemical detection using cuprous oxide modified electrodes 707(1995)335
- Hubbard, J.B., see Cabezas, H. 707(1995)1
- Ip, D.P., see Qin, X.-Z. 707(1995)245
- Ishizawa, S., see Kodama, M. 707(1995)117
- Jones, C., Patel, A., Griffin, S., Martin, J., Young, P., O'Donnell, K., Silverman, C., Porter, T. and Chaiken, I.  
Current trends in molecular recognition and bioseparation 707(1995)3
- Kanaki, T., see Kodama, M. 707(1995)117
- Kitahara, H., see Ôi, N. 707(1995)380
- Kodama, M., Ishizawa, S., Koiwa, A., Kanaki, T., Shibata, K. and Motomura, H.  
Scale-up of liquid chromatography for industrial production of parenteral antibiotic E1077 707(1995)117
- Kohlmann, K., see Basak, S.K. 707(1995)69
- Koiwa, A., see Kodama, M. 707(1995)117
- Kok, W.Th., see Huang, X. 707(1995)335
- Kowalski, K.A., see Goodlett, D.R. 707(1995)233
- Kundu, A., Vunnum, S. and Cramer, S.M.  
Antibiotics as low-molecular-mass displacers in ion-exchange displacement chromatography 707(1995)57
- Kuwamoto, T., see Hirayama, N. 707(1995)384
- Ladisch, M.R., see Basak, S.K. 707(1995)69
- Lafont, F., see Aramendia, M.A. 707(1995)327
- Lam, P., Elliker, P.R., Wnek, G.E. and Przybycien, T.M.  
Towards an electrochemically modulated chromatographic stationary phase 707(1995)29
- Langourieux, S. and Crouzet, J.  
Study of aroma compound-natural polymer interactions by dynamic coupled column liquid chromatography 707(1995)181
- Lee, M.L., see Shen, Y. 707(1995)303
- Lee, S.T. and Olesik, S.V.  
Normal-phase high-performance liquid chromatography using enhanced-fluidity liquid mobile phases 707(1995)217
- Li, S.F.Y., see Wang, T. 707(1995)343
- Li, W., see Shen, Y. 707(1995)303
- Lightfoot, E.N., Athalye, A.M., Coffman, J.L., Roper, D.K. and Root, T.W.  
Nuclear magnetic resonance and the design of chromatographic separations 707(1995)45
- Ling, D., see Zheng, Z. 707(1995)131
- Lociuro, S., see Bonfichi, R. 707(1995)355
- Malik, A., see Shen, Y. 707(1995)303
- Marinas, J.M., see Aramendia, M.A. 707(1995)327
- Martin, J., see Jones, C. 707(1995)3
- Martys, N.S.  
Numerical simulation of hydrodynamic dispersion in random porous media 707(1995)35
- Maruo, M., see Hirayama, N. 707(1995)384
- Matisová, E. and Škrabáková, S.  
Carbon sorbents and their utilization for the preconcentration of organic pollutants in environmental samples 707(1995)145
- Mhatre, R., Nashabeh, W., Schmalzing, D., Yao, X., Fuchs, M., Whitney, D. and Regnier, F.  
Purification of antibody Fab fragments by cation-exchange chromatography and pH gradient elution 707(1995)225
- Morin, Ph., see Baomy, Ph. 707(1995)311
- Mosbach, K., see Nilsson, K.G.I. 707(1995)199
- Motomura, H., see Kodama, M. 707(1995)117
- Mukherjee, T.K., see Goodlett, D.R. 707(1995)233
- Nashabeh, W., see Mhatre, R. 707(1995)225
- Nickless, G., see Sturrock, G.A. 707(1995)255
- Nilsson, K.G.I., Sakaguchi, K., Gemeiner, P. and Mosbach, K.  
Molecular imprinting of acetylated carbohydrate derivatives into methacrylic polymers 707(1995)199
- Ôi, N., Kitahara, H. and Aoki, F.  
Direct separation of carboxylic acid and amine enantiomers by high-performance liquid chromatography on reversed-phase silica gels coated with chiral copper(II) complexes 707(1995)380
- Olesik, S.V., see Lee, S.T. 707(1995)217
- O'Donnell, K., see Jones, C. 707(1995)3
- Patel, A., see Jones, C. 707(1995)3
- Pearlstein, A.J., see Shiue, M.-P. 707(1995)87
- Porter, T., see Jones, C. 707(1995)3
- Przybycien, T.M., see Lam, P. 707(1995)29
- Qin, X.-Z., DeMarco, J. and Ip, D.P.  
Simultaneous determination of enalapril, felodipine and their degradation products in the dosage formulation by reversed-phase high-performance liquid chromatography using a Spherisorb C<sub>8</sub> column 707(1995)245
- Queiroz, J.A., Garcia, F.A.P. and Cabral, J.M.S.  
Hydrophobic interaction chromatography of *Chromobacterium viscosum* lipase 707(1995)137
- Ray, A.D., see Ashton, D.S. 707(1995)367
- Regnier, F., see Mhatre, R. 707(1995)225
- Root, T.W., see Lightfoot, E.N. 707(1995)45
- Roper, D.K., see Lightfoot, E.N. 707(1995)45
- Row, K.H.  
Combined continuous and preparative chromatographic separation 707(1995)105
- Sakaguchi, K., see Nilsson, K.G.I. 707(1995)199
- Sander, L.C., see Emehiser, C. 707(1995)205
- Savage, P.A., see Goodlett, D.R. 707(1995)233
- Schmalzing, D., see Mhatre, R. 707(1995)225
- Schwartz, S.J., see Emehiser, C. 707(1995)205
- Shen, Y., Malik, A., Li, W. and Lee, M.L.  
Packed capillary column supercritical fluid chromatography using SE-54 polymer encapsulated silica 707(1995)303
- Shibata, K., see Kodama, M. 707(1995)117
- Shiota, A., see Hirayama, N. 707(1995)384
- Shiue, M.-P. and Pearlstein, A.J.  
Free-solution electrophoresis with amplification of small mobility differences by helical flow 707(1995)87
- Siebrands, T., see Fischer, C.-H. 707(1995)189
- Silverman, C., see Jones, C. 707(1995)3
- Simmonds, P.G., see Sturrock, G.A. 707(1995)255
- Škrabáková, S., see Matisová, E. 707(1995)145
- Smith, C.J., see Bonwick, G.A. 707(1995)293



- Sofer, G.  
Preparative chromatographic separations in pharmaceutical, diagnostic, and biotechnology industries: current and future trends 707(1995)23
- Spada, A., see Bonfichi, R. 707(1995)355
- Srinivasan, K., see Cole, K.D. 707(1995)77
- Sturrock, G.A., Simmonds, P.G. and Nickless, G.  
Investigation of the use of oxygen doping of the electron-capture detection for determination of atmospheric halocarbons 707(1995)255
- Sun, C., see Bonwick, G.A. 707(1995)293
- Sun, Y., see Zheng, Z. 707(1995)131
- Todd, P., see Cole, K.D. 707(1995)77
- Tolan, J.W., see Goodlett, D.R. 707(1995)233
- Valkó, K., see Ashton, D.S. 707(1995)367
- Velayudhan, A., see Basak, S.K. 707(1995)69
- Viaud, M.C., see Baomy, Ph. 707(1995)311
- Vunnum, S., see Kundu, A. 707(1995)57
- Wang, T. and Li, S.F.Y.  
Migration behaviour of alkali and alkaline-earth metal ion-EDTA complexes and quantitative analysis of magnesium in real samples by capillary electrophoresis with indirect ultraviolet detection 707(1995)343
- Whitney, D., see Mhatre, R. 707(1995)225
- Wnek, G.E., see Lam, P. 707(1995)29
- Yao, X., see Mhatre, R. 707(1995)225
- Young, P., see Jones, C. 707(1995)3
- Zheng, Z., Ling, D. and Sun, Y.  
Production of rare-earth oxides of high purity 707(1995)131



# Carbohydrate Analysis

## High Performance Liquid Chromatography and Capillary Electrophoresis

Edited by **Z. El Rassi**

**Journal of Chromatography Library, Volume 58**

The objective of the present book is to provide a comprehensive review of carbohydrate analysis by HPLC and HPCE by covering analytical and preparative separation techniques for all classes of carbohydrates including mono- and disaccharides; linear and cyclic oligosaccharides; branched heterooligosaccharides (e.g., glycans, plant-derived oligosaccharides); glycoconjugates (e.g., glycolipids, glycoproteins); carbohydrates in food and beverage; compositional carbohydrates of polysaccharides; carbohydrates in biomass degradation; etc.

The book will be of interest to a wide audience, including analytical chemists and biochemists, carbohydrate, glycoprotein and glycolipid chemists, molecular biologists, biotechnologists, etc. It will also be a useful reference work for both the experienced analyst and the newcomer as well as for users of HPLC and HPCE, graduates and postdoctoral students.

### **Contents: Part I. The Solute.**

1. Preparation of carbohydrates for analysis by HPLC and HPCE (A.J. Mort, M.L. Pierce).

### **Part II. Analytical and Preparative Separations.**

2. Reversed-phase and hydrophobic interaction chromatography of carbohydrates and glycoconjugates (Z. El Rassi).

3. High performance hydrophilic interaction chromatography of carbohydrates with

polar solvents (S.C. Churms).  
4. HPLC of carbohydrates with cation- and anion-exchange silica and resin-based stationary phases (C.G. Huber, G.K. Bonn).  
5. Analysis of glycoconjugates using high-pH anion-exchange chromatography (R.R. Townsend).  
6. Basic studies on carbohydrate - protein interaction by high performance affinity chromatography and high performance capillary affinity electrophoresis using lectins as protein models (S. Honda).  
7. Modern size exclusion chromatography of carbohydrates and glycoconjugates (S.C. Churms).  
8. High performance capillary electrophoresis of carbohydrates and glycoconjugates (Z. El Rassi, W. Nashabeh).  
9. Preparative HPLC of carbohydrates (K.B. Hicks).

### **Part III. The Detection.**

10. Pulsed electrochemical detection of carbohydrates at gold electrodes following liquid chromatographic separation (D.C. Johnson,

W.R. LaCourse).  
11. On-column refractive index detection of carbohydrates separated by HPLC and CE (A.E. Bruno, B. Krattiger).  
12. Mass spectrometry of carbohydrates and glycoconjugates (C.A. Settineri, A.L. Burlingame).  
13. Evaporative light scattering detection of carbohydrates in HPLC (M. Dreux, M. Lafosse).  
14. Chiroptical detectors for HPLC of carbohydrates (N. Purdie).  
15. Pre- and post-column detection-oriented derivatization techniques in HPLC of carbohydrates (S. Hase).  
16. Post-column enzyme reactors for the HPLC determination of carbohydrates (L.J. Nagels, P.C. Maes).  
17. Other direct and indirect detection methods of carbohydrates in HPLC and HPCE (Z. El Rassi, J.T. Smith).  
Subject index.

**©1995 692 pages Hardbound**  
**Price: Dfl. 425.00 (US\$250.00)**  
**ISBN 0-444-89981-2**

### **ORDER INFORMATION**

ELSEVIER SCIENCE B.V.  
P.O. Box 330  
1000 AH Amsterdam  
The Netherlands  
Fax: +31 (20) 485 2845

For USA and Canada:  
P.O. Box 945, New York  
NY 10159-0945  
Fax: +1 (212) 633 3680

*US\$ prices are valid only for the USA & Canada and are subject to exchange rate fluctuations; in all other countries the Dutch guilder price (Dfl.) is definitive. Customers in the European Union should add the appropriate VAT rate applicable in their country to the price(s). Books are sent postfree if prepaid.*



**ELSEVIER**

An imprint of Elsevier Science

# Trace Element Analysis in Biological Specimens

Edited by R.F.M. Herber and M. Stoeppler

Techniques and Instrumentation in Analytical Chemistry Volume 15

The major theme of this book is analytical approaches to trace metal and speciation analysis in biological specimens. The emphasis is on the reliable determination of a number of toxicologically and environmentally important metals. It is essentially a handbook based on the practical experience of each individual author. The scope ranges from sampling and sample preparation to the application of various modern and well-documented methods, including quality assessment and control and statistical treatment of data. Practical advice on avoiding sample contamination is included.

In the first part, the reader is offered an introduction into the basic principles and methods, starting with sampling, sample storage and sample treatment, with the emphasis on sample decomposition. This is followed by a description of the potential of atomic absorption spectrometry, atomic emission spectrometry, voltammetry, neutron activation analysis, isotope dilution analysis, and the possibilities for metal speciation in biological specimens. Quality control and all approaches to achieve reliable data are treated in chapters about interlaboratory and intralaboratory surveys and reference methods, reference materials and statistics and data evaluation.

The chapters of the second part provide detailed information on the analysis of thirteen trace metals in the most important biological specimens. The following metals are treated in

great detail: Aluminium, arsenic, cadmium, chromium, copper, lead, selenium, manganese, nickel, mercury, thallium, vanadium and zinc.

The book will serve as a valuable aid for practical analysis in biomedical laboratories and for researchers involved with trace metal and species analysis in clinical, biochemical and environmental research.

## Contents: Part 1. Basic Principles and Methods.

1. Sampling and sample storage (A. Aitio, J. Järvisalo, M. Stoeppler).
2. Sample treatment of human biological materials (B. Sansoni, V.K. Panday).
3. Graphite furnace AAS (W. Slavin).
4. Atomic absorption spectrometry. Flame AAS (W. Slavin).
5. Atomic emission spectrometry (P. Schramel).
6. Voltammetry (J. Wang).
7. Neutron activation analysis (J. Versieck).
8. Isotope dilution mass spectrometry (IDMS) (P. de Bièvre).
9. The chemical speciation of trace elements in biomedical specimens: Analytical techniques (P.H.E. Gardiner, H.T. Delves).
10. Interlaboratory

and intralaboratory surveys.

Reference methods and reference materials (R.A. Braithwaite). 11. Reference materials for trace element analysis (R.M. Parr, M. Stoeppler). 12. Statistics and data evaluation (R.F.M. Herber, H.J.A. Sallé).

**Part 2. Elements.** 13. Aluminium (J. Savory, R.L. Bertholf, S. Brown, M.R. Wills). 14. Arsenic (M. Stoeppler, M. Vahter). 15. Cadmium (R.F.M. Herber). 16. Chromium (R. Cornelis). 17. Copper (H.T. Delves, M. Stoeppler). 18. Lead (U. Ewers, M. Turfeld, E. Jermann). 19. Manganese (D.J. Halls). 20. Mercury (A. Schütz, G. Skarping, S. Skerfving). 21. Nickel (D. Templeton). 22. Selenium (Y. Thomassen, S.A. Lewis, C. Veillon). 23. Thallium (M. Sager). 24. Vanadium (K.-H. Schaller). 25. Zinc (G.S. Fell, T.D.B. Lyon). Subject index.

©1994 590 pages Hardbound  
Price: Dfl. 475.00 (US\$ 279.50)  
ISBN 0-444-89867-0

## ORDER INFORMATION

**ELSEVIER SCIENCE B.V.**  
Order Fulfillment Department  
P.O. Box 211  
1000 AE Amsterdam  
The Netherlands  
Fax: +31 (20) 485 3598  
For USA and Canada:  
**ELSEVIER SCIENCE B.V.**  
P.O. Box 945, New York  
NY 10159-0945  
Fax: +1 (212) 633 3680

US\$ prices are valid only for the USA & Canada and are subject to exchange rate fluctuations; in all other countries the Dutch guilder price (Dfl.) is definitive. Customers in the European Union should add the appropriate VAT rate applicable in their country to the price(s). Books are sent postfree if prepaid.



**ELSEVIER**

An imprint of Elsevier Science

## PUBLICATION SCHEDULE FOR THE 1995 SUBSCRIPTION

### *Journal of Chromatography A and Journal of Chromatography B: Biomedical Applications*

MONTH	1994	J-M	A	M <sup>a</sup>	J	J	
Journal of Chromatography A	Vols. 683-688	689-695	696/1 696/2 697/1 + 2 698/1 + 2	699/1 + 2 700/1 + 2 702/1 + 2 703/1 + 2	704/1 704/2 705/1 705/2	706/1 + 2 707/1 707/2 708/1	The publication schedule for further issues will be published later.
Bibliography Section		713/1			713/2		
Journal of Chromatography B: Biomedical Applications		663-665	666/1 666/2	667/1 667/2	668/1 668/2	669/1 669/2	

<sup>a</sup> Vol. 701 (Cumulative Indexes Vols. 652-700) expected in October.

### INFORMATION FOR AUTHORS

(Detailed *Instructions to Authors* were published in *J. Chromatogr. A*, Vol. 657, pp. 463-469. A free reprint can be obtained by application to the publisher, Elsevier Science B.V., P.O. Box 330, 1000 AH Amsterdam, Netherlands.)

**Types of Contributions.** The following types of papers are published: Regular research papers (full-length papers), Review articles, Short Communications and Discussions. Short Communications are usually descriptions of short investigations, or they can report minor technical improvements of previously published procedures; they reflect the same quality of research as full-length papers, but should preferably not exceed five printed pages. Discussions (one or two pages) should explain, amplify, correct or otherwise comment substantively upon an article recently published in the journal. For Review articles, see inside front cover under Submission of Papers.

**Submission.** Every paper must be accompanied by a letter from the senior author, stating that he/she is submitting the paper for publication in the *Journal of Chromatography A* or *B*.

**Manuscripts.** Manuscripts should be typed in **double spacing** on consecutively numbered pages of uniform size. The manuscript should be preceded by a sheet of manuscript paper carrying the title of the paper and the name and full postal address of the person to whom the proofs are to be sent. As a rule, papers should be divided into sections, headed by a caption (e.g., Abstract, Introduction, Experimental, Results, Discussion, etc.). All illustrations, photographs, tables, etc., should be on separate sheets.

**Abstract.** All articles should have an abstract of 50-100 words which clearly and briefly indicates what is new, different and significant. No references should be given.

**Introduction.** Every paper must have a concise introduction mentioning what has been done before on the topic described, and stating clearly what is new in the paper now submitted.

**Experimental conditions** should preferably be given on a *separate* sheet, headed "Conditions". These conditions will, if appropriate, be printed in a block, directly following the heading "Experimental".

**Illustrations.** The figures should be submitted in a form suitable for reproduction, drawn in Indian ink on drawing or tracing paper. Each illustration should have a caption, all the *captions* being typed (with double spacing) together on a *separate sheet*. If structures are given in the text, the original drawings should be provided. Coloured illustrations are reproduced at the author's expense, the cost being determined by the number of pages and by the number of colours needed. The written permission of the author and publisher must be obtained for the use of any figure already published. Its source must be indicated in the legend.

**References.** References should be numbered in the order in which they are cited in the text, and listed in numerical sequence on a separate sheet at the end of the article. Please check a recent issue for the layout of the reference list. Abbreviations for the titles of journals should follow the system used by *Chemical Abstracts*. Articles not yet published should be given as "in press" (journal should be specified), "submitted for publication" (journal should be specified), "in preparation" or "personal communication".

Vols. 1-651 of the *Journal of Chromatography*; *Journal of Chromatography, Biomedical Applications* and *Journal of Chromatography, Symposium Volumes* should be cited as *J. Chromatogr.* From Vol. 652 on, *Journal of Chromatography A* (incl. Symposium Volumes) should be cited as *J. Chromatogr. A* and *Journal of Chromatography B: Biomedical Applications* as *J. Chromatogr. B*.

**Dispatch.** Before sending the manuscript to the Editor please check that the envelope contains four copies of the paper complete with references, captions and figures. One of the sets of figures must be the originals suitable for direct reproduction. Please also ensure that permission to publish has been obtained from your institute.

**Proofs.** One set of proofs will be sent to the author to be carefully checked for printer's errors. Corrections must be restricted to instances in which the proof is at variance with the manuscript.

**Reprints.** Fifty reprints will be supplied free of charge. Additional reprints can be ordered by the authors. An order form containing price quotations will be sent to the authors together with the proofs of their article.

**Advertisements.** The Editors of the journal accept no responsibility for the contents of the advertisements. Advertisement rates are available on request. Advertising orders and enquiries can be sent to the Advertising Manager, Elsevier Science B.V., Advertising Department, P.O. Box 211, 1000 AE Amsterdam, Netherlands; Tel: 31 (20) 485 3796; Fax: 31 (20) 485 3810. Courier shipments to street address: Molenwerf 1, 1014 AG Amsterdam, Netherlands. UK: T.G. Scott & Son Ltd., Tim Blake, Portland House, 21 Narborough Road, Cosby, Leics. LE9 5TA, UK; Tel: (0116) 2750 521/2753 333; Fax: (0116) 2750 522. USA and Canada: Weston Media Associates, Daniel S. Lipner, P.O. Box 1110, Greens Farms, CT 06436-1110, USA; Tel: (203) 261 2500; Fax: (203) 261 0101.

# Chromatography in the Petroleum Industry

Edited by E.R. Adlard

Journal of Chromatography Library, Volume 56

Petroleum mixtures consist primarily of relatively unreactive complex hydrocarbons covering a wide boiling range. Such mixtures are difficult to separate by most analytical techniques. Therefore, the petroleum industry has for many years played a leading role in the development of chromatographic methods of analysis. Since the last book specifically concerned with chromatographic analysis of petroleum appeared 15 years ago, numerous advances have been made including developments in liquid and supercritical fluid chromatography, the advent of silica capillary columns with bonded stationary phases and the commercial availability of new selective detectors.

The current book contains chapters written by experts concerning the analysis of mixtures ranging from low boiling gases to waxes and crude oils.

Although the volume is specifically aimed at the petroleum analyst, there is much information of general interest which should be of benefit to a very wide readership.

## Contents:

1. The analysis of hydrocarbon gases (C.J. Cowper).
2. Advances in simulated distillation (D.J. Abbott).
3. The chromatographic analysis of refined and synthetic waxes (A. Barker).
4. Hydrodynamic chromatography of polymers (J. Bos, R. Tijssen).
5. Chromatography in petroleum geochemistry (S.J. Rowland, A.T. Revill).
6. The O-FID and its applications in petroleum product analysis (A. Sironi, G.R. Verga).
7. Microwave plasma detectors (A. de Wit, J. Beens).
8. The sulfur chemiluminescence detector (R.S. Hutte).
9. Multi-column systems in gas chromatography (H. Mahler, T. Maurer, F. Müller).
10. Supercritical fluid extraction (T.P. Lynch).
11. Supercritical fluid chromatography (I. Roberts).
12. HPLC and column liquid chromatography (A.C. Neal).
13. Modern data handling methods (N. Dyson).
14. Capillary electrophoresis in the petroleum industry (T. Jones, G. Bondoux).

©1995 452 pages Hardbound  
Price: Dfl. 435.00 (US\$ 255.75)  
ISBN 0-444-89776-3

## ORDER INFORMATION

ELSEVIER SCIENCE B.V.  
P.O. Box 330  
1000 AH Amsterdam  
The Netherlands  
Fax: +31 (20) 485 2845  
For USA and Canada:  
P.O. Box 945, New York  
NY 10159-0945  
Fax: +1 (212) 633 3680



**ELSEVIER**

An imprint of Elsevier Science

US\$ prices are valid only for the USA & Canada and are subject to exchange rate fluctuations; in all other countries the Dutch guildler price (Dfl.) is definitive. Customers in the European Union should add the appropriate VAT rate applicable in their country to the price(s). Books are sent postfree if prepaid.



0021-9673(19950721)707:2;1-2

7 2 0 0 2539